



In this volume are collected the proceedings of the Annual General Meeting of CORILA, held 14th – 16th April 2005 at Palazzo Franchetti, Venice



**SCIENTIFIC RESEARCH
AND SAFEGUARDING OF VENICE
2005**

CORILA Research
Research Program 2004 - 2006

Edit by
PIERPAOLO CAMPOSTRINI

VENEZIA – 2005

© Copyright CORILA. Consorzio per la Gestione del Centro di Coordinamento
delle Ricerche Inerenti il Sistema Lagunare di Venezia

30124 Venezia – Palazzo Franchetti, S. Marco 2847

Tel. +39-041-2402511 – Telefax +39-041-2402512

venezia@corila.it

www.corila.it

Stampa “Multigraf” Spinea, Venezia 2006

INDEX

<i>Valuing the benefits of contaminated sites remediation</i> – A. Chiabai, A. Alberini, M. Turvani, S. Tonin	5
<i>The EL.GI.R.A support system for knowledge building and evaluation in brownfield redevelopment. An application in the ‘Ex Sava Alumix’ area in Porto Marghera (Venice)</i> - D. Patassini, P. Cossettini, E. De Polignol, E. Fabris, M. Hedorfer, E. Rinaldi, E. Verni	21
<i>Support policies for the re-use of abandoned areas: the case of the Venice arsenal</i> - G. Stellin, G. Zoboli	45
<i>The economic reuse of the built heritages a proposal for a set of sustainability indicators</i> – V. Zanatta, M. Dalla Valle, P. Rosato	55
<i>Marmorino plasters in Venice between the XVI and XVIII centuries</i> – M. Piana	71
<i>The maintenance of the urban fabric in Venice in the modern era: gis and archival sources</i> – G. Vertecchi	91
<i>Analysis of the structural behaviour of the historical venetian buildings through theoretical and experimental models: state of the research</i> – D. Chiffi, P. Faccio, A. Vanin	99
<i>Detecting constructive patterns for structural damage interpretation of historic buildings in Venice</i> – F. Doglioni, G. Mirabella Roberti, M. Bondanelli, F. Trovò	115
<i>Venetian building diagnostics information system</i> – L. Marescotti, M. Mascione, S. Maffulli ³	135
<i>Restoration works in the city of Venice geotechnical aspects</i> – A. Mazzucato, A. Dei Svaldi, E. Dalla Corte	146
<i>From the artificial stone to the reinforced concrete: data system project for diagnostics</i> – M. Pretelli, A. Matteini, I. Daga	156
<i>Determination of trace elements and polycyclic aromatic hydrocarbons in the Venice aerosol (PM2.5)</i> - A. Gambaro, L. Manodori, G. Toscano, R. Zangrando, W.R.L. Cairns, G. Capodaglio	171
<i>Fugacity/aquivalence modelling framework of contaminant (pops and heavy metals) fate and transport in the Venice Lagoon</i> – J. Sommerfreund, S. Bhavsar, N. Gandhi, S. Gewurtz, M. Diamond, S. Giuliani, M. Frignani	179

Measurements of pm2.5 concentration and vertical turbulent mass fluxes in the surface layer – D. Contini, A. Donateo, F. Belosi, F. Prodi	193
Size characterization of aerosol in the Venice Lagoon - F.Prodi, F.Belosi , S. Ferrari, G. Santachiara, P. Masia,	207
Time variant tomography monitoring of the salt-water intrusion: geoelectrical survey of the test-site – R. De Franco, G. Biella, G. Boniolo, A. Corsi, A. Morrone, A. Lozej, G. Saracco, B. Chiozzotto, M. Giada, M. Barbeta, V. Bassan, C. Christelle, E. Conchetto, G. Gasparetto-Stori, A. Gaspari, A. Mayer, F. Rizzetto, L. Tosi	217
Radon activity in the southern Lagoon of Venice and the Adriatic Sea -A. Mayer, J. Gattacceca, C. Claude, O. Radakovitch, M. Giada, A. Cucco, C. Vallet-Coulomb, B. Stenni, O; Flora, L. Tosi, F. Rizzetto.	227
Temporal and biotic evolution of “botryllus biocoenosis” in the presence of antifouling paints – F. Cima, P. Burighel, L. Ballarin	239
An integrated approach to biological monitoring in the Lagoon of Venice – F. Giomi, M. Beltramini, G. Fusco, D. Maruzzo, L. Zane, P. Maria Bisol	247
Verification of a pops bioaccumulation model for the Venice Lagoon –T. Lovato, C. Micheletti, R. Pastres, A. Marcomini	259
Vitellogenin induction as biomarker of exposure to xenoestrogenic compounds in the clam tapes philippinarum: experiments with 4-nonylphenol –M. G. Marin, V. Matozzo	273
Microbial production and degradation of organic carbon in the Lagoon of Venice: preliminary results. -A. Pugnetti, F. Aciri, P. Del Negro, M. Giani, F. Bernardi Aubry, D. Berto, E. Crevatin, C. Facca, P. Franceschetti, E. Ravagnan, F. Savelli, A.Valeri, V. Zangrando	283
Nutrient concentration updating in the waters of the Venice Lagoon - A. Sfriso, N. Pellegrino, S. Ceoldo, C. Facca,	291
Comparison between a theoretical model and a numerical simulation of sea-lagoon interaction in the northern Adriatic -D. Bellafiore, G.Ungiesser	301
Assessment of water quality status in the coastal area close to the Lagoon of Venice. first year of activity -M. Bastianini, C. Solidoro, V. Bandelj, D. Bellafiore, R. Codermatz, G. Cossarini, A. Cucco, D. Melaku Canu, E. Ravagnan, G. Ungiesser, M. Vazzoler, A. R. Zogno	311
Quantifying shear stress due to wind waves and tidal currents in	339

<i>the Venice Lagoon</i> –L. Carniello, A. Defina, L. D'alpaos	
<i>Sediment transport model application to lido inlet and treporti canal</i> –F. De Pascalis, G. Umgiesser, C. Ferrarin, C. L. Amos	349
<i>Accuracy of surface current measurements from hf radar</i> –S. Cosoli, M. Gačić, A. Mazzoldi	365
<i>Estimate of the suspended solid matter concentration from the backscatter intensity measured by adcp</i> –F. Arena, V. Kovačević A. Mazzoldi	373
<i>Morphological evolution and sand pathways in northern Venice Lagoon, Italy</i> -R. Helsby, C. L. Amos, G. Umgiesser	388
<i>Assessing long-term changes in the kinematics of inlets of the venetian lagoon</i> -M. Mosquera, M. Gačić, A. Mazzoldi	403
<i>New very high resolution seismic surveys in shallow water to study the subsurface in the Venice Lagoon.</i> –G. Brancolini, L. Tosi, F. Rizzetto, F. Donda, L. Baradello, D. Nieto, F. Fanzutti, N. Wardell, P. Teatini, C. Amos, M. Bonardi.	417
<i>The origin of sand in Venice Lagoon the next step</i> -C.L. Amos, R. Helsby, C.E.L. Thompson, M. Villatoro, V. Venturini, E. Manca, A. Mazzoldi, G. Umgiesser, L. Tosi	429
<i>Experimental researches on the hydraulic behaviour of the ca' di mezzo in codevigo wetland</i> – V. Bixio, A. C. Bixio, M. Cerni, A. Marion, M. Zaramella	455
<i>Tidal simulation in Venice Lagoon</i> - M. Morandi Cecchi, M. Venturin	465
<i>A formulation of convection problems for shallow waters in Venice Lagoon</i> –M. Morandi Cecchi, M. Venturin	477
<i>A 3-D sediment transport model and bed reworking for the Venice Lagoon</i> –C. Ferrarin, G. Umgiesser, C. L. Amos,	491
<i>Environmental data and Venice Lagoon</i> – R. Orsini, F. Dalla Libera, S. De Zorzi, A. Roncato	507

IL SECONDO PASSO È SPESSO PIÙ IMPORTANTE DEL PRIMO

Pierpaolo Campostrini

Direttore CORILA

I fondi di finanziamento per il Primo Programma di Ricerca del CORILA sono stati stanziati dal Comitato interministeriale di coordinamento per la salvaguardia di Venezia e della Laguna, il cosiddetto "Comitatone", prima che il CORILA fosse attivo in città. Il Programma si basava ovviamente sulle linee guida individuate dal Ministero della Ricerca e dalla Comunità scientifica locale e costituiva un contributo fondamentale per l'implementazione dei punti programmatici della Legge Speciale per Venezia. Si trattava, potremmo dire, di una manifestazione di buoni intenti, in cui si sosteneva un qualcosa che ancora non era nato. Il primo finanziamento, di poco superiore a 6 M €, ha reso possibile la selezione e lo sviluppo del Primo Programma di Ricerca i cui risultati sono stati presentati nel 2004.

Alla fine del 2001, quando il Comitatone si riunisce per decidere il finanziamento del Secondo Programma di Ricerca, la struttura del CORILA è nata e il Primo Programma è già partito dimostrando tutta la validità e l'efficacia di questa nuova esperienza ancora in evoluzione. Il merito di questo successo era da attribuire da un lato alla lungimiranza della politica e degli amministratori locali e nazionale e dall'altro alle persone che hanno lavorato e si sono impegnate direttamente sul "campo", a partire dai ricercatori, sino a comprendere i membri del Comitato tecnico e scientifico, i direttori del Consiglio di Amministrazione, il Presidente e tutto lo staff di CORILA.

Questo è il motivo per cui consideriamo questo Secondo Programma di Ricerca molto più importante del primo. Un traguardo che ci rende orgogliosi e allo stesso tempo consapevoli che si apre una nuova fase, per molti versi ancora più difficile, in cui l'attenzione si concentrerà ora su tutti quegli errori che, sino a questo momento, hanno potuto essere accantonati per mancanza di esperienza. Ora saremmo, infatti, giudicati unicamente sulla base dei nostri risultati.

Ma il flusso dei finanziamenti si chiude con il 2001, non a causa di una valutazione negativa dei risultati, bensì per una riduzione dei fondi della Legge Speciale per Venezia che si ripercuote negativamente non solo sul CORILA, ma su numerosi enti ed Amministrazioni Pubbliche in città. Una situazione difficile, generata anche dall'inerzia generale degli anni passati, che ha posto tutti nella necessità di ricercare altrove nuove fonti di finanziamento.

Un percorso tortuoso né breve, né facile, nonostante il notevole finanziamento destinato al CORILA il 6 dicembre 2001 (un po' meno di 6 M €), ci ha condotto alla definizione della struttura del Secondo Programma di Ricerca e all'attuale stato di attività. Sin dall'inizio eravamo consapevoli delle difficoltà di carattere amministrativo che avrebbe implicato gestire un fondo non-standard e abbiamo,

quindi, cercato di redigere un Programma che fosse in sinergia con le priorità individuate dalla comunità scientifica a partire dalle richieste espresse dal Comitato.

Si è proceduto a definire e sviluppare la domanda, selezionare le proposte che meglio potevano dare delle risposte, preparare il quadro tecnico e amministrativo di questo Secondo Programma di Ricerca. Tutte queste attività hanno impegnato le energie e il tempo di molte persone. E' stato scelto di gestire i finanziamenti avendo come obiettivo ultimo quello di sostenere tutti i progetti scelti secondo un approccio globale capace di considerare i singoli progetti in rapporto alle esigenze dei ricercatori e in relazione alle richieste delle Amministrazioni Pubbliche e del Comitato. Questo ha permesso di massimizzare le risorse disponibili rispetto agli obiettivi generali. In molti casi le richieste superavano di gran lunga i fondi a disposizione. La situazione è stata risolta grazie alla costante e attenta collaborazione con i gruppi di ricerca e alla disponibilità di questi ultimi ad integrare i finanziamenti del Programma di ricerca con risorse aggiuntive al fine comunque di arrivare a dei risultati in linea con i fondi utilizzati.

Il 1° gennaio 2004 il Secondo Programma di Ricerca è partito e dovrà essere completato entro tre anni. Questo significa che entrò tre anni dovremmo aver raggiunto risultati importanti sullo studio e l'analisi della qualità dell'ambiente della Laguna di Venezia e che saremmo altresì in grado di fornire all'amministrazione locale strumenti validi di misura e valutazione a supporto delle politiche di intervento e delle scelte legislative.

La Laguna di Venezia da sempre è stata considerata come un laboratorio unico al mondo sia per lo studio del suo habitat naturale che per la sperimentazione di leggi e normative di gestione ambientale. Ma ogni riflessione su Venezia non può, oggi, prescindere dal valutare la dimensione europea: l'esperienza veneziana costituisce, ad esempio, un contributo fondamentale nel contesto della Direttiva Quadro sull'acqua.

Molte delle leggi, delle normative e dei decreti che oggi trovano applicazione nell'ambito della gestione della Laguna sembrano superati e non tengono in considerazione le conoscenze scientifiche acquisite e oggi disponibili. Sicuramente la strada per un rinnovamento della legislazione ambientale non è per nulla semplice e molti sono i "buchi" di conoscenza che le ricerche devono ancora colmare.

Desideriamo comunque presentare in un libro unico questa raccolta di lavori che costituiscono una sintesi dei progetti in via di realizzazione. Si tratta di risultati parziali e di lavori che spaziano in discipline molto diverse ma che danno un'idea dello sforzo e delle competenze che si sono attivate in questi anni. Il lettore trova in questo libro una fonte di notizie nei diversi campi specialistici e uno strumento di comprensione interdisciplinare di ciò che si sta esaminando.

E' un obbligo gradito ringraziare chi ci ha dato fiducia ed incoraggiamento, e soprattutto chi è stato disponibile allo scambio di dati ed informazioni: il

Ministero dell'Istruzione dell'Università e della Ricerca, il Magistrato alle acque di Venezia, il Consorzio Venezia Nuova, la Regione Veneto e l'ARPAV, la Provincia di Venezia, il Comune di Venezia ed in particolare il Servizio Legge Speciale, il Centro Maree ed i Civici Musei, il Comune di Chioggia e gli altri Comuni lagunari, i Consorzi di Bonifica, l'APAT- Servizio Laguna di Venezia, la Sovrintendenza ai Beni Architettonici e Culturali di Venezia. Siamo inoltre grati al personale amministrativo e tecnico dei dipartimenti universitari, degli istituti del CNR e del OGS, che hanno mantenuto la contabilità amministrativa assieme a quello del CORILA. Un ringraziamento del tutto particolare è esteso al Presidente e ai componenti del Comitato Tecnico Scientifico e del Consiglio di Amministrazione, per un impegno profuso con una passione che va al di là dell'obbligo del mandato.

Last but not least, un grazie alle persone che nello staff di CORILA hanno dimostrato non solo impegno ma anche la capacità di costruirsi una professionalità di sapore nuovo e tra essi in particolare l'ing. Stefania De Zorzi che ha curato con pazienza la messa insieme di questo libro.

THE SECOND STEP IS OFTEN MORE IMPORTANT THAN THE FIRST

Pierpaolo Campostrini

Director, CORILA

The funding for the First Research Programme of CORILA was decided by the Inter-Ministry Committee for addressing the intervention on Venice, “Comitatone”, before than CORILA itself was active. It was based, of course, on the serious intent expressed by the Ministry of Research and by the “local” scientific community to perform an activity useful for the issues addressed by the Special Law for Venice. However, in some sense it was an act of good will to support something still not born. The first funding, something more than 6 M€, allowed the First Programme to be developed up the final results presented in 2004.

In the moment of the decision for the second funding (end of 2001), the structure of CORILA was already born, and the First Programme has started. It is clear that this decision of Comitatore was based also on the success of the first experience, even if not concluded yet: therefore the merit in this case should be given not only to the “decision maker” on the political side, who again demonstrated to be long-sighted, but also to the people who worked on the field, starting from the Researchers involved, up to the Scientific Committee, the Board of Directors, the President and the CORILA’s staff.

This is why we consider this Second Research Programme even more important than the first one: we are proud of it and on the other side we know that the “honeymoon period”, where some mistakes could be forgiven for the lack of experience, is definitively over, and we’ll be judged only on the basis of our results.

Unfortunately, also the flux of funding have been stopped since 2001, and in this case it’s not our fault, nor we are alone in being disappointed. The Special Law for Venice is lacking of financial resources, and all the Administrations involved are suffering: as in our case, everybody is running thanks to the inertia of past years’ money, looking forward to finding new resources in future plans or elsewhere.

In any case, considering the important funding decided for us on the 6th Dec of 2001 (something less than 6 M€), the way from there to the actual starting of activities was not short nor easy. We were already aware about administrative problems for managing a non-standard fund and prepared to cope with the scientific issues involving the selection of a Programme, starting from the precise requests of the Comitatore.

However, it took times and energy of many people to develop the requests, to select the proposals, to prepare the administrative framework of this Second Programme. Also in this case, we did not want to distribute the financial resources just to satisfy the needs of many good researchers: the number of

projects selected has been maintained the minimum needed for answering to the “general” questions we received from the Administration represented in the Comitato, maximizing the resources given to each project. Notwithstanding this approach, in some cases the requests from the projects were much higher than the quantity of money available: a careful negotiation and the availability of all the Research Groups to use their additional resources as co-funding, allowed to agree on the ratio results achieved/money spent, which in principle should be quite high.

Finally, the Second Research Programme started the 1st of January 2004, to be completed in three years. At the end of the Program, we should be able to answer to some relevant questions concerning the quality of the environment in the Venice Lagoon, and how to measure it.

This will support important decisions on the interventions, and also on the legislation side. In Italy, the lagoon of Venice has been always a test bed for environmental oriented laws and technical norms: in this new millennium the European dimension should be considered, and the Venice experience can be very helpful in the application of the Water Framework Directive. Many norms, decrees and laws applied on the lagoon environment appears old today, under the light of the present scientific understanding, but the steps needed to renovate them are not trivial at all, and must be based on sound and solid knowledge of the environmental processes.

We still believe it is important to present this collection of works, presenting sometimes only partial results and covering a so large number of disciplines, in a single book. The reader can have an idea of the relevant effort spent and possibly find something of specific interest to use and to discuss, in a interdisciplinary dialogue.

As every year, it is a light and pleasant obligation to thank those who have trusted and encouraged us, especially for the exchange of data and information. They are: the Ministry for Education, University and Research, the Magistrato alle Acque di Venezia, the Consorzio Venezia Nuova, Regione del Veneto and ARPAV, Provincia di Venezia, Comune di Venezia and especially the Servizio Legge Speciale, Istituzione Centro Maree and Civici Musei, Comune di Chioggia and the other lagoon municipalities, the Consorzi di Bonifica, APAT-Servizio Laguna di Venezia, Sovrintendenza ai Beni Architettonici e Culturali di Venezia. We are also grateful to the technical and administrative staff of the University departments, CNR and OGS institutes who kept the administrative records alongside CORILA. A special thanks is extended to members of the Technical Scientific Committee and the Management Board, for profuse commitment and passion which extends beyond the obligations of the role.

Last but not least, thanks to the staff at CORILA who has grown in experience and capabilities and especially to ing. Stefania De Zorzi who patiently put together this book.

AREA 1
Economics

RESEARCH LINE 1.2

Cost-benefits analysis of land reclamation of brownfields in the Venice lagoon

VALUING THE BENEFITS OF CONTAMINATED SITES REMEDIATION

Aline Chiabai¹, Anna Alberini², Margherita Turvani³, Stefania Tonin⁴

¹ FEEM, Venezia ² Agricultural and Resource Economics Department, University of Maryland ³ Department of Planning, Università IUAV di Venezia ⁴ Department of Planning, Università IUAV di Venezia

Riassunto.

La bonifica dei siti contaminati permette di ottenere numerosi benefici di tipo economico, ambientale e sanitario. In questo studio ci siamo concentrati in modo particolare sui benefici derivanti da una riduzione della mortalità per effetto del ripristino ambientale dei siti contaminati in Italia. Per ottenere una valutazione monetaria di questi benefici, abbiamo utilizzato una metodologia basata sul concetto del valore della vita statistica, che è un elemento chiave per riuscire ad ottenere una valutazione dei miglioramenti della salute umana a seguito dell'applicazione di politiche ambientali. Per riuscire ad ottenere una misura del valore della vita statistica abbiamo costruito un questionario di analisi congiunta con lo scopo di indagare la disponibilità a pagare delle persone per una propria riduzione del rischio di morire a causa dell'esposizione a sostanze tossiche. In questo articolo, analizzeremo alcune principali questioni metodologiche relative alla costruzione e al perfezionamento dell'indagine di analisi congiunta e forniremo un'attenta descrizione dei principali temi indagati nel questionario.

Abstract.

Remediation of contaminated sites yield to several economic, environmental and health benefits. In this study we mainly focus on the benefits associated reduction in mortality thanks to the environmental remediation of contaminated soil and groundwater in Italy. In order to calculate the benefits of a public program that saves lives we use a methodology relying on the value of statistical life concept, which is a key factor in valuing human health improvement deriving from environmental policy. To obtain a measure of the value of statistical life we have designed a conjoint choice questionnaire to ask people their willingness to pay for a specific reduction in their risk of dying due to toxic substances exposition. In this paper we provide the main methodological issues of designing and pre-testing a survey of this type and a careful description of the main topics of our conjoint choice questionnaire.

1 Introduction.

Contaminated sites represent a significant problem for nowadays' society, because of the negative impact they have on human health and on the ecosystem in general. There is therefore an urgent need to clean up

contaminated lands.

Contaminated land is a general term to describe sites, and wider areas of land, which have elevated concentrations of chemicals or other substances (contamination), usually resulting from man's use of the land¹. These substances are toxic, corrosive and ignitable. Air, water, land, and even living animals can transmit them. The most common harmful substances causing the contamination of soils are heavy metals (e.g. lead and arsenic), oil products, polyaromatic hydrocarbons, polychlorinated biphenyls, chlorophenols, and pesticides.

Remediation of contaminated soil and groundwater would yield to several benefits for the society. The benefits might relate to health impact, environmental quality, urban environment, stigma elimination and productive reuse of the property. As regards health, contaminated sites have the potential to pose a threat to public health and safety. Exposure to hazardous materials could result in birth defects, respiratory problems, infertility, childhood leukaemia, and heart disease, among others. Remediation should therefore lead to a reduction of mortality and morbidity associated with exposure to hazardous waste. Regarding the environmental quality improvement, it involves soil and groundwater ecosystems improvement, to which an ecological value is attached. Urban environment improvement is linked with aesthetic values and quality of life standards. Contaminated sites remediation would also conduct to an improvement in the market conditions thanks to the elimination of stigma effect, which impacts negatively the perception about a contaminated property by decreasing its value. Other benefits are related to the possibility of a productive reuse of the property. Reuse of these properties of course imply new opportunities for economic and social advancements not only for people leaving in the surrounding areas but for society in more general terms. Last but not least remediation of contaminated land is an important step for a more sustainable development with an eye towards future generations.

Yet, even though many agencies and societies assume the 'polluter pays principle' in practice contaminated land is a legacy of the past forms of urban and industrial developments and remediation necessitates public programmes of intervention for the clean-up of the site Which are often expensive. These interventions involve public policy decisions; economists strongly recommend cost-benefit analysis. This consists of estimating and then comparing the expected costs and benefits associated with the implementation of public programmes. Policy makers should in principle take into account the results of these analysis in deciding whether to implement a program or not.

¹ Sustainable Management of Contaminated Land: An Overview – CLARINET, 2002, Federal Environment Agency, Austria

In this study we focus on the mortality benefits associated with the remediation of contaminated soil and groundwater in Italy. In practice, to obtain an estimate of such benefits one needs to apply a methodology relying to the Value of a Statistical Life concept, which is a key element in assessing health benefits deriving from environmental policy.

The remainder of this paper is organized as follows. In section 2 we introduce the notion of Value of a Statistical Life, the methodology to obtain it using a willingness to pay approach and its application in a public policy context. Section 3 reports the valuation methodology, consisting in the conjoint choice approach. Section 4 describes the questionnaire design, including pre-testing phases and the final structure of the questionnaire. In section 5 we report the conjoint choice valuation scenario. The sampling plan and administration of the survey is illustrated in section 6. Conclusions are reported in section 7.

2 Value of a Statistical Life and Willingness to Pay approach

In order to calculate the benefits of a public program that saves lives, we need the Value of a Statistical Life (VSL); this value is then multiplied by the expected number of lives saved.

The Value of a Statistical Life (VSL) is the marginal value of a reduction in the risk of dying and is calculated as

$$VSL = \frac{\partial WTP}{\partial Risk},$$

where WTP is the beneficiary's willingness to pay for a reduction in the risk of dying, and RISK is the risk of dying, in our case, for exposure to hazardous waste in contaminated sites. The VSL implies the concept of the prevention of a "statistical" death. To illustrate this concept, suppose that a group of 100,000 people enjoys a safety improvement that reduces the risk of death during a certain period by 1 in 100,000 for each member in the group. The expected number of deaths within the group during that period will be reduced by one, so the improvement involves the prevention of one statistical death. Now suppose that people within this group are, on average, willing to pay 5€ for the 1 in 100,000 reduction in the risk on dying. The total willingness to pay will then be given by 5€ X 100,000 or 5€/0.00001=500.000€. This figure is the value of preventing one statistical death or the value of a statistical life (VSL). Notice that since the VSL is essentially the mean willingness to pay divided by the risk reduction concerned, the VSL can alternatively be thought as the mean of individual marginal rates of substitution of wealth for risk.

Willingness to pay in the context of risks to life is defined as "the breakeven payment, per unit reduction in the probability of death, that leaves an individual's overall expected utility unchanged" (Shepard and Zeckhauser, 1982). The willingness to pay approach has its basis in the assumption that changes in individuals' welfare can be valued according to what they are willing to pay to achieve that change. According to this assumption, individuals treat

longevity like any consumption good and reveal their preferences through the choices that involve changes in the risk of death and other economic goods whose values can be measured in monetary terms. Willingness to pay reflects not only the individual's valuation of safety relative to other objects of expenditure but also his or her ability to pay, which is itself a manifestation of society's overall resource constraint. The resultant figure is a clear reflection of what the safety improvement is worth to the society, related to the alternative ways in which each individual might have spent his or her limited income.

The concept of Value of a Statistical Life (VSL) is important for ex ante policy analyses, when the identities of the people whose lives are saved are not known yet.

The VSL can be estimated through several methodologies. One of these methods is the compensating wage approach (Viscusi, 1993), which states that higher wage rates compensate workers for undesirable working conditions, such as an unsafe or unhealthy work environment, characterised by a higher risk of injury or illness. The wage differential are used as proxies of the willingness to pay for reducing the risk of dying. The transfer of these figures in the remediation policy context requires some restrictive assumptions, because the exposure to dangerous substances in contaminated sites does not involve necessarily only workers, but the general population, including children and old persons, who might be more sensitive to health risks. Another weakness of this technique is related to the fact that workers might be poorly informed about the job risks that they face. The relationship between wage and risk in labour markets may also be strongly influenced by regulatory intervention.

Other methods to obtain a measure of VSL rely on Stated Preferences approach, which directly ask individuals what they would do under hypothetical circumstances, using survey-based methodologies, rather than observing actual behaviours on marketplaces. Contingent Valuation or Conjoint Choice Experiments are an example of stated preference methods. In a contingent valuation questionnaire respondents are asked to report their willingness to pay for a specific reduction in their risk of dying. The VSL is then calculated as $WTP / \Delta R$, where ΔR is a finite risk reduction.

In our Conjoint Choice experiments, respondents are asked to choose between different remediation plan scenarios, described by a set of characteristics, like duration, number of avoided deaths, implementation cost, among others. These information are then used to derive the willingness to pay for mortality reductions.

We judged this the most appropriate approach for the purpose of this research, as we explain in next section.

3 Valuation methodology

3.1 The Conjoint Choice approach

Valuation of human health impacts is a complicated task for different reasons. In the case of a commodity that is traded in the market, buyers and sellers reveal their preferences directly through their actions. Even if health is basically a private good, it is not exchanged in regular markets, because the government intervenes in health care sector and the price for a treatment is fixed at an arbitrary level which is kept constant over long intervals of time. This makes it difficult to assess the value of health changes. A further complication is that risk plays a central role within the health field. The use of non market valuation techniques like conjoint choice (stated preference approach) allows to overcome these difficulties because people are asked to react to a hypothetical scenario. In this way it is possible to value resources that are not exchanged in regular market, or when it is difficult to observe market transactions.

The first applications of conjoint analysis were in the fields of marketing research and transportation. Since then, conjoint choice analysis has been applied in several other disciplines. The conjoint choice analysis approach was initially developed by Louviere and Hensher (1982) and Louviere and Woodworth (1983). The approach is derived from Lancaster's theory of demand (1966) which postulates that consumers derive utility not from goods themselves but rather from the attributes or characteristics that the goods possess.

In our context, the conjoint choice questionnaire asks individuals to compare alternative descriptions of described nation wide remediation plans, and to choose the most preferred one. These plans are characterised by different attributes.

Remediation activities to mitigate or solve contamination problems in land and underground water are quite different in scope, costs, and time. The range of the possible techniques is wide and must be chosen carefully by the experts, given the variety of contaminants, their spread, the quality of soil, the possible future use of it, etc...

Furthermore remediation plans may be dictated by laws which may impose different safety standards. That is why an accurate estimate needs to take into account the efficacy of different policy plans with regards to the possible trade offs in term of technical and economic features.

We feel that conjoint choice is more powerful and appropriate for our research goals than other approaches. First, we need to consider several alternative remediation plans, as the clean-up might result in different solutions, depending on the type of pollutant to be removed, the time required for the remediation, the impacts on health, the size of the population involved, the expected time before seeing the health improvement, the accuracy of the results and the costs to be supported, among others. Conjoint choice approach allows to deal with different

valuation scenarios, while on the other side it would be not realistic to focus on one solely program description. In other words, this methodology allows to consider alternative remediation plans or programs, described by different attributes or characteristics, and these scenarios might be especially rich in attribute trade-off information. Another reason for choosing conjoint choice is related to the possibility of constructing any alternative scenario of interest, by choosing different combinations of the characteristics describing the program. This allows to estimate the monetary benefits associated with any hypothetical scenario constructed. Furthermore, the methodology allows us to estimate the marginal willingness to pay of each of the characteristics describing the remediation plan and to state therefore their relative importance for policy decision in this field. Specifically, statistical models will be used to estimate the willingness to pay for a reduction in the risk of dying caused by exposure to hazardous waste. These findings will be further employed for assessing the Value of a Statistical Life (VSL) and for calculating the monetary health benefits produced by remediation plans of soil and groundwater contamination.

A further advantage of conjoint choice is related with flexibility because it is possible to explore how a change in the hypothetical scenario influences people's responses, and to compare the current scenario with many hypothetical alternatives. This is particularly helpful in informing policy decisions before the policy itself has been decided upon (A. Alberini and A. Longo, 2003).

In this specific research conjoint choice approach will allow us to perform the following quantitative analysis:

- monetising the health benefits (in terms of lives saved) associated with the implementation of remediation plans in contaminated sites in Italy, considering different possible valuation scenarios;
- estimating the Willingness to Pay (WTP) for a reduction in the risk of dying due to exposure to hazardous waste in contaminated sites, through implementation of remediation plans;
- estimating the Value of a Statistical life (VSL) which can be used in cost-benefit analysis of environmental remediation policies;
- estimating the marginal values or Willingness to Pay for each attribute defining the remediation plan under consideration.

These analysis results in quantitative measures in monetary terms; yet our purpose is wider and aims at investigating qualitative topics as well, like (i) peoples' knowledge of contaminated sites and related issues; (ii) individual perception of the problems engendered by contaminated sites, like impacts on health and on the ecosystem, latency and altruism effects; (iii) comprehension and familiarity with the health risks related to exposure to hazardous substances in contaminated sites

This study contributes nicely to our broader research program pursuing the valuation of the benefits associated to remediation plans for contaminated site,

by relying on Willingness to Pay (WTP) approach. The valuation of remediation plans and policies by real property developers was investigated in a survey been conducted in 2002 and the results are reported in Alberini et al. (2005).

4 Questionnaire design

4.1 Pre-testing the questionnaire: focus groups

One of the difficulties with conjoint choice approach lies in the description of the hypothetical scenario describing the set of choices. Given that the respondent is asked to make a choice between hypothetical remediation programmes, researchers have to be able to describe scenarios that are credible and easy to be understood. The issue of land contamination and the purposes and possibilities of remediation cannot be considered a familiar topic for most people. Questionnaire design becomes a crucial aspect. Researchers, and our group as well, usually pre-test questionnaire formats, wording, and scenarios comprehension in focus groups sessions.

Focus groups are a somewhat informal technique which makes use of interviews conducted by moderator among a small group of respondents in an unstructured way. Focus groups methodology is a qualitative research technique (Malhotra, 1996). In the context of conjoint choice methodology, they are used early in the questionnaire design process to gain insights about issues of interest and to pre-test the questionnaire. The pre-testing phase is crucial as it is important to ascertain that the respondents are answering the question that the researcher intend to pose.

The group is constituted of six to nine people, recruited on the basis of similar demographics, and the intent is to encourage the participants to interact with each other so that the quality of the output is enhanced. The focus group is implemented using a discussion guide that has been prepared in advance to ensure that the appropriate topics are covered and the proper amount of time is allocated to each topic.

A focus group, which typically lasts about two hours, is normally conducted in a specially constructed facility that includes a discussion room and a "client" observation area, the two places being separated by a one-way mirror so that people watching the session will not be seen by the participants.

In our study, we conducted eight focus groups in four Italian towns, Venice, Milan, Bari and Naples. These towns were chosen because of their proximity to the contaminated sites. Specifically, we chose Venice because of its proximity to Porto Marghera, a contaminated site of national interest; Milan because Lombardy is the region with the highest number of registered contaminated sites; Bari because of the presence of the former Fibronit, a contaminated site of national interest where an important legal action has been recently concluded; and finally Naples because of the presence of Bagnoli where a remediation plan is being implementing with a defined project of reuse.

We report the descriptive statistics of participants in focus groups in table 1

below. The average age is 49 years old, 69% are married and 36% have at least one child. 66% of our participants has an high school certificate and 5% has a college degree. 60% state they are employed and the annual household net income is about 28,000 euro.

Table 1 - Descriptive statistics of focus groups participants.

Variable	Mean	Stand. Devn.
Male (dummy)	0,51	0,50
Age	49	11,72
Married (dummy)	0,69	0,47
High School (dummy)	0,66	0,48
Employed (dummy)	0,61	0,490
Housewife (dummy)	0,20	0,05
Retired (dummy)	0,15	0,04
Household size	3	0,16
Children (dummy)	0,36	0,06
Household income (€/year)	28,196.72	3,101.28
Valid observations	61	

The purposes of these focus groups, conducted in the period from December 2004 to January 2005, were the following:

- To find out the extent to which the residents are aware of the existence of contaminated sites, the risks they pose to health, and the remediation measures. Our intent was to include in the questionnaire the most appropriate questions and definitions aiming at familiarizing the respondents with this issue.
- To analyze how people perceive health risks related to contaminated site exposure, and to find out the appropriate way of communicating to people the concept of health risk associated with exposure to hazardous waste.
- To find out the appropriate attributes and levels of Nation wide remediation plans.
- To define the appropriate valuation scenario and to test the conjoint exercises.

- To analyze possible information bias that could influence respondents' responses.
- To solicit advice on and test question content and order, appropriate wording, form and layout in the questionnaire.

Prior to the final survey, a pre-test was conducted in order to fine-tune the questionnaire. One-on-one interviews were used asking the respondents to interpret the meaning of each question, to explain their answers, and to state any problems and difficulties they may have had. Attention was given also to the software functioning and correct dataset registration.

4.2 Structure of the final questionnaire

The survey was conducted on a computer-based, self-administered questionnaire. This interview mode has the advantage of avoiding interviewer bias and reducing data entry cost and time, as the responses are automatically entered in an Excel spreadsheet.

The questionnaire is structured into 9 sections. In section A we ask the respondents to indicate if and how they have heard of contaminated sites. Some basic information is provided to familiarize the respondent with the contaminated sites issues (definition of contaminated sites, list of the principal hazardous substances, their origins, examples of contaminated sites). Section B asks if in the proximity of the respondent's house or work there exist dumps, incinerators, abandoned or active factories, fuel stations, rivers, lakes or sea; and if he/she knows about contamination problems in these areas. This section presents the map of Italy with the distribution of some of the contaminated sites of national interest, information and data about laws and regulation, the extent of the contaminated sites in Italy and the population living in the proximity of these areas and thus potentially exposed to contamination.

In section C we explain the possible health impacts caused by exposure to hazardous waste, like cancer, respiratory and cardiovascular diseases, cirrhosis, leukemia, asbestosis, and others. Respondents are explained through a picture the possible ways of exposure to the contaminated substances: through the skin, drinking contaminated water, breathing dust containing hazardous substances, or eating contaminated meat or fish once these substances have entered the food chain. The remainder of this section focuses on the number of deaths attributable to exposure to contaminated sites' hazardous substances, and presents a bar chart showing the number of deaths for various causes (cardiovascular, cancer, respiratory system, digestive system, exposition to hazardous waste in contaminated sites, road accidents, carbon monoxide poisoning, plane accident). Respondents are then tested for comprehension of these numbers. Other questions have being included with the purpose of understanding:

- how important is for the respondent to reduce the negative health effects caused by the exposure to hazardous waste in

contaminated sites,

- the possible actions the respondent would undertake if a contaminated site was discovered near his home,
- how useful some proposed government interventions are to tackle contaminated sites problems and to improve the environmental quality (financial incentives to the firms to support clean-up and reuse of contaminated sites, information campaign, enclosing of the contaminated area, among others).

Section D focuses on remediation techniques, explaining that remediation costs and time vary according to the technique used and the type of pollutant. Three possible examples of techniques are described using pictures: removal of contaminated soil and transportation to an authorized treatment facility, use of micro-organisms for natural biodegradation of the substances (bioremediation) and water treatment. For each technique, the time requested for execution, the costs and the type of pollutant are reported.

In section E we present the valuation scenario and the conjoint choice exercises. This section focuses on remediation programs to reduce or eliminate hazardous waste in contaminated sites. Respondents are asked to choose between two remediation programs saving human lives and described with different attributes and levels. The attributes chosen are the number of lives saved every year in 1,000,000 people, the population exposed to the hazardous waste of contaminated sites, the expected time to get evidence of the reduced mortality, duration of the health benefits, and the cost of the program expressed in terms of one-time payment for the nuclear family. A total of four conjoint choice exercises are presented in each questionnaire.

In section F we ask questions that investigate preferences for two cities characterized by a different risk of dying for road accidents and because exposure to hazardous waste in contaminated sites. Section G investigates the inter-temporal rate of preference of the respondents and asks some debriefing questions.

In section H we ask respondents about their habits, like smoking, purchase of organic products, participation in voluntary social or environmental organizations, religious or political activities, among others. Other questions are intended to find out if the respondent has ever been diagnosed to have certain diseases (including cardiovascular diseases, cancer, hypertension, cholesterol, diabetes, chronic bronchitis, emphysema, asthma). We also ask people to tell us about the health of other family members, and to assess their current health, if they think to be in excellent, good or poor health.

Finally Section I concludes with socio-demographic questions.

5 The valuation scenario

In the conjoint exercise, respondents are shown two alternative remediation plans and they are asked to pick their most preferred. Respondents are told that

these plans would be implemented by the government and that they are guaranteed to be effective. Each alternative is characterized by the same number of attributes, but the alternatives differ for the level of one or more attributes.

These plans are defined by a total of 5 attributes: (i) annual number of lives saved in 1,000,000 people (10, 20 or 30), (ii) population potentially exposed to toxic substances (500,000; 1,000,000; 2,000,000), (iii) expected time before seeing the benefits in terms of lives saved (2 years or 10 years), (iv) duration of the health benefits (20, 30, or 45 years), and (v) cost, a one-time tax payment for each household (one-time payment: €50, €100, €200, €500, €950).

We report an example of the conjoint choice exercise in figure 1.

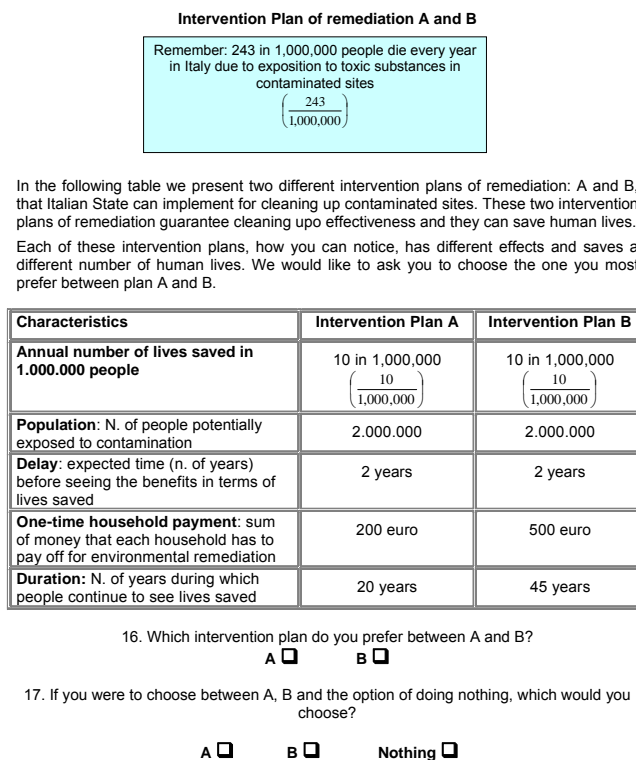


Fig. 1 – A conjoint choice exercise

The design of the conjoint choice exercise was a demanding task, and focus groups played an important role in defining the valuation scenario, and the attributes and their levels. The attributes were selected on the basis of the valuation goal, which is the estimate of the health benefits associated with remediation and the willingness to pay for a reduction in the risk of dying.

The chosen attribute levels span the range over which we expected respondents to have preferences, reported during discussion in focus groups sessions.

When valuing the health impacts entailed by different remediation plans the choice of the measurement unit is crucial. This means that we had first to decide how to measure the health impacts caused by exposure in contaminated sites (number of deaths or lives saved as a rate or in absolute, occurrence or incidence of diseases, etc.). We used the annual number of lives saved in 1,000,000 people as our measurement unit for several reasons. First, we focus on mortality impact while we excluded morbidity effects, and the reason is related to the high scientific and epidemiologic uncertainty surrounding the health impacts associated with the exposure to hazardous waste in contaminated sites. Secondly, because we refer to statistical lives and this was the most understandable way of communicating the concept of risk reduction to people. This task is related with the problem of risk perception and communication, addressed many times during focus groups discussion. Notice that we decided to talk about “lives saved” instead of “reduced deaths”.

The second attribute is the population potentially exposed to hazardous waste, expressed as a total number of people. These are the direct beneficiaries of the remediation plans. This attribute has been included because remediation plans could impact different population sizes, and we want to analyse the individual preferences for the size of the population involved. Population figures combined with the number of lives saved in 1,000,000 people gives the total annual number of lives saved with the proposed program. The way of presenting these two attributes was extensively discussed and pre-tested in focus groups so as to reach a definition understandable to the majority of the respondents.

The expected time before seeing the health improvement (2 or 10 years) was not combined with the other attributes in the conjoint. In other words, the delay time of 2 and 10 years has been randomly assigned to the respondents while being constant within the same choice exercise. This attribute was included in the choice because we wanted to analyse the importance of latency in remediation². On the other hand, people in focus groups have repeatedly addressed this issue, considered as an important determinant for remediation plans.

The duration of the health benefits is another attribute which appeared to be determinant in the choice of remediation plans during focus groups discussions. Moreover, risk reduction cannot be realistically infinite and we were interested in the issue of permanent (and more expensive) versus less permanent.

The cost attribute was included because valuation clearly requires that one of the attributes is the “cost” of the remediation plan. We had also to make sure

² Public remediation plans in contaminated sites addresses the issue of latency between the time an investment is made and the time when the benefits, measured in terms of health risk reductions, are realized.

that the provision mechanism was acceptable to the respondent, and that the payment vehicle was realistic and compatible with the resource (mortality) to be valued. Evidence from focus groups discussion has shown the necessity of expressing the cost as a one-time payment for each household. Note that we do not use terminology like tax or fee to avoid protest. This issue was discussed with participants in focus groups in all the four Italian cities. The main difficulty was related to the negative perception that Italian citizens have about the reliability and efficacy of public intervention.

The order of the attributes as presented to the respondents and the word content were extensively tested during focus groups in order to achieve the most comprehensible scenario presentation.

In our conjoint choice questions, each choice set consists of two hypothetical remediation plans. These have been created selecting randomly two alternatives from all possible combinations of the levels of the attributes. We create 32 different versions of the questionnaire, each with 4 conjoint choice questions. Respondents were randomly assigned to a questionnaire version.

6 Sampling plan and survey administration

The survey was administered in four cities in Italy (Venice, Milan, Bari and Naples) in May 2005, resulting in 800 completed questionnaires (200 people each).

Respondents were recruited by the Istituto Piepoli, a survey firm based in Milan, among the residents of the four cities. The sample is stratified by age using three broad age groups (25-44, 45-54, 55-65), with an equal number of respondents for each of them. The sample is comprised of a roughly equal number of men and women.

The survey was self-administered by the respondents using the computer at centralized facilities, where two interviewers were present at the time to welcome the respondents, introduce the survey to them and provide assistance if requested.

A training session for interviewers was conducted prior to the final survey to inform them about the questionnaire structure and to instruct them on how to address problems that might arise in the course of the administration of the final survey.

7 Conclusions

This work describes two distinct phases of activities of a research program aiming at the estimation of the benefits associated with contaminated sites remediation. During the first phase of work we organized several focus groups in various Italian cities to investigate how people have experience and understanding of the issue of contaminated site and the possibilities of their remediation and redevelopment, how they appreciate health benefits and how they are willing to contribute to public programs aimed at the reduction of health

and mortality risk. The second phase of activities focused on the design of the conjoint choice questionnaire. The purpose of the questionnaire was to introduce and develop a conjoint choice experiments to obtain the willingness to pay for mortality risk reduction thanks to environmental remediation of contaminated sites. In this experiment people are asked to choose between different remediation plan scenarios, described by a set of different attributes: number of lives saved, duration of the health benefits, remediation cost, and expected time before seeing the benefits in terms of lives saved. The computer-based survey was administered in 4 different Italian cities: Venice, Milan, Bari and Naples in May 2005, resulting in 800 completed questionnaires.

Statistical analysis of the data resulting from the survey, and econometric models will be used in the next phase of the project in order to estimate the willingness to pay for mortality risk reduction and the corresponding value of a statistical life. VSL figures will be multiplied by the expected number of lives saved through remediation in order to obtain the monetary health benefits, under different scenarios.

The statistical models will be also produce estimates of the marginal value of each of the attributes of the remediation plan. This will enable us to identify which attributes are judged by the Italian population to be more important for remediation policy. Results are valuable both in term of valuing policy scenario in Italy with reference to the contaminated site problem which is quite diffused in our country and to obtain the VSL that with the appropriate techniques may also be utilized to value other programs affecting human health.

References.

- Alberini, A., Longo, A., Tonin, S., Trombetta, F. and Turvani, M. (2005), *The Role of Liability, Regulation And Economic Incentives In Brownfield Remediation and Redevelopment: Evidence from Surveys of Developers*, *Regional Science and Urban Economics*, N. 35, pp 327-351
- Alberini, Anna and Alberto Longo (2003), "Valuing Environmental Resources Using the Method of Contingent Valuation," CO.RI.LA., Venezia, January.
- Alberini, Anna and Alberto Longo (2003), "Choice Models in Non-market Valuation," draft report to CORILA.
- Alberini, Anna, Alberto Longo and Marcella Veronesi (2005), "Basic Statistical Models for Conjoint Choice Experiments," in *Valuing Environmental Amenities using Choice Experiments: A Common Sense Guide to Theory and Practice*, Barbara Kanninen (ed.), Springer.
- CLARINET (2002), "Sustainable Management of Contaminated Land: An Overview", Federal Environment Agency, Austria.
- Lancaster K. (1971), *Consumer Demand: A New Approach*, Columbia University Press: New York

Louviere, Jordan J., David A. Hensher and Joffre D. Swait (2000), *Stated Choice Methods: Analysis and Applications*, Cambridge, UK: Cambridge University Press.

Malhotra, N.K. (1996), *Marketing research: an applied orientation*, 2nd edition, New Jersey: Prentice-hall International.

Shephard, D.S. and R. Zeckhauser (1982) "Life-cycle consumption and willingness to pay for increased survival" in Jones-Less M.W. (ed) *The value of life and safety: proceedings of a conference held by the general association*, Amsterdam, North-Holland, 95-141.

Tonin S. and M. Turvani, (2005), Report on methodology and focus group findings, in *Scientific Research and Safeguarding of Venice*, Research Programme 2001-03, pp. 21-31

Turvani, M., and S. Tonin, (2005), Economic valuation for contaminated site redevelopment, paper presentato al Convegno Internazionale CABERNET, Belfast 13-15 aprile, in *Atti del Convegno*, pp 390-394

Viscusi, W. Kip (1993), "The value of risks to life and health, *Journal of Economic Literature*, 31(4), 1912-1946.

The EL.GI.R.A support system for knowledge building and evaluation in brownfield redevelopment. An application in the 'Ex Sava Alumix' area in Porto Marghera (Venice)³

Domenico Patassini¹, Paola Cossettini², Enrico De Polignol³, Enrico Fabris⁴, Markus Hedorfer¹, Enrico Rinaldi⁵, Ernesto Verni⁶

¹Planning Department, University of Venice, Faculty of Architecture (IUAV); ²VESTA; Territorial and Environmental Services, Venice; ³Venice Municipality, Environment and Territorial Safety Office; ⁴Environmental engineer, Venice; ⁵CORILA, Lagoon Research Consortium, Venice; ⁶Venice Municipality, Town and Regional Planning Office. Support Policies For The Re-Use Of Abandoned Areas: The Case Of The Venice Arsenal

Riassunto

Il sistema ELGIRA è in fase di sviluppo con test nel "megasito" di Porto Marghera e in altre aree industriali (Patassini et al., 2005a, 2005b, 2005c). Dopo il primo test nell'area "43 ettari" è stato condotto un secondo test nell'area "Ex Sava Alumix", che si estende per circa 35 ettari vicino a Fusina, al margine sud della zona industriale. In quest'area operavano dal 1969 impianti per la produzione dell'alluminio, dismessi nel 1991 con la crisi del settore metallurgico. La Variante del Piano Regolatore Generale di Venezia prevede in quest'area una Zona industriale Portuale di completamento, assoggettandola a strumento attuativo obbligatorio. Nell'area confinante a sud è previsto il nuovo Terminal passeggeri di Fusina. Sono stati approntati alcuni progetti di riqualificazione dell'area con eventuale riuso di manufatti esistenti. La matrice di caratterizzazione del SIS del Comune di Venezia mette in evidenza contaminazioni da oli minerali, idrocarburi policiclici aromatici (IPA), diossine, furani e fluoro.

ELGIRA utilizza un modello di inquinamento del terreno per tutte le sostanze significative, con mappe che evidenziano il superamento dei limiti di legge (D.M. 471/1999). L'analisi del rischio è ancorata ad un progetto architettonico con destinazione per attività portuali e servizi connessi. Le tecnologie di bonifica applicabili (soil washing, desorbimento termico, estrazione con solventi e successiva lisciviazione con acido, incenerimento, capping e discarica) consentono sette tipologie di intervento, singole o in filiera, applicate su tutto il sito o in sub-aree. Per ogni processo sono stati determinati performance e costi, in relazione alla dimensione, alla caratterizzazione e agli scenari d'utilizzo.

³ Translation by Judith McGrath

1 The Ex Sava-Alumix area at Porto Marghera

1.1 Territorial organization and usage cycle of the area

The “Ex Sava-Alumix” site is situated at the southernmost part of Porto Marghera, on the Venetian lagoon and adjacent to the Fusina terminal. It belongs to the area originally known as “Bottenigo”, which borders to the north on the Padua - Venice railway line, to the south on Naviglio Brenta, to the west on the Padua – Mestre main road (provincial thoroughfare), and to the east on the Argine San Marco (St Mark’s Bank).

The area is rectangular in shape, measuring approximately 800 x 400m. The total area measures 35 hectares.

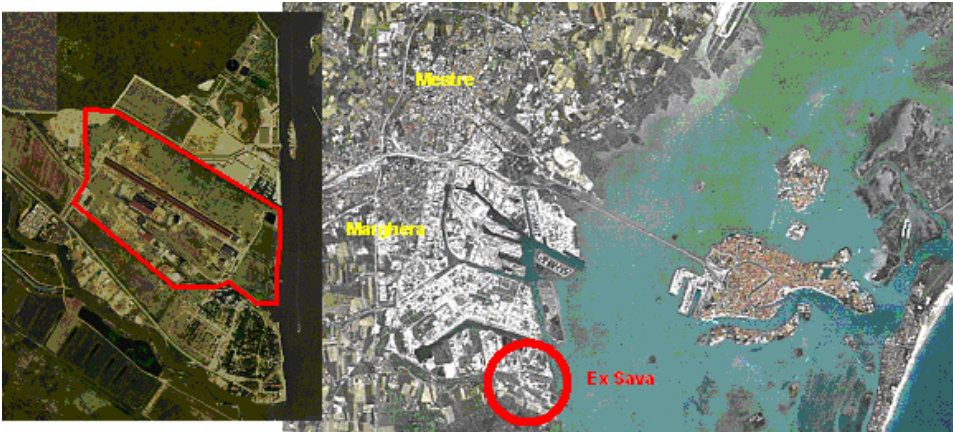


Fig.2. The Ex Sava-Alumix area

The Second World War and the reconstruction in its aftermath signified a period of industrial inactivity, but as of 1950, the economic expansion of Porto Marghera resumed in the shape of the petrol-chemical industry.

In order to accelerate the realization of the second industrial zone, the “Syndicate for the development of the port and industrial zone” was constituted in 1953. Porto Marghera was classified as an industrial zone in the new Master Plan of 1963 (art.#9 of the Implementation Regulations).

The general Plan completed the second industrial zone and two sites were designated to Sava: one which is the area under investigation, and the other which is now called “Alcoa”. The aluminium works were built swiftly and by 1969 had already a near-complete configuration. The buildings within the plant consisted of a 600 metre-long warehouse housing the electrolytic ovens, with an annual capacity of 27,000 tons; a thermoelectric plant, stores, and offices.

The major economic growth of Porto Marghera occurred in the 1960s and 70s, when the workforce reached approximately 31,000, and workers employed in the aluminium plant alone totalled more than 1,200, rising to 3,250 by 1980. Optimistic interpretation of the productive cycle gave rise to an enlargement project for the Sava plant at Fusina, involving a quadrupling of the production facilities. Crises in the sector due to international recession, and the fall in

demand, however, led to the reduction in aluminium production.

In 1981, the name of the plant was changed to SAVA Aluminio Veneto, and formed part of the EFIM/Aluisse group, producing semi-finished laminates. The workforce was reduced to 410. By 1988 this number had dropped to 305, and when, in 1991, the plant changed appellation again to become "Alumix", the factory was already in the process of closure.

1.2 Current and future prospects for the area

The town and regional planning instruments currently implemented in the area are: the PTRC (Regional Plan), PALAV (Master Plan for the Lagoon Area), PTP (Venice Provincial Plan), the Revision of the Master Plan for Porto Marghera (Municipality of Venice, 1996) and the Port Master Plan.

The PALAV sees the area as an industrial zone of generic interest; the PTP, as an area for 'productive installations' that may include compatibly transformable projects such as tourist ports and leisure facilities, within an area dedicated to boating. The Port Master Plan envisages an industrial zone, whereas the Revision suggests a supplementary industrial zone for the port, constrained by a detail plan.

The use of the area by the Venice Port Authority is included in the overall plan. The Venice City Council meeting of 7 April 2003 states in resolution #43 that it accepts the Project Agreement between the Port Authority and Venice Municipality for the expropriation and use of the former Alumix-Sava Fusina.

The agreement stipulates that to start with the Port Authority uphold the declaration of public utility of the areas, so as to be able to expropriate and conjoin them to the existent state-owned maritime properties, while at the same time reserving those areas of interest to the Municipality of Venice for job/asset relocation and the completion of the Fusina terminal. The second commitment undertaken by the Port Authority foresees the realization of docks along the state-owned shorelines for moorings and other uses. The Authority has committed, moreover, to plan and carry out – in accordance with the Agreement Plan for the Chemical Industry of Porto Marghera – the safety and / or reclaim measures required by current legislation.

The new Fusina Passenger Terminal is planned for the southern extremity of the area, which will be built by the winner of a public competition advertised in 1998.

The reclaim scenarios involve a redevelopment project that assigns the area to Port activities (coastal traffic between national ports of ships capable of transporting articulated trucks), parks and gardens, and services (including logistics)⁴.

⁴ The project has been realized during a teaching workshop within the Architectural

Analysis of the survey data, which is collected in the Land Information System (SIS) database of the Venice Municipality, pinpoints the whereabouts of the contaminating agents in the subsoil.

The subsoil is made up of a layer of landfill, whose width varies by just a few decimetres every 2 metres. The typology of the landfill is very heterogeneous and varies from place to place; it usually consists of gravel, pebbles, sand, building refuse, bits of wood, and plastic. Local lenses of black carbon-type material are also present.

Beneath the landfill layer there are banks of mud and slimy sand (grey to yellowish in colour), often alternated with segments of peat.

The former factory area (on the southern side of the site) is heavily contaminated by mineral oils, hydrocarbon polycyclical aromatics (HPA), and, in the one spot subjected to investigation, by dioxins and furans. These two substances were also sought in the north-western part of the site, and very high concentrations were found. Only in one, more confined area at the centre of the site was fluorine contamination found (such as fluoride).

The incidence of pollution by fluoride, hydrocarbon polycyclical aromatics and other agents is present sporadically elsewhere on the site, though much less extensive. Pollution is present in the piles of accumulated materials to the left of the main building. These piles, however, consist of not of land as such, but of refuse (probably resulting from the demolition of the electrolysis cells).

Excavation in the area to the left of the main building, moreover, - the area that looks towards the sea - revealed quantities of solid waste similar to ordinary urban waste: glass bottles, plastic, wood, porcelain insulators, and more besides.

The four piezometres revealed pollution in the waters of the table in the form of fluorine, and to a lesser extent, lead and copper.

The survey results in the Land Information System database (Environment and Territorial Safety Dept., Municipality of Venice) have led to the creation of maps indicating the location of these substances. Not all of these substances appear in the 250 surveys effectuated: some are present in almost all points, and are homogeneously distributed; others occur only in certain and confined points.

In order to prepare the pollution model, the concentration values of the contaminating agents measured at different depths in the samples were brought to a single value at surface level at each point of the survey, as defined by the "ELGIRA vertical interpolation" method. (Hedorfer, 2004)



Fig. 5. Current state of the Ex Sava area.

2.2 Pollution model.

The two-dimensional maps of the points of concentration have been subjected to interpolation (using MoDe software; Patassini et al., 2004) so as to obtain the hypothetical distribution of any substance throughout the area in question. Via the weighted average based on distance, a distribution map of the concentration of each substance is attained whereby a value can be established for every cell.

In this first phase of the survey, only the ground level⁵ is taken into consideration.

The result of the interpolation is visualized with a division into 10 segments of the concentration values in each cell (see map colouring). The segments in this case are the same and have as limits the minimum and maximum values of concentration.

⁵ Further details regarding the methodology and elaboration of the interpolated value maps can be found in “MoDe. A Cellular Automaton Model for the spatial interpolation of values. Applied to the “43 hectare” area in Porto Marghera (Patassini et al., 2004).

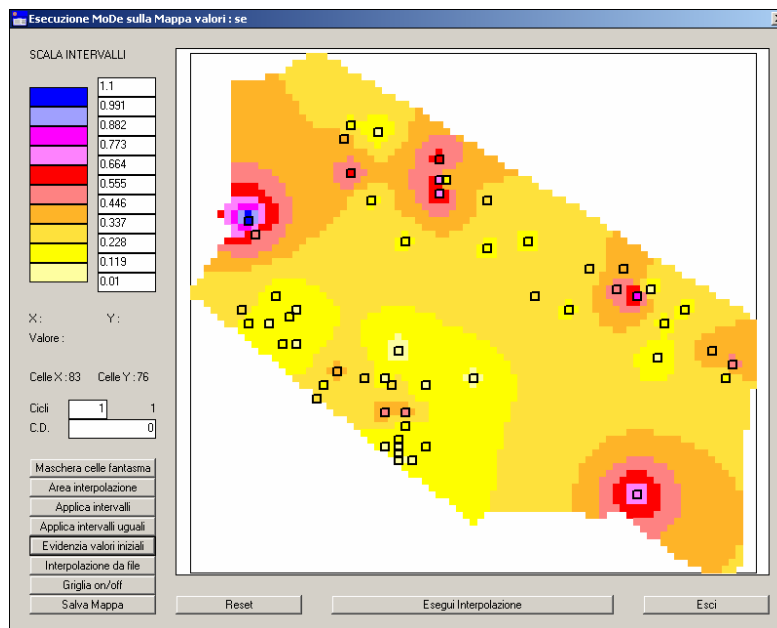


Fig. 6. Interpolation result.

Further maps were produced for each contaminating agent under examination, taking into consideration the relative legislation (Ministerial Decree n. 471/1999), which describes the pollution limits for each site according to its prospected usage (residential or industrial). The maps use normalised values over value limits. Distribution of a substance is described in intervals according to an “attention index” arising from the ratio:

$$C_i = \text{measured concentration value} / \text{legal limit concentration value}.$$

By this means all the concentration values of each map are normalised, and the threshold values are thus inserted on the “normalised” maps. While the map in fig. 7 concerns the legal limit value V_{IA} for public, private, and residential parks and garden areas (type A), the map in fig. 8 concerns commercial and industrial sites (type B). As a result, two C_i indices are obtained; one for each type of site, where V is the concentration value present:

$$C_{IA} = V / V_{IA}$$

$$C_{IB} = V / V_{IB}$$

Therefore, if the measured concentration value is less than the legal limit value, the index is minus 1; conversely, the index is plus 1.

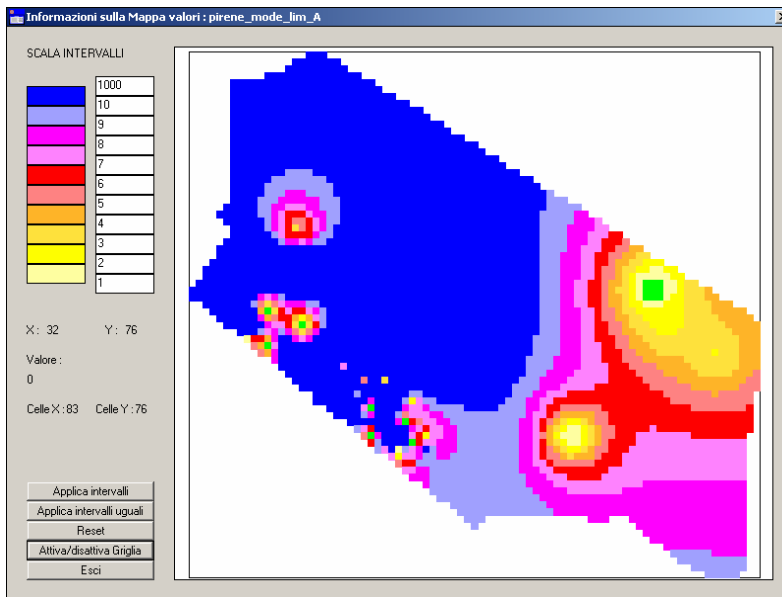


Fig. 7. Threshold value map according to legal limit for type A site (pyrene).

The lowest limit on the scale of intervals is index 1 (legal limit value), after which the scale increases by 1 for every interval, until the ninth interval. The upper limit of the last interval is an enormously high normalised value (theoretically unreachable):

e.g.: 1-2-3-4-5-6-7-8-9-1000

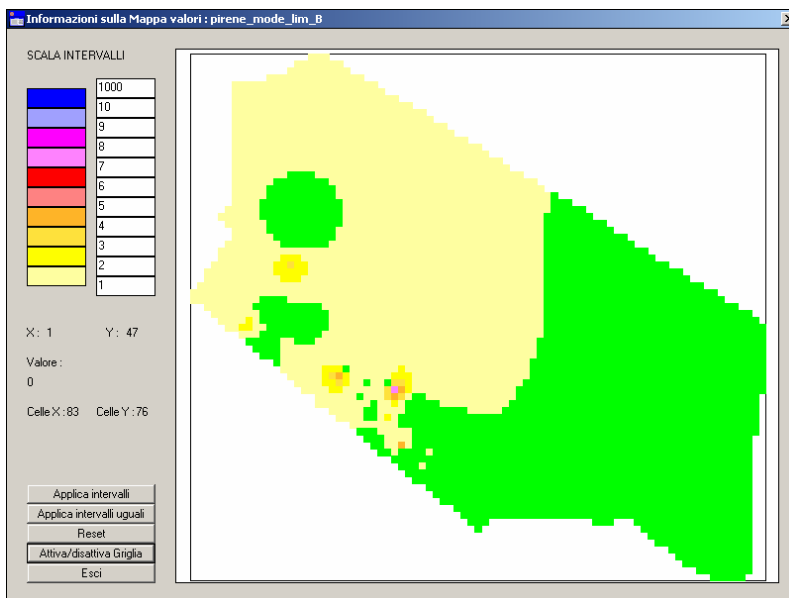


Fig.8. Threshold value map according to legal limit for type B site (pyrene).

The cells of a value less than 1 are coloured green (below the legal limit), with chromatic scale variations up to 9 times the limit value. Values beyond this threshold (considered 'exceptionally' high) are coloured dark blue.

These normalised maps not only identify the surface areas that supersede the

legal limit value, but also aid in estimating the volume of the terrain to be reclaimed. This information is used in later stages of the ELGIRA procedure; particularly in estimating the costs involved in reclaim options, in risk analysis and in the final aggregate evaluation.

By analysing the maps of distribution of concentration values of the various substances as in the surveys, it is possible to see that in some maps, there are sufficient and well-distributed values for a reliable interpolation to be carried out (with the exception of unpredictable 'hot spots').

As regards other substances, however, the available surveys are either insufficient or are localized in just a few zones within the site, thus making a reliable interpolation of the entire area impossible. This is the case with furans and dioxins, for instance, for which there are only a few surveys, concentrated mainly in the north-western part of the site.

Historical knowledge of the site and choices made during the survey campaign make it possible to hypothesise the probable presence of a substance in some areas rather than others. Knowing the manufacturing processes or landfill activities within a given area means that certain substances (such as dioxins and furans) can be presumed in limited portions rather than in the entire area.

On the whole, higher concentration levels are recorded for most of the substances in the western part of the area.

The concentration values of dioxins and furans (described in the processing as 'equivalent toxicity' according to prescriptions by Nato/CCMS, USA-EPA, EC, WHO) are very often much higher than the legal limit established in the Ministerial Decree 471 (both for type A sites and type B sites), and also for 100 and 1000 factors. Such values have a very great bearing on the choice of reclaim processes and risk analysis.

3 Reclaim technologies for the area

3.1 Area zoning according to pollutant families

Contaminating agents that supersede the legal limits for areas earmarked for type B usage (commercial and industrial) were grouped into families, reference being made to the Ministerial Decree 471/99 and to the Porto Marghera Master Plan. The identified substance families are the following:

- inorganic compounds A (nickel, copper);
- inorganic compounds B (mercury);
- inorganic compounds C (cyanides);
- volatile non-halogenated compounds,
- hydrocarbon polycyclical aromatics (HPA: acenaphthene, anthracene, benzo(a)anthracene, benzo(a)pyrene, benzo(g,h,i)perilene, chrysene, dibenzo(a,h)anthracene, phenanthrene, fluoranthene, pyrene, total HPA),.

- dioxines and furans;
- heavy hydrocarbons (oil)
- semi-volatile non-halogenated compounds.

Zoning of the surfaces superseding the limits was carried out according to the above substance families, resulting in the identification of the areas where any of the families present in the site are juxtaposed.

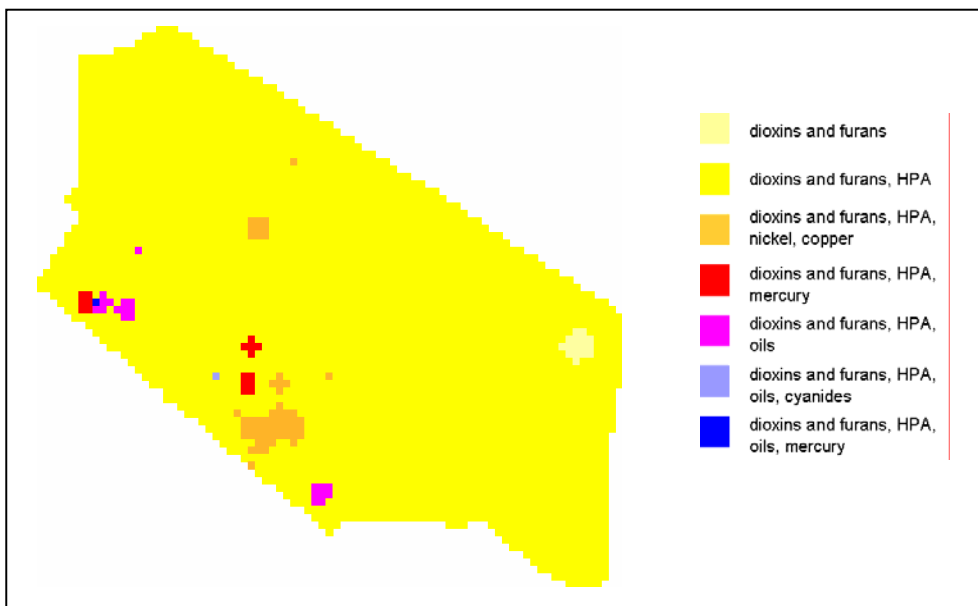


Fig. 9. Zoning of the pollutant families.

The zoning reveals how almost the entire area (dark yellow) is polluted by dioxins and furans with HPA; while small portions are contaminated by other family combinations.

3.2 Pollutant families and reclaim technologies

Relative to the presence, spatial distribution and concentration of the pollutant families discovered in the area, the following application of reclaim technologies is indicated:

- soil washing
- thermic desorption
- incineration
- solvent-based extraction and subsequent acid lixiviation
- bioremediation with selected bacteria groups
- disposal.

Soil washing acts chiefly on HPA and organic and metallic compounds; desorption on HPA and organic material; incineration is recommended mainly in the case of contamination by dioxins and furans; solvent-based extraction and

subsequent acid lixiviation is indicated for metals, and bioremediation with selected bacteria groups for organic materials.

Capping was also taken into consideration. As regards disposal, the dioxin concentration values at the destination point must not be superior to the acceptability limits.

3.3 Types of intervention

The technologies have been divided into six intervention types (singular or group) either in series in the same area or in parallel in diverse areas within the site:

- soil washing + incineration + disposal
- thermic desorption of organics + incineration + disposal
- solvent-based extraction and subsequent acid lixiviation + incineration + disposal
- bioremediation with selected bacteria groups+ incineration + disposal
- incineration
- capping.

Performance and costs of these technologies were established for later evaluation.

4 Risk evaluation

Risk is evaluated in terms of health⁶ and environment. Since they form an integral part of the reclaim and redevelopment scenario, these two elements help define risk within the territory.

The evaluation of health hazards is carried out via the Risk procedure, prior to which, however, an estimate of the volume of contaminated ground soil is made, based on two reclaim options (safety storing or removal) which may be alternative or sequential. Once the soil has been thus treated it is then subjected to further treatments, with the aid of appropriate technologies. These technologies are then analysed with reference to risk, environmental merit, and to financial costs.

4.1 Hydrological model of the ground

The hydrological model taken into account for the mapping of the stratigraphical sequence of topsoil and subsoil is that indicated in the "Operative protocol for site characterization according to the Ministerial Decree 471/99 and the programme agreement for the Porto Marghera chemical industry". In this

⁶ For details see Fabris, 2005.

specific case the following stratigraphy was reviewed:

- top soil consisting of heterometric gravel in mud matrix: 0.0÷-0.3m from the surface level;
- landfill layer consisting of inert materials: -0.3÷-1.5m from the surface level;
- landfill consisting of clayish-sandy mud deriving from excavations of canals and from anomalous levels: -1.5÷-4.0m from the surface level.

Taking into consideration the fact that the samples involved just two layers of terrain - the first between 0.0÷-0.5m from the surface level, and the deeper between -0.5÷-2.5m from surface level - it was assumed that the surface samples could be indicative of contamination in the landfill stratum (0.0÷1.5m from the surface level), while the samples taken further down would be indicative of deep contamination (-1.5÷4.0m from surface level). It was possible thereby to establish a first estimate of the contamination at both ground level and in the subsoil, and of the terrain volume and contaminated material types involved. The subterranean waters in the landfill layer were measured at a depth of -1.0m from the surface level; this measurement is considered the cut-off point between unsaturated and saturated terrain.

4.2 Health risks and exposure

The main means or methods of encountering health risks are the following:

- the volatilization of surface soil;
- the volatilization of subterranean waters;
- the migration of vapours within buildings;
- contact with the soil;
- contact with the water;
- ingestion of the soil;
- ingestion of the waters;
- ingestion of contaminated foodstuffs.

So as to determine the active and most probable means of contamination, the future configuration of the site - according to architectural plans relating to the redevelopment of the area - was taken into consideration and formulated as follows in fig. 10.

<i>source</i>	<i>means of exposure</i>	<i>built up areas</i>	<i>green areas</i>
surface soil	ingestion of soil		x
	skin contact		x
	horticulture		
subterranean waters	domestic use of subterranean waters		
	agricultural use of subterranean waters		
inhalation of vapours	soil and subsoil	x	x
	subterranean waters	x	x
surface waters	ingestion		
	skin contact		

Fig. 10. Active means of contamination.

Superficial and subterranean waters were not taken into consideration since the installation of water wells for animal feeding in the area is not foreseen, and neither is the use of the table waters.

4.3 Software

For the study of risk analysis, RISC WORKBENCH 4.03 software, of Waterloo Hydrogeologic is used. The validity of this software is recognized both nationally and internationally. For those contaminating agents not included in the RISC WORKBENCH 4.03 database, the parameters defined in the GIUDITTA 3.0 software (developed by the Province of Milan offices) are used.

All the indications presented in the "Proposal regarding risk analysis criteria – the National Interest Site of Porto Marghera" (drawn up by APAT, ISS, and ARPAV) are being followed up. Health risk evaluation is being evaluated over an exposure period of 30 years. 'Receivers' are considered those working in the area. The evaluation scenario that has been adopted is that of Reasonable Maximum Exposure. The study is carried out on the basis of all those substances whose concentration is superior to the legal limits imposed by the Ministerial Decree 471/99. The maximum values of the substances outside the legal limits are those used as input data. It is well here to remember the legal limits regarding health risk:

- total risk for carcinogenic substances: 10^{-6} ,
- total risk for non-carcinogenic substances: 1.

4.4 Reclaim hypotheses taken into consideration for health risk analysis

Several alternatives were identified for the reclaim of the area, all of which, however, concurred in the premise of permanent safety enforcement mechanisms, together with the partial or total removal of the contaminated terrain. The possible means of reclaim taken into consideration include the following:

- *permanent safety enforcement of the area consisting in a benthonic diaphragm, pushed to -20m from surface level, and capping with the asphaltting of all non-built areas;*
- *removal of 'hot-spots'; i.e those areas where the concentration of pollutants exceeds 10 times the limits laid specified in column B of table 1 in the enclosure of M.D. 471/99. Capping of the agricultural area and completion of the reclaim intervention together with the margining of the edges of the site that border on the Venetian lagoon, according to the plan laid out by the Venetian Waters Magistrate;*
- *removal of contaminated surface soil (0.0÷-1.5m from surface level) with substitution by agricultural soil; completion of the reclaim intervention with the margining of the edges of the site that border on the Venetian lagoon;*
- *total removal of contaminated soil and completion of reclaim intervention with the margining of the edges of the site that border on the Venetian lagoon.*

For each of these alternatives a maximum estimate was made of the contaminated volumes concerned in the reclaim operations, as well as of the total costs involved. Considering that the eventual destination of the contaminated terrain in either on site or off site treatment plants, or in disposal in appropriate dumps, the overall reclaim costs, including excavation and subsequent filling of the reclaimed areas was calculated at an average €150 per ton. Later, a calculation was made for each of the proposed scenarios regarding residual health risk at the end of the reclaim operations. We should like to add that the estimates made in this study are merely indicative of both the estimate of pollution levels in the area and of reclaim costs.

4.5 Risk analysis results

The following table illustrates the results of the risk analysis for the four options considered:

SOURCE	EXPOSURE AREA	BUILT-UP AREAS		PAVED AREAS	
		Dangerous-ness index	Carcinogenic risk	Toxicity index	Carcinogenic risk
vapour inhalation	soil and	$2,8 \times 10^{-3}$	$6,3 \times 10^{-11}$	not present	not present
	total	$2,8 \times 10^{-3}$	$6,3 \times 10^{-11}$	not present	not present

Fig.11. Risk analysis prior to reclaim.

SOURCE	EXPOSURE AREA	BUILT-UP AREAS		GREEN AREAS	
		Dangerous-ness index	Carcinogenic risk	Toxicity index	Carcinogenic risk
vapour inhalation	soil and	$2,8 \times 10^{-3}$	$6,3 \times 10^{-11}$	$8,3 \times 10^{-4}$	$1,2 \times 10^{-10}$
	subterranean waters	$6,0 \times 10^{-4}$	not present	$5,5 \times 10^{-3}$	not present
	total	$3,4 \times 10^{-3}$	$6,3 \times 10^{-11}$	$6,3 \times 10^{-3}$	$1,2 \times 10^{-10}$

Fig. 12. Risk analysis for reclaim scenario n. 2.

At the end of the reclaim operations there will still be a certain quantity of contaminated soil at -0.5 metres below ground level.

SOURCE	EXPOSURE AREA	BUILT-UP AREAS		GREEN AREAS	
		Dangerous-ness index	Carcinogenic risk	Toxicity index	Carcinogenic risk
vapour inhalation	soil and subsoil	$1,4 \times 10^{-3}$	$6,1 \times 10^{-11}$	$1,1 \times 10^{-4}$	$3,6 \times 10^{-11}$
	subterranean waters	$6,0 \times 10^{-4}$	not present	$5,5 \times 10^{-3}$	not present
	total	$2,0 \times 10^{-3}$	$6,1 \times 10^{-11}$	$5,6 \times 10^{-3}$	$3,6 \times 10^{-11}$

Fig. 13. Risk analysis for reclaim scenario n. 3.

Here also, at the end of the reclaim operations there will still be a certain quantity of contaminated soil at -1.5 metres below ground level.

SOURCE	EXPOSURE AREA	BUILT-UP AREAS		GREEN AREAS	
		Dangerous-ness index	Carcinogenic risk	Toxicity index	Carcinogenic risk
vapour inhalation	subterranean waters	$6,0 \times 10^{-4}$	not present	$5,5 \times 10^{-3}$	not present
	total	$6,0 \times 10^{-4}$	not present	$5,5 \times 10^{-3}$	not present

Fig. 14. Risk analysis for reclaim scenario n. 4.

According to estimates, the health risks post-reclaim fall below the maximum limits set by law. On completion of the study results of the simulations carried out for each of the reclaim scenarios will be published. As regards the evaluation of the variation in the health risk index, the indoor and outdoor areas were considered according to the assumed value of the index itself.

Reclaim intervention	Residual health risk		Quality of re-utilization intervention in the area
	Carcinogenic risk	Risk index	
Capping with asphalt + benthonic diaphragm	3.1E-10	1.7E-02	The reclaim intervention greatly limits the future re-utilization of the area. Since capping involves paving, the area can no longer be dedicated to green areas.
Removal of 'hot spots' + vegetable capping + benthonic diaphragm	2.9E-10	2.2E-02	The reclaim intervention imposes a compulsory raising of the surface ground level by 0.5m in all intended green areas. On the whole there are no changes regarding the development project for the area.
Removal of first metre of contaminated soil + benthonic diaphragm	2.6E-10	7.1E-03	The intervention allows for the reutilization of the area according to the architectural plan. Contamination is still present in the sub soil at a depth of less than one metre from the surface.
Total removal of contaminated soil from the area.	0.0E+00	0.0E+00	The intervention allows for the total removal of contaminating substances and the re-utilization of the area according to the architectural plan.

Fig.15. Summary of the risk analysis results.

5 Reclaim costs, environmental risks and merit

5.1 Application of the REC procedure: Risk, Environment, Cost.

The REC⁷ model is used for the evaluating of risk reduction, environmental merit, and the cost for any one of the intervention options. REC contributes to the forming of hypotheses of future land use, as well as the production of redevelopment scenarios.

REC uses the following information:

1. *the concentration of substances in each cell into which the area is divided;*
2. *maximum concentration values permitted by the MD 471/99 (i, s, t, values according to REC);*
3. *polluted surface area;*
4. *average depth of sub-soil beneath the polluted area;*
5. *average density of the terrain;*
6. *volume of polluted terrain (area times average depth);*
7. *mass of polluted terrain (volume times density);*
8. *minimum concentration in polluted area;*
9. *average concentration in polluted area;*
10. *maximum concentration in polluted area.*

An Attention Index is also calculated, to indicate the ratio between average or maximum concentration and the I value.

As of the first elaboration, a database is formed relating to the polluting agents and their classification based on the attention index, their level of 'dangerousness', and the selection of the first twelve contaminating agents in this latter category.

⁷ For further details on the REC model see Beinart, van Drunen, 2001, and Patassini et al., 2005.

5.2 Results: the classification for R,E, and C

The results are illustrated in Fig. 16, with a 'normalised' version in Fig.17.

Options	Risk reduction		Environmental		Cost (C)	
	value	%	valore	%	mil. Euro	*/-
soil washing + incineration + disposal	4,5295	77	70,36	67	66,788 (1,91/ha)	1,880
thermic desorption of organics + incineration + disposal	4,5295	77	76,7	73	72,689 (2,08/ha)	2,073
solvent-based extraction and subsequent acid lixiviation + incineration + disposal	5,4617	93	76,06	72	43,215 (1,23/ha)	1,134
bioremediation with selected bacteria groups+ incineration + disposal	5,4617	93	78,82	75	84,494 (2,41/ha)	2,464
incineration	5,5154	94	65,79	63	72,689 (2,08/ha)	2,073
capping	2,9271	50	27,61	26	27,579 (0,79/ha)	0,717
disposal	5,5154	94	90,76	86	49,102 (1,40/ha)	1,314
<i>theoretical maximum</i>	<i>5,8807</i>	<i>100</i>	<i>104,95</i>	<i>100</i>	-	-

Fig. 16. The R, E, C indices for intervention options.

As far as risk reduction (R) is concerned, it is clear from the table that the favoured options are incineration and disposal (94% of a theoretical maximum of 100%), solvent-based extraction and subsequent acid lixiviation + incineration + disposal (93%). The least favoured option is capping (50%).

For environmental merit (E) the best option is disposal (86%) and the worst is

capping (26%).

When it comes to cost (C), the least expensive option is that of capping (approximately 27.5 million euros), while the most expensive is bioremediation with bacterial families + incineration + disposal (approximately 84.5 million euros).

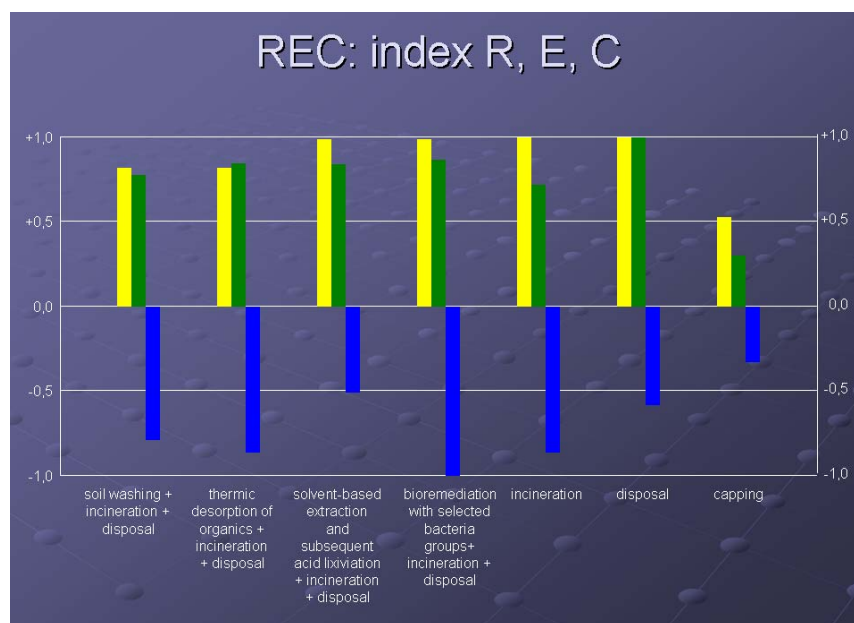


Fig. 17. R, E, C normalized indices for the Ex-Sava area.

6 Conclusions

Literature on the subject highlights several brownfield policy discourses⁸. On the whole, the managerial approach relies on derelict land acts and specific actions in response to the processes of abandonment. This is what happens in Italy, and particularly in the Veneto region with the issuing of reclaim certificates. The neo-liberalist (free trade) approach leads the actions for cities to an attitude of 'urban competition', whereby available areas are used for innovative functions while more importantly, reducing residual risks management in the programmes for real-estate valorisation and environment quality improvement. Environmental laws or environment protection acts entail a very different logic: they define indices and risk or dangerousness thresholds on the basis of scientific results. This sort of logic means the acceptance of the scientific input as it is, contextualising it without doubting its veracity; and giving scientific backing to the brownfield policy discourse – above all in the choice of technologies and during risk analysis. This signifies a standardization of the core of the procedure. Attitudes are more general and integrated within the

⁸ N Karadimitriou, J Deak, 2005.

approaches that place at the centre of the issue themes of sustainability according to a pluralistic, shared vision of a territorial redevelopment that is sensitive to the statutes of the areas involved⁹.

The practice described in this paper proposes a limited approach which is to a certain extent hybrid, in that it combines elements of the technical-scientific domain with managerial issues.

However, the setting up of the ELGIRA procedure remains modular and open, a sort of notebook: it can be adapted to intervention knowledge processes in sites of uncertain conditions or marked by conflict; it may also be deployed in the construction of scenarios by translating into specific redevelopment projects the policies contained in the reclaim Master Plan of Porto Marghera.

References

Beinat E., van Drunen M A (eds) ,2001, The REC decision support system for comparing soil remediation options. A methodology based on risk reduction, environmental merit and cost, REC Consortium, Amsterdam.

Comune di Venezia, Direzione Centrale Ambiente e Sicurezza del territorio, 2001, Accordo di programma per la chimica a Porto Marghera. Dpcm 12.02.99. Quadro conoscitivo di riferimento per la redazione del Master Plan per la bonifica delle aree contaminate di Porto Marghera (a cura di E De Polignol, F Zanetti), Venezia.

Comune di Venezia, 1996, La pianificazione urbanistica come strumento di politica industriale. La Variante al Prg per Porto Marghera, Urbanistica - Quaderni 9.

Fabris E., 2005, "Area Ex-Sava: analisi del rischio eseguita su diversi scenari di bonifica del suolo e sottosuolo", Rapporto interno, Venezia.

Hedorfer M., 2004, Elgira Toolkit 1, Algoritmi di interpolazione verticale delle concentrazioni di inquinanti, rapporto interno.

Karadimitriou N., Deak J., Rethinking brownfields: discourses, networks and space-time relations, Aesop Congress, Vienna, 13-17th, 2005.

Patassini D., Hedorfer M., Rinaldi E., De Polignol E., Cossetini P., Paneghetti C., 2005a, Contextual knowledge generated by a dss for brownfield development- the case of Porto Marghera (Venice), in D. Miller, D. Patassini 2005, Beyond benefit cost analysis. Accounting for non-market values in planning evaluation, Ashgate.

⁹ This theme was introduced within the town and regional planning legislation for the region of Tuscany, and developed in many researches by A Magnaghi.

Patassini D., Hedorfer M., Rinaldi E., De Polignol E., Cossetini P., 2005b, ELGIRA: Support System for Knowledge Building and Evaluation in Brownfield Redevelopment, in *Scientific Research and Safeguarding of Venice*, CORILA Research Programme 2001-03, CORILA.

Patassini D., Hedorfer M., Rinaldi E., De Polignol E., Cossetini P., 2005c, ELGIRA - A Knowledge Support Procedure to reclaim Porto Marghera Brownfields, *Environmental Protection of the Lagoon of Venice: An Economic Valuation*, Elgar Edward.

Provincia di Venezia, www.provincia.venezia.it/proveco/rifiuti/chimica.

Regione del Veneto, Comune di Venezia, 2002, Master Plan delle Bonifiche a Porto Marghera.

Regione del Veneto, 1999, PALAV. Piano d'area della laguna e dell'area veneziana, Cierre Edizioni, Verona.

RESEARCH LINE 1.3

Characteristics and conditions for a model of post-industrial sustainable development for Venice

SUPPORT POLICIES FOR THE RE-USE OF ABANDONED AREAS: THE CASE OF THE VENICE ARSENAL

Giuseppe Stellin¹, Giorgia Zoboli¹

¹ *Dipartimento di Innovazione Meccanica e Gestionale, Università degli Studi di Padova*

Riassunto

La complessità di scenari che si riscontrano nell'affrontare la tematica del riuso economico sostenibile di aree dismesse ha portato alla nascita diversi strumenti che permettono il coordinamento dei numerosi stakeholders. Tali strumenti possono essere ricondotti a tre tipologie: urbanistica, operativa e attuativa, anche se sono tutti finalizzati al confronto tra soggetti pubblici e privati per la realizzazione di opere di rilevante interesse per la collettività. La disamina di tali strumenti convoglia nell'analisi del caso dell'Arsenale di Venezia, area che presenta notevoli elementi di complessità.

Abstract

The complexity of the scenarios when tackling the subject of the economically sustainable re-use of abandoned areas has led to the development of different tools for the co-ordination of the numerous stakeholders. There are three types of tools: urban planning, operative and implementing ones, although all are targeted at a comparison between public and private parties for carrying out works of importance to the community. A survey of these tools is followed by an analysis of the case of the Venice Arsenal - a highly complex area.

1 Introduction

The seriousness of the problem of abandoned sites emerged in the late 1970s, but their resource potential for the process of urban renewal was only fully recognised towards the mid-1990s. The complexity of the possible scenarios is due to many factors, such as: the size of the areas, location, the presence of structures that were an integral part of the pre-existing functions or buildings of historical/architectural interest, the owner situation, the peculiarities of the local property market, and finally the presence of various constraints (such as those imposed by building regulations).

Upgrading projects attract the interest of many directly or indirectly involved parties. These include: the proprietors of the area or buildings to be upgraded; the owners of adjacent areas or buildings, who, if the work is done, may benefit from the positive externalities; the local community, who will be able to make use of any public amenities produced; the developers; the various levels of territorial administration, who are given the chance to gain amenities for the community; scholars of urban economics, valuation and town planning, who have been engaged for some time in an absorbing debate.

A belief in the need for collaboration between interested parties, with the aim of dividing the responsibilities and risks of interventions, is a new concept for public administrations. They should and must stimulate investments in abandoned areas, by implementing measures to render reclamation works competitive. Although the necessity for providing advantages for the private operators cannot be disregarded, it is of fundamental importance that the interests of the public operator are not penalised. Therefore, within the complexity of the decisional process, the public party should play a pivotal role. In other words, within a perspective driven by principles of sustainability, they must act on market incentives, correcting the inefficiencies, to internalise the positive externalities deriving from the works of reclamation and guarantee the sustainability (economic, environmental and social) of the work.

2 Support policies

The first upgrading projects carried out in Italy all agree that the notable difficulties in implementing reclamation operations are due to two main factors: the rigidity and inadequacy of urban planning tools and the lack of straightforward implementation procedures. For this reason, in recent years, forms of collaboration have developed between public and private parties that are leading towards strong innovations in the process of planning and accomplishing upgrading projects. A wide variety of approaches and solutions have been implemented, even if, in a final analysis, the utilisable tools fall into three categories: urban planning, implemental and operative instruments. The specific case study and its socio-economic context allow decision-makers to choose the most suitable tools, the structure of which will be constructed utilising different bargaining incentives. In the specialist literature, the tools described below are commonly considered in some ways similar. On the one hand are the urban planning instruments, which are characterised by the manifestation of the wishes and advantages of the promoters at the planning phase of the upgrading. On the other are the implemental instruments, which are "limited" to managing the complexities of the indications already set out by the urban planning instruments. The operative instruments are in an intermediate position because they can be used either to implement the urban planning instruments by reducing ratification times, or as a substitute for the actual plans in dictating urban planning prescriptions.

3 Urban planning instruments

3.1 Reclamation plan (*Piano di Recupero*)

The reclamation plan, introduced by Law 457/1978, is essentially of an executive nature, with the function of upgrading buildings and areas in already built-up and degraded zones. It can be either a public or private venture, and in the latter case coincides with the reclamation agreement stipulated between the municipal council and the promoters. The prescriptions of this plan, which must respect those of the general urban plan, may in their turn be implemented by private enterprises or the local council.

It should be specified that the reclamation plan was conceived mainly for the upgrading of residential areas with fragmented building ownership and therefore ill-disposed towards investments. It involves placing the co-ordination of the activities and creation of the surrounding conditions in state hands in order to render the areas once again competitive on the market: this takes the form of creating the necessary infrastructures, or financing expenditures and activities that cannot be met by private parties (such as the re-location of residents).

3.2 Complex programmes (*Programmi Complessi*)

Another set of instruments that has recently emerged within the regulatory framework and which are targeted at urban re-conversion and upgrading are those belonging to the group of complex programmes. The name derives from the plurality of aims, contents, parties involved and implementation methods that characterise them. The complex programmes have been successful because they respond to various needs, including: project flexibility, equality between proprietors through a single intervention, integration between public and private functions and between different types of land use, the true feasibility of the state part of the plans - in short the feasibility of urban projects [Urbani et al. 2004].

*3.2.1 Integrated intervention programmes (*Programmi Integrati di Intervento: PII*)*

The complex programmes include different instruments united by their belonging to the family of the integrated intervention programmes, instituted by art. 16 of Law 179/1992. The integrated programme acts with the aim of upgrading the urban, construction and environmental structure of entire areas of the council territory with projects of a sufficient size to have an impact on the organisation of the city or town.

Various parties are qualified to present an intervention hypothesis to the municipal council: public authorities, businesses, individual proprietors - perhaps united in a syndicate or association. Adoption is the concern of the municipal council and, if the programme is not in keeping with the urban planning forecasts, the council's approval is open to criticism from associations, citizens and agencies.

The definition of the relations between the integrated programmes and urban planning instruments is the responsibility of the regional laws. In particular, in Veneto reg. law 11/2004 defines an integrated programme as a level-two urban-planning implementing instrument. Given the possibility of approval of the instrument through recourse to the procedure of programme consent, the integrated programme can constitute a variant to the general urban-planning instruments. The PII involve the integration of public and private resources, indeed they can be financed with regional funds, in particular if they come within the public sector of council house building, whereas the work itself can be supported by a state contribution.

3.2.2 Urban reclamation programme (Programma di Recupero Urbano: PRU).

Law 493/1993 introduced the urban reclamation programmes aimed at integrating the construction of existing urban systems and to carry out maintenance, restoration and renovation on individual buildings. The PRU is thus a detailed urban-planning instrument, based on the involvement of private capital, proposed to the municipal council by public and private parties, sometimes in association. It can be adopted by advancing a 'programme consent' which, once reached, can be followed by specific urban planning conventions between the local administration and the actuating parties of the interventions.

It should be specified that the funds which can be assigned to these programmes are those earmarked for projects for building council houses.

3.2.3 Programme of urban renewal and sustainable land development (Programma di Riqualificazione Urbana e Sviluppo Sostenibile del Territorio: PRUSST)

The D.M. 1169/1998 introduced the programme of urban upgrading and sustainable development of the territory, the objectives of which include expediting funding for projects in urban areas affected by phenomena of degradation, and to encourage sustainable development from the economic, environmental and social points of view. These programmes are launched by the municipal, provincial or regional councils, consistent with the land-use planning and programming instruments. Where these latter are incompatible, the local councils initiate programmes of agreement with the administrations that have the title to these instruments. The programmes can be proposed by the following parties, also united in associations: state land authorities (regions, provinces, mountain communities), other public administrations (universities, companies and businesses with public participation, etc.), private individuals.

Resources from the National Maritime Authority (Direzione generale delle opere maritime) and the National Housebuilding Authority (Direzione generale dell'edilizia statale e dei servizi speciali) can be allocated for these programmes. While funds from the European Union, public administrations and private parties can be assigned for their implementation. The maximum amount that can be allocated for the promotion and carrying out of each programme is more than Euro two million, but it should be specified that the investments for private interventions must cover at least one third of the total investment and that the private parties must contribute a significant quota towards the financing of public works or of public interest, which will be stipulated by the promoter party.

4 Operative instruments

4.1 Urban renewal agreements (convenzioni di recupero)

Reclamation conventions can be finalised either at the time when the urban plans are implemented or when the urban planning prescriptions are identified.

The first type of convention includes those stipulated between the administration and private parties¹ which propose direct implementation of the planned works by a state-venture reclamation plan. These may be stipulated in a few specific cases, including those which wish to spontaneously implement works for the reclamation of the existing building stock where there is strong public interest.

The second type includes conventions that are stipulated in the case of adoption of private-venture reclamation plans, which allow the private parties to contribute towards the fixing of the urban planning regulations.

4.2 Services convention (*conferenza di servizi*)

The services convention is a form of cooperation between public administrations introduced by Law 241/1990 and modified by Law 127/1997 with the aim of simplifying administrative procedures, because it offers administrations the possibility to avoid making pronouncements at different times and locations in cases of particularly complex procedures². Recourse to the services convention is obligatory in cases where the decision-making about public works for an initial total amount of above euro 15 million requires the intervention of more than one administration or agency, i.e. where these are works of national interest or which involve more than one region.

4.3 Programme agreements (*accordi di programma*)

Law 142/1990 introduced the programme agreement as an instrument aimed at the coordination of different municipal, provincial and regional administrations or others for carrying out works and interventions that require integrated action. These parties establish the times, methods and forms of funding the work or intervention to be carried out at a general conference. Its approval involves a declaration of public utility and urgency of the work that, however, ceases to have effect if the work has not begun within three years. In cases where the programme agreement clashes with the urban planning instruments, a variant of the instruments will be constituted.

1 The different categories of parties with which the local council can stipulate the convention include individual owners or owners united in a syndicate, the building cooperatives of which they are members, construction companies or building cooperatives to which the owners or members have given the mandate for doing the work, construction companies or their temporary associations or consortiums, and cooperatives or their syndicates.

2 The services convention is also the place where a programme agreement can be discussed and approved.

5 Implementing instruments

5.1 Public-private partnership (*Società di trasformazione urbana*)

The promotion of a joint-stock company to entrust with urban renewal projects, introduced by Law 127/1997, can be considered as another way to involve building property in projects that fulfil a public utility. The companies are formed by metropolitan cities and local councils, with the participation of regions and provinces, but also by private parties, chosen by means of public evidence procedures. The public authority can decide whether or not to use this instrument for implementing a venture of urban renewal that would be difficult to accomplish with the usual regulatory and market instruments. The company is set up by a municipal council resolution, which also indicates the different partners, areas involved (with the consequent declaration of public utility), the multi-annual company programme and convention schedule between parties.

5.2 Project Financing

The financing project is used to interest private individuals in investing capital and expertise in works of public utility, which can guarantee profitability over time in order to redeem the capital invested. This institution was introduced in the Italian legal system with the passing of Laws 415/1998 and 144/1999 as a method for realising public works that may be obtained from both public and private initiatives. In the case of a private venture procedure the administrations evaluate the feasibility of the proposals presented and take steps to identify those they consider of public interest. The administration then starts up the procedure for evaluating the tenders, which takes place with a system negotiated on the basis of a "double tender". The state venture financing project is instead activated like a normal construction and management concession, with the only difference being that the concessionary is not a business, but a temporary project company formed for that specific task.

6 External bargaining incentives

The incentives on which negotiations between the stakeholders are structured can be of two types: the first is linked to the granting of tax allowances and public funding and the second regards the definition of project choices.

6.1 Tax allowances

In the case of protected buildings, private property is subject to special restrictions in the more general interest of safeguarding the cultural heritage in Italy. As a partial compensation for these limitations, the law grants some important tax advantages. For example, it is possible to deduct maintenance costs (up to a maximum of 19%) from the taxes, to obtain from the State a partial or full contribution to the costs for preservation or restoration work, and also to obtain targeted loans with a contribution of interest on account. In detail, the Ministry has the possibility of contributing up to 100% towards the cost sustained by the proprietors in the case of enforced interventions, and up to

50% for restoration work. In cases where the interventions are of particular importance or are carried out on property which is considered as being of public use or pleasure, the expenditure may be borne in full or in part by the Ministry.

6.2 Negotiation of project choices

For the sake of simplicity, it can be stated that in an operation of urban reclamation the deductible revenue depends mainly on the urban planning parameters, in terms of suitability for building and destinations of use granted, which inevitably define the amount and quality of the offer. These would generally be defined in a feasibility study, but are very often set *a priori* by the planning instruments.

Generally, in abandoned areas the indexes provided by municipal council instruments forbid new high-density building because, in general, a substantial part is set aside as green spaces. Furthermore, most of the urban reclamation work that has been done in Italy is of a functional nature. Therefore the destinations of use frequently accepted, mainly of the residential and services type, have not always reflected the requests of the developers.

It should also not be forgotten that in works of reclamation there are high costs related to any works of pre-urbanisation and demolition that basically depend on the current state of the area. Some authors retain that a *conditio sine qua non* for carrying out works of reclamation is that the costs for rendering the area suitable are borne, at least in part, by the public authority.

7 Venice Arsenal

7.1 Critical aspects

The factors identified above, which describe the complexity of the scenarios regarding the subject of the reclamation of abandoned areas, are particularly evident in the Venice Arsenal. This is an area of approximately 48 hectares, which contains buildings and functions of enormous historical interest to Venice and is not particularly accessible. Regarding this, the recent programme of urban upgrading and sustainable development of the territory (PRUSST) includes, because of the specific location, the provision of a rapid link system between Marco Polo Airport (i.e. the Venetian airport) and the Arsenal. In addition, ownership is problematical, in that the Italian Navy owns 63% of the property and the State owns the remaining 37%. In 2002, the Government Property (Agenzia del Demanio) (51%) and Venice City Council (49%) together set up the company *Arsenale di Venezia s.p.a.* with the specific objectives of the development and optimisation of the property assets of the Arsenal. With the formation of the Company, a convergence of objectives was created between the state and city council, but the divergence between this and the Navy represents an enormous constraint to the identification of the directions to take for the reclamation. Furthermore, in 1986, the area was declared a site of special historical and architectural interest. Another constraint comes from the planning system - the urban planning instrument currently in force refers to the

indications of an instrument of the implemental type which has, however, only been adopted for the northern part of the site.

7.2 *Intervention strategies: possible scenarios*

In order to apply the instruments described to the complex case of the Arsenal different scenarios are proposed, in their turn split into different alternatives.

The **first scenario** considers the presence of various *decision-makers*, who have different aims. In the first alternative it is suggested that the directives to be adopted are made explicit within the ambits of a services convention, during which a programme agreement can be stipulated. In the second and third alternatives the use is suggested of instruments that will also give the possibility of accessing external funding. Therefore, in the second alternative the integrated intervention programmes are indicated. The third alternative instead refers to the PRUSST.

In the delineation of the **second scenario** attention is paid to the problems of access. Indeed, it should not be forgotten that use of the Arsenal by economic players requires that it be reached more easily, which would necessitate sizeable investments. It is for this reason that the most suitable planning instrument is the PRUSST³.

As mentioned above, the current planning structure divides the Arsenal in two parts, so also the situations hypothesised in the third to fifth scenarios differ according to whether there is an implemental tool available. In particular, the third and fourth scenarios have been constructed to describe the possible routes to follow in the northern area: the former involves the designing of a project in agreement with the provisions of the existing urban instruments, and the latter proposes their modification. The **third scenario** is, in its turn, split into two alternatives. In the first, the instrument to use to implement the planning provisions coincides with the constituting of an urban renewal company. The second alternative contemplates the possibility of actuating a financing project procedure.

The **fourth scenario** contemplates the possibility of modifying the indications contained in the current urban planning regulations. Different alternatives can also be identified in this case. In the first alternative, the services convention is indicated as the place where the different public bodies involved can reach a programme agreement, which in this case would lay down the prescriptions to be respected. The second alternative contemplates the possibility of drawing up

³ The Ministry of Infrastructures and Transport has instituted a PRUSST for Venice, the aims of which include that of identifying routes connecting Marco Polo Airport and the Arsenal. However, it cannot be ignored that this proposal would not entirely resolve the problem of access to the area, for which a rail link would also be desirable.

a private or public venture reclamation plan, which would be followed by a reclamation convention to define the responsibilities of the public and private parties. This hypothesis is anyway less probable, given that a detailed planning instrument is already available and that it requires time to draw up an alternative. The third and last alternative of this scenario considers the formation of an integrated programme intervention, to be approved by a programme agreement.

Lastly, the **fifth scenario** is based on the lack of a detailed planning instrument for the southern area. In this case the possibility remains open of structuring the prescriptions in order to best satisfy the stakeholders' requirements. Thus, also according to what is reported in the Veneto Region regulations, the utilisable instruments could be the reclamation plans of public or private ventures and integrated intervention programmes.

8 Conclusions

The system of relations between instruments, aims and partners has highlighted, in a purely schematic way, some "institutional engineering", from which the guidelines can be drawn to identify the framework to which all projects must refer. Once the solution to adopt has been chosen, there must be a careful verification of the feasibility of the projects, especially in terms of quantitative valuations. This paves the way for a second phase of the study of a more operational nature that must be preceded by the definition of the specific implemental instruments. Indeed, what has been described above is just a preliminary to more highly-detailed studies, which will be necessary to reach any type of economic qualification of the project.

References.

Archeologia industriale. Metodologie di recupero e fruizione del bene industriale. Atti del convegno. Prato, 16-17 giugno 2000. A cura di Faustini L., Guidi E., Misiti M.

Barel, B., (2004), a cura di; *La legge urbanistica della Regione Veneto. Commentario alla legge Regionale del Veneto 23 aprile 2004, n. 1*, Grafica Veneta s.p.a., Trebaseleghe (PD).

Bobbio, R. (1999), "Riconversione delle aree dismesse: aggiornamento e spunti di riflessione", in *Urbanistica Informazioni*, 164.

Fusco Girard L. (1987), *Risorse architettoniche e culturali: valutazioni e strategie di conservazione. Una analisi introduttiva*, Franco Angeli, Milano.

Marin, A., (2001) "Il patrimonio storico dell'industria, quali modelli per il riuso?" in *Urbanistica Informazioni*, 180 pag 10-11

Micelli, E., (2004), *Perequazione urbanistica. Pubblico e privato per la trasformazione della città*, Marsilio editori, Venezia.

Micelli, E., (1999) "La riqualificazione delle aree dismesse in Veneto" in

Urbanistica Informazioni, 164 pag 6-7

Nevitt, P. K. (1989), *Project financing*, Euromoney publications.

Reho M., Tonin S., Trombetta F. (2002), "La promozione della bonifica ambientale nelle aree industriali dismesse", in *La valutazione degli investimenti sul territorio*. Atti del XXXIII Incontro di Studio del Ce.S.E.T., Cagliari 24 ottobre.

Stanghellini, S., (2004), a cura di, *La selezione dei progetti e il controllo dei costi nella riqualificazione urbana e territoriale*, Alinea editrice, Firenze.

Stanghellini S. (2003 b), "Funzioni di pubblica utilità e valutazione dell'indennizzo", in *La valutazione degli investimenti sul territorio*, Atti del XXXIII Incontro di Studio del Ce.S.E.T., Cagliari 24 ottobre XXXIII Incontro di Studio del Ce.S.E.T., Cagliari 24 ottobre.

Storto, G., (2004), a cura di, *Le società di trasformazione urbana. Contesto legislativo, caratteri, profili giuridici, problematiche applicative*, Il Sole 24 Ore S.p.a.

Urbani P (2001)., *Nuove regole per la trasformazione urbana*, Relazione tenuta al convegno patrocinato dall'INU – Confcooperative- Federabitazione, Venezia, 23 novembre.

Urbani, P, Civitarese Matteucci, S. (2004), *Diritto urbanistico. Organizzazione e rapporti*, Giappichelli editore, Roma.

THE ECONOMIC REUSE OF THE BUILT HERITAGES A PROPOSAL FOR A SET OF SUSTAINABILITY INDICATORS

Valentina Zanatta¹, Mila Dallavalle² and Paolo Rosato²

¹ *Dipartimento Casa Città, Politecnico di Torino, Torino, Italy, and FEEM* ² *Dipartimento di Ingegneria Civile, Università di Trieste, Trieste, Italy, and FEEM*

This paper is an operative proposal for the application of the sustainability concept to the revitalization and economic re-use of historical buildings. As the ultimate goal of the research project is to assess the potential economic re-use of historical buildings, this paper intends to define a set of indicators able to assess if a certain re-use project on a cultural heritage is sustainable or not.

The research initially introduces the concept of sustainability, which was originally used in the field of environmental economics, and was later applied to social issues and urban development. The efforts to extend the concept of sustainability to cultural heritage has not found a definite operative application in the assessment of renovation and re-use projects of cultural assets. In Italy, the debate about the legal protection of cultural heritage has produced some guidelines to determine the requirements that interventions and re-use projects should have to be considered “sustainable” and the notion of cultural heritage has been gradually extended from individual buildings to the architectural heritage and the building stock, considered as a patrimony. Moreover, the traditional policies for the preservation of cultural heritage through the protection of historical monuments should be included in a broader strategy of sustainable use and management of the buildings: some preliminary studies show some evidence of a “good” economic re-use of the built heritage: the assets that have been used by the owners and/or stakeholders usually have a far greater likelihood of remaining viable than others preserved in the usual ‘top-down’ manner, because they are able to provide for the material maintenance of the asset.

Anyway, the sustainability of the economic re-use of an ancient building requires a delicate balance between use and conservation, able to provide a stream of economic, social and financial benefits. The extensive literature on the sustainability concept is mainly focused on the theoretic definition of the topic and its operative application for the governance of environmental and urban processes. In order to define a sustainable way of re-using built heritage, the effects and impacts of the revitalisation and re-use project on the building’s qualities have to be assessed. These qualities cannot be limited to the building’s visual appearance, but they should consider the range of material and intangible functions that the built heritages produce. The research provides a classification of the different components of the values in terms of material witness, aesthetic and artistic values, symbol of traditions and so on.

Furthermore the research aims to define analysis tools able to evaluate if the

effect of a re-use project is sustainable or not.

Basically, the issue of the economic re-use of cultural heritage derives from the general problem of the lack of public funds for conservation. It is thus necessary to define the economic uses that, avoiding abandonment, could be sustainable for the typological and technological features of the buildings. In fact, as abandonment is a real risk, even an “unbalanced” use may threaten the environmental, cultural features of the building, and produce the loss of the historic nature, complexity and quality of the heritage. In the long term, unsustainable uses are going to clash with the cultural and traditional traits of the asset, involving high external costs. The assessment of the “sustainability” of a re-use project should consider whether the project would provide the economic maximization of the option value of the good. This would involve implementing a transformation in the building which would not rule out the possibility of changing its economic use, without spending too much money on adaptations.

The concept of Same Minimum Standard (Ciriacy-Wantrup, 1955; Bishop, 1979) should provide for a fruitful and well-based approach to the issue, formalising the problem in a trade-off between “transformation” and “preservation” of the asset.

Figure 1 represents a simple model of the relationship between transformation (intensity of the economic use) and conservation. The y axis (ordinates) shows the level of transformation T , while the x axis (abscissas) shows the level of preservation C .

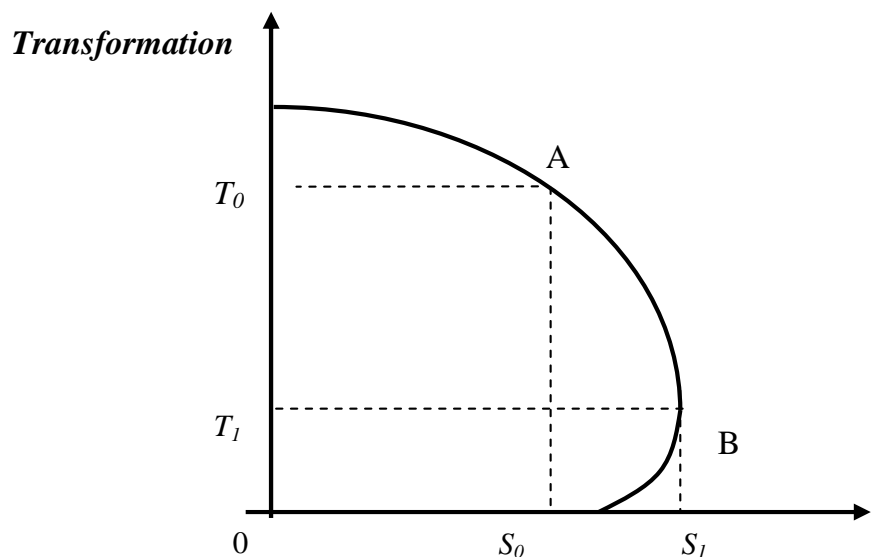


Figure 1 – The preservation/transformation (P/T) threshold

If the economic re-use is very close to the original use of the building, as is the case when a building is restored and used for the purpose it was originally built for, the first part of the preservation/conservation frontier will likely to be

ascending (DB), because of the complementary relation between the preservation of the building and the basic levels of transformation (T_1): the latter correspond to the minimum tasks needed to bring the building to an acceptable level of utilisation and to avoid its degradation. In this situation, the optimal level of preservation is S_1 . When a project which implies greater transformation (for $T_i > T_1$) is implemented, the curve decreases from left to right, expressing the existence of a trade off between the two instances. This formalisation would suggest the existence of a “critical threshold” (T_0) when a re-use or a development project is implemented on a historical building: the threshold defines that minimal level of conservation under which economic use is unsustainable from the conservation point of view. Exceeding the threshold level as a result of unsuitable planning or changes made to the building could imply the loss of both material and immaterial features.

Although the variety of built heritages is such that it is impossible to adopt univocal standards to determine the quality of an architectural renovation process, this paper introduces a set of indicators useful to define the threshold T_0 . As the historic building is mainly a cultural heritage, the coexistence of cultural properties with economic development requires that interventions have adaptive, flexible and reversible characteristics. The output of this research is a set of indicators for the evaluation of the sustainability of a reuse project. These indicators should help to make the sustainability concept operative: they have been selected on the basis of their capability to define and assess five main objectives. These objectives are intended as criteria for evaluating whether the reuse of the built heritage is sustainable or not. The criteria selected are:

- *reversibility*: the possibility of removing the elements that the implementation of the reuse project would add to the building;
- *versatility*: the possibility of easily changing the economic use of the building, yet limiting the costs and the work required to adapt the building to the new use;
- *context respect*: the effects of the project on the environment, the landscape and the general context of the building;
- *invasivity*: the effects of the techniques and technologies of the project on the historic, architectural and artistic characteristics of the building;
- *financial and economic feasibility*: the profitability of the reuse project, also with regard to the distribution.

The set of selected indicators informs, defines and assesses the criteria, making them operative with regard to the material elements of the buildings, and to the different issues (economic, social and environmental) involved in the project, and they are expressed in different scales (quantitative and qualitative / nominal).

The research group is currently working on the elaboration of thresholds for the indicators, supported by a pool of experts. Moreover, the research group is

working on some multiple criteria tools for ordering the indicators and producing an operative path for the evaluation of the sustainability of the reuse projects.

The indicators selected are organised and defined in the tables below.

OBJECTIVE	CRITERIA
Sustainability	Reversibility
	Versatility
	Context respect
	Economic feasibility

CRITERION	INDICATORS	DEFINITION
Reversibility	Historical stratification	Legibility of the historical stratification
		Consistency of the project in relation to the building's history
	Typological pattern	Percentage of volume, which has been demolished
		Internal partition
		Percentage of new construction volume and structures leaning against the historical building
		Maintenance of the key-elements of the typology
	Structures	Use of removable technologies and materials for consolidation of foundations, masonries, floors and roofs
	Finishes	Use of removable and traditional technologies and materials for consolidation or substitution of pavements, interior and exterior partings, casings, iron bars, sills, beds and intradoses
	Decorative elements	Use of removable technologies and materials for consolidation and protection of paints, fillers, marbles, woods, metallic balusters, sculptures, inscriptions, memorial tablets, coats of arms
	Technological systems	Housing of technological systems and ducts in false ceilings and removable walls
		Avoid into chase housing in the presence of decorative elements
		Utility rooms compactness

CRITERIA	INDICATORS	DEFINITION
Versatility	Reuse typology and technological systems	Inflexibility of project plan
		Possibility of removing new superfetations/structures/partitions
		Prevision of enough vertical connection
		Execution of suitable technical room
		Number of plant endings/Number of foreseen rooms
	Typology of the historical building	Monumentality of buildings
		Existence of accessory buildings to the prime building
		Number of accessory buildings
		Existence of external area
	Accessibility	Vehicular accessibility
		Service vehicular accessibility
		Closeness to road or railway infrastructures
		Accessibility by public transport
		Accessibility for disabled person

CRITERIA	INDICATORS	DEFINITION
Context respect	Historic value	Coherence of the new use with the historical ratio articles-context
		Possible access by historic trails
	Landscape quality	Maintenance of the context landscape quality
		Maintenance of the building's aesthetic quality
		Positive externalities on the value of surrounding buildings
	Perception	To share the new functions installed in the articles by the local community
		Public use of area
		Maintenance of the historical building as perceived by the reference community
		Impact of economic benefits of the project on local community
		Increase of the perception of cultural value of the building
	Accessibility	Pedestrian accessibility from city center
		Accessibility with private means of transport
		Closeness to road or railway infrastructures
		Accessibility with public means of transport
		Parking area availability
		Access free to area
		Presence of suitable naturalistic and/or historic trails

CRITERION	INDICATOR	DEFINITION
Economic feasibility	Returns/Benefits	Annual sales of economic business installed in historic building
		Number of employed
		Public benefit
		Number of new economic businesses generated by the re-use of historic complex
		Development of public transport services - new users
		Percentage of maintenance expenditures which are covered by new use
	Costs	Financial costs of project and restoration
		Financial costs to set up and manage economic business installed in the historic building
		Costs to manage the historic complex
		Costs to maintain the historic complex
		Costs to administer the historic complex
	Opportunity	To share costs and benefits of intervention with local community
		Capability of diversification of economic business installed from local economic context activities

References.

Asheim, G.B., Buchholz W. e B. Tungodden (2001), Justifying Sustainability, *Journal of Environmental Economics and Management*, 41(3): 235-251.

Bishop, R.C. (1978), Endangered Species and Uncertainty: the Economics of a Safe Minimum Standard, *American Journal of Agricultural Economics*, 57 (Feb): 10-8.

- Bishop, R.C. (1979), Endangered Species, Irreversibility, and Uncertainty: A Reply, *American Journal of Agricultural Economics*, 61(2): 376–79.
- Buchanan, M. e W. Stubblebine (1962), Externality, *Economica*, 29: 371-84.
- Carbonara, G. (2001), *Trattato di restauro architettonico*, Torino, UTET.
- Castle, E.N. e R.P. Berrens (1993), Endangered Species, Economic Analysis, and the Safe Minimum Standard, *Northwest Environmental Journal*, 9: 108-30.
- Ciriacy-Wantrup, S.V. (1964), The “New” Competition for Land and Some Implications for Public Policy, *Natural Resources Journal*, 4: 252-67.
- Ciriacy-Wantrup, S.V. 1968[1952], *Resource Conservation: Economics and Policies*, Berkeley, University of California Press, California.
- Chichilnisky, G. (1997), What is sustainable development?, *Land Economics*, 73(4): 467-91.
- Culyer, A.J. (1971), *Merit Goods and the Welfare Economics of Coercion*, Public Finance, 4: 546-62.
- D'Alpaos C., Rosato P. e V. Zanatta (2001), Il riuso economico degli edifici storici, un modello di valutazione gerarchica, *Riconversione di manufatti storici in musei. I musei di oggi negli edifici di ieri*, a cura di Ientile R., atti delle giornate di studio, Torino 7-8- maggio 2001.
- Dezzi Bardeschi, M. (1991), *Restauro: punto e da capo. Frammenti per una (impossibile) teoria*, Milano, Franco Angeli.
- Dogliani, F. (1997), *Startigrafia e restauro. Tra conoscenza e conservazione dell'architettura*, Trieste, LINT.
- Fusco Girard, L. (1987), *Risorse architettoniche e culturali: valutazioni e strategie di conservazione*, Milano, Franco Angeli.
- Fusco Girard, L. (a cura di) (1989), *Conservazione e sviluppo: la valutazione nella pianificazione fisica*, Milano, Franco Angeli.
- Fusco Girard, L. (1993), *Estimo ed economia ambientale. Le nuove frontiere nel campo della valutazione. Studi in onore di Carlo Forte*, Milano, Franco Angeli.
- Franceschi, S. e L. Germani (2003), *Manuale operativo per il restauro architettonico*, Roma, DEI.
- Giannini, M.S. (1976), I beni culturali, *Rivista Trimestrale di Diritto Pubblico*, cit. in Alibrandi T., Ferri P. (1995), *I beni culturali e ambientali*, Milano, Giuffrè, p. 17.
- Head, J.G. (1966), On Merit Goods, *Finanzarchiv*, (1): 1-29.
- Head, J.G. (1968), Merit Goods Revisited, *Finanzarchiv*, (3): 215-25.
- Heal, G. (1998), *Valuing the Future: Economic Theory and Sustainability*, Columbia University Press.
- Howarth, R.B. (1997), Defining Sustainability, *Land Economics*, 73(4): 445-621.

Krutilla, J.V. (1967), Conservation Reconsidered, *American Economic Review*, 57(4): 777-86.

Marconi, P. (1993), *Il restauro e l'architetto. Teoria e pratica in due secoli di dibattito*, Venezia, Marsilio.

Mason, R. (2002), Assessing values in conservation planning: methodological issues and choices, *Assesing the values of cultural heritage*, Los Angeles, The Getty Conservation Institute.

Mishan, E.J. (1971), The Post-war Literature on Externalities: an Interpretative Essay, *Journal of Economic Literature*, (2): 1-20.

Musgrave, R.A. (1971), Provision for Social Goods in the Market System, *Public Finance*, (2): 304-20.

Norton, B.G. e M.A. Toman (1997), Sustainability: Ecological and Economic Perspectives, *Land Economics*, 73(4): 553-68.

Pearce, D. e R.K. Turner (1991), *Economia delle risorse naturali e dell'ambiente*, Il Mulino, Bologna.

Pezzey, J. (1997), Sustainability Constraints Versus "Optimality" Versus Intertemporal Concern and Axioms versus Data, *Land Economics*, (73): 448-66.

Raccomandazioni Normal. Alterazioni dei materiali lapidei e trattamenti conservativi - Proposte per l'unificazione dei metodi sperimentali di studio e di controllo. Normal 1/88: alterazioni macroscopiche dei materiali lapidei: lessico. Normal 20/85: Interventi conservativi: progettazione, esecuzione e valutazione preventiva.

Randall, A. (1986), Human preferences, economics, and the preservation of species. In Norton, B.G. (eds.), *The Preservation of Species. The Value of Biological Diversity*, Princeton University Press, Princeton, pp.79-109.

Randall, A. (1991), Total and Non Use Values. In: J.B. Braden e C.D. Kolstad (eds.), *Measuring the Demand for Environmental Quality*, North Holland, Amsterdam.

Randall, A. e Stoll, J. (1983), Existence values in a total valuation framework. In Row, R. D., e L. G. Chestnut, *Managing Air Quality and Scenic Resources at National Parks and Wilderness Areas*, Boulder: Westview Press.

Ready, R.C. e Bishop, R.C. (1991), Endangered species and the safe minimum standard, *American Journal of Agricultural Economics*, 73 (2), pp. 309-12.

Romano, S. (2002), La stima del valore di opzione e del valore di esistenza delle risorse naturali: il caso del *Pinus leucodermis* del Pollino, *Aestimum*, (41): 27-64.

Roskamp, K.W. (1975), Public Goods, Merit Goods, Pareto Optimum and Social Optimum, *Public Finance*, (30): 61-9.

Salmen, L.F. (1998), Toward a Listening Bank: A Review of Best Practices and the Efficacy of Beneficiary Assessment. Social Development Papers,

Environmentally and Socially Sustainable Development, Paper No.23 (September).

Serageldin, I. e J. Martin-Brown (eds.) (1999), *Culture in Sustainable Development. Investing in Cultural and Natural Endowments*, Conference Sponsored by the World Bank and the UNESCO. Proceedings.

Smelser, N.J. (1997), *Social Dimensions of Economic Development*. Environment Department Papers. Social Assessment Series, Environmental Sustainable Development. The World Bank, Paper No. 048 (February).

Seidl, I. e C.A. Tisdell (2001), *Neglected features of the Safe Minimum Standard: Socio – Economic and institutional dimensions*, *Review of Social Economy*, 59 (4): 417-42.

Stellin, G. e P. Rosato (1998), *La valutazione economica dei beni ambientali: metodologia e casi di studio*, Torino, Città Studi.

The World Bank (2001), *Cultural Properties in Policy and Practice: A Review of World Bank Experience*. Operations Evaluation Department. Sector and Thematic Evaluation Group. Report No. 23369 (December).

Throsby, D. (2001), *Economia e cultura*, Bologna, Il Mulino.

Throsby, D. (2002), *Cultural capital and sustainability concepts in the economics of cultural heritage, Assessing the values of cultural heritage*, Los Angeles, The Getty Conservation Institute.

Woodward, R.T. (2000), *Sustainability as Intergenerational Fairness: Efficiency, Uncertainty, and Numerical Methods*, *American Journal of Agricultural Economics* 82(3): 581-93.

Woodward, R.T. e R.C. Bishop (1997), *How to Decide When Experts Disagree: Uncertainty-Based Choice Rules in Environmental Policy*, *Land Economics* 73(4): 492-507.

AREA 2

Architecture and Cultural Heritage

RESEARCH LINE 2.2

Catalogue of Venetian plasters and historical interventions for high water defense

MARMORINO PLASTERS IN VENICE BETWEEN THE XVI AND XVIII CENTURIES

MARIO PIANA

Dipartimento di Storia dell'Architettura, Università IUAV di Venezia

Riassunto

L'affermarsi del classicismo in ambito architettonico segnò una svolta precisa, un mutamento delle abitudini e dei sistemi costruttivi del cantiere medievale. I rivestimenti esterni risentiranno di questo cambio di gusto e proprio all'inizio del XVI secolo si metteranno in pratica nuove tecniche e nuovi materiali come per gli intonaci a marmorino che, emulando i più preziosi rivestimenti lapidei, cambiarono in parte il colore alla città.

I marmorini, per la loro capacità di aderire al linguaggio dell'architettura classicista e per le loro indubbie qualità di resistenza all'aggressione delle intemperie, nel corso di tre secoli trasformeranno la fisionomia della città imprimendo quel tono bianco-rosato che ancor oggi l'edilizia lagunare, sia pure parzialmente, conserva.

Abstract

The success of classicism in the architectural field constituted a definite change, in habits and construction systems, in mediaeval construction sites. External plasters were also involved in this change in tastes, and right at the beginning of the XVI century, new techniques and new materials shall be adopted, such as marmorino plasters that, by imitating the most precious stone coatings, contributed to change the colour of the city.

Marmorinos, thanks to their adaptability to the language of classicist architecture, and thanks also to their undoubted resistance to weathering, shall, in the course of three centuries, change the face of the city, conferring to it that rosy-white shade that has, partly survived to the present day.

1 Introduction

Rationalisation, simplification, unification of building procedures and building materials: these seem to be the main characteristics of the evolutive trend in building on the Lagoon in the second half of the XV century.

An analysis of the whole complex of buildings erected between the XVI and the XVII centuries in the lagoon area shows technical and system continuity of building prevailing over the novelty elements. It is possible to detect a slow evolution, a prudent change in building techniques that are only a secondary characteristic, as an answer to the needs of the new architectural language. A cautious adjustment can be seen mainly through the rationalisation of static schemes and the normalisation of building materials.

The reasons of the extraordinary continuity in the use of materials, techniques and static systems in city buildings can be found mainly in the formidable opposition to the erection of new buildings adopted by the lagoon's city and in the consequent building contrivances and ploys, both singular and effective, found and applied by the skilled workers from the very first centuries of Venetian building. Balancing problems derived from the unavoidable need to lay the foundations in marshy grounds, incapable of supporting significant loads, could not be faced and solved unless long-proven procedures were adopted.

2 The appearance of terrazzos in Venice

Some techniques, unknown until then, were introduced and new materials were also used; among these the one that was maybe the most interesting is *stucco*, called also *terrazzo* or *terrazzetto* – today's marmorino plaster – as it was the most intimately linked to the new architecture (Fig. 1)



Fig. 1 - Venice, Dorsoduro, Foscari Palace at Carmini.

The term *terrazzo*, and the accompanying verb, *terrazzar*, can be found already during the second half of the XV century. Its first known appearance dates back to 1473, in a contract drawn by the Santa Chiara Nuns of Murano with regard to

the construction of the church, where it is stipulated that “ditj murj tutj belizar smaltar e terazar si dentro come de fuora”¹ (the walls shall be finished, internally and externally, with enamel and terrazzo finishes). The term is used consistently in the building papers from the XVI and XVII² centuries, and remains in use until the XVIII century: as an example, see the “terrazzo da Rovigno fregato in buona forma”(Rovinj *terrazzo*, well polished)³ applied in 1734 to the façade of the Scuola della Carità, where there is also an interesting reference to the Istrian city of Rovinj, the main source of *pietra d'Istria*.

Marmorinos appear in the city between the XV and XVI centuries, at the same time as the diffusion of the new architectural language. In the centuries of classicism marble was considered a noble material, to be preferred above all others in the construction of a building⁴. In the lagoon the *Pietra d'Istria*, for its characteristics of compactness and resistance, but also for the aesthetic qualities derived from its fine grain and remarkable whiteness, was considered the first choice of lithotype, comparable only to the finest marbles. In *Venetia, città nobilissima e singolare*, for instance, it is said that “bella et mirabil cosa è la materia delle pietre vive, che sono condotte da Rovigno et da Brioni, castella della Dalmatia, sono di color bianco et simili al marmo: ma salde et forti di una maniera che durano per lunghissimo tempo a i ghiacci et al Sole: onde se ne fanno statue: le quali polite col feltro a guisa del marmo, poi che sono pomiciate, hanno sembianza di marmo”(the stones brought from Rovinj and Brioni, Dalmatian cities, are quite beautiful, white and similar to marble; they are

¹ P. Paoletti, *L'architettura e la scultura del Rinascimento in Venezia: Ricerche storico-artistiche*. Parte I, Venezia 1893, p. 92.

² The first known instance of the use of this term in the XVI century dates back to 1534: the proto Antonio Scarpagnino, explaining the plans for the construction of a housing block in Santa Maria Zobenigo specifies that: “tute ditte muragie de bone piere ben cotte de bona tera padovane overo trevixane, con bone calzine bene lavorade et smaltade e biancizado de dentro via et di fuora ben interazado per modo che tuti stiano bene”. (ASVe, Scuola Grande di S. Rocco, II delivery, b. 46, c. 27, 14th January 1534. Published by G. GIANIGHIAN, *Appunti per una storia del cantiere a Venezia (secoli XVI-XVIII)*, in G. CANIATO, M. DAL BORGO, *Le arti edili a Venezia*, Roma 1990, pp. 244-45).

³ Quoted from P. MODESTI, *Le trasformazioni storico-costruttive del complesso della Carità*, in *Progettare un museo. Le nuove gallerie dell'Accademia a Venezia*, Milano 2005, p. 23.

⁴ Marcantonio Sabellico, for instance, at the end of the XV century, and referring to the recently completed church of San Fantin, describes it as follows “frons aedis nitida, candidoque saxo nuper instaurata” (Quoted in G. VIO, *I “mistri” della chiesa di S. Fantin in Venezia*, in “Arte Veneta”, 31, 1977, p. 225).

compact and strong, so that they are resistant to the action of ice and sun for a long time; they are used for statues that, polished with felt, like it happens with marble, and after being buffed with pumice, look like marble)⁵.

In Venice, in the transition decades between the Middle Ages and the Modern Age, Istrian limestone became the only, or virtually so, stone used for structural elements and for the architectural framework of buildings⁶; from the beginning of the XVI century onwards, furthermore, and in the course of a few decades only, *pietra d'Istria* completely replaced red Verona marble, Greek marbles and Carrara marbles, as well as breccia marbles, red and green porphyries, which

⁵ F. SANSONO, *Venetia, città nobilissima e singolare*, Venezia 1581, pp.140-41. This is neither the first nor the last instance of the appreciation of this material; the writings of Pietro Coppo in 1540 should not be forgotten: "La Isola di Breoni e quasi davanti el Porto de Pola (...) boni taiapiera si atrovano qui per esser Isola copiosa de bella sorte de piera bianca: manco dura che quella de Rovigno. (...) In questi doi lochi si attrova gran rompitori di grosse & ponderose piere bianche. de qual se fano belli lavori da gran edifitii et sumptuose fabriche per Venetia & altre Citta opulente" (P. COPPO, *Del sito de listria*, Venezia 1540, p. 17). Giorgio Vasari, in the first chapter of his *Vite*, underscores its advantages: "Cavasi ancora in Istria una pietra bianca livida, la quale molto agevolmente si schianta; e di questa sopra di ogni altra si serve non solamente la città di Vinegia, ma tutta la Romagna ancora, facendone tutti i loro lavori e di quadro e d'intaglio (...) e porte, finestre, cappelle et altri ornamenti che lor vien comodo di fare, non ostante che da Verona per il fiume dello Adige abbiano comodità di condurvi i mischi et altra sorte di pietre, delle quali poche cose si veggono, per aver più in uso questa" (G. VASARI, *Le Vite*, chapt. I "Dell'Architettura". Modern edition by C. RAGGHIANI, Milano 1971, pp. 122-123). At the beginning of the XV century, Vincenzo Scamozzi reminds that "le cave vecchie [che] si veggono alla marina sotto Orsera (...) vero è, che la maggior quantità, e bonta di essa [pietra d'Istria] si ritrova nelle cave di Leme, e Mondelago: perche e l'une, e l'altre sono molto bianche, e fine, e sonore, salde, e dure" (V. SCAMOZZI, *L'idea dell'Architettura Universale*, Venezia 1615, p. 198).

⁶ Very few constructions shall not adhere to the new taste, thus avoiding standardisation; among these, a notable, practically unique instance is the Palladio Peristyle of the Carità complex, built at the beginning of the second half of the XVI century: "Questo edificio è tutto fatto di pietre cotte, cioè mattoni, salvo le base delle colonne, i capitegli, l'imposte degl'archi, le scale, le superficie delle cornici e le finestre tutte e le porte"⁶, mentioned Vasari, who had probably visited the construction yard during his brief sojourn in Venice in May 1566. This quite pertinent notation underscores that the dominant role played by structural tiles is the main constructive characteristic of the building. Clay appears not only as a constituent material of the construction's many walls and members, as was common usage in Venice, but is also used as a substitute for stone, to form the great majority of the orders elements. Column shafts, architraves, friezes, cornices, moulded fascias are built in structural tile, modelled with great precision and finished with an extremely thin coloured layer.

had been quite common in mediaeval and first Renaissance architecture, in face coatings⁷.

However, modern era constructions, built with direct bearings entirely made of stone are rare: the instances of the Zecca and of the building of the Prigioni Nuove are significant, and isolated, exceptions. Equally rare are the constructions with stone primary members (like the great arching of the Rialto bridge, for instance) or the architectures with face structural blocks associated with the underlying structural tiles. (remember the instances of Codussi's San Pietro di Castello bell tower and of the San Fantin church). A reason for this might lie in the fact that the spreading of the new architectural language, inspired by Roman classicism, could not have a significant impact on the mental attitudes and the habits of a building culture which, like the Venetian one, had to look for maximum lightness in building: in this city, the vast majority of constructions continued therefore to be based on the use of structural tiles.

Stone members would have required a greater building effort, having a higher weight density, starting with the pilings and the lower brickwork, with the consequent increased expenditure. Moreover, such a structure would have drastically reduced one of the fundamental characteristics offered by structural tiles, namely, the ability to adapt themselves plastically to the inevitable relative settlements suffered by Venetian buildings, always of considerable absolute degree, thus reducing the development of crack systems, which would, on the contrary, have been exalted by stone walls. Structural tile buildings completely plated with thin stone slabs are also isolated instances, given the very high costs of such workmanship. With the exclusion of the faces of many church buildings, of some public buildings and of some palaces, where stone was used only on the main façade, and, even here, only as a coating laid over a cotto member, the church of Santa Maria dei Miracoli and the Palazzo dei Camerlenghi are the only buildings with the whole external facades coated with marble *tables*.

3 Marmorinos

In order to overcome these building limitations and obstacles, and spurred by the new requirements of the "ancient style" language, the local building culture found an answer by perfecting a new plaster that allowed brickwork to resemble stone walls. It can be said that *marmorinos*, by avoiding a not inconsiderable difficulty, that is, by allowing builders to continue with structural tile septa which

⁷ In those same decades the practice of painting and gilding the structural and coating stones, for aesthetic and protective purposes, still flourishing at the end of the XV century, ceases. Such practice is still visible today – even though in traces – on several buildings, and is confirmed by abundant iconography, as witnessed by some surviving construction documents.

were much lighter than stone, but which could be given a “stone” look, eliminated one of the technical obstacles that might have hindered the spreading of the new architecture in the Lagoon.

There qualities and advantages were clearly described by Alvise Cornaro, around 1560, when he, in his visionary proposal for the construction of a theatre in the St. Mark’s basin area, theorised a “Theatro in pietra grande, ma non di pietra da scalpello ma di cotta, che non costerà la metà e sarà opera durabile come di pietra da scalpello, perché la cotta hora che si ha trovato il stucco se istuccherà e, come si vede, tal stucco si converte in sasso perché è fatto di sasso” (a theatre made of stone, but not solid stone, rather of bricks, that shall cost less than half as much and that shall be as enduring as a stone one, because bricks, now that we have discovered how, shall be plastered and, as can be seen, such plaster shall transform into stone, because it is made of stone)⁸.

The reason of the rapid and immense success of *marmorinos* since the XVI century, first in Venice, then all over the Venice territory, must be found in their ability to recall effectively and sometimes mimic the look and substance of stone⁹. Indeed, where normally *marmorinos* tend to recall only the appearance of stone, sometimes, in some stringcourses, window frames or fake angular ashlar-work, there is a clear intention of reproducing faithfully also the typical processing of hewn stone, down to the grain created by hacking and to the perimetric *cordellina*, the thin, polished band with which the lapicides finished the hewn stones’ edges¹⁰ (Fig. 2).

⁸ A. CORNARO, *Scritti sull’architettura*, (edited by) P. CARPEGGIANI, Padova 1980.

⁹ M. PIANA, *Tecniche edificatorie cinquecentesche: tradizione e novità in Laguna*, in *D’une ville à l’autre: structures matérielles et organisation de l’espace dans les villes européennes (XIII-XVI siècle)*, atti del convegno École Française de Rome, Roma 1989, p. 639. For further information on materials and execution techniques of *marmorinos* and on their chemical-physical properties, consult: G. BISCONTIN – M. PIANA – G. RIVA, *Research on Limes and Intonaco of the historical Venetian Architecture*, in *Mortars, Cements and Grouts used in the Conservation of Historic Buildings*, proceedings of the Symposium ICCROM, Roma 1982, pp.359–371; G. BISCONTIN - M. PIANA - G. RIVA, *Aspetti e durabilità degli intonaci “marmorino” veneziani*, in “*Restauro e Città*”, n° 3/4, 1986, pp. 117–126.

¹⁰ Some construction documents explicitly refer to this imitative purpose: see, for instance, the XVII century work specification of the Scuola di San Giorgio dei Greci to far di diverse case (build several houses), according to the project by Baldassarre Longhena: “Far tutti li soffitti di dette scale et patti questi inerazzatti di terazo roso et poi slissati di bianco con le sue fase atorno, cioè de arte suo et questi li sarà misuratti et ridotti a passo quadro (...) stabelliti il tutto ponto et fase finte di pietra viva”¹⁰. (Archives of the Hellenic Institute of Byzantine and Post-Byzantine Studies, Venezia, reg. 55, cc.



Fig. 2 - Venice, Castello, Palazzo Cavanis. Detail of the band window post.

There are more than a few examples of whole facades realised with this method, including the plaster that still exists on the sides of the Gesuati Church at the Zattere (Fig. 3), where the whole panels, fascias, bands and bull edged mouldings show a remarkable variety of degrees of beating and dressing.



Fig. 3 - Venice, Dorsoduro, Gesuati Church. Detail of the band and the panels.

101-2, 1658, 13 July (Published G. CRISTINELLI, Baldassarre Longhena architetto del '600 a Venezia, Venezia 1978, p.169).

Part of these plasters, however, such as the white ones that were worked over until a perfect polish was obtained and then subjected to the final oil or wax finish, seems to have been obtained using a filler constituted not by stone fragments, but by *cocciopesto*, even though, often, a fraction of such mixtures was constituted by rare shards of *pietra d'Istria* (Fig. 4).



Fig. 4 – Venice, Cannaregio, Palace in *fondamenta della Senza*.

Although less frequent than the white ones, these reddish *terrazzos*, sometimes, quite intensely so, are probably to be considered as a tribute to tradition, as they originated from a wish to reproduce the colours that had dominated in the city since the end of the XV century and due to the almost ubiquitous presence of the *regalzieri*, plasters applied with a *fresco* technique that reproduce the colour and look of a wall curtain¹¹.

The colour intensity of *cocciopesto marmorinos* is due to the application, in the final phases of work, of paint strata with a red ochre base. These colours were applied with a *fresco* technique or, more often, easily fixed through the use of oleoresin binders, as can be inferred from a drawing contained in Giovanni Antonio Rusconi's treatise¹² (Fig. 5), rather than from the text attached thereto, that fails to describe the technique: "la seguente figura (...) ci mostra il modo del dare il minio sottilmente alle pareti con la vernice, come s'usa spetialmente in

¹¹ Fondamenta dei Frari, S. Polo 2557-2560.

¹² G. A. RUSCONI, *Della Architettura*, Venezia 1590, VII, p. 111.

Venetia, la qual cosa essendo comunissima, et chiara nel disegno, non ricerca maggior dichiarazione”(the following picture (...) shows how to apply red lead to the walls in a thin layer, together with paint, as is the use, especially in Venice, a procedure that is so widespread and clear in the picture that it does not require any further explanation)¹³.

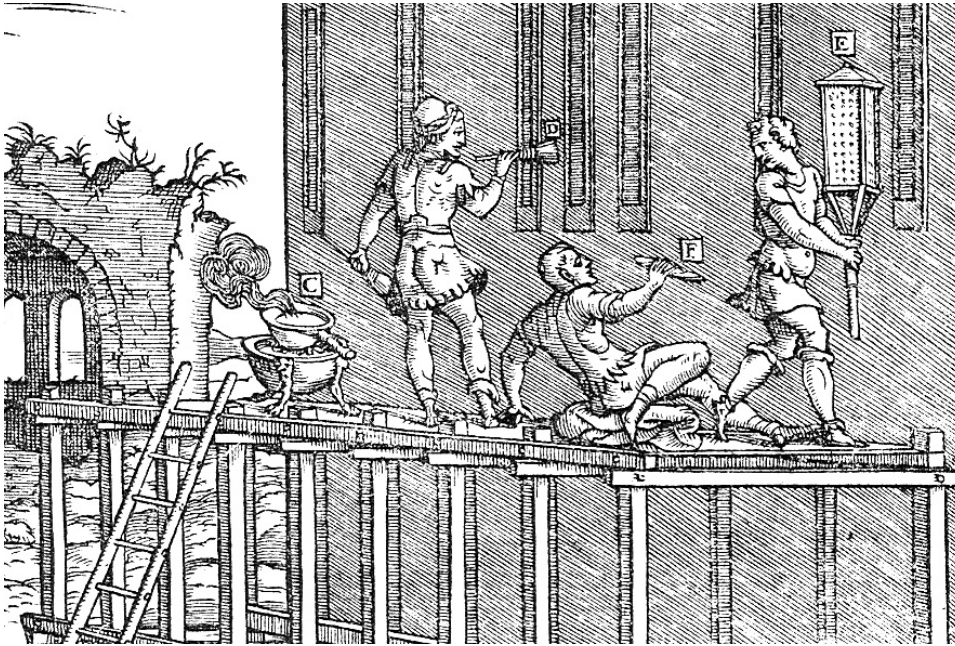


Fig. 5 – Drawing from Rusconi, *Della Architettura*, Venezia 1590.

The xylograph shows three masters working on a scaffolding: the first one is applying colour with a brush dipped in a container set on a brazier, the second one is rubbing the surface of the face with a rag, the third one is holding a lamp, apparently right against the plastered face, maybe to heat it. This image, it must be remembered, was meant to illustrate an edition of the Vitruvian treatise, in particular, a passage of charter nine of Tome Seven¹⁴, but, given that it had

¹³ *Idem*, p. 110.

¹⁴ “At si qui subtilior fuerit et voluerit expolitionem miniaceam suum colorem retinere, cum paries expolitus et aridus fuerit, ceram punicam igni liquefactam paulo oleo temperatam saeta inducat, deinde postea carbonibus in ferreo vase compositis eam ceram a proximo cum pariete calfaciundo sudare cogat, itaque ut peraequetur, deinde tunc candela linteisque puris subigat, uti signa marmorea nuda curantur. Haec autem γανωσις graece dicitur. Ita obstans cerae punicae lorica non patitur nec lunae splendorem nec solis radios lambendo eripere ex his politionibus colorem”. (“Ma chi fosse più accurato e volesse una decorazione col cinabro che conservi il colore originario, dovrà applicare con un pennello, dopo che la parete sarà stata dipinta e sarà asciutta, della cera punica liquefatta al fuoco e stemperata con un po’ d’olio. Poi, continuando, servendosi di carboni messi dentro un recipiente di ferro, porterà questa cera a trasudare assieme alla parete, riscaldandola da vicino, in modo da uguagliarne la

been composed on the basis of the technical culture Rusconi was familiar with, it seems very likely that it shows a practice that was well known in Venice in the second half of the XVI century. The heating of the colouring materials suggests the use of an oleoresin substance as binder for the pigment; high application temperatures, which would be useless and even detrimental with water-based paints, increases oil and resin fluidity, favouring their penetration. The unknown commentator of Rusconi's drawings makes references to red lead (a colouring substance artificially obtained from lead), even though it seems much more likely that the term used referred to red ochre, the only pigment that would have reasonably been used for large surfaces, given its modest cost¹⁵. Construction documents referring to the red variant of *marmorinos* are relatively late; a contract dating back to the end of the XVI century, for instance, executed between the nuns of the Saints Cosmas and Damian, at the Giudecca, and master Andrea, *murer*, of Camposampiero, for the building of four *case da statio in contrà de san Anzolo* (houses in the san Anzolo quarter), requires that "Le fazzade siano terrazade de terrazzo rosso, overo bianco, come alli procuratori sopradetti parerà, che sii ben fregado et lissado con il suo oglio de lin de sopra" (the façades be treated with red or white *terrazzo* plaster, according to the wish

superficie, infine la strofinerà con una candela e con panni di lino puliti, nello stesso modo in cui vengono trattate le statue nude di marmo. Questo procedimento si chiama in greco *gánōsis*. In questo modo il rivestimento protettivo di cera punica, facendo da ostacolo, impedisce tanto allo splendore della luna quanto ai raggi del sole di portar via a queste decorazioni, sfiorandole, il colore" – "However, if someone wished to be more accurate and wished for a decoration made with cinnabar that shall maintain its original colours, this someone shall have to apply, with a brush, some liquefied beeswax diluted with some oil. Then, to continue, using embers in an iron pail, shall bring the wax to sweat next to the wall, by warming it, so that the surface shall be uniform, finally the wall shall be rubbed with a candle and clean linen rags, like it is done with marble statues. This procedure is called *gánōsis* in Greek. In this way the beeswax protective coating acts as an obstacle to the moon's and sun's rays so that the colours shall remain intact"). M. VITRUVIUS, *De Architectura*, VII, 9, 3-4. The Italian translation was extracted from the critical edition edited by Pierre GROS, Torino 1997.

¹⁵ The term *minum* is used by Vitruvius (VII, 8, 1) to define cinnabar (mercuric oxide), whereas for red ochre the word he uses is *sil*: "Colores vero alii sunt qui per se certis locis procreantur et inde fonditur, nonnulli ex aliis rebus tractationibus aut mixtionibus temperaturis compositi perficiuntur, uti praestent eandem in operibus utilitatem. Primum autem exponemus quae per se nascentia fodiuntur, uti sil quod graece *ωχρα* dicitur" M. VITRUVIO, *De architectura*, VII, 7, 1 "Quanto ai colori (...) tratterò innanzitutto di quelli che si estraggono allo strato naturale, come il *sil*, detto in greco *ōchra*" ("As for colours (...), I shall speak first of all of those that are extracted in their natural state, such as *sil*, or *ōchra* in Greek").

of the workers, well rubbed and polished with a coating of linseed oil)¹⁶.

The use of *marmorinos* with a reddish base can be found on some constructions, however, already in the mid-XVI century, in important buildings such as the San Giorgio Maggiore Palladian Refectory and Church, where, on the right side, which was spared the XX century renovations, the red *terrazzo* faces are modulated by the pilaster shafts and by white *terrazzo* bands, as well as by an intense red colour applied to the polished bricks connected to the architrave. In many later constructions, too, the *cocciopesto terrazzo* is often associated with whitish bands and parts, the latter meant to suggest a partial use of stone in the architectural elements (Fig. 6).



Fig. 6 – Venice, S. Croce, Bell tower of S. Zan Degolà's Church.

¹⁶ ASVe, Monastero di santi Cosma e Damiano, b. 6, file. 506, 1585, 5 December, contract between the nuns of the Saints Cosmas and Damian, at the Giudecca, and master Andrea, *murer*, of Camposampiero, for the building of four *case da statio in contrà de san Anzolo* (houses in the san Anzolo quarter). Published by G. GIANIGHIAN, *Appunti per una storia del cantiere a Venezia (secoli XVI-XVIII)*, in G. CANIATO, M. DAL BORGIO, *Le arti edili a Venezia*, Roma 1990, pp. 249-50.

External coloured *marmorinos* are much rarer, and are usually associated with vegetable black and confined to the stringcourses or contour bands, like those found in the three left panels of Campiello di San Giovanni Evangelista (even though they date back to a XVII century renovation), that were built in clear imitation of the grey-cerulean blue bardiglio marble set in the central marble sept, while variations in matching tones of white appear more frequent and are used, almost always, to highlight the stringboards, edge hewn stones or the contours of openings (Fig. 7).



Fig. 7 – Venice, S. Croce, *Campiello* S. Giovanni Evangelista.

4 Technical variables in the execution of marmorinos

Marmorinos, since their appearance in the first decades of the XVII century, are invariably realised in a single layer, directly applied on the structural tile face. Starting from the XVII century, on the contrary, the *terrazzo* is applied only after laying a preparatory *cocciopesto* layer: this is a constant, that shall continue to the present era (Fig. 8).

The first known document referring to this double layer dates back to 1658, and directs to “Far tutti li soffitti di dette scale et patti questi inerazzati di terazo roso et poi slissati di bianco con le sue fase atorno, cioè de arte suo (...) stabelliti il tutto ponto et fase finte di pietra viva”¹⁷.

¹⁷ Archives of the Hellenic Institute of Byzantine and Post-Byzantine Studies, Venezia, reg. 55, cc. 101-2, Work specifications of Scuola di San Giorgio dei Greci to “far di diverse case” (build several houses) according to a project by Baldassarre Longhena, 1658, 13 July. Published by G. CRISTINELLI, *Baldassarre Longhena architetto del '600 a Venezia*, Venezia 1978, p.169.



Fig. 8 – Venice, S. Croce, Scuola of the S. Giovanni Evangelista.

The reason of this technical evolution is almost certainly the general drop in the quality of walls in the lagoon's construction after the XVI century. *Marmorino*, more than any other kind of plaster, must be laid in a layer of even thickness, otherwise the polishing process can be severely hindered, to the point of becoming impossible. Indeed, if the thickness is uneven, mortar's setting speed, which is directly proportional to the layer's thickness, would lead to an alternation of plaster areas with different thickness, some already set, some others still in the plastic phase, and this would obstruct the even sliding of the *ferro*, thus voiding the setting action. As long as wall surfaces resulted strongly coplanar, made of structural tiles laid in perfect alignment, *marmorinos* continued to be applied and worked in a single layer ; when the structural tile surfaces resulted less homogeneous, evening out the irregularities was carried out through the application of the *cocciopesto* substrate, that could therefore receive the even thickness of the subsequent finish.

There are three main factors characterising *marmorinos*: the use of artificially produced fillers, the execution, accurate and time-consuming, and the final treatments with linseed oil or soap and wax.

4.1 The artificial fillers

Differently from any other plaster used in the lagoon's area, the inert of *marmorinos*, that combines with lime, is not constituted of sands, but of stone fragments (or *cotto*, in the case of red ones), crushed in a mortar and sifted (Fig. 9).



Fig. 9 – Venice, detail of stone fragments.

It is possible that the unknown skilled workers of the Veneto who first used artificially produced inerts were influenced – indirectly, rather than directly – by the Vitruvian text that prescribes the use of marble powder in plasters' final layers: “Il marmo non si trova dappertutto della stessa qualità: in alcune zone ne esistono blocchi che contengono blocchi che pestati e macinati si rivelano utili nelle lavorazioni. Ma dove non si trovano questi blocchi si pestano e si macinano i rottami di marmo o, come vengono chiamate, le schegge che i marmisti lasciano cadere durante il loro lavoro, e dopo averle passate al setaccio si adoperano nei lavori a stucco” (Marble is not found everywhere with the same quality: in some areas there are block of it which, when crushed and round, are useful for several proceedings. However, where such blocks are not found, marble debris, or the shards that marble workers let fall during their work, as they are called, are crushed and round instead and the results, after being sieved, are used for plaster works)¹⁸. The considerable quantity of waste

¹⁸ “Marmor non eodem genere omnibus regionibus procreatur, sed quibusdam locis glaebae ut salis micas perlucidas habentes nascuntur, quae contusae et molitae praestant operibus deiciunt, contunduntur et moluntur, et cum est subcretum in operibus utuntur”. M. VITRUVIUS, *De Architectura*, VII, 6, 1. The translations are drawn from the critical edition edited by Pierre GROS, Torino 1997.

produced in the working of Istrian limestone would therefore be collected and recycled for the production of *marmorinos*, as well as for the *terrazzo* floors: the identity of the material was a guarantee of a good reproduction of the stone look.

There are also instances, although rare in the city, of inerts different from *pietra d'Istria*. On the right side of Ca' Vendramin Calergi, for instance, there are still two wide areas where the preserved original plaster was realised with fillers rich in macrocrystalline marble clasts: the same lithotype, Carrara statuary, present in the encrustation on the prospect facing the Canal Grande¹⁹. In addition, *marmorinos* realised on the mainland evidence fillers obtained from the fragmentation of the local stones used for the construction process: the *Nanto* in the Padua area, white stone in Vicenza, the *biancone* in the Verona area, etc.. Some sources mention also other substances that might be used in the *marmorino* mixes. In the "Della pratica delle malte" chapter (The practice of mortars) of his treatise on architecture, Paduan Gioseffe Viola Zannini mentions the "smaltature di calcina bianca di lucido splendore, dentro alla quale in cambio di arena si pone granzolo di vetro, qual si compra a murano, et in altri luoghi dove è la maccina da farlo" (white lime enamels, brightly polished, in which glass fragments are used instead of sand, bought in Murano or in other places equipped with the appropriate machines)²⁰, or "la scolatura del ferro, che sono gocce, che cascano nel fuoco a modo di liquida cera, mentre il ferro bolle, le quali ammassate insieme si convertono in pietra, che marogna si chiama; et questa minutamente pesta a modo di terrazzo, et mescolata con la calce fa la smaltatura molto forte, et dura" (iron refuse, that is to say, molten iron drops that fall into the fire, like liquid wax, while iron boils, which, accumulating together, transform into a stone called *marogna*; this stone, finely ground like *terrazzo*, and mixed with lime, makes the enamel very strong and hard)²¹. Glass fragments (the *granzolo di vetro*) that should increase layer resistance and silicate fillers (the *marogna*) that, combining with lime, can confer some hydraulicity to the binding agent. As far as we know, these materials seem not to have ever been used in the Lagoon. On this theme, it must be remembered that in Venice hydraulic or semi-hydraulic limes had never been used, at least, not in outdoor *marmorinos*, even though a new, slightly hydraulic binding agent had been available since the second half of the XV century: this was the so-called *calce padovana*, also known as *calce negra* or *brovada*, that was obtained by cooking marly stones extracted from the Euganean Hills, which, in the city, was used only in city walls²².

¹⁹

²⁰ G. VIOLA ZANNINI, *Della Architettura, libri due*, Padova 1629, I, VXi, p. 94.

²¹ *Idem*, p. 96.

²² With regard to the sporadic use of Padua lime in the preparation of bases for internal

4.2 The process

The realisation of this kind of plaster requires quite long and tiring procedures. The extremely long processing of the mix was the secret of the decisive characteristics of the *marmorino* layer.

Its application was preceded by abundant soaking of the faces, necessary in order to slow the setting of the binding agent as much as possible: the imbibition to the point of overflow of the structural tiles prevented the dryness of the walls underneath to subtract water from the mix, thus prolonging the formability of the plaster. The continuous application of mortar implied a settling of clasts, which were characterised by high dimensional variability (from some tenths of millimetre to several millimetres) that gradually got nearer to each other, thus leading to the optimal compaction of the layer. Together with the reduction volume of the mortar due to water evaporation, this process reduced the formation of shrinkage cracks significantly, increasing plaster resistance to weathering. Moreover, the settling of the filler's grains, obtained by repeated application of the *ferro*, a small trowel with a thick and slightly convex blade, compelled the water in the mix (the so-called *pacciarina*) to migrate outside. The liquid transported hydraulic lime in solution and enriched the plaster surface with binding agent; the plaster surface then hardened, thus making its "skin" more resistant to weathering. It must also be remembered that a fraction of the inert, in the instance of fillers obtained from *pietra d'Istria*, was constituted by slivers that, while being extremely thin, might be even a centimetre wide²³. Thanks to the compacting action of the *ferro*, these slivers, previously random, oriented themselves practically parallel to the wall surface, overlapping one another and strengthening the layer significantly. The slivers, always present in the more ancient *marmorinos*, tend to disappear in the XVIII century. Generally speaking, with the passing of time the dimensions of clasts in the filler was constantly reduced, until, in the XIX century, we have works realised with fine

plasters, we know of only one case: "Far tutte le smaltadure di drento via in tutte le stanze tagliando le sue malte alle pietre vive, come si fava ancho nelle sopradette terazadure et queste smaltadure bugando benissimo li muri et poi smaltatte di dui mano di malta una di sotto negra et poi di sopra slisatta di calcina bianca et dandoli sopra di penello et questa benissimo avalitta" (Archives of the Hellenic Institute of Byzantine and Post-Byzantine Studies, Venezia, reg.55, cc. 101-2, Work specifications of Scuola di San Giorgio dei Greci to "far di diverse case" (build several houses) according to a project by Baldassarre Longhena, 1658, 13 July. Published by G. CRISTINELLI, *Baldassarre Longhena architetto del '600 a Venezia*, Venezia 1978, p.169.

²³ A characteristic of *pietra d'Istria* is that it breaks into slivers if hit; other lithic materials used in the area of the Veneto disaggregate by producing spheroid clasts, with more or less sharp faces. The latter, therefore, during the compacting of plaster, can get nearer to each other, but not overlap each other.

granulometry and uniform sorting inerts.

4.3 The final finish

The treatments applied to these plasters in the last phases of their laying process constitute another one of the peculiarities that characterise *marmorinos*. There were two basic finishes, either on a linseed oil base or a soap and was base.

There were several reasons for this treatment. The final finishes had a fundamental task, aesthetic in nature: with these treatments the plastered surfaces lost their chalky, dull and opaque look and, thanks to the different refraction, acquired a “wet”, partially translucent and almost horny, thus better to assume the consistency and aspect of *pietra d'Istria*. Moreover, the included substances, by hindering the absorption of rain water without at the same time reducing the permeability in any significant way, developed a clear protective action, making the plaster better resistant to weathering in a particularly aggressive environment, such as the one of the Lagoon. Another important aspect is also the increased cementation of the layer induced by such organic substances. Oils, in particular, can chemically interact with the binding agent, favouring its slow, but sure transformation in oxalates, the most stable and resistant crystalline forms that calcium can acquire²⁴. Finally, it must be remembered, always with regard to the application of both raw and cooked linseed oil, that glycerine, being one of the few substances that is soluble both in water and oil, improved the absorption capacity of marmorino, that still had a considerable percentage of humidity at the moment of its laying.

Imbibition of surfaces with oil obtained from linseed is an extinct practice in this period, unknown to the last marmorino artists still working in the city²⁵, but the treatment is recorded in some XVI-XVII century construction documents. At the end of 1585, for instance, a contract executed between the nuns of the Saints Cosmas and Damian, at the Giudecca, and master Andrea, *murer*, of Camposampiero, for the building of four “case da statio in contrà de san Anzolo” (houses in the san Anzolo quarter), requires that the *terrazzo* “sii ben fregado st lissado con il suo oglio de lin de sopra” (shall be well polished and treated with linseed oil)²⁶. In the mid-XVII century, the work specifications by the Scuola

²⁴ The two possible forms of calcium oxalate are Wewellite and Wedellite, calcium monohydroxide and calcium dihydroxide, respectively.

²⁵ Actually, the linseed oil treatment has been successfully revived for some decades now, in some *marmorino* restoration works starting from the integrations dating from the second half of the Eighties at Palazzo Grimani, in Santa Maria Formosa.

²⁶ ASVe, Monastero di santi Cosma e Damiano, b. 6, file. 506, 1585, 5 December, contract between the nuns of the Saints Cosmas and Damian, at the Giudecca, and master Andrea, *murer*, of Camposampiero, for the building of four *case da statio in*

di San Giorgio dei Greci to “far di diverse case” (build several houses) according to a project by Baldassarre Longhena, requires “far tutte terazzature di fora via di detta fabrica (...) et dandoli poi il suo oglio de lino. (...) Far li camini dalli copi in suso (...) et questi smaltatti cioè interazzatti (...) dandoli il suo oglio de lino stabelliti di tutto ponto” (treat all the external walls of the construction with *terrazzo* plaster (...), then treated with linseed oil (...). To build the chimneys, from the roof upwards, and enamel them, that is, apply *terrazzo* plaster and apply linseed oil)²⁷. Again, the practice seems still known in the mid-XVIII century: in 1734 the facade of the Scuola della Carità was covered with “terrazzo da Rovigno fregato in buona forma (...) con anco il suo oglio di lino per difenderla dalla tramontana” (with Rovinj terrazzo, well polished (...) with its linseed oil treatment, to protect it from the north wind)²⁸. The application had to be carried out once the polishing phase had been completed, presumably some time after completion of the layer, as the presence in the fresh plaster of considerable quantities of water was an obstacle to the penetration of the oily substance. It is also possible that the oil was diluted with *rasa* (turpentine), in order to make it more fluid and favour better absorption; it is equally likely that the surfaces would be “dusted” with rags, some hour after the oil application, to redistribute the oil and remove it from accumulation areas, in order to avoid the formation of undesirable films, as it used to be done for *terrazzo* floors.

An alternative to the practice, common in Venice in the XVI and XVII centuries, that entailed the use, in the final phase, of cooked linseed oil²⁹, marmorino treatment with “damaschino” soap (better known to us as Marseilles soap) and beeswax is well described in the first years of the XVII century by Paduan Gioseffo Viola Zannini: “et detta smaltatura deve esser benissimo lisciata con la cazzola, fino à tanto che s’indurisca poi si piglia sapon da maschino, et distemperasi nell’acqua à modo di liquido bianco; per imbiancare i muri, et con quello si vadi con il pennello spianzando la smaltadura: un poco per volta, et così spianzata di fresco si vadi con la cazzola lisciando con diligentia; et quando tutta sarà lisciata la si lasci impassire, et poi piglisi un panno di lino, et

contrà de san Anzolo (houses in the san Anzolo quarter). Published by G. GIANIGHIAN, *Appunti per una storia del cantiere a Venezia (secoli XVI-XVIII)*, in G. CANIATO, M. DAL BORGO, *Le arti edili a Venezia*, Roma 1990, pp. 249-50.

²⁷ Archives of the Hellenic Institute of Byzantine and Post-Byzantine Studies, Venezia, reg. 55, cc. 101-2, 1658, 13 July. Published by G. CRISTINELLI, *Baldassarre Longhena architetto del '600 a Venezia*, Venezia 1978, p.169.

²⁸ Quoted from P. MODESTI, *Le trasformazioni storico-costruttive del complesso della Carità*, in *Progettare un museo. Le nuove gallerie dell’Accademia a Venezia*, Milano 2005 (pp. 20-69) p. 23.

²⁹ There are no known documents or construction documents from the XVI-XVII century relating to lagoon’s construction that prescribe treatment with soap and wax.

freghesi benissimo, poi piglisi cera di formelle, et con quella in cambio di cazzola si vadi benissimo con diligentia per tutto lisciando, et poi fregghisi un'altra volta con panno di lino” (such enamelling shall be well smoothed with the trowel, until it hardens, then Marseilles soap must be dissolved in water, until a whit liquid is obtained; the liquid shall then be splashed with a brush over the enamel, slowly and, passing the trowel over it; once the liquid has been completely spread, it shall be left to dry and afterwards, with a linen rag, it shall be well polished; then wax blocks shall be passed on the surface, and, once the whole surface has been treated, it shall be polished again with a linen rag)³⁰. This latter operation has also the goal of obtaining a perfectly polished surface, “la qual nelle colonne le fa come di marmo, maggiormente se venate con colori, l'esempio delle quali ho veduto nelle colonne della rotonda appresso Vicenza, che da molti sono tenute per marmo” (which, if applied to columns, makes them look like marble, all the more so if they have coloured veneers, such as the columns of the rotunda near Vicenza, which are though by many to be marble)³¹.

References

- VITRUVIO M. *De Architectura*, VII, 9. Le traduzioni sono tratte dall'edizione critica curata da Pierre GROS, Torino 1997.
- VASARI G. *Le Vite*, cap. I “Dell'Architettura”. Edizione moderna a cura di C. Ragghianti, Milano 1971.
- COPPO P. (1540) *Del sito de listria*, Venezia.
- SANSOVINO F. (1581) *Venetia, città nobilissima e singolare*, Venezia.
- RUSCONI G. A. (1590) *Della Architettura*, Venezia.
- SCAMOZZI V. (1615) *L'idea dell'Architettura Universale*, Venezia.
- VIOLA ZANNINI G. (1629) *Della Architettura, libri due*, Padova.
- CORNARO A. *Scritti sull'architettura*, (a cura di) P. CARPEGGIANI, Padova 1980.
- PAOLETTI P. (1893) *L'architettura e la scultura del Rinascimento in Venezia: Ricerche storico-artistiche. Parte I (periodo di transizione)* Venezia .
- VIO G. (1977) *I “mistri” della chiesa di S. Fantin in Venezia*, in *Arte Veneta*, 31, p. 225.
- CRISTINELLI G. (1978) *Baldassarre Longhena architetto del '600 a Venezia*, Venezia.

³⁰ Viola Zanini, *Della Architettura, libri due*, Padova 1629, I, XVI, p. 94.

³¹ Ibidem.

BISCONTI G. – PIANA M. – RIVA G. (1982) *Research on Limes and Intonaco of the historical Venetian Architecture*, in *Mortars, Cements and Grouts used in the Conservation of Historic Buildings*, atti del Symposium ICCROM, Roma, p. 359–371.

ARMANI E. - PIANA M. (1984) *Primo inventario degli intonaci e delle decorazioni esterne dell'architettura veneziana; indagine e classificazione degli intonaci colorati di una città che fu policroma*, in "Ricerche di Storia dell'Arte", 24, p. 44-54.

PIANA M. (1984) *Una esperienza di restauro sugli intonaci veneziani*, in: "Bollettino d'Arte", Ministero per i Beni Culturali e Ambientali, 6, p. 103-106.

ARMANI E. - PIANA M. (1985) *Le superfici esterne dell'architettura veneziana, in Facciate dipinte, conservazione e restauro* (a cura di G. ROTONDI TERMINIELLO) atti del convegno, Genova, p. 75-78, figg. 101-103.

CHAROLA A. - LAURENZI TABASSO M. - LAZZARINI L. (1985) *Caratteristiche chimico-petrografiche di intonaci veneziani del XIV-XX secolo*, in: "L'intonaco: storia, cultura e tecnologia", atti del Convegno di Bressanone, Padova, p. 211-21.

BISCONTIN G. – PIANA M. – RIVA G. (1986) *Aspetti e durabilità degli intonaci "marmorino" veneziani*, in *Restauro e Città*, 3/4, p. 117–126.

PIANA M. (1988) *Convento di S. Salvador; gli intonaci del secondo chiostro*, in: "Il colore della città", atti del convegno, Roma, p.135-139.

PIANA M. (1988) *Edificio tardo cinquecentesco al Ponte di Rialto: gli intonaci esterni*, in: "Il colore della città", atti del convegno, Roma, p.140-145

PIANA M. (1989) *Tecniche edificatorie cinquecentesche: tradizione e novità in Laguna*, in *D'une ville à l'autre: structures matérielles et organisation de l'espace dans les villes européennes (XIII-XVI siècle)*, atti del convegno école Française de Rome, Roma, p. 639.

GIANIGHIAN G. (1990) *Appunti per una storia del cantiere a Venezia (secoli XVI-XVIII)*, in CANIATO G. - DAL BORGIO M. *Le arti edili a Venezia*, Roma, p. 244-45.

ROSSI MANARESI R. (1992) *Intonaci e stucchi in area padana*, in: "Bollettino d'Arte del M.B.C.A.", 73, VI, p. 133-46.

DANZI E - PIANA M. (2002) *The Catalogue of the External Plasters in Venetian Building*, in "Scientific research and safeguarding of Venice". Corila, Venezia, 87-95.

FERRIGHI A. (2002) *The Plasters Data Base*, in "Scientific research and safeguarding of Venice". Corila, Venezia, p. 97-108.

MODESTI P. (2005) *Le trasformazioni storico-costruttive del complesso della Carità*, in *Progettare un museo. Le nuove gallerie dell'Accademia a Venezia*, Milano.

THE MAINTENANCE OF THE URBAN FABRIC IN VENICE IN THE MODERN ERA: GIS AND ARCHIVAL SOURCES

Giulia Vertecchi

Dipartimento di Storia dell'Architettura, IUAV

Riassunto

Obiettivo della ricerca è quello di individuare le procedure di manutenzione urbana e le strategie di intervento per la difesa dalle acque alte nell'età della Repubblica. Lo studio mette in luce la metodologia e il percorso di ricerca adottati per rendere le informazioni archivistiche fruibili dal sistema GIS. La complessità del dato 'documento d'archivio' ha comportato che una gran parte del lavoro fosse dedicata alla selezione e all'organizzazione dei dati. Il sistema elaborato consente di analizzare aspetti legati alla distribuzione spaziale dei dati d'archivio offrendo la possibilità di studiare la città e le sue trasformazioni.

Abstract

The goal of this research is the identification of the urban maintenance works and intervention strategies for the protection of the city's buildings from the waters in the Age of the Republic. This study highlights the methods and research areas that were adopted in order to make the archival information available for use with the GIS system. The complexity of the "archival document" data entailed dedicating a relevant part of the work to data selection and organisation. The resulting system makes it possible to analyse characteristics linked to the spatial distribution of archival data, and thus gives the opportunity to study the city and its transformations.

1 Introduction

The historical research, co-ordinated by Ms Donatella Calabi required considerable organisation. In its first phase, the research involved the systematic examination of the archival collections of the three Venetian offices entrusted with the control of the urban area and of the lagoon's status, namely, the *Savi ed Esecutori alle Acque*, the *Giudici del Piovego* and the *Provveditori di Comun*. Further, the research examined the collection of the Senate, the highest government body, in order to carry out a thorough analysis of the historical framework.

Duties, judicial and operating tasks and responsibilities of each of the people working in the office of the *Provveditori di Comun* were analysed (by Stefano Zaggia) in the long term, together with the more evident transformation phases [Crouzet-Pavan, 1992; Gasparini, 1993; Crouzet-Pavan 1996]. The *Provveditori di Comun*, as judges, had the task of defining disputes of a mercantile nature or concerning the management of the charity schools, but also of deciding and

ordering concrete protection and maintenance interventions regarding the urban fabric. The intervention forms of the magistrates remained unchanged in the 16th and 17th centuries, but underwent considerable changes during the 18th century, when the ordinary and extraordinary maintenance activities regarding the urban structures (building of bridges, street maintenance and paving, excavation of *rii* and wells) started being organised through preventive plans divided by *sestiere* and entrusted to the execution of private concerns [Zaggia, 2004].

The analysis (carried out by Silvia Moretti and Giulia Vertecchi) of a series of licences issued by the *Giudici del Piovego* with regard to the addition of one floor to existing buildings or the addition of a chimney, the enlargement of a riva (bank) or the restoration of a front evidences how, with time, tasks of a judicial nature and tasks concerned with the protection against usurpation by private subjects (families or religious orders) and with the promotion of urban development and the supervision of reclamation works came to be added to the original tasks of conservation of public waters and of internal land and sea links [Calabi, 2003; Moretti 2004]. The Piovego magistrate office records, especially around the end of the 18th century, all the changes taking place in the houses of the nobility and, more slowly, in the secondary building industry, such as the elimination of the more evident asymmetries, the frequent increases in the height of buildings without following any standard rules, the opening of doors, windows, external staircases, balconies and small terraces, sometimes “squared” and linear, chimneys, roof-terraces, water sewage systems [Cavazzana Romanelli, 1986].

The analysis of the collection of the *Savi ed Esecutori alle Acque* (by Elena Svalduz), highlighted the two directions in which the intervention policy of the magistrate was developed: on the one hand, there are the great “plans” for the city, the wide-ranging interventions, on the other hand there are the detailed works [Gasparini, 1993]. Among the wide-ranging interventions are the building of the new Zattere fondamenta (started in 1520) and of the Fondamenta Nuove (started in the last decade of the 16th century), two great works that define the southern and northern outline of the city, respectively. As far as the detailed, more circumscribed, works are concerned, there are several examples thereof. It is indubitable, for instance, that the lack of stone banks in open spaces, such as in the vineyards around the city, and in the nearby islands was considered by the *proti* as one of the worst “enemies” of the lagoon, as it was seen as a degradation factor that would, in the end, compromise the lagoon’s very existence [Svalduz, 2004].

In order to determine to what extent it is possible to speak of Venetian specificity, Antonio Brucculeri, through a study of the *Senato Terra* collection, analysed the importance of the Arsenale di Stato in the production and exportation of techniques at the service not only of navy and ship-building, but also of the city itself. It is clear from the Brucculeri study that the circulation of skilled workers, techniques and materials, the use of devices and machines usually destined to the maintenance of waterways, to water supply and to the

practice of urban construction was in reality an experiment in subsidising, in the laying down of materials or of parts of building units, with a permeable use of “ingenia” that was capable of reciprocal influences between canal excavation, ships or mills building, swamp reclamation, fountain functioning or building maintenance of the city’s convents [Aymard, 1980; Concina 1984 e 1990].

The excavation and backfill of the *rii*, the paving of the *calli* and the *campi*, the restoration of the *fondamenta* and of wells, as well as the modifications of houses and palaces are only some examples of the slow, continuous process of urban transformation and maintenance characterising the history of the city of Venice. The archival work has led, therefore, to the collection of a considerable amount of data on the management activities of public spaces and the urban planning control activities in the city [Concina, 2001]. A computer card was created, for data collection, so that each researcher would be able to input information derived from the archival collection studied.

2 The “archival document” datum and the computer card

The archival document constitutes an extremely complex datum: it includes chronological and topographic information, information on the types of materials used, the names of owners and work principals and, sometimes, even drawings. The researchers have found themselves faced with the need to create a card which would allow them, at first, to collect the highest number of data. This is why the first database was built with a very flexible structure. This made for quicker implementation activities and, at the same time, ensured that no information would be lost; however, it also meant that the database could not be optimised for GIS.

In the second phase of the research, the work addressed the issue of data rationalisation and harmonisation, in order to make the database ready to be linked with the map. Substantially – basing the database structure on an E-R conceptual construct – the “document-entity” (containing the archival coordinates, the date and an abstract of the text of the archival document) was associated with the “topographic indication-entity” (with a 1:1 relationship) and with the “type of intervention-entity” (with a 1:N relationship).

Indeed, each archival document contains, in the great majority of cases, several types of intervention: for instance, the *Giudici del Piovego*, in their licences, could authorise, within the context of the restructuring of a front, also the elevation of the building. For this reason, in the archival data input form an ample space was dedicated to the description of the type of interventions. The issue of the localisation of a document is more complex; the choice of a 1:1 relationship between the document and the relevant topographic data entails some limitations. Indeed, all the documents showing maintenance works in a vast, difficult to identify clearly area of the city, such as, for instance, the interventions ordered by the *Provveditori di Comun* for the restoration of wells located in various areas of the city, were excluded. Not all of the documents can be used with the GIS system: if the document does not show the topographic information, but refers generically to the whole city, it is not possible

to connect it with the map. Furthermore, precedence was given to those documents which, thanks to their clear topographic information, made it possible to define an immediate connection with the geographical object present in the GIS.

3 Geo-referencing of archival documents

The main premise for the use of GIS is the localisation of the information, that is, the possibility to associate a descriptive attribute to a geographical object that describes its spatial position (geographical co-ordinates). The archival document can be represented and analysed by GIS through the topographic information in the text of the document itself. Then the document's topographic information is associated with the geographical entity on the map of Venice; geometry and the GIS levels that are necessary for the localisation correspond to the three levels built into the Geomedia program, namely, Land Area, Built Area and Rii.

In order to obtain the link between the archival documents database and the map, the documents were divided into three main categories, according to the respective reference areas with regard to the existing GIS levels; the documents of the *Savi ed Esecutori alle Acque* collection were associated to Geomedia's Rii level, the documents of the *Giudici del Piovego* to the Built Area level and, finally, the documents of the *Provveditori di Comun* to the Land Area level.

Subsequently, attention was focused on the Built Area level, because the city's building fabric is also the object of the investigation of the workgroup dealing with the plasters census: by using the same geographical objects, that is, the buildings, as common reference, it was possible to verify the consistency of the archival documents database and to start the first cross checks.

The building permits issued by the *Giudici del Piovego* in the second half of the 18th century are a good starting point for geo-referencing work, not only because, through them, it is possible to deepen the knowledge of Venetian building industry – including the one that is considered minor – but also because, as they are concentrated in the last period of the Republic, they are easier to find. Indeed, there is a reliable correspondence between the archival data of the late 18th Century and present day cartography, while the documents that date back to a much earlier period create some difficulties, because of the transformations that have occurred in the city.



Fig. 1 – .Georeferenced archival documents

The geo-referencing work often requires an accurate text analysis and some surveys, as the topographic indications of a certain building are often insufficient in order to identify it: for instance, if a text said that the building was located in the “fondamenta e calle dette de’ Sartori in contrada di SS. Apostoli” (ASVe, *Giudici del Piovego*, b. 16, c. 72), it would be necessary, in order to create a GIS link, to identify precisely what building is referred to.



Fig. 2 – Identified building in the fondamenta de’ Sartori

Once the building has been identified, there is the problem of the repetition of some Venetian toponyms (e.g., “del Forno”, “della Malvasia”, etc.), that has to be solved in order to be able to associate the document with the correct GIS localisation. Then, it is necessary to extract the aggregated GIS map toponyms and to modify the database data input form, so that if the “sestiere San Marco” string is chosen, only the islands included in said “sestiere San Marco” can be

chosen; similarly, once the island has been identified, it must be possible to choose only among all the *calli*, *campi* and *corti* that belong to that island. The process continues in this way until it is possible to identify the code of the building, which, in turn, makes it possible to create the link with the map.

4 Problem issues and research development hypotheses

The organisation of the archival documentation database and the georeferencing of some of them opened new prospects for research and analysis. Historical and archival data are a great resource, not only for a study of the city, but also for the management and valorisation of its architectural heritage. On the other hand, the creation of the database of urban maintenance documents in the Age of the Republic has evidenced the city's continuous physical transformations [Concina, 2001]. However, in order to be able to benefit fully from the archival information within the GIS system, it is necessary to tackle two problem issues: the first one concerns the localisation of the document and the second, which is directly connected to the first one, concerns the possibility of representing said document in geographical terms.

As of today, the reference cartographical support, representing the city as it is today, does not offer the possibility of localising, and, therefore analysing from the spatial point of view, part of the documents; indeed, there are instances in which the historical toponym does not coincide with the current one; there are also instances in which the city's structure has been altered, as against the one existing in the historical period of the document, because of demolitions, transformations, or filling ups.

The best procedure would be exploiting the potential offered by the Geographic Information System, while starting to work on historical maps, so that several different maps of the city could be superimposed. This solution, successful in other Italian and European cities, would allow historians to form a global view of the urban transformation processes, and would also provide the municipal authorities or superintendences to acquire a deeper knowledge of the building fabric [Gauthiez, 2004].

5 Conclusions

The next goal of the work is the completion of the database, with the inclusion of information on urban maintenance with regard to open spaces and *rii* (that is, protection from high tides interventions, pavings, restoration of wells, *fondamenta*, excavation of *rii*, etc.). In this way, with a map of soil structure, it shall be possible to analyse data from a spatial point of view and to know, for instance, what types of intervention were used in the past in order to deal with urban maintenance with regard to soil structure.

Thanks to the possibility of carrying out geographical searches, it shall therefore be possible to make historical information available to all GIS users. Indeed, a deeper knowledge of events and transformations concerning the urban structure leads the way to the acquisition of useful competences in terms of

maintenance and protection of the building heritage.

References

Aymard M., 1980. L'arsenale e le conoscenze tecnico-marinaresche. Le arti, in G. Araldi e M. Pastore Stocchi (a cura di), *Storia della cultura veneta: dal primo Quattrocento al Concilio di Trento*, 3//II, Vicenza, neri Pozza, pp. 289-315;

Concina E., 1984. *L'arsenale della Repubblica di Venezia*, Milano, Electa;

Cavazzana Romanelli F., 1986. Restauri a Venezia nel Settecento: le "licenze" dei Giudici del Piovego, in «*Restauro e città*», II, 3/4, pp. 34-56.

Concina E., 1990. *Navis. L'umanesimo sul mare (1470-1740)*, Torino, Einaudi.

Gasparini, S. 1993. La disciplina giuridica dei lavori pubblici a Venezia nell'età moderna. I fondi archivistici del Magistrato alle Acque e dei Provveditori di Comun. *Ricerche e ipotesi*.

Crouzet-Pavan E., 1992. «Sopra le acque salse». *Espaces, pouvoir et société à Venise à la fin du Moyen Age*, Paris.

Crouzet-Pavan E., 1996. La maturazione dello spazio urbano, in *Storia di Venezia*, V, Il Rinascimento. Società ed economia, Roma, pp. 3-100.

Concina E., 2001. Trasformazioni della struttura urbana attraverso fonti d'archivio. Analisi e restituzione grafica delle fonti fiscali descrittive per la città di Venezia, in *Estimi e Catasticazioni Descrittive, Cartografia Storica, Innovazioni Catalografiche. Metodologie di rilevamento e di elaborazione in funzione della conoscenza e dell'intervento nell'ambiente urbano*, a cura di Molteni E., Regione Veneto-Università Ca' Foscari Venezia, pp. 103-143.

Calabi D., 2003, *Trasformazioni urbane a Venezia: Santa Maria Formosa*, in "Quaderni di Insula", settembre.

Gauthiez B., 2004. Des unités pertinentes pour mesurer la ville concrète, in "Histoire et Mesure", XIX – 3/4, pp. 295-316.

Mazzi G., Zaggia S. (a cura di), 2004. "Architetto sia l'ingegniero che discorre". *Ingegneri, architetti e protti nell'età della Repubblica*, Venezia.

Moretti S., 2004. La professione di un funzionario pubblico al servizio della Dominante. Giuseppe Benoni tra Venezia e Friuli nel XVII secolo, in "Architetto sia l'ingegniero che discorre", cit.

Svalduz E., 2004. Al servizio del magistrato. I protti alle acque nel corso del primo secolo d'attività, in "Architetto sia l'ingegniero che discorre", cit.

Zaggia S., 2004. Ruoli e competenze dei "periti pubblici" in ambito veneto, in "Architetto sia l'ingegniero che discorre", cit.

Abbreviation:

ASVe = Archivio di Stato di Venezia

ANALYSIS OF THE STRUCTURAL BEHAVIOUR OF THE HISTORICAL VENETIAN BUILDINGS THROUGH THEORETICAL AND EXPERIMENTAL MODELS: STATE OF THE RESEARCH

Chiffi Donato¹, Faccio Paolo¹, Vanin Alessia¹

¹ *Dipartimento di Storia dell'Architettura, Università Iuav di Venezia*

Riassunto.

Lo studio presentato indaga sulle modifiche indotte sul funzionamento strutturale degli edifici storici veneziani dall'interazione tra acqua e struttura. Con questa finalità si sviluppano modelli previsionali analitici e numerici che consentono di analizzare l'alterazione del funzionamento strutturale in relazione al grado di danneggiamento dei singoli elementi strutturali e delle relative connessioni. Ad essi seguirà una valutazione sperimentale eseguita su prototipi costruiti in scala reale.

Abstract.

A study of the modifications of the structural functioning due to the interaction between the lagoon water and the structure of the historical Venetian buildings is presented. Forecasting numerical and analytical models that permit to analyse the alteration of the structural functioning at varying of the decay of the structural elements are developed. Moreover an experimental evaluation on some prototypes built in the real scale will be realized.

1 Introduction.

The influence of the environmental variables on the structural behaviour of the buildings is usually a not much investigated problem.

In many cases the solution with respect to the alteration of their original structure due to the decay and to the natural ageing is the substitution of some existing parts with new constructive details, that are often repetitive and that often have nothing to do with the historical and constructive reality of the building. The result of this design procedure is the levelling down and the standardization of the constructive characteristics, and widely the progressive loss of the identity of the buildings.

So a cognitive effort about the relation between the environmental variables and the behaviour of the structure is necessary. In the case of Venice this is the relation between the lagoon water and the preservation of the materials and of the structural functioning of the buildings.

The qualitative evaluation of the problems is combined with a quantitative evaluation through theoretical and analytical models.

The knowledge of the real incidence of the alteration of the structures on their

efficiency permits to define some hypothesis and technical solutions for the restoration in the draft of the conservation design.

2 Alteration of the structural functioning of the historical venetian buildings due to the interaction with the lagoon water.

It is well known that the environmental circumstances conditioned the art of building in every time. In the case of Venice the particular relation with the water influenced the building process imposing the adoption of specific technical solutions to preserve the integrity of the structures.

These solutions are briefly summarized.

The side of the foundation wall in contact with the water was covered with Istrian stone blocks to preserve the bricks below. Some continuous courses of Istrian stone blocks, called “cadene”, were arranged to create some waterproof layers to preserve the wall also from the rising damp. These courses were collocated at regular intervals in height, up to a level above the “comun marino”, that is to say up to a level above the middle sea level [Piana, 1984] (Fig. 1).

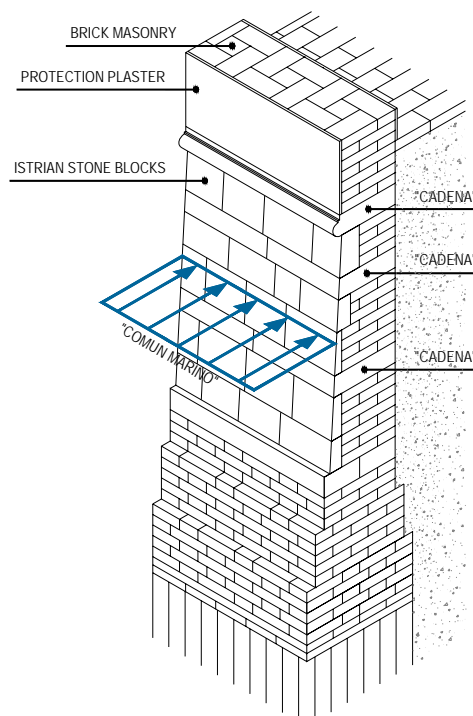


Fig. 1 – Scheme of the foundation system.

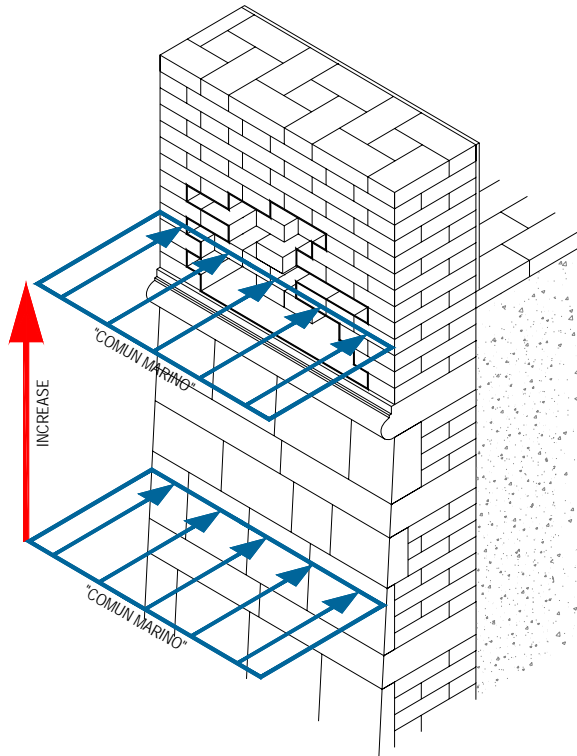


Fig. 2 – Alteration of the brick walls.

The increase of the sea level over the centuries, added to the sinking of the foundation ground, determined the inadequacy of these technical solutions.

Nowadays many historical buildings show a severe damage of their load-bearing structures. This damage, added to the natural decay of the structures due to ageing, modifies the original structural functioning, submitting the structural elements to additional or different stress with respect to which they were designed [Zuccolo, 1975].

The direct contact with the lagoon water of the brick walls causes the wash of the protection plaster, and then the wash of the bricks below.

The consequences of this phenomenon are serious: in many cases a consistent reduction of the thickness of the wall appears at the base, that is to say in the part of the buildings where the compressive stress reach the greatest value (Fig. 2). Moreover, as referred from the literature, the Venetian walls were built with a very big height to thickness ratio, in order to contain the loads transferred from the foundations to the ground, generally constituted by non-homogeneous layers of sand, silt and clay and characterized by low values of the compression strength: in this way the reduction of their thickness becomes a more relevant problem.

The absorption of the salt water causes also the alteration of the mechanical

properties of the masonry [Biscontin *et al.*, 1981; Zago *et al.*, 1981a,b].

The first part of this research – CORILA Research Programme 2000-2004 - investigated the variations of the mechanical properties of the brick, with reference to its contents of water and salts. Some samples of bricks, obtained from historical Venetian bricks, were subjected to different treatments of drying, saturation and washing in order to vary their contents of water and salts (Fig. 3). Subsequently they were crushed (Fig. 4), and a qualitative relation between the compression strength and the contents of water and salts of the brick was obtained (Fig. 5).

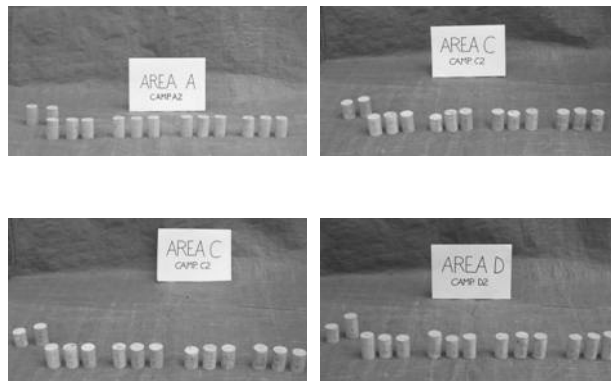


Fig. 3 – Samples involved in the tests.

Fig. 4 – Crushing test.

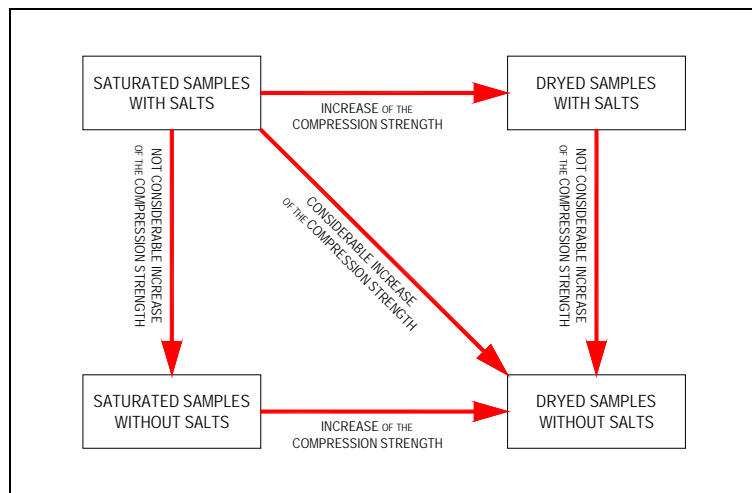


Fig. 5 – Results of the tests.

The increase of the stress and the reduction of the resistance of the wall, because of the modification of the geometrical shape and the reduction of the mechanical properties of the constitutive material cause in many cases the appearance of local crushing.

In second place the rising damp also determines a heavy damage of the horizontal structures [Zuccolo, 1975].

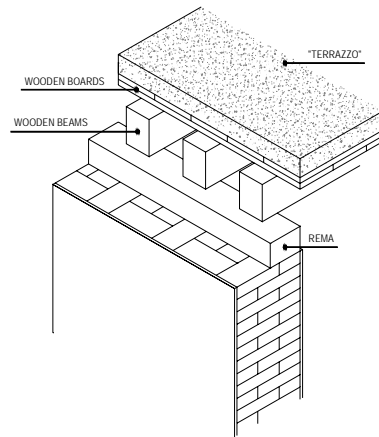


Fig. 6 – Scheme of the floor.

The floors of Venetian buildings were almost always built with wooden beams, either to contain the loads transferred from the foundations to the ground, or to avoid the transmission of horizontal actions to the walls, which is dangerous for the equilibrium (Fig. 6). For this reason also the vaulted ceiling were built with wooden beams, to which a layer of reed mat covered with plaster was connected [Piana 1984] (Fig. 7).

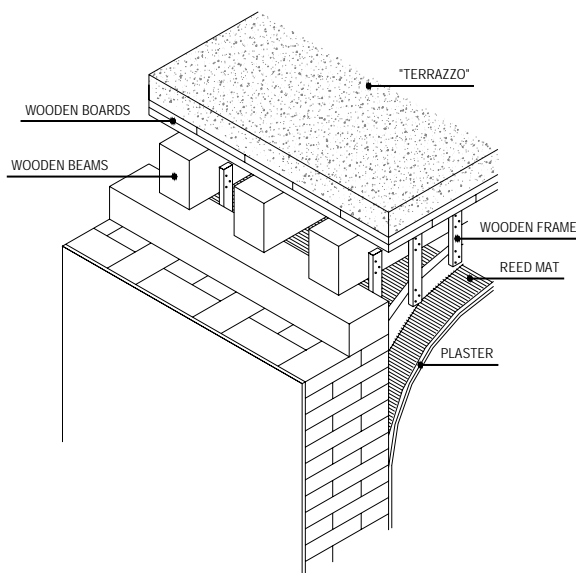


Fig. 7 – Scheme of the vaulted ceiling

The rising damp causes the decay of the part of the wooden beams that rests

on the walls. Sometimes an element called "rema" was placed below the wooden beams, in order to distribute the loads transferred to the wall and to preserve the integrity of the head of the wooden beams. Nevertheless the decay interests also this element.

The consequences of this phenomenon are the reduction of the contact area between the beams and the wall, that is to say an increase of the eccentricity of the action transferred from the beams to the wall, and therefore an increase of the stress of the masonry. On the other hand it is to note that, in a not damaged condition, the connection with the floors improves the structural behaviour of the slender walls, because it contrasts the phenomenon of instability reducing the length of their possible inflexion in consequence of the transmission of the vertical loads. The alteration of the connection between the floor and the wall prevents this collaboration. Finally in some cases the deformation of the wooden beams in consequence of their inflection determines the transmission of a horizontal component of the force to the wall, with the above described problems.

The rising damp determines also the corrosion of the tie rods, that play an important role for the structural functioning of the historical Venetian buildings (Figs. 8 and 9).

It is to note that the walls of the Venetian buildings are built without a connection with the orthogonal walls, in order to guarantee the independence of their vertical translations in front of the sinking of the ground (Fig. 10). The tie rods placed at the level of each floor prevent the overturning of the external walls, especially of the façades, that cannot benefit of the bond of the floors because of the disposition of the beams, fixed only with the criterion of the transmission of compression stress approximately homogeneous to the ground; for this reason the façade, that usually supports the roof load, is relieved of the load of the floors, supported by the lateral-walls [Piana, 2000] (Fig. 11).

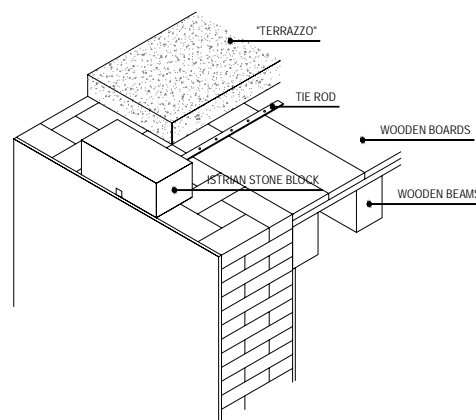


Fig. 8 – Connection between the wall and the floor.

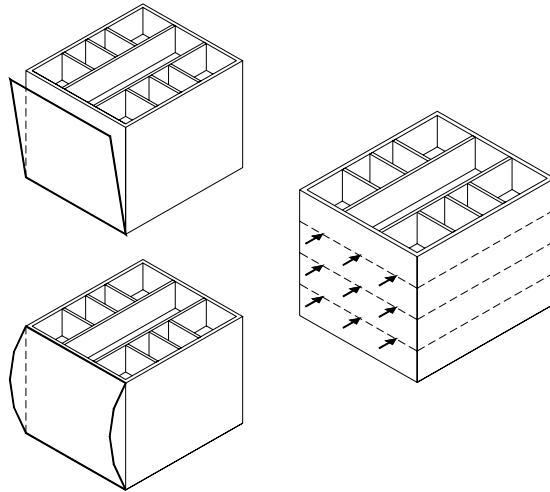


Fig. 9 – Function of the tie rods.

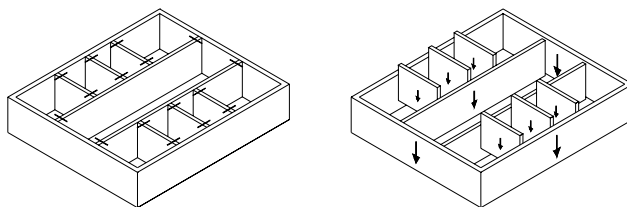


Fig. 10 – Relation among the load-bearing walls

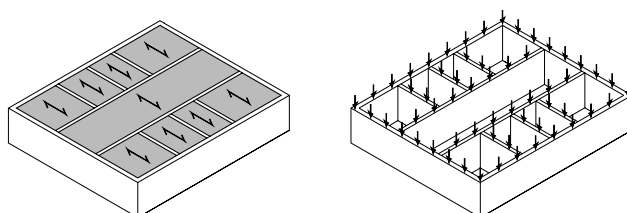


Fig. 11 – Texture of the floors and loads distribution on the walls

This second part of the research investigates the modifications of the structural functioning of the Venetian buildings, in consequence of the decay of their

structures.

3 Modelling phase: definition of the prototypes

The analysis of the modifications of the structural functioning of Venetian buildings with respect to the original one is developed through both the theoretical and the experimental approach.

A model of the system masonry walls-wooden floors –“detailed model”- is defined to this purpose (Fig. 12). Its geometrical shape was conceived so that it can be reproduced in laboratory in the real scale.

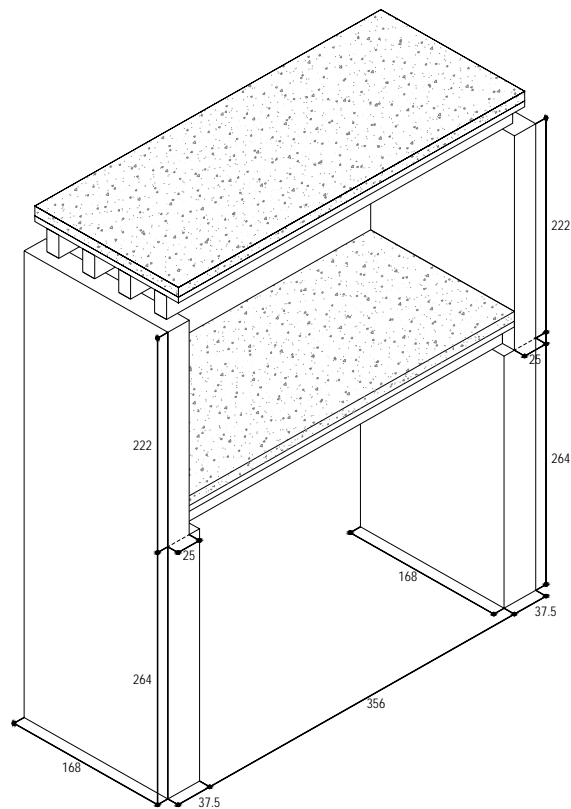


Fig. 12 – Geometrical shape of the detailed model.

The theoretical analysis results in forecasting numerical and analytical models.

The numerical model is developed through the Straus calculation code. The structural elements are represented using brick elements with 8 vertex nodes (Fig. 13).

On the base of the walls some continuous springs are collocated, in order to simulate the interaction between the ground and the structure.

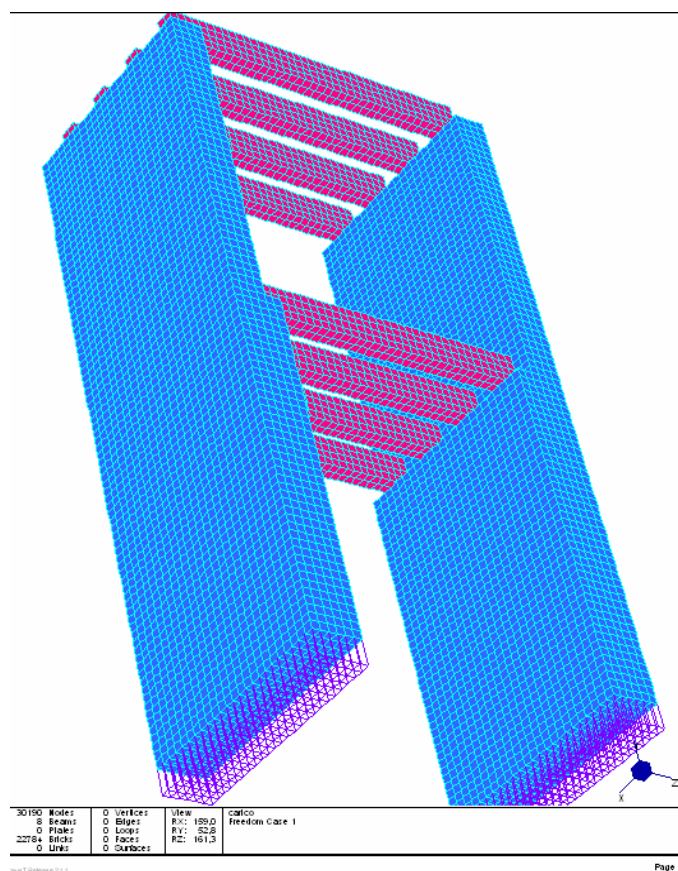


Fig. 13 – Mesh F.E.M. for the detailed model.

For the definition of the boundary conditions on the lateral sides of the walls a general model of the building –“building model”- in which the load - bearing walls and the main openings are taken into account is defined. This model utilizes shell elements, with bending and membrane stiffness. The mesh cannot be much precise, to not exceed the potentiality of the software. The external actions that interest the structure are applied, and the strains of the whole building are determined.

A second model of the façade of the building –“façade model”- is created. The strains resulting for the boundary points of the façade wall from the “building model” are applied to the same points in the “façade model”.

The strains determined with this model, loaded with the external actions, permits to define the boundary condition of the “detailed model”.

In a first phase of the analysis the constitutive materials of the structural elements, that is to say the brick masonry for the walls and the wood for the beams, are modelled with reference to their elastic behaviour. In a second phase it is possible to introduce constitutive laws that take into account of the non-linear behaviour of the materials.

The external actions that can be applied to the structure are the weight of the

structural elements, vertical distributed or concentrated loads depending on the utilization, horizontal forces due to the drift of the roof, arches or vaulted ceilings, but also to the wind or to the earthquake.

Through this model all the described effects of the decay of the structural elements, that is to say the reduction of the thickness of the walls, the presence of breaks and discontinuities on the body of the wall, the alteration of the bond between the floor and the wall and finally the sinking of the ground, can be simulated.

Moreover the model permits to find the stress and the strains of the analysed structure caused by the external actions, and so to locate the fields with the best stress concentration.

The results are expressed either with numerical list or with coloured stresses and displacements graphs. These stresses are yielded from the applied actions, but also from the strains and from the displacements due to the decay of the original functioning of the structure.

The applied actions can be increased until to the collapse of the structure, in order to evaluate the security degree of the structure and the coefficient of the security with reference to the break of the structure.

The analytical model is developed through the Matlab calculation code, but because of its simplicity it can also be run with most common calculation codes, or even with the manual calculation.

This model renounces to a local description of the stress and the strains in the body of the structural elements, and focuses its attention on the global behaviour of these.

The evaluation of the global behaviour is based on equations, that express the equilibrium of the structure or that quantify the stress and the displacements of the structure with reference to a functioning of the structure that is fixed a-priori. The materials mechanical parameters play a less important role.

The external actions that can be applied to the structure are the same described for the numerical model. The variations of the geometry of the structural elements due to the decay can be easily taken into account; the same cannot be said about the sinking of the ground, and about other displacements imposed to the structure.

As in the numerical model the applied actions can be increased until to the collapse of the structure, in order to evaluate the security degree of the structure and the coefficient of the security with reference to the break of the structure.

The theoretical approach permits to simulate a very big number of real situations, because of the easy reproducibility of the models. Moreover it requires the definition of some hypothesis that can only approach the real case.

This aspect gains a primary importance in the case of the modelling of the

historical buildings. For these the knowledge of the geometrical shape, of the mechanical properties of the materials, of the real connection of the structural elements, is very doubtful. The same can be said about the knowledge of the loads and the displacements. So even a refined modelling approach can lead to aleatory results.

This study evaluates the potentialities of the numerical and the analytical approach in the forecast of the structural behaviour of the structures, with respect to the computational request.

The experimental analysis results in laboratory tests on some models that reproduce the most significant problems stood out from the theoretical analysis. For this reason the number and the type of the samples are not still defined.

4 Conclusions.

On the base of the results carried out from experimental models, the theoretical models will be calibrated, in order to obtain the greatest reliability in the forecast of the structural functioning of the buildings.

The investigation continues with the analysis of some prototypes of the buildings, in particular with the study of an existing masonry building, that is to say Palazzo Contarini del Bovolo, of which a precise geometrical relief and some chemical and physical analysis of the materials were executed (Figs. 14 and 15).

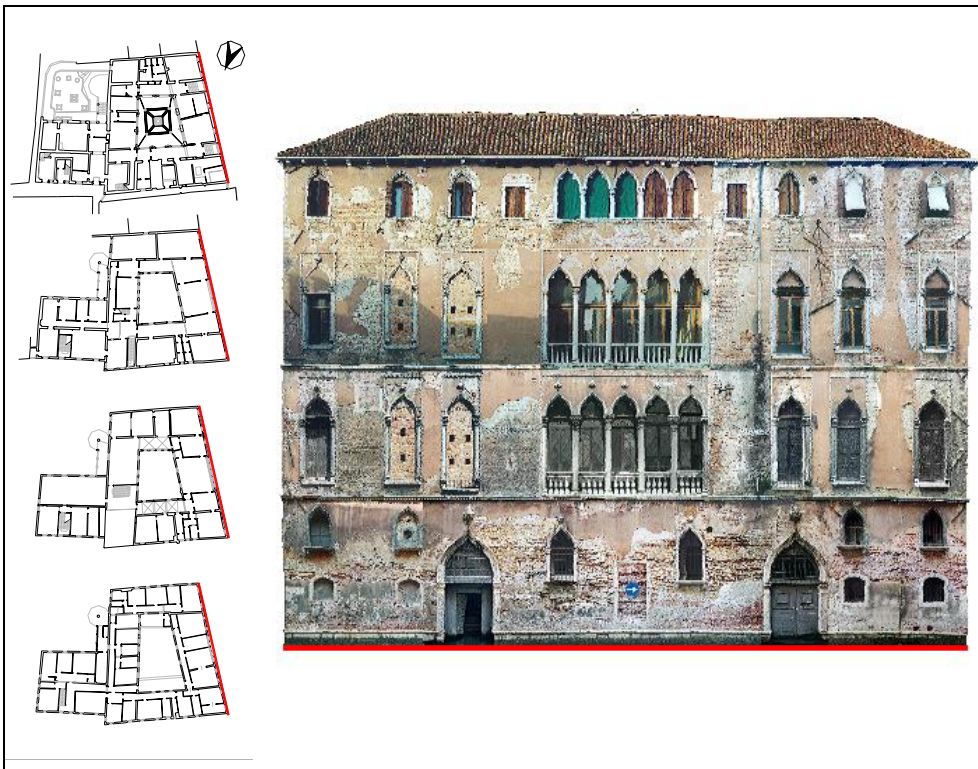


Fig. 14 – Palazzo Contarini del Bovolo: façade.

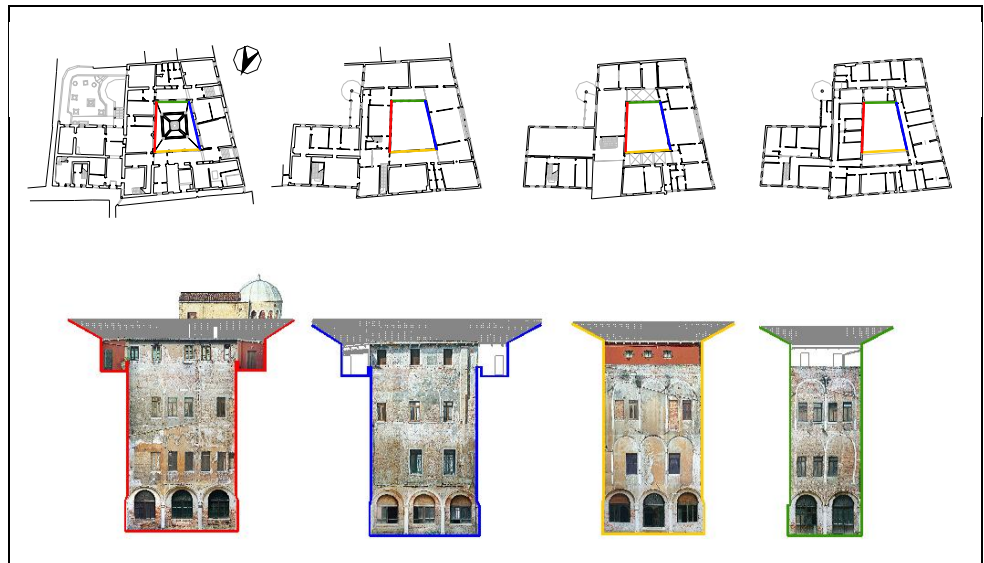


Fig. 15 – Palazzo Contarini del Bovolo: internal yard.

Finally, this study will permit to evaluate the effects of the decay of the structural elements with respect to the structural functioning and with respect to the reserve of the security with reference both to a global and to a local point of view.

The potentialities of each modelling approach in the forecast of this functioning are evaluated, in order to define a methodology of investigation for the study of the peculiar problems of the Venetian buildings.

References.

Piana M., 1984, Accorgimenti costruttivi e sistemi statici dell'architettura veneziana, in *"Dietro i palazzi, Tre secoli di architettura minore a Venezia 1492-1803"*, by G. Gianighian, P., Pavanini, Arsenale editrice, Venezia.

Piana M., 2000, Note sulle tecniche murarie dei primi secoli dell'edilizia lagunare, in *"L'architettura gotica veneziana: atti del Convegno Internazionale di studio, Venezia, 27-29 novembre 1996"*, Istituto Veneto di Scienze, Lettere ed Arti, Venezia.

Zuccolo G., 1975, *Il restauro statico nell'architettura di Venezia*, Istituto Veneto di Scienze Lettere ed Arti, Venezia.

Biscontin G., Riva G., Zago F., 1981, Indagine sulla degradazione chimico-fisica e meccanica delle murature in laterizio a Venezia, in *"Ceramurgia"*, 2, pp. 49-54.

Zago F., Riva G., 1981, Proprietà fisico-meccaniche dei mattoni e comportamento della muratura del centro storico di Venezia. Parte prima: il

mattone, *Atti dell'Istituto di Scienza delle Costruzioni, Istituto Universitario di Architettura di Venezia*, Scuola Tipografica Emiliana Artigianelli, Venezia.

Zago F., Riva G., 1981, Proprietà fisico-meccaniche dei mattoni e comportamento della muratura del centro storico di Venezia. Parte seconda: la muratura, *Atti dell'Istituto di Scienza delle Costruzioni, Istituto Universitario di Architettura di Venezia*, Scuola Tipografica Emiliana Artigianelli, Venezia.

RESEARCH LINE 2.3

Methodologies and technologies for conservation and restoration of historical Venetian buildings

DETECTING CONSTRUCTIVE PATTERNS FOR STRUCTURAL DAMAGE INTERPRETATION OF HISTORIC BUILDINGS IN VENICE

Francesco Doglioni, Giulio Mirabella Roberti, Michele Bondanelli, Francesco Trovò

*Dipartimento di Storia dell'Architettura, Università IUAV di Venezia S. Polo 2468, 30125
Venezia*

Riassunto

Gli edifici storici veneziani, a causa delle condizioni ambientali, adottarono nel passato tecniche costruttive peculiari, e ora manifestano specifiche condizioni di danno, evidenziate da quadri fessurativi e deformativi particolari, spesso effetto di meccanismi di danno agenti in un arco di tempo molto lungo, a volte a partire già dalla fase di costruzione. Perciò la ricognizione del processo di deterioramento per il patrimonio architettonico è un punto fondamentale della ricerca ora in atto nella linea 2.3 dell'Area "Architettura e Beni Culturali", incentrata su *Organizzazione della conoscenza per la diagnosi e la conservazione degli edifici storici veneziani*.

Abstract

Due to environmental conditions, historic buildings in Venice adopted in the past very particular construction techniques and show now some characteristic damage appearance, highlighted by different crack and deformation patterns. These patterns are often the result of damage mechanisms acting on the building during a very wide time span, starting sometimes already during the construction. So the deterioration process recognition for the architectonic heritage of the historical centre is a fundamental point of the research now in progress, belonging to line 2.3 of the Area "Architecture and Cultural Heritage", focused on diagnosis and knowledge organization for the historic building conservation in Venice.

1 Introduction

In the framework of the 2nd CORILA research program 2004-2006 (at the moment in the second year of activity), line 2.3 of the Area "Architecture and Cultural Heritage" has been focused on diagnosis and knowledge organization for the historic building conservation in Venice.

Due to environmental conditions, historic buildings in Venice adopted in the past very particular construction techniques and show now some characteristic damage appearance, highlighted by different crack and deformation patterns. These patterns are often the result of damage mechanisms acting on the building during a very wide time span, starting sometimes from immediately after the construction time.

So the deterioration process recognition for the architectonic heritage of the historical centre is a fundamental point of the research now in progress, with the aim of pointing out the existing relationships among constructional techniques and damage processes.

The constructional feature detection has to be achieved as a result of a well structured and articulated inquiry, very different from those developed in other Italian historical urban centres hinted by the earthquake. It is almost impossible in Venice to set up a comparative study, starting from huge damage situations that bring to light the internal layers and constructional patterns. In recent years only three partial building failures have been recorded, due to some erosion problems on water channel banks. In fact, in catastrophic situations where even partial failures have occurred, damage mechanism appears clearly, as the expected outcome of a partially identifiable process, connected to the constructional features of the building as well as to the seismic intensity.

The research involves an extended reading of historical buildings in Venice, in order not only to go beyond the diffused practice of acting according to the circumstances, that clearly affect most of the interventions in the buildings of the town, but also to soundly rely on methodological approaches based on the analysis of the distribution and the frequency of the various observed situations, collecting and classifying the information under objective parameters of several categories.

In this approach, it is clear that setting up an “expert system” for the damage diagnosis appears more as an expected goal than as a working tool, the complexity of which depends by the study of the case history (the *anamnesis*) and the relationship system that characterizes the purposive sample, that can be further extended but must be yet representative: this sample will be the source for an epidemiologic analysis aimed towards the detection of clear relationships among constructional features, damage and deterioration appearances.

A central point of the process is the diagnostic interpretation of the sequence construction – transformation – deterioration – damage by means of the recognition of the compatibility among the acting mechanisms and the damage appearance (deformation and crack pattern). By the comparison of the outcomes obtained in different buildings, some meaningful and repeated relationships will be outlined, in order to set up tools (as operating standards) useful for the damage interpretation in any specific case.



Fig. 1. Partial failure of a building with wall on the channel bank (*rio di Ca' Rezzonico, Dorsoduro*)



Fig. 2. A case of a whole building collapse (*rio di Ognissanti, Dorsoduro*).

2 Choice of the investigation sample

The systematic collection of the information about the first 130 buildings situated in the six *sestieri* of the historical centre of the town (i.e. *Dorsoduro*, *S. Croce*, *S. Polo*, *S. Marco*, *Cannaregio*, *Castello*) allows a first effective definition of some themes of interest, that can be observed and analyzed, useful to achieve the proposed goals.

2.1 Relational data-base for geo-photographic recording

The selection of the initial sample has been based on the choice of some objective parameters, related to macroscopic aspects, environmental as well as architectonic:

- environmental parameters: the building referred to its physical position inside the town, with respect to the channels, the banks, the paths (*calli*) and the squares (*campi*);
- architectural and urban characterization parameters (the building related to the dimensional characters of the surroundings);
- morphological and stylistic character parameters (description of the intrinsic constructional characteristics, based on their recognition and also on the formation of typological categories for particular building configurations, like angular solutions, basement solutions, cantilever roofs)
- stratigraphic and age-dimensional characterization parameters for the wall panel, (description of the degree of stratigraphic complexity of the wall panel, also related to the other materials; description of the brick bond and characterization by shape, dimensions and clay mix of the bricks);
- description and localization of the particular connections of the building (connections stone/brick/wood on the corner system, the shops at the ground level and the special retaining elements at the floor level);
- description of the previous strengthening interventions (survey on the original systems and repair of the previous structural damages).

The systematic recording of information collected during the survey is supported by using a reading form, which must be filled on site. This tool –that is the bases for structuring an expert information system– can guide the operator also to file the collected information. It is possible to reference the observed buildings in a GIS related way, so that specific queries can be made on selected parameters.

In this way an extensible data-base of information will be set up, that allow performing comparison analysis based on similarities observed or suspected. The compilation of a catalogue, that will include also information deduced by archive documentation, will allow also performing diachronic observations, when documents related to interventions of the past or simply to the building conditions in different times are available.



Fig. 3. Example of recording in HTML format of the collected data.



Fig. 4. Example of interactive cartographic visualization in HTML format of sestiere San Polo, with the localization of the sample buildings

2.2 Main themes of interest for the research

Starting from the studies made on bricks and walls in Venice in the last 30 years, particularly adopting archaeological approaches, such as dimensional chronology, a first check on the sample has been performed on the possibility of dating bricks and wall bond. In Venice the dimensional chronology plot shows such a fluctuation that bricks with the same base area (taken as reference in the study) can belong to different ages, also far off each other. The first trial suggested that this plot has to be modified firstly taking into account volume measurement (ranging from about 700 cm^3 to more than 3.000 cm^3) and also looking for more refined relationships among metric components. The more significant results are expected from the association of dimensional-chronological with morphological parameters, concerning for example the clay

mix, for which a comparative study is requested to focus some reference morphologies. A correlation being supposed among dimensions of the bricks, the consequent bond, and the appearance of damage in the masonry, a research has been started on the bond and texture appearance that will take into account the great dimensional scattering of the bricks.

Other topics of the research concern the nature and the shape of stone elements, particularly in the case of corner structures, for which a first classification has been made, and the devices connecting walls and floors (mainly the so-called *fiube*). The different configuration of the corner stones is associated to particular failure mechanisms – observed as discontinuities in the brick panels – that indicates his intrinsic weakness, and to some typical repairing or containing devices.

A particular attention is deserved to the buildings having the base floor partially made by monolithic columns, showing frequently out-of-plumb configuration in this zone. A correlation is sought with the laying of the first floor beams, to detect the factors that increase this defect. Another main subject of the research is the detection of the initial configuration of the buildings, in order to verify the origin and the nature of the inward out-of-plumb frequently found in Venetian buildings, and to assess if and in what proportion it can be referred to an intentional original design or to a subsequent deformation.

2.3 Topographic survey of selected buildings

In order to characterize and to partially verify the thematic statements that were firstly assumed, selected topographic surveys have been made that enrich and complete the information in the data-base and become crucial points for setting up an interpretation model of some typical structural damages found in the research. Vertical and horizontal outlines have been surveyed in order to quantify the configuration and the behaviour connected to failure mechanisms, so that constructional configurations can be discriminated from geometrical modifications.

Hereafter the type of data collected is specified:

- deformation and displacements reading (inward and outward out-of-plumb)
- displacements in the correspondence of containing devices (such as the *fiube*, the stone – brick – wood connections)
- deformations associated to peculiar architectonic solutions (buildings with corbelled façade, associated to a shop gallery at ground floor)
- individuation of constructional geometric characteristics that can be referred to intentional design (as in the case of buildings with the front or the lateral wall showing a lack of verticality inward, growing to the top).

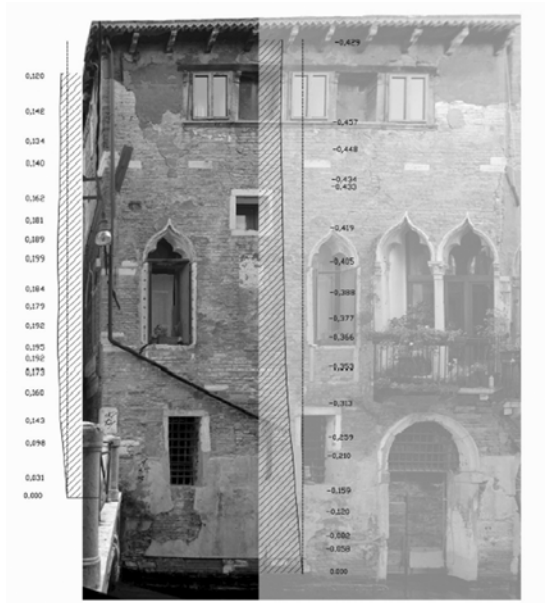


Fig. 5. Topographical survey of some vertical profiles of a gothic house near *campo S.Barnaba*, in *sestiere di Dorsoduro*

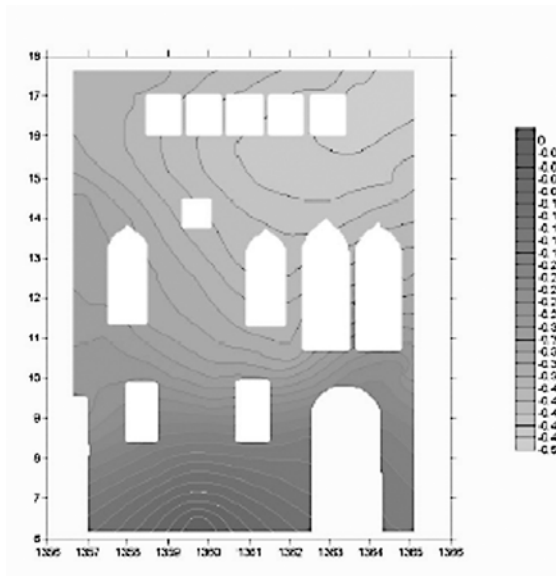


Fig. 6. Contour plot of horizontal deformations of the façade plan, building of fig. 5.

3 Investigation topics: the wall panel

The studies on historic buildings in Venice are characterised by specificity and geographic confinement: building system brittleness is linked to the constructional techniques (such as the frequent use of thin wall panels, together with wooden beams floors etc.) that were adopted to fit the lagoon environment.

The examination of the masonry surface, belonging to a wall panel expected to support building loads, is a central topic in the study of constructional patterns

and its mechanical consequences. The nature of these relationships is directly influenced by the wall panel characteristics showing different heterogeneity degrees in constructional patterns as well in the appearance. This heterogeneity is strictly connected to structural, functional and formal transformations. In this approach great importance is attached to the identification of discontinuities and to the detection of constructional elements in stone or wood, as well as the analysis of the brick bond in the parts where it appears belonging to homogeneous building phases.

3.1 Identification of different bond patterns belonging to a specific building-phase: the contribution of dimensional-chronology and micro-stratigraphic reading

Different brickwork patterns have been classified according to morphological and stylistic criteria, in order to highlight the expected relationships between the masonry appearance and the related mechanical behaviour:

- *altinelle* masonry (XII – XIII cent.): made using small dimension bricks, whose use in Venice is documented across XII and XIII century both in flooring and in masonry works. The *altinelle* bricks are 15,5÷18 cm long, 7÷8 cm large and 4,5÷5 cm thick. This kind of brick is produced with *caranto*, which is a very stiff, yellow-grey clay from the lagoon. The bricks are laid alternating headers and stretchers in each course, or alternating stretcher courses with rowlock courses;
- gothic masonry (XIV – XV cent.): in this kind of masonry the units are 26÷28 cm long, 12,5÷14,5 cm large and 5,5÷8 cm thick. The bricks are laid out on horizontal regular courses alternating headers and stretchers, although this arrangement may be different;
- renaissance masonry (XVI cent): noteworthy is the fact that renaissance walls show the same Gothic brick bond, but usually altogether less refined and with brick arrangement not always regular. Bricks are 27 cm long, 13 cm large and 6 cm thick;
- masonry across XVII – XVIII centuries: in this kind of masonry bricks are in the average 26 cm long, 11÷12 cm large and 5÷6 cm thick. These dimensions remained the same across the whole XVII century till the beginning of XVIII, when the minimal dimensions recorded are 5,5×11,6×23,5 cm. At the end of XVIII century the brick size changes into 5×12×24 cm;
- modern masonry (XIX cent): starting from the end of XIX century, the brick size tends to a standard and approaches to that is still used nowadays. Bricks are 24 cm long, 12 large and 5 cm thick.

According to the previous dimensional-chronological researches, a linear decrease in brick dimensions has usually been observed (from 28 to 24 cm).

For Venetian bricks, the dimensional-chronological plot shows two fundamental points, the first among XII and XIII centuries and the other on mid XV century (VAROSIO, 2001). The fluctuation in brick dimensions limits the possibility of identifying masonry morphology by using only constructional parameter, so that it is more appropriate to rely on more complex volume measurement or clay mix observation. A strict correlation is forwarded between dimension-chronological individuation and the analysis of brickwork, which probably involves mechanical behaviour.



Fig. 7. Frari Church. Macrophotograph showing the particularity of clay mix.



Fig. 8. House in *ramo del Tentor*, S.Croce. Macrophotograph showing the particularity of clay mix.



Fig. 9. Frari Church. Masonry specimen outlining brickwork. Headers and stretchers are alternated very regularly (from the practice of Restoration classes at IUAV, prof. F. Doglioni – year 2004/05).

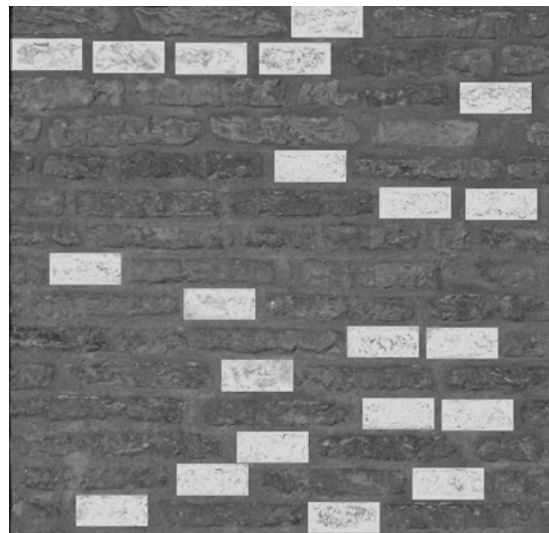


Fig. 10. Madonna dell'Orto Church. Masonry specimen outlining brickwork. Lack of regularity in the alternance of headers and stretchers (from the practice of Restoration classes at IUAV, prof. F. Doglioni – year 2004/05).

3.2 Identification of masonry damage patterns

Investigation on material deterioration is another topic of masonry study. Diagnostic interpretation may follow the path construction – transformation – deterioration – severe damage or failure that marks each workmanship. So that particularly meaningful are some typical deterioration pattern of masonry panels, for shape, dimensions and clay mix of the units as well as brickwork pattern. Moreover, some damage and deterioration patterns can play an important role in modifying the static efficiency of the building.

An example is the salt efflorescence matching constructive discontinuities: the

under-wall construction, or the partial substitution of bricks with new ones with high salt content or different porosity, can be source of punctual weakness modifying the overall mechanical response. Among other elements that attract the efficiency-loss processes, the connection links wood – iron – stone – bricks that are typical of the Venetian constructive tradition, and the formation of capillarity-rise front, particularly on walls aside the channels, where bricks appear often totally disintegrated.

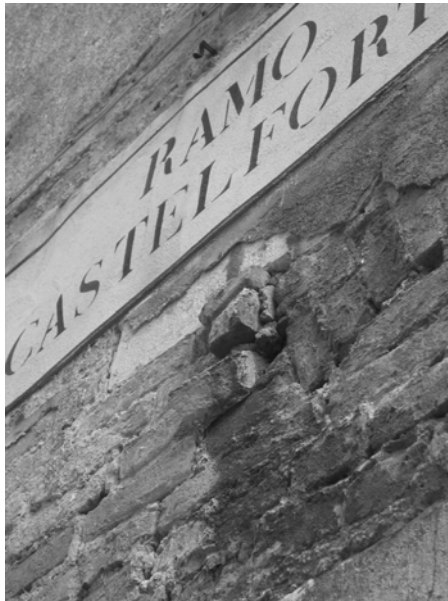


Fig. 11. *Castelforte San Rocco*: the oxidation of the internal iron tie beneath the stone anchor, and the consequent increase in volume, cause the bulking of adjacent bricks.



Fig. 12. Masonry panel where local substitution are evident, determining discontinuity patterns that can reduce masonry efficiency.

3.3 Simplified stratigraphic-constructive survey: discontinuity detection

Also a simplified stratigraphic survey may enable to read the main transformation of the building in the course of time.

The detection of the main discontinuities and the assessment of their impact on the diagnostic interpretation may become a reference step for the individuation of local vulnerabilities. As example, the basement part of the buildings in historic centre, very often substituted, show the connection between static overstress on the wall panels and constructional discontinuities.

4 Investigation topics: reading the structural damage process of the buildings

The historical buildings in Venice show very heterogeneous constructional characters and structural damage processes, which reveal to surface by means of various crack and deformation patterns, according to specific geomorphologic characteristics of each building body where damage mechanisms can have been originated, in some cases, also in the very first times of life of the building, if not already during construction.

4.1 Detection of previous repair intervention

The appearance of structural problems time after time and the relatively fast developing of failure mechanisms conducted in Venetian context to the development of repair techniques and methods that kept in use in the course of time, although with some technological or material modification, assuming in this way an aesthetic worth but also becoming itself a constructional character.

Tie-rods with visible bolts, iron cramps, stirrups, hoops are so diffused that they become a precious reading code for the interpretation of the structural damage modifications and of the dynamic loads possibly applied on buildings. For Venetian buildings, in fact, a comparative study on damage mechanisms can be reliably based on the assessment of the compatibility among damage appearance, loads acting on the building and previous strengthening interventions, so that the interpretation of the process building – transformation – deterioration – failure can be based also on the detection of similar strengthening intervention repeated in the time.



Fig. 13. Tie-rod bolt made by an iron bar substituting the previous stone anchor system (*fiuba*) in the connection between wall and floor, when the efficiency was lost for the deterioration of the external part.



Fig. 14. Deterioration and efficiency loss of the external iron bolt. The lack of an anchor system in the wall-floor connection caused a buckling effect on the wall at the floor level and eventually the extraction of floor beam heads.

Also from outside (on the façades bordering the paths, the squares, the channels, or the shops and the porches) the survey can reveal the incoming and the repetition of damage mechanisms cycles, strictly connected to specific constructive solutions that characterize the building system. So, the damage states can be read as the relationships among the effects (crack and deformation pattern) and the repair interventions depending from the specific constructional solutions, where the cause may be of various and uncertain source: very different situation from the damage produced by seismic actions,

where the cause is clearly detectable and often also numerically defined.

5 Investigation topics: selection of constructional characters at the building scale

The direct investigation on the buildings allows the selection of some specific constructional characters, for which a dedicated reading will be proposed, with the aim of increasing knowledge on these systems. The frequency of appearance of these details makes them very meaningful for our purposes, even if they seem of limited dimensions compared to the whole building. On the other hand, a relationship is suspected among some failure mechanisms and the constructional details. For example, the effects of live and dead load distribution will be observed in correspondence of the corners that usually mark a particular stress concentration, depending on the constructional morphology.

Also some particular distributive and morphological solutions have been investigated, such as the use of stone pillars at the ground floor, often found for the presence of shops, and the adoption of corbelled construction for cantilevering the first floor.

5.1 Survey of quoin systems

The constructive solutions for the quoins in historical buildings of Venice change with reference to the architectural style of the time but also to the architectonic significance and the building dimensions. The variety of quoin systems can be classified with reference to the material and to the overall disposition: the detection of the constructional systems can begin at the ground floor of the buildings.

There are solutions with the corner mainly in brick masonry, both at the ground floor and at the upper levels; in these situations stone ashlar and connectors are found at the floor level. In other cases stone ashlar – regular or irregular in shape – are disposed at the ground level continuing also at the upper levels, sometimes sustained by a pillar.

Often this pillar is one floor high, and in the more important buildings it reaches also the *cornice* or belt course, but there are situation where in the upper floors the pillar is replaced by brickwork or stone ashlar.

Finally, there are some cases where the corner pillar does not reach the first floor level, and the corner is completed by different materials.

The most critical situations from the damage point of view are represented by corner systems where the stone pillar ends at the first floor level: horizontal components of loading may determinate local displacements of stone element, frequently causing fracturing of the pillar or of the lintel of adjacent openings. In the mixed stone – brickwork systems the damage more frequently observed is connected to the different stiffness of the two materials involved: some cracks

appears vertically on the masonry near the corner, and in some cases the phenomenon is more evident, showing also a deflection of the wall corresponding to the corner.

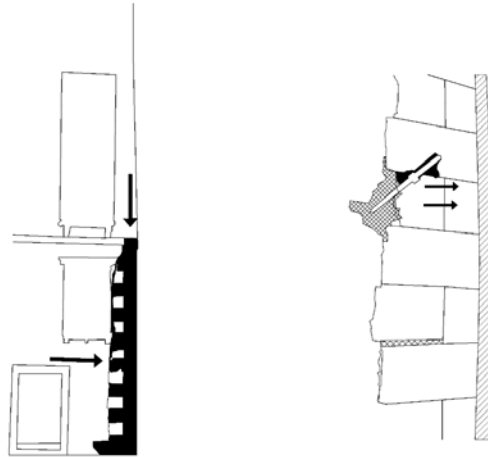


Fig. 15. *Dorsoduro*, 3908. Gothic building where the coin is made by stone ashlar regularly laid until the first level. The inflection mechanism can be noticed on the left, and on the right the detachment of brick elements caused by localized compression near the tie-rod bolt (from the practice of Restoration classes at IUAV, prof. F. Doglioni – year 2004/05).

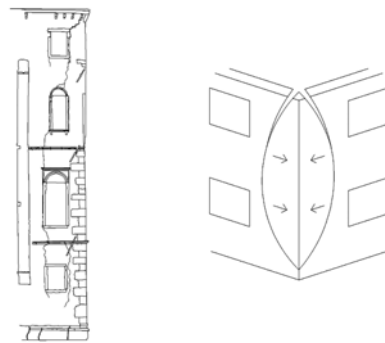


Fig. 16. *Ca' Bernardi*, sestiere di san Polo. The crack pattern near the quoin is shown. Cracks involve the masonry as well as the stone elements, such as the lintels and the haunch of the openings (on the left). On the right, the arch expulsion mechanism is shown. (from the practice of Restoration classes at IUAV, prof. F. Doglioni – year 2004/05)

The appearance of deterioration pathologies, like the plaster detachment or the erosion of mortar joints or of the same *Istria* stone, can increase the disconnection among elements reducing the efficiency of the corner node.

Among other recorded phenomenon, connected more frequently but not only to the mixed stone/brick corner systems, also an “arch mechanism” with corner

ejection can be observed, made possible by the combined action of loads acting on the wall and the top constraint.

The brickwork quoin, sometimes strengthened by stone ashlar, is the most sensitive to the deterioration induced by capillary rise and salt efflorescence, starting from lower levels. The lack of regular stone ashlars or continuous stone pillars facilitates in this case a crushing failure of the masonry.

5.2 Base systems with stone pillars

Obvious functional needs determined the development of townhouse morphology with the shops at the ground level. The display window openings require a particular static solution that is characterized by the presence of pillars in *Istria* stone, connected on the top by wood lintels over which the overhanging wall is laid. These systems, clearly recognizable, show some typical weakness characteristics, often outlined by particular and also important deformation patterns. This constructive type can be subdivided in two categories: corner and row houses. Each type show particular damage mechanisms, depending from specific constructional character, the transformation processes, the lack of structural connections.

On the basis of a consistent sample analyzed, it is possible to state that out of plane deformation is less frequent in the case of corner house with roof beams laid parallel to the main front compared to the cases when the beams are laid perpendicularly. The inward displacement – which can be found at the upper levels – is observed more frequently in the front perpendicular to the floor framework. Also in the case of row houses, the majority of the observed cases show an out of plane deformation when the floor framework is perpendicular to the front.



Fig. 17. Building system with pillar at the base. In this case, the deformation appears frequently outwards until the first level, changing inwards in the upper part (from the practice of Restoration classes at IUAV, prof. F. Doglioni – year 2004/05).

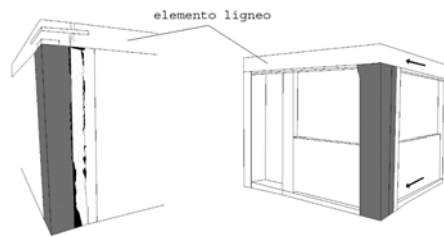


Fig. 18. Building in *calle del Tabacco, sestiere di San Polo*. The corner base system is shown, where a stone pillar is adopted together with a wood beam. In particular, a brick repair is a proof of a past damage, as well as the insertion of iron cramps on the lintel (from the practice of Restoration classes at IUAV, prof. F. Doglioni – year 2004/05)

5.3 Buildings with cantilevering floors of corbel type

The constructive type of these buildings can be well represented by the peculiarity of the connections, the sophistication of the manufacturing of wood and stone parts, and the general efficiency of the whole system.

Referring to the materials adopted, their placement and the way of constituting the cantilever of the floor, it is possible to distinguish some categories, also characterized by the observed damage.

A homogeneous structural response can be expected from this system, made only by wood corbels: on the contrary, the presence of stone elements (generally corresponding to the walls perpendicular to the front) gives rise to crack and deformation patterns related to diversified stress responses.

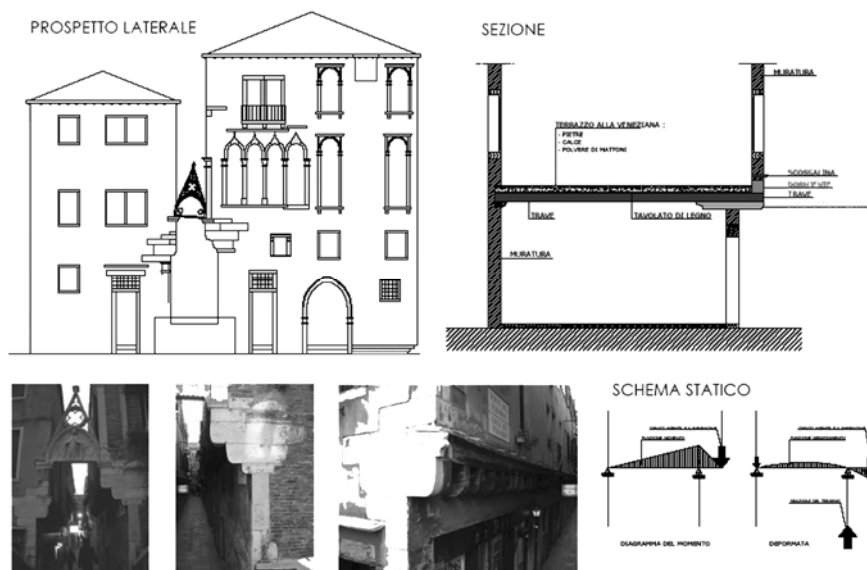


Fig. 19. Buildings in *calle del Paradiso, sestiere di Castello*. In the cross section on the right, the corbelled system configuration is described (from the practice of Restoration classes at IUAV, prof. F. Doglioni – year 2004/05)

5.4 Foundation systems

Another important investigation topic concerns the knowledge of the foundation systems in Venice. The effects of the soil–structure interaction is highly conditioned by different foundation systems adopted, also in the same building, and by the stratigraphic heterogeneousness of the soils where Venice lies. (see MAZZUCATO – DEI SVALDI, 2005). The variability of environmental conditions (bank walls on the channels, walls on calli and campi), the different volume of the buildings, the various age of construction and also the zone of the town (sestiere) to which the building belongs are all parameters to take into account in the prosecution of the research.

6 Conclusions

The research involves an extended reading of historical buildings in Venice, in order to collect and classify the information under objective parameters, relying on methodological approaches based on the analysis of the distribution and the frequency of the various observed situations. So the deterioration process recognition for the architectonic heritage of the historical centre is a fundamental point of the research now in progress, with the aim of pointing out the existing relationships among constructional techniques and damage processes. By the comparison of the outcomes obtained in different buildings, some meaningful and repeated relationships have been outlined, in setting up tools and procedures useful for the damage interpretation in any specific case.

References

- AA.VV., 2000. Venezia - Forma Urbis, il fotopiano digitale, Produzione IUAV-CIRCE, Ed. Marsilio, Venezia.
- AA.VV., 2003. Danneggiamento, conservazione e manutenzione di strutture murarie e lignee: diagnosi e modellazione con riferimento alle tipologie costruttive ed edilizie, Atti del workshop, Politecnico di Milano, 16-17 gennaio 2003.
- Doglionì F., Moretti A., Petrini V., 1994. Le chiese e il terremoto, Ed. Lint, Trieste.
- Doglionì F., con contributi, tra gli altri di Moretti A., Marino F., 2000. Codice di pratica - Linee guida per la progettazione di interventi di riparazione, miglioramento sismico e restauro dei beni architettonici danneggiati dal terremoto umbro-marchigiano del 1997, Bollettino Ufficiale della regione Marche, ed. straordinaria n. 15 del 29/09/2000
- Fazio G., Hreglich S., Lazzarini L., Pirredda U., 1982, Le altinelle a Venezia: problemi storici, caratterizzazione chimico fisica, cause di deterioramento, in "AA.VV., Il Mattone a Venezia, Convegno presso Ateneo Veneto del 29 ottobre 1982", by Comune di Venezia, a cura dell'Istituto per lo studio della dinamica delle grandi masse del CNR.

Giuffrè A., 1988. *Lettura sulla meccanica delle murature storiche*, Ed. Kappa, Roma.

Gurrieri F., a cura di, 1999. *Manuale per la riabilitazione e la ricostruzione postsismica degli edifici: Regione dell'Umbria*, Dei, Roma

Maretto P., 1986. *La casa veneziana*, Ed. Marsilio, Venezia

Trincanato E.R., 1948. *Venezia minore*, Filippi Editore, Venezia.

Valcanover F., Wolters W., a cura di, 2000. *L'architettura gotica veneziana: atti del convegno internazionale di studio, 27-29 novembre 1996*, Venezia, Istituto Veneto di scienze, lettere ed arti, Venezia.

Varosio F., a.a. 2000/2001. *Tesi di Laurea in Rilievo e analisi tecnica dei monumenti antichi*, relatore Ferrando I., correlatore Varaldo C., Mannoni T., *Ricerca per una mensiocronologia dei laterizi a Venezia*, Università degli studi di Genova, Facoltà di Lettere e Filosofia, Corso di Laurea in Conservazione di Beni Culturali, indirizzo archeologico, architettonico e per l'ambiente.

Zuccolo G., 1975. *Il restauro statico dell'architettura di Venezia*, Istituto Veneto di scienze, lettere ed arti, Venezia.

VENETIAN BUILDING DIAGNOSTICS INFORMATION SYSTEM

Luca Marescotti¹, Maria Mascione², Stefano Maffulli³

¹.Professore, Dipartimento BEST, Politecnico di Milano ².Assegnista di ricerca, Dipartimento BEST, Politecnico di Milano, ³Libero professionista

Riassunto

Il progetto concettuale del sistema informativo per la diagnostica dell'edilizia veneziana affronta due principali livelli: il livello territoriale e il livello locale (edificio).

I due livelli operativi richiedono la capacità di muoversi con dettagli diversi passando dalla piccola alla media e alla grande scala in termini geografici e alfanumerici senza perdere l'integrità degli oggetti e garantendo, soprattutto, il mantenimento della congruenza territoriale e temporale delle informazioni. La questione di fatto, non si limita alla georeferenza del singolo elemento ma risiede nella continuità dei dati nel sistema informativo durante tutti i passaggi di scala.

L'approccio alla progettazione del sistema informativo è stato avviato su due fronti principali: l'individuazione dei requisiti funzionali, l'analisi dei materiali e delle interazioni tra utenti e sistema. In merito ai requisiti funzionali sono state definite due aree: quella relativa alla fase d'inserimento dei dati nel sistema e quella della consultazione. Le interazioni sono state definite in relazione ai requisiti e ai materiali e alle attività dei gruppi di ricerca. Sono stati così individuati cinque principali gruppi di dati: 1.edifici; 2.tecniche costruttive; 3.strutture e materiali, dissesti e meccanismi di danno, fenomeni di degrado; 4.rilievi e analisi geometriche; 5.procedure, norme, capitolati.

Il prodotto, ancora in corso di definizione, è il modello UML (Unified Modeling Language) del sistema informativo formalizzato in casi d'uso e diagrammi classi e oggetti.

La finalità di tale approccio progettuale, fondato sull'individuazione corretta dei gruppi di utenti e delle classi d'informazione, è la garanzia nel tempo della flessibilità e della vitalità del sistema come corollario della sua utilità: questi principi sono, di fatto, le condizioni necessarie e sufficienti anche per un aggiornamento continuo.

Abstract

The conceptual design of an information system for a diagnostic survey of Venetian buildings tackles two main levels: territorial (spatial) level and local (building) level.

The two operational levels require the ability to move across small, average and large-scale in geographic and alphanumeric terms, changing details without

losing object integrity. The system must assure spatial and chronological congruency maintenance of the information. The main question, of fact, is not limited therefore to a single object georeference, but it resides in the continuity of data during all the passages of scale.

The approach to design of the information system has been started on two main foreheads: identification of functional requirements; analysis of materials and interactions between customers and information system. With respect to requirements two areas have been defined: that one relative to the phase of data entry and that one of the consultation. The interactions have been defined in relation to requirements and the materials and the activities of the research units. Five main data sets were been therefore identified: buildings; constructive technologies; structures and materials, damage and mechanisms of damage, phenomena of deterioration; metric and geometric survey; rules of procedure, norms and specifications.

The product, still in progress, is the UML model (Unified Modelling Language) of the information system formalised in use cases and diagrams classes and objects.

The information system will be founded on identifying correctly users groups and defining taxonomies and information classes. The purpose of such an approach, is to assure along the time flexibility and vitality like corollary of information system usefulness: these principles are, of fact, the necessary and sufficient conditions also for a continuous updating.

1 Introduction

In the phase of the conceptual design of whichever information system resides winning elements, because here requirements are defined, users characterised with theirs requirements, too, contents are analysed and well described.

The requirements to deepen such phase, relative to the approach of the design the system as like as essential activity, demands, therefore and necessarily, the communication between those who produces data and the designers of the system. The designers are not exactly software developers, but the interface between users and software developers.

At the same time the deepening of regarding methodological and theoretical aspects involved in the design of an information system purposely addressed to support the architectural preservation, involves the development of new reflections on the preservation plan. One opens a dialectic relationship among design, data flows, and knowledge and information system. The argument concerns on the operative principles of the intervention, and also on their relationship with the urban and regional planning.

The information system is not placed like alternative to the knowledge model of acquaintance of the architecture represented from the preservation plan and design, therefore as it is proposed from part of the updated architectural culture. It is one of the job instruments and of research; it contributes to that "operational

knowledge”, who generates other knowledge. For its characteristics it is dedicated to the management, to data sharing and data flows and is this aspect that one must privilege.

The preservation plan is already a system of information because its contents are defined in the essential parts and in the relations with others. The formulation of the geometric survey, of investigations like structural analysis and materials (points of sample and analyses of laboratory) analysis and characterization, rather than the role of the documentary research, or the stratigraphic analysis of elevates, are all by now acquired on the methodological and operational plan.

It will be however necessary to define specific topics in order to avoid a generic and unfruitful result because if their contents are conceptual clear, it is equally clear amplitude, complexity and troubles to transform in database the relations generated from the contributions of the several disciplines. Of necessity it comes down to work by a modular approach that it inquires the topics of base of the preservation plan and the users objectives, and “it receives” developments dictates from future questions, always with the conscience that the information system is not exhaustive of the consistency of the analyses and results, but can address to the informative resources.

2 Territory and architecture in the levels of planning

The conceptual plan of information system for the diagnostic survey of Venetian building tackles two main levels: the territorial (spatial) level and the local level (building).

The spatial level allows to organise environmental problems that are only meaningful to this scale, but that are lend to determine informative requirement and deepening of investigations to the local and building scale. To this level it is necessary to have specialized information, even if general, to the aim of correct operating, in order to plan the intervention, in order to program the resources, to achieve strategic and main objectives and to understand relations between the parts, that constitute the territory in its unity, singularity and complexity. To the spatial level they compete, however, other information of general character that are intimately connected with the local level: The geologic and hydrographical conditions and those seismic that, influencing the mechanics of the ground and therefore the structural answer of the buildings, address the diagnostic techniques. Just as the general level and that particular one do not have clean borders, in so far as the construction of the information system must allow the coherent management of the levels and the interoperability of data.

The local level, in specific “the building”, is indispensable for the data acquisition with an appropriated level precision suitable to supporting the restitution of information for the plan of preservation and the consequent planning activities. The participation to this scale demands detailed diagnostic and project action, supported from general knowledge about the context and other ones detailed of the building, aimed to resolve in the best way problems “reasonably” defined.

The work progress previews the definition in the detail of the levels territorial and local in function of requirement, the users and geographical and alphanumeric data.

3 Materials and data sets

The materials available for the total development of the plan are of varied nature: geographic and alphanumeric data, images, documents of text. Part of them derives from the analysis of documentary sources and cataloguing of examples in several of the fields of the research (degradation and damage phenomena catalogue, abacuses). Others depend on investigation on the field dedicated to specific cases study: they are the structural diagnostic tests in situ and laboratory, the characterization of the materials, the building survey, the ground/building interaction in the foundation structures.

The location of the data set comes down from the contents of the entire project and it is articulated in the analysis of the data typology, of their form and contents, and of their relations.

The project is much articulating. Its complexity is reflected also from the making competences reference to as many work groups. The first phase of analysis of the complex of the activities of the WP (Work Packages) has carried to characterize the following main data set:

- Buildings.
- Constructive technologies/techniques.
- Structures and material.
- Damage and mechanisms of damage, phenomena of deterioration.
- Geometric and photogrammetric survey.
- Rules of procedures, norms and specifications.

The information system therefore will be constituted from one first size of data, deriving from the acquisition and organization of existing sources and new data on the field according to specific formats.

A second size of data will regard the study of sample buildings from which acquiring specific data. The representation of results of diagnostic (the structures in masonry, armed concrete and ferrous materials, wood) is from defining in modality 2D and 3D in function of the level of deepening of the information.

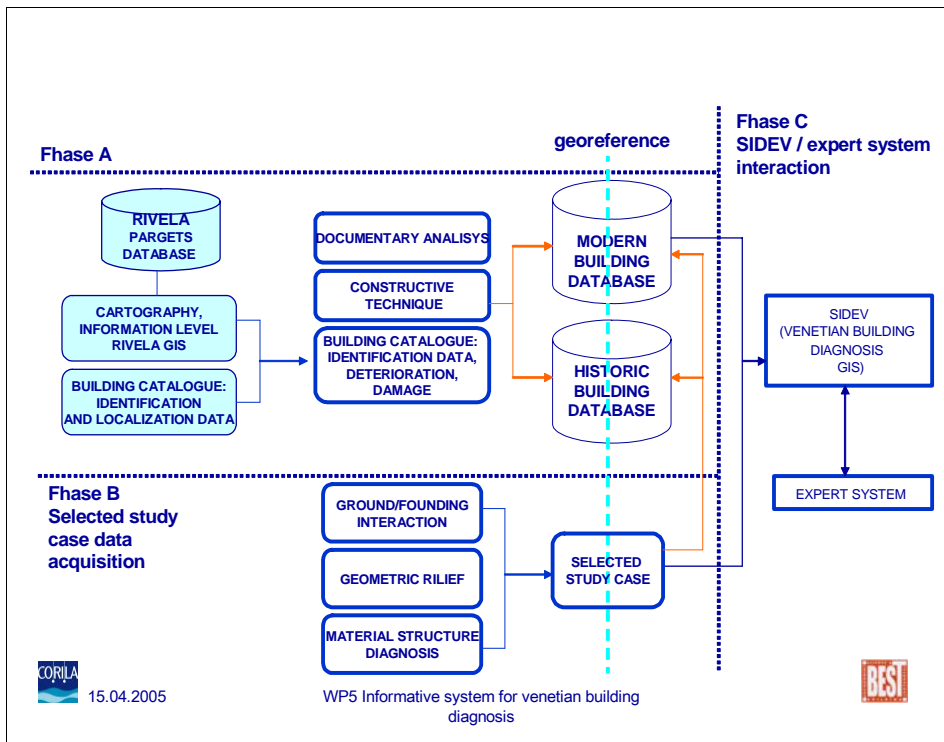


Fig. 1 – General scheme of the information system planning. The A phase regards the relations between the specific materials of the research and the geographic and alphanumeric database of the RIVELA system. The B phase evidences integration of the database of the A phase with data set deriving from the study cases; geographic localization of the building is the element that unifies the system. The C phase is dedicated to the interactions between the SIDEV (Information System for the Diagnostic of the Venetian Building) and the VMDS (Venice Monument Diagnostic System).

4 Analysis of functional requirements

This activity constitutes the premise for the conceptual organization of the database, through the appraisal of the information to insert, the location of the bases of external connected database, the query formalization to which the system must answer. Its development happens at least on two sides:

The first one interests the contents of the information system;

The second one regards the technologies of the information: data typology (alphanumeric, geographic, iconographic) and software for the implementation of the prototype on geographic base.

For both it will not leave out off consideration the integration with the Corila/RIVELA database (database for the Searches on Venice and the Lagoon).

The complexity of the plan and the non-uniformity in the research development

ways do not allow defining beforehand requirements. The process of development of will follow "adactive" approach mostly. The interactions will be characterized that appear simpler definition and if others suggest some on the supply of the information and the requirements emerged from talks had with the investigators of the WP The development of the plan will follow a iterative and multidisciplinary way, refining gradually the methods and the procedures of the researcher.

4.1 Main requirement

- Data entry from the groups of research through web interface resident on the Corila server.
- Possibility of geographic and alphanumeric search.
- Location of a building, or same buildings, based on specific search keys: typology of building, damage and (or) degradation typology, materials, resistant elements, address.
- Further indications on diagnostic survey and rules of diagnostic procedure according with degradation and damage phenomena first survey.
- Further indications on the access to the expert system to forehead of determined situations of damage according with SIDEV users outcome.
- Integration with the existing systems.

4.2 Requirement to deepen

- Cross-sectional relations between the several DB of the SIDEV.
- Criteria of search
- Representation of the deterioration and the damage associated to the quality and by piece in the geometric and cartographic representation of the building.
 - Localization of the points of withdrawal of money of the champions for the characterization of the materials.
 - Localization of the points or fronts for the diagnostic in situ (masonries, wood).
 - Geometric survey of the cases study (restitution 2D and 3D).
 - Representation of damage and deterioration (restitution 2D and 3D).
- Relation between the table of the deterioration and that one of the damage, that is their integrated reading to determinate the state of preservation of the building.

- Regarding the variety of the produced materials and which will produce, it must define which will be organized in database, which will be managed like enclosure and which others are products that will not make part of the SIDEV.

5 Users groups

In the case of an information system dedicated to architectural preservation plan, the first analysis are about users (agencies, institutions, until to the physical persons) that they will use the system; in the second place it inquires the identified users for the tasks that are called to carry out through specific professional competences. It is implicit, but it is always better to remember it, that this phase is in tightened relation to specific well defined objects for the entire information system and to requirement, therefore to the contents and to the quality of data.

The determination of users, or user groups, is tackled in the respect of two main requirements.

The first one regards the access to data therefore like previewed from Corila.

The second one, inside to logic of the I.S., interests the location of data sets in relation to some typologies of users:

- Corila, client, administrative and technician referring and of the having plan role of validation of data and of the system.
- Researcher of the Institutions partners of the Corila.
- Agencies, Institutions or single researchers (user subscribed and authorized from Corila).
- Researchers of the specific project of research. They are specialized users because they are professional operators of the field and researchers.
- Skilled professional operators. It comprises various skilled professional operators with competences and different interests in relations to the building scale intervention.
- Common of Venice (urban and building scale). One characterizes from a part for the capacity of the institutional tasks (decisions, planning, allocation of resources). From the other it is part of the "Skilled professional operators" category as far as the activity of the technical offices (plan evaluation, control of the building activity, drafting of plans...).
- Superintendence to the Architectonic assets, the Landscape and the Historical, Artistic and Demoethnoanthropological Heritage of Venice and lagoon (BAPPSAD). It has institutional tasks in quality of supervisory body for the participations on buildings and architectonic wholes, subordinates to the State protection, with the

advanced competences of preservation skilled professional operator.

- Province of Venice (territorial scale).
- Magistrate to waters of Venice (territorial scale).
- Insula S.p.A, Corporation for the urban maintenance of Venice (urban scale).

They are users bearers of various requirements of information for which, to forehead of the interest for the entire complex of data of the SIDEV, some groups can be more meant or important of others. In some cases, draft then to inquire the usefulness to determine priority of display, or distances of search dedicates to you.

6 UML model of information system for the diagnostic one of the Venetian building

For the requirements understanding and their code implementation the information system works with UML language, useful to describe with graphical formalisms the complex systems operation. Through the use cases, based on a description in text and graphical shape, is possible to describe the interactions between the components of the system. The diagrams of classes are of use to list in way sufficiently detailed the same components. Other diagrams, like the diagram of the flows, will be realized subsequently, during the implementation of the system.

The first phase (illustrated in figure 2) regards the identification of elementary data deals you from the several WP. From the cataloguing system developed has been extrapolated the necessary generalizations to rationalization both of data entry and use. They had been identified all the elements that need of the definition of a thesaurus shared between all WP. It's important in fact to share a common set of definitions that it is widest possible, in way of being able to increase the possibility to lead analysis on the information collections.

Therefore some scenes have been described step by step: they are the sequence that characterize a determined interaction between customer and system, or subsystem and system.

Corila databases interoperability

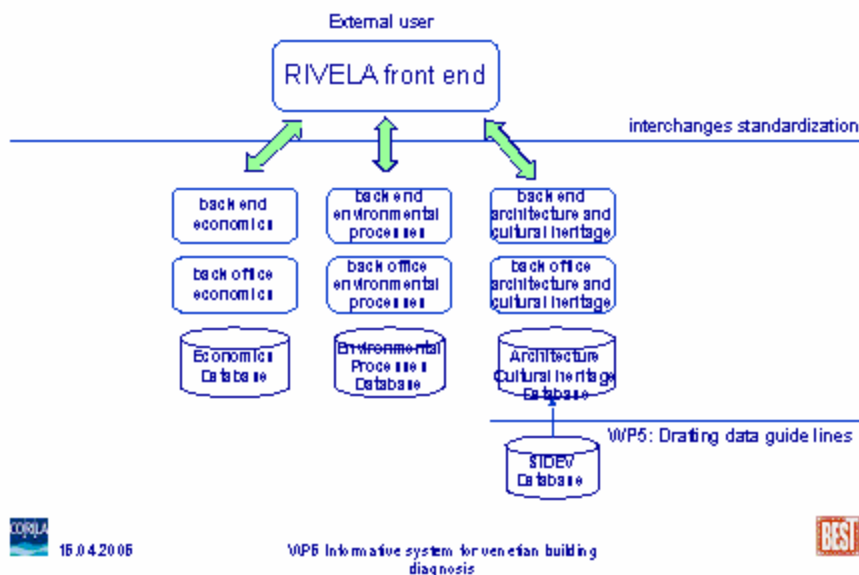


Fig. 2 – Work phases, from the analysis of the members of the information system is gone in the detail of the database, comprised the thesaurus. The application of the I.S. integrates the data supplies them to the customers, after the authorizations to the access. For the date entry they come *ad hoc* developed interfaces.

7 Conclusion

The conceptual plan demands not only the acknowledgment of the groups of users and the mutual collaboration, but the first interpretation of the relations between spatial information and local information.

To the definition of the users of information system often corresponds a directory of typologies reported to competences, roles, positions that are inside of processes. In truth beyond to the competences and roles, the communication between the groups is faced also and the possibility to surf inside various data set, as like as database users, or database processors.

To use data set and information from other user groups, must be offer a level of interoperability that does not force in rigid cages the job, but that it allows to share mutual the acquaintances on geographic and alphanumeric base. It is necessary an open system that allows trying new relations between observed phenomena, independently from observation scale.

Diagnostic and metric surveys, techniques, technologies and interventions will be stored updating information systems. Knowledge so collected can be worked by appropriate data mining. This way will be like one of the more interesting ways in order to develop theoretic and operational approaches to preservation of architectonic heritage, where every case is singular but not cut off from

context, so much that it will be, at the same time, exemplary of building and framework texture, where all is intimately and structural connected.

Corila databases interoperability

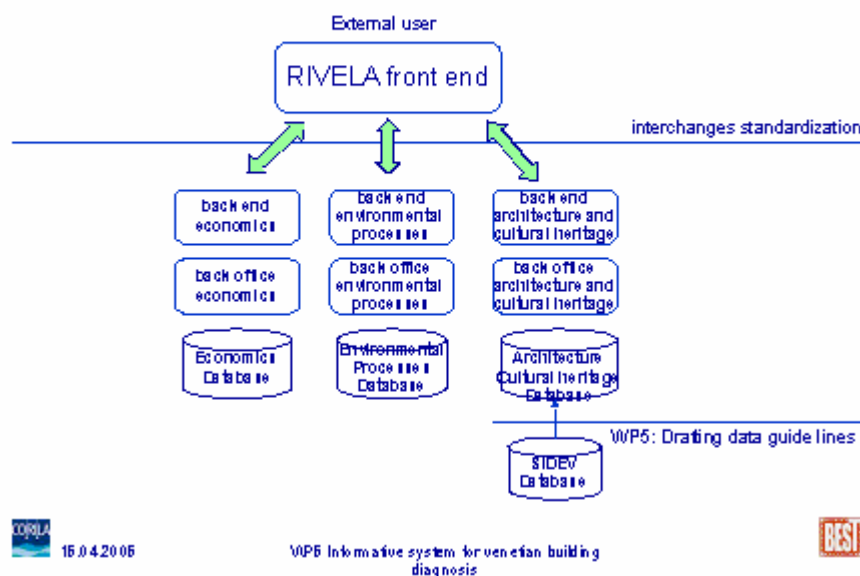


Fig. 3 – Corila database interoperability.

It is essential that the final product of the research is opened to other groups of users and decisional levels. The definition of objects passes from the phase of proposal to the operating phase through the work groups that of it articulate the definition.

This process must obviously recognize same ties:

- a) pluralism data processing;
- b) limited resources;
- c) cooperation in the management of the procedures and the combined developments.

These inner and external aspects to the system require answers in terms of interoperability of data, whose existence will be guaranteed alone if to the technologies (hardware, net and software abundantly involved in operations derived from norms and standard as how much product from ISO-International Organization for Standardization and OGC-Open Gis Consortium) will place side by side positively a turned semantic activity to the use trans- and interdisciplinary.

All the system will be subordinate to a political interoperability, revolt to sanction the legal value and the legal protection of the data. The interoperability will guarantee not by a unique System (comparable to the old hypothesis of a mainframe with several terminals), but a friendly front-end, accessible to all

workstations from a network.

RESTORATION WORKS IN THE CITY OF VENICE GEOTECHNICAL ASPECTS

Alberto Mazzucato¹, Andrea Dei Svaldi¹, Eleonora Dalla Corte¹

¹ Dipartimento DCA, Università IUAV di Venezia

Riassunto

Nello studio degli interventi di restauro e consolidamento riveste un ruolo fondamentale la conoscenza dei fenomeni d'interazione terreno-struttura che hanno caratterizzato il comportamento dell'opera nel tempo.

Tali aspetti assumono particolare rilevanza quando si interviene nella città di Venezia, dove le costruzioni sono in genere caratterizzate da cedimenti totali e differenziali elevati, conseguenza dell'eterogeneità stratigrafiche, delle diverse tipologie di fondazioni adottate (anche nell'ambito di uno stesso manufatto) e dell'entità delle tensioni trasmesse al terreno.

In tale ambito assume un ruolo fondamentale la definizione del modello geotecnico del sottosuolo con particolare riferimento alle caratteristiche stratigrafiche, alle proprietà fisico-meccaniche dei materiali ed alla distribuzione delle pressioni interstiziali.

Nell'articolo si presenta l'inquadramento generale del sottosuolo, sulla base dei risultati delle indagini geotecniche condotte nei diversi sestieri della città. Gli strati superficiali sono costituiti da argille limose di consistenza da molle a media, talvolta con sostanze organiche. In profondità sono presenti alternanze di argille compatte o di media consistenza e sabbie fini.

Viene infine affrontato il problema d'interazione terreno-struttura con riferimento al campanile di San Marco mediante l'impiego di modelli numerici in ambito elasto-plastico.

Abstract

In restoration and consolidation design the knowledge of the interaction between soil and structure plays a major role in structural behaviour over time. This aspect is particularly important when dealing with the city of Venice, where the buildings are generally characterized by important total and differential settlements as a result of stratigraphic variability and the pressure induced by different types of foundation.

The interaction between the construction and foundation as they develop over time must take the building's history into consideration making full use of archive sources and on-site inspections.

In this paper a general outline of the subsoil is presented, based on results from geotechnical investigations carried out in different areas of the city (sestrieri),

where the shallow layers consisting of soft medium silty clays and peaty soil alternate between deeper layers of compact medium clay and fine sand.

An attempted historical reconstruction of consolidation settlements relating to St. Mark's bell tower will be presented, as an example of soil structure interaction within the framework of critical state soil mechanics.

1 Introduction

Venice represents an example of architectural complexity due to its physical environment, construction materials and strong connection between stone and water. One of the basic considerations in analysing structure behaviour has to begin with foundation type as well as the dimensions, materials and state of decay.

A study of the existing foundations presents serious difficulties as a result of limited information concerning their construction and modifications undergone over time.

To carry out this type of analysis we need to adopt a multidisciplinary approach which will include geotechnical and structural aspects as well as an examination of the building's history.

2 Geotechnical characterization of the soil

Soil profiles concerning different parts of the city show remarkable differences. As an example of the stratigraphic variability of the city of Venice two different soil profiles are presented, one relating to the sestiere of Cannaregio, and the other referring to area of Dorsoduro (Fig.1).

The shallow normally consolidated cohesive layer is characterized by a compression index of $C_c=0.30-0.35$ and recompression index of $C_r=0.05-0.08$. For the deep layer the indices are $C_c=0.28$ and $C_r=0.05$.

The cone penetration resistance q_c of the underlying medium to dense sand and silty sand layers ranges from 4 MPa to 10 MPa. (Colombo 1971; Mazzucato 2004).

CANNAREGIO

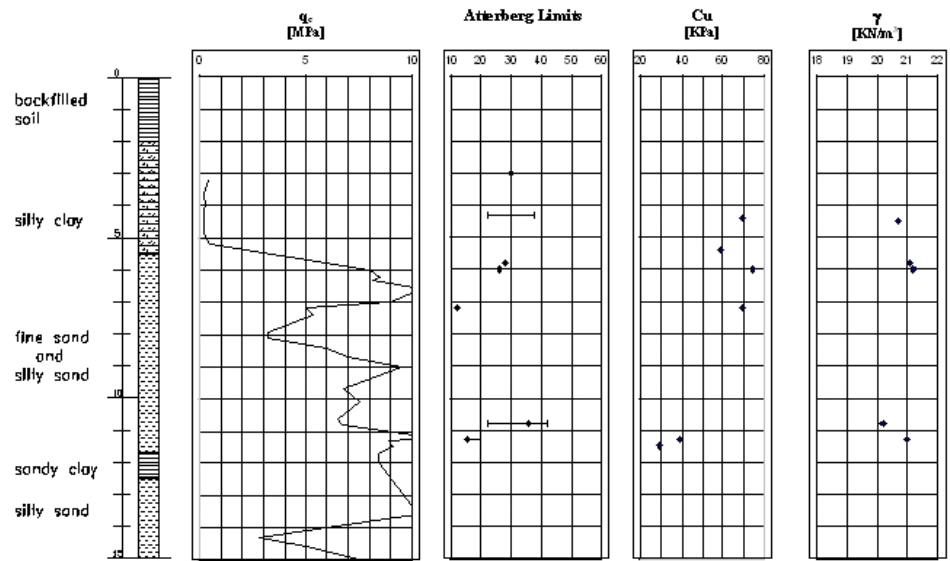


Fig. 1 - Cannaregio soil profile.

DORSODURO

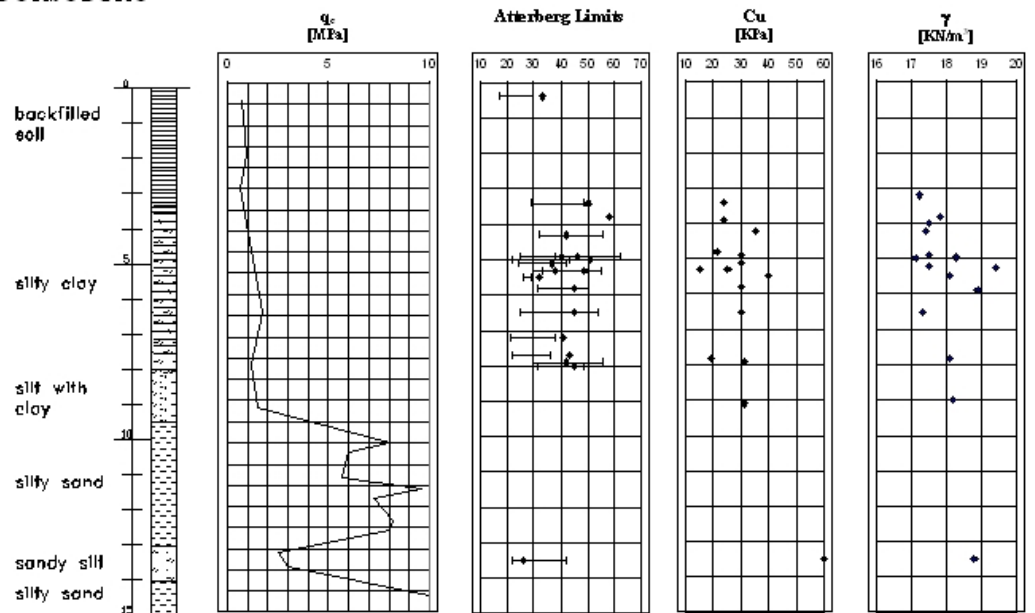


Fig. 2 - Dorsoduro soil profile.

3 Foundation typologies

Venetian foundations do not always evolve continuously along the building walls and often shallow and pile foundations are used under the same structure (Colombo, Colleselli 1997; Mazzucato 2004).

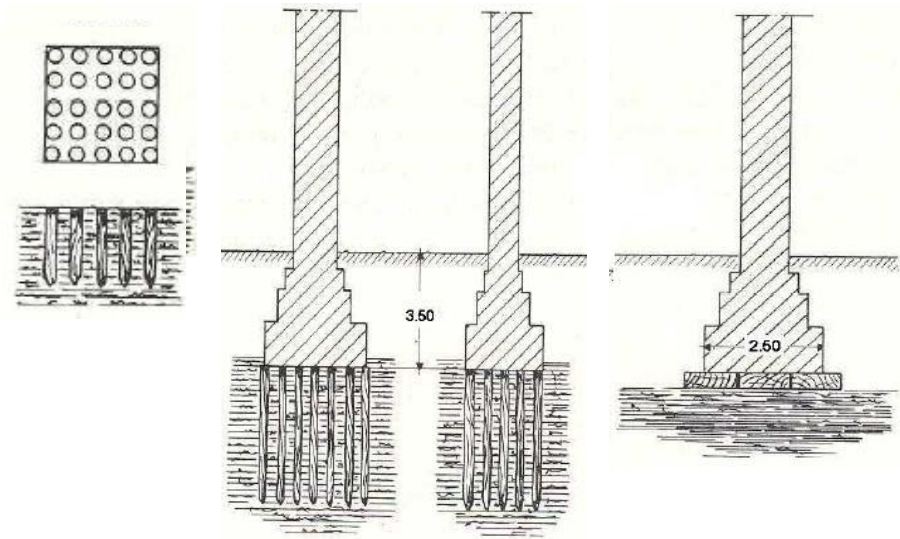


Fig.3 - Foundation typologies.

Generally the outer walls are built on wooden piles (larch, fir or alder), of 15–20 cm in diameter with lengths varying between 1.5m and 5 m in 9-10 number per m², connected by a wooden raft made up of two or three layers of 5-10 cm thick planks.

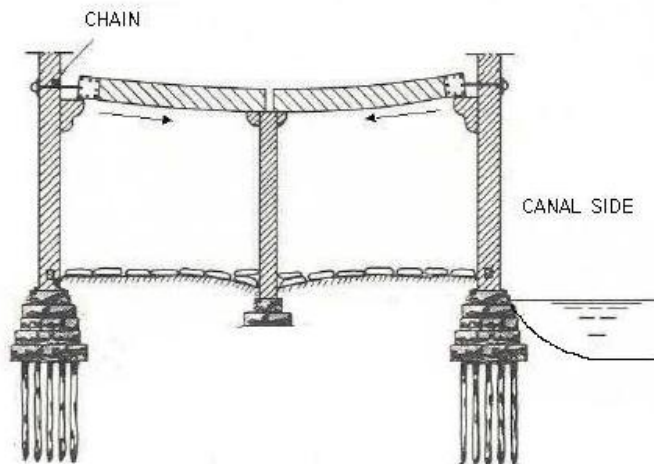


Fig.4 - Typical structural building scheme.

Pile length depends on stratigraphic variability and in particular on the depths of layers with better mechanical characteristics.

An in-depth historical investigation is useful in determining the geometry of the structure and foundation (depth and width), as well as the materials and building methods employed. It also enables us to estimate load distribution over time in addition to carrying out a soil structure interaction study. It is important to underline the contribution of the various disciplines concerning building approaches when applied to the unique case of Venice.

4 Analisi dei carichi e cedimenti

Once the structural scheme is defined, load evaluation allows us to calculate the pressure at the foundation level and any consequent settlements.

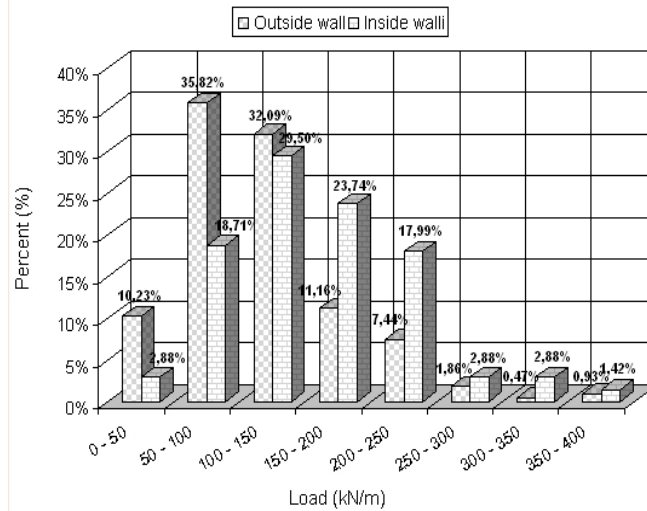


Fig. 5 - Range of foundation loads.

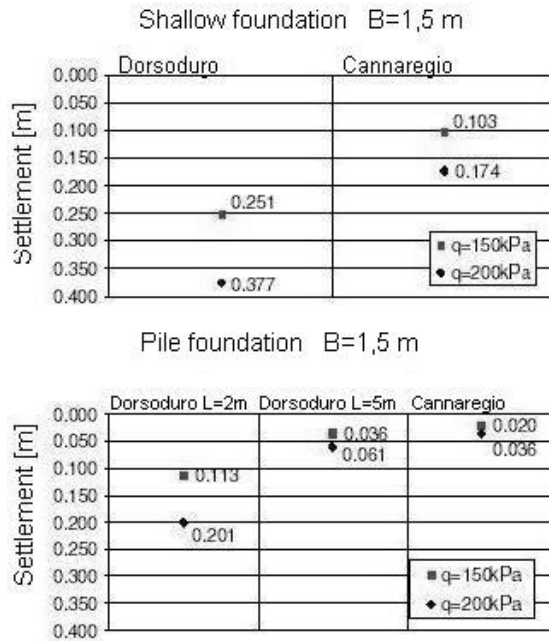


Fig. 6 – Settlements.

As far as Venetian buildings are concerned wall load generally ranges from 150 to 200 kN/m (Zuccolo 1975) (Fig.5).

Fig 6 reports an estimate of shallow and pile foundation settlements based upon the stratigraphy of Cannaregio and Dorsoduro.

In the case of Dorsoduro piles of 5 m in length, driven below the foundations,

reach sandy layers to greatly reduce settlements.

5 Settlement of St. Mark's bell tower

A numerical analysis to calculate the settlement relating to St. Mark's bell tower was carried out based on the soil characteristics around St. Mark's church (Gajo *et al.* 1997; Dei Svaldi *et al.* 2001). Foundation dimensions and estimated load history were similarly taken into account.

In Fig.7 the foundation section of the bell tower and soil profile are reported before 1912 and after reconstruction as published by D. Donghi (1912).

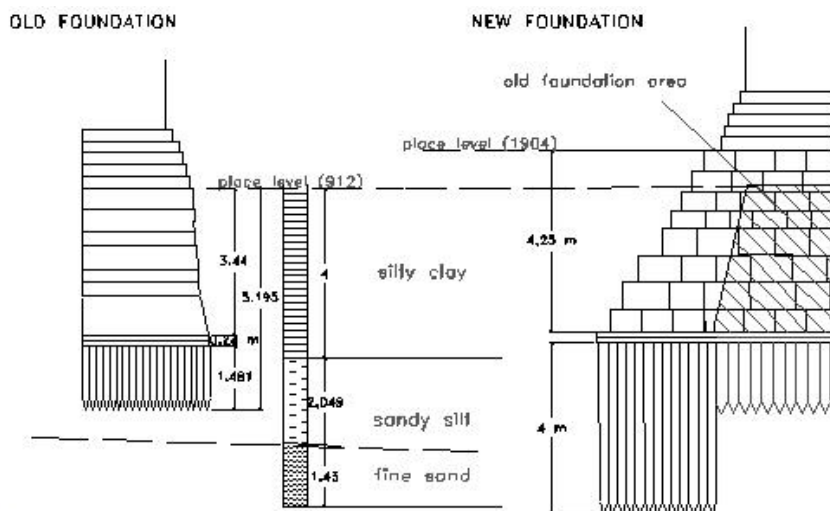


Fig.7 - Sections of the bell tower foundations before and after its collapse.

An axial symmetrical analysis was made based on an equal circular surface of 222 m² relating to the earlier foundation and 405 m² for the reconstructed one.

Fig.8 shows the finite element mesh and parameters of the isotropic hardening elastoplastic constitutive model (Modified Cam Clay) adopted to represent mechanical soil behaviour. In the analysis no account was taken of secondary settlement.

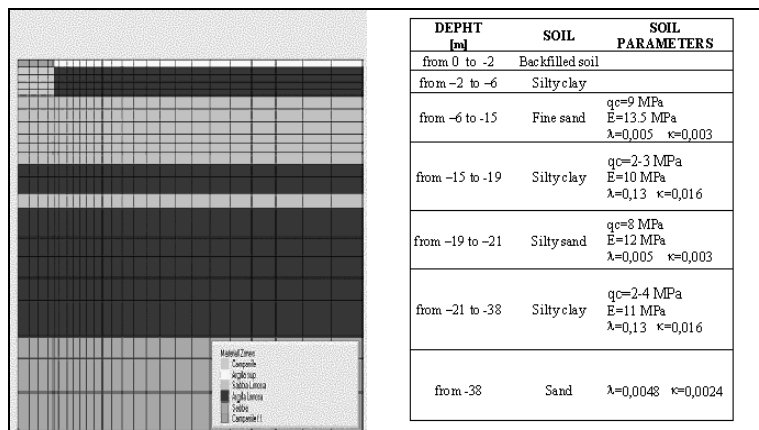


Fig 8 - Mesh and soil stratigraphy.

Load history relating to both before and after the collapse were based on various sources and data published by G.Gattinoni (1904) and G.A.Fradeletto (1912).

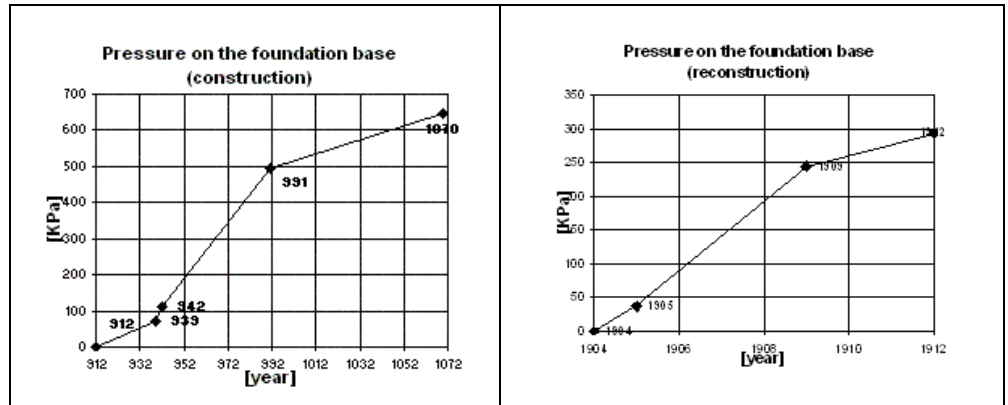


Fig.9 - Reconstruction of load history.

Fig.10 reports the time-settlement curve obtained by numerical simulations. Settlement estimated after the building's completion in 1072 is 45 cm. In 1904 the tower fell down for structural reasons and, following rubble removal, a ground swell of 10 cm resulted. The settlement calculated for the successive reconstruction is about 7 cm.

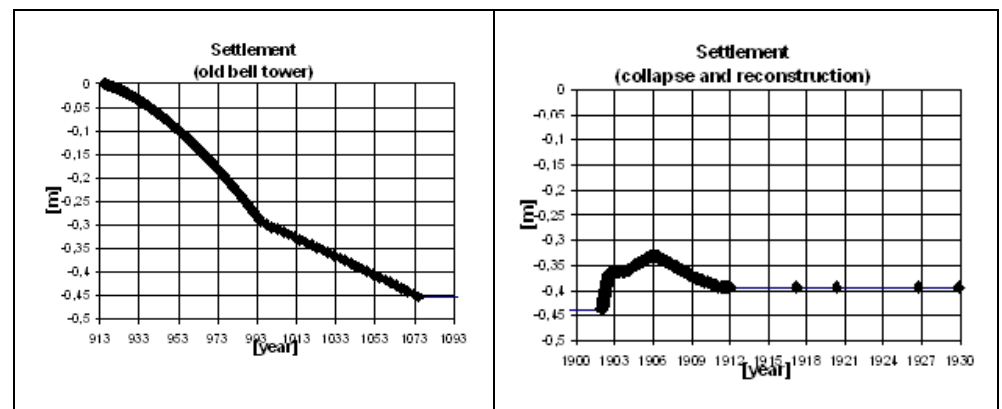


Fig. 10 - Bell tower settlement calculations.

6 Final remarks

A correct approach for studying foundation works in the city of Venice involves various aspects to define load distribution. In addition historical investigation, providing construction method and material information, allows for an understanding of how the building developed over time.

Such data and a detailed geotechnical investigation made the soil structure interaction study possible in order to define the preservation and restoration activity.

Fig.11 reports the possible contribution made by various disciplines involved in the conservation of Venetian buildings.

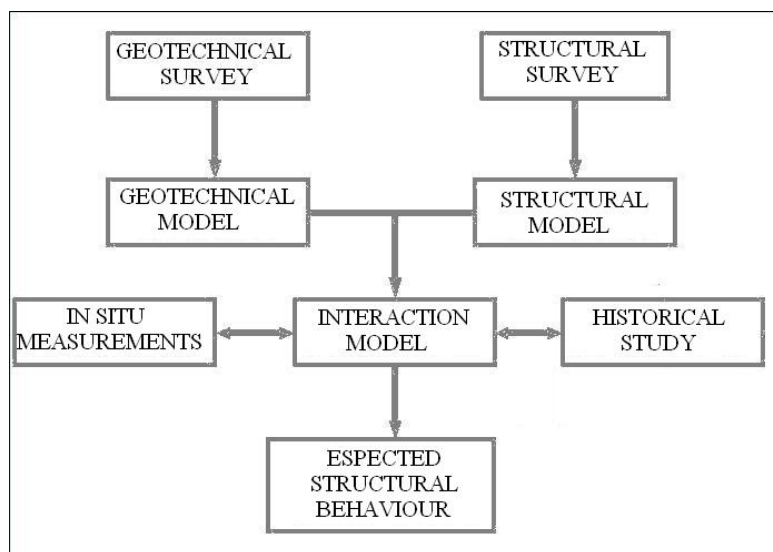


Fig. 11 – Contribution of different disciplines in soil structure interaction analysis.

References

- Colombo P.,1969. Il sottosuolo ed i problemi geotecnici di Venezia Mestre e Marghera.VII Convegno Nazionale di Geotecnica, Cagliari.
- Colombo P.,Colleselli F.,1997. Preservation problems in historical and artistic monuments in: Geotechnical engineering for the preservatinon in Historic sites, Viggiani (ed) , Balkema,Rotterdam.
- Dei Svaldi A., Mazzucato A., Soranzo M., 2001.A survey of the situation of three Basilicas situated in North Italy – Proceedings 2nd International Congress on Studies in Ancient Structures, Istanbul.
- Donghi, D.,1913. La ricostruzione del campanile di S. Marco a Venezia, Roma, Stab. tip. del genio civile, 1913 ,Estr. da: Giornale del genio civile, anno 1913.
- Fradeletto A.,1912. Il campanile di San Marco riedificato : studi, ricerche, relazioni .
- Gaio A., Soranzo M., Vitaliani R., 1997. Subsoil characteristic and foundation settlement analysis of St.Mark's basilica in Venice, in: Geotechnical engineering for the preservatinon in Historic sites, Viggiani (ed) , Balkema,Rotterdam.
- Gattinoni G.,1912.Il campanile di San Marco in Venezia Venezia , Tip. libreria emiliana.
- Mazzucato A., 2004. Consolidamenti e sottofondazioni nella città storica, Istituto Veneto di scienze, lettere ed arti, Venezia.
- Zuccolo G., 1975. Il restauro statico nell'architettura di Venezia ,Venezia, Ist.

veneto di scienze, letter ed arti.- Commissione di studio dei provvedimenti per la conservazione e difesa della laguna e della città di Venezia; 6.

FROM THE ARTIFICIAL STONE TO THE REINFORCED CONCRETE: DATA SYSTEM PROJECT FOR DIAGNOSTICS

Marco Pretelli¹, Alice Matteini², Isabella Daga²

¹*Soprintendenza di Venezia per i Beni Architettonici e per il Paesaggio*, ²*Dipartimento di Storia dell'Architettura, Università IUAV di Venezia*

Riassunto

La ricerca è finalizzata a definire un corretto percorso di analisi dello stato di conservazione di manufatti realizzati in pietra artificiale cementizia che, partendo dall'analisi delle forme di degrado, aiuti a definire metodologie e tecniche di intervento che rispettino la natura del materiale.

Il materiale, nella sua particolare funzione decorativa, è stato studiato dal punto di vista chimico-mineralogico, tecnologico, funzionale e in rapporto ad un ambiente aggressivo come quello lagunare.

L'ampio impiego di questo materiale nell'edilizia veneziana dei primi decenni del Novecento e la mancanza di una adeguata trattazione scientifica dei problemi conservativi del materiale cementizio con funzione decorativa hanno reso necessario definire un protocollo per la raccolta dei dati geometrici e materici e una fase di verifica sperimentale dei dati raccolti in situ.

Abstract

The research is oriented to define the correct procedure to analyse the good state of artificial stone decorations in order to determine, beginning from the deterioration, the methodologies and the techniques of intervention to respect the material.

The artificial stone has been analysed from a chemical-mineralogical, technological, functional point of view with a special attention to the aggressiveness of the lagoon environment.

The large use of concrete material in the decoration of venetian buildings of the early XX century and the lack of scientific treatment of artificial stone conservation made a protocol for data collection and experimental data control necessary.

1 Introduction

The technologies of the artificial stone making that have been used at the beginning of its utilisation, between the end of the XIX century and the early XX century, have been studied and analysed through the bibliographic and documentary research.

The realisation of a real artificial stone became possible just with the introduction of the cement: the new binding permitted to obtain a product marked by resistance and durability that are similar to the ones of the lithoid materials.

Moreover, the cementitious mortar, unlike the common lime, could tolerate the standard surface finishing of the lithoid materials such as the stone-cutter's chisel and the stone dressing.

During the first years of the utilisation of the concrete with a decorative function the imitation of natural stone was essential not only at an aesthetic level: the artificial stone was used with functions that were common to lithoid materials both for what concerns the decorative elements (coating, jamb, etc..) and the static elements (bracket, architrave, etc..).

Basically, the utilization of the concrete decorations is referable to two different tendencies: the "coating artificial stone", which aims to obtain surfaces similar to the ones made by natural stone in all its different kinds and the "sculptured cement" which, beginning from the imitation of traditional shapes of the natural stone, defines an application field, a technical process and a new figurative repertoire.

The "coating artificial stone"(Fig.1), as the ashlar-works and the "bozzati" and the linear frames were realized directly in the building yard using the "modine" whereas the "sculptured cement" (Fig.2), as the bass-relief and the full-relief, were realized in the cementer's laboratories through the utilization of moulds. The technique consisted in the creation of a model, usually made by clay, from which they made the mould for the mixture.

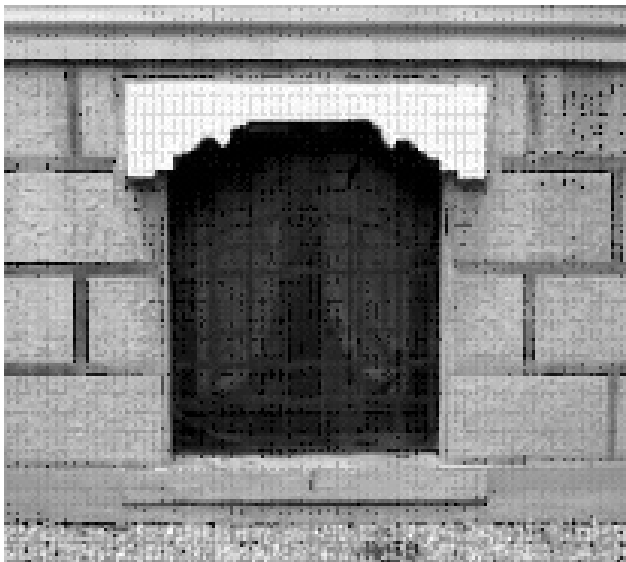


Fig.1- Example of "bozzato" realized in the building yard

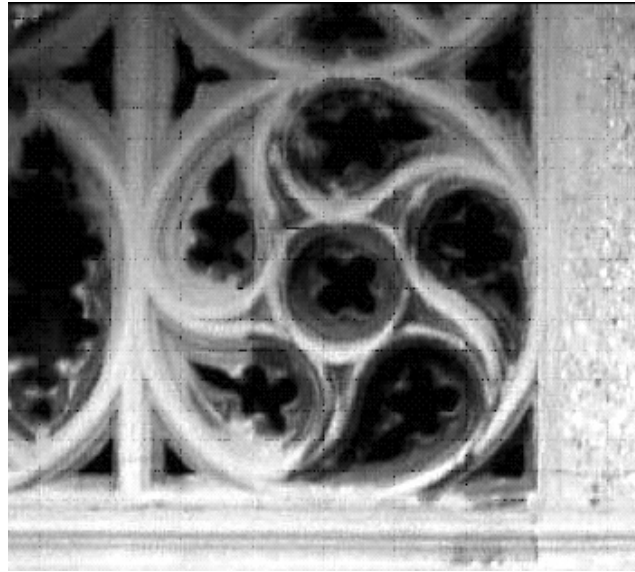


Fig.2- Example of "sculptured cement" realised in cementser's laboratories.

The mould (Fig.3) was made with different kinds of material: plaster, glue, sand, wood, metal, wax and clay.

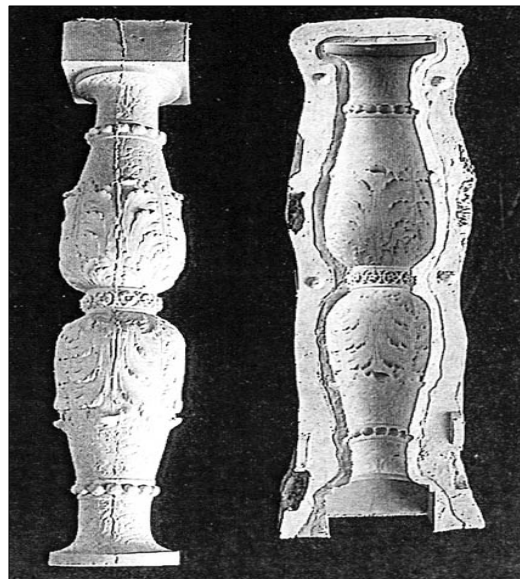


Fig.3- Mould made with plaster.

When the mould opened, the concrete could appear unhomogeneous, spotted or covered by a green coat of cement that settled on the surface of the concrete during the setting.

In order to remove the green coat they used mechanical instruments such as metal brushes, sharp chisels or corrosive solutions as sulphuric, nitric and muriatic acid.

The surface finishings, as the "bocciardatura" or the "martellinatura", were normally done after 15-20 days from the concrete casting, when the hardening

was not completed yet and they gave to the concrete a look similar to the lythoid one.

2 Studied object

The “Casa Bizantina” in rio del Gaffaro (Fig.4) was built between 1905 and 1907 and was based on a project drawn by Giuseppe Torres(1872-1935) some years before. The venetian architect, one of the most important planners of the early XX century, repropose the theme of the Middle Age house, through elements evidently ispirated to the byzantine and late gothic style.

The decorative elements as the frames of the double lancet windows or the stone denticulate take inspiration from the historicism but are freely disposed and combined following a personal and original rethinking.

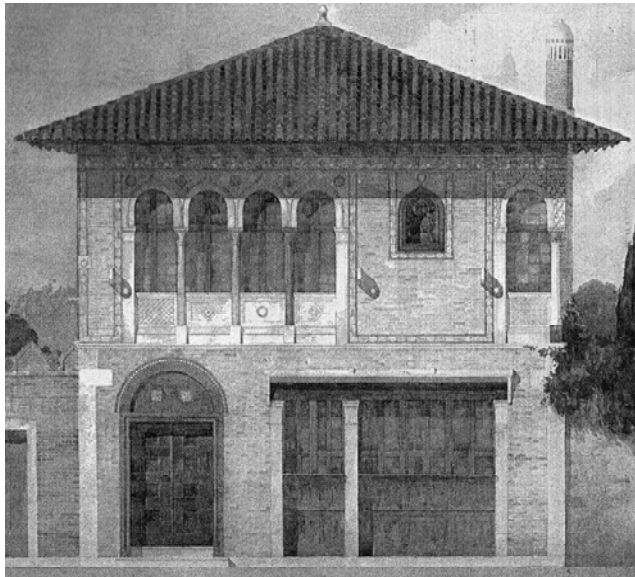


Fig.4- “Casa Bizantina” in Rio del Gaffaro, Venice.

The fencing parapet is the only element made by artificial stone (Fig.5).

It is articulated in three modules framed by 4 little smooth pillars realized in artificial stone (Fig.5). The parapet is characterized by the alternation of a wheel decor (Fig.6) composed by 5 fretworked drops which are disposed around a circle motif and a fretworked eye decoration.

The whole element was produced in different parts in a cementser’s laboratory probably through the technique of the clay mould, and afterwards collected in the building yard as it appears from the jointing lines.



Fig.5- Parapet in artificial stone, Casa Bizantina in Rio del Gaffaro, Venice



Fig.6- Detail of the wheel décor, Casa Bizantina in Rio del Gaffaro, Venice.

3 Protocol for data collection

In order to collect the geometrical and materic data of the studied object, we have used a cataloguing system that has permitted a standard reading of all its characteristics.

The cataloguing is divided in three parts: general informations about the object, the macroscopic description of the concrete and the weathering. Each part is referred to different aspects that give a detailed description of the phenomena through a standard key.

For example, the general information paper shortly analyses each element (wall, floor, door, pillar, etc...), its exposure characteristics (area, environment,

etc...), its location (ground, overhang, joint, etc...), its structural behaviour (compression, traction, etc...) and its mix design (reinforced, not reinforced, covered, etc...).

4 Experimental data control

The experimental data control section consisted of the production of 8 sample made by artificial stone following different recipes taken from the specialistic reviews of the early XX century.

The samples that have been realized in collaboration with the “Centro di Formazione Maestranze Edili Mestre”, were put in wooden formworks (Fig.7) that have the sizes of 1m x 0,2m x 0,2m with a volume of 0,04m³ reinforced with 6mm iron rod.



Fig.7- Wooden formwork

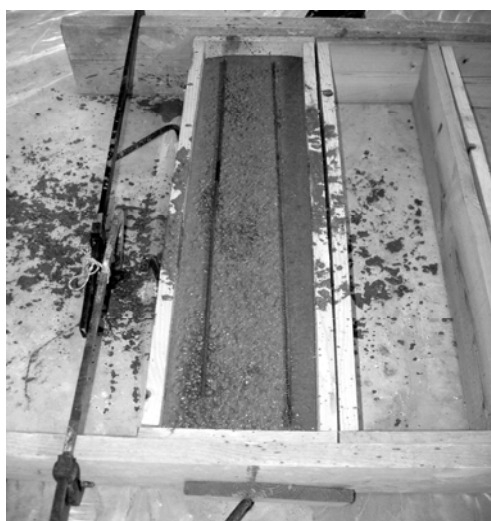


Fig.8- Iron rod.

- Sample 1. Recipe taken from *La resistenza delle pietre artificiali in cemento*, "Il Cemento", IX, n.2, 1912, pag. 29-30: "450kg di Portland, 0,4m3 di sabbia silicea setacciata, 0,8m3 ghiaietto siliceo, impiegata per cornicioni di sporgenza considerevole". The sample has been realized with the following proportions: 14kg Portland, 22Kg siliceous sand, 43Kg siliceous gravel.
- Sample 2. Recipe taken from *La resistenza delle pietre artificiali in cemento*, "Il Cemento", IX, n.2, 1912, pag. 29-30: "350kg di Portland, 0,4m3 di sabbia silicea setacciata, 0,8m3 ghiaietto siliceo, correntemente adoperata". The sample has been realized with the following proportions: 12kg Portland, 23Kg siliceous sand, 45Kg siliceous gravel .
- Sample 3. Recipe taken from *La resistenza delle pietre artificiali in cemento*, "Il Cemento", IX, n.2, 1912, pag. 29-30: "300kg di Portland, 0,4m3 di sabbia silicea setacciata, 0,8m3 ghiaietto siliceo, impiegata per costruzione di edifici meno importanti". The sample has been realized with the following proportions: 10kg Portland, 23Kg siliceous sand, 46Kg siliceous gravel.
- Sample 4. Recipe of Edoardo Campese, a cementser who worked in Venice in the early XX century (oral testimony): "1 sacco di cemento, 3 carriole di sabbia". The sample has been realized with the following proportions: 25Kg Portland, 80Kg siliceous sand.
- Sample 5. Recipe of Edoardo Campese, a cementser who worked in Venice in the early XX century (oral testimony): "1 sacco di cemento, 3 carriole di sabbia, selce". The sample has been realized with the following proportions: 25Kg Portland, 80Kg siliceous sand, 2% firestone.
- Sample 6. Recipe taken from *Alcune miscele per pietre artificiali in cemento*, "Il Cemento", X, n.1, 1913, pag. 14-15: "Pietra d'Istria: 2 parti in volume di granelli di Pietra d'Istria, una parte in volume di cemento bianco, polvere di marmo". The sample has been realized with the following proportions: 60Kg di Istrian stone(0,6-1,5mm), 30Kg white cement, marble powder.
- Sample 7. Recipe taken from *Manuale pratico per la lavorazione della pietra artificiale*, Firenze, 1936: " 200Kg cemento bianco, 0,37Kg arancio di cadmio, 0,13Kg giallo di Cadmio, sale grosso, polvere di marmo". The sample has been realized with the following proportions: 30Kg pigmented cement, 30Kg white cement, 30Kg marble powder, coarse salt, 0,1Kg cadmium orange, 0,06Kg cadmium yellow.
- Sample 8. Recipe taken from *Le pietre artificiali nell'architettura*, "Il Cemento", IV, n.1, 1908, pag. 17-18: "il nucleo interno è formato da 1 parte in di cemento e una parte di ghiaietta mista a sabbia, il

rivestimento esterno da 1 parte di cemento, 1 parte e mezzo di sabbia. The sample has been realized with the following proportions: inside 20Kg Portland, 20Kg siliceous sand and siliceous gravel, outside 10Kg Portland, 30 Kg siliceous sand.

The 8 samples have been treated with the typical surface finishings of the natural stone and afterwards they will be subjected to the following artificial ageing tests: chill-thaw cycles (-5°C - 35°C), imbibition with salts coming from the ground (nitrates, sulphates, chlorides) and wetting-drying cycles with salty solutions.

5 Conclusions

The research has the aim to define an approach to the artificial stone restoration problem that will guarantee the best conservation and the respect of the material.

The bibliographic and documentary research, the protocol for data collection and the experimental data control will concur to the creation of a data system about the diagnostics and the strategy of intervention in order to preserve the artificial stone elements.

References

AA.VV., 1993. Calcestruzzi antichi e moderni: storia cultura e tecnologia, Atti del convegno di studi di Bressanone 6-9 luglio 1993, Padova.

Biscontin G., Driussi G., 2004. Architettura e materiali del Novecento. Conservazione, Restauro, Manutenzione, Atti del convegno di Studi Bressanone 13-16 Luglio 2004, Venezia.

Bossaglia R., 1987. Archivi del Liberty Italiano, Architettura, Milano.

Cavallini M., Chimenti C., 1996. La pietra artificiale. Manuale per il restauro e il rifacimento delle decorazioni plastico-architettoniche delle facciate, Firenze.

Domenichini R., 2001. Giuseppe Torres 1872-1935, inventario analitico dell'archivio, Venezia.

Giola V., 2001. Per una caratterizzazione dei cementi decorativi Liberty, in "Lo stucco. Cultura, tecnologia, conoscenza", Atti del Convegno di Studi Bressanone 10-13 Luglio 2001, Venezia, pag.358-363.

Nelva R.,1995. Calcestruzzi armati e pietre artificiali nei primi anni di applicazione del "béton armé" in Italia. Recupero e conservazione, anno I, n. 3 , pag. 29-39.

Perocco G., 1977. Aspetti del Liberty a Venezia. In "Situazione degli studi sul Liberty", Atti del convegno internazionale di Salsomaggiore Terme by Bossaglia R., Cresti C., Savi V., Firenze, pag. 153-158.

Pretelli M., 2002. Il liberty e l'architettura eclettica al Lido di Venezia. Un

patrimonio a rischio, in "Tra Tardo Eclettico e Liberty: Architettura, decorazione e arredo nel territorio lagunare, Itinerari storico-artistici" , IV Settimana per la Cultura 15-21 aprile 2002, Soprintendenza di Venezia per i Beni Architettonici e per il Paesaggio, Venezia, pag. 22-23.

Romanelli G., 1972. Architetti e architetture a Venezia tra Otto e Novecento. *Antichità viva*, XI, n.5, pag. 25-48.

Romanelli G., 1977. L'architetto Torres e il liberty, in "Situazione degli studi sul Liberty, Atti del convegno internazionale di Salsomaggiore Terme", Firenze, pag.245-253.

Romanelli G., 1985. Nuova edilizia veneziana all'inizio del XX secolo. *Rassegna*, n.22, pag.10-17.

Romanelli G. 1985. Il sogno secessionista di Giuseppe Torres, in "Le Venezie possibili, Da Palladio a Le Corbusier", by Puppi L., Romanelli G., Milano, pag. 260-265.

Le pietre artificiali nell'architettura. *Il Cemento*, anno IV, n.1, 1908, pag.17-18.

La colorazione dei marmi artificiali. *Il Cemento*, anno IX, n.5, 1912, pag.77-78.

Gli utensili pneumatici applicati alla lavorazione delle pietre artificiali. *Il Cemento*, anno V, n.3, 1908, pag.67.

Il rifinimento delle superfici in cemento. *Il Cemento*, anno I, n.7, 1904, pag.221.

Finimento delle superfici in calcestruzzo. *Il Cemento*, anno IV, 1907, pag.68.

Colori per cemento. *Il Cemento*, anno VII, n. 21, 1910, pag.23.

Il trattamento esterno delle superfici in cemento. *Il Cemento*, anno VII, n.24, 1910, pag.379-383.

Il trattamento esterno delle superfici in cemento. *Il Cemento*, anno VII, n.23, 1910, pag.17.

La preparazione delle forme in gesso e altre in uso. *Il Cemento*, anno IX, n. 3, 1912, pag.38-40.

La preparazione delle forme in gesso ed altre in uso. *Il Cemento*, anno IX, n. 4, 1912, pag.58.

Impasto per pietra artificiale. *Il Cemento*, anno XII, n.4, 1915, pag. 62.

Posa in opera della pietra artificiale. *Il Cemento*, anno XII, n.7, 1915, pag. 98.

Confezione di malte e impasti per pietre artificiali. *Materiali da costruzione*, anno I, 1914, pag. 57.

AREA 3

Environmental processes

RESEARCH LINE 3.8

Speciation and flow of pollutants

Determination of trace elements and polycyclic aromatic hydrocarbons in the Venice aerosol (PM_{2.5})

A. Gambaro^{1,2}, L. Manodori¹, G. Toscano¹, R. Zangrando², W.R.L. Cairns², G. Capodaglio^{1,2}

¹Department of Environmental Sciences, University Ca' Foscari of Venice, ²Institute for the Dynamics of the Environmental Processes-CNR, Venice

Riassunto

In questo lavoro vengono presentati i risultati sulla determinazione di microinquinanti organici (IPA) ed inorganici (Li, Na, Mg, K, Ca, Cr, Ni, Rb, Sr, Cs, Ba, Pb, U, Cd, Al, V, Mn, Fe, Cu, Zn, Co) presenti nell'aerosol atmosferico PM_{2.5} della laguna di Venezia. Il campionamento è stato effettuato nell'estate 2004 in un sito presso l'isola di Mazzorbetto nella Laguna Centrale di Venezia.

Questo studio è parte di una ricerca più ampia che si propone di studiare i processi che contribuiscono all'apporto di microinquinanti alle acque della Laguna di Venezia e focalizza l'attenzione sulla valutazione dei flussi all'interfaccia acqua-atmosfera. L'analisi degli elementi in tracce ha rilevato delle concentrazioni comparabili a quelle ottenute in studi precedenti condotti nella Laguna di Venezia. Di particolare interesse sono i risultati ottenuti per Cd, Pb e Zn, che, oltre a presentare dei valori di concentrazione elevati, mostrano un andamento temporale diverso da quello degli altri elementi.

I risultati ottenuti per gli IPA indicano un diverso comportamento a seconda dei composti considerati. L'analisi temporale evidenzia l'esistenza di due gruppi di composti, il primo formato dagli IPA più "leggeri" e il secondo dagli IPA più "pesanti".

Abstract

The aim of this study is to establish the trace elements and PAH concentrations in aerosol (PM_{2.5}) in the Venice lagoon. Sampling was conducted at Mazzorbo, a small island at the centre of the Venice lagoon, during the summer of 2004. The study is a part of a bigger project titled "Balance of fluxes of organic and inorganic pollutants at the water-air interface of the lagoon of Venice". Comparison with the literature shows that the element concentrations obtained in this study are similar to those obtained in previous studies on the Venice lagoon. Cd, Pb and Zn concentrations are high and show a temporal trend different to other elements. The temporal evolution of PAH shows the existence of two groups, the "lightest" and "heaviest" PAH.

1 Introduction

Recent investigations indicate the following processes among those responsible for contaminating the Venice lagoon system: direct injection of industrial effluents in water, the atmosphere water exchanges, the water sediment

min at 0W, 20 min at 400W, 2 min at 0W, 20 min at 500W, 2 min at 0W, 3 min at 650W. The final solution was transferred in to LDPE bottles and diluted to 30 ml with ultrapure water. Concentrations of the trace elements were determined by an Inductively Coupled Plasma Quadrupole Mass Spectrometer (ICP-QMS, Agilent 7500) using an external calibration curve using multielemental standard solutions (ULTRAscientific, North Kingstown). The elements analyzed were: Li, Na, Mg, Al, K, V, Mn, Fe, Co, Ni, Cu, Zn, Rb, Sr, Cd, Cs, Ba, and Pb.

For PAH analysis the airborne particles were collected on quartz fiber filters that are cleaned at 400 °C for 5 hours. The sample filters were extracted 3 times with dichloromethane/n-hexane (3:1, v/v) in a PSE-ONE instrument (Labservice, Bologna), using a static phase of 10 min, a temperature of 100°C and a pressure of 120 bar. For quantitative determination, before the extraction, 50 ng of ¹³C-labeled phenanthrene (Cambridge Isotope Laboratories Inc., Austin) in n-hexane was added to the samples. Sample extract volumes (about 90 mL) were reduced to 0.5 mL under a gentle nitrogen flow in a Turbovap II instrument (Zimark, Massachusetts), and diluted to 5 mL with n-hexane. Clean up was performed by adding the sample to neutral silica columns in a Power Prep instrument (Labservice, Bologna), and eluting with 30 mL n-hexane and 20 mL dichloromethane/n-hexane (1:1, v/v). The eluates were reduced to 100 µl and 13 PAH in 13 chromatographic peaks (acenaphtylene (Acy), acenaphthene (Ace), fluorene (F), phenanthrene (Phe), anthracene (An), fluoranthene (Flt), pyrene (Py), benzo(a)anthracene (BaA), chrysene (Ch), benzo(b)fluoranthene (BbF), benzo(k)fluoranthene (BkF), benzo(a)pyrene (BaP) and benzo(g,h,i)perylene (BghiP)) were analyzed by a Hewlett Packard 5890 series II GC coupled with a MAT 95 XP, high resolution mass spectrometer (Thermo Finnigan). Gas chromatographic separation was performed on a fused silica capillary column (J&W Scientific DB-5MS, 60m × 0.250 mm × 0.25 µm). Data were acquired in the electron impact (EI) mode (45eV) using the Multiple Ion Detection (MID) mode. The operating conditions for PAH analysis were: injector temperature, 300°C; oven temperature program 1.5 min at 70°C, 10°C min⁻¹ to 150°C, 10 min at 150°C, 3°C min⁻¹ to 280°C, 55 min at 280°C; carrier gas (helium), constant flow, 1 mL min⁻¹, injection mode splitless (split valve open after 1 min) with purge flow 50 mL min⁻¹. Acquisition was made in MID mode, using the masse ranges: 151.5-152.5, 153.5-154.5, 165.5-166.5, 177.5-178.5, 183.5-184.5, 201.5-202.5, 227.5-228.5, 251.5-252.5, 275.5-276.5.

3 Results and discussion

3.1 Quality control

Quality control for the analytical procedure for trace elements analysis was performed by evaluating repeatability and recoveries, using a NIST Standard Urban Dust Reference Material (SRM-1648), and by determining the values of the blank. The repeatability of the method was obtained by element analysis of 4 aliquots (about 11mg) of NIST, using the methodology previously reported. The relative standard deviation (RSD%) of metal concentrations obtained ranged from 0.1% (Mg) to 20.3% (Cs) and were < 5% for 15 of the 19 elements.

The recoveries ranged from 84% (V) to 105% (Na) and generally all recoveries are greater than 80%, and for 10 of the 14 elements bigger than 90%. To evaluate and control possible sample contamination we analysed 6 "field-blanks". Greatest values were found for K (1.0 µg), Fe (0.50 µg), Na (0.3 µg), Mg (0.36 µg) and Al (0.27 µg), whereas lowest were found for Li (0.0004 µg), Rb (0.0004 µg), Cd (0.0009 µg) and Cs (0.0002 µg). The values obtained are comparable with those reported in the literature (Heal et al. 2005; Pekney et al. 2005). The limit of detection (LOD, ng) was calculated as the arithmetical mean concentrations of the field blank mass plus 3 standard deviations. The lowest value of LOD was found for Cs (0.00049 µg) while the highest value was found for K (1.5 µg). Comparison between trace element amounts in samples, in the field blanks, the repeatability and LOD show that all elements are present in quantities greater than the LOD, the field blanks aren't negligible and range from 1% (Pb) to 60% (Co) of the sample amount so the concentrations in the samples must be blank corrected.

For the PAH analysis, quality control was performed by evaluating repeatability and recoveries, by using the NIST Urban Dust (SRM-1649a), and by analyzing the field blank. The repeatability of the method was evaluated by the determination of PAH in 5 aliquots (about 75 mg) of NIST using the methodology previously reported. Relative standard deviations (RSD%) obtained ranged from 6% (Phe) to 19% (BaP) and it was < 15% for most PAH compounds. The recoveries are greater than 65% for all compounds and the lowest values were peculiar to PAHs with a smaller number of rings (F 68%, Phe 68%) whereas the highest values are typical of PAH with a major number of rings (Ch 99%, BkF 137%). To evaluate possible sample contamination during the whole procedure, 8 field-blanks were analyzed as samples. The greatest values were found for Py (28 ng) and Flt (6.2 ng) while the lowest values were found for BkF (0.07 ng), BbF (0.11 ng), BaP (0.11 ng) and Ch (0.12 ng). The lower values of LOD (mean blank amounts +3 standard deviation) were found for BkF (0.13 ng) and BaA (0.13 ng) whereas greater values were found for Py (34 ng) and Flt (7.1 ng). These values are comparable with those reported in literature (Gambaro et al. 2004b; Caricchia et al. 1999; Lee and Jones 1999).

Comparison between PAH amounts in samples, the field blanks and LOD show that all compounds are present in quantities greater than the LOD and the field blank are not negligible so the concentrations in the samples must be blank corrected.

3.2 Concentrations

Average concentrations and standard deviations of elements and PAH (13 identified compounds) in PM_{2.5} obtained in this study are reported in Tab. 1 and 2.

Tab. 1: Average concentrations and standard deviations of PAH in PM_{2.5}

PAH compounds	Mean concentration (ng/m ³)	Standard deviation (ng/m ³)
Acn	0.024	0.031
Ace	0.017	0.032
Fl	0.027	0.039
Phe	0.119	0.115
Antr	0.011	0.014
Ft	0.134	0.173
Py	0.504	0.705
B(a)A	0.010	0.015
Chr	0.027	0.016
B(b)F	0.044	0.022
B(k)F	0.013	0.008
B(a)P	0.021	0.021
B(g,h,i)P	0.028	0.015
ΣIPA	0.983	1.057

Tab. 2: Average concentrations and standard deviations of elements in PM_{2.5}

Element	Mean (ng/m ³)	Standard deviation (ng/m ³)
Li	0,04	0.03
Na	73	16
Mg	12	5
Al	20	17
K	99	74
V	5,1	3.2
Mn	2,6	1.7
Fe	36	25
Co	0,02	0.03
Ni	3,32	1.46
Cu	2,76	1.55
Zn	31	43
Rb	0,24	0.12
Sr	0,35	0.22
Cd	3,33	4.16
Cs	0,01	0.01
Ba	1,42	0.76
Pb	10	11

Temporal concentration profiles of PAH (ng m^{-3}) shows the existence of two groups. The first, composed of acenaphtylene, acenaphtene, fluorene, phenanthrene, fluoranthene and pyrene, shows a generally decreasing trend during the period of study. The second, composed of benzo(a)anthracene, chrysene, benzo(b)fluoranthene, benzo(k)fluoranthene, benzo(a)pyrene and benzo(g,h,i)perylene, shows a generally constant trend. In the first group there are PAHs with 3 or 4 rings and with a higher vapour pressure, whereas in the second group there are PAHs with 4,5,6 rings and with lower vapour pressure. A particular case is anthracene that has a temporal trend different from all others.

Fig. 3 shows the temporal trends of fluorene and benzo(a)anthracene.

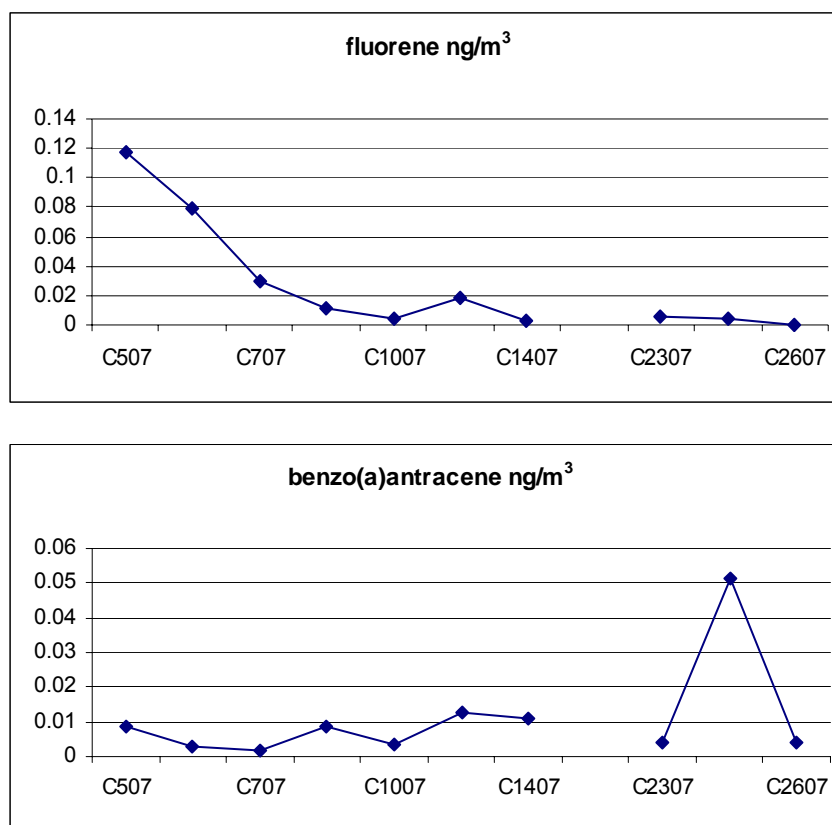


Fig. 3: Temporal trends of fluorene and benzo(a)anthracene.

The temporal trend of element concentrations (ng m^{-3}) shows a similar evolution for Li, Na, Mg, K, Mn, Ni, Cu, Fe, Ba, Rb and Sr, with the higher value at 22 July and a decreasing from 23 July. Also Zn has a similar temporal evolution but with a very high value concentration at 01 August. The same peak is present in the trend for Pb, but however, for the period from 16 July to 23 July it is unlike that of any other elements. Cd, Cs and V show a temporal trend different from all others.

Fig. 4 shows the temporal trends of Na, Cd and Pb.

Results obtained indicate the presence of different source for Cd, Zn, Pb and V

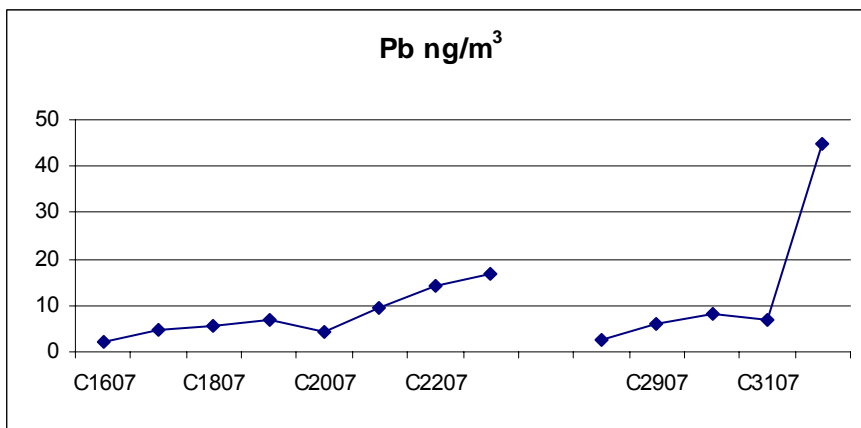
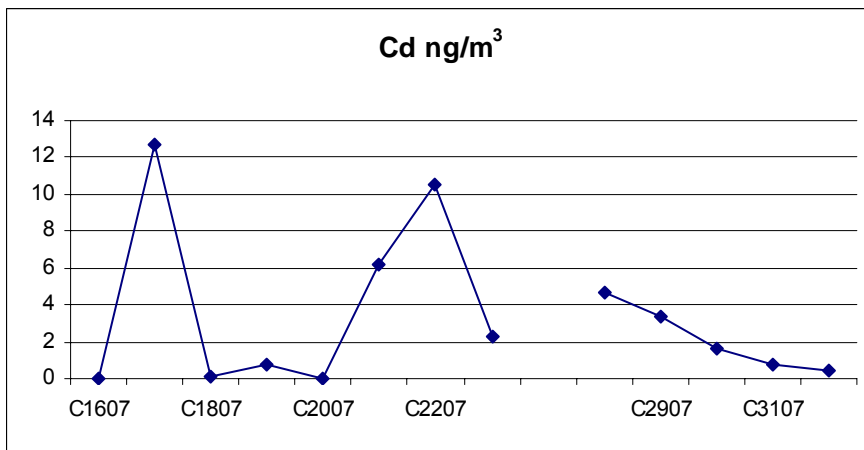
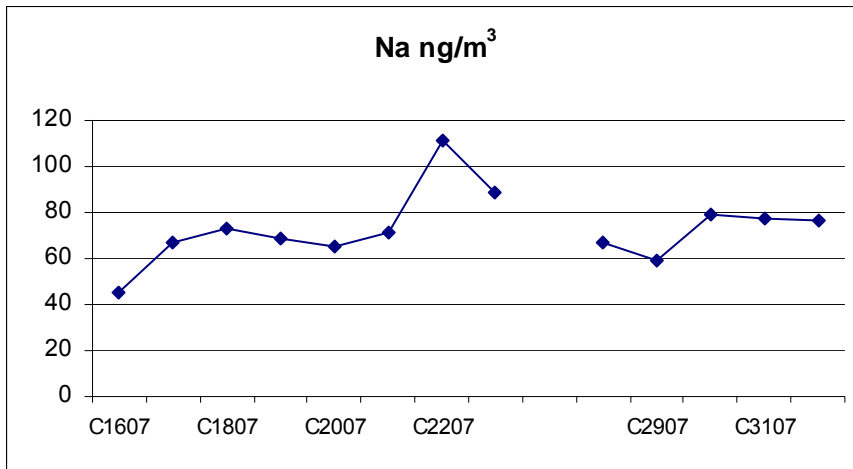


Fig. 4: Temporal trends of Na, Cd and Pb.

4 Conclusions

Trace elements and PAH concentrations in the PM_{2.5} were investigated for about a month at a site of the Venice Lagoon.

The study of the temporal evolution shows two groups of elements. The first consist of K, Fe that probably has a crustal origin. The second group including V and Cu probably have an anthropogenic origin. The temporal evolution of PAH shows the existence of two groups; the "light" and "heavy" PAH.

Acknowledgement

This work was supported by CORILA under the project 'Balance of fluxes of organic and inorganic pollutants at the air-water interface of the Venice lagoon' and by the National Research Council of Italy (CNR). They are also grateful to Valter Zampieri and Erika Mattiuzzo for technical support.

References

- Caricchia AM, Chiavarini S, Pezza M (1999) *Atmos Environ* 33:3731-3738.
- Gambaro A., Manodori L., Toscano G., Ferrari S., Varga A., Moret I., Capodoglio G. (2004a) *Environ. Sci. Technol.*, 38, 5357-5364.
- Gambaro A, Manodori L, Moret I, Capodaglio G, Cescon P (2004b) *Anal Bioanal Chem* 378:1806-1814
- Heal MR, Hibbs LR, Agius RM, Beverland IJ (2005) *Atmos Environ* 39:1417-1430
- Lee R.G.M., Jones K.C. (1999) *Environ Sci Technol* 33:705-712
- Pekney N.J., Davidson C.I. (2005). *Anal. Chim. Acta* 540:269-277

FUGACITY/AQUIVALENCE MODELLING FRAMEWORK OF CONTAMINANT (POPS AND HEAVY METALS) FATE AND TRANSPORT IN THE VENICE LAGOON

Julie Sommerfreund¹, Satyendra Bhavsar¹, Nilima Gandhi¹, Sarah Gewurtz², Miriam Diamond^{*1,2}, Silvia Giuliani³ And Mauro Frignani³

¹Department of Chemical Engineering and Applied Chemistry University of Toronto, TORONTO, Canada M5S 3E5 ²Department of Geography University of Toronto, TORONTO, Canada M5S 3G3, *Corresponding Author, ³ Istituto di Scienze Marine – Sezione di Geologia Marina, BOLOGNA, Italia 40129

Abstract

The sediment and water of the Venice Lagoon, mostly those of the industrial canals, have elevated concentrations of persistent organic pollutants (POPs) and trace metals. Present contamination levels in the lagoon are still of concern due to the potential for elevated concentrations in consumable species, namely clams and fish. In order to effectively manage the risk associated with elevated concentrations of contaminants in any system, it is essential to identify their main sources and dominant fate pathways. This paper outlines an integrated modelling framework developed for POPs and metals in the Venice Lagoon. The framework consists of models for metal speciation-complexation, chemical fate and transport, and POP transfer through the aquatic food web. The fate model uses fugacity-aquivalence as equilibrium criteria suitable for volatile and non-volatile compounds (Diamond et al., 1992), respectively. For metals, we use TRANSPEC, in which a geochemical model such as MINEQL+, which estimates metal speciation and complexation assuming equilibrium conditions, is loosely coupled to the fate model (Bhavsar et al., 2004a,b). For POPs, we use a mechanistic food web model (Gewurtz et al., in press) that uses water and sediment concentrations estimated by the fate model. The framework is mechanistically-based and generally applicable to POPs and metals in a variety of aquatic systems. Here we adapt it to include the hydrodynamic characterization of Solidoro et al. (2004b) and processes unique to the lagoon environment.

1 Introduction

The Venice Lagoon is a complex aquatic environment that is under pressure due to numerous competing current uses and past stresses. Among the stresses are past and present chemical emissions from industrial and municipal sources within the lagoon, in addition to inputs from tributaries (Secco et al., 2005) and atmospheric deposition (Guerzoni et al., 2004; Gambaro et al., 2004) (Figure 1). As a result, the sediment and water have elevated concentrations of persistent organic pollutants or POPs (e.g., polychlorinated biphenyls or PCBs and polychlorinated dibenzodioxins and furans or PCDD/Fs) (Secco et al., 2005) and trace metals (e.g., As, Pb, Zn) (Bellucci et al., 2002). Due to

improved technologies and enhanced emission controls over the last two decades, industrial inputs have been significantly reduced. Present contamination levels in the lagoon are still of concern due to elevated concentrations in consumable species, namely clams and fish (Secco et al., 2005).

In order to effectively manage the risk associated with elevated concentrations of contaminants in any system, it is essential to identify their main sources and dominant fate pathways. This can be achieved through fate and transport modelling in concert with measured data. Dalla Valle et al. (2003) developed a fugacity model to describe the fate of polychlorinated dibenzodioxins and furans (PCDD/F) in the Central Basin of the Venice Lagoon, assuming a single, well-mixed basin. Recent monitoring studies, however, have identified the lagoon as a heterogeneous environment with many varying physical chemical factors (Solidoro et al., 2004a). Dalla Valle et al. (2003) estimated that 99% of PCDD/Fs present in the model environment were contained in the top layer of the sediment and fugacity ratios suggested a net transfer of PCDD/Fs from sediment to water. Their analysis indicated a high degree of model sensitivity to active sediment depth, deposition and resuspension rates, in addition to, external loadings. Carrer et al. (2005) developed a "hybrid" deterministic-statistical model to estimate the fate and trophic transfer of PCDD/F, PCBs and selected metals in 516 grid squares (1 km width) in the lagoon. Their results showed the importance of external loadings as the main factor controlling the distribution of As and a representative PCB congener for which concentrations are highest in the north-central part of the lagoon and lowest nearby the lagoon outlets.

This paper presents a modelling framework developed for POPs and metals in the Venice Lagoon. We take an approach that builds on the fugacity approach used by Dalla Valle et al. (2003) and also incorporates hydrodynamic information (Umgiesser et al., 2004; Solidoro et al., 2004b) similar to Carrer et al. (2005). Our modeling framework uses fugacity-equivalence as equilibrium criteria suitable for volatile and non-volatile compounds, respectively, and speciation-complexation calculations from a loosely coupled geochemical model (Bhavsar et al., 2004a,b). For POPs, we use a mechanistic food web model that is loosely coupled to the fugacity fate model (Gewurtz et al., in press). As such, the framework is mechanistically-based and respects the chemistry of organic compounds and metals, tailored to the lagoon through the hydrodynamic characterization of Solidoro et al. (2004b).

1.1 Modelling Background

Over the last 10 years numerous advances have been made in modeling contaminant behaviour of POPs (Wania and Mackay, 1999) and trace metals (Diamond, 1995; Bhavsar et al. 2004a,b), in aquatic environments. A fugacity-based fate model for aquatic systems was first introduced by Mackay et al. (1983, 1991) as the Quantitative Water Air Sediment Interaction (QWASI) model. The purpose of the model is to describe the dominant fate processes and distribution of organic contaminants, identify transport rates between

compartments, and estimate contaminant persistence. The model considers the fate of a contaminant in the environment distributed between three, well-mixed compartments (air, water and sediment) and their associated sub compartments (e.g., dissolved and particulate phases). The model assumes that the contaminant adopts this distribution instantaneously, with the particular distribution and fate processes depending on the contaminant's physical-chemical properties and the characteristics of the environment. The QWASI model has been applied and evaluated in many systems including arctic lakes (Freitas et al., 1997; Helm et al., 2002), the Great Lakes and its bays (Mackay and Diamond, 1989; Ling et al., 1993; Diamond et al., 1994) and estuarine systems (Lun et al., 1998).

Fugacity is the equilibrium criterion used for chemicals with a measurable vapour pressure POPs. In order to consider metals, equivalence was developed as an alternative equilibrium criterion (Mackay and Diamond, 1989). Models using either equilibrium criterion, fugacity or equivalence, consider the fate and transport of dissolved and particulate forms of chemical. Whereas this is reasonable for POPs which occur as single chemical entities, it is not satisfactory for metals that exist as multiple, interconverting species in water amongst truly dissolved, colloidal and particulate phases. The ability to distinguish amongst these forms and species is important due to their different physical chemical properties and toxicological effects. The limitation of the "traditional" fugacity/ equivalence model was addressed through the multispecies fugacity/ equivalence concept in which a mass balance is constructed for each species in each compartment (Diamond et al., 1992). Diamond et al. (2000) evaluated the multispecies model with mercury in the Lahontan Reservoir.

The first applications of the multispecies fugacity/equivalence model relied on measured fractions of metal species/forms (e.g., Diamond et al., 2000). This restricted the use of the model for predictive purposes and required ambient measurements of species fractions which can be difficult to obtain. Bhavsar et al. (2004a,b) improved upon the model by developing TRANSPEC which loosely couples a geochemical model that estimates metal speciation and complexation, with the multispecies fugacity/equivalence fate and transport model (Diamond et al., 1992). The first version of TRANSPEC coupled MINEQL+ (Schecher and McAvoy, 2001) to estimate the equilibrium concentrations of dissolved, precipitated and complexed fractions of cationic metals as governed by pH, alkalinity, redox potential and ionic strength. The estimated species fractions (for example fraction of ZnSO_4^0 relative to total Zn) are used by the fate and transport model which estimates the distribution of these species amongst the compartments. TRANSPEC has been successfully evaluated using steady-state and dynamic versions for Ross Lake (Bhavsar et al., 2004a,b).

Fugacity/equivalence mass balanced models have been shown to be a useful tool for identifying the critical factors in contaminant dynamics (e.g., Freitas et al., 1997), the estimation of contaminant concentrations of unmeasured contaminants in the long term (e.g., Diamond et al., 1994) in the absence of

empirical measurements (due to technical know how or cost), and to develop testable hypotheses on unknown conditions. Mass balance models lend themselves to synthesize large datasets into an understandable picture capable of testing and interpreting. Although, these models are limited by their assumptions, they provide an effective management tool to be used in conjunction with field and observational data. In addition, the models can provide valuable insight into the relative significance of transport pathways in the system of interest.

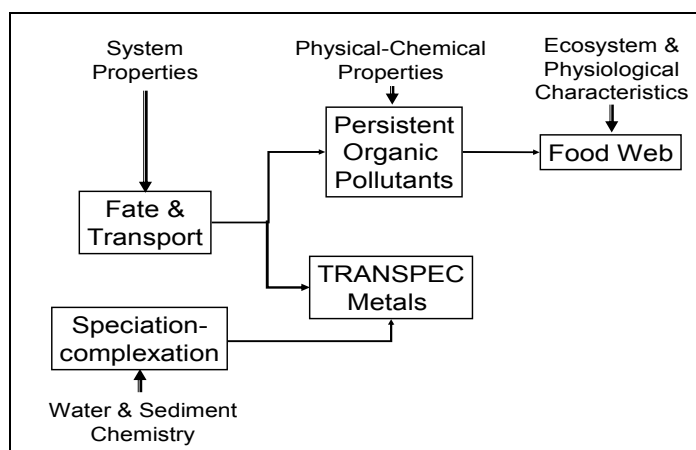


Fig. 1- Conceptual Model Framework.

2 Model Framework

The contamination of the Venice Lagoon requires the exploration of both POPs and trace metals. In order to elucidate the dominant fate and transport pathways and sources, as well as estimate concentrations, we use two modelling approaches. First, POPs are evaluated using a fate and transport model loosely coupled to a food web model (Gewurtz et al., in press). Second, the trace metals are modelled using TRANSPEC, for which the fate and transport model is the same as that used for POPs (Figure 1). In the first generation of models, we assume steady-state conditions that “average” diurnal variations due to tidal flows and seasonal variations in temperature.

2.1 Fate and Transport Model

A mass balance fugacity/aquivalence fate and transport model (QWASI based) was constructed and parameterized for the Venice Lagoon. We initially assume that the system is in steady-state in order to estimate long term conditions in the Lagoon given constant loadings. For each geographic segment, the model consists of three well-mixed compartments (water, upper sediment layer and deeper sediment layer) and their respective sub compartments (suspended sediments, pore water) (Figure 2) that are in equilibrium within the bulk compartment. Air is considered to have an infinite volume with a specified concentration, i.e., air concentrations are controlled by conditions external to the lagoon. The active upper sediment layer is 5 cm deep, as assumed by Dalla Valle et al. (2003). This depth represents the sediments that exchange directly

with the water column (Secco et al., 2005). Underlying the upper sediment layer is a lower sediment layer which exchanges via sediment mixing that is due to bioturbation and physical mixing processes.

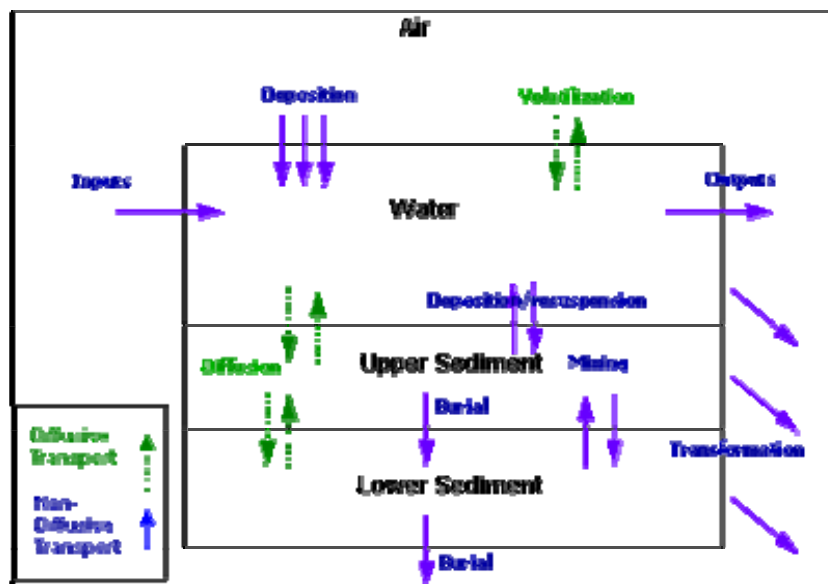


Fig. 2 – Processes considered in each geographic segment of the fate model of the Venice Lagoon.

A chemical moves vertically among compartments by diffusive (e.g., volatilization-absorption, sediment-water diffusion) and non-diffusive (e.g., atmospheric deposition, sediment deposition and burial) processes. It is ultimately lost via chemical transformation (e.g., biodegradation, hydrolysis) and burial to deep sediment.

In order to represent the heterogeneous environment of the Venice Lagoon, we have adopted the segmentation scheme developed by Solidoro et al. (2004b) in which they defined 10 segments (Fig. 3). This segmentation is based on the analysis of the spatial distribution of physical properties (salinity and water residence time) simulated by the model. The segmentation scheme is consistent with that suggested based on water quality parameters that indicate the heterogeneous nature of the lagoon (Solidoro et al., 2004a). Solidoro et al. (2004b) quantified the circulation pattern amongst the 10 segments using a 2-dimensional hydrodynamic finite flow model. This circulation model has been extensively evaluated and tested elsewhere (Umgiesser et al., 2004). Based on this flow regime, Solidoro et al. (2004b) estimated the residence times, water volume and areas of each segment, values which we use in our model.

The circulation model of Solidoro et al. (2004b) provides net flow amongst segments. In order to account for mixing among segments, we have calculated the gross flow in the dominant flow direction and backflow in the opposite direction. We approximated values for “forwards” and “backwards” flow among segments via calibration using chloride as a conservative tracer.

The fate and transport model requires input data for both environmental and chemical properties in addition to transport rates. These parameters include

ambient air concentration, suspended solids concentration, sediment porosity etc. Transport rates include atmospheric wet and dry deposition, rain rate, particle deposition, resuspension, burial and bioturbation rates. These values have been obtained from field studies, the literature, and calibration. To model POPs, we require the organic carbon content of each phase in each compartment of each segment. We also require the physical-chemical properties of each compound, including transformation rates which are poorly known.

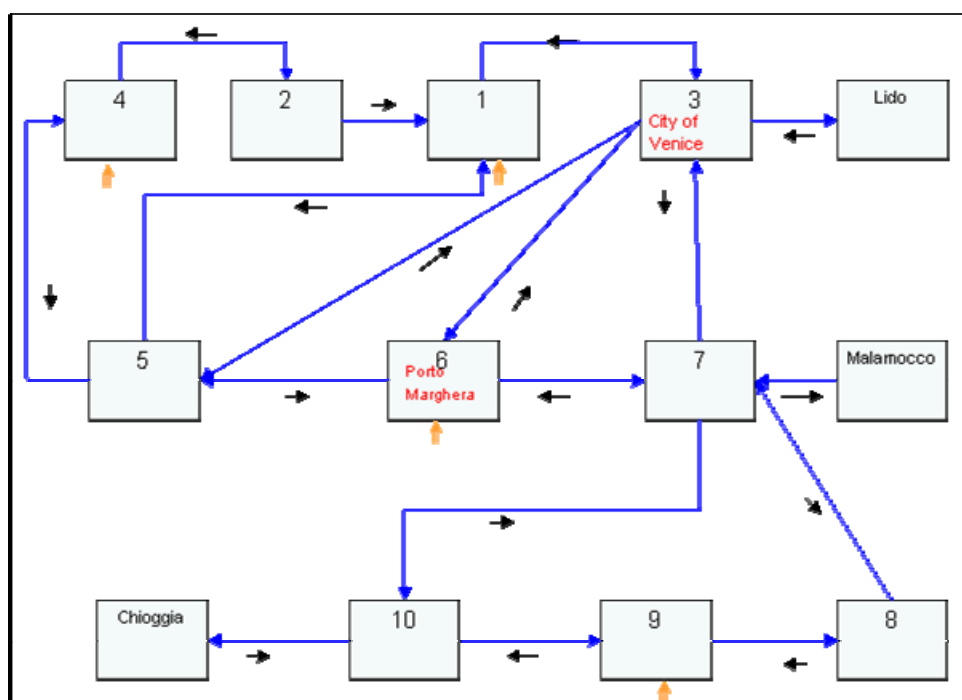


Fig. 3 – Circulation pattern and box numbers derived from Solidoro et al. (2004b). Segments 1-5 are located in the North Basin, 6&7 are located in the Central Basin, and, 8-10 are located in the Southern Basin. Large arrows indicate the dominant flow direction between segments while small arrows indicate back flow. Double arrows indicate tributary input.

2.2 Food web Model

The purpose of the food web model is to estimate the concentration of organic contaminants in the clams and fish consumed from the Venice Lagoon. The food web model is based on that by Campfens and Mackay (1997) and revised by Arnot et al. (2004) and Gewurtz et al. (in Press). The model considers chemical uptake and loss at each trophic level (bioconcentration and bioaccumulation) as well as trophic transfer (biomagnification). For each organism (except phytoplankton), chemical enters and is lost to and from the water through respiration (e.g., gill ventilation) and food (ingestion and egestion) (Figure 4). Water and sediment fugacities are inputs used to calculate the fugacities of phytoplankton and benthos, respectively, and uptake due to gill ventilation.

In the modelling framework, the food web model is constructed for two

segments. The first is Segment 6 due to proximity to the industrial area Porto Marghera and the availability of data. In addition, this area is subject to illegal clam fishing. Segment 2 is modeled in order to represent a “cleaner” region in the northern part of the lagoon. The model is parameterized and evaluated using data collected for polychaetes, clams and gobi (CORILA Research Line 3.8).

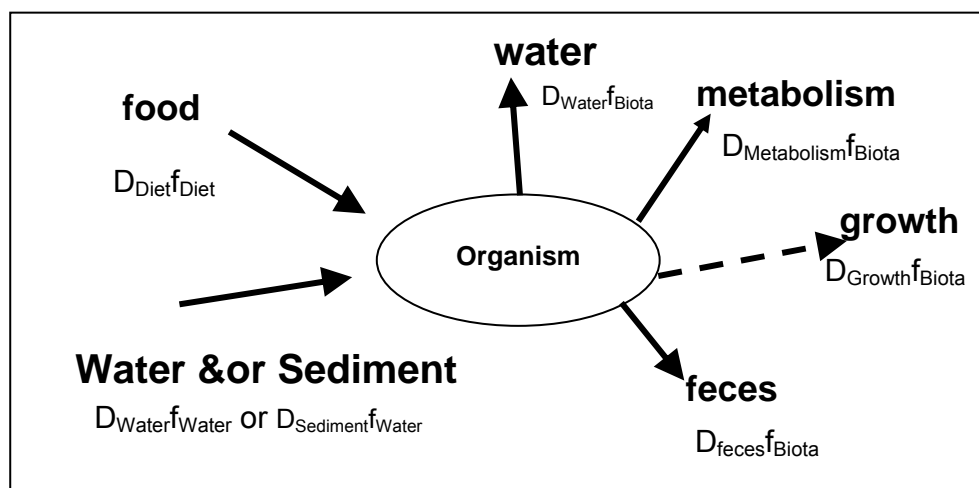


Fig. 4 – Schematic of conceptual food web model. D represents transport parameters ($\text{mol h}^{-1} \text{Pa}^{-1}$) and f is fugacity (Pa), the product of which is a rate (mol h^{-1}) of contaminant movement according to the process indicated by the subscript. From Arnot et al. (2004).

2.3 TRANSPEC

In order to evaluate the fate and transport of metals in the lagoon it is necessary to account for metal chemistry and the distribution of species among dissolved, colloidal and particulate phases. To accomplish this, we have applied TRANSPEC to estimate the fate of cationic metals in the water and sediment compartments defined above. As described earlier the complexation/speciation model estimates the equilibrium concentration of dissolved, precipitated and adsorbed fractions of chemical complexes. Input data for the model include pH, alkalinity, redox potential and ionic strength. To approximate steady-state conditions in the lagoon we take time-averaged measurements of salinity in each geographic segment.

Whereas the geochemical speciation model performs well in oxic conditions, estimates of dissolved-particulate partitioning (K_d) are less certain under anoxic conditions that can prevail in the sediments. To address this uncertainty we compare model estimates of K_d with estimates obtained from field studies and adjust the values used in the model accordingly.

3 Discussion

The complexity of the Venice Lagoon requires the integrated modelling approach presented here to answer a number of research questions governing the fate and transport of contaminants. The shallow nature and the intricate

circulation pattern suggest that both lateral and vertical particle transport may play a role in contaminant fate. The modelling approach presented here will be applied to answer several related research questions.

The first question concerns the dominant transport process in the Venice Lagoon. High concentrations of suspended particles are transported laterally with water currents and vertically via deposition and resuspension. The lagoon is subject to strong diurnal tidal flushing and significant exchange with the Adriatic Sea through its three outlets (Solidoro et al., 2004b). In addition, nine rivers discharge into the lagoon causing estuarine-like mixing. In addition, the water flows entrain dissolved and colloidal-phase contaminants. It is unclear which process (lateral versus vertical movement) dominates overall chemical fate and the extent to which this varies depending on the particular segment and chemical. This leads to the second research question.

The Venice Lagoon is subject to several physical disturbances resulting in enhanced resuspension of bottom sediment. These disturbances include boating and illegal clam fishing of the Manila clam (*Tapes philippinarum*) using "rusca", primarily in the Central basin of the lagoon (Pranovi et al., 2003). However, the presence of the Manila clam throughout the lagoon acts in opposition to these erosive processes through its filter feeding, enhancing water-to-sediment transfer of contaminants. The framework will be used to evaluate the impact of these processes on contaminant fate in the Venice lagoon.

Third, contaminant fate is not limited to sediment-water interface but is also subject to air-water exchange. Air-water exchange is governed by the dissolved fraction of the contaminant which is subject to volatilization. Due to the large surface area of the lagoon relative to its mean depth of 1 m, air-water exchange could be significant for the less hydrophobic POPs. However, the high concentrations of suspended particles in the lagoon reduce the truly dissolved fraction of POPs and thereby reduce rates of volatilization. Thus, we will explore estimated rates of chemical loss or gain via air-water exchange and the magnitude of this process relative to other processes contributing to chemical losses and gains.

The fourth question concerns the sources of contaminant loads to the lagoon – the locations, magnitude and contaminants emitted. The Venice Lagoon receives contaminant loadings from direct discharges from industry and the City of Venice, loads from the rivers that discharge into the lagoon, non-point source loadings from boats, etc., and atmospheric deposition that is promoted by the large surface area of the lagoon. Emission rates from each source are uncertain, as they are for many water bodies (e.g., Ling et al., 1993). Historically emitted contaminants that have accumulated in the sediment of the Porto Marghera provide an internal loading source however quantifying this load requires knowledge of loads from the other sources. The canals in the City of Venice are responsible for the 85% of the water exchange between the segment receiving direct industrial input (Porto Marghera, segment 6) and the segment containing the City of Venice (Segment 3). The dominant circulation

pattern results in water flow from segment 3 to 6 suggesting that, emissions from the city of Venice may contribute to contaminant levels in the segment 6. Clarifying the magnitude and location of emissions will assist with evaluating the impact of measures taken to mitigate emissions from industry and the municipality.

4 Conclusions

The modelling framework presented here contributes to the knowledge of the Venice Lagoon by incorporating new knowledge regarding environmental modelling and new knowledge about the lagoon. The models can be used as effective means of estimating concentrations, pathways and persistence of contaminants (POPs and metals) in sediment and water compartments. These data are useful for risk assessment and to evaluate current emission standards against benchmarks. In addition, these media estimates can be used in conjunction with a food web model to estimate concentrations in the consumable biota (fish and clams). The models presented here are especially useful in elucidating the dominant fate and transport pathways in the Venice Lagoon, information which is crucial to making informed decisions regarding contaminant management.

References

- Arnot, J. and F. Gobas (2004). A food web bioaccumulation model for organic chemicals in aquatic ecosystems. *Environmental Toxicology and Chemistry*. 23: 2343-2355.
- Bhavsar, S.P, Diamond, M.L., Evans, L.J., Gandhi, N., Nilsen, J., and P. Antunes (2004a). Development of a coupled metal speciation-fate model for surface aquatic systems. *Environmental Toxicology and Chemistry*. 23: 1376-1385.
- Bhavsar, S.P, Diamond, M.L., Evans, L.J., Gandhi, N. and J. Nilsen (2004b). Dynamic coupled metal transport-speciation model: Application to assess a zinc-contaminated lake. *Environmental Toxicology and Chemistry*. 23: 2410-2420.
- Bellucci, L., Frignani, M., Paolucci, D. and M. Ravanelli (2002). Distribution of heavy metals in sediments of the Venice Lagoon: the role of the industrial area. *Science of the Total Environment*. 295: 35-49.
- Campfens, J., and D. Mackay (1997). Fugacity-based bioaccumulation in complex aquatic food webs. *Environmental Science and Technology*. 31: 577-583.
- Carrer, S., G. Coffaro, M. Bocci, and A. Barbanti (2005). Modelling partitioning and distribution of micropollutants in the lagoon of Venice: a first step towards a comprehensive ecotoxicological model. *Ecological Modelling*. 184: 83-101.
- Dalla Valle, M., Marcomini, A., Sfriso, A., Sweetman, A. and K. Jones (2003). Estimation of PCDD/F distribution and fluxes in the Venice Lagoon, Italy:

combining measurement and modelling approaches. *Chemosphere*. 51: 603-616.

Diamond, M.L., Mackay, D., and P.M. Welbourn (1992). Models of multi-media partitioning of multi-species chemicals: The fugacity/aquivalence approach *Chemosphere*. 25:1907-1921.

Diamond, M.L., D. Mackay, D.J. Poulton and F.A. Stride (1994). Development of a mass balance model of the fate of 17 chemicals in the Bay of Quinte. *Journal of Great Lakes Research*. 20: 643-666.

Diamond, M.L. (1995). Application of a mass balance model to assess in-place arsenic pollution. *Environmental Science and Technology*. 28: 29-42.

Diamond, M., Ganapathy, M., Peterson, S. and C. Mach (2000). Mercury dynamics in the Lahontan Reservoir, Nevada: Application of the QWASI fugacity/aquivalence multispecies model. *Water, Air, and Soil Pollution*. 117: 133-156,

Freitas, H., Diamond, M., Semkin, R. and D. Gregor (1997) Contaminant fate in high Arctic lakes: Development and application of a mass balance model. *Science of the Total Environment*. 201: 171-187.

Gambaro, A. Manodori, L., Moret, I., Capodaglio, G. and P. Cescon (2004). Determination of polychlorobiphenyls and polycyclic aromatic hydrocarbons in the atmospheric aerosol of the Venice Lagoon. *Analytical and Bioanalytical Chemistry*. 378: 1806-1814.

Gewurtz, S.B., Gandhi, N., Christensen, G.N., Evenset, A., Gregor, D. and M.L. Diamond. Application of a food web model to determine the relative influence of lake morphology, nutrients, and contaminant loadings on the dynamics of polychlorinated biphenyls in a high arctic food web. *Chemosphere*. In press.

Guerzoni, S., Rossini, P., Molinaroli, E., Rampazzo, G. and S. Raccanelli (2004). Measurement of atmospheric deposition of polychlorinated dibenzo-p-dioxins and dibenzofurans in the Lagoon of Venice, Italy. *Chemosphere*. 54:1309-1317.

Helm, P.A., Diamond, M.L., Semkin, R., Strachan, W.M.J., Teixeira, C., and D. Gregor (2002). A mass balance model describing multiyear fate of organochlorine compounds in a high Arctic lake. *Environmental Science and Technology*. 36 (5): 996-1003

Ling, H., M. Diamond and D. Mackay (1993). Application of the QWASI fugacity/aquivalence model to assessing the fate of contaminants in the water and sediments of Hamilton Harbour. *Journal of Great Lakes Research*. 19: 582-602.

Lun R, Lee K, De Marco L, Nalewajko, C. and D. Mackay (1998) A model of the fate of polycyclic aromatic hydrocarbons in the Saguenay Fjord, Canada. *Environmental Toxicology and Chemistry*. 17: 333-341.

Mackay, D., Joy, M. and S. Paterson (1983). A quantitative water, air, sediment interaction (QWASI) fugacity model for describing the fate of chemicals in lakes.

Chemosphere. 12: 981-997.

Mackay, D. and M. Diamond (1989). Application of the QWASI (Quantitative Water Air Sediment Interaction) fugacity model to the dynamics of organic and inorganic chemicals in lakes. Chemosphere. 18: 1343-1365.

Mackay, D. (1991). Multimedia Environmental Models. The fugacity approach. Lewis Publishers.

Pranovi, F., Libralato, S., Raicevich, S., Granzotto, A., Pastres, R., and O. Giovanardi (2003). Mechanical clam dredging in Venice lagoon: ecosystem effects evaluated with a trophic mass-balance model. Marine Biology. 143: 393-403.

Secco, T., Pellizzato, F., Sfriso, A., and B. Pavoni (2005). The changing state of contamination in the Lagoon of Venice. Part 1: organic pollutants. Chemosphere. 58: 279-290.

Schecher W. D. and McAvoy D. C. (2001). MINEQL+ - A Chemical Equilibrium Modelling System, version 4.5 for windows User's Manual. Environmental Research Software.

Solidoro, C., Pastres, R., Cossarini, G. and S. Ciavatta (2004a). Seasonal and spatial variability of water quality parameters in the lagoon of Venice. Journal of Marine Systems. 51: 7-18.

Solidoro, C., Pastres, R., Cossarini, G. and S. Ciavatta (2004b). A partition of the Venice Lagoon based on physical properties and analysis of general circulation. Journal of Marine Systems. 51: 147-160.

Umgiesser, G., Melaku Canu, D., Cucco, A. and C. Solidoro (2004). A finite element model for the Venice Lagoon, development, set up, calibration and validation. Journal of Marine Systems. 51: 123-145

Wania, F. and D. Mackay (1999). The evolution of mass balance models of persistent organic pollutant fate in the environment. Environmental Pollution. 100: 223.

RESEARCH LINE 3.9

Pollutant flows in the lagoon carried by aerosols and atmospheric fall-out

MEASUREMENTS OF PM_{2.5} CONCENTRATION AND VERTICAL TURBULENT MASS FLUXES IN THE SURFACE LAYER

Daniele Contini¹, Antonio Donateo¹, Franco Belosi², Franco Prodi²

¹ *Istituto di Scienze dell'Atmosfera e del Clima, CNR, Sez. di Lecce, SP Lecce-Monteroni km 1.2, 73100 Lecce,* ² *Istituto di Scienze dell'Atmosfera e del Clima, CNR, Via Gobetti 101, 40129 Bologna*

Riassunto

In questo lavoro si presenta uno studio della dinamica locale di aerosol nella laguna di Venezia, sull'Isola di Mazzorbetto, utilizzando una stazione di misura basata su di un anemometro ultrasonico ed un rivelatore ottico di PM_{2.5}. Il sistema permette di rilevare le fluttuazioni del campo di concentrazione e di velocità del vento che sono utilizzate per il calcolo dei flussi verticali turbolenti di massa di PM_{2.5}. Tali informazioni, correlate con i parametri meteorologici, permettono una più approfondita analisi della dinamica dell'aerosol atmosferico migliorando l'interpretazione dei dati di qualità dell'aria. Sono state svolte due campagne di misura: una nel periodo estivo e l'altra durante l'inverno, tuttavia i risultati presentati si riferiscono prevalentemente alle misure svolte nel periodo estivo in cui le concentrazioni sono mediamente più basse di quello invernale. In estate si instaura una circolazione a mesoscala con vento proveniente dalle Alpi nelle ore notturne ed una brezza di mare nelle ore diurne. Durante questa circolazione i valori maggiori di concentrazione ed i flussi verticali turbolenti negativi si hanno prevalentemente nel periodo notturno ed alle prime ore del mattino e sono associati alla direzione del vento NE.

Abstract

In this work an analysis of the local aerosol dynamics is presented. Measurements have been carried out on the Mazzorbetto Island in the Venice Lagoon using a measuring station based on an ultrasonic anemometer and a real-time PM_{2.5} optical detector. Measurement system allows to detect fluctuations of the concentration and velocity fields that are used to evaluate the vertical turbulent fluxes of PM_{2.5}. The information obtained, correlated with local meteorological parameters, gives insights about local aerosol dynamics that are useful to interpret air quality data. Two measurement campaigns have been carried out: the first during the summer and the second one during the winter, however the results presented refer mainly to measurement taken in the summer period in which concentration levels are lower with respect to the ones measured in the winter. In the summer it is present a general circulation with wind coming from the Alps during the night and a sea breeze during the day. During this circulation the largest concentration values as well as the periods of negative fluxes are mainly associated to nocturnal and early morning hours with

wind coming from NE.

1 Introduction

Atmospheric aerosol is nowadays an important topic in air quality monitoring both in urban and rural environments. The fine particulate fraction of aerosol is recognized to be the most dangerous for its potential impact on human health (Schwarz et al., 2002). The atmospheric parameters that mainly influence aerosol concentrations and size-distributions, like emissions characteristics of the sources, temperature, relative humidity, wind direction, wind speed, atmospheric stability and mixing height, vary on time scales substantially smaller than 24 hours that is the typical averaging time used in gravimetric detections of atmospheric aerosol. Therefore, it is useful to employ real time monitoring systems because they can improve the understanding of traditional air quality data and furnish detailed information about local dynamics of aerosol. Additional information about aerosol dynamics in the surface boundary-layer can be achieved from the analysis of vertical turbulent fluxes of particulate matter, that indicate periods (or eventually areas) of sink or source of particle, and from the correlation between these periods and the parameters that characterise local micrometeorology.

In this work we describe a methodology for real-time detection of the PM_{2.5} fraction of atmospheric aerosol with a measuring station, based on an ultrasonic anemometer and a compact portable optical detector, which allows measurement of concentration fluctuations (at 1 Hz) and the evaluation of vertical turbulent fluxes of aerosol. A new procedure to correct the effect of relative humidity on optically measured PM_{2.5} is employed. Results show a good correlation between gravimetrically and optically measured daily concentrations after the application of the correction procedure on the measured instantaneous data. Results indicate that PM_{2.5} levels are larger in the winter period with respect to the summer however there are similarities in the aerosol dynamics. Results indicate that PM_{2.5} concentration decreases when wind velocity increases as consequence of a more efficient mixing of pollutant. In particular, on average, concentration is about 38% lower in summer and about 44% lower in winter for wind speed greater than 3m/s with respect to the average value measured for wind speed lower than 3 m/s. Concentration levels are lower during the day with respect to nocturnal hours. Results indicate that the average concentration during the day (from 8 am to 8 pm) is about 24% lower than the average values measured during the night in the summer. This reduction is basically the same (about 25%) in the winter period.

Results indicate that in the summer period it is present a general circulation with wind blowing from the Alps (NE - mainly during the night) and from the Adriatic Sea (SE - mainly during the day). In these conditions the concentration levels are larger when the wind is blowing from NE and also the largest negative peaks in the vertical fluxes are observed with NE winds. This circulation is not present in the winter period.

2 Experimental equipment, measurement site and post-processing procedure

Data has been collected in the Mazzorbetto Island in the Venice Lagoon in two measurement campaigns: the first one in the summer period (July 2004) and the second one in the winter period (February-March 2005). However the results reported in this paper refer mainly to the summer period being the second measurement campaign still under analysis. Data has been collected with a measuring station, placed on an horizontal bar at the top of a telescopic mast (Clark Mast SQT9/M) at 9.6m above the ground. The station is based on a Gill R3 ultrasonic anemometer, operating at 100 Hz in calibrated mode (Gill Instruments, 1999), a Rotronic (Campbell Scientific MP100A) termo-igrometer, a bi-axial inclinometer (Microstrain FAS-A) and an infrared (880 nm) optical detector Mie pDR-1200. A photograph of the measuring station as well as a view of the measurement site is reported in Figure 1. The signals of the different instruments are sampled by the anemometer synchronously with velocity and sonic temperature measurements. The termo-igrometer gives ambient temperature and relative humidity (RH) that is necessary in order to correct PM_{2.5} measurements for the effect of hygroscopic growth of particle (McMurry 2000, Chakrabarti et al 2004). The inclinometer fixed to the base of the anemometer is used to continuously monitor the inclination of the anemometer with respect to the gravity vector. The pDR-1200 was placed inside a small aerated metal box and it was operating in active mode with air sampled through a 40 cm tube placed near (about 30 cm) the sampling volume of the ultrasonic anemometer. The optical detector operates at 1 Hz in active sampling (air flow-rate equal to 4 l/min) and it is equipped with a 2.5 μm cut-off cyclone. The air flow was maintained using a Bravo Plus pump of Tecora.





Fig. 1 – Photo of the measurement site (left) and of the real-time measuring station (right).

Raw data series are post-processed to evaluate the different turbulent parameters, including vertical turbulent mass-fluxes of PM2.5, using 30 minutes averages. A first analysis is performed on the different signals in order to eliminate unphysical spikes that are sometimes presents because of electric interferences. Afterwards the instantaneous velocity vectors are rotated into the streamlines system by performing three successive rotations (McMillen, 1988). After rotation the PM2.5 concentration signals are corrected for the relative humidity effect as described in detail later on. All the time-history measured (concentration, wind velocity and sonic temperature) are linearly detrended to limits the effect of slow changes (with respect to the averaging time) of the measured quantities (Rannik & vesala 1999). After detrending the vertical turbulent fluxes F_C of PM2.5, with mass concentration C , is calculated using the eddy-correlation method (Stull 1988): $F_C = \langle w'c' \rangle$ where c' are the fluctuations of the PM2.5 concentration C . The same method is used to evaluate kinematic turbulent momentum fluxes $F_M = \langle w'u' \rangle$, the friction velocity

$$u^* = \left(\langle u'w' \rangle^2 + \langle v'w' \rangle^2 \right)^{1/4}$$

and kinematic sensible heat fluxes $F_H = \langle w'Ts' \rangle$ using fluctuations Ts' of the sonic temperature Ts as usual (Moncrieff et al 1997). Vertical turbulent fluxes are used to calculate the deposition velocity V_d defined as $V_d = -F_C/C$.

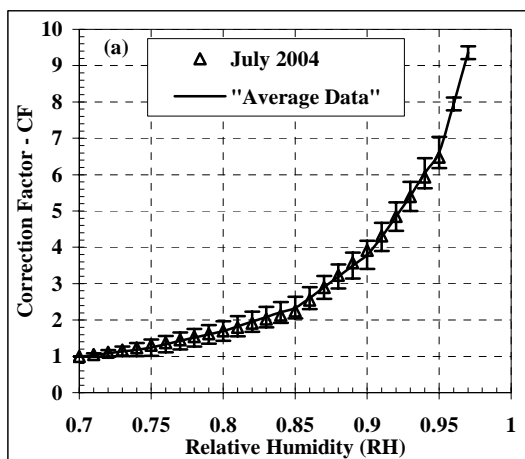
The mentioned correction for the RH effects on PM2.5 measurements is carried out with a new mathematical procedure (Donateo 2004) based on the analysis of correlation between RH and C . The concentrations measured with the pDR-1200, and in general the measurements of optical photometers, are influenced by the environmental relative humidity. Particulate matter absorbs water vapor changing dimension, density and optical properties. It is generally shown that the output of optical nephelometers increases with RH (Sloane, 1984; Sioutas et al., 2000; Chakrabarti et al., 2004). This is due to the quick growth of particle smaller than the wavelength of the light used that change the size distribution of aerosol measured shifting an important fraction of the total number of particles towards dimensions similar to the wavelength used thereby increasing the scattering efficiency and, consequently, the signal measured by the optical

detector. An inspection of concentration measured with the pDR-1200 in different field campaigns showed that a correction is necessary for RH>70%. The correction factor CF(RH), used on instantaneous concentration data, is reported in Figure 2(a). In the figure it is reported the curve found in the measurements carried out in the summer period and also a curve, with error bars, that represent the average correction factor calculated over three different measurement campaigns. A fourth-order polynomial fit of experimental results is actually used to correct raw-data:

$$CF = \frac{C(RH)}{C(RH = 0.7)} = 4330.8282774RH^4 - 13628.3399181RH^3 + 16102.7519624RH^2 - 8456.2021129RH + 1664.7397809$$

All the data reported in this paper have been corrected according to Eq. (1) used on the instantaneous optical measurement of PM_{2.5} concentration. To test the quality of optical measurements of PM_{2.5} a comparison of the results obtained with the pDR-1200 with measurements taken using gravimetric analysis has been performed. Gravimetric measurement of PM_{2.5} concentrations have been performed, on a 24 hours basis, using an impactor inlet operating at the standard flow-rate of 2.3 m³/h and collecting aerosol on 47mm filters. Filters were conditioned in laboratory before and after exposition in order to limit the effects of RH on calculated concentrations. Results of comparison are reported in Figure 1(b). The correlation is reasonably good and it is similar to what has been reported in the scientific literature (Chakrabarti et al. 2004). The average concentration value of all the gravimetric measurements is 21.6 µg/m³ and the corresponding average for RH-corrected optical measurements is 18.3 µg/m³. This is restricting the analysis to the period in which both measurements (gravimetric and optical) were available. A preliminary analysis shows that a similar level of correlation is also found in winter measurements that are characterised by larger concentration levels than the summer period. During the winter the average (over about 1 month period) of RH-corrected optical concentration is 41.8 µg/m³.

3 Discussion of results



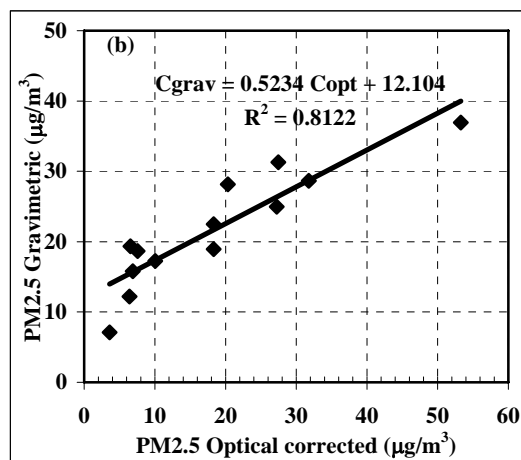


Fig. 2 – (a) Correction factor used to take into account the effect of RH on PM2.5 concentration measurements. (b) Scatter plot of gravimetric and RH-corrected optical measurements of daily concentration of PM2.5 measured during the summer period in July 2004.

In Figure 3(a) it is reported the wind speed and in Figure 3(b) the wind direction measured in the summer period. The wind direction is compared to the hourly wind direction measured at 160m above the ground with a sodar system placed at Porto Marghera. Results indicate a good agreement between the two independent measurements indicating that the wind direction is usually quite stable in the Surface Layer. The results show that the largest wind speeds are in the period before 14/7/2004. The average wind speed during all the measurement period was 2.82 m/s with a peak (on 30 mins average) of about 10 m/s. That happens in the afternoon of 13/7/2004 and there are also several wind velocity peaks over 8 m/s.

The behaviour of wind direction put in evidence a general circulation (after 13/7/2004) with wind blowing from NE during the night and wind blowing from SE during the day. This circulation is linked to the presence of a circulation with wind coming from the Alps and the Adriatic sea (Camuffo, 1981). The transition from NE to SE is usually happening between 9am and 11 am and the opposite transition from SE to NE is usually happening between 23pm and 01am. In the period in which circulation from NE and SE is present the wind speed is generally lower: 2.3 m/s on average between 13/7/2004 and 21/7/2004 with respect to 3.2 m/s on average between 2/7/2004 and 12/7/2004). During the measurement campaign the air temperature was ranging between 15 °C and 30 °C and relative humidity is ranging between 36% and 97%. In Figure 4 it is reported the temporal behaviour of 30-minutes average PM2.5 concentration measured by the optical detector. The average concentration in all measurement period is 16.7 µg/m³ and the maximum peak is about 125 µg/m³ (on 30 mins average) and it happens the 9/7/2004. Results indicate that the average concentration during the day (from 8 am to 8 pm) is about 24% lower than the average values measured during the night in the summer. This reduction is basically the same (about 25%) in the winter period. Results also

indicate that concentration levels are larger, on average, in the first measurement period (before 12/7/2004) with respect to the second period in which the stable circulation between Alps and Adriatic Sea is established. In Figure 5 the calculated vertical turbulent PM_{2.5} fluxes and the relative deposition velocities are reported as function of measurement time. Results show that it is not possible to find a periodic pattern in the turbulent PM_{2.5} fluxes but a greater activity in diurnal periods that are often characterised by unstable atmosphere.

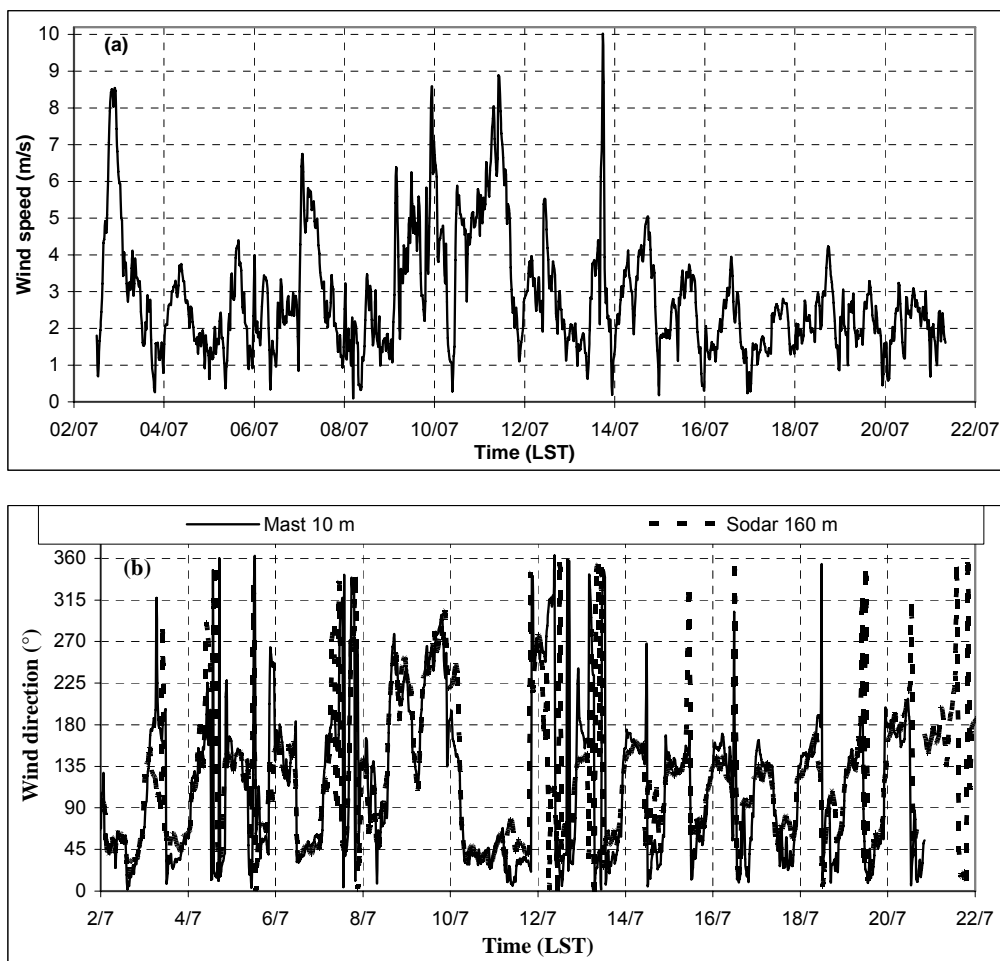


Fig. 3 – Wind velocity (a) and wind direction (b) measured in the summer 2004.

Measured concentration show a peak in the PM_{2.5} level (about 100 $\mu\text{g}/\text{m}^3$ in concentration) during the day of 8/7/2004. This is also the day with the maximum daily average concentration of all the measurement period. During this day the wind speed at 10m is relatively low (about 2 m/s) and the wind direction at 1500m above the ground, as measured by the radio soundings in Udine, indicates that the wind is blowing mainly from SO. Therefore the high concentration level could be due to a long range transport from Pianura Padana or from Africa dust transported over the northern part of Italy and brought

towards the ground partly as consequence of convective mixing in the boundary-layer. Another brief and evident concentration peak is present in the morning of 9/7/2004 and it is associated to a negative vertical turbulent flux during the build-up of the concentration peak and to a successive positive flux during the decreasing part of the concentration peak indicating a mixing with cleaner air present above the measurement height. During the concentration peak the wind direction (at 10m above the ground) was compatible with the position, with respect to the measurement site, of the industrial site of Porto Marghera and the peak could be interpreted as a short range transport.

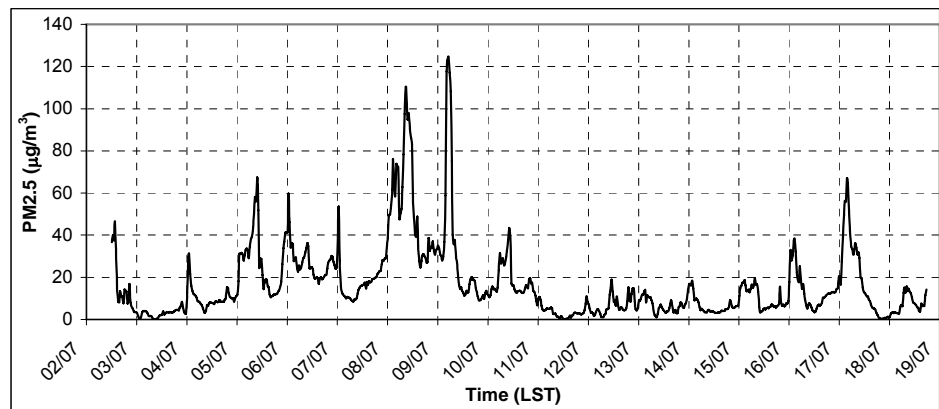


Fig. 4 – PM2.5 concentration measured in the summer 2004.

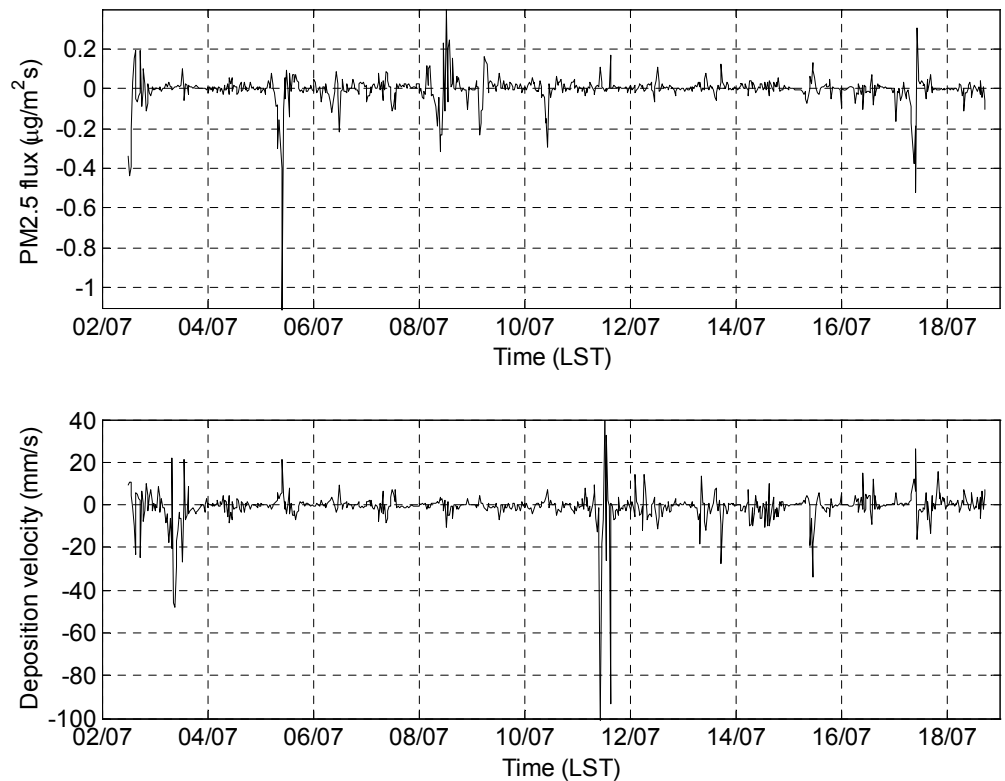


Fig. 5 – PM2.5 vertical turbulent fluxes (top) and deposition velocities (bottom)

A similar behaviour of deposition followed by successive positive fluxes has also been observed the 6/7/2004, the 8/7/2004 and during a small concentration peak that happens during 17/7/2004. The largest deposition has been observed during the day of 5/7/2004 with concentration peaks entirely associated to negative fluxes and starting during the first hours of the morning possibly indicating a mixing with polluted air present above the measurement height. In order to obtain more detailed information about aerosol dynamics the concentration levels as well as the vertical turbulent fluxes have been correlated with wind speed and direction. In Figure 6 is reported the scatter-plot of measured concentrations against the wind velocity U_v for both periods summer and winter. On average, for U_v greater than 3 m/s, PM_{2.5} concentration is reduced of about 38% with respect to cases in which U_v is lower than 3 m/s. This behaviour is observed also in the winter period with an average reduction of about 44%.

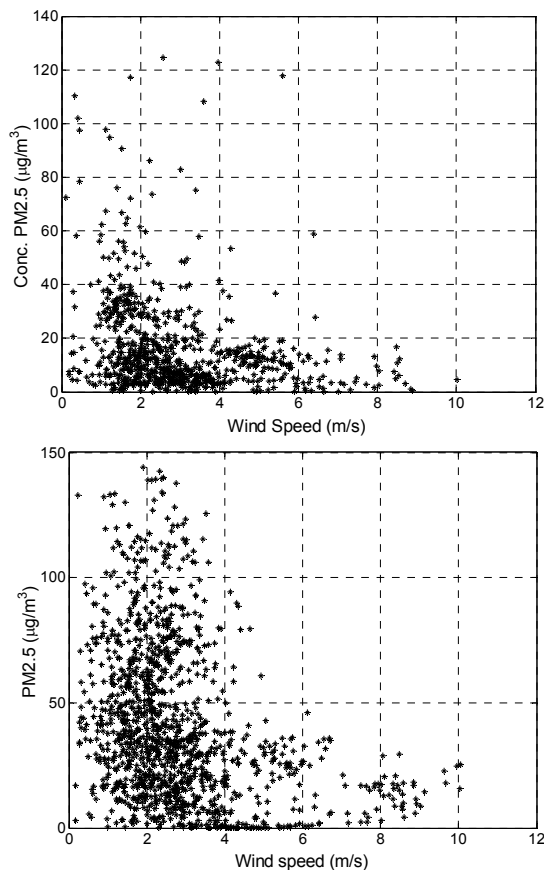


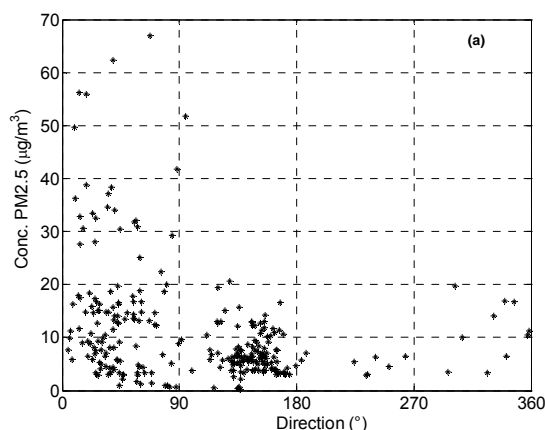
Fig. 6 – PM_{2.5} concentration against wind velocity during summer period (left) and winter period (right)

In the period starting from 13/7/2004 when the general circulation from Alps and Adriatic Sea is present the PM_{2.5} concentrations and the relative vertical turbulent fluxes are correlated to wind direction as shown in Fig. 7. In this period maximum concentrations have been found associated to wind direction of about 50° corresponding to air masses coming from the Alps mainly during the night and the first hours of the morning. Wind directions associated to air masses

coming from the Adriatic Sea are characterised by lower levels of atmospheric PM2.5. A similar difference is also found in the vertical turbulent fluxes with values mainly negative during the night or in the first hours of the morning. In Figure 8 it is reported an analysis of the standard deviation of PM2.5 concentration σ_C evaluated on 30 minutes averages. In Figure 8 the relative fluctuations σ_C / C are reported, as function of C, for all the measurement period. The maximum relative fluctuations are found at very low concentration values (during 3/7/2004 and 11/7/2004). The relative fluctuations are usually within 10% for concentration values larger than 25 $\mu\text{g}/\text{m}^3$. A similar behaviour has also been observed in measurements carried out in the winter 2005 (not shown). In Figure 9 the deposition velocity are plotted against the friction velocity u^* separating the cases of sink of PM2.5 ($V_d > 0$) and source of PM2.5 ($V_d < 0$). Results indicate an increment of deposition velocity with u^* in a similar way to what has been found over vegetated surfaces (Gallagher et al, 1997).

Conclusions.

In this work some results of real-time measurements of PM2.5 concentration and vertical turbulent fluxes over the Venice Lagoon are presented. Results indicate that there is a good correlation between RH-corrected optical measurements of daily PM2.5 concentration and gravimetric results. The average concentration levels are lower during the summer period (about 16.7 $\mu\text{g}/\text{m}^3$) with respect to the winter case (about 41.8 $\mu\text{g}/\text{m}^3$). Despite this difference in the concentration levels there is some similarity in aerosol dynamics. Results indicate that concentration levels are, on average, lower during the day (from 8am to 8pm), with respect to the average values of the night and this reduction is about 25% in winter and 24% in the summer. Concentration levels decrease when the wind velocity increases as consequence of a more efficient mixing of air masses. Results indicate that the average values measured in cases in which the wind is above 3 m/s is 38% lower than the average values measured in cases in which the wind is lower than 3 m/s. This reduction is about 44% in the winter measurement campaign.



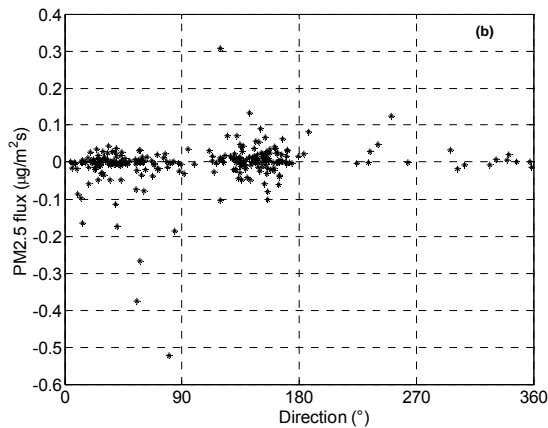


Fig. 7 – (a) Correlation between PM2.5 concentration and wind direction. (b) Correlation between PM2.5 turbulent flux and wind direction. Results refer to measurement taken starting from 13/7/2004.

During the summer period results indicates that there are some concentration peaks (also larger than $100 \mu\text{g}/\text{m}^3$) in meteorological conditions compatible with the presence of a contribution from Porto-Marghera and from Pianura Padana. Several concentration peaks are associated to a structure of the vertical turbulent fluxes in which a deposition is observed during the build-up of the concentration peaks followed by positive fluxes indicating a mixing with clean air present above the measurement height. The day of 5/7/2004 present the maximum deposition of all the measurement period with a concentration peak associated to a period of negative vertical flux. Meteorological data indicates that in the summer period it is present a general circulation, stable in the first layers of the atmosphere as it is also confirmed by sodar measurements, in which wind is blowing from the Alps (mainly during the night) and from the Adriatic Sea (mainly during the day). In these conditions the concentration levels are larger when the wind is blowing from the Alps and also the largest negative peaks in the vertical fluxes are observed when the wind is blowing from the Alps. This circulation is not present in the winter period. Typical PM2.5 concentration fluctuations are within 10% (as ratio between the standard deviation of concentration and the concentration itself) for concentration levels larger of about $25 \mu\text{g}/\text{m}^3$ and this happens in both measurement periods: during the summer and during the winter. Results indicate that the absolute values of the deposition velocity increase when the friction velocity increase in a similar way to what has been observed in measurements taken over vegetated surfaces (Gallagher et al, 1997). This behaviour is present in both measurements sets: the one taken in the summer and the one taken during the winter.

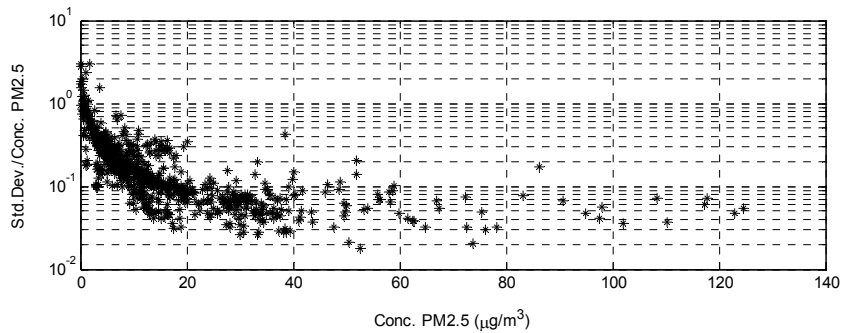


Fig. 8 – Relative concentration fluctuations of PM2.5 against concentration

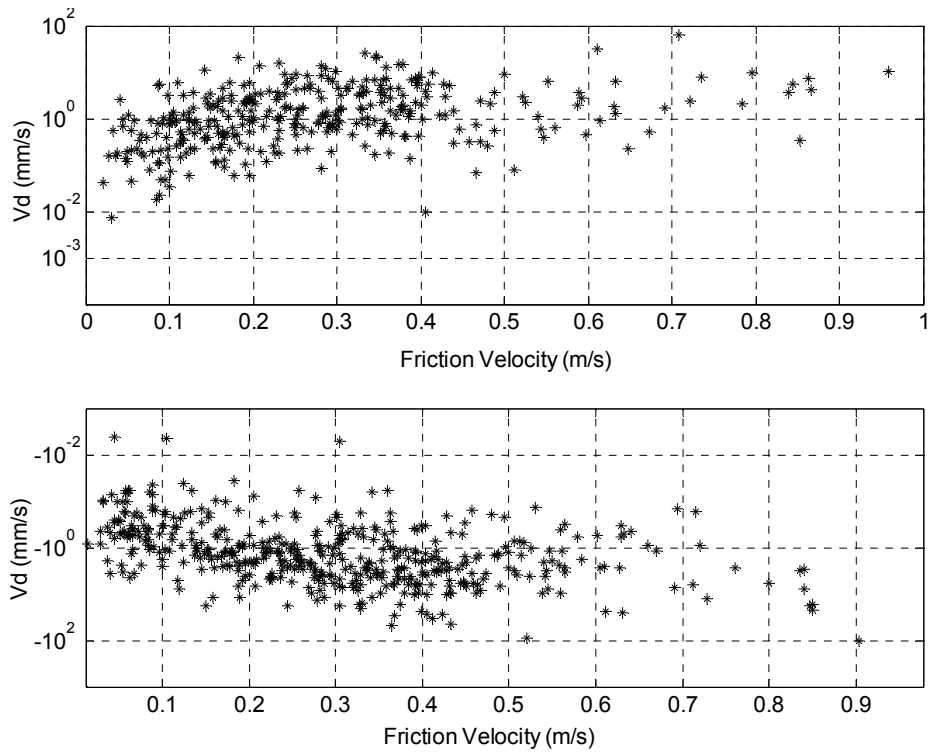


Fig. 9 – Deposition velocity against friction velocity. (a) cases with $V_d > 0$. (b) Cases with $V_d < 0$.

Acknowledgements

Authors wish to thank Dr. A. Gambaro, Dr. L. Manodori and Mr. I. Ongaro of the University of Venice for their help in the research. Many thanks to Dr. S. Ferrari of ISAC-CNR. Authors wish to thank Mr. E. Rampado of the Ente Zona Industriale di Porto Maghera for providing some meteorological data and also sodar measurements.

References.

Camuffo D., 1981. Fluctuations in wind direction at Venice, related to the origin of the air

masses. *Atmospheric Environment* 15, 1543 -1551

Chakrabarti B., Fine M.P., Delfino R., Sioutas C., 2004. Performance evaluation of the active-flow personal DataRAM PM2.5 mass monitor (Thermo Anderson pDR-1200) designed for continuous personal exposure measurements. *Atmospheric Environment* 38, 3329-3340.

Donateo A. 2004. Misure di Flussi Verticali Turbolenti di Particolato e Traccianti Gassosi nello Strato Limite Superficiale. PhD Thesis, Università degli Studi di Urbino.

Gallagher M.W., Beswick K.M., Duyzer J., Westrate H., Choularton T.W., Hummelshoj P., 1997. Measurements of aerosol fluxes to Speulder forest using a micrometeorological technique. *Atmospheric Environment* 31, 359-373.

Gill Instruments, 1999. Omnidirectional (R3) & Asymmetric (R3A) Research Ultrasonic Anemometer User Manual and Product Specification. Gill Instruments Ltd, Lymington, UK.

McMillen R.T., 1988. An eddy correlation technique with extended applicability to non simple terrain. *Boundary Layer Meteorology* 43, 231-245.

McMurry P. H., 2000. A review of atmospheric aerosol measurements. *Atmospheric Environment* 34, 1959-1999.

Moncrieff J.B., Massheder J.M., de Bruin H., Elbers J., Friborg T., Heusinkveld B., Kabat P., Scott S., Soegaard H., Verhoef A., 1997. A system to measure surface fluxes of momentum, sensible heat, water vapour and carbon dioxide. *Journal of Hydrology* 188-189, 589-611.

Rannik U. & Vesala T., 1999. Autoregressive filtering versus linear detrending in estimation of fluxes by the eddy covariance method. *Boundary Layer Meteorology* 91, 259-280.

Schwarz J., Laden F., Zanobetti A., 2002. The concentration-response relation between PM2.5 and daily death. *Environmental Health Perspective* 110 (10), 1025-1029.

Sioutas C., Kim S., Chang M., Terrell L.L., Gong H. Jr, 2000. Field evaluation of a modified DataRAM MIE scattering monitor for real-time PM2.5 mass concentration measurements. *Atmospheric Environment* 34, 4829-4838.

Sloane C.S., 1984. Optical properties of aerosols of mixed composition. *Atmospheric Environment* 18, pp. 871-878.

Stull, R.B., 1988. An introduction to *Boundary Layer Meteorology*. Kluwer Academic Publishers, 666 pp.

SIZE CHARACTERIZATION OF AEROSOL IN THE VENICE LAGOON

F.Prodi, F.Belosi, S. Ferrari, G. Santachiara, P. Masia,

CNR-Istituto di Scienze dell'Atmosfera e del Clima, Via Gobetti 101, 40129, Bologna, Italy

Riassunto

In questo lavoro vengono presentati i risultati di una campagna di misure finalizzata alla valutazione degli effetti dell'aerosol atmosferico sul sistema lagunare veneziano e alla individuazione delle sorgenti (mare, attività antropogenica, suolo).

I campionamenti di aerosol sono stati effettuati a Mazzorbetto, nella Laguna nord di Venezia, nel periodo estivo (giugno-luglio 2004), utilizzando i seguenti strumenti: uno spettrometro inerziale (Inspec), un campionatore basato sulla diffusione della luce da parte delle particelle (Las-X) ed una batteria a diffusione (TSI, modello 3040) accoppiata ad un contatore di nuclei (TSI, modello 3020). Lo spettrometro inerziale (Prodi V., 1979) permette di campionare l'aerosol su filtro, effettuando contemporaneamente una separazione in base al diametro aerodinamico. Le particelle di aerosol raccolte sui filtri di policarbonato sono state analizzate per mezzo del microscopio elettronico a scansione (SEM-EDAX). Le analisi elementari sono state eseguite nei seguenti intervalli dimensionali: < 1.5 μm ; 1.5-2.7 μm ; 3.5-4.5 μm ; 4.7-5.5 μm and 6.3-7.5 μm .

Il Las-X misura in tempo reale la concentrazione dell'aerosol, classificandolo in 15 intervalli dimensionali, da 0.1 μm a 7.5 μm .

La batteria a diffusione accoppiata con il contatore di nuclei è stata utilizzata per determinare la concentrazione e la distribuzione dimensionale delle particelle di aerosol ultrafini (<100 nm).

I dati raccolti dai differenti strumenti sono stati correlati con i parametri meteorologici (temperatura, direzione e velocità del vento, ecc) e alle misure dei flussi verticali turbolenti dell'aerosol PM_{2.5}.

Abstract.

In this work some results of a sampling campaign, aimed to understand the role and contribution of aerosol on the Venice lagoon system and to assess the possible sources (anthropogenic, crustal or marine), are presented. Aerosol samplings were carried out at Mazzorbetto, in the north Venice Lagoon, during summer 2004 (June-July), by using the following devices: the inertial spectrometer (Inspec), the light particle scattering sampler (Las-X, PMS inc.) and the diffusion battery coupled (TSI, mod. 3040) with a condensation nucleus counter (TSI, mod. 3020). The inertial spectrometer (Prodi V., 1979) allows to sample aerosol on a filter and to separate particles based on aerodynamic

diameter. The aerosol was collected on polycarbonate filters and analyzed with SEM-EDAX device. The elemental analysis were performed in the following size intervals: < 1.5 μm ; 1.5-2.7 μm ; 3.5-4.5 μm ; 4.7-5.5 μm and 6.3-7.5 μm .

The Las-X light scattering covers a size range of 0.1 to 7.5 μm and gives the particle number concentration divided in 15 interval ranges. The diffusion battery coupled with a condensation nucleus counter (CNC) gives the concentration and size distribution of ultrafine aerosol particles (< 100 nm).

The data collected from the different instruments have been correlated with the meteorological parameters (direction, speed, vertical profile of wind, etc) and with vertical PM_{2.5} turbulent fluxes.

1 Introduction

Recent investigations indicate the following processes among those responsible of contaminating the Venice lagoon system: direct injection of industrial effluents in water, the atmosphere-water exchanges, the water-sediments exchanges, the inflow of rives. Previous researches performed under the 2000-2004 Corila program were aimed to understand the role and contribution of aerosols to the pollution of the lagoon, but results were partial. Further efforts should then be devoted to obtain more complete results. The investigation will be performed with a global approach through the estimation of the individual transfer processes at water-air interface by identification and quantification of organic (PCB, IPA, etc) and inorganic (Pb, Cd, Zn, Cu, etc) to the aquatic system (dry and wet deposition measurements), by means of high volume size separation samplers, capable of collecting particles according to wind direction and intensity, and chemical trace elements evaluation, measurements of the microlayer pollution content and by PM_{2.5} vertical turbulent fluxes assessment.

In this work the relevant results dealing with aerosol size characterization and composition are shown.

2 Experimental

The measurements were carried out in Mazzorbetto from 30th June to 21st July 2004. The site is located in an island of north part of Venice Lagoon, far 5 Km from the airport. The Venice Lagoon is a shallow basin, located along the northwest coast of the Adriatic Sea, and it is subjected to pollution from industrial, agricultural and urban sources.

The sampling devices were lodged in a small wood home, where a conditioning system was working (Fig.1). The aerosol size distribution, concentration and the elemental analysis were performed by means of the Inertial Spectrometer (Inspec), the light particle scattering sampler (Las-X, PMS inc.) and the diffusion battery coupled with a condensation nucleus counter. The flow rates were chosen in order to assure isokinetic conditions.

The Inspec (Prodi V., 1979) samples the aerosol on a filter and separates the aerosol particles on the basis of their aerodynamic size; the smallest particles

being deposited on the filter at the greatest distance from the inlet in the deposition chamber. The optimum operating conditions for the best size resolution are high winnowing air flow rate combined with the lowest aerosol flow rate. The Inspec was calibrated in laboratory by using Latex particles and the winnowing flow rate was 420 L/h, while the aerosol sample flow rate was 21 L/h. During experimental campaign filter sampling lasted from 12 to 24 hours.

The Nuclepore filters (0.1 μm porosity) were subsequently analysed by SEM interfaced with EDAX. Five strips were cut at increasing distance from the inlet of the aerosol and put on stubs, which were coated with a thin film of carbon.

According to calibration curve, the range of aerodynamic diameter on each stub was: 0-1.5 μm , 1.5-2.7 μm , 3.5-4.5 μm , 4.7-5.5 μm and 6.3-7.5 μm .

The Las-X sampler is a optical particle counter and measures the size and number concentration of aerosol particles in a limited size range by measuring the light scattered by single particles. For this purpose a stream of aerosol is drawn through a condensed light beam. Light flashes scattered from single particles are received by a photodetector and converted into electrical pulsed. The light power scattered from an individual particle is a function of its size. The Las-X measure the aerosol particles concentration in the range 0.1 –7.5 μm , divided in 15 intervals.

The diffusion battery (TSI, mod. 3040) coupled with a condensation nucleus counter (TSI, mod. 3020) gives the concentration and size distribution of ultrafine aerosol particles (< 100 nm) converting the diffusion coefficient of particles to particles size. Sinclair and Hoopes (1975a) designed a ten-stage unit using stainless steel 635-mesh screens of uniform diameter. Penetration through screens can be predicted by fan model filtration theory (Cheng and Yeh 1980; Cheng et al., 1980).

The condensation nucleus counter is used to measure the number concentration of aerosol particles. It accomplishes this by passing each particle through vapour of n-butyl alcohol. It is based on the principle of thermal cooling to induce the supersaturation of a working fluid and the particles are detected, after growing by condensation, with a light scattering system.

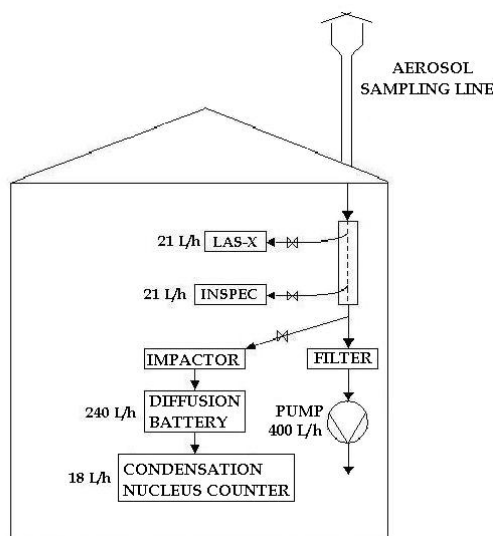


Fig. 1. Experimental apparatus.

2.1 Meteorological condition

The winds at the Venice are due to a combination of large-scale and local effects associated with the Alps, the plain, the lagoon and the Adriatic Sea. The most frequent large-scale flows in the area are the north-easterly Bora and southerly Scirocco, while the most frequent daytime small-scale flow is the summer sea breeze. The large-scale flows are generally associated with high wind speeds, producing low pollutant concentrations in Venice; the small-scale flows (breezes) are associated with low speed anticyclonic regimes, producing high pollutant concentrations. During these latter periods the circulations in Venice are due to land-sea temperature differences. The most frequent daytime flow has a SSE direction (local sea breeze), while the most frequent night-time flow has a NE direction. The sea-breeze circulation continued until about midnight (Camuffo et al., 1979; Camuffo D., 1981).

3 Results and discussion

The local meteorological conditions are estimated by means of an ultrasonic anemometer Omnidirectional R3 (Gill Instruments Ltd, Lymington, UK), placed at 10 m above the ground, while the Sodar, located in Porto Marghera gives the local wind profile up to 400 m altitude.

The mesoscale conditions are estimated by the radiosoundings in Udine (up to 3000 m altitude)(<http://weather.uwyo.edu/upperair/europe.html>) and the BOLAM mapps (850 hPa; <http://www.cmirl.ge.infn.it/MAP/BOLAM/Bolamin.html>).

During the Inspec sampling, 13th July-14th July, the wind was mostly coming from north-eastern direction. Radiosoundings and BOLAM mapps pointed out a NE wind direction in the atmospheric layer between 800 m and 1500 m (probably due to a local breeze circulation), while up to 3000 m the flow direction is NW. Sodar data showed that the wind mainly flows from NE,

excluding the period from 00 a.m. to 01 a.m. (14th July) in which is NW. Therefore nocturnal breeze, reinforced by wind coming from NE up to 1500 m, is the prevailing condition.

The elemental analysis (SEM-EDAX) of the aerosol particles sampled on Nuclepore filters is shown in Table 1. In the size range < 1.5 µm it is observed mainly the presence of Cr, Fe and Ni, that can indicate an industrial source. The presence of Mg, Al, Si and Ca, detected in 1.5-2.7 size range, can show a crustal source. In size ranges 3.5-4.5 µm, 4.7-5.5 µm and 6.3-7.5 µm mixed aerosol particles were detected: Mg, Al, Si and Ca can point out a crustal source, while again Cr, Fe, Ni and Mo can indicate an industrial source, and finally Na and Cl can indicate a marine source.

Table 1. Percent of particles containing the indicated element.

Size range	C	Na	Mg	Al	Si	P	S	Cl	K	Ca	Ti	Cr	Fe	Ni	Cu	Mo
<1.5 µm	24				4							24	24	24		
1.5-2.7 µm	4		4	19	23	8	11		8	15						8
3.5-4.5 µm	6	4	11	13	10	5	8	9	7	10	1	1	9	1	5	
4.7-5.5 µm	10	10	10		5		10	5		25		5	10	5		5
6.3-7.5 µm		4	10	4	10	4	11	7	7	27		4	4	4		4

Figure 2 shows two particles, collected on the filter in the aerodynamic range 3.5-4.5 µm. Particle 1 is rich in Mg, P, S, Cl and K and probably has a biological source (e.g. marine source), while particle 2 has a marine source (33% Na and 51% Cl). Both of them have the same percentage of Al (4%). Further efforts should be devoted to define the composition of marine spray. A coordinated surveying of microlayer, column water, sediment and pollutants of photochemical origin in atmosphere is necessary.

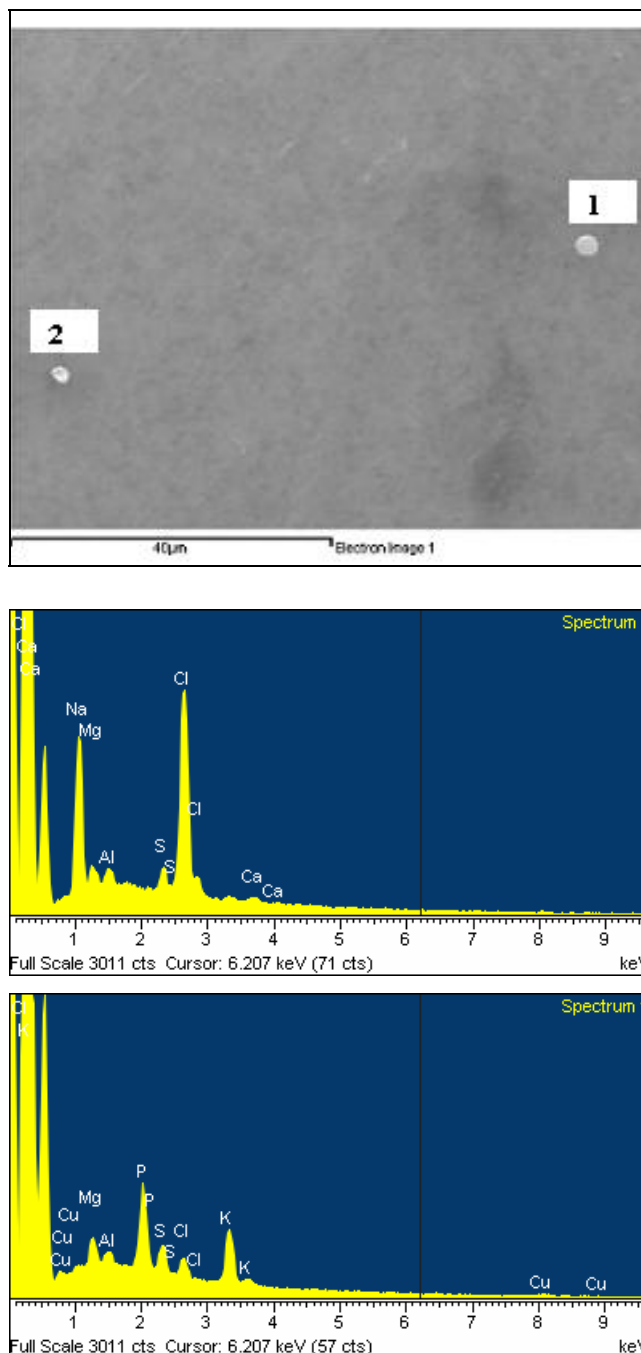


Fig. 2. Aerosol particles image and spectrum by SEM-EDAX.

Figure 3 shows two particles, in the same aerodynamic size range, with different shape and volume. The evident size difference is due to chemical composition of particles. Particle 4 contains 90% weight of Ca, while particle 3 contains mainly Fe (71%) and Cr (13%).

Their geometric sizes are respectively about 1.6 µm (particle 3) and 3.6 µm (particle 4); the latest is the average of four geometric diameters since its shape is not spherical. Their aerodynamic diameter d_a is given by the following relationship:

$$d_a = d_g \sqrt{\rho_p}$$

where d_g is the geometric diameter and ρ_p is the particle density.

The density of particle 3 is computed by the weight average of the density of Fe and Cr (about 7.7 g/cm³); the density of the particle 4 is simply given by the Ca density (1.5 g/cm³). The computed aerodynamic size of the particles becomes 4.5 μm for particle 4 and 4.4 μm for particle 3; that confirms what above mentioned that their difference in shape and volume is due to their density.

Furthermore it confirms the good calibration of Inspec because these particles are deposited in the aerodynamic size between 3.5-4.5 μm .

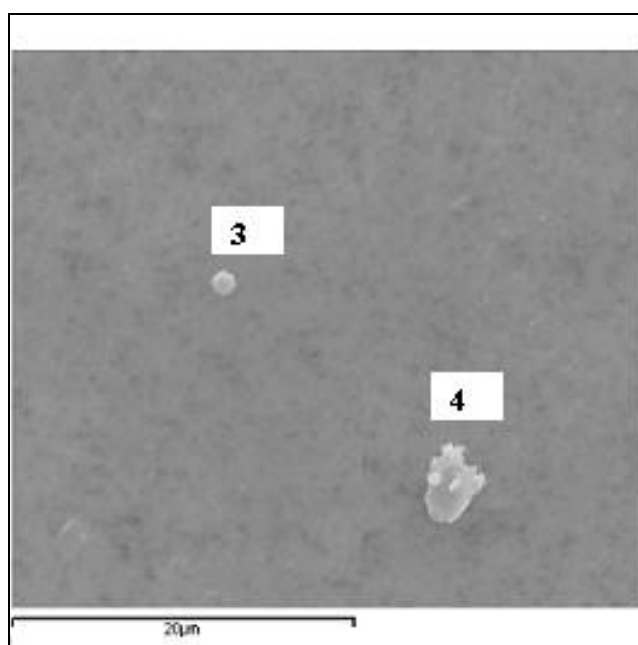


Fig. 3. Aerosol particles imaged by SEM-EDAX.

The Las-X size distribution, expressed as particles number concentration (particles number/m³) normalized for the interval width (by dividing the particles number concentration in each size interval by the width of considered interval), was similar for all samplings. The size distribution shows a maximum peak in the 0.10-0.12 μm size range. A crude comparison between aerosol mass concentration, obtained from particles number (assuming density 1 g/cc) and optical system placed 8 Km far was carried out (Punta Sabbioni). Trends were in good qualitative agreement.

The diffusion battery shows a monomodal distribution with the peak in size range 30-60 nm.

4 Conclusions

The experimental results show a correlation between aerosol composition and wind direction:

- Marine aerosol in the considered events is due prevalently to

particle with an high aerodynamic diameter, and in the presence of wind blowing from the Adriatic sea

- Antropogenic aerosol is present specially in the size range lower than $1.5 \mu\text{m}$ independently from the wind direction, with an increase in the percentage in the bigger size ranges when the wind is coming from the NW sectors (where is located the industrial area of Marghera)
- Crustal aerosol is present in all size range (except below $1.5 \mu\text{m}$), again with an increase in the percentage when the wind is coming from the NW sectors

A second sampling campaign was carried out on winter 2005 (February-March), but the data elaboration is still in progress. In this campaign a microLIDAR was used for the study of the aerosols concentration profile in the atmospheric layer (0-5 Km) and a cyclone, for sampling aerosol particles below $1 \mu\text{m}$ for increasing the information about inorganic anionic and cationic species, that are important to define the aerosol origin.

Acknowledgements

This work was supported by Corila under the Project "Pollutants flows in the lagoon carried by aerosol and atmospheric fall-out". The authors thank Dott. Rampado of Ente Zona of Porto Marghera for Sodar data, Dott. Di Donfrancesco for the microLIDAR and Mr I. Ongaro, Mr M. Tercon, Mr C. Nobile for their technical support.

References

- Camuffo D., Tampieri F., Zambini G., 1979. "Local mesoscale circulation over Venice as a result of the mountain-sea interaction 1979". *Boundary-layer Metreology*, 16, pp. 83-92.
- Camuffo D., 1981. "Fluctuations in wind direction at Venice, related to the origin of the air masses". *Atmospheric Environment*. 15, 1543-1551.
- Cheng Y. S., Keating J. A. and Kanapilly G. M., 1980. Theory and calibration of screen-type diffusion battery. *Journal Aerosol Science*, 11, 549-556.
- Cheng Y.S. and Yeh H.C., 1980. Theory of screen-type diffusion battery. *Journal Aerosol Science*, 11, 313-320.
- Prodi V., Melandri C., Tarroni G., De Zaiacomo T., Formignani M., Hochrainer D., 1979. An Inertial Spectrometer for Aerosol Particles. *Journal Aerosol Science.*, 10, 411-419.
- Sinclair D. and Hoopes G.S. (1975a). A novel form of diffusion battery. *Am. Ind. Hyg. Assoc. J.* 36:39-42.

RESEARCH LINE 3.10

**Groundwater flows in the Venice lagoon
system**

TIME VARIANT TOMOGRAPHY MONITORING OF THE SALT-WATER INTRUSION: GEOELECTRICAL SURVEY OF THE TEST-SITE

Roberto De Franco¹, Giancarlo Biella¹, Graziano Boniolo¹, Adelmo Corsi¹, Antonio Morrone¹, Alfredo Lozej², Ginette Saracco³, Barbara Chiozzotto⁴, Marco Giada⁴, Massimo Barbetta⁶, Valentina Bassan⁵, Christelle Claude³, Enrico Conchetto⁵, Giuseppe Gasparetto-Stori⁶, Antonio Gaspari⁷, Adriano Mayer³, Federica Rizzetto⁷, Luigi Tosi⁷

¹ IDPA-CNR, Milano, ² Dip. Scienze della Terra, Università degli Studi di Milano, Milano, ³ CEREGE, Aix en Provence, France, ⁴ Morgan Srl, Marghera (VE), ⁵ Provincia di Venezia-Servizio Geologico, Venezia, ⁶ Consorzio di Bonifica Adige-Bacchiglione, Padova, ⁷ ISMAR-CNR, Venezia

Riassunto

Vengono qui illustrati i risultati dell'elaborazione dei dati geoelettrici acquisiti nel campo sperimentale istituito nel bacino scolante meridionale della laguna veneta, in prossimità del margine lagunare, in località Casetta. L'obiettivo del campo sperimentale consiste nel monitorare in continuo l'interfaccia acqua dolce-acqua salata per conoscere la relazione tra i flussi dolci sotterranei provenienti dal bacino scolante verso la laguna, quelli salati che viceversa giungono dalla laguna e si intrudono nel sottosuolo della pianura e quelli di dispersione dall'alveo del Bacchiglione-Brenta, i quali, a seconda delle condizioni idrauliche e meteo-marine, possono essere di acqua dolce o salata. Attualmente è in corso la caratterizzazione geofisica del sito, al fine di individuare i parametri ottimali per lo stendimento elettrotomografico permanente a picchetti indirizzabili e tele-controllato, che consentirà l'acquisizione tomografica a scala oraria. Si è predisposto il seguente programma di misure:

- esecuzione di due sondaggi elettrici verticali di controllo le cui interpretazioni mostrano uno strato più superficiale con resistività di 15-25 Ωm e spessore di 1.5-2.5 m, seguito da uno strato a bassa resistività con valori compresi tra 3 e 6 Ωm , osservati alla profondità media di 3m. L'elettro-stratigrafia mostra una crescita della resistività fino a valori massimi di circa 14 e 10 Ωm alle profondità rispettive di 25 m e 35 m nei due SEV. La prima discontinuità geoelettrica dovrebbe corrispondere al tetto del cuneo salino, che si dovrebbe estendere ad una profondità di circa 30-40 m, ipotizzandone valori di resistività inferiori a 6-7 Ωm ed inglobando in esso anche la zona di transizione ad acqua salmastra.

- esecuzione di sondaggi elettrotomografici a interdistanza elettrodica compresa tra 2.5 e 10 m, per acquisire informazioni sulla distribuzione spaziale della resistività lungo una sezione bidimensionale. Tutte le elettro-tomografie indicano una tendenza all'aumento della resistività proseguendo da nord a sud.

In tal modo viene ben delineato il cuneo salino, che, dall'inizio del profilo, si estende fino a circa 350 m a sud, ha il tetto a pochi metri di profondità e spessore che, da circa 35 m all'inizio del profilo, diminuisce gradualmente verso

sud allontanandosi dal margine lagunare.

Abstract

In order to evaluate the time variant salt water intrusion extent in coastal aquifers south of the Venice lagoon, a test site has been chosen near Casetta, a pumping station of the Consorzio di Bonifica Adige-Bacchiglione. In this paper the data and interpretation of a geophysical survey performed in the test site are presented. Aim of the study was the electrical characterization of the test site, to define the physical parameters of the permanent tomographic array. Two vertical electrical soundings (VES) have been acquired in order to depict the distribution of the electrical field, together with three tomographic sections, with electrode spacing of 2.5, 5 and 10 m respectively and maximum offset of 730m in order to obtain the spatial distribution of the resistivity, both laterally and in depth.

The VES interpretation shows an upper layer of 15-25 Ωm of resistivity and 1.5 to 2.5 m thick, followed by a conductive layer with resistivity of 3 to 6 Ωm and extending at 25-35 m depth, where the resistivity values increase to 10-14 Ωm . The conductive layer should correspond to the seawater intrusion, including both salt and brackish water. From the tomographic images the saline wedge seems to extent vertically from few meters up to 35 m depth near the lagoon, extending southward, far from the coast line, up to 350 m offset, showing a gradual decrease in thickness.

1 Introduction

Saline water intrusion into aquifers of many coastal areas has resulted in acute environmental problems. Excessive withdrawal of ground water, as well as significant decrease in recharge of the aquifers due to less rainfall, has largely aggravated the hazard. At the interface between the freshwaters of the aquifers and the encroaching seawaters a natural wedge or saline intrusion occurs due to contrasts in the two water body volume and density (Fetter, 1994). These are in turn influenced by the nature of geological formations present, hydraulic gradient, rate of withdrawal and recharge of ground water (Choudhury et al., 2001). The resulting pressure gradients produced by these influences is an active phenomenon that regulates the storage and flow of freshwaters within the aquifers. Moreover it has been shown that the natural external processes of the tidal fluctuations in seawater levels influence the pressure gradients within the aquifers (Ataie-Ashtiani et al., 2000). This in turn results in a proportional change in the mean water table levels due to the movement of the saline intrusion into and out of the aquifer over tidal periods (Choudhury et al., 2001).

In the framework of the second CORILA Research Programme, Line 3.10 has the aim of studying the groundwater flows in the Venice lagoon system, starting from its southern sector. The investigated area is characterized by well developed paleo-river systems, intersecting the lagoon edge and the close coastline. Permeable sediments, bounding two salt-water bodies, represent

preferential pathway of communication among waters with different salinity, resulting in a critical unconfined aquifer contamination by salt water intrusion from the sea and the lagoon (Carbognin and Tosi, 2003). It is reported by Galgaro and Tosi (1999) that the two dimensional extent of the saline wedge is strongly related to the different morphology of the littoral (3 m a.s.l.) and the inland (3 m b.s.l.) sectors. Reclaimed land constitutes the inland area, where pumping is required to maintain the water level below the land surface. The critical ground elevation, the water pumping and the marine water seepage during high tides, together with exceptional dry summer seasons, are the factors that allow the salt water contamination of the agricultural soil (Galgaro and Tosi, 1999). Resistivity surveying is one of the best non-invasive techniques in groundwater investigations because of its capability to detect changes in pore-water salinity, thus allowing a distinction between fresh and saline water. A test site has thus been chosen near Casetta (Fig. 1), a pumping station of the Consorzio di Bonifica Adige-Bacchiglione, in order to detect, map and consequently monitor the saline intrusion within the southern coastal area of the lagoon by using the geoelectrical imaging survey technique (electrical resistivity tomography). Time variant monitoring using this non-intrusive method would allow an assessment of the occurrence and movements of hydrological processes related to the natural and anthropogenic processes at different time scales from daily to seasonal.

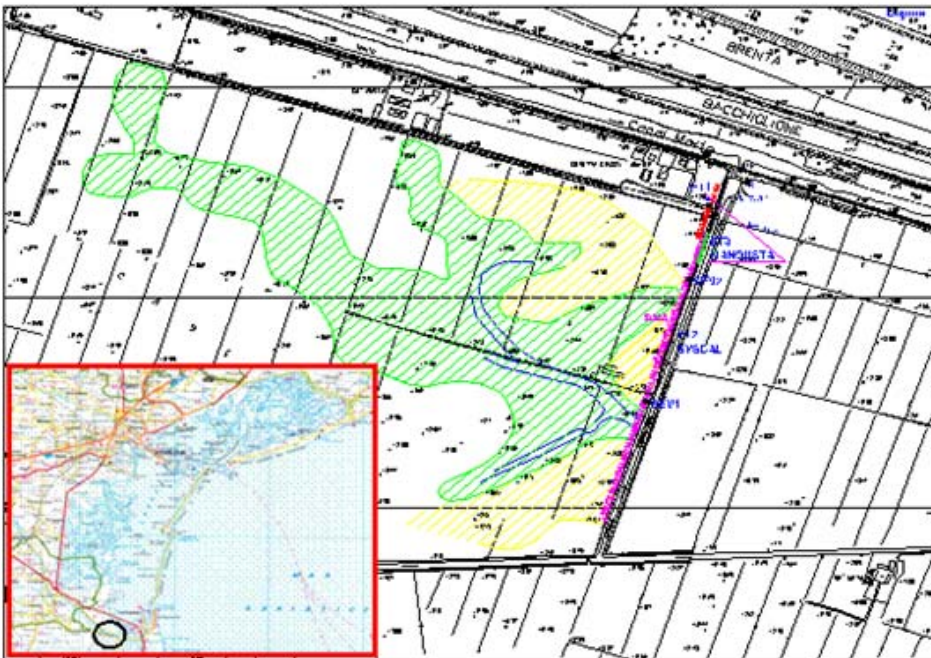


Fig. 1 – Location map of the test site area and the resistivity survey (VES and tomography lines). Green lines represent a paleo-river (Carbognin and Tosi, 2003).

In this paper we present the results of a preliminary geophysical survey devoted to highlight the electrical character of the test site and to define the physical parameters of the outgoing permanent continuous monitoring tomographic

array. Two vertical electrical soundings (VES) have been acquired in order to depict the distribution of the electrical field, together with three electrical resistivity tomography lines, with electrode spacing of 2.5, 5 and 10 m respectively and maximum offset of 730m, in order to obtain the spatial distribution of the resistivity, both laterally and in depth.

2 Data and interpretation.

Two vertical electrical soundings have been carried out along the chosen line in order to depict the distribution of the electrical field and to understand the geological structure of survey area, together with three tomographic sections, with electrode spacing of 2.5, 5 and 10 m respectively and maximum offset of 730m in order to obtain the spatial distribution of the resistivity, both laterally and in depth. (Fig. 1).

2.1 Vertical electrical soundings (VES)

The two VES were acquired near Casetta and 300 m southward. The Schlumberger electrode array was used, with a maximum current electrode spacing of 600 m and 400 m respectively. Figure 2 shows the apparent resistivity curves with superimposed the data obtained by inversion of the interpreted models shown in Figure 3.

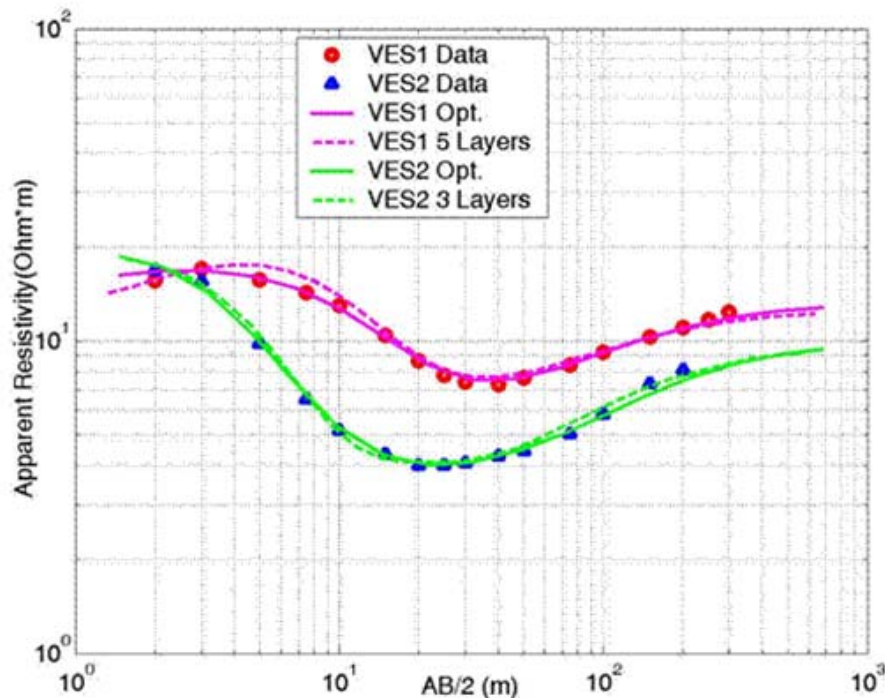


Fig. 2. VES's data with superimposed the calculated curves on the basis of models shown in figure 3.

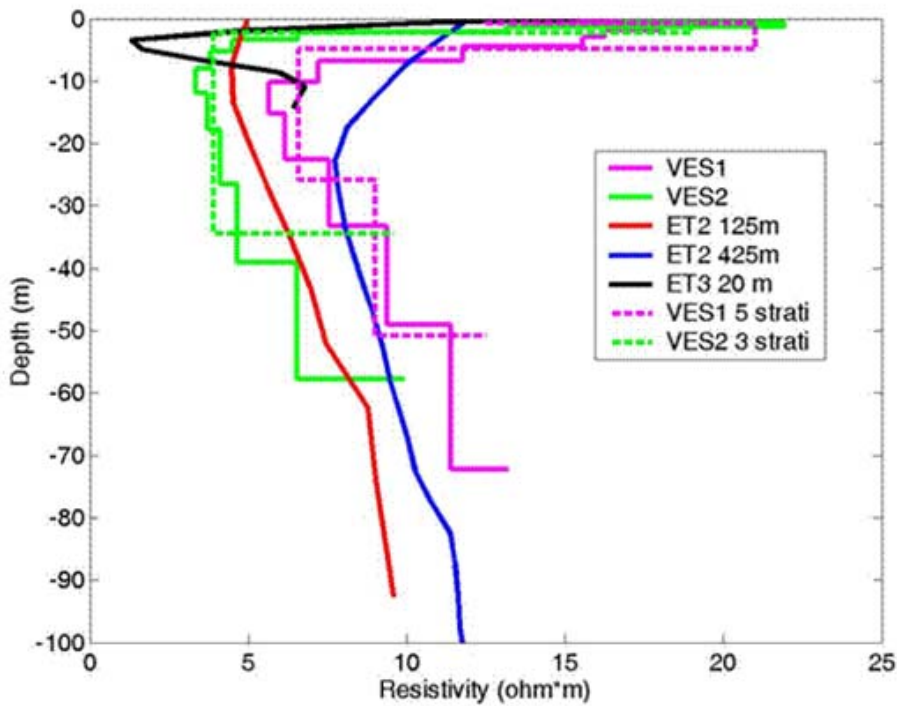


Fig.3. Interpreted models from VES and electrical tomographies ET2 and ET3.

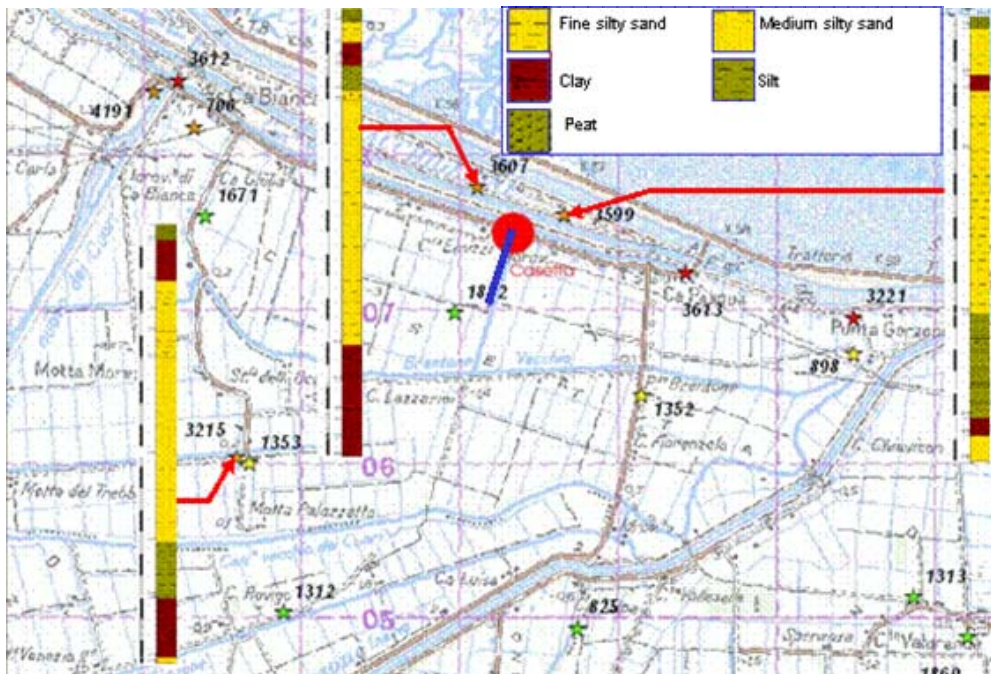


Fig. 4. Site map of selected borehole stratigraphies.

The VES curves were initially interpreted using the Orellana and Mooney (1966) Master Curves with a trial and error procedure obtaining an average electrostratigraphy of 3 and 5 layers respectively (dashed lines). A standard inverse modelling program has been then used to get the parameters of the

best fitted model (Fig. 3, continuous lines). The obtained models show on average a three layers stratigraphy, with an upper layer 1.5-2.5 m thick and 15-25 Ωm of resistivity. The intermediate layer, 25-35 m thick, shows resistivity values of 3 to 6 Ωm , followed by a basal layer with resistivity of 10-14 Ωm . According to the selected borehole data (Fig. 4) and the reported fluid conductivity (Carbognin and Tosi, 2003, and references therein), the upper layer is composed of peat and silty clay, followed by silty sand saturated with salt water, representing in fact the saline wedge. The third layer represents a transition from salt to fresh water in sandy clayey deposits.

2.2 Geoelectrical imaging survey (Electrical resistivity tomography, ET)

A conventional electrical imaging technique, which uses a limited number of electrodes, becomes impractical and uneconomical when surveys are to be conducted over long traverses. For efficient coverage, large electrode spacing is used but information from the near-surface of the surveyed area is missing. Consequently ambiguous sections would result from such surveys. Therefore, it is necessary to find alternative survey techniques that lead to rapid data acquisition while simultaneously increasing the resolution of the resulting section. In order to overcome this problem a multiscale survey technique has been proposed to be used (Griffiths et al., 1990 and 1993). In this technique, information from various depth levels is gained by conducting a series of measurements using different electrode spacing over the same survey line.

In order to obtain the spatial distribution of the resistivity, both laterally and in depth, at the proposed site three electrical resistivity tomography lines were performed, with electrode spacing of 2.5, 5 and 10 m respectively and maximum offset of 730m (Fig. 1). The apparatus chosen for the survey consisted of both the IRIS-Syscal System and a self constructed computer controlled system (Mangusta System; Morrone, 2003). The Wenner configuration was used as the most efficient in terms of the ratio of received voltage per unit of transmitted current (Roy and Apparao, 1971). The Wenner array has also the lowest number of measurements compared with the other arrays employed in geoelectrical imaging survey (Xu and Noel, 1993). The data gathered in this survey were then interpreted quantitatively using the rapid inversion algorithm of Loke and Barker (1996) to provide the inverse resistivity sections that approximate the actual subsurface structure.

The first line (ET1, Fig.1) was acquired using the Mangusta system, with an electrode spacing of 5 m and offset of 125 m, and conducted starting from the road bordering northward the lagoon shoreline. This part of the profile is characterized by the presence of an electric power cabin and a little bridge crossed by the line. Figure 5 shows the data and the result of the inversion. The saline water/fresh water boundary is fairly well mapped. The blue colour is related to the saline water intrusion, with resistivity values less than 1.5 Ωm , overlaid by the brackish water zone with resistivity around 4.5-6 Ωm . Resistivity values above 6 Ωm are thought to represent the fresh water zone in silty sand

deposits. The high resistivity plume at 90 m offset is related to the bridge, where to electrodes were placed, and the underlying void, that cause the high RMS value of the inversion.

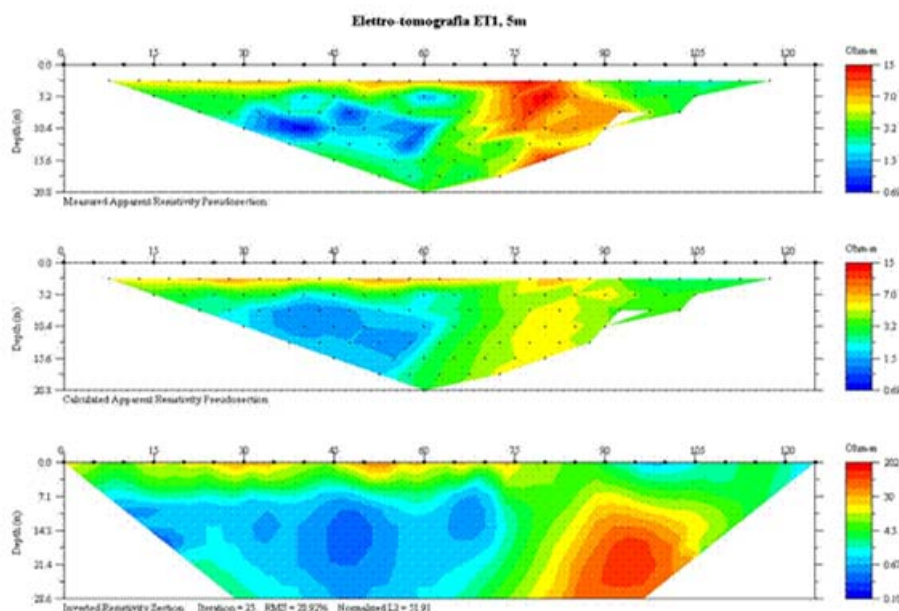


Fig. 5. Electrical resistivity tomography ET1.

The second line (ET2, Fig 1) is situated behind the bridge southwards and the data were collected using the IRIS-Syscal System, with an electrode spacing of 10 m and a maximum offset of 710 m, in order to obtain the best vertical and lateral resistivity distribution. Figure 6 shows data and obtained image. Despite the loss of resolution in the shallower part, due to the electrode spacing, a low resistivity wedge is fairly well depicted up to 280 m offset and depth ranging from 30 m to the surface southward. This is thought as the saline wedge, even though some ambiguities remain about the underlying portion of the model, with resistivity around $6 \Omega\text{m}$, which could represent both clay/sandy clay and sand saturated with brackish water. The relative high resistivity between 420 m and 490 m offset is related to a paleo river, as part of the paleo-river system reported in Carbognin and Tosi (2003).

On the basis of the results of the previous discussed two ET lines, a third line ET3 (Fig. 1) has been acquired using the Mangusta system, with electrode spacing of 2.5 m and maximum offset of 65 m. This geometrical configuration was chosen in order to overcome the loss of information from the near surface of the surveyed area. Measured apparent resistivity pseudosection and inverted tomography section are shown in figure 7. This image represents a good detail of the saline wedge outlined in the first part of the section ET2. A thin (less than 2m thickness) resistive superficial layer is followed in depth by a high conductive salty layer (blue colour) bounded by terrains probably saturated of brackish water, along all the extension of the line both laterally and in depth. The very well mapped bottom of the conductive layer could represent an

impermeable terrain, for which the conductive layer itself represents a preferential way of saline water intrusion from the lagoon.

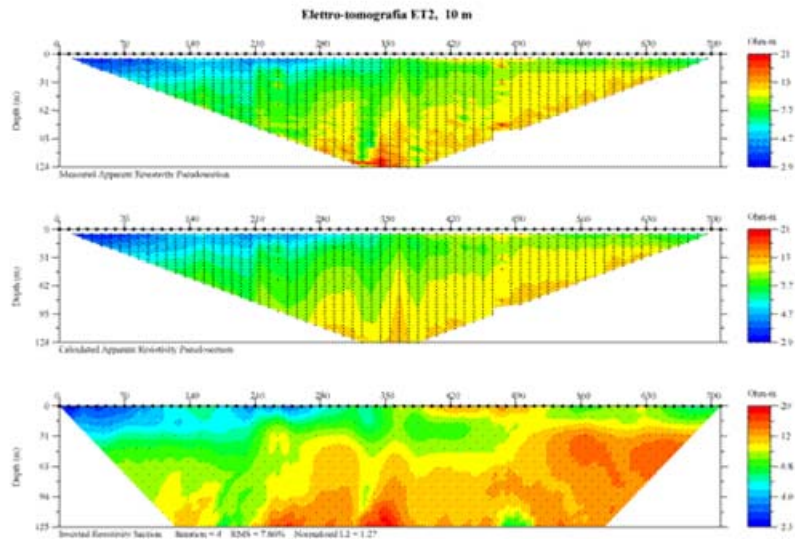


Fig. 6. Electrical resistivity tomography ET2.

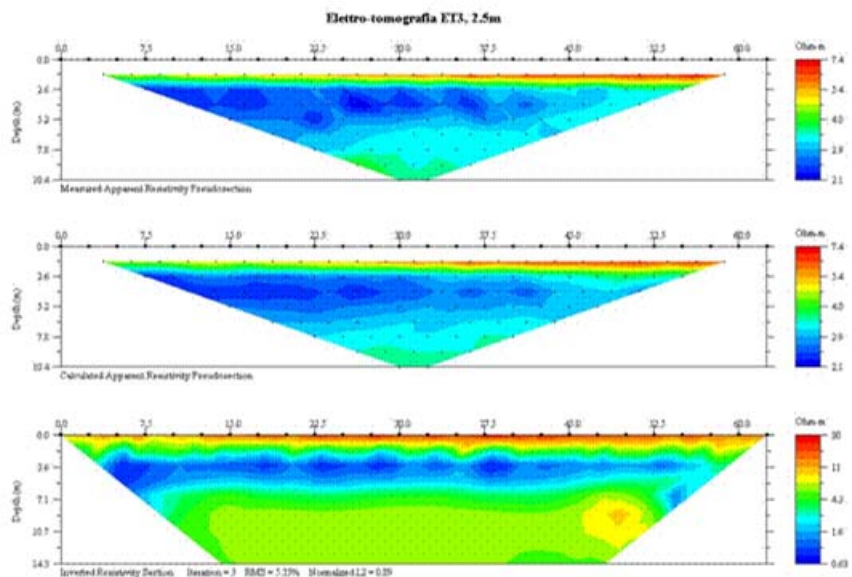


Fig. 7. Electrical resistivity tomography ET3.

3 Conclusions.

The geoelectrical survey carried out in the test area of Casetta has outlined the hydrogeophysical characters of the subsurface and delineated the boundary between the aquifer and the saline/brackish ground water zones. Some ambiguities remain about the extension of the brackish zone both laterally and vertically. They should be addressed by drilling some piezometers along the profile, as already planned. The electrical resistivity tomography technique has

demonstrated, in coastal settings, to be able to detect and consequently monitor hydrogeological processes such as the saline intrusion and its changes at different time scale, from daily tidal variations to seasonally varying rainfall regimes.

With respect to the best experimental parameters to be adopted in the continuous monitoring survey, the following consideration can be made:

-the Wenner configuration is the most efficient and a transmitted current of 300 mA will allow reliable voltage measurements in order to reach depth up to 100 m.

-the maximum offset of 400 m has to be adopted, in order to sample the possible extension of the brackish zone both southward and in depth, as outlined by ET2 tomography section and confirmed by figure 8, in which the inversion has been performed excluding the data acquired behind 400 m offset.

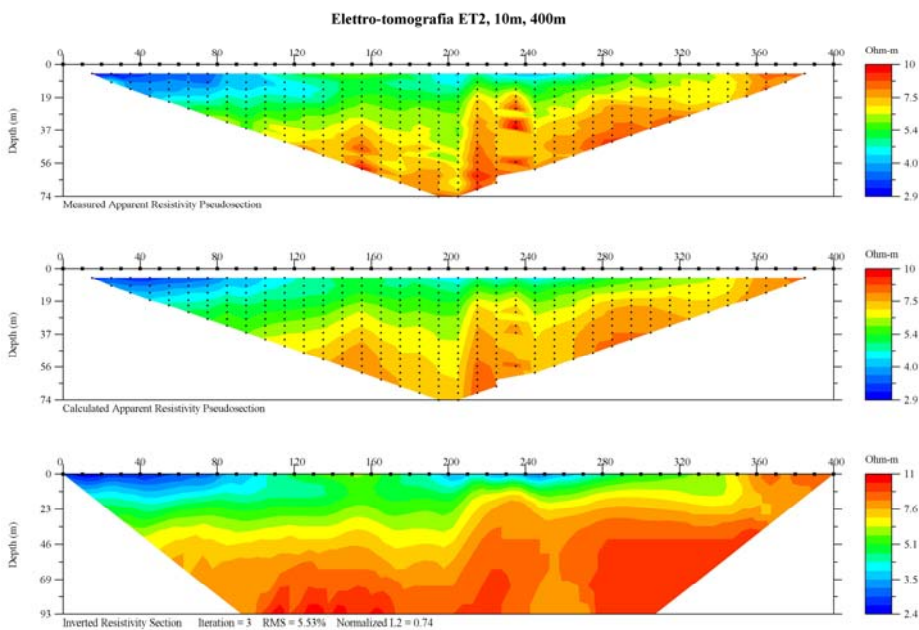


Fig. 8. Electrical resistivity tomography ET2 obtained with data up to 400m offset.

-the electrode spacing should be of not more than 2.5 m in order to detail the near surface portion of the area, as shown by ET3 (Fig. 7). Using this spacing for all the 400 m of the profile would require an acquisition time of about four hours that is too much with respect to the tidal cycle of six hours. A good compromise is to adopt an electrode spacing of 2.5m up to 95 m, the offset to which the less resistivity values are encountered (Fig. 8). From 95 m to 400 m offset the electrode spacing could be of 5 m, thus allowing an acquisition time

less than 3 hours, as required to sample the effects of tidal cycle.

Acknowledgments

This study was carried out within the framework and with the financial support of the second research programme of CORILA. The authors wish to thank Andrea Vitturi for his continuous support

References

Ataie-Ashtiani B.R., Volker R.E. and Lockington D.A., 2000. Tidal effects on groundwater dynamics in unconfined aquifers. *Hydrological process*, 15, 655-669.

Carbognin L. and Tosi L., 2003. Il progetto ISES per l'analisi dei processi di intrusione salina e subsidenza nei territori meridionali delle province di Padova e Venezia. Grafiche Erredici-Padova.

Choudhury K., Saha D.K. and Chakraborty P., 2001. Geophysical study for saline water intrusion in a coastal alluvial terrain. *Applied Geophysics*, 46, 189-200.

Fetter C.W., 1994. *Applied Hydrogeology*, 3rd edition, prentice-Hall.

Galgaro A. and Tosi L., 1999. Studio dell'intrusione salina negli acquiferi costieri del comprensorio meridionale veneziano: risultati preliminari. *Geologia tecnica & ambientale*, 2, 39-45.

Griffiths D.H. and Barker R.D., 1993. Two-dimensional resistivity imaging and modelling in areas of complex geology. *Journal of applied geophysics*, 29, 211-226.

Griffiths D.H., Turnbull J and Olayinka A.L., 1990. Two-dimensional resistivity mapping with a computer controlled array. *First break*, 8, 121-129.

Loke M.H. and Barker R.D., 1996. Rapid least-squares inversion of apparent resistivity pseudosection by a quasi-Newton method. *Geophysical Prospecting*, 44, 131-152.

Morrone A., 2003. Funzionamento hardware del sistema elettro-tomografico Mangusta. Rapporto interno IDPA-CNR, Milano.

Orellana E. and Mooney H.M., 1966. Master tables and curves for vertical electrical sounding over layered structures. Madrid Interciencia, 150 pp., 66 tables.

Roy A. and Apparao A., 1971. Depth of investigation in direct current methods. *Geophysics*, 36, 943-959.

Xu B. and Noel M., 1993. On the completeness of data sets with multi-electrode systems for electrical resistivity survey. *Geophysical prospecting*, 41, 791-801.

Radon activity in the southern Lagoon of Venice and the Adriatic Sea

A. Mayer¹, J. Gattacceca², C. Claude², O. Radakovitch², M. Giada³, A. Cucco⁴, C. Vallet-Coulomb², B. Stenni⁵, O. Flora⁵, L. Tosi⁴ and F. Rizzetto⁴.

¹ CNR - IDPA, Sezione di Milano. IDPA-CNR, Milano, ² CEREGE, Aix en Provence, France, ³Morgan Rilievi Srl, Marghera (VE), ⁴ CNR - ISMAR, Venezia, ⁵Dipartimento di Scienze Geologiche, Ambientali e Marine - Università degli Studi di Trieste

Introduction

In the frame of the line 3.10 research we are investigating the possibility that groundwater sources exists in the Lagoon of Venice (LV), either in the form of localised springs or as diffuse seepages. The knowledge of the rate of submarine groundwater discharge (SGD) into the LV is important for many practical issues related to land use in the surrounding watershed but also for several environmental aspects of the lagoon ecosystem, such as flux of nutrients (nitrates), algal blooming, land subsidence and mobilisation of heavy metals in sediments due to changes in pore-water salinity. Hydrological modelling of water circulation in the lagoon usually does not take into account changes in salinity due to SGD. Umgiesser et al 2004 however pointed out that unknown components of freshwaters discharge may be responsible of some discrepancy between the salinity distributions predicted for the LV with hydrodynamic models and salinity data.

Although the inputs of surface freshwaters entering the LV is well know from previous studies (for instance DRAIN), a global estimate of SGD into the LV has never been attempted. In the northern part of LV, and in some central parts between Venice and Marghera, freshwaters in localised springs have been historically known from anedoctic observations of fishermans. Changes in salinities are also due to diffuse seepages in the Cona zone. For the southern parts of LV, instead, no data or historical records on the existence of SGD seems to be available. We remind however the fact that in the past, several "casoni" in the lagoon islands of the southern part of the LV where permanently inhabited. In many of these settlements, wells existed to provide potable freshwaters from the shallower aquifer. It is reasonable therefore to presume that at shallow level an aquifer occurs and that at least in some of the deeper bathymetries of the LV (such in canals or through formed by tide currents) this aquifer is actually intercepted. Depending on the piezometric heads, these zones of exchange could represent sources of SGD or entry points of seawater into the first aquifer. Groundwater sources are also known offshore the LV, in the zone of the Tenue (Chioggia) and more to the north (offshore Jesolo - Cavallino).

The quantification of the SGD fluxes with classical hydrological methods is notoriously difficult due to the dispersive character of the groundwater seepage.

A volume- integrated estimate is however possible using appropriate natural tracers such as radium and radon. The ^{222}Rn (hereafter called "radon") activity in particular is an ideal natural tracer to study diffuse SGDs. This noble gas is produced by decay of the parent isotope ^{226}Ra present in traces in sediments and it decays with a half-life of 3.82 days into ^{218}Po . The concentration of radon in surface waters (lacs, rivers, sea and lagoons) are almost invariably very low, due to the relatively fast radioactive decay and the dispersion into air and offshore waters. Conversely, in the aquifers, an equilibrium tends to be reached between the rate of emanation of radon from the solids and the rate of its removal by diffusion, advection and radioactive decay. As a result, concentrations of radon in groundwaters of any salinity are much higher (up to several ten or hundreds thousand of Bq/m³), than those of surface waters (10 to 100 Bq/m³). This clear difference in concentration allows a distinction between freshwater inputs via-surface or via-SGD. Several other important reasons justify to use radon as tracer: its behaviour as a noble gas, chemically and biologically inert; its half-life of 3.82 days, appropriate to study a variety of hydrologic, oceanographic and diffusive processes (estimates of fluxes, transit times, diffusivities of water masses, benthic exchanges, bio-irrigation).



Figure 1: sites investigated in this study

Here we report the radon data obtained during the first two campaigns (February 2005 and April 2005) in the southernmost basin of the Lagoon of Venice (Chioggia Sub-basin) and in the Adriatic Sea. Radon activity in lagoon- and coastal waters have been continuously monitored during the change of tides with an alpha spectrometer RAD7 and other equipments described below, for five localities: Petta di Bo, Millecampi, Grisa, Pellestrina and the CNR-platform (figure 1). The study was conducted in these periods in order to highlight possible seasonal changes of SGD. The end of February is typically the end of the driest period of winter, while the end of April is at the end of the wettest period in springtime, corresponding to the minimum and maximum possible SGD, respectively.

1 Methods

In the studied sites we used the same standard equipment for radon data acquisition. A 12-V immersion pump connected with a PE tubes was deployed in the lagoon water always at 25 cm from the sediments. The pump provides a constant flow (2.5 litre/min) of bottom lagoon- or sewerwater into a gas exchanger. We used an immersion pump to avoid the problems of remobilization of sediments and possible degassing of radon into the tubes (seawater is not sucked from surface in our case). Before to enter the gas-exchanger, water is filtered at 80 micron to remove suspended particles. Radon originally present as dissolved gas in seawater diffuses with known rate into the air present in the gas exchanger. During acquisition, the gas exchanger is permanently connected in series to 1) a nafion membrane that strip the excess of water vapor, 2) a drierite column that further dries the air, 3) a series of filters that remove the aereosols, and 4) the alpha spectrometer. The air outgoing the spectrometer then returns into the gas exchanger forming a closed loop. A pump assure the air circulation within the closed loop. In the spectrometer, radon decays in ^{218}Po that is suddenly ionized as Po^+ and then conveyed into a silicon detector by using an electrostatic field of 2100V. The silicon detector measures the energy decay of ^{218}Po and, after reaching secular equilibrium, that of ^{214}Po . Radon concentrations are then calculated from the activity of the polonium isotopes and various calibrations. Since the water is constantly flowing into the gas exchanger while the spectrometer monitors the activity of ^{218}Po and ^{214}Po , and also the gas loop is never in contact with external air, radon activity can be calculated in continue without the need to collect discrete samples. The water discharged from the gas exchanger is then measured for salinity. Temperatures are also measuerd in continuous within the gas exchanger (necessary for the calibrations) and by the MORGAN doppler currentometer.

Before to enter the gas exchanger, a fraction of the water supplied by the immersion pump is deviated into another apparatus. Water is there filtered to remove 40- and then 0.4- micron sediment-plancton fraction. Afterwards the water passes through two acrylic fibers coated with MnO_2 that collect radium dissolved in seawater with known efficiency. Acrylic fibers have been kindly

provided by Ms. Gandolfi, Montefibre - Marghera. ^{224}Ra has a half-life of 3.4 days and decays into ^{220}Rn that is easily measurable using the radon alpha spectrometer. At the end of the radon data acquisition in the lagoon or at sea, fibers are mounted into a glass container connected in closed loop with the alpha spectrometer. From the measured activity of ^{220}Rn it is possible to calculate the ^{224}Ra concentrations in seawater knowing the volume of water passed through the fibers. To calculate the volumes, flow counters are installed at the outlet of the last MnO_2 fiber and at the inlet of the gas-exchanger. In addition, after storing for 2 weeks the fibers into closed glass containers, the radon emanated from the ^{226}Ra adsorbed into the fibers is also analysed with the alpha spectrometer. From this second radon measurement, we are then able to obtain the concentration of ^{226}Ra dissolved in seawater. The ensemble of the apparatus, that is fully portable, has been developed with CORILA and CEREGE founding. In summary, the apparatus allows the measurements of radon, ^{224}Ra and ^{226}Ra in the same mass of water without the need to collect discrete samples. The knowledge of the concentration of ^{226}Ra in the same water mass also allows an evaluation of the true "excess" of radon, i.e. the difference between the total radon present in water (measured using the gas-exchanger) and the radon supported by decay of ^{226}Ra dissolved in water. Also, the knowledge of the activity ratio ^{224}Ra - ^{226}Ra allows an evaluation of the residence time of water masses, as this activity ratio changes with time but not with dilutions. We also collected samples of seawater in the same localities in order to obtain minor and trace elements concentrations, Sr, O, H isotopes and ^{226}Ra and ^{228}Ra activity measured by thermal ionisation mass spectrometry. Data obtained for radium and other tracers will be discussed in another report.

2 Experiment at Petta di Bo

Radon activity of the water was monitored during the passage through the minimum ebb phase at the Petta di Bo mareograph. Continuous measurements of current direction and intensity, water level, temperature and salinity were made with instruments of the MORGAN-RILIEVI. At Petta di Bo, the bathymetry is 1 m, a typical values for the LV. The point of measurement is located 50m outside a navigation canal. By time-integration of the measured currents we reconstructed the displacement of the water mass during radon data acquisition. Water mass travelled for about 850 m before to inverse its direction of movement due to the change of tide. At the fixed point of the Petta di Bo mareograph we actually measured radon two times for the same water flowing in the two directions. The currentometric data obtained in situ by MORGAN-RILIEVI (portable doppler currentometer) well compare with OGS-CORILA current data obtained by Perini (OGS) at the lagoon mouth of Chioggia by applying the tide delay-time and amplification factors calculated by Cucco for the Petta di Bo using the hydrodynamic model of LV (figure 2). This almost coincidence of results confirmed that for the southern part of the LV, in normal meteorological conditions such as those of this experiment, currents, tide-high and water-mass displacements can be reliably reconstructed using OGS-CORILA data obtained at the mouth of Chioggia and the hydrodynamic model

of Cucco and Umgessier. The good agreement in both time of tide inversion (about 12 minutes of difference) and tide level in respect to Z (Punta della Salute) also implies that the LV was in "ideal" condition during the course of these radon measurements.

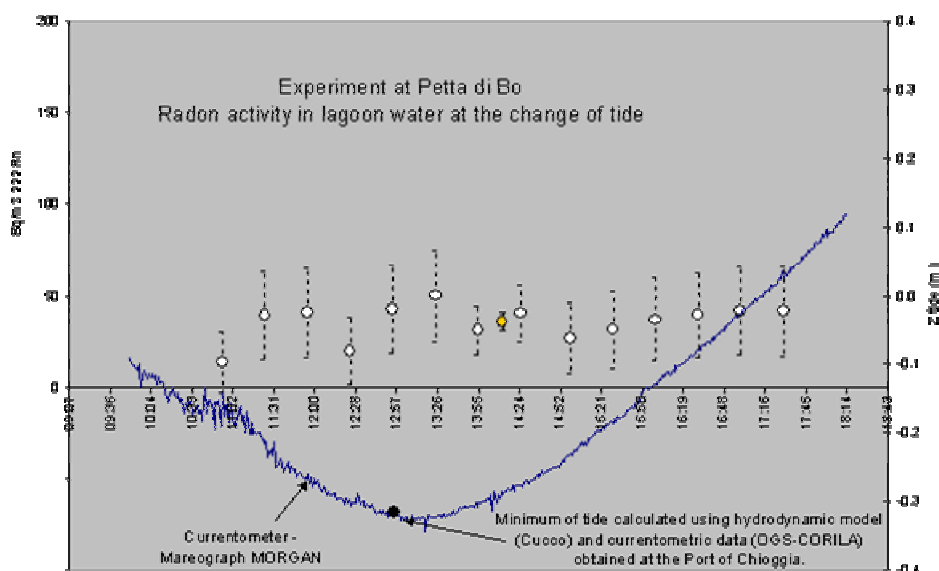


Figure 2: radon concentrations monitored during the change of tide at Petta di Bo.

At Petta di Bo radon data was obtained every 30 minutes (figure 2). The activity resulted very low, and no significant change is observed at the tide inversion. This water mass was therefore well homogenised in respect to radon at this scale (800m). Radon activity reported in figure 2 and following figures, have 2 sigma error-bars. The mean square of weighted deviates of the data is 1.03. The probability that the analytical errors alone justify the observed scattering of data is 42 per cent. This value is quite high and justify, from a statistical point of view, the pooling of all data into a weighted mean value of 33.4 ± 5.3 Bq/m³. Error here is expressed as 95% confidence limits, taking into account the observed data scattering. However, in order to compare data obtained with different counting times in other experiments, we combined the data obtained every 30 minutes in order to get one value as it would be obtained from a single counting experiment lasting the total counting time. In this case, the concentration of radon at Petta di Bo deducted pooling 388 minutes of counting time is 35.7 ± 4.7 (2 sigma) Bq/m³. This is the value we will refer to for Petta di Bo.

3 Experiments at Millecampi

At Millecampi, we analysed radon during the ebb and flood phases in February and during one ebb phase at the end of April. We deployed the immersion pump at a depth of 5 meters in a canal linking the innermost parts of the Southern-western LV with the zone of "water divide" between the Chioggia Sub

Basin and the Malamocco Basin. Water passing through the canal derives from a much wider area in respect to that passing at Petta di Bo. These areas have also a typical bathymetry of 1m. Radon concentration found at the ebb phase are similar to those measured at the Petta di Bo: $28.0 \pm 4.9 \text{ Bq/m}^3$ in February and $26.2 \pm 3.1 \text{ Bq/m}^3$ in April. As in Petta di Bo, no discernible changes in concentrations of radon are found within the 2 hours before and the 2 hours after the inversion of tide. However a significantly lower radon concentrations, $14.5 \pm 5.8 \text{ Bq/m}^3$ is found at the full flood tide of February. Thus, during ebb phases, water contains about 13.5 Bq/m^3 more radon than in case of flood phases.

Some preliminary calculation on the fluxes of radon and possible SGD in this part of the LV can be done by assuming these concentrations as valid for the entire water column not affected by radon escape into the atmosphere (at the bottom of the canals, waters deriving from large areas are often well mixed because of the intensity of the currents). Assuming that at every cycle of tide the difference in radon activity of 13.5 Bq/m^3 is renewed, the radon flux from the bottom of the lagoon would be $\sim 18 \text{ Bq/day/m}^2$. This flux of radon should be considered as a combination of radon exhaled directly from the sediments, radon carried by pore water via diffusion mechanisms, and radon transported by groundwaters displacements. To have an idea of the SGD involved in the calculated flux of radon, we may assume that radon concentration of the groundwater below the LV is the same as the radon equilibrium concentration measured in groundwater of the shallower confined aquifer of the LV watershed, i.e. 10 kBq/m^3 (obtained from our work on ISES piezometer). With this assumption, the input of groundwater would be of 0.00125 liters per minute per square meter of lagoon. Considering a porosity of 0.7 for the initial layers of sediments (a typical value), the calculated discharge rate implies a vertical displacement of groundwater of about 0.25 cm/day. Before to take any conclusion about these value of SGD, however, we must evaluate precisely the diffusive flux of radon from sediments. A dedicated sub-research is ongoing to estimate diffusive fluxes and diffusivities constants. As a preliminary estimate we may assume that lagoon sediments contain about 50 Bq/kg of ^{226}Ra (as in the average suspended sediments measured by Degetto and Cantaluppi (2004, CORILA)). Diffusion from this type of sediment would supply a flux of radon into bottom lagoon water in the range between 7 and $30 \text{ Bq/m}^2/\text{day}$, the precise value being depending on the constant of effective diffusivity chosen. Sediment diffusion alone therefore could supply a flux of radon of the same order of magnitude of the flux of radon necessary to re-establish the radon excess in the inventory at every cycle of tide. The evasion of radon to the atmosphere, here neglected, should also be evaluated in future.

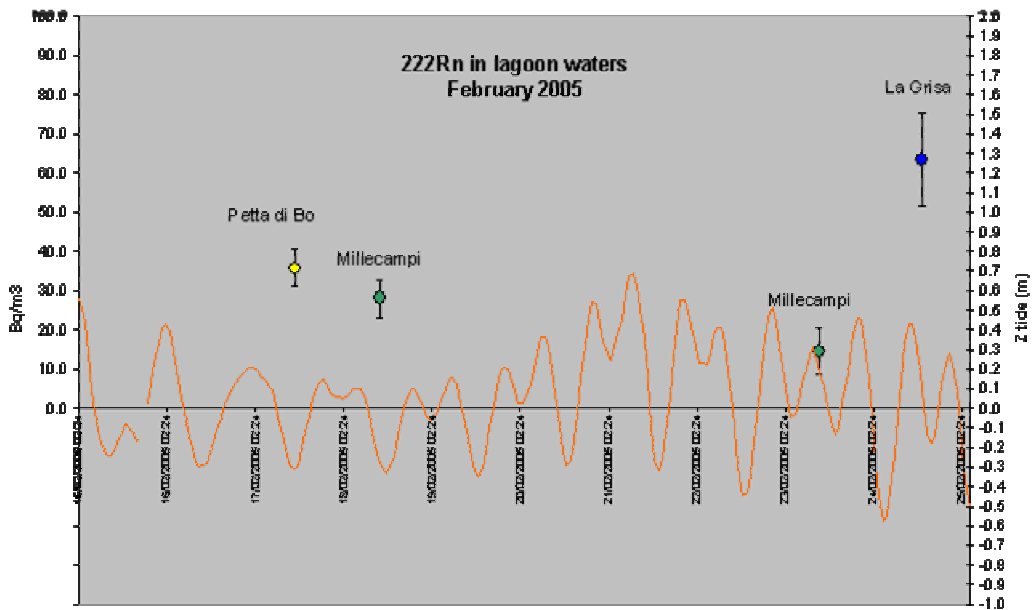


Figure 3: radon concentrations in different sites and tides of the LV at the end of February

4 Other experiments

In "La Grisa" we analysed radon during the ebb phase in a shallow pond. In this site we have found the highest concentrations of radon (about 70Bq/m3). We also analysed radon 1.7 km offshore the beach of Pellestrina and at the CNR oceanographic platform.

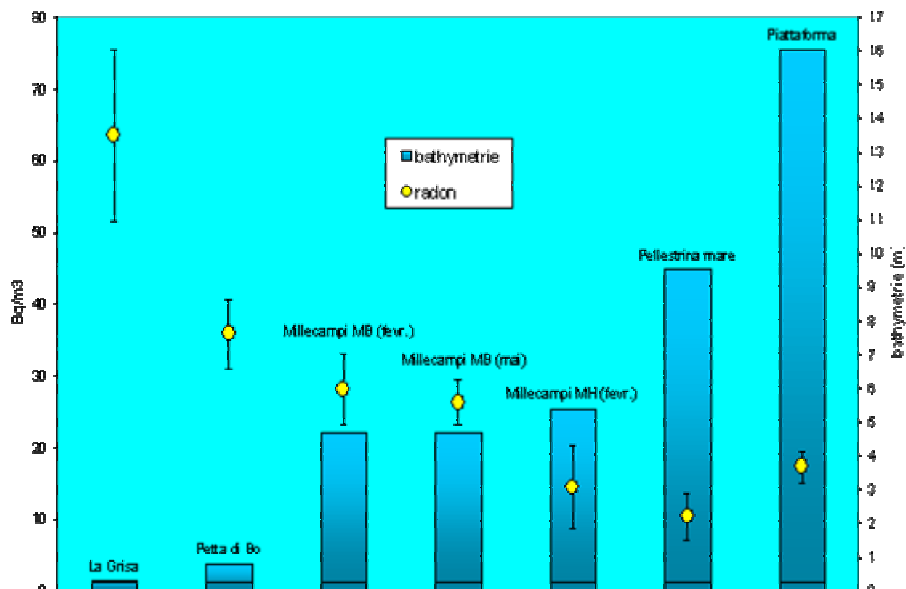


Figure 4: comparison of radon concentrations and bathymetry. Radon has been always analysed at 25cm from the sediments.

In figure 4, radon concentrations are compared together with the depth of the

water columns. Higher concentrations are found at the bottom of shallower water masses, i.e. at lower hydrostatic pressures. This fact is a clear indication that radon inventories in water columns within the LV must be corrected for the effects of dilution due to tidal changes of water levels, i.e. addition or removal of water masses having different radon concentrations. Moreover, as the data refers always to the water at 25 cm from the sediments and not to an inventory integrated to the entire water column, the inverse correlation observed between concentrations and bathymetry should not be the result of a simple dilution. On the contrary, fluxes of radon from the bottom sediments may somehow be dependent on the pressure that the water column exerts to the sediments.

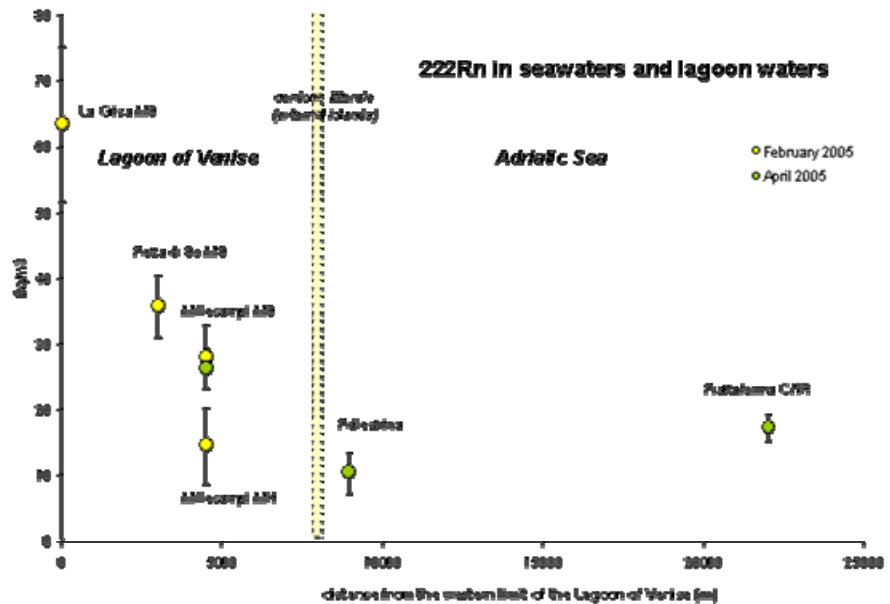


Figure 5. Radon concentrations plotted against distances starting from the inner border of the LV.

In figure 5 we finally compare the radon data with the distances from the coast. Offshore Pellestrina we measured the lowest radon concentrations (10.3 ± 3.2 Bq/m³). Such low concentration suggests that in this area water masses are relatively "older" in respect to time they abandoned their radon sources (the radon recharge areas in the lagoon). This interpretation is in agreement with the results of hydrodynamic modelling that envisage a zone of "devide" offshore Pellestrina, between the areas of influence of the Chioggia and Malamocco mouths. We may also note that waters present in the lagoon at the high tide (Millecampi) have almost the same radon concentration of the seawaters outside the influence of the lagoon (17.3 ± 2.1 Bq/m³ measured at the CNR oceanographic platform). This finding points for a long residence time of the lagoon waters, as predicted by hydrodynamic models.

Acknowledgements

We thank Ms. Perini (OGS) to kindly provide the currentometric data for the Port of Chioggia, Barbara Chiozzotto (MORGAN) for the data elaboration of the MORGAN doppler currentometer. We thanks also to the Captain A. Penzo and the crew of the Litus for the techical support during the experiments at the CNR Platform and offshore Pellestrina. We warmly thanks Ms. Gandolfi of Montefibre for providing us the acrylic fibers necessary for this study. This contribution has been financed be CORILA program 2005-2007, line of research 3.10.

RESEARCH LINE 3.11

Ecological quality indices, biodiversity and environmental management for lagoon areas

TEMPORAL AND BIOTIC EVOLUTION OF “*Botryllus* BIOCOENOSIS” IN THE PRESENCE OF ANTIFOULING PAINTS

Francesca Cima, Paolo Burighel, Lorian Ballarin

Dipartimento di Biologia, Università di Padova

Riassunto

E' stato affrontato il problema dell'azione destrutturata sulla comunità a *Botryllus*, un'associazione bentonica a macrofouling di substrato duro di varie specie di ascidiacei tra cui dominano le specie coloniali, da parte di nuove vernici antivegetative ampiamente usate su scafi e vari manufatti sommersi nell'area lagunare. Sono stati scelti e quindi utilizzati alcuni indici descrittivi della biodiversità (ricchezza in specie, struttura della comunità, indice di copertura-abbondanza, indice di similarità) per descrivere l'evoluzione della biocenosi su pannelli di legno e acciaio trattati con vernici antivegetative e immersi per un anno in tre stazioni della laguna di Chioggia con diverse caratteristiche idrodinamiche e di torbidità. I principi attivi presi in considerazione sono stati Sea-Nine 211, Diuron, TCMS piridina, Zinco piritione, Zineb ed Endosulfan. Il confronto di questi indici ha permesso di valutare le alterazioni della comunità e proporre le possibili cause destrutturate che portano alla selezione di specie dominanti spesso diverse da quelle del climax naturale.

Abstract

We investigated the disturbing action on “*Botryllus biocoenosis*”, a benthic association of various ascidians where the colonial species are dominant, by new antifouling paints today largely used on boat hulls and various structures submerged in the lagoon area. Some biodiversity indexes (species richness, biocoenosis structure, covering-abundance index, similarity index) were used to describe the evolution of biocoenosis on wooden and steel panels immersed for one year in three stations of Chioggia with different hydrodynamic and turbidity characteristics. The biocidal compounds taken into consideration were Sea-Nine 211, Diuron, TCMS pyridine, Zinc pyrithione, Zineb and Endosulfan. The comparison of biodiversity indexes allowed us to evaluate the alterations of biocoenosis and suggest the disturbing causes which result in selection of dominant species often different to those of the natural climax.

1 Introduction

The term biofouling refers to sessile marine animals and plants fixed on submerged hard substrata and encrusting steady structures such as stony harbour structures, wooden and steel parts of the boat keels as well as rope fishnets, plastic objects of every type and even other organisms. The association of organisms on a submerged surface can develop various features

depending on geographic place, type of substratum, physico-chemical characteristics of the seawater and seasonal climatic conditions. In the biocoenosis succession, a temporal sequence, depending on duration of immersion, a seasonal sequence, depending on the course of seasons and, finally, a biotic succession depending on the ecological niche occupied by various species, can be distinguished [Redfield and Delvy, 1952]. In the lagoon of Venice, the climax of the macrofouling biocoenosis of hard substratum is reached in summer and is represented by colonial ascidians of the Styelidae family as dominant species: it is the benthic "*Botryllus biocoenosis*".

Indeed, macrofouling growing on artificial objects constantly immersed in the seawater causes severe economic damages, which result in continuous maintenance of the structures and high costs due to hydrodynamic loss of the boats. The latter also involves a sensitive increase in fuel consumption with a consequent introduction in atmosphere of more than 201 t millions of carbon dioxide per year and 5.2 millions t of sulphur dioxide. A layer of only 100 µm of fouling on a boat keel provokes an increase of fuel consumption of 6% and, at a worldwide scale, the surplus of fuel consumption is estimated around 70 millions t. Therefore, the study of antifouling compounds is fundamental for the future of naval engineering with which it parallelly evolved.

The entrance of antifouling paints in the field of technology occurred in 1970s with the introduction of organotin compounds as principal biocides, which presented remarkable functional and economic advantages as well as numerous and severe disadvantages for their environmental impact so that in the course of the last years their employment was regulated and reduced with the purpose of reaching their total elimination within 2008.

As a consequence, from 1990s, the research of alternative biocides, to be applied as antifouling in paints for covering immersed objects, remarkably increased aiming to produce new chemical formulations effective on the fouling and also compatible with the preservation of marine ecosystem.

The purpose of our research was to evaluate the effects of some new antifouling paints in commerce, based on biocides alternative to organotins, on the "*Botryllus biocoenosis*" of the southern basin of the lagoon of Venice. Systems of wooden and steel panels coated with various antifouling paints, as previously described [Cima et al., 2005], were placed in constant immersion in three stations of Chioggia harbour (Venice) and representing three types of microenvironment of the lagoon biome which differ for bathymetric and hydrodynamic characteristics: station 1 was an abandoned mussel breeding along the Perognola canal, in front of the harbour entry in a zone far from the inhabited centre, where the depth of seawater was about 3 m; station 2 was sited near the dry coast land, in front of the Isola dei Cantieri, in a zone of low depth and considerable wave motion caused by traffic of the numerous fishing boats directed to the fish market; station 3 was sited along the Sottomarina canal in an internal zone in respect with the harbour entry, characterized by a scarce wave motion, where the seawater often appeared turbid. Panels were

permanently immersed for a period of a year and controlled monthly. Data collected during this period were elaborated and expressed by means of the biodiversity indexes at biocoenosis level, i.e., *species richness*, *biocoenosis structure*, *Benninghoff's covering-abundance index*, *Sørensen's similarity index*, with the aim of evaluating the effect of biocides on some target-species, the consequent alteration of the ecological succession on artificial hard substratum and possible ecological damage on the macrofouling biocoenosis. We have chosen paints containing various biocides formulated exclusively for an antifouling function, like Sea-Nine 211, or previously used as pesticides in agriculture, like Diuron, TCMS pyridine, Zinc pyrithione and Zineb. The biocidal efficacy of these paints was compared with a TBT-containing paint (Tab. 1).

We have then evaluated the disturbing activity of these new generation paints on the macrofouling biocoenosis. Generally, on the panels treated with antifouling paints the covering of fouling appeared always later and with minor extension than that on control panels.

2 Paint A

On panels coated with the reference TBT-containing paint an ecological succession was never recognisable, but only organisms resistant to biocidal activity as chlorophytae (*Enteromorpha* sp.) and cirripeds appeared. The similarity index (Fig. 1a), with the exception of a little peak value in September on wooden panels, trends downwards to zero similarly to what happens on steel panels in stations 1 and 2, whereas in station 3 this index generally shows a discontinuous trend.

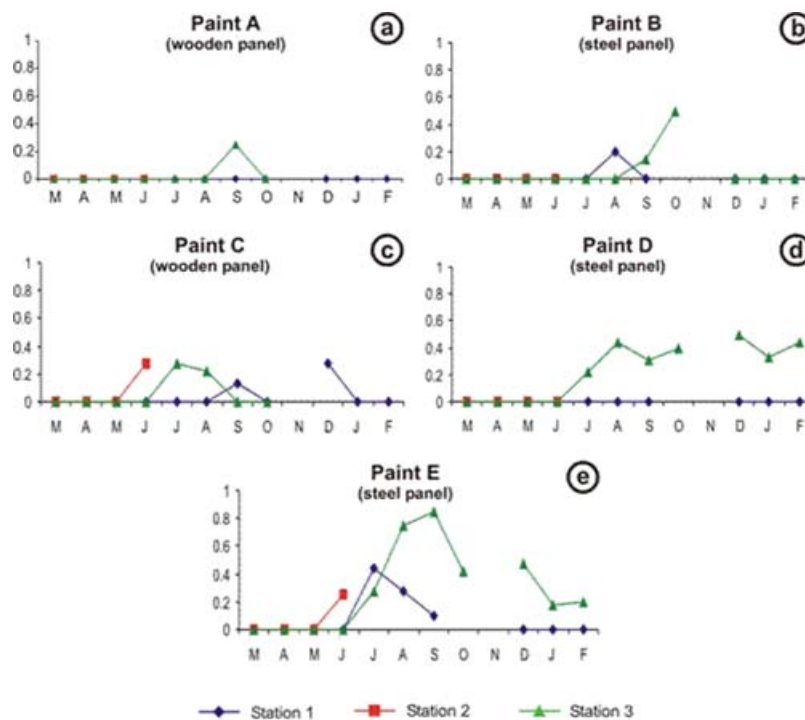


Fig. 1 - Sørensen's similarity index on panels coated with different paints.

Tab. 1 - Antifouling paints used on wooden and steel panels of the systems immersed in the environment.

PAINT		BIOCIDES	MATRIX	USE
A	Sigmaplane Antifouling HB	TBT methacrylate	Self-polishing with methacrylate copolymers	Fishing boats and freighters >25 m in length (hulls in steel, tarred wood, coated with epoxy resins)
B	Marlin Antivegetativa Velox TF	Zn pyrithione (5-10%), Zineb (5-10%), Endosulfan (1-5%)	Hard matrix with colophony	Fishing boats (helixes, boards, stern feet)
C	Veneziani Antialga	Sea-Nine 211 (2.7%) Diuron (7.6%)	Hard matrix	Sailing boats, motorboats (water line band)
D	Veneziani Propeller	Zn pyrithione (7-10%), Diuron (7-10%), Sea-Nine 211 (1-3%)	Hard matrix	Sailing boats, motorboats (helixes, boards, stern feet, flaps)
E	Veneziani Even 2 Extreme	TCMS pyridine, Diuron	Self-polishing with two components and Biomatrix technology	Sailing boats for competition (hulls in plastic reinforced by incorporated fiberglass, wood, steel)
F	Sikkens Super Gloss (Control paint)	–	Silicone alkylic resins	Fishing and sailing boats (craft waterline)

3 Paint B

The comparison with control panel shows a disturbing activity on the macrofouling biocoenosis, which appears consequently to be less complex and with a less number of species. Colonisation did not include more than three or four taxa at the same time. The most resistant organisms were bryozoans (*Bugula neritina*, *Bugula stolonifera* and *Cryptosula pallasiana*), tunicates (*Botryllus schlosseri*, *Botrylloides leachi*, *Botrylloides violaceus*, *Styela plicata*, *Ciona intestinalis*, *Asciella aspersa*), hydrozoans (*Tubularia crocea*), chlorophytae (*Bryopsis plumosa*, *Cladophora pellucida*, *Ulva lactuca*, *Enteromorpha prolifera*) and rhodophytae (*Polysiphonia sertularioides*, *Gracilaria verrucosa*, *Ceramium ciliatum*), while serpulids like *Hydroides dianthus* and porifers like *Sycon ciliatum*, *Halichondria panicea*, *Halichondria bowerbanki*, *Aplysina aerophoba*, *Hymeniacidon sanguinea*, which are common in fouling biocoenoses of the lagoon were occasionally present. As regards the difference among the structures of the biocoenosis in the various stations, station 1 was the most variously colonised on steel panels, followed by station 3 and station 2, while for wooden panels, which resulted generally more populated than those of steel, the order for colonisation extension was station 3, station 1 and station 2. The index of similarity shows, for steel panels, values similar as those of the corresponding panels coated with paint A, whereas for wooden panels the values are higher, with a peak of 0.7 in June on panel of station 2 (Fig.1b).

4 Paint C

In this case, the biocoenosis had a behaviour similar as that on the B paint, mainly as regards the tolerant and resistant species to which some serpulids (*Hydroides dianthus*, *Janua pagenstecheri*) and, to a lesser extent, cirripeds (*Balanus sp.*, *Balanus improvisus*, *Balanus amphitrite communis*), porifers (*Haliclona cinerea*, *Halichondria bowerbanki*, *Aplysina aerophoba*) and bivalves (*Ostrea edulis*, *Mytilus galloprovincialis*) were added. Hydrozoans were particularly sensitive towards the biocides. The number of taxa represented was high, with a climax of six-seven taxa which remained also for three months. As regards the structure of the biocoenosis on both wooden and steel panels, station 3 showed the highest taxonomic variability, followed by station 2 and station 1. The index of similarity shows very low average values although not comparable with those of panels coated with paint A, mainly in station 1 where the values are always close to zero. However, very high peak values which reached 0.9 were obtained from steel panels (Fig. 1c).

5 Paint D

The panels showed a minor delay in their colonisation in comparison with those treated with paint B and C and a covering lasting for the entire experiment, although a disturbing effect on the structure of biocoenosis was observed. The

taxa present on the panels seldom persisted with stable associations for more than two months and the number of total taxa was also low and represented by the same species. Cirripeds (*Balanus improvisus*, *Balanus amphitrite communis*), chlorophytae (*Cladophora pellucida*, *Ulva lactuca*, *Enteromorpha intestinalis*), bryozoans, hydrozoans and tunicates were dominant. Instead, rhodophytae (*Polysiphonia sertularioides*, *Gracilaria verucosa*), porifers (*Aplysina aerophoba*) and serpulids (*Janua pagenstecheri*, *Hydroides dianthus*) were represented by scarce covering. As regards differences among the structures of biocoenosis in the various stations, station 3 was the most variously colonised, followed in order by station 1 and station 2. The index of similarity shows on steel panels an average value similar as that of the paint A, whereas the values for wooden panels are clearly higher, with peak values of 0.7 (Fig. 1d).

6 Paint E

The colonisation began already from May and continued with typical associations of hard substratum till September when the climax was reached. Hydrozoans (*Tubularia crocea*) and bivalves (*Ostrea edulis*, *Mytilus galloprovincialis*) appeared to suffer drastically the effect of biocide presence. Therefore, the species richness was generally high, always showing higher values in comparison with those of the other antifouling paints. Also in this case, the variability of the structure of biocoenosis on both wooden and steel panels showed the same dependence on the station location, i.e. station 1 was the most various whereas station 2, like in the other cases, resulted the less colonised. The similarity index shows high values for all panels with peak values close to 1 (Fig. 1e).

7 Conclusions.

We have established an order of biocidal efficacy of the assayed antifouling paints by means of our direct observations of the panels during the course of a year and on the basis of the results expressed with the four biodiversity indexes used:

$$E < D < C < B < A$$

As regards the effect on the biodiversity of biocoenosis of hard substratum, it is remarkable that none of the paints assayed is more powerful than that which contains TBT. For its moderate impact on marine environment, Sea-Nine 211 has been decorated of the "Green Chemistry Challenge Award" by the U.S.A. Environmental Protection Agency (EPA) in 1996. Although the use of this biocide is not restricted by any legislation in many world countries, its toxicity was demonstrated on bacteria, aquatic plants and crustaceans [Fernandez-Alba et al., 2000], echinoderms [Kobayashi and Okamura, 2002] and teleosts [Okamura et al., 2001]. Organozinc compounds recently showed a high affinity with TBT in the toxic effects, in particular as concerns the values of LC50 in teleosts already at low concentrations [U.S. EPA, 2000]. In Europe, the use of this compound is regulated by the directive of Biocidal Products n. 98/8/EC.

Data on toxicity and environmental fate of TCMS pyridine are very scanty and only regarding laboratory animals. For the herbicide Diuron, evidence of high toxicity was reported on not-target marine invertebrates, as echinoderms [Kobayashi and Okamura, 2002] and amphipods [Nebeker and Schuytema, 1998], and also on vertebrates as teleosts [Okamura et al., 2001] and amphibians [Schuytema et al., 1998]. The above-mentioned directive of Biocidal Products n. 98/8/EC banned Diuron from the biocides usable in the antifouling paints, but Italy doesn't yet conform its normative to the European one. Analogously, after the occurrence of severe teratogen effects in 1994 in Indian persons living in villages where the cultivated fields were sprayed with Endosulfan [EJF, 2002], the use of this compound was forbidden in many countries and in Italy its use is regulated by D.M. 19 May 2000 and directives n. 2000/42/EC and n. 2000/48/EC.

Therefore, considering that three of the four antifouling paints assayed which should replace the organotin compounds contain Diuron and Endosulfan as biocides representing so harmful substances that their use has been strictly regulated all over the world, it is necessary today to make efforts to i) a wider monitoring activity supported by an adequate legislation in particular fragile areas like the Lagoon of Venice, ii) the research of new antifouling systems which don't use chemical biocides and iii) the revival of a more careful study of the paints already in commerce.

References

- Cima F., Ballarin L. and Burighel P., 2005 Macrofouling ecological succession on hard substrata in the Lagoon of Venice: effects of copper-containing antifouling paints, in: "Scientific Research and Safeguarding of Venice – Vol. III", by P. Campostrini Ed., Istituto Veneto di Scienze, Lettere ed Arti, Venezia, 429-435.
- EJF, 2002. "End of the road for Endosulfan: a call for action against a dangerous pesticide". Environmental Justice Foundation, London, UK.
- Fernandez-Alba A.R., Hervando M.D., Pietra L. and Chisti Y., 2002. Toxicity evaluation of a single and mixed antifouling biocides measured with acute toxicity bioassays. *Analytica Chimica Acta*, 456, 303-312.
- Kobayashi N. and Okamura H., 2002. Effects of new antifouling compounds on the development of sea urchin. *Marine Pollution Bulletin*, 44, 748-751.
- Nebeker A.V. and Schuytema G.S., 1998. Chronic effects of the herbicide Diuron on freshwater cladocerans, amphipods, midges, minnow, worms and snails. *Archives of Environmental Contamination and Toxicology*, 35, 441-446.
- Okamura H., Watanabe T., Aoyama I. and Hasobe M., 2001. Toxicity evaluation of new antifouling compounds using suspension-cultured fish cells. *Chemosphere*, 46, 945-951.
- Redfield L.W. and Delvy E.S., 1952. "Temporal sequences and biotic

succession. Marine fouling and its prevention". Wood Hole Oceanographic Institute Ed., Wood Hole, 42-47.

Schuytema, Gerald S. and Nebeker A.V., 1998. Comparative toxicity of Diuron on survival and growth of Pacific tree frog, bullfrog, red-legged frog, and African clawed frog embryos and tadpoles. Archives of Environmental Contamination and Toxicology., 34, 370-376.

U.S. EPA, 2000. Notice of filing a pesticide petition to establish an exemption from the requirement of a tolerance for a certain pesticide chemical in or on food federal register: September 20, 65, 56895-56901.

AN INTEGRATED APPROACH TO BIOLOGICAL MONITORING IN THE LAGOON OF VENICE

Folco Giomi, Mariano Beltramini, Giuseppe Fusco, Diego Maruzzo, Lorenzo Zane, Paolo Maria Bisol

Dipartimento di Biologia, Università degli Studi di Padova

Riassunto

Nell'ambito delle ricerche per l'identificazione di specie indicatrici e lo sviluppo di metodologie affidabili di biomonitoraggio della qualità ambientale e dell'impatto antropico sugli ecosistemi, abbiamo sviluppato un approccio metodologico integrato, potenzialmente in grado di fornire indicazioni su possibili alterazioni ambientali che influiscono su processi biologici a diversa scala temporale. Attraverso l'analisi del polimorfismo di proteine respiratorie, misure di instabilità nello sviluppo e la stima della diversità genetica, è possibile ottenere un quadro delle variazioni ambientali a breve, medio e lungo termine. Per mettere alla prova questo approccio composito, è stata scelta la specie indicatrice *Carcinus aestuarii*, un crostaceo decapode. L'ampia diffusione di questo granchio nella laguna veneta e nella fascia costiera dell'Adriatico consente la comparazione tra popolazioni provenienti da diversi contesti locali.

Abstract

Within the course of researches for the identification of qualified keystone species, and the development of reliable methodologies for the biological monitoring of the environmental quality and the human impact on the ecosystems, we have developed an integrated approach that may provide indications of possible environmental alterations that affect biological processes at different temporal scales. Through the analysis of respiratory protein polymorphisms, measures of developmental instability, and the evaluation of genetic variation within and between populations, it is possible to get a picture of the environmental variations at short, middle and long term scale. To test this method, we chose *Carcinus aestuarii* as keystone species. This decapod crustacean, broadly diffused in the Venetian lagoon and along the cost of the Adriatic sea, seems to be optimal for comparing populations from different local contexts.

1 Introduction

The strict relationships that link the environment with human activities prompt for the necessity to devise a reliable net of environmental screenings to measure, prevent and restore the effects of environmental perturbations. Beside classical chemical and physical analysis, biological monitoring data can provide information about the cumulative impact of contaminants and other kinds of environmental changes. Biological monitoring consists in the study of selected

traits of a community or a single keystone species that can be associated to environmental changes, both in spatial and temporal dimensions. The complexity of interactions between environment and biological communities requires the integration of different approaches and methodologies, in order to get a detailed picture of several environmental conditions.

Here we describe a biological monitoring approach that aims to an accurate evaluation of environmental conditions through the comparison of different populations. The novelty of our approach consists in the integration of different lines of investigation (physiological, morphological and genetic) performed on the same specimens.

In particular, this study evaluates the possibility of using the decapod crustacean *Carcinus aestuarii* Nardo, 1847, the common shore crab, as a bioindicator. This crab is broadly diffused in the Venetian lagoon and along the coast of the Adriatic sea, and seems to be a good candidate for comparing populations from different localities.

1.1 Measures of hemocyanin heterogeneity

In many arthropods and molluscs the hemolymph oxygen transport process is achieved by freely dissolved copper proteins: the hemocyanins. Arthropod hemocyanins are high molecular weight oligomers resulting from a multimeric aggregation of single polypeptide chains, each one encoded by a different gene. A considerable heterogeneity in level of the different subunits synthesis, both within and between species, have been recorded. This heterogeneity provides the basis for intraspecific hemocyanin polymorphisms and constitutes a mechanism of physiological adaptability [DeFur et al., 1990]. Different researches have pointed out the influence of environment, together with life stages and moult cycle, to determine the hemocyanin phenotypic polymorphism [Bellelli et al., 1988; Terwilliger and Ryan, 2001]. Several chemical and physical factors (e.g. salinity, dissolved oxygen, temperature) are clearly involved in subunit composition change, and it was suggested that this capability for hemocyanin modulation is strongly related to the physiological adaptation process of the whole animal [Mangum and Rainer, 1988; Mangum, 1990]. The potentiality to shift from different hemocyanin phenotypes according to the environmental factors makes this physiological aspect a reliable character for biological monitoring of environmental changes.

1.2 Measures of developmental instability

Nijhout and Davidowitz [2003] distinguish two main kinds of phenotypic variation in natural populations. The first is the systematic variation of the target phenotype (the phenotype specified by a given genetic makeup and environmental conditions) with genetic or environmental variation. The second is the variation around the target phenotype, caused by stochastic events in ontogeny not compensated by the developmental system. The source of this non-heritable variation is known as 'developmental instability'. From the opposite view, developmental stability is a property of the organism

developmental system reflecting its ability to resist deleterious effects of possible environmental perturbations during development, so to produce a consistent target phenotype.

Several environmental factors have been proven to be effective in biasing the stability of embryonic and post-embryonic development in several animal taxa [Møller and Swaddle, 1997]. Different types of environmental stress can reduce the regulative power of the developmental system, producing phenotypic alteration of different kind and magnitude.

Measures of developmental instability depend on explicit hypotheses on the characters of the target phenotype. This is in general non-predictable in detail, but limiting the view to the study of body symmetry offers operational workable hypotheses. For an organism, the specific symmetry of its body plan (e.g. bilateral, translational, or radial symmetry) can be regarded as the idealized outcome of unperturbed development. Thus, any kind of deviation from symmetry, detectable as morphological irregularity, can potentially be exploited for studying developmental stability [Freeman et al., 1993].

The random and non-inheritable deviation from perfect bilateral symmetry is known as 'fluctuating asymmetry' (FA) [Van Valen, 1962]. Measures of FA are routinely used as indexes of developmental instability. When the latter is caused by environmental factors, measures of FA are considered significant indicators of the level of environmental stress that organisms experience during their life [Hoffmann and Woods, 2003].

1.3 Measures of genetic diversity

Natural selection and genetic drift can produce variation of allele frequencies in space and time. For this reason, the genetic approaches may be interesting in the aquatic toxicology context, where they allow to investigate the effect of genetic diversity on biomarker response and to study the relationships between genetic polymorphism, pollution and demographic dynamics.

In general, population genetics studies suggest an higher than expected complexity in populations of marine organisms [Carvalho and Hauser, 1998]. For example, despite the potential for dispersal particularly at the larval stage, these organisms can achieve a strong genetic differentiation, even at the local scale. Examples of genetic differentiation at the micro-geographic scale include differentiation between adjacent islands in species with extended larval duration [Taylor and Hellberg, 2003], differentiation between adjacent estuaries [Maltagliati et al., 2003; Ikeda et al., 2003], and differentiation inside the same lagoon [Planes et al., 1998]. Moreover, investigation of temporal change in allele frequencies show both the existence of long term trends of variation [Hutchinson et al., 2003], than the existence of genetic heterogeneity between cohorts in population samples taken from the same area [Lenfant and Planes, 2002]. This, in turn, can be linked with the complexity of recruitment and with the large variance in reproductive success [Hedgecock et al., 1992], that can lead to overrepresentation of individuals of the same family group.

On the other hand, genetic variation at adaptive loci can have significant effects on the population dynamics of a species, and can therefore as well as affect other species in the food web. These processes involve the recursive interaction of different elements: a) variation in allele frequencies, b) variation in morphological or physiological design, c) variation in ecological performance, d) variation in demographic output [Feder and Watt, 1992].

Taken together, local genetic differences and temporal changes in the genetic constitution of populations can be per se indicators of environmental effects when caused by selective effects; alternatively they can act as confounding factors in bioindicator studies, inducing differences in biomarkers response caused by genetic differences between individuals rather than pollutant exposure.

2 Experimental procedures

2.1 Field sampling

Specimen collection was performed by sampling populations from different local contexts. A highly perturbed site was selected and compared with two control sites. Live animals were collected either by hand or using creel nets, taking care to avoid damages to the exoskeleton. Several environmental parameters (water temperature, pH, salinity, dissolved oxygen) were recorded at the time of specimen collection. Two sampling campaigns were planned for each site during the year.

2.2 Measures of hemocyanin heterogeneity

Antibody development. Native hemocyanin was purified from the *C. aestuarii* hemolymph following the procedure described by Bubacco et al. [1992]. Dodecameric hemocyanin fraction was purified by gel filtration chromatography using a Superose 6 HR 10/30 analytical column in a FPLC apparatus (Pharmacia). A 50 mM Tris/HCl buffer containing 10 mM CaCl_2 at pH 7.5 was used throughout.

Following a preliminary blood sample, which constitutes the pre-immunized serum, a solution containing 400 μl of dodecameric hemocyanin at 3.11 $\mu\text{g}/\mu\text{l}$, 200 μl of distilled water and 150 μl of PolyA-PolyU 20 $\mu\text{g}/\mu\text{l}$, was injected in a rabbit to obtain the primary response. Three weeks later a second injection was performed reintroducing the antigen in the primed animal. One week later the antibodies anti-hemocyanin were isolated from the blood by through sedimentation of the cellular component and isolation of the serum. Tertiary and subsequent injections were performed at the same intervals to increase the amount of serum stored. Antibodies were tested at several dilution factors to optimize the immunological staining.

Hemolymph sampling. To avoid clotting reaction and inhibit proteolytic degradation during sampling an extracting buffer solution composed by Tris 50 mM, EDTA 20 mM, sucrose 20%, protease inhibiting cocktail (Sigma-Aldrich

Art. P2714), pH 9.2, was employed. Individual samples of hemolymph were obtained from living specimens with a 1 ml syringe, preventively filled with 0.1 ml of extracting buffer solution. The hypodermic needle was insert in the intersegmental membranes of the abdominal region and approximately 0.1 ml of hemolymph was withdrawn from the pericardiac cavity. Samples, stored in 0.5 ml eppendorf, were immediately frozen for the subsequent analyses.

Sample preparation. Towed samples were centrifuged for 15 min at 14.000 rpm and analyzed for hemocyanin concentration determination. Each value protein concentration were estimated spectrophotometrically using the Bradford total protein assay [Bradford, 1976] (Bio-Rad) and the extinction coefficient of $1.21 \text{ M}^{-1} \cdot \text{cm}^{-1}$ calculated for *C. aestuarii* hemocyanin [Dainese et al., 1998] in order to evaluate the concentration of the total freely dissolved proteins and the hemocyanin component, respectively. Individual samples for gel electrophoresis, were prepared by adding to the hemolymph an amount of sample buffer, composed by Glycine 50 mM, EDTA 1 mM, glycerole 20%, pH 9.6, in order to achieve a resulting protein concentration of $0.5 \mu\text{g}/\mu$. The hemolymph proteins were incubated overnight in this alkaline conditions to obtain a dissociated subunit profile.

Electrophoresis and Western Blot. Polyacrylamide gel electrophoresis was carried out in vertical gel according to the methods of Markl et al. [1979] using Biorad Mini Protean® 3 apparatus. Discontinuous gels composed of a stacking gel, 4% pH 9.6, over a resolving gel 9% pH 9.6, (Acrylamide/bis-acrylamide ratio 48:1.5) were performed at alkaline pH employing a running buffer composed by Glycine 50 mM, EDTA 1 mM, pH 9.6. Three microliters of diluted hemolymph were loaded into each well and the electrophoresis was carried out at constant current 40 mA per two gels for 75 min (Fig. 1, Panel A).

For western blotting, the proteins were transferred from the Native-PAGE to a PVDF membrane (Immobilon -P) by tank transfer blotting at $40 \cdot \text{V}$, overnight at 4°C using Bio-Rad Trans-Blot cell®.

Alkaline phosphatase staining. Membranes were blocked in milk/TTBS (20 mM Tris-HCl, pH 7.5; 150mM NaCl; 0.1% Tween 20) at 5% w/v for 1•h and incubated for 2 h with the polyclonal antibody anti-*C. aestuarii* hemocyanin at room temperature. Subsequently, a 6•min washing step with milk/TTBS was repeated five times, and the membranes were incubated with a polyclonal secondary antibody coupled to peroxidase (Goat anti-Rabbit IGG, Sigma) for 1•h at room temperature. After another 5•6•min washing step with milk/TTBS, the antibody complex was detected using the substrate Bromo-chloro-indolyl-phosphate/Nitro Blue Tetrazolium (BCIP/NBT) (Sigma) incubated at room temperature for 10-15•min.

Densitometric scan and statistical analyses. The membranes were further digitalized at $1200 \cdot \text{d.p.i.}$ resolution. Density profiles were obtained from the western blot membranes using Adobe Photoshop 6.0 software and from the intensity values were calculated the relative contribution of each subunits to the whole profile (Fig. 1, Panel B). Statistical analyses were be performed

evaluating the difference of the mean value and the variance of each subunit applying the Levene test between groups of samples.

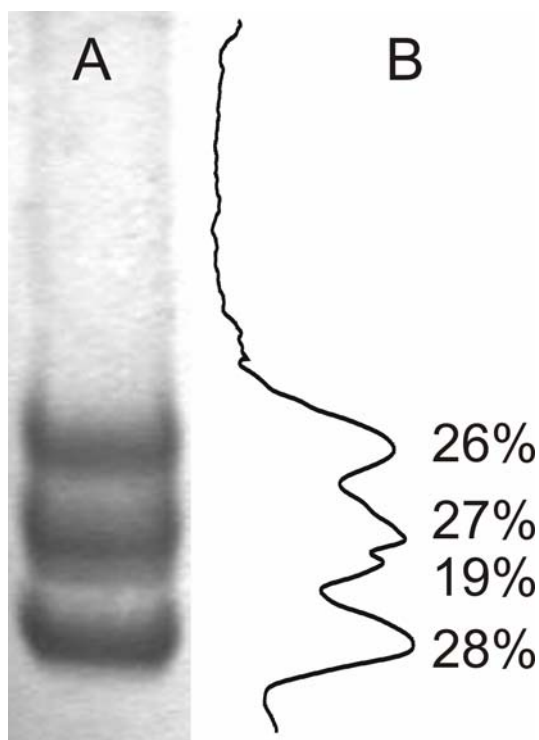


Fig. 1. Hemocyanin subunits analysis. Panel A: subunit pattern obtained from whole hemocyanin by PAG-electrophoresis under dissociating conditions. Panel B: densitometric profile of PAGE; the percentages of each subunit relative to the whole hemocyanin are indicated in correspondence with the peaks.

2.3 Measures of developmental instability

Morphometric data acquisition. Digital images of each specimen, fixed and preserved in 70% ethanol, were taken using a digital camera, and subsequently processed by a specific software for morphometric analysis (TPS, Stony Brook, USA). Measures of each morphological character (right and left sides) were obtained from the coordinates of a set of landmarks placed on the digital images in homologous anatomical positions between individuals.

Character choice was limited to body structures that are not easily lost and regenerated, as it is likely to occur to legs and chelipedes (claws). We measured five characters on the dorsal carapace and five characters on the ventral side the thorax (Fig. 2). These are not all geometrically independent from each other, because some characters share one landmark, but this bias is accounted for in subsequent analyses (see below). Acquisition of a second morphometric dataset, concerning the maxillipedes, is still in progress.

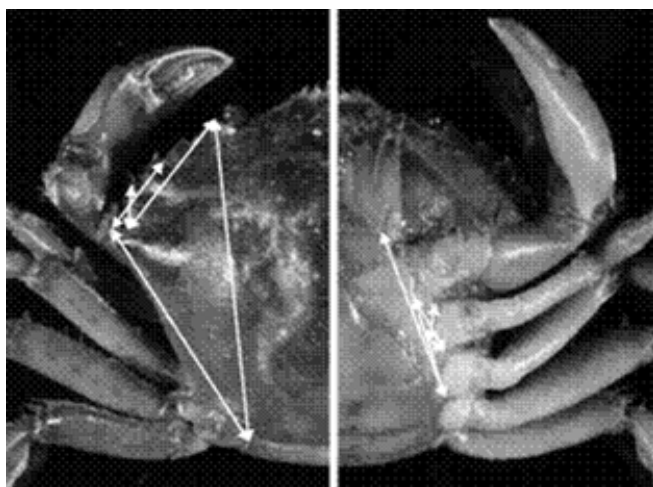


Fig. 2 - Dorsal and ventral characters used for the analysis of fluctuating asymmetry.

Measures of fluctuating asymmetry. For FA calculation we used the following metrics:

$$\text{mean } |\ln(R) - \ln(L)|$$

where $\ln(R)$ is the natural logarithm of the character on the right side, and $\ln(L)$ is the natural logarithm of the same character on the left side. This metrics offers several advantages [Palmer and Strobeck, 2003]: a) produces adimensional indexes that allow to compare symmetry between traits of different size; b) the frequency distribution of $\ln(R)-\ln(L)$ is not affected by trait size; c) it is possible to combine several indexes of asymmetry in a single analysis to test differences between groups of characters or groups of specimens.

For each specimen we calculated on the whole 13 indexes of asymmetry. Ten are relative to individual characters, one to the dorsal side of the animal (combining three independent characters of the carapace), one to the ventral side of the animal (combining three independent ventral characters), and one is comprehensive of the whole specimen (combining six independent dorsal and ventral characters).

2.4 Measures of genetic diversity

Microsatellite isolation. Chelipeds were detached from living specimens and preserved in liquid nitrogen. Genomic DNA was extracted from muscle tissue using standard methods, and a enriched genomic library was constructed following FIASCO protocol (Fast Isolation by AFLP of Sequences Containing repeats, [Zane et al., 2002]). DNA was digested with MseI and ligated to MseI AFLP adaptor [Vos et al., 1995], amplified with AFLP adaptor-specific primers and enriched using a biotinylated (AC)₁₇ probe. Amplified DNA was hybridized with the biotinylated oligonucleotide, and hybridized DNA molecules were captured by streptavidin-coated beads, and repeatedly washed. Elution was

performed by treating beads with NaOH, followed by neutralization and isopropanol precipitation. DNA was dissolved in appropriate volume of water and amplified by 30 cycles of PCR. PCR products were cloned and recombinant clones were PCR amplified using primers on the vector. Positives identified in the screening were purified and both strands were sequenced. Primers were designed on microsatellites containing clones and used for population analysis.

Population analysis. A total of 60 colonies were sequenced, providing about 50% of microsatellite containing clones. Primers for 7 loci were designed, and all proved to amplify genomic DNA of *C. aestuarii*; this result allowed to perform a preliminary population study, currently in progress.

So far, total genomic DNA has been extracted using a salting out protocol from 80 individuals collected in the Venice lagoon. Genomic DNA has been quantified and diluted to a working concentration of 50 ng/ul.

The forward primer of each pair has been labelled with fluorescent dyes, which allowed detection on ABI sequencers. PCR amplifications have performed in 20 μ l using the following conditions: Taq buffer 1X (Promega), $MgCl_2$ 1.375 mM, 250 nM of each primer, 100 μ M dNTP's, 1 unit of Taq, and 50 ng of genomic DNA. A hot-start touch-down PCR profile was used as follows: 1) pre-denaturation 94 °C 2 min; 2) thirty cycles of denaturation 94 °C 30 sec, annealing 52 °C 40 sec, extension 72 °C 1 min; 3) an additional extension for 5 min at 72 °C. Electrophoresis of loci is currently being performed with an ABI Prism 3100 or 3700 automated sequencer, using standard conditions. Sizing is obtained by comparison with the internal standard GS 400 Hd Rox (Applied Biosystem), and scoring is performed using the program Genotyper 3.7 (Applied Biosystem) that allow to reconstruct individual genotypes.

Genotypic data will allow to calculate classic population genetic statistics and to draw indications about genetic differentiation of samples.

Number of alleles, heterozygosity, departure from Hardy-Weinberg (HW) equilibrium, and linkage disequilibrium will be calculated using GENEPOP ver3.1b [Raymond and Rousset, 1995]. Pattern of population differentiation will be investigated by analysis of molecular variance (AMOVA, [Excoffier et al. 1992]). Φ_{ST} , the percentage of molecular variation attributable to sample subdivision, will be calculated subdividing individuals by site, date of collection, and by sex. In all cases, statistical significance will be tested by multiple permutations of the original data set.

3 Conclusions

By means of the integrated approach we suggest here, it is possible to evaluate a wide range of environmental perturbations that the sample might have experienced. Physiological, morphological and genetic analyses are combined to perform an accurate biological monitoring at different time scales.

Comparing the hemocyanin subunit patterns and applying statistical measures to evaluate the differences in protein expression, it is possible to infer adaptive

process toward stressful events that occur in short term intervals. Following an environmental modification such a shift in physical parameters the protein synthesis is conformed to furnish, with a delay of 15-45 days, a better adapted phenotype.

Throughout the measurement of fluctuating asymmetry is possible to estimate the disruptive effects of environmental factors during the ontogenesis, which are reflected in the level of developmental instability in the population. In arthropods, the analysis of FA can detect 'developmental noise' affecting the production of the exoskeleton at any earlier developmental stage, thus covering a temporal interval that in *Carcinus* spans from days to months.

Finally, the genetic study provide an extensive database on the genetic heterogeneity of a population. Comparing the allele frequencies among populations is possible to infer processes of genetic drift caused by the environmental pressure. This approach has proved to be particularly useful when data from different generations are available, enabling to estimate the effective population size and to unveil genetic signature of population bottlenecks.

References

- Bellelli A., Giardina G., Corda M., Pellegrini M.G., Cau A., Condò S.G. and Brunori M., 1988. Sexual and seasonal variability of lobster hemocyanin. *Comparative Biochemistry and Physiology*, 91A, 445-449.
- Bradford M.M., 1976. A rapid and sensitive method for the quantitation of microgram quantities of protein utilizing the principle of protein-dye binding. *Analytical Biochemistry*, 72, 248-54.
- Bubacco L., Magliozzo R.S., Beltramini M., Salvato B. and Peisach J., 1992. Preparation and spectroscopic characterization of a coupled binuclear center in cobalt(II)-substituted hemocyanin. *Biochemistry*, 31, 9294-9303.
- Carvalho G.R. and Hauser L., 1998. Advances in the molecular analysis of fish population structure. *Italian Journal of Zoology*, 65, 21-33.
- Dainese E., Di Muro P., Beltramini M., Salvato B. and Decker H., 1998. Subunits composition and allosteric control in *Carcinus aestuarii* hemocyanin. *European Journal of Biochemistry*, 256, 350-358.
- DeFur P.L., Mangum C.P. and Reese J.E., 1990. Respiratory responses of the blue crab *Callinectes sapidus* to long-term hypoxia. *Biological Bulletin*, 178, 46-54.
- Excoffier L., Smouse P. and Quattro J., 1992. Analysis of molecular variance inferred from metric distances among DNA haplotypes: application to human mitochondrial DNA restriction data. *Genetics*, 131, 479-491.
- Feder M.E. and Watt W.A., 1992. Functional biology of adaptation, in "Genes in ecology", by Berry R.J., Crawford, T.J. and Hewitt, G.M., The 33rd Symposium

of the British Ecological Society, University of East Anglia 1991, Oxford, Blackwell Scientific Publications.

Freeman D.C., Graham J.H. and Emlen J.M., 1993. Developmental stability in plants: symmetries, stress and epigenesis. *Genetica*, 89, 97-119.

Hedgecock D., Chow V. and Waples R.S., 1992. Effective population numbers of shell-fish broodstocks estimated from temporal variance in allelic frequencies. *Aquaculture*, 108, 215-232.

Hoffmann A.A. and Woods R.E., 2003. Associating environmental stress with developmental stability: problems and patterns. In "Developmental instability: causes and consequences", by Polak M., Oxford University Press, New York.

Hutchinson, W.F., van Oosterhout C., Rogers S.I. and Carvalho G.R., 2003. Temporal analysis of archived samples indicates marked genetic changes in declining North Sea cod (*Gadus morhua*). *Proceeding Royal Society London ser B: Bio Sci*, 270, 2125-2132.

Ikeda M., Nunokawa M. and Taniguchi N., 2003. Lack of mitochondrial gene flow between populations of the endangered amphidromous fish *Plecoglossus altivelis ryukyuensis* inhabiting Amami-oshima Island. *Fishery Sciences*, 69, 1162-1168.

Lenfant P. and Planes S., 2002. Temporal genetic changes between cohorts in a natural population of a marine fish, *Diplodus sargus*. *Biological Journal of the Linnean Society*, 76, 9-20.

Maltagliati F., Domenici P., Fosch C.F., Cossu P., Casu M. and Castelli A., 2003. Small-scale morphological and genetic differentiation in the Mediterranean killifish *Aphanius fasciatus* (Cyprinodontidae) from a coastal brackish-water pond and an adjacent pool in northern Sardinia. *Oceanological Acta*, 26, 111-119.

Mangum C.P. and Rainer J.S., 1988. The relationship between subunit composition and oxygen binding of blue crab hemocyanin. *Biological Bulletin*, 174, 77-82.

Mangum C.P., 1990. Inducible O₂ carriers in the crustaceans. In "Animal Nutrition and Transport Process: Transport, Respiration and excretion", by Truchot J.P. and Lalou B., Karger Basel.

Markl J., Markl A., Schartau W. and Linzen B., 1979. Subunit heterogeneity in arthropod hemocyanins. I. Chelicerata. *Journal Comparative Physiology*, 130, 283-292.

Møller A.P. and Swaddle J.P., 1997. *Asymmetry, developmental stability, and evolution*, Oxford University Press, New York.

Nijhout H.F. and Davidowitz G., 2003. Developmental perspectives on phenotypic variation, canalization, and fluctuating asymmetry. In "Developmental instability: causes and consequences", by M. Polak, Oxford University Press, New York.

Palmer A.R. and Strobeck C., 2003. Fluctuating asymmetry analyses revisited. In "Developmental instability: causes and consequences", by Polak M., Oxford University Press, New York.

Planes S., Parroni M. and Chauvet C., 1998. Evidence of limited gene flow in three species of coral reef fishes in the lagoon of New Caledonia. *Marine Biology*, 130, 361-368.

Raymond M. and Rousset F., 1995. GENEPOP version 1.2: population genetics software for exact tests and ecumenism. *Journal of Heredity*, 86, 248-249.

Taylor M.S. and Hellberg M.E., 2003. Genetic evidence for local retention of pelagic larvae in a Caribbean reef fish. *Science*, 299, 107-109.

Terwilliger N.B. and Ryan M., 2001. Ontogeny of crustacean respiratory proteins. *American Zoologist*, 41, 1057-1067.

Van Valen L., 1962. A study of fluctuating asymmetry. *Evolution*, 16, 125-142.

Vos P., Hogers R., Bleeker M., Reijans M., van de Lee T., Hornes M., Frijters A., Pot J., Peleman J. and Kuiper M., 1995. AFLP: a new technique for DNA fingerprinting. *Nucleic Acids Research*, 23, 4407-4414.

Zane L., Bargelloni L. and Patarnello T., 2002. Strategies for microsatellite isolation: a review. *Molecular Ecology*, 11, 1-16.

VERIFICATION OF A POPs BIOACCUMULATION MODEL FOR THE VENICE LAGOON

Tomas Lovato¹, Christian Micheletti², Roberto Pastres¹, Antonio Marcomini²

¹ Dipartimento di Chimica Fisica, Università di Venezia, ² Dipartimento di Scienze Ambientali, Università di Venezia

Riassunto.

Viene presentata l'applicazione all'ecosistema lagunare veneziano di un modello recentemente proposto per valutare il bioaccumulo di POP in ecosistemi acquatici. Il modello è stato implementato inizialmente per valutare le concentrazioni di nove congeneri persistenti di PCB in invertebrati e pesci della Laguna di Venezia. I valori modellati sono stati confrontati con i dati sperimentali per quattro specie della rete trofica: *Tapes philippinarum*, *Carcinus mediterraneus*, *Chelon labrosus* e *Zosterisessor ophiocephalus*. Successivamente, il modello è stato utilizzato per stimare il tasso di biotrasformazione, k_M , per 20 congeneri tra PCB, dibenzo-p-diossine policlorurate (PCDD) e dibenzo-p-furani policlorurati (PCDF), potenzialmente metabolizzabili. I valori ottenuti, compresi tra 0.001 e 0.3 d⁻¹, risultano in buon accordo con la recente letteratura. In generale, le capacità predittive del modello appaiono soddisfacenti, sebbene i valori predetti di BAF siano sovrastimati rispetto ai valori di BAF osservati.

Abstract.

A food web bioaccumulation model recently proposed in the specific literature was applied to the Venice lagoon ecosystem. The model was first set up, in order to fit the concentrations of nine persistent PCB congeners in four species, i.e. *Tapes philippinarum*, *Carcinus mediterraneus*, *Chelon labrosus* and *Zosterisessor ophiocephalus*. Subsequently, the model was used to estimate the chemical biotransformation rates, k_M , for potentially metabolised PCB, polychlorinated dibenzo-p-dioxin (PCDD), and polychlorinated dibenzo-p-furan (PCDF) congeners. The estimated biotransformation rates varied between 0.001 and 0.3 d⁻¹, generally, in fair agreement with the results previously obtained in other models studies. Overall, the model performance was good, even though the BAFs predicted by the model led to overestimate the observed BAFs.

1 Introduction

The results of recent studies (Frignani et al., 2005; Secco et al., 2005), indicate that the concentrations of organic micropollutants belonging to POPs (polychlorinated biphenyl, dibenzo-p-dioxins and dibenzo-p-furans) in both the sediment and water in the Lagoon of Venice have been decreasing from the early 90es. On the other hand, it is recognized that the processes of

bioaccumulation and biomagnification along the food web maintain the concentrations in the biota at a high level, also for low concentrations of these toxicants in the environment (Gobas and Morrison, 2000). These findings are a source of concern, since the results of recent studies (COM 2001/C, 332/02) suggest that even low dose of dibenzo-p-dioxins and furans can be highly toxic.

In order to relate the level of POP contamination in water and sediment to the potential risks for human health and for the ecosystem, it is necessary to investigate the bioaccumulation processes, i.e. the processes of uptake and retention of a chemical by an aquatic organism from all surrounding media like water, sediment and food (EPA-822-R-03-030).

The tendency of a given pollutant to bioaccumulate in a given "compartment" of the trophic web (i.e. a species or a group of species with similar ecological role and biological characteristics) is usually specified by means of two indexes: the bioconcentration factor, BCF, which is the ratio between the concentration in the compartment and the concentration in the water, and the bioaccumulation factor, BAF, which is the ratio between the chemical concentration in the organism and that dissolved concentration in water. These factors can be estimated from experimental data, but analytical data are often incomplete or not available for technical or economic reasons. As was demonstrated in a number of recent publications (EPA-822-B-98-005; Mackay and Fraser, 2000; van der Oost et al., 2003) mathematical models represent a viable alternative for the evaluation of BAFs. Furthermore, since analytical data usually describe the concentrations in few fish and shellfish species, the estimation of these factors by means of numerical models is often the only way to perform integrated environmental risk assessments. Such models can also support the elaboration of water quality headlines, the definition of maximum anthropogenic loading, the characterization of potentially hazardous substances (Canadian Environmental Protection Act, 1999).

Since the pioneering work of Neely et al. (1974), a variety of bioaccumulation models, of increasing complexity, have been proposed (Lake et al., 1990; Thomann et al., 1992; Gobas, 1993; Morrison et al., 1996; Shea, 1998). In this paper, we present the application of a recent bioaccumulation model to the evaluation of the concentrations of PCBs and PCDD/Fs in the Venice Lagoon aquatic biota. The main features and the parameterization of the model are described in the second section. The model set up and main results are presented and discussed in the third section, which is divided into three parts. In the first part, we present the verification of the model for nine non-metabolized PCBs congeners, by comparing the simulated and observed data concerning four organisms: *Tapes philippinarum*, *Carcinus mediterraneus*, *Chelone labrosus* and *Zosterisessor ophiocephalus*. Subsequently, the results of the estimation of the metabolic rates concerning metabolized PCB's, dioxin and furan congeners are given and in the third part, we show the results of model validation, by comparing the model output with a set of independent data. Some concluding remarks are put forward in the last section of the paper.

2 Material and methods

2.1 Model description

The food web bioaccumulation model described by Arnot and Gobas (2004) was used to predict PCBs and PCDD/Fs congeners concentrations in Venice Lagoon aquatic biota.

The main features of the model are: i) a model for the partitioning of chemicals into the organism, ii) an enhanced description of chemical concentrations in algae, phytoplankton and zooplankton, iii) a set of allometric relationships, which allows one to estimate species-specific parameters for a wide range of aquatic organisms and iv) a mechanistic module for the prediction of the gastrointestinal magnification of chemical concentrations.

The model is based on the following assumptions: (i) the chemical is homogeneous distributed within the organism as long as differences in tissue composition and phase partitioning are taken into account, (ii) organisms are considered as compartments, (iii) the system is assumed to be at a steady state, since most organisms are usually exposed for a long time to the chemicals, in comparison to their life-cycle.

At steady state, the overall rate of chemical uptake equals the depuration one and, for a given chemical, the model mass-balance equation reads as:

$$C_{B,i} = [k_1 \cdot C_W + k_D \cdot C_{D,i}] / [k_2 + k_E + k_G + k_M] \quad (1)$$

where $C_{B,i}$ (g/kg), C_W (g/L) and $C_{D,i}$ (g/kg) represent the concentration of a chemical, respectively, in the i^{th} organism in water and in the diet. The parameters k_1 (L/kg·d) and k_D (kg/kg·d) are, respectively, the assumption rates for respiration and diet. The terms k_2 , k_E , k_G and k_M (d⁻¹) represent the respiration, excretion, growth dilution and biotransformation rate.

2.2 Field data

The contamination of sediment in the Lagoon of Venice present a high spatial variability, depending on the distance and the typology of source, the morphology and the hydrodynamism (Dalla Valle et al., 2003; Carrer et al., 2005). In spite of such complexity, it's possible to operate a division in more homogeneous subregions, according to achieved knowledge about the lagoon environment: in Figure 1 is represented the adopted division and are highlighted the model verification sites and the test site.

A large set of data, concerning PCBs and PCDD/F concentrations in 100 sediment samples, was collected by the Venice Water Authority in 1999 (MAV-CVN, 1999; Micheletti et al., 2004). The chemicals content of the top sediment (0-15 cm) was taken as representative of the reactive layer, adopting whenever the concentrations were below the detection thresholds a value equal to half of

the limits.

The total concentrations of chemicals in water were measured at 15 monitoring stations in the framework of the Venice Water Authority monitoring program in 2002 (MAV-SAMA, 2002). Because of the lack of field data about dissolved concentrations, we estimated the bioavailable concentrations on the basis of total water concentration using the partition formula proposed in Gobas (1993). The partitioning of hydrophobic substances between sediment and water plays a primary role in the transfer mechanism across the trophic web (Burkhard, 2000; Gobas and MacLean, 2003), since the dissolved fraction is also the bioavailable one.

The experimental datasets information have been grouped following the sites subdivision and the chemicals inputs value for the bioaccumulation model were the median of concentrations in sediment and the mean of total concentrations in water.

The biota concentrations used to verify and validate the model were determined in 1999 (MAV-CVN, 1999) and were grouped as previously specified for inputs. The data concern the following species: *Tapes philippinarum*, *Carcinus mediterraneus*, *Chelon labrosus* and *Zosterisessor ophiocephalus*. The organic micropollutants investigated in this study are listed in Table 1.

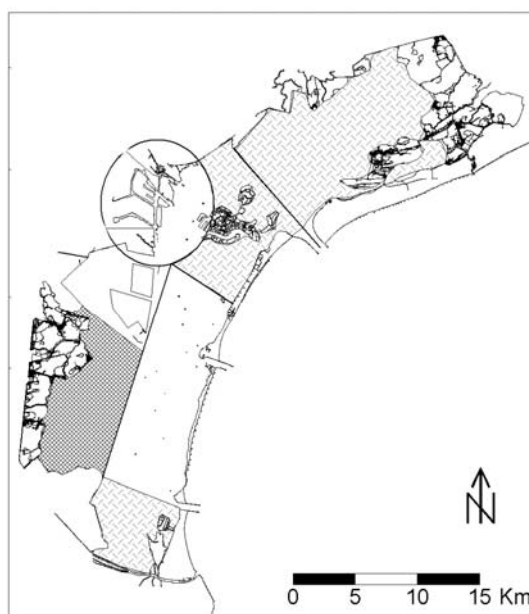


Fig. 1 Map of theoretical division of the Venice Lagoon. The model verification was carried out using the data collected in the light grey shaded areas. The model validation was carried out using the data collected in the dark grey shaded area.

2.3 Evaluation of model performance

The model performance was evaluated by computing the overall model bias,

MB_o , (Arnot and Gobas, 2004):

$$MB_o = 10^{\left[\frac{\sum_{j=1}^n \frac{\sum_{i=1}^m \log BAF_{P,i,j} - \log BAF_{O,i,j}}{m}}{n} \right]} \quad (2)$$

where BAF_P is the model predicted BAF, BAF_O the observed BAF, and the subscripts i and j refer to the number of chemicals and the number of species. The overall model bias, i.e. the geometric mean of the residual between the logarithms of simulated and field data., represents the general tendency to overestimation ($MB_o > 1$) or underestimation ($MB_o < 1$) of the model in predicting concentrations. For example, a value of $MB_{i,j}$ equal to 10 means that the bioaccumulation factors is overestimated by one order of magnitude. Conversely, a value $MB_{i,j} = 0.1$ means that the model underestimate the BAFs empirical value by one order of magnitude.

3 Results and discussion

3.1 Model setup and verification for non metabolized PCB congeners.

The main environmental parameters that characterize the Lagoon of Venice were determined during the project MeLA1 (MAV-CVN, 2001): the mean temperature of 17°C, annual dissolved oxygen saturation of 110 %, the annual averaged concentrations of dissolved organic carbon for 2.7 mg of C·L⁻¹ and particulate organic carbon of 0.62 mg of C·L⁻¹.

In order to estimate the feed intake of chemicals, namely $C_{D,i}$ in eq. (1), one needs to define the food web and specify each organism diet. Based on the results already presented (Carrer and Opitz, 1999; Libralato et al., 2002; Pranovi et al., 2003; Sorokin et al., 2002 and 2004), the food web used in this study includes 3 planktonic, 9 benthonic and 6 nektonic organisms, which are listed in Table 2. Organisms belonging to the lower trophic levels (i.e. microzooplankton, macroinvertebrates), were grouped on the basis of common habitat and feeding similarities, since their ecological role is similar. As one can see, in some instances juveniles and adults are also considered as different compartments, in order to account for the differences in their metabolism internal tissues composition and feeding habits. The diet matrix, was defined on the basis of the previously cited literature. Organism or group specific parameters, such as the gill ventilation rate or the feeding efficiency, were estimated by means of the allometric equations proposed in Arnot and Gobas (2004).

Tab. 1 – List of PCB and PCDD/F and logK_{OW} considered in the study. ^a Arnot and Gobas, 2004. ^b Mackay et al., 1992.

Non metabolized congeners	logK _{OW}
PCB 81	6.36 ^a
PCB 105	6.65 ^a
PCB 114	6.65 ^a
PCB 118 / 123	6.74 ^a
PCB 156 / 157	7.18 ^a
PCB 167	7.27 ^a
PCB 170	7.37 ^a
PCB 180	7.36 ^a
PCB 189	7.3 ^a
Metabolized congeners	
PCB 77	6.36 ^a
PCB 126	6.89 ^a
PCB 169	7.42 ^a
2,3,7,8-TetraCDD	7 ^b
1,2,3,7,8-PentaCDD	7.4 ^b
1,2,3,4,7,8-HexaCDD	7.8 ^b
1,2,3,6,7,8-HexaCDD	7.8 ^b
1,2,3,7,8,9-HexaCDD	7.8 ^b
1,2,3,4,6,7,8-HeptaCDD	8 ^b
1,2,3,4,6,7,8,9-OctaCDD	8.2 ^b
2,3,7,8-TetraCDF	6.4 ^b
1,2,3,7,8-PentaCDF	6.7 ^b
2,3,4,7,8-PentaCDF	6.7 ^b
1,2,3,4,7,8-HexaCDF	7 ^b
1,2,3,6,7,8-HexaCDF	7 ^b
1,2,3,7,8,9-HexaCDF	7 ^b
2,3,4,6,7,8-HexaCDF	7 ^b
1,2,3,4,6,7,8-HeptaCDF	7.4 ^b
1,2,3,4,7,8,9-HeptaCDF	7.4 ^b
1,2,3,4,6,7,8,9-OctaCDF	8 ^b

Tab. 2 – The Lagoon of Venice food web used in this model application.

Sediment/Detritus
Phytoplankton
Phytobenthos
Bacterioplankton
Zooplankton
Micro-MeioBenthos
MacroBenthos detritivorous
MacroBenthos herbivorous/detritivorous
MacroBenthos omnivorous/filter feeders
Tapes philippinarum Juv.
Tapes philippinarum
MacroBenthos omnivorous/mixed feeders
Carcinus mediterraneus
MacroBenthos omnivorous predator
Mugilidae Juv.
Mugilidae
Atherina Boyeri
Zosterisessor ophiocephalus
Nekton carnivorous / benthic feeders
Spaurus aurata Juv.
Spaurus aurata
Dicentrarcus labrax Juv.
Dicentrarcus labrax

The results obtained for the persistent PCBs are presented in the scatter plot shown in Figure 2. The model bias ($MB_0=0.8$), indicates that the, in general,

the predicted values underestimate the field ones. However, Fig. 2 shows that the results are poorer for *Carcinus med.*, but the predictions concerning *Chelon l.*, *Zosterisessor oph.* and *Tapes phil.* are in good agreement with the data since, for these species, the MBs are respectively 0.97 and 0.96 and 0.70. The modelled values for the logarithm of the bioaccumulation factor ranged between 4.6 and 7.2. The 95% of data are within the confidence boundaries of factor 10.

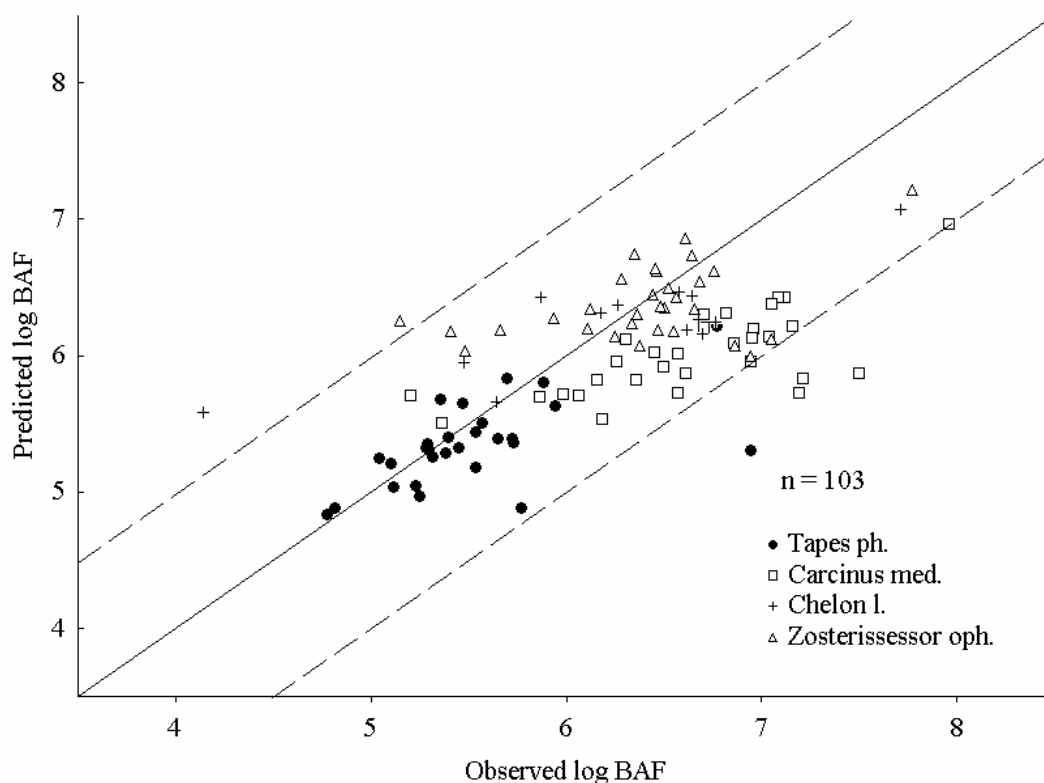


Fig. 2 – Observed vs predicted log BAF for the non metabolized PCB. The dotted lines represent the boundary of factor 10.

3.2 Estimation of chemical metabolic rates

Marine organisms are able to metabolize some POPs (Metcalf and Metcalfe, 1997). The biotransformation is related to the chemical structure of these compounds: in particular, the non-ortho chlorine substituted PCBs are considered similar to the 2,3,7,8 dibenzo-p-dioxin since it has been shown (Goerke and Weber, 2001) that macroinvertebrates and fish can metabolized them

The KM values were calculated using as a goal function the minimization of the sum of relative squared errors between observed (C_O) and simulated (C_P) ($SRSE = \sum((C_O - C_P)/C_O)$). Literature concerns (Goerke and Weber, 2001; Van der Linde et al., 2001) give a KM range for benthonic and nektonic organisms between 0.01 and 0.5 d^{-1} and these were set as boundaries for the model's exploration domain.

The results are summarized in Table 3, which shows the estimated

biotransformation rates for non-ortho PCBs congeners, dioxins and furans.

	Tapes ph.	Carcinus med.	Chelon L.	Zosterisessor oph.
PCB 77	0.01	0.001	0.05	0.075
PCB 126	0.01	0.001	0.01	0.01
PCB 169	0.01	0.001	0.001	0.001
2,3,7,8-TetraCDD	0.125	0.05	0.15	0.1
1,2,3,7,8-PentaCDD	0.125	0.05	0.15	0.1
1,2,3,4,7,8-HexaCDD	0.075	0.025	0.2	0.05
1,2,3,6,7,8-HexaCDD	0.075	0.025	0.2	0.05
1,2,3,7,8,9-HexaCDD	0.075	0.025	0.2	0.05
1,2,3,4,6,7,8-HeptaCDD	0.01	0.025	0.25	0.05
1,2,3,4,6,7,8,9-OctaCDD	0.01	0.025	0.25	0.05
2,3,7,8-TetraCDF	0.05	0.01	0.1	0.175
1,2,3,7,8-PentaCDF	0.075	0.05	0.1	0.175
2,3,4,7,8-PentaCDF	0.075	0.05	0.1	0.175
1,2,3,4,7,8-HexaCDF	0.1	0.05	0.3	0.15
1,2,3,6,7,8-HexaCDF	0.1	0.05	0.3	0.15
1,2,3,7,8,9-HexaCDF	0.1	0.05	0.3	0.15
2,3,4,6,7,8-HexaCDF	0.1	0.05	0.3	0.15
1,2,3,4,6,7,8-HeptaCDF	0.1	0.1	0.3	0.175
1,2,3,4,7,8,9-HeptaCDF	0.1	0.1	0.3	0.175
1,2,3,4,6,7,8,9-OctaCDF	0.05	0.1	0.3	0.075

Tab. 3 –Estimated values for biotransformation parameter, k_M (d^{-1}).

The predicted log BAFs ranged from 3.6 to 6.03. The value MB_O equal to 1.3

indicates that the model has a tendency to overestimate the field data. Such tendency was more pronounced in regard to *Chelon l.* (MB=1.7), whereas the model bias for *Carcinus med.* was close to 1. Overall, the performance of the model was still good, with a 98 % of data falling within the factor 10 of confidence (Fig. 3).

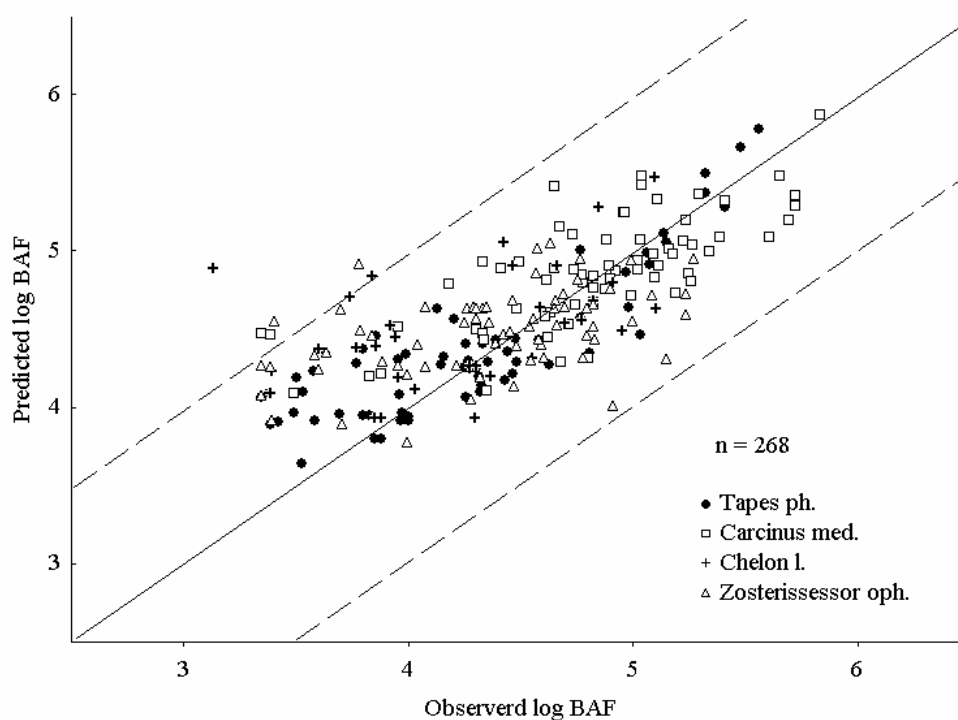


Fig. 3 - Observed vs predicted log BAF for the metabolized non-ortho PCBs and PCDD/Fs. The dotted lines represent the boundary of factor 10.

3.3 Model validation

The estimates presented in Tab. 2 were validated by comparing the model output with an independent data set, concerning the dark grey area in Fig. 1. The predicted log BAF values (Fig. 4) ranged between 3.8 and 5.7, while the overall model bias indicated an overestimation of the field data ($MB_0=1.53$). In particular, the bias for *Tapes ph.*, *Carcinus med.*, *Chelon l.* and *Zosterisessor oph.* were respectively 1.15, 1.18, 1.8 and 2. As expected, the model performance was poorer than that obtained using the verification data set, but in 95 % of the cases the model was still able to correctly predict the order of magnitude of the observed BAFs.

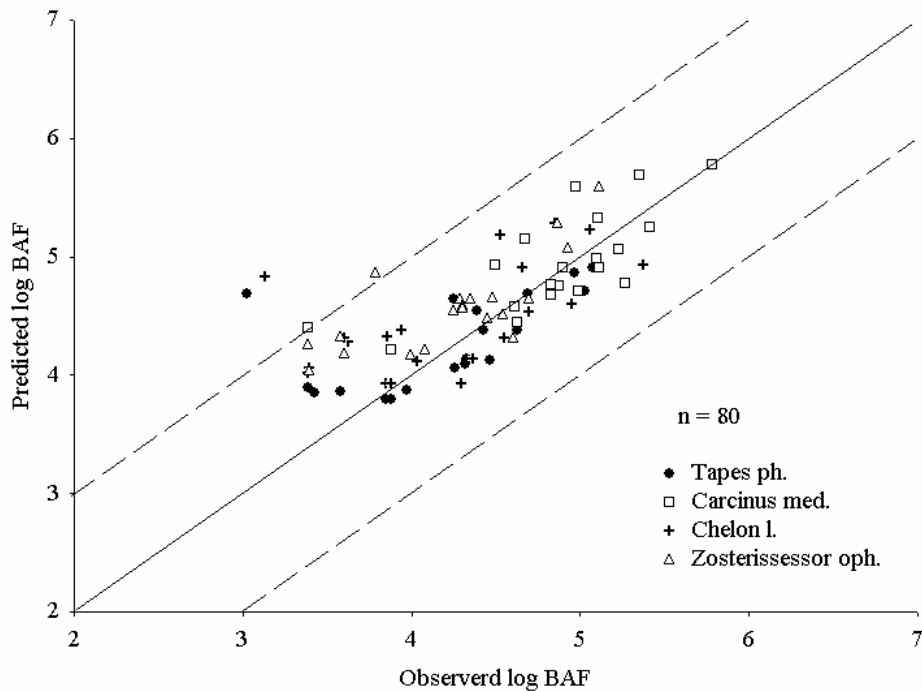


Fig. 4 - Observed vs predicted log BAF of the metabolized non-ortho PCBs and PCDD/Fs for the test site. The dotted lines represent the boundary of factor 10.

4 Conclusions.

The results presented in the previous section indicate that the model here presented allows one to predict with sufficient accuracy the bioaccumulation of PCBs and PCDFs in the Venice lagoon biota. In fact, the predicted bioaccumulation factors are in good agreement with the observed ones, since the model correctly predicted the order of magnitude of the observed BAFs in 95% of the cases. Furthermore, the ranges of the BAFs are in good agreement with other experimental data concerning similar organisms (Morrison et al., 1997, 1998; Metcalfe and Metcalfe, 1997). The model partially failed in predicting the bioaccumulation in *Chelon l.*: this could be due to the lack of empirical information concerning the chemical concentrations and to the uncertainties on the organism-specific parameters, which were estimated using allometric regression.

Model performance could be enhanced when the data which are being collected in the framework of the CORILA project will be available, since the analysis of these data should improve our knowledge of the food web. In this perspective, the model which has been set up and tested in the present work can be considered a useful tool for the evaluation and the analysis of impacts on ichthyic species ecologically and economically significant in the lagoon of Venice.

References

- Arnot, J.A., and Gobas, F.A.P.C., 2004. A food web bioaccumulation model for organic chemicals in aquatic ecosystems. *Environ. Toxicol. Chem.*, 23, 2343-2355.
- Burkhard, L. P., 2000. Comparison of two models for predicting bioaccumulation of hydrophobic organic chemicals in a great lakes food web. *Environ. Toxicol. Chem.*, 17, 383-393.
- Canadian Environmental Protection Act, 1999. <http://laws.justice.gc.ca/en/C-15.31/29610.html>
- Carrer, S., and Opitz, S., 1999. Trophic network model of a shallow water area in the northern part of the Lagoon of Venice. *Ecol. Model.*, 124, 193-219.
- Carrer, S., Halling-Sorensen, B., Bendoricchio, G., 2000. Modelling the fate of dioxins in a trophic network by coupling an ecotoxicological and Ecopath model. *Ecol. Model.*, 126, 210-223.
- Carrer, S., Coffaro, G., Bocci, M., Barbanti, A., 2005. Modelling partitioning and distribution of micropollutants in the lagoon of Venice: a first step towards a comprehensive ecotoxicological model. *Ecol. Model.*, 184, 83-101.
- COM 2001/C, 332/02, 2001. Comunicazione della commissione al Consiglio, al Parlamento Europeo e al Comitato Economico e sociale – Strategia comunitaria sulle diossine, i furani e i bifenili policlorurati. *Gazzetta ufficiale delle Comunità europee*.
- EPA-822-B-98-005 – US Environmental Protection Agency, 1998. Ambient water quality criteria derivation methodology Human Health, Technical support document.
- EPA-822-R-03-030 – US Environmental Protection Agency, 2003. Methodology for Deriving Ambient Water Quality Criteria for the Protection of Human Health (2000). Technical Support Document Volume 2.
- Gobas, F.A.P.C., 1993. A model for predicting the bioaccumulation of hydrophobic chemicals in aquatic food-webs: application to Lake Ontario. *Ecol. Model.*, 69, 1-17.
- Gobas, F.A.P.C., e Morrison, H.A., 2000. Bioconcentration and biomagnification in the environment. In: Boethling, R.S., Mackay, D., eds. 1999. *Handbook of property estimation methods for chemicals: environmental and health sciences*. CRC, Boca Raton, FL, USA.
- Gobas, F.A.P.C., and MacLean, L.G., 2003. Sediment-water distribution of organic contaminants in aquatic ecosystem: the role of organic carbon mineralization. *Environ. Sci. Technol.*, 37, 735-741.
- Goerke, H, and Weber, K., 2001. Species-specific elimination of polychlorinated biphenyls in estuarine animals and its impact on residue patterns. *Mar. Env. Res.*, 51, 131-149.

- Lake, J.L., Rubinstein, N.I., Lee, H.I., Lake, C.A., Helste, J., Pavignano, S., 1990. Equilibrium partitioning and bioaccumulation of sediment-associated contaminants by infaunal organisms. *Environ. Toxicol. Chem.*, 9, 1095-1106.
- Libralato, S., Pranovi, F., Raicevich, S., Da Ponte, F., Giovanardi, O., Pastres, R., Torricelli, P., and Mainardi, D., 2004. Ecological stages of the Venice Lagoon analysed using landing time series data. *J. Mar. Sys.*, 51, 331-344.
- Libralato, S., Pastres, R., Pranovi, F., Raicevich, S., Granzotto, A., Giovanardi, O., Torricelli, P., 2002. Comparison between the energy flow networks of two habitats in the Venice Lagoon. *Mar. Ecol.*, 23, 228-236.
- Mackay, D., and Fraser, A., 2000. Bioaccumulation of persistent organic chemicals: mechanisms and models. *Env. Poll.*, 110, 375-391.
- Mackay, D., Shiu, W.Y., Ma, K.C., 1992. Illustrated handbook of physical-chemical properties and environmental fate for organic chemicals, Vol. II. Lewis Publishers, Boca Raton, Ann Arbor, London.
- MAV-CVN, 1999. Interventi per il recupero ambientale e morfologico della laguna di Venezia - Mappatura dell'inquinamento dei fondali lagunari, Final report of Magistrato alle Acque di Venezia – Consorzio Venezia Nuova.
- MAV-CVN, 2001. Attività di monitoraggio ambientale della laguna di Venezia "Mela1". Final report.
- MAV-SAMA, 2002. Monitoraggio delle acque della Laguna di Venezia – Dati relativi al 200-2001. Magistrato alle Acque di Venezia – Sezione Antinquinamento del Magistrato alle Acque, December 2002, Venice.
- Metcalfe, T.L., and Metcalfe, C.D., 1997. The trophodynamics of PCBs, including mono- and non-ortho congeners, in the food web of North-Central Lake Ontario. *Sci. Tot. Env.*, 201, 245-272.
- Micheletti, C., Critto, A., Carlon, C., Marcomini, A., 2004. Ecological risk assessment of persistent toxic substances for the clam *Tapes philippinarum* in the Lagoon of Venice, Italy. *Environ. Toxicol. Chem.*, 23, 1575-1582.
- Morrison, H.A., Gobas, F.P.A.C., Lazar, R., Haffner, D.G., 1996. Development and verification of a bioaccumulation model for organic contaminants in benthic invertebrates. *Environ. Sci. Technol.*, 30, 3377-3384.
- Morrison, H.A., Whittle, D.M., Niimi, A.J., Metcalfe, C.D., 1998. Application of a food web bioaccumulation model for the prediction of polychlorinated biphenyl, dioxin, and furan congener concentrations in Lake Ontario aquatic biota. *Can. J. Fish. Aquat. Sci.*, 56, 1389-1400.
- Neely, W.B., Branson, D.R., Blau, G.E., 1974. Partition coefficients to measure the bioconcentration factor of chemicals in fish. *Environ. Sci. Technol.*, 8, 1113-1115.
- Pranovi, F., Libralato, S., Raicevich, S., Granzotto, A., Pastres, R., Giovanardi, O., 2003. Mechanical clam dredging in Venice Lagoon: ecosystem effects evaluated with a trophic mass-balance model. *Mar. Biol.*, 143, 393-403.

Thomann, R. V., Connolly, J. P., Parkerton, T. F., 1992. An equilibrium model of organic chemical accumulation in aquatic food webs with sediment interaction. *Environ. Toxicol. Chem.*, 11, 615-629.

Secco, T., Pellizzato, F., Sfriso, A., and Pavoni, B. 2005. The changing state of contamination in the Lagoon of Venice. Part 1: organic pollutants. *Chemosph.*, 58, 279-290.

Shea, D. , 1998. Developing national sediment-quality criteria. *Environ. Sci. Technol.*, 22, 1256-1261.

Sorokin, P. Yu., Sorokin, I. Yu., Zakuskina, O. Yu., and Ravagnan, G.-P., 2002. On the changing ecology of the Venice lagoon. *Hydrobiologia*, 487, 1-18.

Sorokin, P. Yu., Sorokin, I. Yu., Boscolo, R., Giovanardi, O., 2004. Bloom of picocyanobacteria in the Venice lagoon during summer-autumn 2001: Ecological sequences. *Hydrobiologia*, 523, 71-85.

Van der Linde, A., Hendricks, A.J., Sijm, D.T.H.M., 2001. Estimating biotransformation rate constants of organic chemicals from modelled and measured elimination rates. *Chemosph.*, 44, 423-435.

VITELLOGENIN INDUCTION AS BIOMARKER OF EXPOSURE TO XENOESTROGENIC COMPOUNDS IN THE CLAM *TAPES PHILIPPINARUM*: EXPERIMENTS WITH 4-NONYLPHENOL

Maria Gabriella Marin, Valerio Matozzo

Dipartimento di Biologia, Università di Padova

Riassunto

Lo studio di fenomeni di alterazione endocrina in molluschi bivalvi (*Tapes philippinarum*) è stato affrontato attraverso esperimenti di laboratorio con lo scopo di validare l'induzione di proteine vitellogenina (Vg)-like, precursori delle componenti proteiche del tuorlo, come risposta biologica all'esposizione a sostanze estrogeniche. Tra queste si è scelto il 4-nonylfenolo (NP), sulla base della sua nota estrogenicità in altri organismi acquatici, nonché della sua presenza ambientale. I risultati ottenuti evidenziano che il NP può indurre la sintesi di proteine Vg-like in animali in fase di riposo sessuale e tale azione si esplica a concentrazioni più basse del contaminante aumentando i tempi di esposizione.

Abstract

With the aim of validating vitellogenin (Vg)-like proteins induction as biomarker of exposure to xenoestrogenic compounds in bivalve molluscs, laboratory experiments were performed on the clam *Tapes philippinarum*. Among contaminants, 4-nonylphenol was chosen, because of its well-known estrogenic potential to aquatic organisms and widespread presence in aquatic environments. The results obtained highlight that NP can induce Vg synthesis in clams far from their reproductive period, acting at lower concentrations when the time of exposure to the contaminant increases.

1 Introduction

Vitellogenins (Vgs) are precursors of the egg-yolk proteins, vitellins, which provide energy reserves for embryonic development in oviparous organisms. They are glycolipophosphoproteins having Ca and Zn ligands, and exhibit similar characteristics in vertebrates, such as fish (Nagler et al., 1987), and invertebrates, molluscs in particular (Blaise et al., 1999). In females, Vgs are produced in the liver, or equivalent organs, in response to endogenous estrogens, released into the bloodstream and stored in developing oocytes. Vg levels increase in sexually mature females, generally being lower in juveniles. In males, the Vg gene, although present, is normally not expressed. However, it may be activated by xenoestrogens (Flouriot et al., 1995): Vg levels, generally undetectable in male plasma, may significantly increase in estrogen-exposed males.

Xenoestrogens belong to a large and heterogeneous group of environmental contaminants, termed endocrine disruptors, which are able to influence and modify endocrine functions in animals. Among these substances NP is widespread in aquatic ecosystems, due to its use in several industrial productions, such as those of nonylphenol ethoxylates, NP phosphites and aminocarb insecticide sprays. NP phosphites are commonly used as stabilisers and antioxidant agents in both rubber and plastic industries; NPEs are nonionic surfactants largely employed in lubricating oils, emulsifiers, plastics, latex paints, household and industrial detergents, and paper and textile industries. NPEs are generally discharged in large quantities into aquatic environments, either directly from untreated effluent or indirectly from sewage treatment plants (STPs). In both aquatic ecosystems and STPs, NPEs are biodegraded to de-ethoxylated intermediates (NP_(n-1)Es), of which NP is the final product (Maguire, 1999). Because of its low solubility in water, NP is more persistent to degradation than NPEs (Ekelund et al., 1993; Heinis et al., 1999). Moreover, NP is highly lipophilic and may consequently be accumulated both in sediment and aquatic organisms (Ekelund et al., 1990; Ahel et al., 1993). In particular, NP is known to be responsible for estrogenic effects in aquatic organisms, being able to mimic the action of endogenous estrogens and thus inducing Vg synthesis (Arukwe et al., 1997; Madigou et al., 2001). Estrogenic effects are well recognised in fish, whereas limited knowledge is available on invertebrates (Marin and Matozzo, 2004).

On the basis of the relevant environmental presence of NP, also in the Lagoon of Venice, as demonstrated by recent studies of Marcomini et al. (2000) and Pojana et al. (2004a,b), we decided to choose this compound to evaluate possible effects of endocrine disruption, such as induction of Vg synthesis. As model organism *T. philippinarum* was chosen, an infaunal bivalve which, due to its filter-feeding habit, can be considered a good indicator of both sediment and overlaying water conditions. Lastly, the wide spread of *T. philippinarum* in the Lagoon of Venice and its economical importance as fishing and harvesting product represent essential elements supporting the use of this species in laboratory studies, which are necessary premises for further field studies.

2 Materials and Methods

Specimens of *T. philippinarum* (3.0-3.5 cm shell length) were collected in December 2004-January 2005 from a licensed area for clam culture in the southern basin of the Lagoon of Venice and acclimatized in the laboratory for 7 days before exposure to NP. They were kept in large aquaria provided with a sandy bottom and aerated sea water (salinity of $35 \pm 1\text{‰}$ and temperature $17 \pm 0.5^\circ\text{C}$). Clams were in sexual resting phase, thus not identifiable as males or females. They (20 per concentration) were exposed for 7 days to 0, 0+acetone, 0.0125, 0.025, 0.05, 0.1 and 0.2 mg NP/L and for 14 days to 0, 0+acetone, 0.0125, 0.025, 0.05 and 0.1 mg NP/L. Sea water, NP and food (*Isochrysis galbana*) were daily renewed.

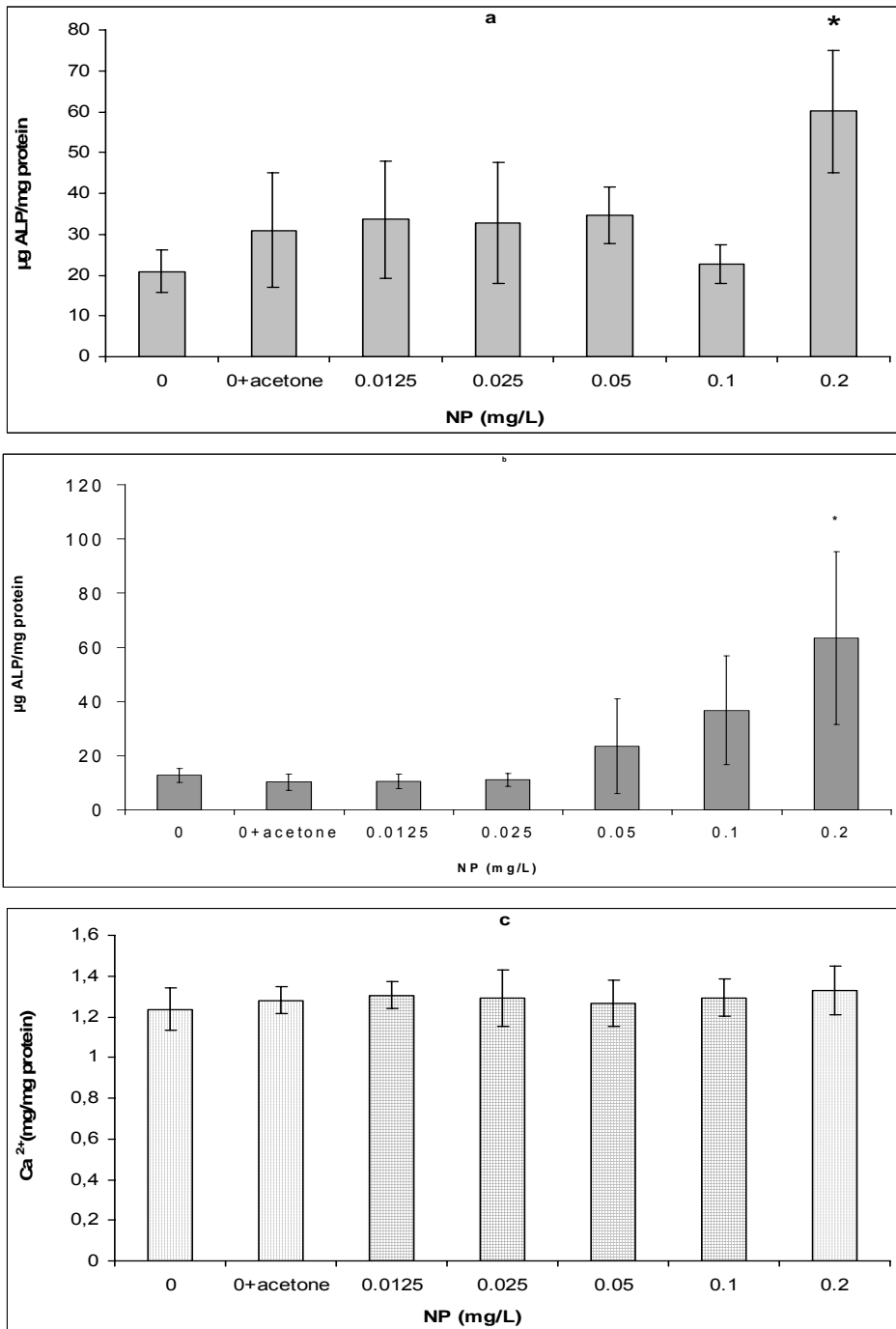


Fig. 1. Vitellogenin-like protein levels (expressed as $\mu\text{g ALP/mg proteins}$) in hemolymph (a) and digestive gland (b), and Ca^{2+} concentrations (expressed as $\text{mg Ca}^{2+}/\text{mg protein}$) in hemolymph (c) of *T. philippinarum* exposed for 7 days to NP. Asterisks: significant results, in comparison with controls. Values are means \pm standard deviation; * $P < 0.05$.

Vg was determined in both haemolymph and digestive gland by the alkali-labile phosphate (ALP) assay, according to Blaise et al. (1999) and Gagné et al. (2001, modified). In the haemolymph Ca^{2+} levels were also measured using the

“Calcium C” (o-cresolphthalein complexon) method (Pekkarinen and Suoranta, 1995). In both hemolymph and homogenized digestive gland protein concentration was quantified according to Bradford (1976).

The results of all assays were compared using a one-way ANOVA, followed by a post hoc Duncan’s test.

3 Results and Discussion

Exposure of *T. philippinarum* for 7 days to 0.2 mg NP/L resulted in significant ($p < 0.05$) increases in Vg-like proteins, expressed as $\mu\text{g ALP/mg protein}$, in both haemolymph and digestive gland with respect to controls (Fig.1a,b). Ca^{2+} level in the haemolymph, expressed as $\text{mg Ca}^{2+}/\text{mg protein}$, did not show any variation (Fig.1c), although its measurement has been suggested to complete the evaluation of Vg-like proteins, particularly rich in calcium (Blaise et al. 1999, Verslycke et al., 2002).

After 14-days exposure, Vg significantly ($p < 0.05$) increased in digestive gland from 0.05 and 0.1 mg NP/L-exposed clams (Fig.2b), whereas increases in Vg content measured from 0.025 mg NP/L in haemolymph were not significant, due to high variability among replicates (Fig.2a). Conversely, Ca^{2+} levels significantly ($p < 0.05$) increased at 0.025 and 0.05 mg NP/L (Fig.2c), exhibiting the same pattern observed in ALP values of haemolymph at the various NP concentrations tested.

In a previous work (Matozzo and Marin, 2005), 7-day exposure to NP was performed, at the same concentrations here tested, on sexually mature clams, resulting in a dose-dependent Vg induction in both haemolymph and digestive gland of males. No significant change was observed in treated females, high levels of Vg, naturally induced by endogenous hormones, masking any possible xenoestrogenic effect of NP. In this regard, we can note that mean ALP values, which provide an estimation of Vg-like protein content, decreases from 260 and 675 $\mu\text{g PO}_4/\text{mg protein}$ in haemolymph and digestive gland of control mature female (Matozzo and Marin, 2005) to 21 and 16 $\mu\text{g PO}_4/\text{mg protein}$, respectively, in control resting clams (this study). Our present results confirm the sensitivity of ALP method in detecting induction of Vg-like proteins also when exposure is carried out on clams far from their reproductive phase. In this case, a further advantage have to be considered: clam sex cannot be distinguished and consequently analytical procedure becomes easier and faster. When the duration of exposure increased, significant effects were detected at lower NP concentrations. However, a different responsiveness was shown in the two tissues analysed, this probably depending on their prevailing role in production or transport of Vg-like proteins. The results obtained in the present study indicate digestive gland as particularly suitable to discriminate differing conditions of exposure. Lastly, digestive gland in both mature males (Matozzo and Marin, 2005) and resting clams showed a similar increase in ALP values after 7-day exposure to 0.2 mg NP/L, they being 4-5 times higher than those of controls.

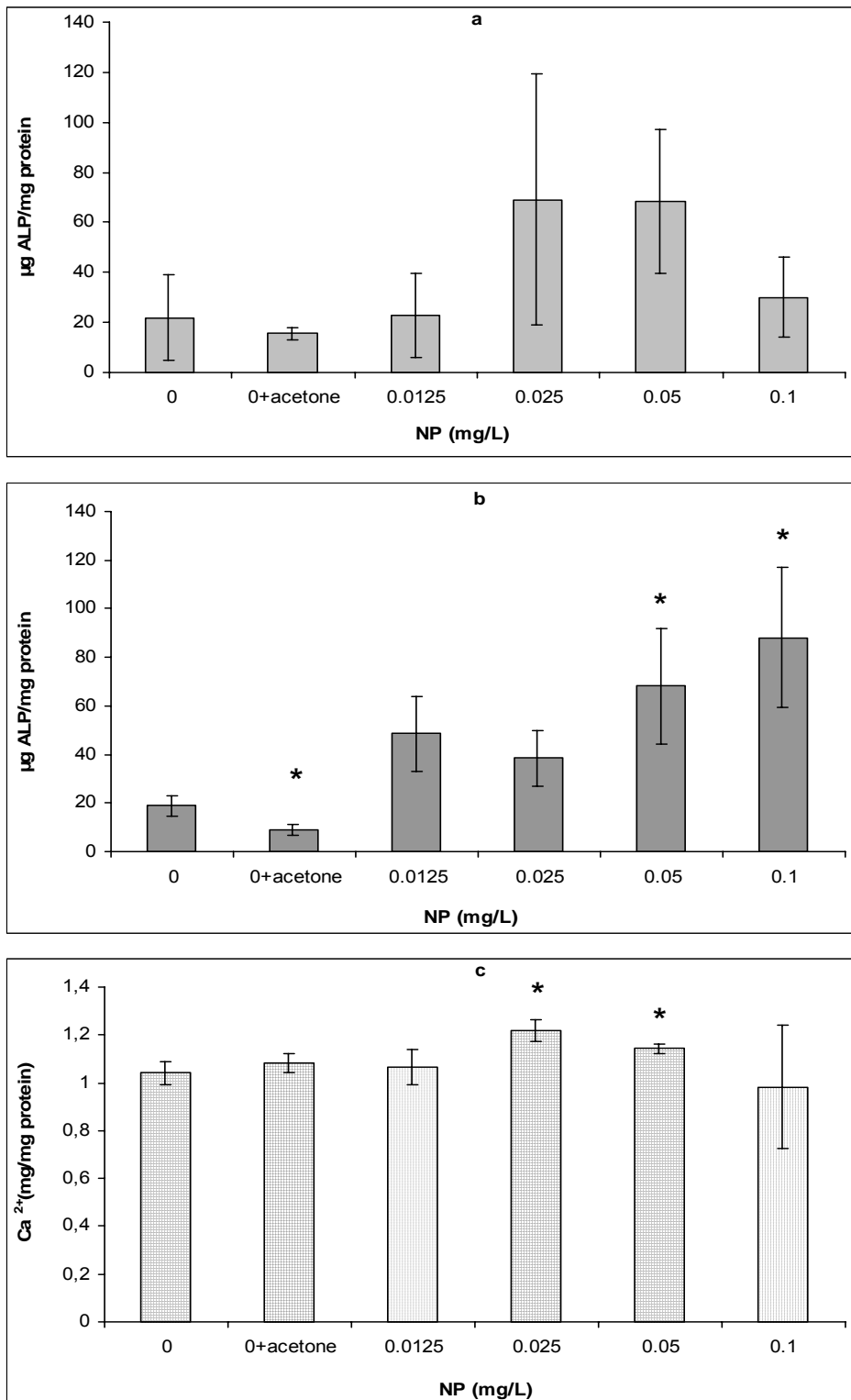


Fig. 2. Vitellogenin-like protein levels (expressed as µg ALP/mg proteins) in hemolymph (a) and digestive gland (b), and Ca²⁺ concentrations (expressed as mg Ca²⁺/mg protein) in hemolymph (c) of *T. philippinarum* exposed for 14 days to NP. Asterisks: significant results, in comparison with controls. Values are

means \pm standard deviation; * $P < 0.05$.

4 Conclusions

Results from laboratory study can provide useful information for the application of Vg-like protein induction as specific biomarker of exposure to xenoestrogenic compounds. To this end, responsiveness of the ALP method in *T. philippinarum* should be further demonstrated after exposure to other contaminants, such as natural or synthetic estrogens, known to produce similar effects, mostly in fish. As in the case of NP, also these substances may be discharged into aquatic environments from many sources: municipal effluents, livestock wastes and STPs, in particular. In lagoon waters, many contaminants having feminising effects may interact producing differing responses of the animals, depending on species sensitivity, endogenous constraints, mainly related to reproductive cycle, and environmental changes. The responses obtained in the laboratory in several conditions of exposure (type of contaminant, concentrations, duration of exposure, reproductive conditions of clams) will be essential to the validation of the proposed biomarker in the field, to the comprehension of the field data till now collected, as well as to the setting-up of future biomonitoring programmes.

References

- Ahel, M., McEvoy, J., Giger, W., 1993. Bioaccumulation of the lipophilic metabolites of nonionic surfactants in freshwater organisms. *Environmental Pollution*, 79, 243-248.
- Arukwe, A., Förlin, L., Goksøyr, A., 1997. Xenobiotic and steroid biotransformation enzymes in Atlantic salmon (*Salmo salar*) liver treated with an estrogenic compound, 4-nonylphenol. *Environmental Toxicology and Chemistry*, 16, 2576-2583.
- Blaise, C., Gagné, F., Pellerin, J., Hansen, P.D., 1999. Determination of vitellogenin-like properties in *Mya arenaria* hemolymph (Saguenay Fjord, Canada): a potential biomarker for endocrine disruption. *Environmental Toxicology*, 14, 455-465.
- Ekelund, R., Bergman, Å., Granmo, Å, and Berggren, M., 1990. Bioaccumulation of 4-nonylphenol in marine animals. A re-evaluation. *Environmental Pollution*, 64, 107-120.
- Ekelund, R., Granmo, Å., Magnusson, K., Berggren M., and Bergman, Å., 1993. Biodegradation of 4-nonylphenol in seawater and sediment. *Environmental Pollution*, 79, 59-61.
- Flouriot, G., Pakdel, F., Ducouret, B., Valotaire, Y., 1995. Influence of xenobiotics on rainbow trout liver estrogen receptor and vitellogenin gene expression. *Journal of Molecular Endocrinology*, 15, 143-151.
- Gagné, F., Blaise, C., Salazar, M., Salazar, S., Hansen, P.D., 2001. Evaluation of estrogenic effects of municipal effluents to the freshwater mussel *Elliptio*

complanata. *Comparative Biochemistry and Physiology*, 128C, 213-225.

Heinis, L. J., Knuth, M. L., Liber, K., Sheedy, B. R., Tunell, R. L., and Ankley, G. T., 1999. Persistence and distribution of 4-nonylphenol following repeated application to littoral enclosures. *Environmental Toxicology and Chemistry*, 18, 363-375.

Madigou, T., Le Goff, P., Salbert, G., Cravedi, J.P., Segner, H., Pakdel, F., Valotaire, Y., 2001. Effects of nonylphenol on estrogen receptor conformation, transcriptional activity and sexual reversion in rainbow trout (*Oncorhynchus mykiss*). *Aquatic Toxicology*, 53, 173-186.

Maguire, R. J., 1999. Review of the persistence on nonylphenol and nonylphenol ethoxylates in aquatic environments. *Water Quality Research Journal of Canada*, 34, 37-78.

Marcomini, A., Pojana, G., Sfriso, A., and Alonso Quiroga, J-M., 2000. Behaviour of anionic surfactants and their persistent metabolites in the Venice lagoon, Italy. *Environmental Toxicology and Chemistry*, 19, 2000-2007.

Marin M.G. , Matozzo V., 2004 – Vitellogenin induction as a biomarker of exposure to estrogenic compounds in aquatic environments. *Marine Pollution Bulletin*, 48: 835-839.

Matozzo V., Marin, M.G., 2005. Can 4-nonylphenol induce vitellogenin-like proteins in the clam *Tapes philippinarum*? *Environmental Research*, 97: 43-49.

Nagler, J.J., Ruby, S., Idler, D.R., So, Y.P., 1987. Serum phosphoprotein phosphorus and calcium levels as reproductive indicators of vitellogenin in highly vitellogenic mature female and estradiol-injected immature rainbow trout (*Oncorhynchus mykiss*). *Canadian Journal of Zoology*, 65, 2421-2425.

Pekkarinen M., Suoranta R., 1995. Effects of transportation stress and recovery and sample treatment on Ca²⁺ and glucose concentrations in body fluids of *Anodonta anatina* (Linnaeus). *Journal of Shellfish Research*, 14, 425-433.

Pojana, G., Bonfà, A., Buseti, F., Collarin, A., Marcomini, A., 2004a. Estrogenic potential of the Venice, Italy, Lagoon waters. *Environmental Toxicology and Chemistry*, 23, 1874-1880.

Pojana, G., Bonfà, A., Buseti, F., Collarin, A., Marcomini, A., 2004b. Determination of natural and synthetic estrogenic compounds in coastal lagoon waters by HPLC-electrospray-mass spectrometry. *International Journal of Environmental Analytical Chemistry*, 84, 717-727.

RESEARCH LINE 3.12

Trophic chain and primary production in the lagoon metabolism

MICROBIAL PRODUCTION AND DEGRADATION OF ORGANIC CARBON IN THE LAGOON OF VENICE: PRELIMINARY RESULTS.

A. Pugnetti⁴, F. Aciri⁴, P. Del Negro¹, M. Gianì¹, F. Bernardi Aubry, D. Berto², E. Crevatin¹, C. Facca³, P. Franceschetti², E. Ravagnan, F. Savelli², A. Valeri¹, V. Zangrando²

⁴ C.N.R. Istituto di Scienze Marine (ISMAR), Sezione di Venezia, Castello 1364/A, 30122 Venezia, ¹ Laboratorio di Biologia Marina, Trieste, ² Istituto Centrale per la Ricerca scientifica e tecnologica Applicata al Mare (ICRAM) Chioggia, ³ Dipartimento di Scienze Ambientali, Università di Venezia

Riassunto

Vengono presentati i primi risultati dell'attività di ricerca della Linea 3.12 "Struttura, dinamica e caratteristiche funzionali delle comunità biologiche dominate da macrofite e da alghe planctoniche nella Laguna di Venezia", svolta nell'ambito del 2° Programma di Ricerca CORILA 2004-2006.

La ricerca avrà il suo svolgimento completo nel biennio 2005-2006 e ha come obiettivo principale lo studio della produzione del carbonio organico da parte dei più importanti organismi autotrofi della Laguna di Venezia e del ruolo funzionale della componente microbica in relazione alla degradazione della sostanza organica, in aree lagunari e in momenti stagionali diversi.

Vengono presentati alcuni risultati relativi alle prime due campagne, effettuate in ottobre 2004 e in gennaio 2005, in tre stazioni della Laguna di Venezia.

L'attività fotosintetica del fitoplancton ha mostrato i valori più alti in ottobre, nelle due stazioni a più elevato impatto antropico (23 mg C m⁻³ h⁻¹ a Marghera, 14 mg C m⁻³ h⁻¹ a San Giuliano), mentre sono state registrate produzioni estremamente basse (< 1 mg C m⁻³ h⁻¹) in gennaio, in tutte e tre le stazioni. La comunità microfitorbentonica, risospesa in colonna, ha mostrato valori assoluti di produzione molto simili a quelli della comunità fitoplanctonica. La produzione specifica ($P^b = PP/Chl\ a$) è risultata, però, nettamente più alta per la comunità fitoplanctonica.

Le abbondanze batteriche sono risultate elevate (1,3 – 5,1 x 10⁹ cell l⁻¹): i massimi sono stati osservati nella stazione di Marghera (in ottobre) ed i minimi nella stazione di San Giuliano (sempre in ottobre). Alle minime abbondanze sono corrisposti, però, i più elevati valori di produzione batterica (92 µg C l⁻¹ h⁻¹), indicando un'intensa attività di crescita. Le attività esoenzimatiche batteriche sono state più intense in gennaio quando la limitata attività fotosintetica ha determinato, verosimilmente, una riduzione nell'apporto di substrato labile da parte del fitoplancton. La leucina aminopeptidasi è risultato l'enzima più attivo, seguito da lipasi e fosfatasi alcalina.

I valori più elevati di DOC (295 ± 55 µM), POC (89 ± 3 µM) e TPN (11 ± 1 µM) sono stati osservati in ottobre nella stazione di San Giuliano. Il rapporto Corg/N

(6 ± 1) è stato mediamente molto vicino al rapporto di Redfield (6,6).

Abstract

The preliminary results of the research line (3.12): "Structure, dynamics and functional characteristics of the biological communities dominated by macrophytes and planktonic algae in the Lagoon of Venice" (2nd CORILA Research Programme, 2004-2006) are presented.

This work focuses on the study of the photosynthetic organic carbon production by phytoplankton and microphytobenthos, of the degradation of organic carbon by the microbial communities and of some quali-quantitative aspects of the organic matter.

Two experimental campaigns were carried out in October 2004 and January 2005.

The highest photosynthetic activity was recorded in October (up to $23 \text{ mg C m}^{-3} \text{ h}^{-1}$), the lowest in January ($< 1 \text{ mg C m}^{-3} \text{ h}^{-1}$). The specific production (P^b) was noticeably higher for the phytoplankton community ($4 - 5 \text{ mg C mg chl a}^{-1} \text{ h}^{-1}$) than for the microphytobenthos ($< 1 \text{ mg C mg chl a}^{-1} \text{ h}^{-1}$).

Bacterial abundance ranged between $1.3 - 5.1 \times 10^9 \text{ cell l}^{-1}$; the lowest value corresponded to the highest bacterial production (up to $92 \text{ } \mu\text{g C l}^{-1} \text{ h}^{-1}$). The bacterial esoenzymatic activity was highest in January, when primary production was at the minimum rate, and it could indicate the lack of labile organic matter in the waters. The most active enzymes were leucine-aminopeptidase, lipase and alkaline phosphatase.

The highest organic matter concentrations were recorded in October 2004 at San Giuliano (DOC: $295 \pm 55 \text{ } \mu\text{M}$; POC: $89 \pm 3 \text{ } \mu\text{M}$; TPN: $11 \pm 1 \text{ } \mu\text{M}$). The average Corg/N (6 ± 1) was close to the Redfield ratio (6.6).

1 Introduction

The dynamics and the mechanisms that control and govern the production and the degradation of the organic carbon have important ecological implications, in terms of energy flux and trophic state of aquatic ecosystems.

Ecological information about these functional aspects in the Lagoon of Venice is sporadic.

In this paper we present the preliminary results of a research focused on the study of the photosynthetic organic carbon production, by the main autotrophic communities of the lagoon (fanerogams, macroalgae, phytoplankton and microphytobenthos), and of the degradation of organic carbon by the microbial communities. The research aims at giving a contribution useful to: (i) estimate the range of temporal and spatial variations of primary production, in relation with nutrient concentrations; (ii) define the relative importance of macrophytes, phytoplankton and microphytobenthos for the autotrophic carbon production; (iii) evaluate the functional role of the microbial community in relation with the

degradation of the organic matter and its temporal and spatial variations; (iv) assess the organic matter composition, in the different seasonal periods, considering the relative importance of dissolved and particulate fractions, the humic substances and the terrestrial contribution.

The research will be carried out in the years 2005-2006, in the framework of the 2nd CORILA research program (2004-2006). In this paper some preliminary results of the first two experimental campaigns are presented, concerning the microbial communities and the organic matter.

2 Materials and methods

Six sampling stations (Fig. 1), distributed in the northern and central basins, have been chosen, in relation to the influence of seawater, the impact of human activities and the distribution of the main primary producers. During each experimental campaign, the following parameters are considered: temperature and salinity (CTD probe Idronaut 316), transparency (Secchi disk), PAR irradiance (Li-COR sensor LI-192), dissolved macronutrients (N-NH₄, N-NO₂, N-NO₃, P-PO₄, Si-SiO₄) [Hansen and Koroleff, 1999], phytoplankton and microphytobenthos chlorophyll a [Holm Hansen et al., 1965], size structure [Utermöhl, 1958; Maugeri et al., 1990; Zingone et al., 1990], taxonomic composition [Tomas, 1997] and photosynthetic activity [Steeman Nielsen, 1952; Richardson, 1987], viral abundance [Noble and Fuhrman, 1998], bacterial abundance [Porter and Feig, 1980], production [Fuhrman and Azam, 1982] and enzymatic activity [Hoppe, 1983], dissolved organic carbon [Sugimura and Suzuki, 1988], particulated organic carbon and nitrogen [Nieuwenhuize et al., 1994] and extraction of aquatic humic and fulvic acids [Thurman et al., 1981]. Spectroscopic analyses and High-Pressure Size Exclusion Chromatography (HPSEC) were performed on humic fractions extracts. Absorbance ratios A_{272}/A_{407} and A_{465}/A_{665} were used to differentiate origin [Fooker and Liebezeit, 2000] and the degree of condensation of the humic substances [Schnitzer, 1971], respectively.

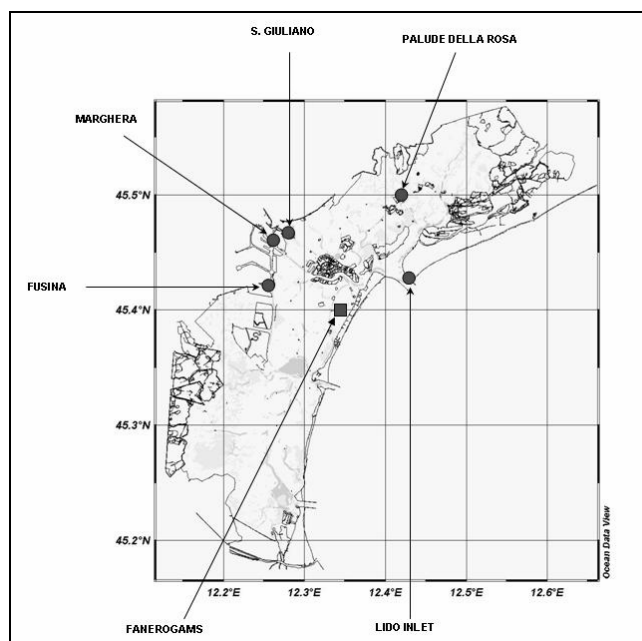


Figure 1 – The lagoon of Venice. Location of the sampling stations.

3 Results

In this paper we will present some preliminary results obtained during the first two experimental campaigns (October 2004 and January 2005). Attention is focussed on the production and degradation of the organic matter by the microbial communities (phytoplankton, microphytobenthos and bacteria) and on some quali-quantitative aspects of the organic matter, at three stations of the Lagoon of Venice (Fig. 1; Marghera, San Giuliano e Palude della Rosa).

3.1 Photosynthetic activity

The studies on the photosynthetic activity in the Lagoon of Venice are quite sporadic [Vatova, 1960; Battaglia et al., 1983; Degobbis et al., 1986; Creo et al., 1995; Sorokin et al., 1996; Bianchi et al., 2000; Sorokin et al., 2002; Bernardi Aubry and Pugnetti, 2005]. The main results indicate an elevated variability of phytoplankton primary production, covering two orders of magnitude. The highest values (up to $500 \text{ mg C m}^{-3} \text{ h}^{-1}$ e $5000 \text{ mg C m}^{-2} \text{ d}^{-1}$) have been generally recorded in the inner areas of the lagoon, in spring and summer, in relation to high phytoplankton biomass. No information is available on the photosynthetic activity of the microphytobenthos community in the lagoon.

During the present research the highest phytoplankton production were recorded in October at the stations Marghera ($23 \text{ mg C m}^{-3} \text{ h}^{-1}$) and San Giuliano ($14 \text{ mg C m}^{-3} \text{ h}^{-1}$). Phytoplankton production decreased markedly in January: in all the stations it was lowest than $1 \text{ mg C m}^{-3} \text{ h}^{-1}$. Phytoplankton production was significantly correlated with chlorophyll a ($r = 0,95$; $N = 8$; $p < 0,05$).

The microphytobenthos production, measured after the resuspension of the

community in the water, matched quite closely the phytoplankton photosynthetic activity. However, the specific production (P^b : production normalized to chlorophyll a) was noticeably higher for the phytoplankton community ($P^b = 4 - 5 \text{ mg C mg chl a}^{-1} \text{ h}^{-1}$) than for the microphytobenthos ($P^b < 1 \text{ mg C mg chl a}^{-1} \text{ h}^{-1}$).

3.2 Microbial community

Very few information are available on the microbial community of the Lagoon of Venice. The studies carried out in the past [Sorokin et al., 1996; 2002; 2004] emphasize the importance of the bacterial community and of the microbial loop in the lagoon: bacterial abundance ranged between 2 and $7 \times 10^6 \text{ cell ml}^{-1}$ and the bacterial production was quite close to, or even higher than, the phytoplankton production.

During this study the bacterial abundance ranged between $1.3 \times 10^9 \text{ cell l}^{-1}$ (October, San Giuliano) and $5.1 \times 10^9 \text{ cells l}^{-1}$ (October, Marghera). The temporal variations of bacterial abundance were different at the three stations: Marghera and Palude della Rosa showed the highest values in October, San Giuliano in January. The lowest abundances were generally associated with the highest bacterial production, as a consequence of increased cellular duplication in low abundance populations. In particular, the highest bacterial production ($92 \mu\text{g C l}^{-1} \text{ h}^{-1}$) was observed in October at San Giuliano.

The bacterial esoenzymatic activity was highest in January, when primary production was at the minimum rate, and it could indicate the lack of labile organic matter in the waters. The most active enzymes were leucine-aminopeptidase, lipase and alkaline phosphatase.

3.3 Organic matter

Past studies indicated a high variability of dissolved organic carbon (DOC), particulate organic carbon (POC) and total particulate nitrogen (TPN) in the lagoon of Venice [Bianchi et al., 1987; 2003; 2004]. In general the maximum values were recorded at low tide and in areas characterized by a marked anthropogenic impact.

In the present study, the highest DOC concentrations were recorded in October 2004 at San Giuliano ($295 \pm 55 \mu\text{M}$) and Marghera ($272 \pm 26 \mu\text{M}$). Also POC and TPN attained the highest concentrations in October, at San Giuliano ($89 \pm 3 \mu\text{M}$ and $11 \pm 1 \mu\text{M}$, respectively). The atomic ratio between organic carbon and particulate nitrogen (C_{org}/N) ranged between 4 (Marghera, January 2005) and 8 (San Giuliano, October 2004). The average C_{org}/N (6 ± 1), calculated considering the whole data set, was close to the Redfield ratio (6.6).

High values of A_{272}/A_{407} ratio of humic (8.4 ± 2.5) and fulvic (5.6 ± 0.6) acids and low A_{465}/A_{665} ratios (4.8 ± 2.5 and 3.4 ± 2.7 of humic and fulvic acids, respectively) showed a terrestrial contribution and high degree of condensation of humic fractions.

The molecular weights of the isolated humic fractions were low, ranging from 1276 to 1878 Da.

4 Conclusions

The information about the autotrophic community production and the organic matter degradation in the lagoon of Venice, which will be provided by this research in the years 2005-2006, will be useful for the general understanding of the lagoon ecosystem functioning. They will also be suitable for ecological modelling, in particular as it regards the trophic state evaluation and ecotoxicology. These data could also be used to evaluate future changes related to tide and lagoon/sea exchange control.

References

Battaglia B., Datei C., Dejak C., Gamabarello G., Guarise G.B., Perin G., Vianello E. and Zingales F., 1983. Indagini idrotermodinamiche e biologiche per la valutazione dei riflessi ambientali del funzionamento a piena potenza della centrale termoelettrica dell'Enel di Porto Marghera. Regione Veneto, Venezia.

Bernardi Aubry F. and Pugnetti A., 2005. Phytoplakton and primary production at the inlets of the Lagoon of Venice. *Scientific Research and safeguarding of Venice. Research programme 2001-2003*, vol. III: 343- 349.

Bianchi F., Aciri F., Alberighi L., Bastianini M., Boldrin A., Cavalloni B., Cioce F., Comaschi A., Rabitti S., Socal G. and Turchetto M., 2000. Biological variability in the Venice lagoon. In: Lasserre, P. and Marzollo, A. (Eds) *The Venice Lagoon Ecosystem. Inputs and interactions between land and sea. Man and the biosphere series volume 25*. UNESCO and Parthenon Publishing Group: 97-125.

Bianchi F., Boldrin A., Cioce F., Rabitti S. and Socal G., 1987. Variazioni stagionali dei nutrienti e del materiale particolato nella laguna di Venezia. bacino settentrionale. Estratto da: *Rapporti e studi*, Volume XI.

Bianchi F., Aciri F., Bernardi-Aubry F., Berton A., Boldrin A., Camatti E., Cassin D. and Comaschi A., 2003. Can plankton communities be considered as bio-indicators of water quality in the lagoon of Venice? *Marine Pollution Bulletin*, 46, 964-971.

Bianchi F., Ravagnan E., Aciri F., Bernardi-Aubry F., Boldrin A., Camatti E., Cassin D. and Turchetto M., 2004. Variability and fluxes of hydrology, nutrients and particulate matter between the Venice lagoon and the Adriatic Sea. Preliminary results (years 2001-2002). *Journal of Marine Systems*, 51, 49-64.

Creo C., Russo P., Mitola M., Poggi M., Signorini A., Silvestri C. and Izzo G., 1995. *SiTE, Atti*, 16: 83-86.

Degobbis D., Gilmartin M. and Orio A.A., 1986. The relation of nutrient regeneration in the sediments of the Northern Adriatic to eutrophication, with special reference to the Lagoon of Venice. *The Science of the Total*

Environment, 56, 201-210.

Fooker U. and G. Liebezeit., 2000. Distinction of marine and terrestrial origin of humic acids in North Sea surface sediments by absorption spectroscopy. *Marine. Geology*, 164, 173-181.

Fuhrman J.A. and Azam F., 1982. Thymidine incorporation as a measure of heterotrophic bacterioplankton production in marine surface waters: evaluation and field results. *Marine Biology*, 66, 109-120.

Hansen H.P. and Koroleff F., 1999. Determination of nutrients. In Grasshoff, K., Cremling, K., Erhardt, M. (eds), *Methods of seawater analysis*, Wiley-VCH Verlag: 159-228.

Holm-Hansen O., Lorenzen C.J., Holmes R.W. and Strickland J.D.H., 1965. Fluorimetric determination of chlorophyll. *Journal du Conseil International pour l'Exploration de la Mer*, 30: 3-15.

Hoppe H.G., 1983. Significance of exoenzymatic activities in the ecology of brackish water: measurements by means of methylumbelliferyl substrates. *Marine Ecology Progress Series*, 11, 299-308.

Maugeri T.L., Acosta Pomar M.L.C. and Bruni V., 1990. Picoplankton. *Metodi nell'ecologia del plancton marino*. Nova Thalassia, 11, 199-205.

Nieuwenhuize J., Maas E. M. and Middelburg J. J., 1994. Rapid analysis of organic carbon and nitrogen in particulate materials. *Marine Chemistry*, 45, 217-224.

Noble R.T. and Fuhrman J.A., 1998. Use of SYBR Green®1 for rapid epifluorescence counts of marine viruses and bacteria. *Aquatic Microbial Ecology*, 14, 113-118.

Porter K.G. and Feig Y.S., 1980. The use of DAPI for identifying and counting aquatic microflora. *Limnology and Oceanography*, 25, 943-948

Richardson K. (ed.), 1987. Primary production: guidelines for the measurement by ¹⁴C incorporation. ICES, *Techniques in marine environmental sciences*, 5.

Schnitzer, M. ,1971. Characterization of humic constituents by spectroscopy. In *Soil Biochemistry*, Vol. 2 (McLaren, A. D. & Skujins, J., eds). Marcel Dekker, New York, pp. 60–95.

Smith D.C., Azam F. 1992. A simple economical method for measuring bacterial protein synthesis rates in seawater using ³H-leucine. *Marine Microbial Food Webs* , 6 (2), 107-114.

Sorokin Yu. I., Sorokin P.Yu., Giovanardi O. and Dalla Venezia L., 1996. Study of the ecosystem of the lagoon of Venice with emphasis on anthropogenic impact. *Marine Ecology Progress Series*, 141, 247-261.

Sorokin P. Yu., Sorokin Yu. I., Zakuskina O. Yu. and Ravagnan G.-P., 2002. On the changing ecology of Venice lagoon. *Hydrobiologia*, 487, 1-18.

Sorokin P. Yu., Sorokin Yu. I., Boscolo R. and Giovanardi, O., 2004. Bloom of

picocyanobacteria in the Venice lagoon during summer-autumn 2001: ecological sequences. *Hydrobiologia*, 523, 71-85.

Steeman-Nielsen E., 1952. The use of radioactive carbon (^{14}C) for measuring organic production in the sea. *Journal du Conseil International pour l'Exploration de la Mer*, 18, 117-140.

Sugimira Y., Suzuki Y. 1988. A high-temperature catalytic oxidation method for the determination of non-volatile dissolved organic carbon in seawater by direct injection of a liquid sample. *Marine Chemistry*, 24, 105-131.

Thurman, E.M., and Malcolm R.L., 1981. Preparative isolation of aquatic humic substances. *Environ. Sci. Technol.* 15, 463-466.

Tomas C.R., 1997. *Identifying Marine Phytoplankton*. Academic Press, Arcourt Brace & Company.

Utermöhl H., 1958. Zur Vervollkomnung der quantitativen Phytoplankton-Methodik. *Mitt. Int. Verein. Limnol.*, 9: 1-38.

Vatova A., 1960., Primary production in the High Venice Lagoon. *Journal du Conseil International pour l'Exploration de la Mer*, 26, 148-155.

Zingone A., Honsell G., Marino D., Montresor M. and Socal G., 1990. Fitoplancton. In: Lint, Trieste (Ed.). *Nova Thalassia*, 11, Ministero dell'Ambiente.

NUTRIENT CONCENTRATION UPDATING IN THE WATERS OF THE VENICE LAGOON

Adriano Sfriso, Nicola Pellegrino, Sonia Ceoldo, Chiara Facca,

Department of Environmental Sciences, Calle Larga Santa Marta 2137, 30123 Venezia.

Riassunto

Vengono presentati i risultati della variazione delle concentrazioni dell'azoto inorganico disciolto (DIN= somma di ammonio, nitrito e nitrato) e del fosforo reattivo (RP) nella colonna d'acqua di tre stazioni (Tresse, Celestia e San Nicolò) campionate mensilmente tra luglio 2001 e giugno 2002 nella parte centrale della laguna di Venezia.

Inoltre, in estate 2003, mediante il campionamento di 163 stazioni omogeneamente distribuite nei bassifondali lagunari sono state rilevate e mappate le distribuzioni del DIN e RP nella colonna d'acqua di tutta la laguna e successivamente in settembre–ottobre 2003 ed in gennaio ed aprile 2004 sono state effettuate 3 campagne in 30 stazioni localizzate all'interno delle aree assegnate dalla Provincia di Venezia per l'allevamento delle vongole filippine (*Tapes philippinarum*, Adams & Reeve).

I dati sono stati analizzati e discussi in funzione della normativa (Decreto Ronchi-Costa, 23 Aprile 1998) che stabilisce valori di riferimento per le concentrazioni di azoto e fosforo totali nelle acque lagunari.

Abstract

Annual sampling results of Dissolved Inorganic Nitrogen (DIN = sum of ammonium, nitrite, nitrate) and the Reactive Phosphorus (RP) concentration changes in the water column of three stations (Tresse, Celestia and San Nicolò) which were sampled on a monthly basis between July 2001 and June 2002 in the central part of the Venice lagoon are studied in the present paper. The DIN and RP concentrations in the water column of the whole Venice lagoon were obtained and mapped by monitoring 163 stations homogeneously spread in the shallow bottoms in summer 2003. The same nutrients were also recorded in September-October 2003, January and April 2004 in 30 stations located in the areas assigned by the Province of Venice for clam-farming (*Tapes philippinarum* Adams & Reeve). Data were analysed and discussed according to the benchmark values for the total dissolved nutrients established by the Ronchi-Costa decree (23 April 1998).

1 Introduction

The variations of the nutrients and pollutant concentrations in the Venice lagoon have been the object of many studies. Their seasonal and annual trends have been monitored and compared with the "Imperative" and "Guide" values

established by the Ronchi-Costa decree to evidence possible reductions. Although surface sediments have experienced a significant reduction in the last 15 years [Sfriso et al., 2003], in the water column only RP displayed a significant decrease whereas DIN concentrations remained quite unchanged [Sfriso et al., 2005].

The present paper shows updated results (2001-2004) of the nutrient determinations in single areas sampled annually on a monthly basis and in seasonal samplings in the whole lagoon. Spatial and time concentration changes are discussed and compared with the benchmark values established by the law.

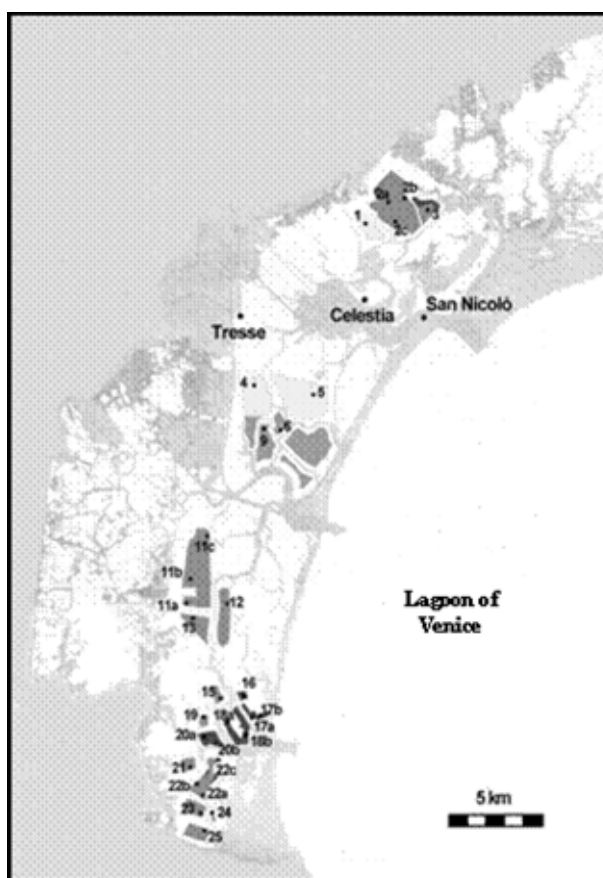


Fig. 1 – Three areas (Tresse, Celestia and San Nicolò) sampled annually on a monthly basis and 30 stations placed in the areas assigned for clam-farming.

2 Materials and methods

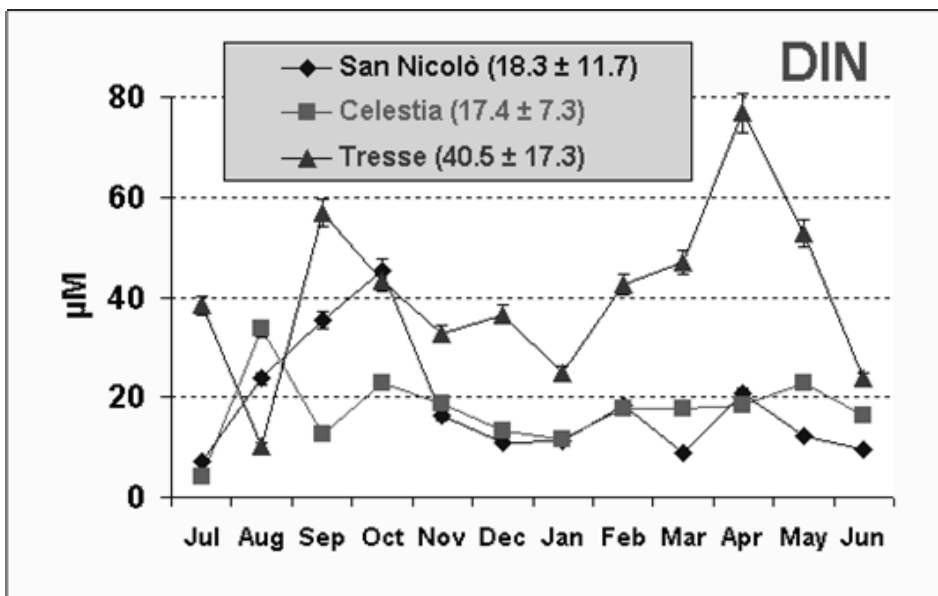
2.1 The Study area

Nutrient concentrations have been sampled in three areas (Tresse, Celestia and Samn Nicolò) of the central lagoon for one year on a monthly basis (Fig. 1) and in summer in 163 stations spread over the whole lagoon.

Table 1 – Nutrient concentrations in the water column of the three stations.

Nutrients in the Water Column (Three stations)							
2001-02	Samples	Ammonium	Nitrite	Nitrate	DIN	RP	
Stations	N°	µM					
S. Nicolò	12	mean	9.80	0.66	7.82	18.3	0.75
		std	12.90	0.37	3.31	11.7	0.65
Celestia	12	mean	9.10	0.87	7.43	17.4	0.93
		std	10.20	0.40	4.02	7.3	1.05
Tresse	12	mean	17.80	1.95	20.80	40.5	1.85
		std	7.52	0.68	10.10	17.3	3.01
Total mean			12.23	1.16	12.02	25.41	1.18

Moreover three seasonal (autumn, winter, spring) campaigns have been carried out in 30 sites placed in the areas assigned to clam-farming by the Province of Venice (Fig. 1).



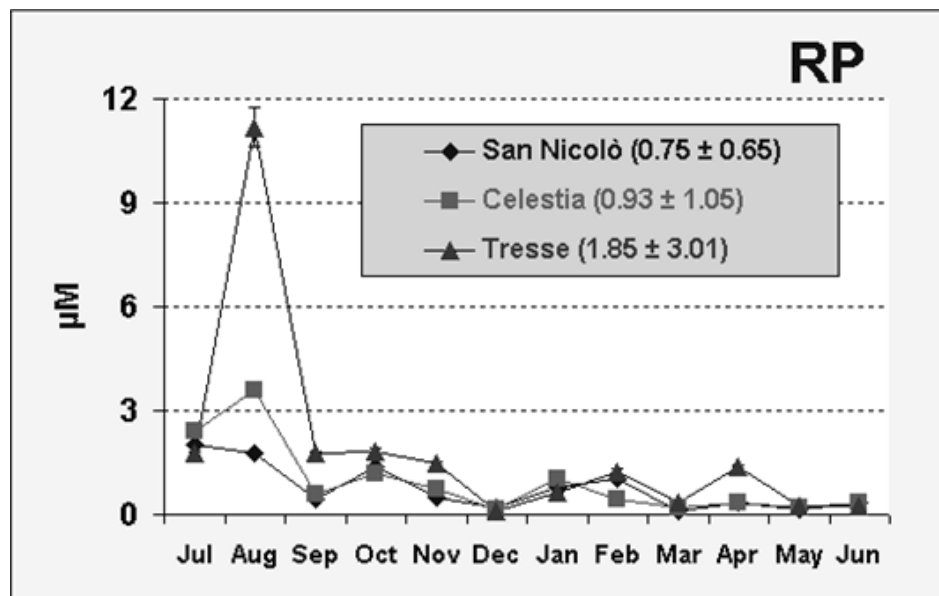


Fig. 2 – Trends of DIN and RP in the water column of the three stations.

2.2 Water analyses

Water samples were obtained by mixing together 5-6 sub-samples of the entire water column collected by means of a home-made bottle (height 150 cm, diameter 4 cm). Water aliquots were filtered through GF/F glass fibre filters (ca. 0.7 µm) and frozen at -20°C till nutrient determination. Nutrient analyses were carried out according to the analytical procedures reported in Strickland & Parsons [1972].

3 Results and discussion

3.1 Three stations

On average, total DIN and RP concentrations were ca. 25.4 and 1.2 µM. Ammonium and nitrate display concentrations quite similar (ca. 12 µM) whereas nitrite is ca. one order of magnitude lower than the other nitrogen species (ca. 1.2 µM). At San Nicolò and Celestia stations, which are affected by the urban untreated sewages of Venice historical centre, nutrient concentrations were quite similar whereas they were ca. 2 times as high at Tresse which is placed near the industrial area of Porto Marghera (Tab. 1). During the annual trends strong changes were found with two peaks in August-October (all the three stations) and in April (Tresse) for DIN and a peak in August for RP (Fig. 2). At Tresse DIN and RP reached 76.8 and 11.2 µM, respectively.

At Celestia RP (0.93 ± 1.05 µM) and at Tresse both DIN (40.5 ± 17.3 µM) and RP (1.85 ± 3.01 µM) showed mean concentrations higher than the "Imperative values" quoted by the Ronchi-Costa decree for the total dissolved nutrients (Tab. 2).

Tab. 2 – Regulatory Water Criteria for nutrients in river basins and lagoon waters (Ronchi-Costa decree, 23/04/1998).

Regulatory Water Criteria						
	River Basin		Lagoon Waters			
Nutrients	Value					
	Guide		Imperative		Guide	
	$\mu\text{g L}^{-1}$	μM	$\mu\text{g L}^{-1}$	μM	$\mu\text{g L}^{-1}$	μM
Total Dissolved Nitrogen	400	28.6	350	25	200	14.3
Total Phosphorus	30	1.0	25	0.8	10	0.3

3.2 Total lagoon (163 sites in summer)

On the whole, DIN and RP concentrations were 8.77 μM and 0.22 μM , respectively, but important differences were found when considering both the three morphological basins and the areas near the mainland or the lagoon inlets (Tab. 2). The central basin closed between the Malamocco-Marghera canal and the Burano-Torcello tidal lands exhibited the highest mean concentrations of both DIN (ca. 15.5 μM) and RP (ca. 0.25), while the southern basin showed the lowest mean values (DIN: ca. 4.53 μM , RP: ca. 0.20 μM). The northern basin showed concentrations close to those of the southern basin (DIN: ca. 5.24 and 4.53 μM ; RP ca. 0.21 and 0.20 μM , respectively).

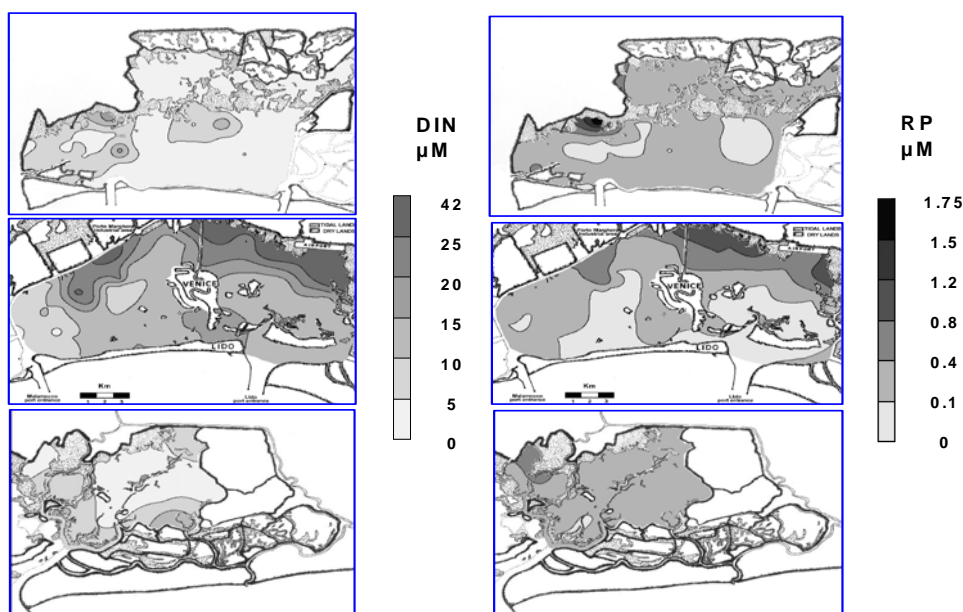


Fig. 3 – Total Dissolved nitrogen (DIN) and Reactive Phosphorus (RP) in the Venice lagoon in summer 2003.

Tab. 3 – Nutrient concentrations in the whole lagoon

Nutrients in the Water Column (Total lagoon)							
2003	Samples		Ammonium	Nitrite	Nitrate	DIN	RP
lagoon	N°		µM				
north	19	mean	2.29	0.28	2.67	5.24	0.21
		std	1.47	0.14	2.52	11.70	0.11
central	63	mean	4.62	0.68	10.23	15.53	0.25
		std	2.88	0.38	5.68	7.28	0.27
south	81	mean	2.22	0.28	2.03	4.53	0.20
		std	2.06	0.11	1.94	17.30	0.20
Total	163		3.12	0.43	5.22	8.77	0.22

In the central lagoon RP showed concentrations higher than 0.8 µM, the imperative value quoted by the Ronchi-Costa decree (Table 2), in many areas close to the mainland (Fig. 3). Reactive phosphorus exceeded that concentration also in the southern lagoon at Sacca dell'Aseo, north of the Romea translagoon bridge, while in the northern lagoon RP concentrations were below 0.52 µM. Similarly, DIN exceeded 25 µM in most of the central lagoon areas situated in proximity of the mainland, whereas the concentrations found in the other basins were below the Ronchi-Costa Imperative value. However, those concentrations were recorded in the summer period when nutrients are taken up by macrophytes and phytoplankton. In autumn and winter nutrients usually show concentrations which, on average are higher than the values recorded in summer.

Therefore in those areas RP exceeded the imperative values of the Ronchi-Costa decree all the campaigns whereas DIN was higher in winter and in spring.

Comparisons between the four groups of stations show that the central (DIN: 29.8 µM, RP 1.35 µM) and north (DIN: 23.6 µM, RP: 1.58 µM) basins displayed the highest mean values. In contrast the lowest DIN (ca. 20.6 µM) and RP (ca. 0.90 µM) concentrations were recorded in the Chioggia area.

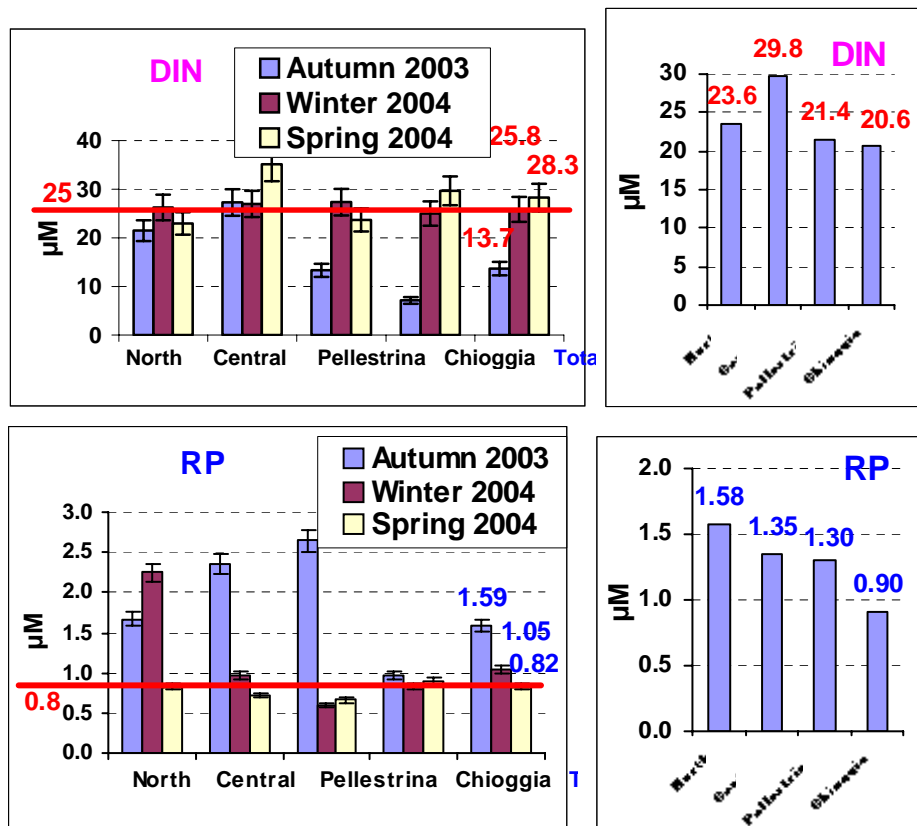


Fig. 4 – Concentrations of DIN and RP in the 30 stations divided into 4 groups and all together.

3.3 Total lagoon (30 sites in autumn, winter and summer)

The 30 stations have been divided into 4 groups corresponding to the north (sts.: 1, 2a, 2b, 2c, 3) and central (sts.: 4, 5,6 ,9) basins and to the areas of Pellestrina (sts.: 11a, 11b, 11c, 12, 13) and Chioggia (sts.: 15, 16, 17a, 17b,18a, 18b, 19,2c,20b, 21, 22a, 22b, 22c, 23, 24, 25) but also all together (Fig. 4). Significant differences were found especially between the autumn and the winter-spring campaigns. On an average DIN increased from 13.7 µM in autumn to 25.8 µM in winter and to 28.3 µM in spring, whereas RP showed an opposite trend. The highest RP mean concentration was 1.59 µM in autumn, but it dropped to 1.05 µM in winter and 0.82 µM in spring.

4 Conclusions

Dissolved inorganic nitrogen and reactive phosphorus concentrations in the water column show high spatial and temporal variability and, on the whole, exceed the “Imperative values” expected for the total dissolved nutrients (Ronchi-Costa decree) even without considering the organic fractions. In fact the lagoon receives ca. 24 small rivers and canals which drain about 1800 km² of intensively cultivated areas and the untreated sewages of the historical centre of Venice and the minor islands which are not provided with treatment plants. Moreover, intense clam-harvesting activities re-suspend high amounts of fine

sediment releasing the nitrogen and phosphorus trapped in the surface sediments [Sfriso et al., 2005].

As a consequence, whereas the sediments are experiencing a significant nutrient decrease [Sfriso et al., 2003], RP and DIN in the water column show again a high pulsing trend and concentrations which hardly correspond to the regulatory criteria also by considering the highest values established as "Imperative values".

Acknowledgements

This work was partly supported by the Consortium of Research Activities concerning the Venice lagoon System (Co.Ri.La) and partly by the Province of Venice. The authors are grateful to Dr. Orietta Zucchetta for the English editing.

References

Sfriso A., Facca C., Ceoldo, S., Silvestri S. and Ghetti P.F., 2003. Role of macroalgal biomass and clam fishing on spatial and temporal changes in N and P sedimentary pools in the central part of the Venice lagoon. *Oceanol. Acta.*, 26, 3-13.

Sfriso A., Facca C. Ceoldo S. and Marcomini A., 2005. Trophic level changes in the lagoon of Venice during the last 15 years. *Environ.Int.*, in press.

Strickland J.D.H., Parsons, T.R., 1972. *A Practical Handbook of Seawater Analyses*. Fish. Res. Board Can. Bull., Ottawa, p. 310.

RESEARCH LINE 3.13

Meteo-oceanographic conditions and coastal zone water quality

COMPARISON BETWEEN A THEORETICAL MODEL AND A NUMERICAL SIMULATION OF SEA-LAGOON INTERACTION IN THE NORTHERN ADRIATIC

Debora Bellafiore¹, Georg Umgiesser²

¹Università degli Studi di Padova, ²Istituto di Scienze Marine ISMAR, CNR, Venezia

Riassunto

Si presenta qui un confronto tra le evidenze prodotte da esperimenti in laboratorio, basati sul modello teorico di Wells, e i risultati dell'implementazione di un modello numerico tridimensionale agli elementi finiti, SHYFEM, creato all'Ismar-CNR di Venezia, nella ricostruzione dei fenomeni d'interscambio laguna-mare aperto.

L'osservazione delle evidenze è stata compiuta nell'area di Nord Adriatico, all'interno ed in prossimità delle bocche di porto di Lido e Malamocco, che collegano la Laguna di Venezia con il Mar Adriatico.

Si è analizzata l'asimmetria tra la fase di influsso e quella di efflusso, dovute al ciclo mareale, osservando la formazione di strutture vorticali a piccola scala ai lati delle bocche di porto.

Sono state verificate, nell'area di studio, le condizioni geometrico-morfologiche necessarie, secondo il modello di Wells, per l'accoppiamento dei vortici a formare un dipolo capace di propagarsi al largo e si è proceduto con l'analisi dei dati da simulazione numerica.

Abstract

A comparison between laboratory studies, based on a theoretical model, and results of a three-dimensional finite element model implementation is presented. The numerical model is called SHYFEM and has been created and implemented at Ismar-CNR Institute, Venice.

The study is focused on the phenomena of Lagoon-Open Sea Interaction, analysing the evidences connected with the inflow-outflow cycle.

The area considered for this study is the Northern Adriatic, in proximity of Lido and Malamocco inlets. These channels link the Venice Lagoon to the open sea.

The asymmetry between the inflow and the outflow phase, which is due to the tidal cycle, has been studied, paying attention to the formation of small scale vortex formations near the Venice inlets.

In the study area, looking at the theoretical model, the geometrical-morphological conditions, which are necessary for the vortex coupling to create

a dipole, have been verified. Finally the simulation results have been interpreted.

1 Introduction

The interaction between the Venice Lagoon and the Adriatic Sea can be studied both by the experimental approach and model simulations.

The structure and the physical basis of the interaction between two basins connected by a narrow channel have been investigated, in a theoretical way, by M. G. Wells [Wells and Van Heijst, 2003] and it's now of interest trying to apply this knowledge of these phenomena to a real natural situation, the one in front of the Venetian Lagoon.

There is a great scientific interest close to the inlet areas and to their fluid dynamic processes and huge efforts have been made for years to investigate them. Some experimental campaigns have taken place in the Venetian Inlets: ADCPs (Acoustic Doppler Current Profilers) have been put near the bottom of the Lido inlet, where a linear correlation between the inlet flow rate and the vertically averaged current over a unit column area was established [Gačić et al., 2004]. It has been possible to obtain information about the tidal impact at the inlets and about the tidal phases correlated with maximum current values [Gačić et al., 2004].

Now we want to analyze not only the impact but also the shape, scale order and evolution of phenomena connected with the tidal cycle and with the interaction between two basins. For this reason a simulation of surface currents has been produced for the period February 2004, implementing the 3D SHYFEM model [Umgiesser and Bergamasco, 1995, Umgiesser et al., 2004]. All predominant forcings have been introduced to produce realistic simulation results.

2 Phenomenology

The area near and inside the channel connecting two basins, as in the North of Adriatic Sea in proximity of the Venetian Lagoon, has a variety of fluid dynamic processes linked to the tidal cycle and to other external forcings such as wind and thermohaline gradients.

Both Lido and Malamocco Inlets are under the predominant influence of tides, 80% of variability is linked to them [Gačić et al., 2004]. There is also a dependence in the water level rise connected to the wind action, in particular, the Sirocco wind, from South-East. Also the influence of the North-East wind, Bora, is felt at the inlets.

The channel which connects the two basins is the point where the water masses are exchanged. The tidal cycle carries water into the narrow link and creates a periodical movement of water masses. Tides and bathymetrical-geometrical characteristics are at the basis of the asymmetry in the phases of inflow of new water into the Lagoon system and outflow of lagoon water into the Open Sea. There is the formation of small scale vortex structures during the

outflow process. They are present in the northern and southern area outside the inlet, on both sides of the jets, which propagate hundreds of meters offshore. These processes are visible from remote sensed images (Fig. 1).



Fig.1 – Sat image of Lido Inlet. The small scale vortex structures, due to the inflow-outflow cycle, are evident. This is the first phase of outflow; later there is the jet formation.

3 Methods

Because of the scale of phenomena here studied (500 m), they are not observed by HF Radar, which is the instrument used to investigate surface currents in Northern Adriatic (resolution 750 m) [Kovačević et al., 2004].

This work is preliminary to a possible comparison with measurements which will give extra information about sea-lagoon interaction. For the moment we just want to verify if what is theoretically expected can be numerically simulated.

3.1 Theoretical Model

The movements due to the inflow-outflow cycle have been the object of theoretical studies. A model has been developed by M. G. Wells [Wells and Van Heijst, 2003], on the basis of evidences from previous studies in Japan [Kashiwai, 1984].

The cycle creates an asymmetry between the inflow and the outflow phase, shown in Fig. 2. At the beginning of the outflow phase the ejection of water from the channel produces a small scale vortex formation, at the sides of the inlet. The transition from a narrow channel to the open basin helps the formation of coherent structures, jets, which propagate offshore. The temporal evolution of vortices is dependent on the inlet's geometry and from viscosity characteristics of lateral boundary, the so called no slip condition. If vortices are able to maintain a self coherent structure over many cycles their coupling in a dipole propagating offshore is possible.

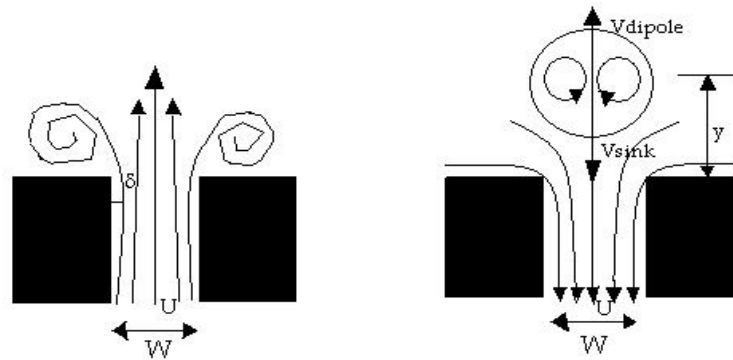


Fig. 2 – The channel outflow can induce a dipole formation, caused by the boundaries' vorticity advection. The inlet is as a sink for the inflow phase. There can be, under geometrical-morphological conditions, a dipole propagation offshore.

Calling Γ the total vorticity advected from the nozzle at time t , a the distance between the point vortices, the translation velocity can be written as

$$V_{dipole} = \frac{\Gamma}{2\pi a} \quad (1)$$

while the sink velocity, in the inflow phase, dependent on the distance in transversal direction from the inlet y , is

$$V_{sink} = \frac{UW}{4\pi y} \quad (2)$$

where U is the maximal velocity in the inlet and W the channel width.

Obtaining the condition of dipole formation and propagation one considers the relation

$$V_{dipole} > V_{sink} \quad (3)$$

or, expressing it with a dimensionless quantity W/UT , T the tidal period

$$\frac{W}{UT} < 0.13 \quad (4)$$

Wells has tried to verify this relation in the laboratory introducing a periodical forcing, with the same effects of tides. He has imposed a laminar flow observing that three-dimensional effects are not so relevant. This model has been applied to oceanographic context and preliminary evidence of its validity

has been recorded in the flushing of the Venice Lagoon [Gačić et al., 2002]. In this work the modeling of this phenomenon considering the geometrical-morphological characteristics of Lido and Malamocco inlets is presented.

3.2 SHYFEM Model

The three-dimensional primitive equation finite element model SHYFEM has been implemented to simulate the Lagoon-Open Sea Interaction Phenomena. The model has been utilized for many studies in the Venice Lagoon Area, to investigate fluid dynamics.

It is based on the momentum conservation equations and on the continuity equation. The complete transport equations, considering also the baroclinic terms are:

$$\frac{\partial U_i}{\partial t} - fV_i = Adv_i^x - g \frac{\partial \zeta}{\partial x} h_i - \frac{gh_i}{\rho_0} \frac{\partial}{\partial x} \int_{-H_i}^{\zeta} \rho' dz - \frac{1}{\rho_0} \frac{\partial p_a}{\partial x} + \frac{1}{\rho_0} (\tau_x^{i-1} - \tau_x^i) + A_H \left(\frac{\partial^2 U_i}{\partial x^2} + \frac{\partial^2 U_i}{\partial y^2} \right) \quad (5)$$

$$\frac{\partial V_i}{\partial t} + fU_i = Adv_i^y - g \frac{\partial \zeta}{\partial y} h_i - \frac{gh_i}{\rho_0} \frac{\partial}{\partial y} \int_{-H_i}^{\zeta} \rho' dz - \frac{1}{\rho_0} \frac{\partial p_a}{\partial y} + \frac{1}{\rho_0} (\tau_y^{i-1} - \tau_y^i) + A_H \left(\frac{\partial^2 V_i}{\partial x^2} + \frac{\partial^2 V_i}{\partial y^2} \right) \quad (6)$$

i indicates the vertical layer, (U, V) Horizontal Transports, g gravitational constant, p_a atmospheric pressure, ζ sea level, $\rho = \rho_0 + \rho'$ water density, h_i layer thickness, H_i total depth, A_H horizontal eddy viscosity.

The advective terms are expressed as

$$Adv_i^x = \left(-U_i \frac{\partial U_i}{\partial x} - V_i \frac{\partial U_i}{\partial y} \right) h_i \quad Adv_i^y = \left(-U_i \frac{\partial V_i}{\partial x} - V_i \frac{\partial V_i}{\partial y} \right) h_i \quad (7)$$

The stress terms, for each vertical interface, can be written as

$$\begin{aligned} \tau_x^i &= -k \left(\frac{\partial u}{\partial z} \right)_i \\ \tau_y^i &= -k \left(\frac{\partial v}{\partial z} \right)_i \end{aligned} \quad (8)$$

The boundary conditions for stress terms are

$$\tau_x^{\text{sup}} = c_D \rho_a w_x \sqrt{w_x^2 + w_y^2} \quad \tau_y^{\text{sup}} = c_D \rho_a w_y \sqrt{w_x^2 + w_y^2} \quad (9,10)$$

$$\tau_x^{bottom} = c_B \rho_0 u_L \sqrt{u_L^2 + v_L^2} \quad \tau_y^{bottom} = c_B \rho_0 v_L \sqrt{u_L^2 + v_L^2} \quad (11,12)$$

c_B is bottom friction coefficient, c_D wind drag coefficient, ρ_a air density, ρ_0 constant water density, (w_x, w_y) wind velocity, in zonal and meridional direction, (u_L, v_L) bottom velocity.

The boundary conditions applied to the whole system are

$$\text{At surface layer} \quad w_0 = \frac{d\zeta}{dt} \quad (13)$$

$$\text{At bottom layer} \quad w_L = - \left(u_L \frac{\partial H_L}{\partial x} + v_L \frac{\partial H_L}{\partial y} \right) \quad (14)$$

w_0 and w_L are vertical velocities at the surface layer and at the bottom layer respectively and H_L is the undisturbed water depth.

In this work two peculiar aspects have been developed. The first is the coupling of two basins, the Venice Lagoon and the Adriatic Sea, leading to a possible study of interaction flushing. The second is concerned with the increase of resolution in proximity of the inlets and in the coastal area between them, to simulate small scale phenomena.

The work on the grid consisted in modifying the high resolution Adriatic Sea grid, used for previous studies on the Venetian Lagoon [Cucco and Umgiesser, 2004a,b]. It has a resolution of 100 m inside the inlets and, for this study, that resolution has been extended also outside the channels and in the coastal area. An area, including the two Malamocco and Lido Inlets, has been chosen and an automatic mesh generator has been applied to insert a higher number of finite elements, increasing the resolution (Fig. 3). After that the bathymetric information has been inserted to create the new grid for the model.

The new grid was tested with respect to the computational weight and the stability analysis of the model and it was verified that increase in resolution did not introduce numerical instability.

To simulate the sea-lagoon interaction phenomena external forcings have been introduced into the model: astronomical tides, wind, temperature and salinity gradients. The first of these is the most effective to simulate the small scale vortical formations. We can say that the presence of the other forcings can lead to results that do not reproduce the laboratory results, in which they are not considered. Their description is the topic of another paper [Bellafiore et al., this issue].

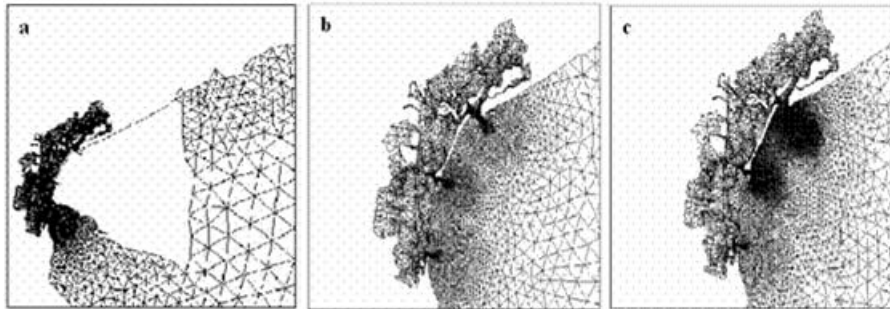


Fig. 3 – Particular of the Adriatic basin finite element grid. a) The chosen area for an increase in resolution; b) the high resolution grid used before this study; c) the new grid.

4 Results

First of all the geometrical-morphological characteristics of Lido and Malamocco Inlets have been verified.

Tab. 1 – Parameters of the Lido and Malamocco inlets: W, width of the inlet, U, maximal velocity inside the inlet, T, tidal period and dimensionless number W/UT.

	W (m)	U (m/s)	T (s)	W/UT
Lido	900	1	43200	0.02
Malamocco	400	1.5	43200	0.006

From Tab. 1 one can note that both of the inlets have properties which lead to values of the dimensionless quantity W/UT under the critical value of 1.3. So the small scale vortex formations and their coupling in a dipole propagating offshore are expected.

The simulation covers February 2004. Attention has been focused on temporal ranges in which wind forcing is not predominant and the direct tidal connected phenomena were possible to see (Fig. 4).

In the first outflow phase there is the jet formation and subsequently, on both sides of the inlet, two small scale vortices form. They have a diameter of 200 m and small internal velocity.

These vortex structures propagate offshore and during the first inflow phase they begin coupling. The formation and the attenuation of a dipole going offshore are sequential.

The evidences connected with jets, from the simulation, show structures which propagate offshore less than what seen from remote sensed images. Also in this case we suppose that forcing characteristics can influence this aspect. The fact that used thermohaline values, MFStep data from OPA-Interannual, are

given in the open sea but do not describe the real gradients present along the coast and near the inlets, can be one reason of the underestimation of the phenomenon. We did also not consider T/S contributions from rivers.

Moreover, real bathymetry does certainly change the ideal laboratory situation and will lead to different results. However, jets are evident from simulation but wind and T/S forcings, which are not considered in lab experiments, can divert the propagation direction (Fig. 4).

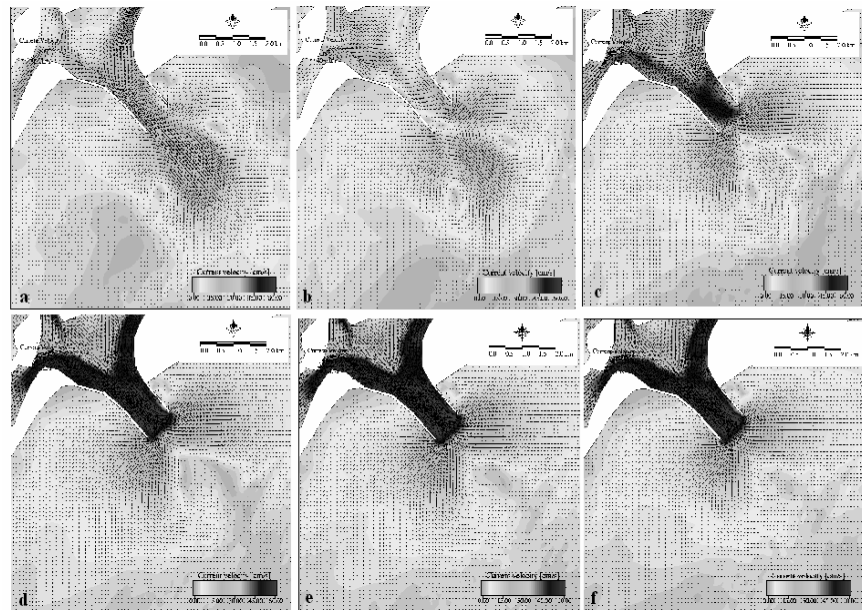


Fig. 4 – Simulation plots. Small scale vortex formation during and after the maximum outflow (a). When out flowing velocity decreases vortices begin moving offshore (b and c). In the final phase vortices tends to couple maintaining the two senses of rotation (d). In the first phase of inflow the two vortex structures show fusion into a dipole propagating and attenuating offshore (e and f).

5 Conclusions

The qualitative comparison between a theoretical model and numerical simulations present evidence of the same phenomena. The situations of major agreement are the one in which external forcings are acting low.

So far, it is possible to suppose a valid future comparison between the simulation results and the measured ones. In CORILA Projects a new campaign of Radar measurements are planned for September 2005. A VHF Radar, transmitting at a frequency of 152 MHz, will measure surface currents and collecting data over a new CODAR grid with a resolution of 100 m will be possible. Interaction phenomena will be investigated with measured data.

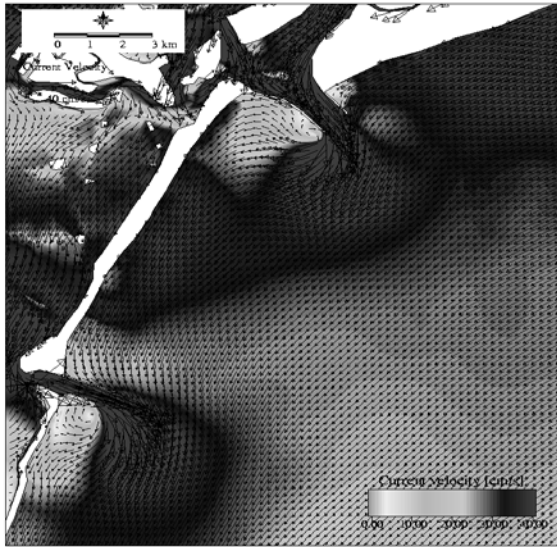


Fig. 5 – Surface current near Lido and Malamocco Inlets. A strong wind phenomenon from North deviates out flowing water masses. The jet propagation is directed to the South.

Acknowledgements

The authors want to thank Dr. Gačić for the help in finding connection between the Wells model and the results of SHYFEM simulations near the Venice Inlets.

Thanks to Dott. Cucco for the precious suggestions in implementing SHYFEM Model.

Thanks to INGV Institute for Temperature and Salinity data.

This work was carried out with the financial support of CORILA in the framework of the CORILA Project 3.13 “Condizioni meteo-oceanografiche e qualità delle acque della zona costiera”.

References

Bellafiore D., Umgiesser G., Kovačević V., Cucco A., Cosoli S., Simulation of Surface Currents in Northern Adriatic and Comparison with HF Radar Data Measurements, Present Issue.

Cucco A., Umgiesser G., 2004. Modeling the Venice Lagoon Residence Time. Submitted to Journal of Marine Systems.

Cucco A., Umgiesser G., 2004. Modeling the water exchange between the Venice Lagoon and the Adriatic Sea. Submitted to Journal of Marine Systems.

Kashiwai M., 1984. Tidal residual circulation produced by a tidal vortex, Part 1, Life history of a tidal vortex.. J. Ocean. Soc. JPN, 40, 279-294.

Kovačević V., Gačić M., Mancero Mosquera I., Mazzoldi A., Marinetti S., 2004. HF radar observation in the northern Adriatic: surface current field in front of the

Venetian Lagoon, *Journal of Marine Systems*, 51, 1-4, 95-122.

Umgiesser G., Bergamasco A., 1995. Outline of a Primitive Equation Finite Element Model, *Istituto Veneto di Scienze Lettere e Arti, Rapporti e Studi*, XII, 291-320.

Umgiesser G., Melaku Canu D., Cucco A., Solidoro C., 2004. A finite element model for the Venice Lagoon. Development, set up, calibration and validation, *Journal of Marine Systems*, 51, 123-145.

Wells M.G., Van Heijst G.-J.F., 2003, A model of tidal flushing of an estuary by dipole formation, *Dynamics of Atmospheres and Oceans*, 37, 223-244.

ASSESSMENT OF WATER QUALITY STATUS IN THE COASTAL AREA CLOSE TO THE LAGOON OF VENICE. FIRST YEAR OF ACTIVITY

Mauro Bastianini¹, Cosimo Solidoro², Vinko Bandelj², Debora Bellafiore¹, Raffaella Codermatz², Gianpiero Cossarini², Andrea Cucco¹, Donata Melaku Canu², Elisa Ravagnan¹, Georg Umgiesser¹, Marina Vazzoler³, Anna Rita Zogno³

¹ Istituto Scienze Marine ISMAR-CNR, Venezia, ² Istituto Nazionale di Oceanografia e di Geofisica Sperimentale - OGS, Sgonico(TS), ³ ARPAV, Osservatorio Alto Adriatico, Padova

Riassunto

Il manoscritto descrive i risultati principali conseguiti nel corso del primo anno di attività del progetto CORILA 3.13, "Climatologia e qualità delle acque costiere della Regione Veneto". La ricerca si propone di fornire un contributo alla valutazione della qualità delle acque in zona costiera ed alla comprensione delle interazioni fra questa e la qualità delle acque interne alla laguna. L'obiettivo principale è raccogliere e sintetizzare in un quadro unitario i risultati provenienti da diversi progetti ed attività di monitoraggio che hanno, o hanno avuto, per oggetto l'area in questione, così da costruire una condizione tipica di riferimento (climatologia) e poter valutare le scale di variabilità, spaziale e temporale, dei principali parametri che caratterizzano il corpo d'acqua.

Abstract

In this manuscript we describe major results of the first year of activities of CORILA project 3.13. The project aims to contribute to the assessment of water quality status in the coastal area that is connected to the lagoon and to a deeper understanding of the interaction between the lagoon of Venice and this coastal area.

The main goal is to synthesize and integrate results coming from different research projects and monitoring activities, so to eventually provide 'typical condition' and scales of variability for the area.

Here we illustrate how we constructed the project data set, by collation, comparison and check, of different data sets, and we present results of first elaborations.

1 Introduction

Venice is one of the most studied sites in the world, but up to few years ago most of the projects consisted in individual researches, and there was a lack in concerted basin-wide efforts, as well as in attempts to integrate existing knowledge in a common frame and from a systemic viewpoint.

This research aims at partially filling this gap, by providing a contribution to the

assessment of water quality status in the coastal area that is connected to the lagoon, and to a deeper understanding of the interaction between the lagoon of Venice and this coastal area. The research will result as an important piece of information in the analysis of the integrated system composed by the drainage basin, the lagoon and the coastal area, and might provide interesting indications of the role played by lagoon systems in buffering impacts of drainage basin on coastal sea. Results will also provide a contribution to management of coastal area by local authorities.

Main goal is to synthesize and integrate results coming from different research projects and monitoring activities. Historical data referring to the coastal area will be collected in a common database, and a retrospective analysis will be performed in order to identify 'typical condition' of the area, as well as typical variability around it, also depending on space (distance from tributaries and/or lagoon inlets) and time of the year. Analysis of long term trends will be performed too.

The emerging picture will be confronted with those of similar ecosystems, and discussed also with reference to existing legislation and to indexes proposed in scientific literature to assess water quality or status. This should give some elements to local authorities too, about water quality standards and maximum permissible load to be enforced in future regulation.

Indeed, local authorities are active participants of the project, through their technical chapters that are in charge of monitoring water quality parameters in coastal area.

Finally we'll consider the possibility to evaluate an integrated biogeochemical budget of the Lagoon-coastal system.

In this manuscript we resume the first year of activities, which consisted mainly in the identification of the project data set, by collation, comparison and check, of different data sets, and in a first characterization of scale of variabilities for major parameters.

2 Identification of the Data Set

The dataset is composed of two main parts: the first one was collected by ARPAV (regional agency for environmental prevention and protection in Veneto) and contains data about the coastal area within 3 nautical mile from the coastline, lasting from 1985 until now, Fig. 1a, while the second part is relative to off shore data of the North Adriatic Sea, starting from the beginning of the last century, Fig. 1b.

In the present paper we focus on the second dataset that consists of a large collection of published and unpublished data, 113.986 records, covering the area of the Northern Adriatic Sea comprised between 44° 30' and 45° 45' of latitude and 12° 18' and 13° 56' of longitude. The oldest datasets were collated in the ATOS dataset, spanning from 1911 to 1980 (Russo et al., 2002), then from 1990 to 1994 data were collected in the frame of a monitoring project

named “Progetto Alto Adriatico”. Other data come from the PRISMA II project for the period 1995-1998 and the most recent data, from 1999 to 2001, were gathered in the frame of Interreg II project.

Only surface data, the first measurement of each cast profile but above the depth of 2 meters, were considered in the present dataset. Then, the resulting dataset comprises a total of 6322 casts that are distributed all over the basin, Fig. 1b. The density of casts increases along few transects, while the areas less covered are the Croatian coast and the area in front of the Grado-Marano lagoon.

The list of variables includes physical parameter as temperature, salinity, dissolved oxygen, pH and Secchi disk, and six trophic parameters: as nitrate, nitrite, ammonia, phosphate, silicate, chlorophyll a.

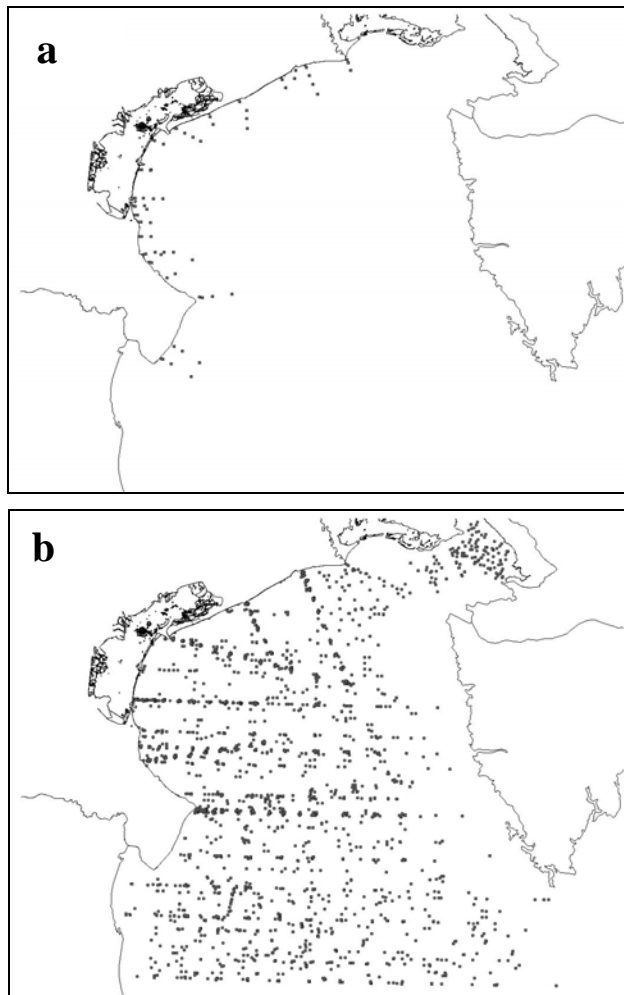


Fig. 1a, b. Casts location maps for the two parts of the dataset: a) coastal dataset, b) off-shore dataset.

3 Modelling circulation in the coastal area

Understanding the circulation pattern in the coastal area facilitates the interpretation of the spatial distribution of dissolved substances, as well as the set up of an integrated biogeochemical budget of the Lagoon-coastal system. For this reason a primitive equation, three-dimensional finite element model will be applied to the area, to simulate and investigate the current field. Presently the model is being tested, after the introduction of a better parameterization of baroclinic pressure gradients into the conservation momentum equations [Cucco and Umgiesser, 2004; Bellafiore, 2005], and implementation of boundary conditions [Bellafiore and Umgiesser, 2005 this issue]

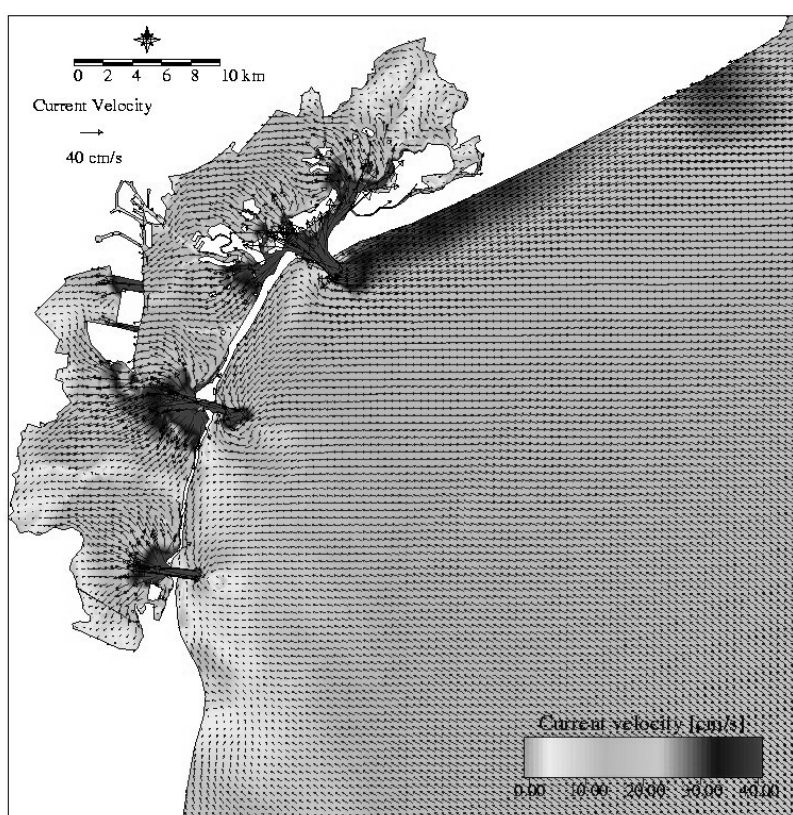


Fig. 2: Surface velocity map in the Northern Adriatic area near the Venetian Lagoon for realistic wind conditions. Velocity values are produced by the implementation of the primitive equation three-dimensional finite element model SHYFEM.

4 Analysis of the dataset and assessment of the scales of variabilities

4.1 Numerical abundance and spatial coverage of the dataset

The annual and monthly distributions of the number of casts are presented respectively in Figs. 3a and 3b. The dataset includes historical data from the period 1911-1916, but the number of samples is relevant only after 1971, and only after 1986 it is homogenously high. During the last decade, at least 250

casts per year were collected, except during 1991 and 1997, when only 178 and 140 were gathered. The 'richest' year is 1993, with about 600 casts, but also in years 1987, 1992 and 2001 there are more than 400 data. Most of the data were collected during spring and summer months, with usually more than 600 casts per month, while January, with less than 200 casts, is the less rich month, Fig.3b.

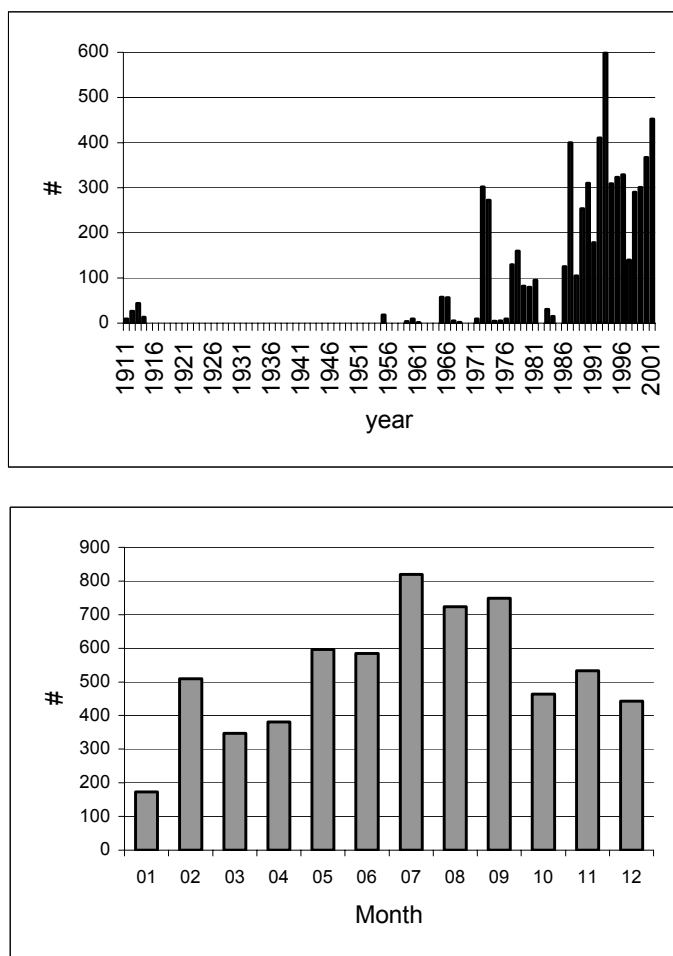


Fig. 3a, b: annual and monthly cast distributions.

Fig. 3 shows that the availability of data varies greatly from year to year and from month to month, but also the spatial distribution of casts varies greatly from a period to another period. As an example, Fig. 4, underlines well the differences in spatial distribution and data coverage in casts collected during summers 1976 and 2001, as a result of different sampling strategies adopted in different studies. Furthermore, coverage varies from month to month, and it is quite poor if a temporal interval shorter than one year is considered. The consequence is that, in order to get a reasonably homogeneous coverage both in space and in time, one needs to aggregate the data over longer temporal window, to be selected on the basis of abundance of data during the years, Fig 3, and temporal evolution of some selected variables, Fig. 5.

Fig. 3 shows that a continuous dataset could be constructed with data down to 1986, even if 1986 and 1988 have less than 130 casts. The graphics of fig.5 indicate that during this period no trend is clearly detectable from time evolutions of statistical indexes which describe the frequency distribution of data. However, we decided to consider data starting from 1990, when the PPA project started, since from then there should be a standardization of sampling and analysis methodologies.

Therefore data of the period 1990-2001 had been aggregated and analysed as a homogeneous pool of data for calculating the reference annual mean and the reference seasonal evolution for the variables. As a result of the selection, the analysed dataset consists of 4007 casts, and since the number of data depends on the variable, the present dataset contains almost 4000 observations for salinity, temperature and density, but less than 800 observations for nutrients and chlorophyll, Tab.1.

	Number of observations
Temperature	3979
salinity	3996
Density	3977
Nitrate	689
Phosphate	709
Silicate	726
Chlorophyll	522

Tab.1: number of valid observations in the 1990-2001 dataset for each variable.

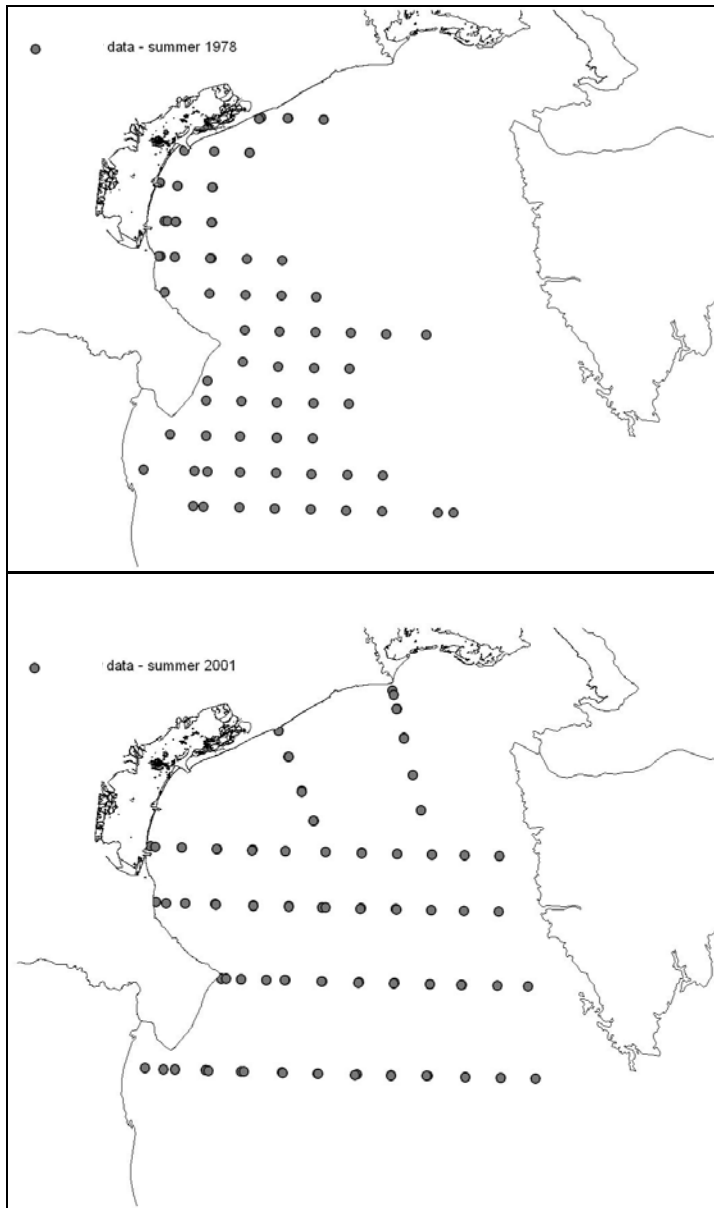
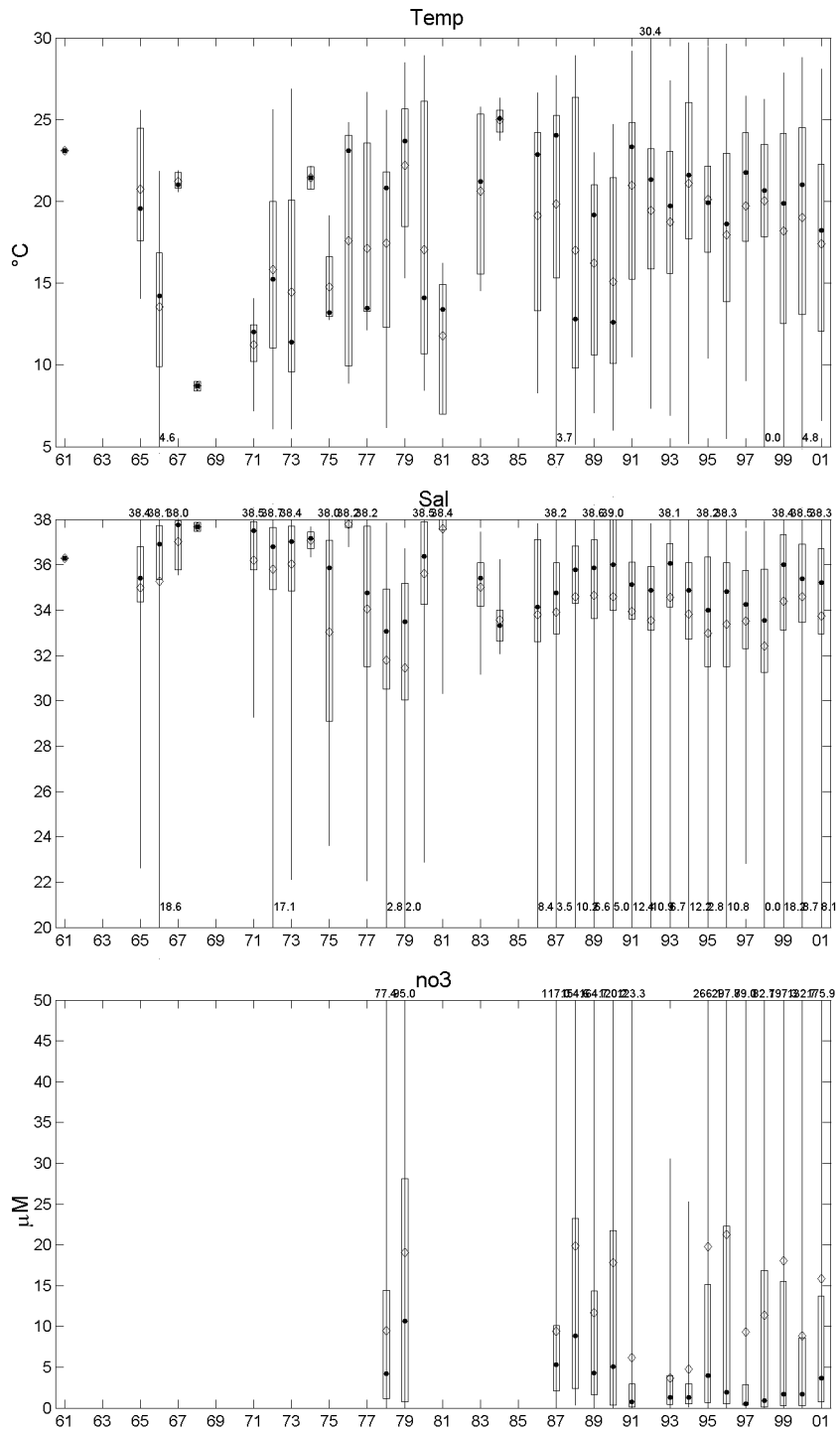


Fig. 4: spatial distribution of casts collected during summer of 2001 (DX) and of 1978 (SX)



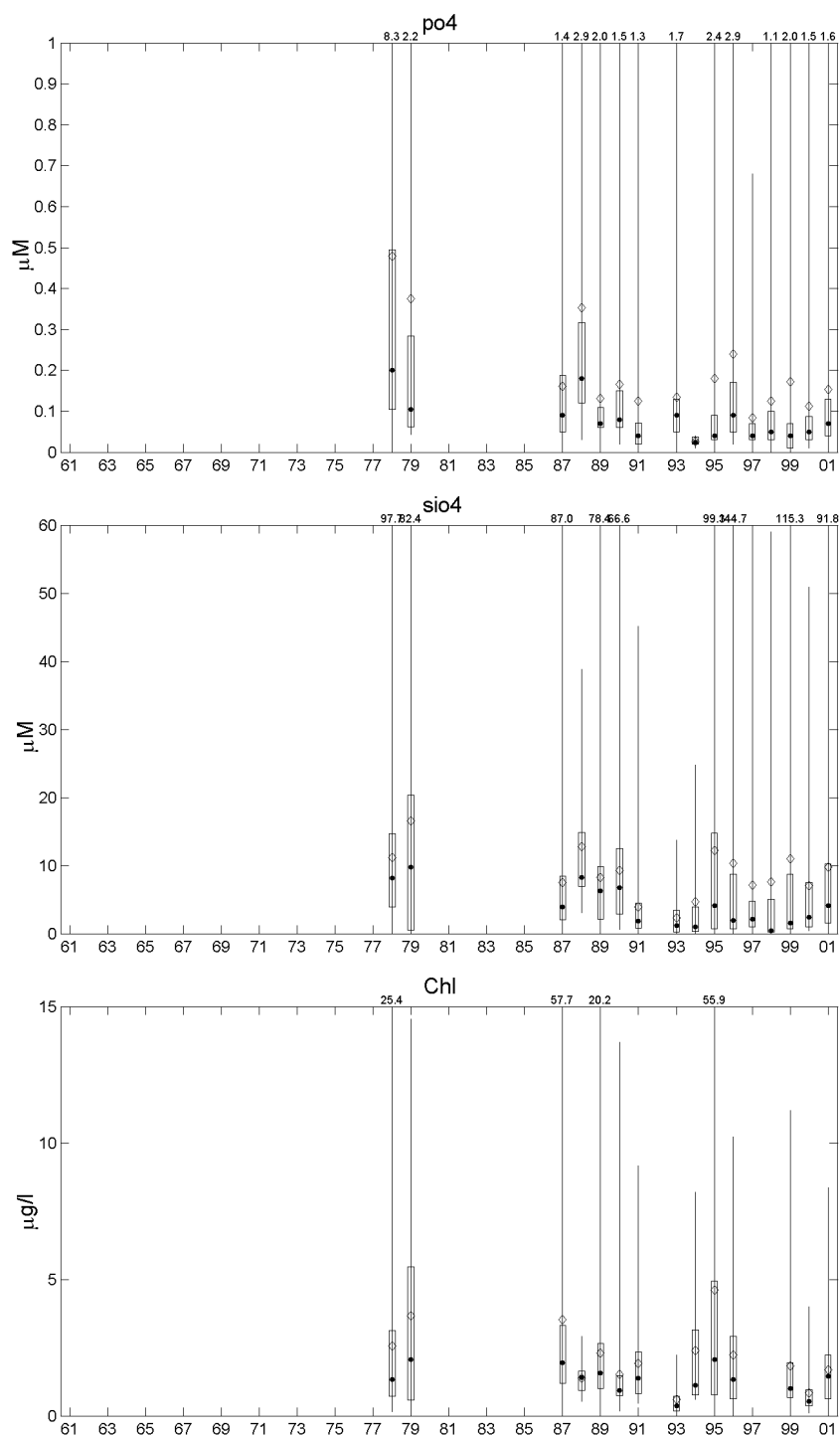
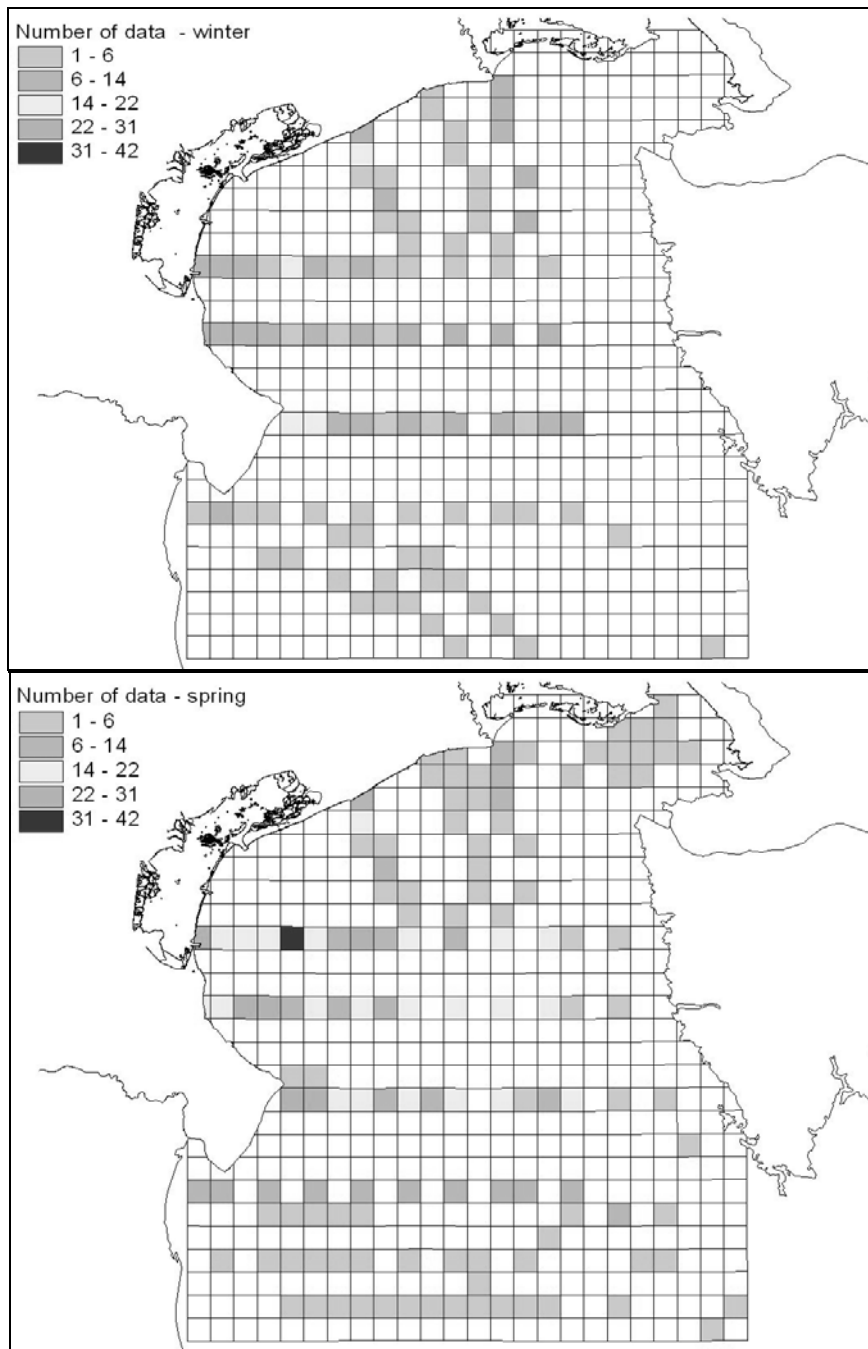


Fig. 5: evolutions of box-plot of the annual distribution of data over the whole basin for temperature (Temp), salinity (Sal), nitrate (no3), phosphate (po4), silicate (sio4) and chlorophyll (chl). Each box-plot reports the median (black dot), the mean (empty diamond), the interquartile range (box) and the range min-max (vertical black bar) of the distribution of all the data collected in the study area during each year from 1961 to 2001.

Data were aggregated spatially, too, in order to provide a homogeneous base for geostatistical analysis. The Northern Adriatic Sea domain was subdivided in a grid of 5x5 km, as in Fig. 6, and casts which fall in each of the bins pooled. This size of the grid enable one to get a minim number of data in each 'active' bin, and therefore a 'robust' data set, while preserving the possibility to observe spatial variability. Of course there are bins in which no data are present, as illustrated in fig. 6 and fig. 7, in which coverage and abundance for respectively salinity and nitrate are illustrated, as proxies for database consistence of physical and trophic parameters.

The analysis of the 4 maps of Fig. 6 and 7 makes clear that most of salinity data is collected along 3 meridian and 4 parallel transects and that the area in front of the Po delta has the greatest number of data. Spatial coverage of nitrate data is quite poor when compared to the one of physical variables. Three transects are detectable, and again the area in front of Po delta is the most sampled one.



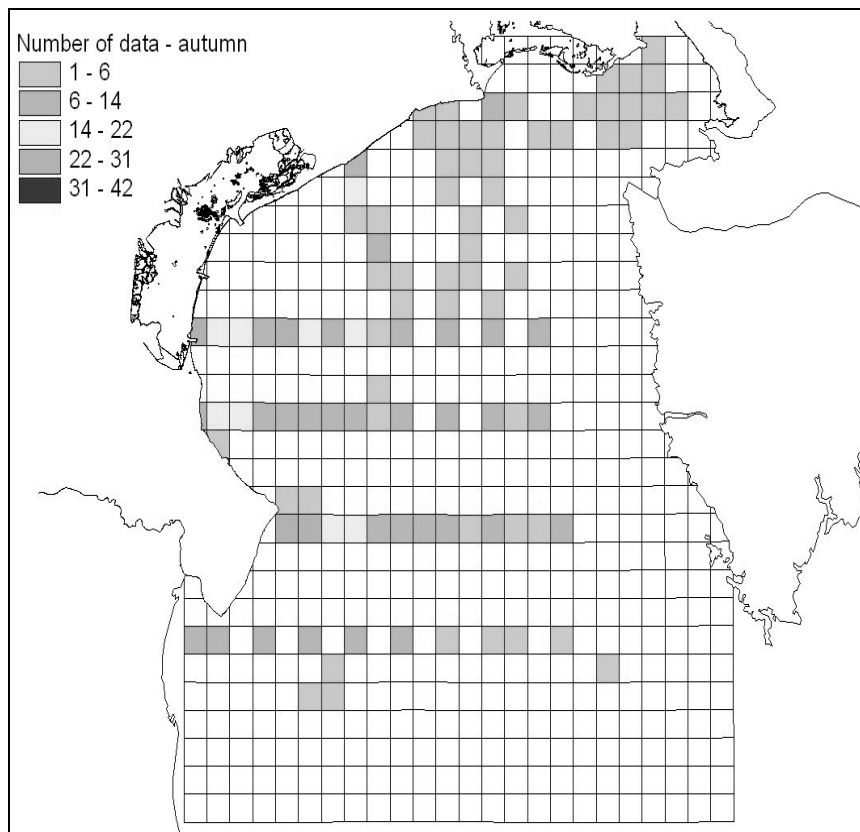
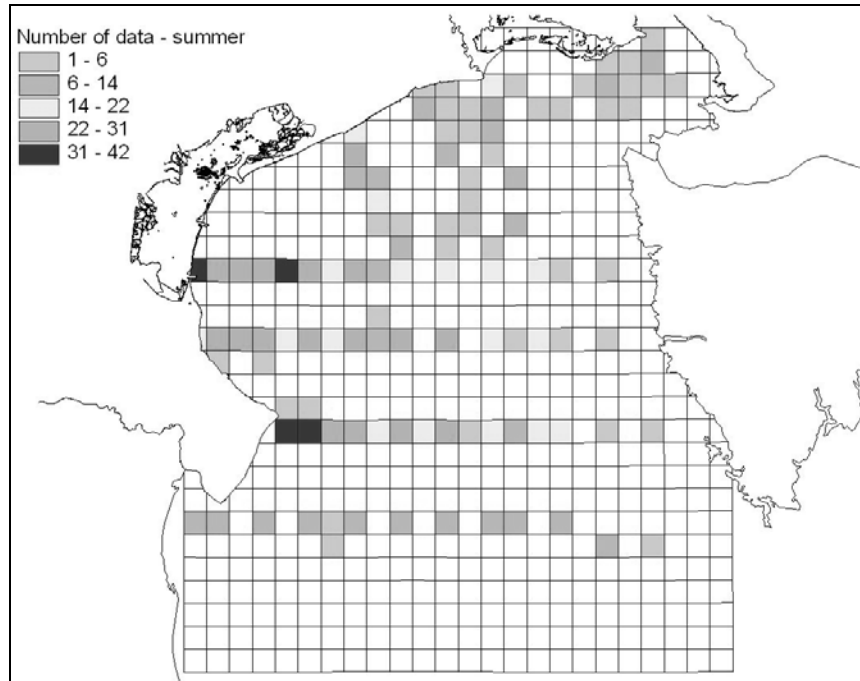
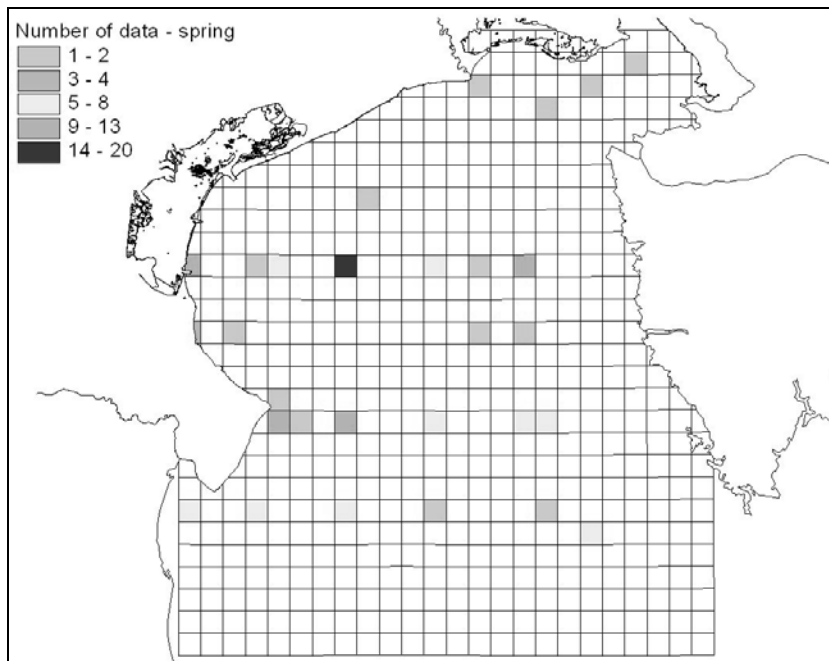
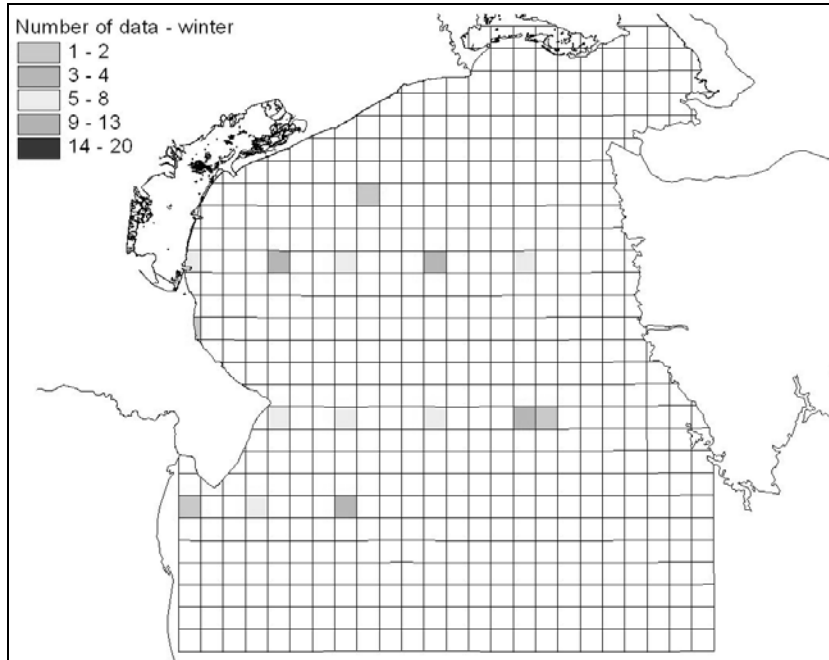


Fig. 6: number of salinity data in each cell of the grid of 5km for the four

seasons (winter, spring, summer and fall) of the 1990-2001 data.



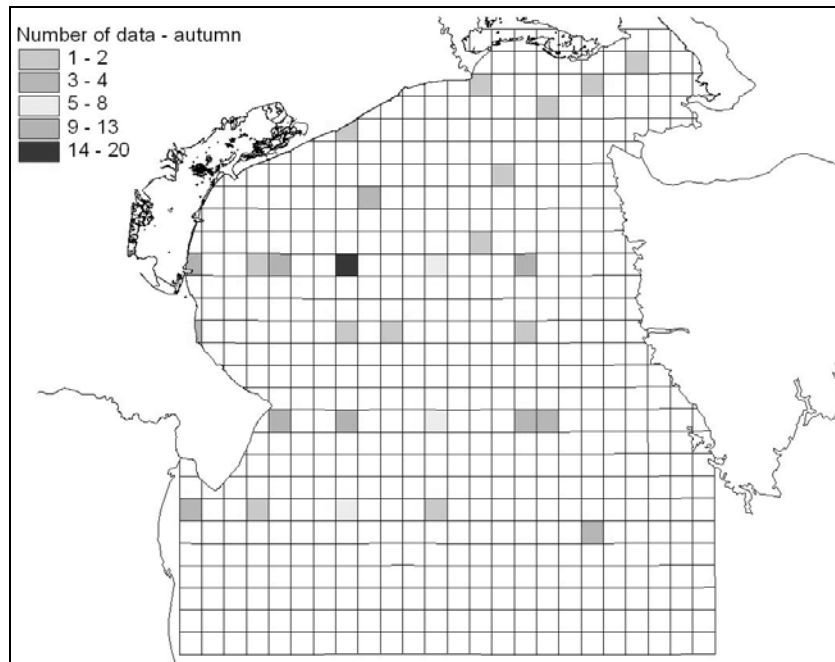
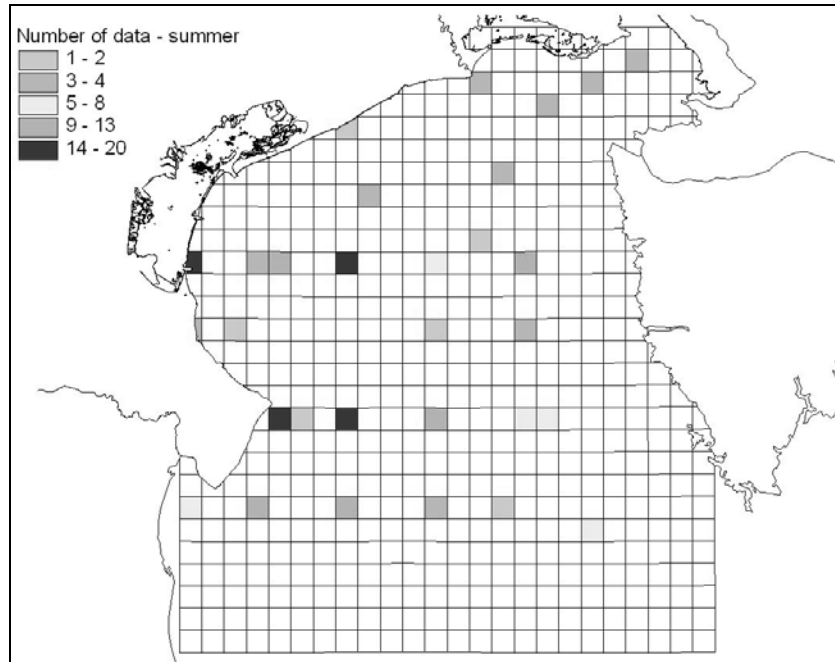
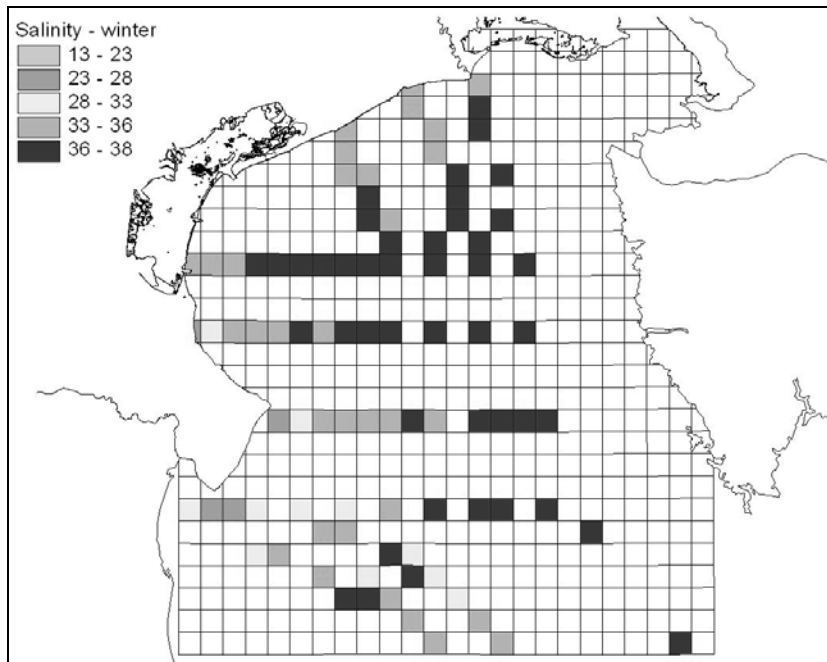


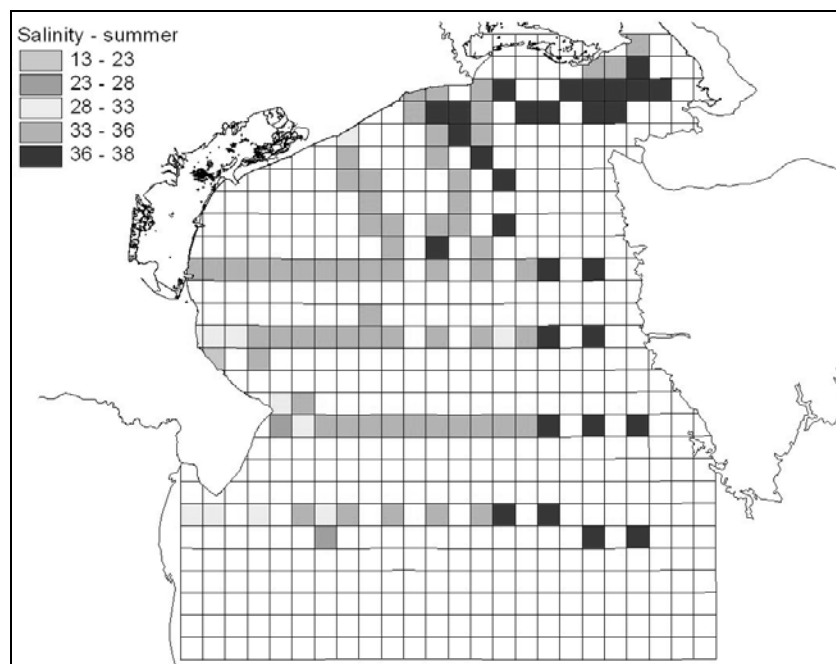
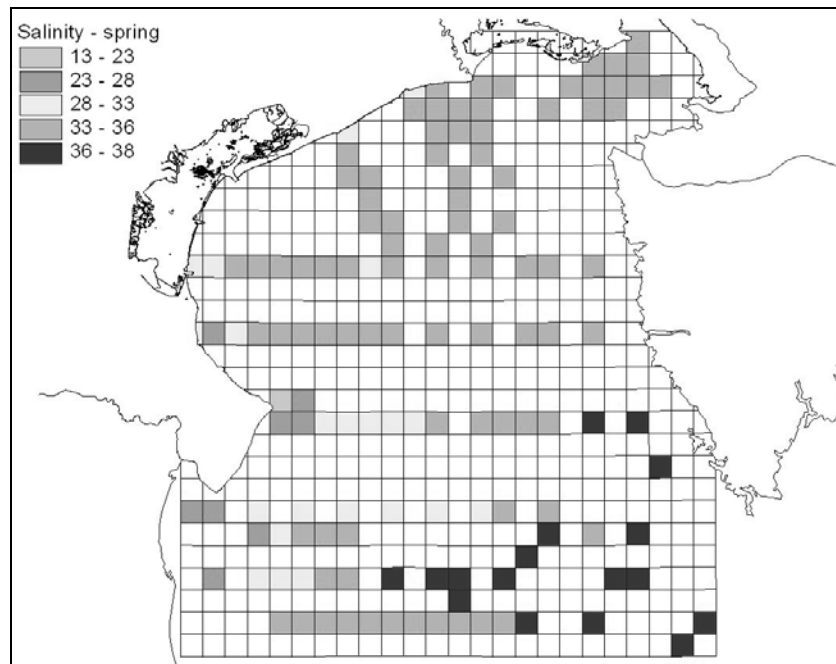
Fig. 7: number of nitrate data in each cell of the grid of 5km grid for the four seasons (winter, spring, summer and fall) of the 1990-2001 data.

4.2 Spatial distribution and seasonal variability

A first representation of spatial distribution of water quality parameters can be obtained by plotting the median of the observations falling within each bin. Examples for seasonal sea surface distribution salinity and nitrate are given in the maps of Fig. 8 and 9 respectively. Cells without data are blanked in the maps. The median was preferred to the mean because it is a more robust statistical index when the distribution of the data is not normal.

Maps of salinity show the presence of a gradient from the coast to off shore mainly due to rivers runoff during all the four seasons. The area in front of Po river presents the most marked gradient, but the signature of other rivers are also recognizable. In fact, low salinity values are visible in the area close to the Isonzo, in the gulf of Trieste, mainly in fall, and in the most coastal cells close to Tagliamento, Livenza and Adige-Brenta rivers.





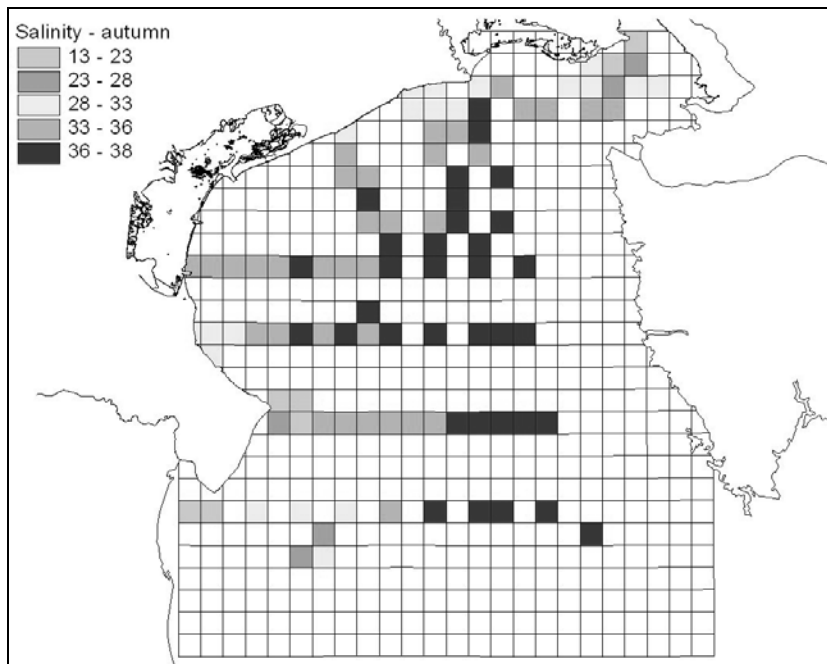
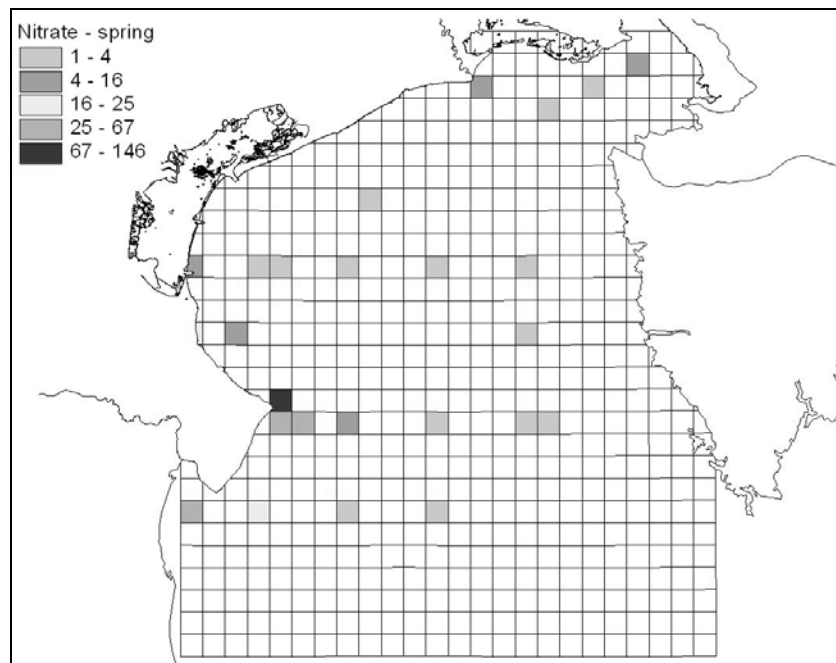
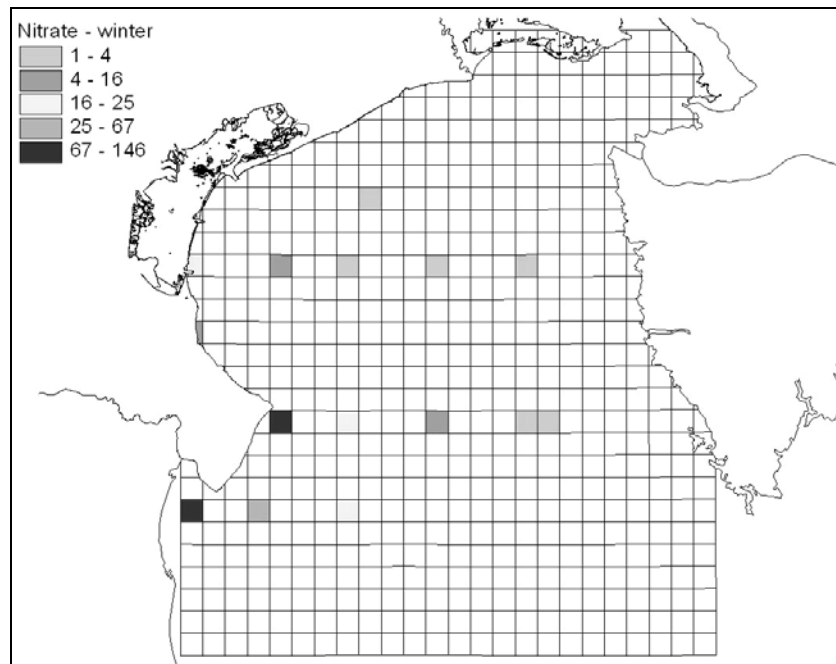


Fig. 8: seasonal sea surface salinity distribution; the value of each cell was calculated as the median of the 1990–2001 data.

The number of bins without data, blanked in the figure, is higher when considering maps of nitrate, fig.9, and therefore spatial patterns of nutrient concentration are harder to identify. Nevertheless, the influence of nutrient input from the Po river (higher concentration) is clearly visible in all the four seasons, and the impact of other rivers can be recognized from season to season: Isonzo on the right end of coastline in the map of fall, the Adige-Brenta at the left of the Venice lagoon during all the season, and the Piave and Livenza at the right of Venice lagoon in the summer and fall maps.



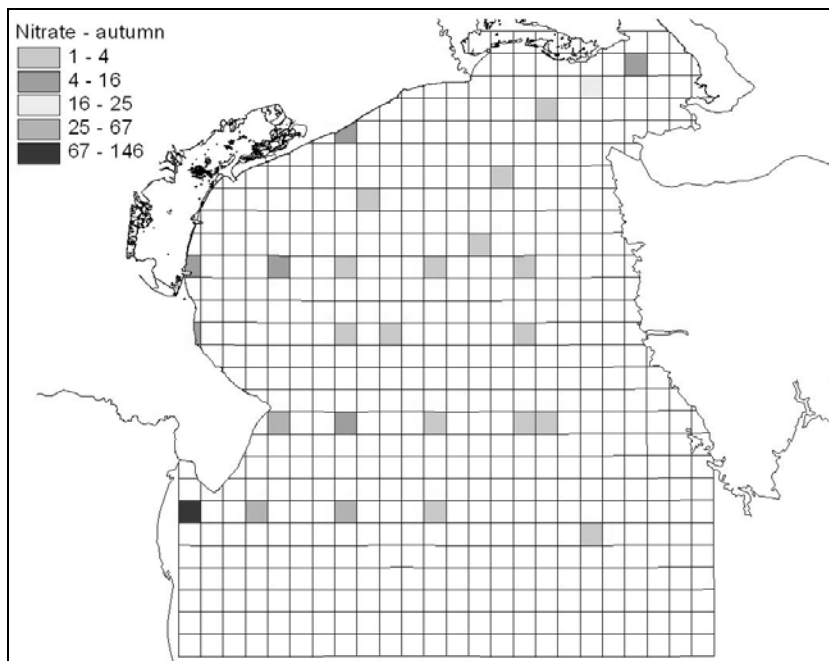
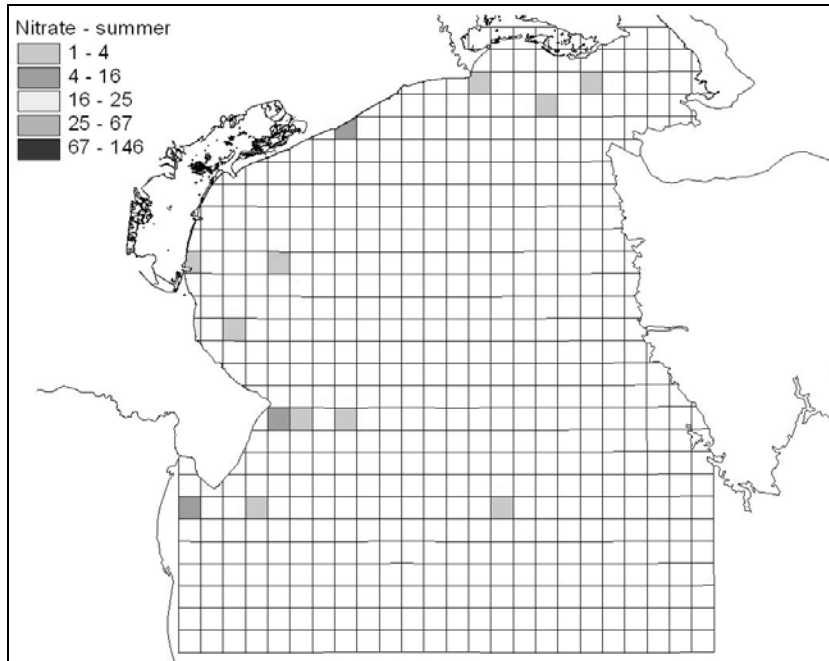


Fig.9: seasonal sea surface nitrate distribution; the value of each cell was calculated as the median of the 1990–2001 data.

Results depicted in fig. 8 and 9 can be used also for assessing scale of spatial variability over the whole basin. In particular, for each of the seasons it is

possible to compute a measure of dispersion, as the ratio between half of interquartile range and the median value of the distribution of bin values.

The comparison among spatial variability in the different seasons is presented in Fig. 10 for 13 variables. The figure puts in evidence that the variability of trophic variables (right panel in the graph, right axis) can be twice as great as the variability of physical variables (left panel, left axis). In particular variability of nutrients and chlorophyll is always higher than 50% and can reach values up to 250%, while the variability of physical parameters, is always less than 10%, with the noticeable exception Secchi disk.

The variability of all the nutrients, except NO₂, is maximum during fall due to the gradients induced by river input, while the highest variability for chlorophyll is observed during spring. This compare well with analysis of monthly Po river runoff in the period 1988-1999 (Russo et al., 2002), which shows that the maximum outflow occurs in October and November. Spatial variability of temperature is instead maximum during winter and spring, when heat flux and intrusion of southern water mass generate the highest spatial gradients

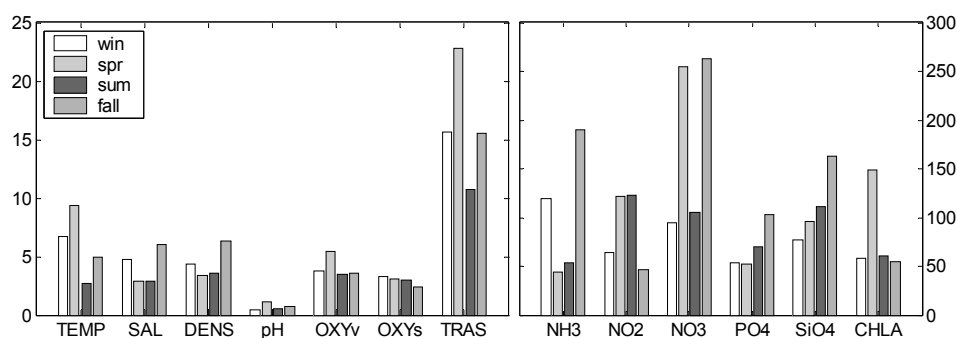


Fig. 10: spatial variability over the whole basin for the four seasons (colored gray bars). The variability index is calculated as the ratio between the half of interquartile range and the median value of the distribution of cell values.

4.3 Spatial interpolation of gridded data

Spatial distribution of median values such as the ones reported in fig. 8 and 9 can be spatially interpolated, in order to provide more intuitive representation of the field. Different geostatistical methodologies are available for this elaboration, including kriging, objective analysis, and gridding techniques.

As an example of possible result, and a first attempt on spatial interpolation of data, we have utilized ordinary kriging in the present application. This is an interpolation procedure that generates an estimated surface from a scattered set of points with z values, basing on the assumption that the spatial variation in the phenomenon represented by the z values is statistically homogeneous throughout the surface; that is, the same pattern of variation can be observed at all locations on the surface (regionalized variable theory). The spatial variation is quantified by the semi-variogram, that is estimated by the sample semi-variogram, in turn computed from the input point data set by fitting a theoretical function. Confidence (error bands) in the interpolation can be quantified.

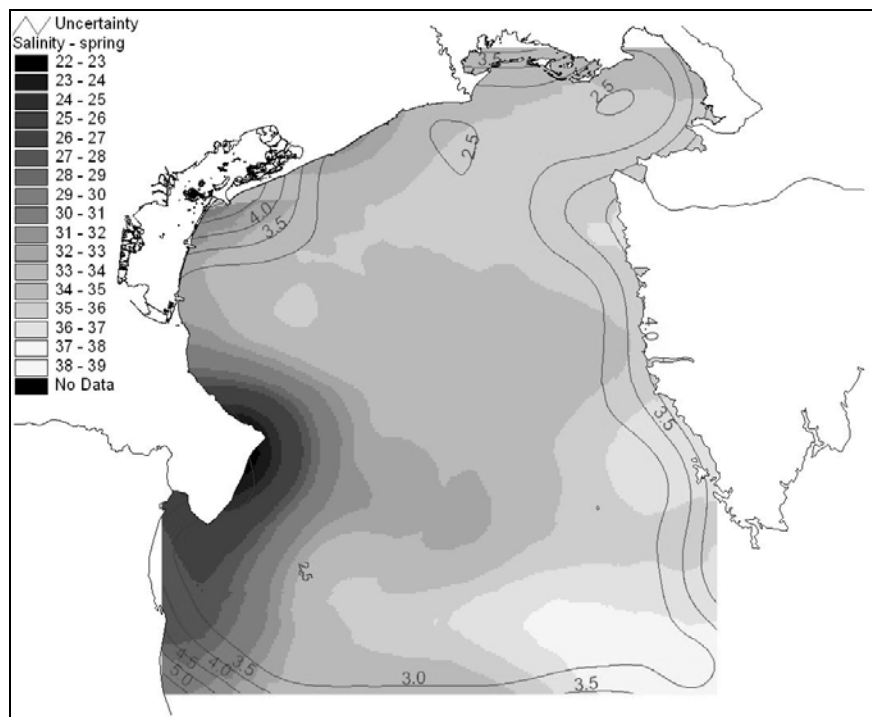
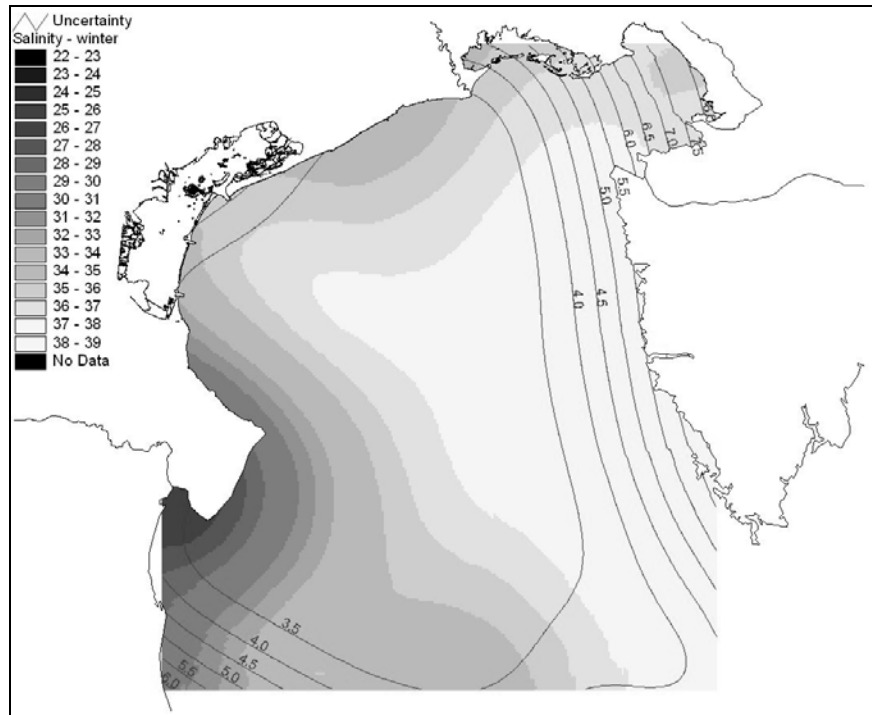
Here we present interpolation performed using ordinary kriging algorithms. The parameter needed in the interpolation were set, after some numerical experiments, as in tables 2.

Parameter	Salinity	nitrate
lag	10km	20 km in winter, 10 km in the other seasons
semi-variance model	Gaussian	exponential
Seach radius	50 km	50 km
Minimum number of data	5	5

Tab. 2: values of kriging parameters for salinity and nitrate.

The figures 11 and 12 show the estimated surfaces of salinity and nitrate seasonal data and the uncertainty associated with the data. The spatial patterns roughly evidenced in the discrete maps of Fig. 9 and 10 are clearly visible in the interpolated ones (figures 11 and 12).

Contours lines superimposed to the property field give a measure of uncertainty. It is easy to see that the estimations of salinity maps is more reliable than that ones of nitrate. In fact, the uncertainty values associated with the salinity data are much lower than the salinity values; whereas the uncertainty values associated with nitrate data often exceed data themselves. This is due to the better coverage of salinity data with respect to that of nitrate data and to the much lower variability range of salinity data compared to that of nitrate data.



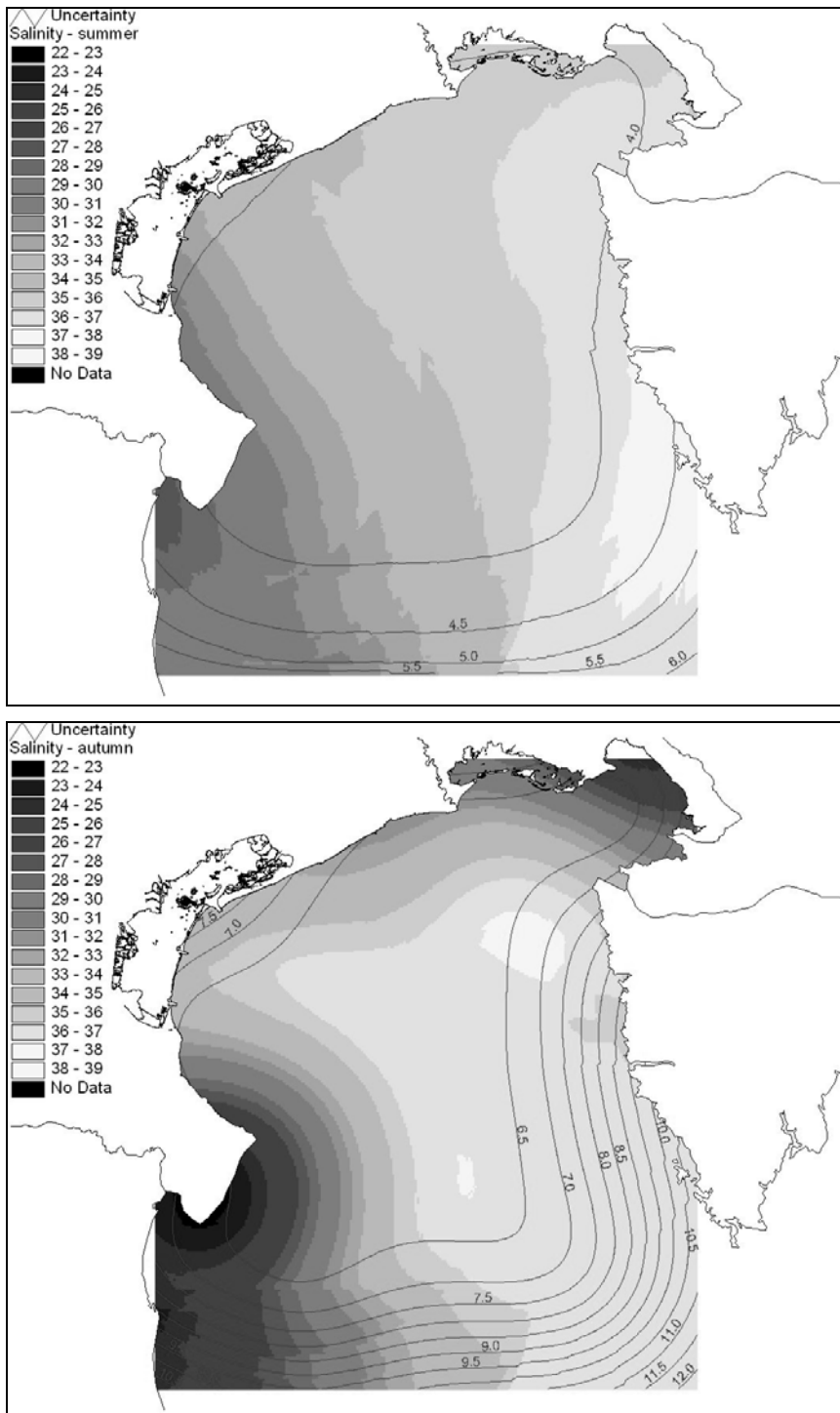
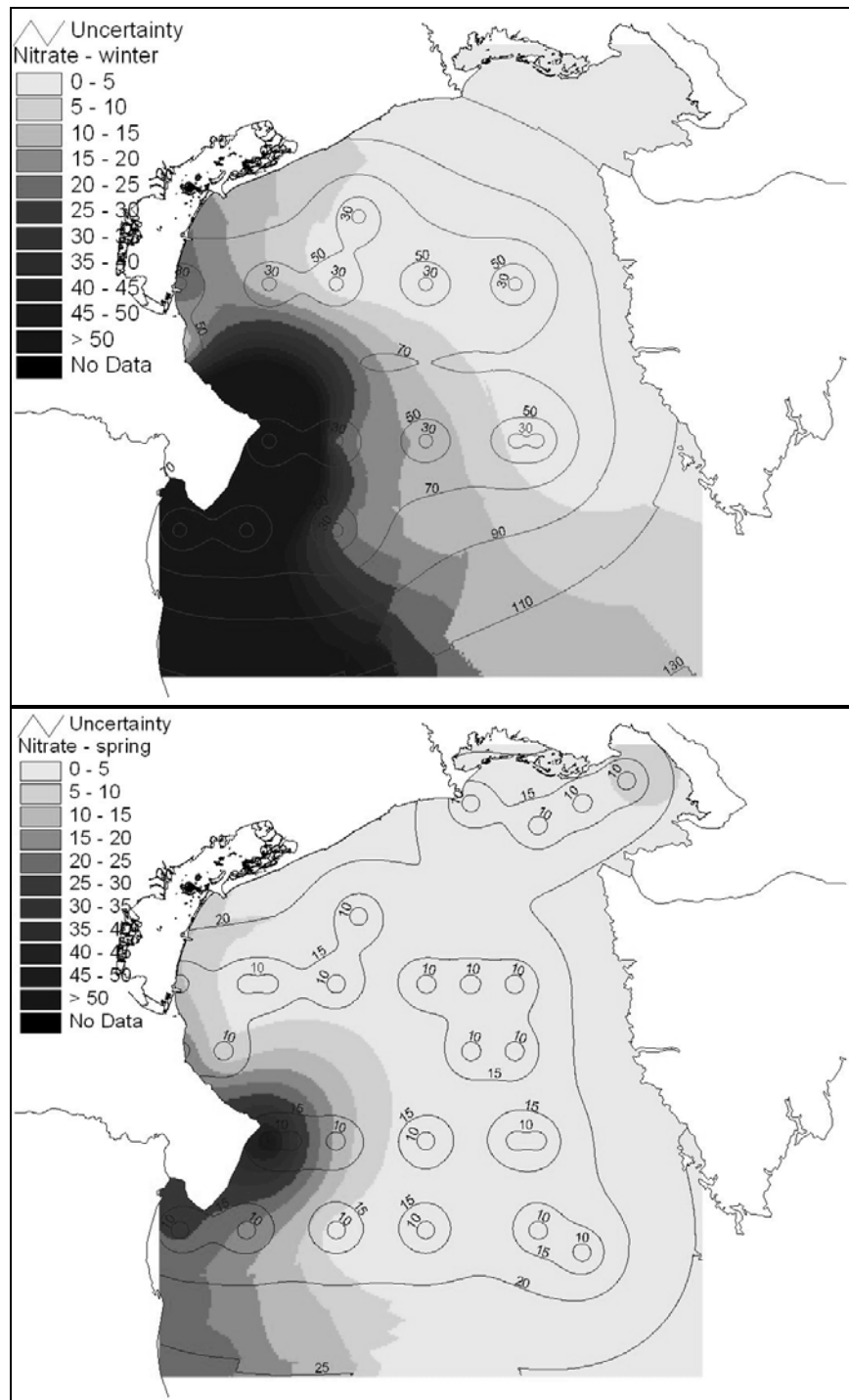


Fig. 11: kriging of the seasonal salinity distribution for 1990-2001 data. The maps report the uncertainty associated to the reconstructed fields, (red line contour).



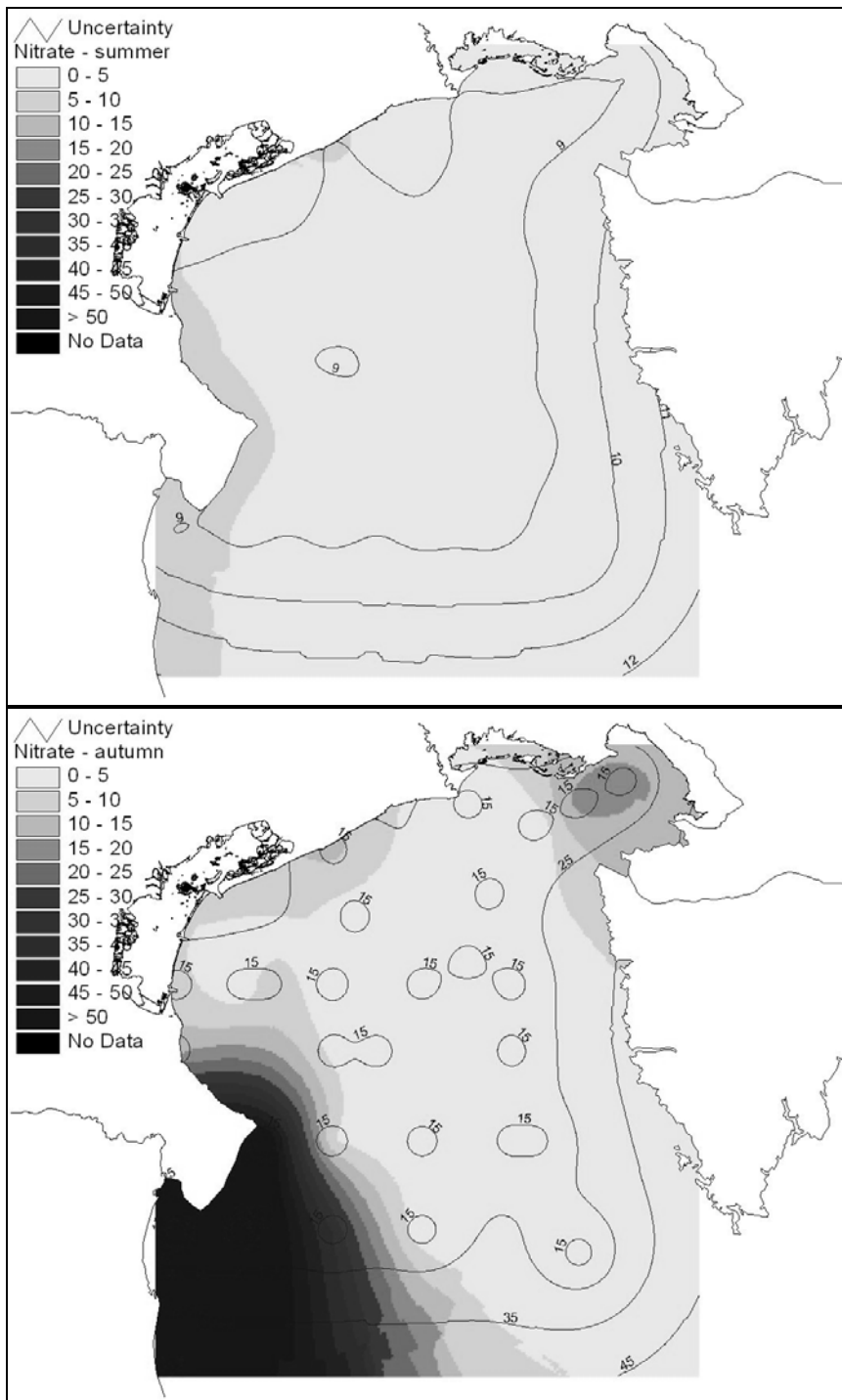


Fig. 12: kriging of the seasonal nitrate distribution for 1990-2001 data. The maps report the uncertainty associated to the reconstructed fields, (blue line contour).

References

Cucco and Umgiesser, 2005 Modelling fluxes among the lagoon of Venice and the Adriatic Sea. *Ecological Modelling.* (in press)

Bellafiore, 2005 . Tesi di laurea Università di Padova

Russo A., Rabitti S., and Bastianini M., 2002. Decadal climatic Anomalies in the Northern Adriatic Sea inferred from a new oceanographic data set. *Marine Ecology*, 23 supplement 1, pp. 340-351.

Artegiani A., Bregant D., Paschini E., Pinardi N., Raicich F., and Russo A., 1997. The Adriatic Sea general circulation. Part I: Air-Sea interaction and water mass structure. *Journal of physical oceanography* 27(8), pp.1492-1514.

RESEARCH LINE 3.14

**Erosion and sedimentation processes in the
Venice lagoon.**

QUANTIFYING SHEAR STRESS DUE TO WIND WAVES AND TIDAL CURRENTS IN THE VENICE LAGOON

Luca Carniello, Andrea Defina, Luigi D'alpaos

*Dip. di Ingegneria Idraulica Marittima Ambientale e Geotecnica, Università di Padova,
Padova*

Riassunto

L'oggetto del presente lavoro è un modello accoppiato in grado di descrivere le onde da vento e la propagazione della marea all'interno di un bacino lagunare. Il modello idrodinamico risolve le equazioni delle onde lunghe in acque basse utilizzando uno schema agli elementi finiti mentre il modello del moto ondoso risolve l'equazione delle conservazione dell'azione d'onda con uno schema ai volumi finiti. Entrambe i modelli lavorano sul medesimo reticolo di calcolo. L'applicazione alla laguna di Venezia, caratterizzata da una batimetria estremamente irregolare con presenza di canali, bassifondi e barene emergenti ha suggerito l'introduzione di ipotesi semplificative per le equazioni che governano i processi descritti. Ciò ha prodotto notevoli vantaggi in termini di efficienza e robustezza dell'algoritmo implementato.

Per verificare il funzionamento del modello proposto sono state condotte simulazioni caratterizzate da diverse forzanti meteorologiche e di marea. I risultati del calcolo presentano un buon accordo con le misure raccolte all'interno della laguna di Venezia. In conclusione sono presentate evidenze relative all'importanza dell'effetto combinato di onde da vento e correnti di marea sul processo di risospensione dei sedimenti.

Abstract

A numerical model that combines wind waves with tidal fluxes in a tidal basin is presented and validated. The model couples a hydrodynamic finite element module based on the shallow water equations with a finite volume module that accounts for the generation and propagation of wind waves. The wave module solves the wave action conservation equation on the same triangular mesh used in the hydrodynamic module, thus efficiently reproducing the physical relationships between waves and tide propagation. The combined wind wave-tidal model is applied to the Venice lagoon. The highly irregular bathymetry of this tidal environment, characterized by deep channels, emergent salt marshes, and extensive tidal flats, suggests the introduction of ad hoc hypotheses that simplify the governing equations with a noteworthy increase in efficiency and robustness of the algorithm.

Simulations of wave fields generated under specific wind conditions are presented and discussed. The model results are compared, with good agreement, to field data collected in different stations inside the lagoon of

Venice. Finally, evidence of the effect of tidal currents and wind waves on sediment resuspension is presented using the results of different simulations.

1 Introduction

Recent studies and field campaigns have shown that the saltmarshes and tidal flats within the Venice lagoon are under erosion with a net sediment loss for the entire tidal basin. The global sediment loss is the result, firstly, of the diversion of the rivers Brenta and Sile brought about by the “Serenissima Repubblica di Venezia” during the seventeenth century to prevent the infilling of the lagoon. Secondly, the lagoon was modified by the construction of large inlet jetties at the end of the nineteen century. These two manmade modifications interfered with the supply of sediments both from the watershed and from the sea. Furthermore, recent studies have demonstrated that the asymmetric flow during a tidal cycle produces an overall loss of sediments through the three inlets [D’Alpaos and Martini, 2003]. This trend is further enhanced by subsidence and sea-level rise.

Because of the above considerations it is clear that a correct description of the in-situ sediment resuspension is very important in understanding and assessing the evolution trend of the Venice lagoon. The tidal currents alone are not able to explain the destruction of salt marshes and the flattening of the lagoon bottom. Tidal currents produce shear stresses large enough to carry sediments into suspension only in the large channels near the three inlets, where velocities are high. On the contrary, sediment resuspension on salt marshes and tidal flats is mainly caused by shear stress induced by wind waves.

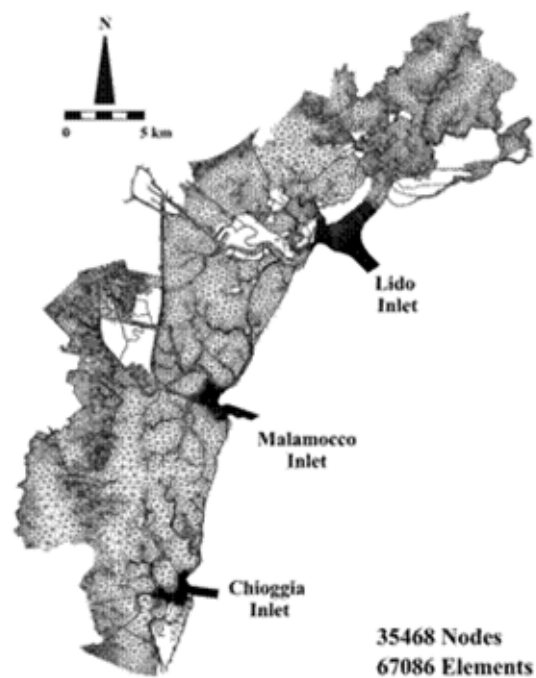


Fig. 1 – Mesh reproducing the lagoon of Venice used in the simulations.

Since shallow tidal basins have a very irregular morphology with large and sudden changes in bottom elevation, islands, and temporarily dry areas, a specific model must be developed to assess wind wave generation and propagation within these involved environments.

Given the irregular bathymetry of the Venice lagoon, and the uncertainties affecting the modeling of non linear wave interactions, a simplified, computationally efficient model, which propagates a monochromatic wave, is here presented.

The model reproduces the wind wave generation and propagation inside the lagoon of Venice by solving the wave action conservation equation on a unstructured triangular mesh of arbitrary shape with a first order finite volume explicit scheme. The wave model is coupled with a hydrodynamic model for tide propagation inside the basin solved with a finite element technique [D'Alpaos and Defina, 1995]. Sharing the two models the same grid (Fig. 1) enables us to correctly account for the interactions between waves and tides since the main physical quantities are shared on the same grid.

The main purpose of our model is to evaluate the significant wave height produced by a given wind field in each element of the domain. Special attention is given to describing all the physical phenomena producing or dissipating energy in the wave field. Wind waves are then combined to tidal currents in order to determine bottom shear stresses and describe sediment resuspension.

Numerical simulations reproducing the wind wave field inside the Venice lagoon under different wind and tidal conditions are presented and the results are compared with recent data collected in two field stations.

Finally, the bottom shear stress is evaluated to assess the effects of tidal currents and wind waves on sediment resuspension in tidal basins.

2 Wind Wave – Tidal Model

The hydrodynamic model solves the two-dimensional shallow water equations modified to deal with flooding and drying processes and very irregular domains. [Defina et. al., 1994; D'Alpaos and Defina, 1995; Defina, 2000].

The averaged equations are:

$$\frac{\partial q_x}{\partial t} + \frac{\partial}{\partial x} \left(\frac{q_x^2}{Y} \right) + \frac{\partial}{\partial y} \left(\frac{q_x q_y}{Y} \right) - \left(\frac{\partial R_{xx}}{\partial x} + \frac{\partial R_{xy}}{\partial y} \right) + \frac{\tau_{bx}}{\rho} - \frac{\tau_{wx}}{\rho} + gY \frac{\partial h}{\partial x} = 0 \quad (1)$$

$$\frac{\partial q_y}{\partial t} + \frac{\partial}{\partial x} \left(\frac{q_x q_y}{Y} \right) + \frac{\partial}{\partial y} \left(\frac{q_y^2}{Y} \right) - \left(\frac{\partial R_{xy}}{\partial x} + \frac{\partial R_{yy}}{\partial y} \right) + \frac{\tau_{by}}{\rho} - \frac{\tau_{wy}}{\rho} + gY \frac{\partial h}{\partial y} = 0 \quad (2)$$

$$\eta \frac{\partial h}{\partial t} + \frac{\partial q_x}{\partial x} + \frac{\partial q_y}{\partial y} = 0 \quad (3)$$

where t denotes time, q_x , q_y are the flow rates per unit width in the x , y (planform) directions respectively, R_{ij} are the Reynolds stresses (i, j denoting

either the x or y co-ordinates), $\tau_{b,curr}=(\tau_{bx}, \tau_{by})$ is the stress at the bottom produced by the tidal current, $\tau_w=(\tau_{wx}, \tau_{wy})$ is the wind shear stress at the free surface, ρ is fluid density, h is the free surface elevation, g is gravity. Y is the equivalent water depth and η is the local fraction of wetted domain.

For the case of a turbulent flow over a rough wall, the bed shear stress can be written as [Defina, 2000]:

$$\frac{\tau_{b,curr}}{\rho Y} = g \left(\frac{|\mathbf{q}|}{K_s^2 H^{10/3}} \right) \mathbf{q} \quad (4)$$

where $\mathbf{q}=(q_x, q_y)$, $|\mathbf{q}| = \sqrt{q_x^2 + q_y^2}$, K_s is the Strickler bed roughness coefficient, and H is an equivalent water.

The wind shear stress at the free surface τ_w , is evaluated as:

$$\tau_w = \rho_a c_d U_{wind}^2 \quad (5)$$

where ρ_a is the air density, c_d is drag coefficient and U_{wind} is wind speed. Moreover, in the present work Reynolds stresses and convective terms are neglected.

At each time step, the hydrodynamic model yields nodal water levels which are used by the wind wave model to assess wave group celerity and bottom influence on wave propagation. Moreover, depth integrated velocity and water depth computed with the hydrodynamic model are used to evaluate the bottom shear stress produced by the combined action of tidal currents and wind waves.

The wind wave model is based on the conservation of the wave action N , which is defined as the ratio of wave energy E to the relative wave frequency σ .

The wave action conservation equation, in the most general spectral formulation is [Hasselmann et al., 1973]:

$$\frac{\partial N}{\partial t} + \frac{\partial}{\partial x} c_{gx} N + \frac{\partial}{\partial y} c_{gy} N + \frac{\partial}{\partial \sigma} c_{\sigma} N + \frac{\partial}{\partial \theta} c_{\theta} N = \frac{S}{\sigma} \quad (6)$$

The first term of (6) represents the local rate of change of action density in time, the second and third terms represent the propagation of wave action in the space (c_{gx} and c_{gy} are the x and y components of the wave group celerity). The fourth term represents shifting of the relative frequency σ due to variation in depth and currents. The fifth term represents depth induced and current induced refraction, θ being the wave direction). The S term on the right-hand side of (6) is the source term which includes wave growth by wind and wave decay by bottom friction, whitecapping, and depth-induced breaking.

Some terms of equation (6) can be neglected on making some justifiable simplifications. Given the relatively poor performance of spectral models in

shallow tidal basins [see *Lin et al.*, 2002], we prefer to utilize a monochromatic wave which allows for a noteworthy reduction of computational effort and to neglect the fourth term in (6). Moreover the model assumes that the direction of wave propagation instantaneously complies to the wind direction. Since the model considers only waves generated within the lagoon the assumption turns out to be feasible. Only a small fraction of wave coming from the Adriatic Sea enters the lagoon through the inlets. This is neglected in the model.

The above hypothesis is supported by the results of a numerical study on the decay of wave energy in the lagoon of Venice. Further evidence supporting the hypothesis can be found in *Lin et al.* [2002], where wind and wave data collected in the Chesapeake Bay show that mean wave direction closely follows the wind direction.

With the above assumption we implicitly neglect refraction. Indeed, it is basically impossible to correctly evaluate wave refraction in a very irregular domain with sharp and frequent discontinuities of the bottom, when using a comparably coarse grid.

Finally it is important to note that the wave action conservation equation cannot reproduce diffraction. Because diffraction affects wave field in a region of 1~2 wavelengths in size behind an obstacle, and because the wave length inside the lagoon of Venice is far smaller than the grid size, diffraction can be neglected.

The term S on the right hand side of equation (6) describes all the external physical phenomena contributing to wave energy. They can be either positive e.g. wind energy input, or negative e.g. bottom friction, whitecapping, and depth induced breaking. Details can be found in [*Carniello et al.*,2005]

3 Results and discussion

The hydrodynamic model was described and validated elsewhere [Defina et. al., 1994; D'Alpaos & Defina, 1995; Defina, 2000]. Some additional model validation focusing on the importance of the wind action on the free surface displacement can be found in [*Carniello et al.*,2005].

Recent measurements of wind speed and direction and wave heights are provided by the Ministero delle Infrastrutture e dei Trasporti—Magistrato alle Acque di Venezia through Consorzio Venezia Nuova. These field measurements were taken at two different stations: the first (1BF) is on a shoal in the northern part of the lagoon (San Felice marsh) and the second (2BF) is in a deeper area in the southern part of the lagoon (Fondo dei Sette Morti). Available data at these stations consists of contemporaneous significant wave height and averaged wind speed and direction. In addition, the water level at the stations is given.

To give a complete validation of the whole model and to asses the importance of a hydrodynamic model working together with the wind wave model here we present the results of a simulation forcing the model simultaneously with real

hydrodynamic boundary conditions at the three inlets and assuming a real wind field blowing on the lagoon. The period of time reproduced by the model is 16-17 February 2003, characterized by wind blowing more or less from 60°N with a velocity in the range between 10 to 12 m/s. To define the wind field forcing the model, data collected at 2BF station are used being this station more or less in the middle of the lagoon.

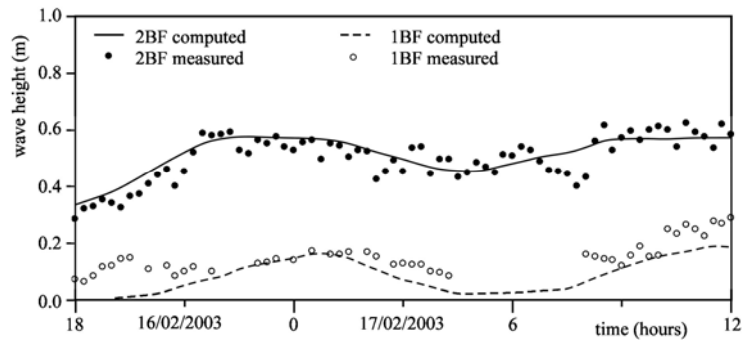


Fig. 2 – comparison of the measured (circles) and computed (solid lines) wave height at 1BF (dashed line and white circles) and 2BF (solid line and black circles) stations during 16-17 2003

Fig.2 reproduces a diagram comparing the significant wave height measured at 1BF and 2BF station with the wave height evaluated by the model. The agreement is quite good. Looking at the results it is evident a sinusoidal like variation of the significant wave height following the tidal oscillation. This confirm the importance to know exactly the water level to correctly evaluate the wave height.

4 Wind Waves effect on sediment resuspension

In the model we evaluate the bottom shear stress indicating the resuspension capacity of tidal currents and wind waves during different simulations, focusing on resuspension capacity without going into detail on suspended sediment concentration.

There are two contributions to the production of a bottom shear stress. To evaluate the tidal current contribution ($\tau_{b,curr}$) we use the current speed value from the hydrodynamic model and equation(4). For the waves contribution ($\tau_{b,wave}$) we use the expression:

$$\tau_{b,wave} = \frac{1}{2} f_w \rho_w u_m^2 \quad (7)$$

Here u_m is the maximum horizontal orbital velocity associated with the wave propagation and f_w is the wave friction factor [Soulsby.,1997].

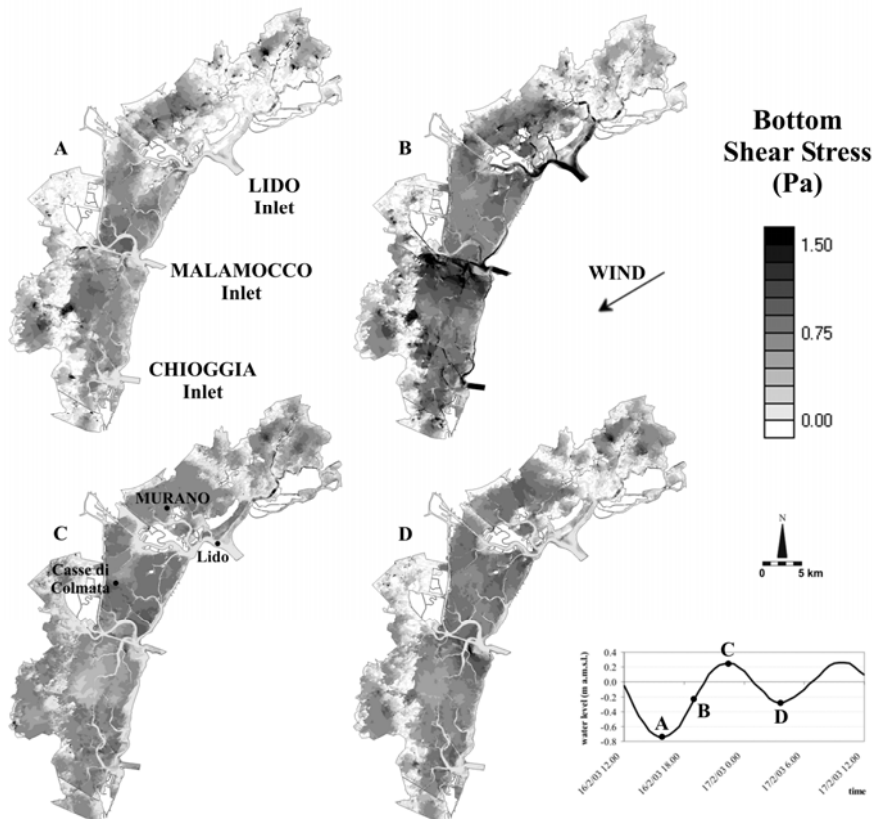


Fig. 3 – 16-17 February 2003: bottom shear stress spatial distribution evaluated by the model inside the Venice lagoon during tide propagation. A very low tide slack water condition (A), a high tidal current flow condition (B), a high tide slack water condition (C) and a second low tide slack water condition (D) are reproduced.

Actual bed shear stress under the combined action of waves and currents is enhanced beyond the sum of the two contributions. This occurs because of the non-linear interaction between the wave and current boundary layers. In the present model the empirical formulation suggested by *Soulsby*, [1997] is adopted.

Fig. 3 shows the spatial distribution of bottom shear stress computed with the model inside the lagoon of Venice at four different times during 16-17 February 2003. The plot in the figure shows the tidal level at the Lido inlet. The wind field above the lagoon is characterized by a 10~12 m/s wind blowing from approximately 60 °N. High shear stress values are recognizable in the large channels departing from the three inlets only during ebb and flood (Fig. 3B) while it is completely absent during times of high water slack and low water slack. Besides shear stress intensity and spatial distribution is extremely sensitive to water level inside the lagoon.

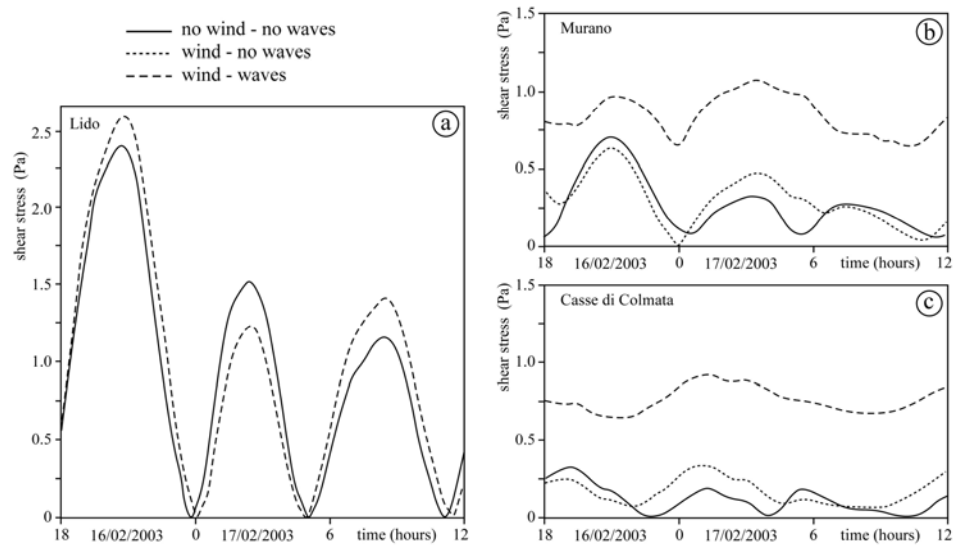


Fig. 4 – 16-17February 2003: comparison of the shear stress at the bottom produced by the combined effect of wind waves and tidal current (black circles), the tidal currents alone (grey circles) and the tidal currents neglecting the wind shear stress at the free surface (white circles). The comparison refers respectively to the Lido Inlet (a), a tidal flat close the Murano Island (b) and a tidal flat close the “Casse di Colmata” (c).

Fig. 4 shows the time evolution of the bottom shear stress at three different sites within the lagoon. Sites were chosen respectively inside a big channel close the Lido inlet (Fig. 4a), on a tidal flat close to the Murano island (Fig. 4b), and on a tidal flat next to the Casse di Colmata (Fig. 4c). Location of these sites are shown in Fig. 3C. Each plot compares model results obtained with three different simulations, i.e. a) after switching off wind wave module and neglecting wind shear stress; b) same as a) but accounting for wind shear stress; c) same as b) but after switching on the wind wave module. Fig. 4a, shows the same behavior for shear stress computed in the second and third simulations confirming that inside deep channels wind waves negligibly affects bottom shear stress. Some difference can be observed when comparing results obtained including and neglecting the wind shear stress on the free surface. This result confirm the importance of this process on the lagoon hydrodynamics. The latter conclusion is supported also by results obtained at Murano (Fig. 4b) and Casse di Colmata (Fig. 4c). In these sites, however, bottom shear stress is strongly enhanced when wind waves are accounted for in the model.

Considering a critical value for sediment erosion inside the lagoon of Venice ($\tau_{cr} \cong 0.7$ Pa according to *Amos et al.* [2004]) it is worth noting that in the presence of wave effects bottom shear stress exceed τ_{cr} . On the contrary the stress remains always smaller than the critical value when wind waves are excluded from the model.

5 Conclusions

A model describing the generation and propagation of wind waves inside a tidal basin is presented which solves the wave action conservation equation using a finite volume scheme. The wave model is coupled with a hydrodynamic model that uses the same domain discretization, thus optimizing the transfer of data between the tidal and the wave components.

The wind wave model is validated with wave measurements taken within the lagoon of Venice, Italy. Even though the physical processes described by the model are very complex and the model is comparably simple, a good agreement between the model results and the field data is found. The influence on the wave field of time changing water levels is assessed and confirms the importance to have a hydrodynamic model working together with the wind wave model.

The complementary effect of tidal currents and wind waves on bed shear stress is shown. The importance of including wind waves effects to model sediment resuspension on tidal flats and salt marshes is demonstrated as well.

References

- Amos, C.L., A. Bergamasco, G. Umgiesser, S. Cappucci, D. Cloutier, L. DeNat, M. Flindt, M. Bonardi, and S. Cristante (2004), The stability of tidal flats in Venice Lagoon – the results of in-situ measurements using two benthic, annular flumes, *Journal of Marine Systems*, 51, 211-241.
- Carniello, L., A. Defina, S. Fagherazzi and L. D'Alpaos (2005), A combined Wind Wave-Tidal Model for the Venice Lagoon, Italy. *Journal of Geophysical Research – Earth Surface*, in press.
- D'Alpaos, L. and A. Defina (1995), Modellazione matematica del comportamento idrodinamico di zone a barena solcate da una rete di canali minori, *Estratto da Rapporti e Studi, Ist. Veneto di Scienze, Lettere ed Arti*.
- D'Alpaos, L. and P. Martini (2003), The influence of inlet configuration on sediment loss in the Venice Lagoon, *Proc. of Flooding and Environmental Challenges for Venice and its Lagoon: State of Knowledge 2003, Cambridge*.
- Defina, A., L. D'Alpaos, and B. Matticchio (1994), A new set of equations for very shallow water and partially dry areas suitable to 2D numerical models, in *Proceedings of the Specialty Conference on "Modelling of Flood Propagation Over Initially Dry Areas", Milan (Italy) 29 June -1 July 1994, edited by P. Molinaro and L. Natale, 72-81*.
- Defina, A. (2000), Two-dimensional shallow water equations for partially dry areas, *Water Resour. Res.*, 36, 3251-3264.
- Hasselmann, K., T.P. Barnett, E. Bouws, H. Carlson, D.E. Cartwright, K. Enke, J.A. Ewing, H. Giennapp, D.E. Hasselmann, P. Kruseman, A. Meersburg, P. Muller, D.J. Olbers, K. Richter, W. Sell, and H. Walden (1973), Measurements

of wind-wave growth and swell decay during the Joint North Sea Wave Project (JONSWAP), *Dtsch. Hydrogr. Zeit. Suppl.*, 12(A8), 1-95.

Lin, W., L.P. Sanford, B.J. and S.E. Suttles (2002), Wave measurements and modeling in Chesapeake Bay, *Continental Shelf Research*, 22, 2673-2686.

Soulsby, R.L., (1997), Dynamics of marine sands. A manual for practical applications. Thomas Telford Ed. 248 pp.

SEDIMENT TRANSPORT MODEL APPLICATION TO LIDO INLET AND TREPORTI CANAL

Francesca De Pascalis¹, Georg Umgiesser^{1*}, Christian Ferrarin¹, And CARL L. AMOS²

1. Institute of Marine Science, ISMAR-CNR, S. Polo 1364, 30125 Venezia, Italy.,

2. Southampton Oceanography Centre, SOC, Empress Dock, Southampton, Hampshire, UK.

Riassunto

In questo lavoro si è tentato di approfondire la conoscenza dei meccanismi di trasporto dei sedimenti nella laguna di Venezia, attraverso l'utilizzo di tre modelli accoppiati: il modello idrodinamico SHYFEM, il modello di trasporto SEDTRANS e un modello empirico d'onda. La zona indagata è stata quella della bocca di Lido e del canale di Treporti.

Lo scopo del lavoro è stato quello di studiare il movimento delle sabbie di diverse granulometrie applicando un modello a box. I criteri di suddivisione dei box sono stati scelti in base alla morfologia e alla batimetria della zona.

La griglia di calcolo, utilizzata dal modello idrodinamico, è stata modificata per avere una maggiore risoluzione spaziale nelle zone di basso fondale. Inoltre è stata inserita nel modello una nuova batimetria e sono state aggiunte le sezioni sulla bocca di Lido.

Le simulazioni sono state effettuate utilizzando i dati reali di un anno tipo per la laguna di Venezia (il 1987). Oltre al trasporto è stato successivamente effettuato un bilancio di sedimenti per avere una stima di erosione e deposizione.

I risultati rivelano che nel canale di Treporti i sedimenti vengono prevalentemente trasportati verso il mare. La bocca di Lido presenta invece un comportamento particolare in quanto il canale di S. Nicolò e quello di Treporti sembrano avere dinamiche differenti a causa dei riflussi che si hanno nella zona di bocca. Qui il trasporto è diretto verso il mare sul lato di Punta Sabbioni mentre è contrario sul lato di S. Nicolò.

Abstract

The aim of this work was to study in depth the sediment transport dynamics in Venice Lagoon, using three models. Finite element hydrodynamic model (SHYFEM), an empirical wave model and sediment transport model (SEDTRANS). The investigated area was northern lagoon, in particular, Treporti canal and Lido inlet.

A type of linked box model was created by combining main model's elements and subsequently computing water and sediment fluxes for the so-created boxes. Several grain size classes were simulated.

The computing grid, used by hydrodynamic model, has been modified to have more spatial resolution on the studied area. Moreover a new section and bathymetry have been inserted.

The total transport through all sections was computed for one year. Sediment mass balance was determined and the resulting trends of erosion and deposition were computed. The year of reference is 1987, where forcing data exists.

The results reveal that into Treporti canal the sediment transport is directed to Adriatic Sea. At Lido inlet two different behaviors have been found for two inlet sides. In southern side (S. Nicolò) the transport is directed towards lagoon, instead in northern side is seaward directed.

1 Introduction

The Venice lagoon is an extremely complex ecosystem. In this environment the sand transport has an important role for the morphological transformations.

The coastal lagoon development is closely connected to the barrier islands system formation due to the long-shore currents. The sandy sediment is transported along the seacoast to form a shore spits that are transformed into barrier islands.

The type of coastal setting and its morphological manifestation is governed by the relative proportions of sand to mud (EMPHASYS Report 2000). When mud dominates, then fringing tidal flats and wetlands dominate the coastal landscape and barrier islands are largely absent; when sand dominates, then beaches, barriers and lagoons dominate. The fact that Venice is located within a lagoon immediately illustrates the dominating role of sand in the evolution of this coastal setting.

Submerged beaches form a significant part of the margins to the canal system. These beaches attenuate wave motion and thus protect the marshes from erosion. The beaches are composed of fine sand in dynamic equilibrium with the passage of waves, and also host colonies of *Cymadocea* that attenuate wave energy. The origin of the fine sand is unknown, but is thought to come from reworking of the canal bed and perhaps from the Lido entrance.

This work aims to give a contribution to these questions. Here a sediment transport model has been applied, together with an hydrodynamic model and a wave model to study the sand transport in one of the major canals in the lagoon, close to the northernmost inlet. The model has been set up as a box model, and the net transport of the sandy material and the mass balance has been determined.

2 Modeling

Three numerical models have been applied to the Treporti canal and Lido inlet in order to study the sand behavior in this area. The models used were the hydrodynamic model SHYFEM, an empirical wave model and the sediment

transport model SEDTRANS96.

2.1 Hydrodynamic model (SHYFEM)

The hydrodynamic data used in the simulations with the sediment transport model have been derived from the numerical model SHYFEM, developed at ISMAR-CNR of Venice. SHYFEM is a finite element program that can be used to resolve the hydrodynamic equations in shallow water. The program uses finite elements for the spatial resolution of the equations and an effective semi-implicit time resolution algorithm, which makes this program especially suitable for the application to complicate geometry and bathymetry.

The subdivision of the system in triangles, varying in form and size, allows the simulation of shallow water flats, tidal marches that in tidal cycle may be covered with water during high tide and then fall dry during ebb tide.

The equations used in the model are the well known vertically integrated shallow water equations in their formulation with water levels and transports:

$$\frac{\partial U}{\partial t} - fV + gH \frac{\partial \zeta}{\partial x} + RU + X = 0 \quad (1)$$

$$\frac{\partial V}{\partial t} + fU + gH \frac{\partial \zeta}{\partial y} + RV + Y = 0 \quad (2)$$

$$\frac{\partial \zeta}{\partial t} + \frac{\partial U}{\partial x} + \frac{\partial V}{\partial y} = 0 \quad (3)$$

where ζ is the water level, u , v the velocities in x and y directions, U , V the vertical integrated velocities

$$U = \int_{-h}^{\zeta} u dz, \quad V = \int_{-h}^{\zeta} v dz \quad (4)$$

g the gravitational acceleration, $H = h + \zeta$ the total water depth, h the undisturbed water depth, t the time and R the friction coefficient. The terms X , Y contain all other terms that may be treated explicitly by the semi-implicit algorithm like the wind stress or the non-linear terms. (Umgiesser, 2004).

The grid of the Venice lagoon model is constructed by a subdivision of the area into 4000 nodes and almost 8000 triangular elements to describe the lagoon's geometry and bathymetry. Thanks to the flexible size of the elements it is possible to have a higher spatial resolution for the three inlets and the small canals.

2.2 The wave model

Resuspension of sediments due to wind-generated waves is an important source of sediment to the water column. The wave sub-model utilizes empirical formulations which provide approximate estimates of significant wave height and period. This model does not take into account refraction, dispersion or wave breaking effects.

The formulation of the significant wave height (H_{m0}) and period (T_p) is based on the well know empirical prediction equations for shallow water (U.S. Army Engineer Waterways Experiment Station, 1984):

$$\frac{gH_{m0}}{U_A^2} = 0.283 \tanh \left[0.530 \left(\frac{gh_a}{U_A^2} \right)^{3/4} \right] \tanh \left[\frac{0.00565 \left(\frac{gX}{U_A^2} \right)^{1/2}}{\tanh \left[0.530 \left(\frac{gh_a}{U_A^2} \right)^{3/4} \right]} \right] \quad (5)$$

$$\frac{gT_p}{U_A} = 7.54 \tanh \left[0.833 \left(\frac{gh_a}{U_A^2} \right)^{3/8} \right] \tanh \left[\frac{0.0379 \left(\frac{gX}{U_A^2} \right)^{1/3}}{\tanh \left[0.833 \left(\frac{gh_a}{U_A^2} \right)^{3/8} \right]} \right] \quad (6)$$

where U_A is the wind speed [m/s], g is the gravity [m_2/s], h_a is the averaged water depth along the fetch and X is the wind fetch [m]. h_a is the weighted average of the element water depth along the fetch using the each element part of the fetch distance as the weights. Using the averaged water depth along the fetch it could appear that the calculated wave height is higher than the real depth. To avoid this overestimation the wave height has been limited to the breaking wave height $H_{br} = 0.78h$ with h the element depth.

This empirical formulation assumes that the wind blows with essentially constant direction, over a fetch for sufficient time to achieve steady-state fetch limited values.

2.3 Transport model (SEDTRANS96)

The processes of sediment erosion, transport and deposition essentially occurs in the bottom boundary layer which forms the interface between the seabed and the water column. These processes greatly affect seabed stability, the dispersal of particulate material and benthic communities.

SEDTRANS96 is a two-dimensional computer model that can be used to predict the transport rate and direction of sand or mud under either steady currents or combined waves and currents outside the breaking zone. SEDTRANS96 adopts the Grant and Madsen (1986) continental shelf bottom boundary layer theory (GM86 hereafter) to predict bed shear stresses and the velocity profile in the bottom boundary layer. The model uses the algorithms of Einstein-Brown (Brown, 1950) and Yalin (1963) for bedload prediction. The methods of Engelund and Hansen (1967) and Bagnold (1963) are used to determine total load transport (bedload plus suspended load). At the present, SEDTRANS96 uses the median grain size of bottom sediment in its calculations and does not deal with the effect of grain size distribution. The prediction of cohesive sediment transport adopts a new algorithm proposed by Li and Amos (1997).

(Li, & Amos, 2001)

2.4 Calculation of critical shear stresses

As bed shear stress increases, sediment particles will first be entrained from their inert positions and then go through three distinctive modes of transport, bedload, suspension and sheet-flow transport. In this work the sheeflow effect has not been considered. From bottom conditions the critical shear stresses and critical shear velocity are computed for every transport mode.

BEDLOAD TRANSPORT:

$$\tau_{cr} = \mathcal{G}_{cr} (\rho_s - \rho) g D \quad [\text{Pa}] \quad (7)$$

The Yalin's metod according to Miller et al. (1977) has been used to obtain the dimensionless critical Shields parameter \mathcal{G}_{cr} :

$$\log \mathcal{G}_{cr} = 0.041 (\log Y)^2 - 0.356 \log Y - 0.997 \quad Y < 100 \quad (9)$$

$$\log \mathcal{G}_{cr} = 0.132 \log Y - 1.804 \quad 100 < Y < 3000 \quad (10)$$

$$\mathcal{G}_{cr} = 0.045 \quad (11)$$

$$u_{cr}^* = \sqrt{\frac{\tau_{cr}}{\rho}} \quad [\text{m s}^{-1}] \quad (12)$$

where τ_{cr} the critical shear stress, u_{cr}^* is the critical shear velocity, \mathcal{G}_{cr} is the Shields parameter, Y is the Yalin parameter that is defined as

$$\left[(\rho_s - \rho) g D^3 / \rho \nu^2 \right]^{0.5},$$

ρ is the fluid density, ρ_s is the sediment density, g is the gravity acceleration, D is the (median) grain diameter, and ν is the Kinematic fluid viscosity

SUSPENSION TRANSPORT:

in this case the settling velocity W_s (Gibbs et al., 1971) of a sediment grain of diameter D is first calculated:

$$W_s = \frac{\left\{ -3\mu + \left[9\mu^2 + (gD^2/4)\rho(\rho_s - \rho)(0.0155 + 0.0992D) \right]^{0.5} \right\}}{[\rho(0.0116 + 0.0744D)]} \quad [\text{m s}^{-1}] \quad (13)$$

where μ is the dynamic viscosity of the transporting fluid.

The critical shear stress τ_{crs} is than computed from Bagnold (1966):

$$\tau_{crs} = 0.64 \rho W_s^2 \quad [\text{kg m}^{-1} \text{s}^{-2}] \quad (14)$$

$$u_{crs}^* = 0.8W_s \quad [\text{m s}^{-1}] \quad (15)$$

These critical values are compared with the bottom stress value produced by flow conditions in order to determine the start and duration of three transport modes. After that SEDTRANS96 computes transport rates only when the bottom stress goes past one of the critical values.

2.5 Calculation of flow conditions in the boundary layer

Through the bottom boundary layer theory of waves and currents the model computes the velocity profile and the bottom stress. The model uses the Grant & Madsen method (1986) to estimate the friction factor and the combined-flow stress. This method determines first the bottom boundary layer velocity profile and than the shear velocity is calculated in this way:

$$u_{cw}^* = u_w^* C_r^{0.5} \quad [\text{m s}^{-1}] \quad (16)$$

where C_r is the relative strength ratio of wave to current, estimated through:

$$C_r = \left[1 + 2 \left(\frac{u_c^*}{u_w^*} \right)^2 \cos \phi_b + \left(\frac{u_c^*}{u_w^*} \right)^4 \right]^{0.5} \quad (17)$$

ϕ_b is the angle between wave and current in the boundary layer. The wave shear velocity u_w^* is obtained by:

$$u_w^* = (C_r f_{cw} u_b^2 / 2)^{0.5} \quad [\text{m s}^{-1}] \quad (18)$$

The friction factor f_{cw} can than be obtained by iteration from:

$$\frac{1}{(4f_{cw}^{0.5})} + \log \left[\frac{1}{(4f_{cw}^{0.5})} \right] = \log \left(\frac{C_r u_b}{\omega z_0} \right) + 0.14(4f_{cw}^{0.5}) - 1.65 \quad (19)$$

where $z_0 = \frac{k_b}{30}$ is the bottom roughness.

The procedure described above is repeated three times, using different roughness heights, to obtain various friction factors and shear velocity.

- At the first step SEDTRANS96 uses the grain roughness height $k_g = 2.5D$ to estimate the friction factor and skin-friction velocities (u_{cs}^* , u_{ws}^* , u_{cws}^*);
- At the second step the sum of predicted bedload roughness height and the grain roughness height is used to obtain bedload friction factor and bedload shear velocities (u_{cb}^* , u_{ws}^* , u_{cwb}^*);
- At the third step the model derives the ripple roughness height $k_r = 27.7 \eta (\eta / \lambda)$ which is added to the grain roughness height and bedload roughness height to give the total roughness height. Through this value the model computes the total friction

factor and total bed shear velocities (u_c^* , u_w^* , u_{cw}^*).

2.6 Duration of transport

SEDTRANS96 calculates the time during a wave cycle when the respective threshold criteria are exceeded. A vectorial sum is used to obtain the instantaneous combined shear stress τ_{cws} from:

$$\tau_{cws}(t)^2 = [\tau_{ws} \cos(\omega t) + \tau_{cs} \cos(\phi_b)]^2 + [\tau_{cs} \sin(\phi_b)]^2 \quad (20)$$

where ϕ_b is the angle between τ_{cs} and τ_{ws} . The duration of bedload transport t_b is obtained by solving the following equation:

$$[\tau_{ws} \cos(\omega t_b) + \tau_{cs} \cos(\phi_b)]^2 + [\tau_{cs} \sin(\phi_b)]^2 \geq \tau_{crb}^2 \quad (21)$$

The same procedures are repeated using τ_{crs} to derive the time for suspended load transport.

2.7 Sediment transport

The model calculates sediment transport only if the flow velocity at the seabed exceeds one of the critical values. The instantaneous sediment transport is integrated though a wave cycle to obtain the time-averaged net sediment transport rate. Five transport algorithms are available in SEDTRANS96 (Engelund-Hansen total load equation, Einstein-Brown bedload equation, Bagnold total load equation, Yalin bedload equation, cohesive sediment transport). In this work, the Engelund-Hansen algorithm is used. The original Engelund-Hansen equation was based on unidirectional flume experiment data and was derived for dune-covered beds with mean grain size larger than 150 μm . This equation modified for continental shelf conditions reads:

$$q = 0.05 u_{100}^2 \rho^2 u_*^3 / D(\Delta\rho g) \quad [\text{m}^2 \text{s}^{-1}] \quad (22)$$

Where q is the volume rate of sediment transport per unit width of bed, $\Delta\rho = (\rho_s - \rho)$ and u_* is a general form skin-friction shear velocity.

2.8 Application of models

Three models have been applied not only to Treporti canal (Umgiesser, et al. 2005) but also to whole Lido inlet, in order to compute the hydrodynamic data necessary for transport simulations. First step was to modify the existing grid of the finite element model. The old grid has an inadequate spatial resolution therefore elements' number has been increased on the whole study area. The old bathymetry (1962) of Lido inlet has been replaced with new depth data of 1970 and 1990. The new data of 1990 is available until sections 3, 4, the sections 5, 6, 8 are based on 1970 depth data.

The second step was to choose a new section for the Lido inlet and S. Nicolò canal. In preceding work (Umgiesser, et al. 2005) used sections were only from

1 to 8. Seven sections have been added (9-15) in order to understand sediments' behaviour into whole inlet. From this division resulted 7 boxes. (Fig. 1)

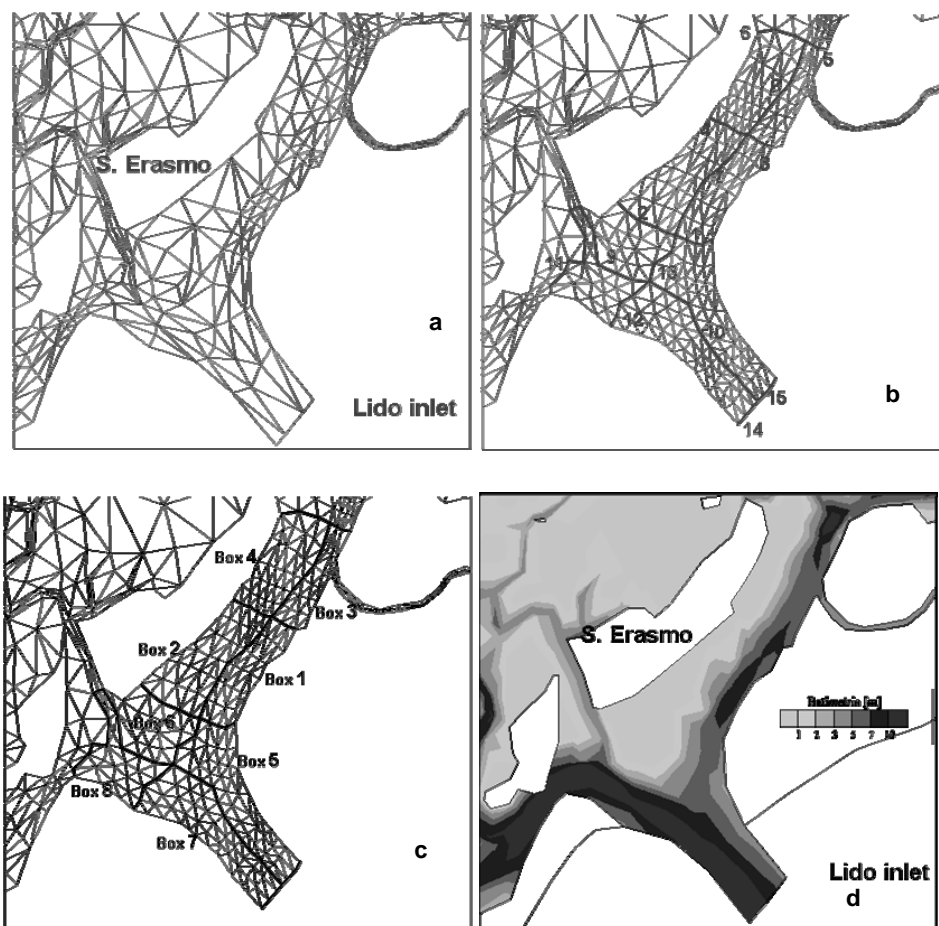


Fig. 1 – Finite elements grid and box model of the studied area. (a) Old grid. (b) New grid and new sections. (c) new boxes. (d) new bathymetry.

The hydrodynamic input parameters needed for Sedtrans96 were flow conditions on every node of each section. These were computed through several simulations with Shyfm. All simulations were carried out with a time step of 300 s. The hydrodynamic model was calibrated prior to this study and all parameters (bottom friction, etc.) have been adopted in these simulations.

Real tidal and wind data by an entire year(1987) were used in the simulation. The wind field statistics during the year 1987 are shown in Fig. 2.

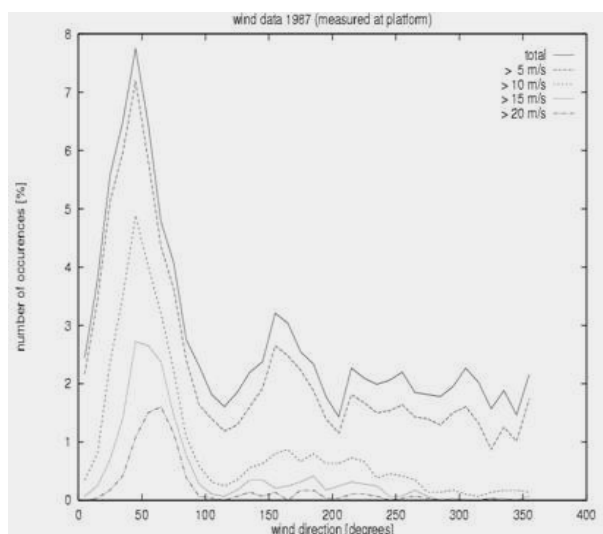


Fig. 2 – Wind distribution of year 1987.

Two peaks can be distinguished clearly: the first one, between 40-70° N, represents the bora events, frequently during the winter season. The second peak, with direction 140-170° N, represents the scirocco wind that blows mostly during summer (Coraci, 2003).

The sediment transport model has been run for several grain size distributions (500, 250, 200, 150 μm). The Engelund-Hansen algorithm ($q = 0.05u_{100}^2 \rho^2 u_*^3 / D(\Delta\rho g)$) was used because this method is valid for grain sizes greater than 150. A mass balance was carried out and the bottom variation in each box due to erosion and deposition was computed.

3 Results

3.1 Simulation of one year (1987)

Simulation for year 1987 has been carried out. In a preceding work (Umgiesser, et al. 2005) the same year has been simulated but in this study many changes were done. The grid has been modified and new bathymetry and new sections have been added. New sediment transport through the 15 sections and the mass balance between the 7 boxes are shown in Fig. 3.

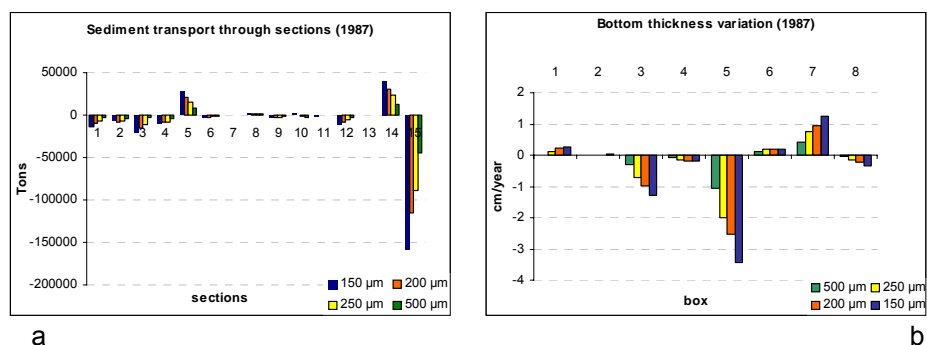


Fig. 3 – Simulations results of year 1987 for the Treporti canal (sections 1-8) and Lido inlet (9-15). (a) Transports through sections, negative values represent a seaward transport. (b) Bottom thickness variation, negative values represent an erosion into the box.

In the transport plot it's clear that smaller grain size (150 µm) are more transported than greater grain size (500 µm). For Treporti canal sections (1, 2, 3, 4, 5, 6) the sediment transport is more balanced. Specially, transport through this sections is directed to Adriatic sea but into section 5 the direction of transport is opposite to the others. This problem could be caused by two different bathymetries in this area. Depth data of year 1990 are available only until sections 3, 4 and sections 5, 6, 8 are based on 1970 depth data.

Sediment transport through sections 7, 8, 9, 10, 11, 12 is almost zero. Instead 14 and 15 sections' behaviours are opposite. In section 14, on southern inlet side, transport is directed toward the lagoon. Transport through section 15 is seaward.

In order to justify this situation a simulation for one tide cycle has been carried out on these sections. Old and new grid have been used to show possible differences of current velocity between two grids. Velocity module has been computed in 4 nodes on both grids (Fig. 4).

In Fig. 5 current velocity module plots for old and new grid are showed.

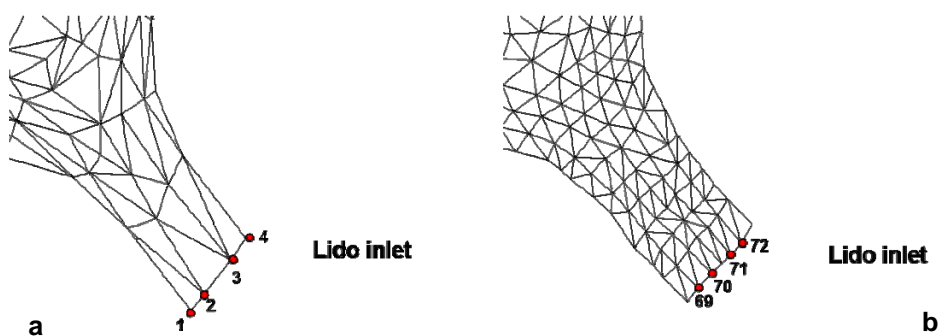


Fig. 4 – Nodes used to compute current velocity module. a): old grid, nodes 1, 2 are in section 14 and nodes 3, 4 in section 15. b) new grid, nodes 69, 70 are in section 14 and nodes 71, 72 in section 15.

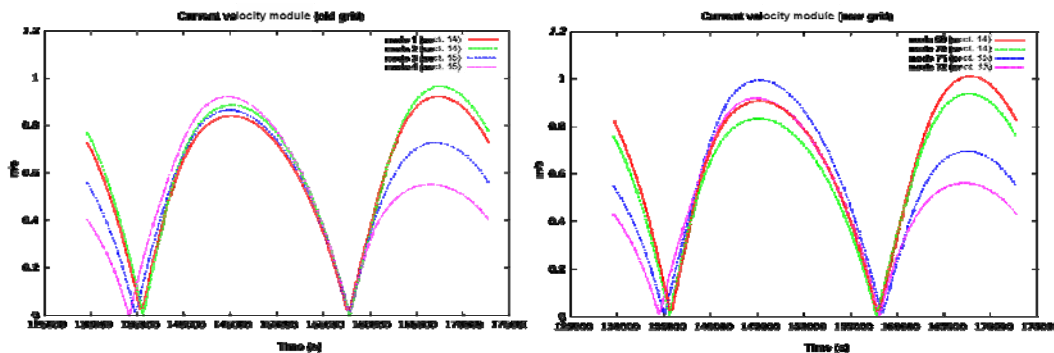


Fig. 5 – Current velocity plots.

The plots show that for nodes in section 14 (1, 2 old grid and 69, 70 new grid) current velocity module landward (second peak) is higher than seaward (first peak). For nodes in section 15 the situation is reversed. Seaward directed velocity values are higher than toward lagoon.

Sediment transport follows current behavior and then the simulation results for year 1987 are confirmed.

4 Conclusions

In this work sediment transport in Venice Lagoon has been studied by means of finite element hydrodynamic model, wave model and sediment transport model. In this study, compared with preceding works (Umgiesser, G., et al. 2005), there are some changes.

Treporti canal and Lido inlet areas are investigated. In order to obtain major spatial resolution old grid has been modify and bathymetry has been changed. Moreover new sections have been added on Lido inlet both to Punta Sabbioni side than to S. Nicolò side. Simulation's results for whole year 1987 show that the sediment transport into Treporti canal is directed toward Adriatic Sea instead in Lido inlet there is a more complex situation.

For S. Nicolò inlet side transport is landward directed instead for Punta Sabbioni side transport is seaward directed. This condition is probably due to the different direction of current velocity and to bathymetry differences between two inlet sides.

The aim of next study will be to apply 2D hydrodynamic model with sediment transport model in order to obtain erosion/deposition maps.

References

Amos, C. L., Helsby, R., Umgiesser, G., Mazzoldi, A., and Tosi, L. 2005. Sand transport in northern Venice lagoon. CORILA 3.2 – Idrodinamica e morfologia della laguna di Venezia (VELMA). *In Scientific Research and Safeguarding of Venice*. Volume III, Corila, Venice.

- Amos, C.L., Umgiesser, G., Helsby, R.A. and Friend, P.L. 2004. Final Report - CORILA 3.2 – Idrodinamica e morfologia della laguna di Venezia (VELMA). In *Scientific Research and Safeguarding of Venice*. Volume II, Corila, Venice: 189-202.
- Bagnold, R.A., 1963. Mechanics of marine sedimentation. In: Hill, M.N. (Ed.), *The Sea*, 3. Wiley-Interscience, New York, 507-527.
- Bagnold, R.A., 1966. An approach to the sediment transport problem from general physics. *US Geological Survey Professional Paper*, 4421, 37p.
- Brown, C.B., 1950. In: Rouse, H. (Ed.), *Engineering Hydraulics*. Wiley, New York, 1039
- Bruun, P. 1978. Stability of Tidal Inlets, Theory and Engineering. *Elsevier Scientific Publishing Company*, 506p
- Carter, R.W. G. 1988. Coastal Environments. An Introduction to the Physical, ecological and Cultural Systems of Coastlines. *Publ. Academic Press, London*.
- Chick, K. 2002. A sidescan survey of Lido Entrance, Venice Lagoon. Unpublished B.Sc. thesis, University of Southampton.
- Coastal Engineering Manual. 1998. Engineering Design. COASTAL GEOLOGY. *Publ. Dept. of the Army, Washington, Manual No. 1110-2-1810*
- Coraci E., Umgiesser G., Sclavo M., Amos C.L., 2003. Modeling sand transport in the Venice Lagoon inlets, In *Scientific Research and Safeguarding of Venice*. Volume II, Corila, Venice.
- De Pascalis, F., 2003. Applicazione di un modello di trasporto di sedimenti ai canali principali della laguna di Venezia: il canale di Treporti. *Master thesis. Università Ca'Foscari Venezia*.
- EMPHASYS Consortium. 2000. A Guide to Prediction of Morphological Change within Estuarine Systems. *MAFF Project FD1401 Publication: 53p + Appendixes*.
- Engelund, F., Hansen, E., 1967. A monograph on sediment transport in alluvial streams. *Teknisk Forlag, Copenhagen Denmark*, 62p.
- Gazzi, P., Zuffa, G.G. Gandolf, G. and Paganelli, L. 1973. Provenienza e dispersione litoranea delle sabbie delle spiagge adriatiche fra le foci dell'Isonzo e del Foglia: inquadramento regionale. *Memorie della Societa Geologica Italiana* 12: 1-37.
- Gibbs, R.J., Mathews, M.D., Link, D.A., 1971. The relation-ship between sphere size and settling velocity. *Journal of Sedimentary Petrology* 41, 7-18.
- Gibbs, R.J., Mathews, M.D., Link, D.A., 1971. The relation-ship between sphere size and settling velocity. *Journal of Sedimentary Petrology* 41, 7-18.
- Grant, W.D., Madsen, O.S., 1986. The continental shelf bottom boundary layer. *Annual Review of fluid Mechanics* 18, 265-305.

Hubbard, D.K., Oertel, G. and Nummedal, D. 1979. The role of waves and tidal currents in the development of tidal-inlet sedimentary structures and sand body geometry: examples from North Carolina and Georgia. *Journal of Sedimentary Petrology* 49: 1073-1092.

Kjerve, B. and Magill, K.E. 1989. Geographic and hydrodynamic characteristics of shallow coastal lagoons. *Mar Geol* 88:187-199

Li, M.Z., Amos, C.L., 1997. SEDTRANS96: Upgrade and calibration of the GSC sediment transport model. *Geological Survey of Canada Atlantic Open File Report* 3512, 140p.

Li, M.Z., Amos, C.L., 2001. SEDTRANS96: the upgraded and better calibrate sediment transport model for continental shelves. *Computers & Geosciences* 27, 619-645.

Li, M.Z., Amos, C.L., 2001. SEDTRANS96: the upgraded and better calibrate sediment transport model for continental shelves. *Computers & Geosciences* 27, 619-645.

Miller, M.C., McCave, I.N., Komar, P.D., 1977. Threshold of sediment motion under unidirectional currents. *Sedimentology*, 24, 507-527.

Shepard, F.P., 1954. Nomenclature based on the sand-silt-clay ratios. *J. Sedim. Petrol.*, 24, n. 3, 151-158.

U.S. Army Engineer Waterways Experiment Station, 1984. Shore Protection Manual. *U.S. Government Printing Office*, Washington DC, U.S.

Umgiesser, G., 2000. SHYFEM Finite element model for coastal Seas - User manual

Umgiesser, G., Melaku Canu, D., Cucco, A., Solidoro, C., 2004. A finite element model for the Venice Lagoon. Development, set up, calibration and validation. *Journal of Marine Systems*, 51, 123-145

Umgiesser, G., Ferrarin, C., De Pascalis, F., Amos, C. L., 2005. Modeling sand transport in a canal system, northern Venice Lagoon. *In Scientific Research and Safeguarding of Venice*. Volume III, Corila, Venice.

Wentworth, C.K., 1922. A scale of grade and class terms for clastic sediments. *J. Geol.* 30, 377-392

Yalin, M.S., 1963. An expression for bedload transportation. *Journal of Hydraulics Division, Proceedings ASCE* 89 (HY3), 221-250.

RESEARCH LINE 3.15

Solid transport and circulation of the upper layers in the inlets and the coastal zone.

ACCURACY OF SURFACE CURRENT MEASUREMENTS FROM HF RADAR

Simone Cosoli¹, Miroslav Gačić², Andrea Mazzoldi¹

¹ C.N.R. - Istituto di Scienze Marine, Sezione di Ricerca di Venezia (ISMAR), Italy,

² Istituto Nazionale di Oceanografia e di Geofisica Sperimentale (OGS), Trieste, Italy

Riassunto

Le misure di corrente superficiale da Radar costiero HF vengono confrontate con serie temporali di corrente subsuperficiali da correntometro ADCP. Il periodo considerato si estende da Settembre ad Ottobre 2002. Nonostante differenze intrinseche alle tecniche di misura, l'analisi evidenzia un buon accordo tra le correnti superficiali e sub-superficiali. Le differenze tra le registrazioni sono dovute sia ad incertezze nelle misure, sia all'azione del vento su scala temporale diurna (regime di brezza).

Abstract

Surface currents from HF radar network in front of the Lagoon of Venice and subsurface currents from a bottom-mounted ADCP are compared. Results show good agreement between current time series, despite intrinsic differences in the measurement techniques. Major differences between surface and subsurface currents are due to uncertainties in the measurements, and wind forcing on a diurnal time scale (sea-breeze forcing).

1 Introduction

Surface currents play a fundamental role in coastal environments, due to their influence on ecology, recreation and shipping. HF Doppler techniques allow for continuous, nearly real-time measurements of the surface current on wide areas, which would be otherwise impossible with more conventional techniques. The reliability of these measurements has to be confirmed by comparing HF radar currents to measurements obtained with more conventional instruments.

High frequency coastal radar measure currents by transmitting electromagnetic waves on the radio frequency band along the sea surface, and analyzing the Doppler shifted spectrum of the sea-surface echo. The mechanism is based on Bragg scattering phenomena, a positive interference occurring when transmitted electromagnetic waves are backscattered by waves traveling on the rough sea surface and having comparable wavelength. Due to the presence of wave trains approaching to and receding from the transmit site, two peaks in the Doppler spectrum are present (see Fig.1). The frequency at which Bragg peaks will appear is related to the phase speed of the sea waves. Any displacement of the Bragg peaks from their expected position is proportional to the component of water velocity moving radially to the radar station. Two or more radar stations allow for the surface motion field to be measured.

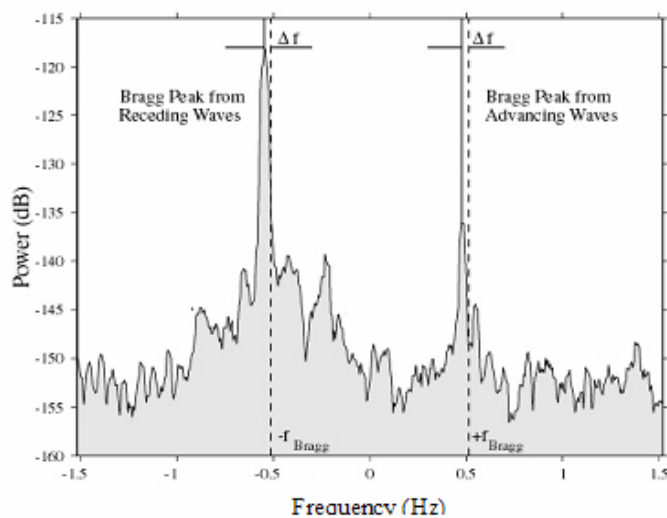


Fig 1 – Spectrum of the sea echo showing the two Bragg peaks due to receding and advancing wave trains.

Differences between current measurements are to be expected even when radar and more conventional currentmeters are properly setup and perfectly operating. Radar-derived currents represent an average value of the near-sea surface motion field, typically on 1 km² footprint, while currentmeters measure pointwise currents at distances from the surface of more than 2 meters. The so-called “geophysical noise”, that’s to say the ensemble of physical processes occurring at the measurement site, also contributes to differences between current time series. The contributions to the overall differences must thus be estimates on a statistical basis, and explained in terms of both instrument errors or limitations, and physical phenomena.

This preliminary accuracy estimate is attempted by comparing the total current vector obtained combining radial current from the two sites of Lido and Pellestrina to subsurface currents along the water column as measured by a bottom-mounted ADCP. Figure 2 shows the position of the two radar sites, the ADCP mooring and the Oceanographic Tower. The analyzed data set covers the two-months period from September to October 2002.

2 Data and methods

Surface currents are obtained from a 25 MHz shore-based HF CODAR-type radar network managed by CNR-ISMAR, within a regular grid with spatial resolution of 750 m and temporal resolution of 1 hour. Nominal accuracy is 7 cm/s and 10° for current speed and direction, respectively. Subsurface currents are obtained from a 1200 kHz bottom-mounted ADCP moored close to the Oceanographic Tower at 18 m, with a vertical resolution of 35 cm and temporal resolution of 1 hour. Nominal accuracy for current speed and direction are 1 cm/s e 1°, respectively.

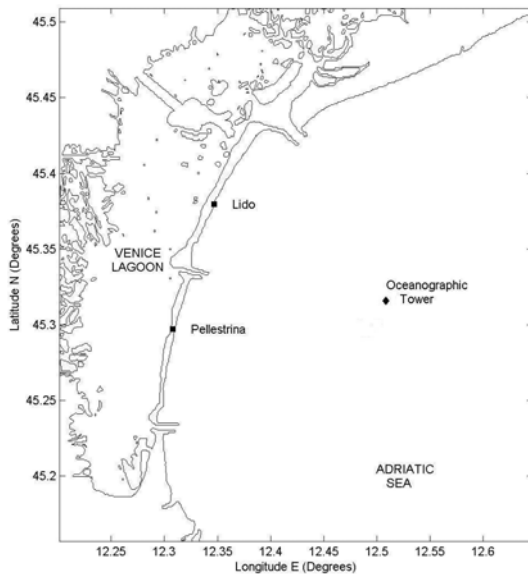


Fig. 2 – Location of the Radar sites of Lido and Pellestrina (black squares) and the Oceanographic Tower (black diamond) .

Wind time series at the Tower are also analyzed; hourly time series of wind stress are obtained according to Large and Pond formulation. (JPO, 1981). Tidal currents in surface and subsurface currents are extracted using Matlab code “t_tide” [Pawlowicz et al., 2002]. Tidal contribution to the overall variability is expressed in terms of variance explained by the astronomical forcing. A complex correlation coefficient is used in order to compute the relationship between couples of vectors [Kundu, 1976]:

$$R = \rho \exp(i\alpha) = \frac{\langle w_1 \circ w_2 \rangle}{\langle w_1 \circ w_1 \rangle^{1/2} \langle w_2 \circ w_2 \rangle^{1/2}}$$

The magnitude represents a measure of the correlation between the two vectors, while the phase angle gives the average difference in direction (veering) of the two vectors.

3 Results

According to scatterplot of the horizontal components for surface and subsurface current estimates, measurements are quite nicely clustered around the line of equal velocity. Scalar correlation coefficients between velocity components are .68, .49 respectively for the U (E-W), V (N-S) components, and significantly increase (.72, .58, for U, V components respectively) after low-passing time series, in order to cut off high-frequency signals (time scale 1 day) and random errors. Vector correlation coefficient is .63, with a veering angle between surface and subsurface currents for the shallowest bin of 15°; after low-passing data, vector correlation slightly increases while the veering angle decrease to 12°.

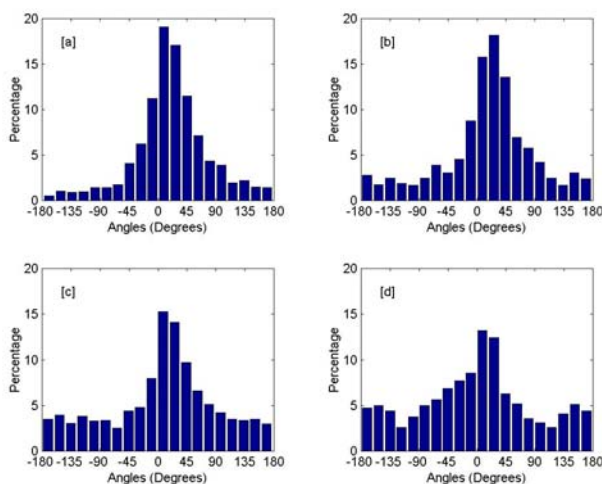


Fig – 3 Frequency distribution of angles between Codar and ADCP measured currents at four different levels ([a] depth 2.37m; [b] depth 5.87 m; [c] depth 9.37 m; [d] 16.37 m)

Distribution of the angles between surface and subsurface currents depicted in Fig – 3 show that on the average current direction differ by 20°, sub-surface ADCP estimates being to the right of the HF surface time series.

Differences between the horizontal current components are small, being 4 cm/s, 1 cm/s for the U, V component respectively, as shown by histograms depicted in Fig – 4. The root-mean-square of the differences is 9.3 cm/s (9.8 cm/s for V component), and decreases to 6.9 cm/s (6 cm/s) after low-passing time series. According to the sample cumulative distribution function (not shown), more than 50% of the differences between current component estimates is less than 7 cm/s, and this percentage significantly increases after low-passing current time series. A similar behavior holds for current direction differences; moreover, differences in direction larger than 45° are associated with current speed significantly lower than 7 cm/s.

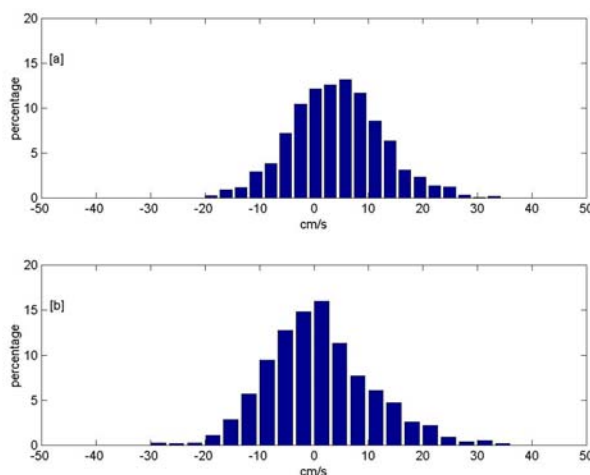


Fig – 4 Histograms of the differences between ADCP and Codar measured U ([a]) and V ([b]) velocity components.

Rotary spectra of HF-surface and ADCP sub-surface currents along the water column, together with results from least squares tidal analysis, differences are mainly due to wind forcing. Low frequency oscillations have the same amount of variance, and no significant variation in amplitude with depth is found in the semidiurnal band. Significant differences are present in the diurnal band. Fig. 5 shows rotary spectra for surface, sub-surface and near-bottom currents: a variance reduction with depth in the frequency band spanning from 12 to 24 hours is clear. Least squares harmonic analysis results confirm, as far as the semidiurnal and the diurnal tidal band are concerned, the vertical shear in the diurnal K1 tidal ellipse major axis, which is not present at the semidiurnal tide M2. Figure 6 depicting the vertical profiles of K1 and M2 tidal ellipse major axes, shows the 50% reduction of K1 amplitude occurring within 3-4 m from the surface. The presence of a significant peak in wind stress rotary spectrum at the diurnal frequency suggest that wind forcing on a daily time scale (diurnal sea-breeze) might explain part of the differences between HF-surface and ADCP sub-surface currents.

4 Conclusions

In this work, preliminary results of the assessment of accuracy of HF radar current measurements are shown, and differences with sub-surface currents from a bottom-mounted ADCP are discussed in terms of physical forcing in the area. The analyzed data set spans two months over the period September-October 2002. Despite intrinsic differences in the sampling techniques, good agreement is found between current estimates. Currents are significantly correlated, as shown by the scalar correlation coefficient between velocity components, and the vector correlation coefficient. Differences between time series of current components are small.

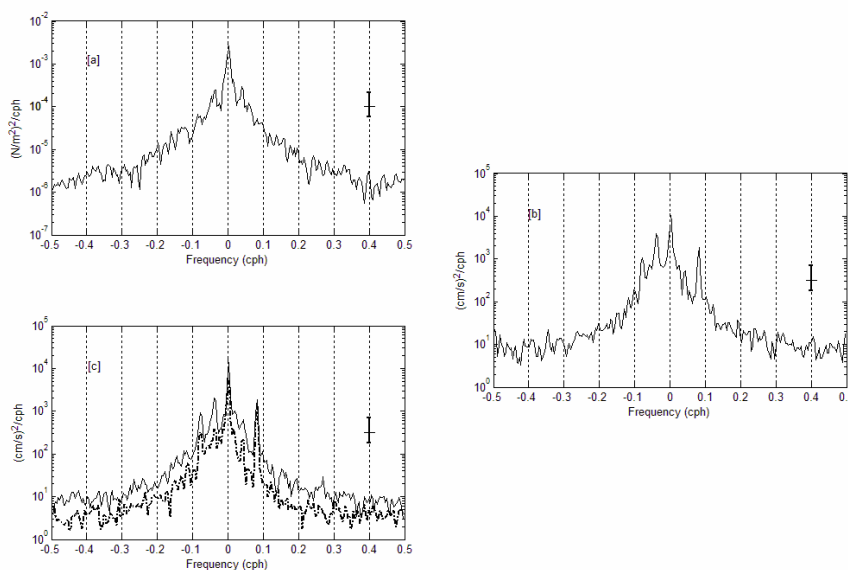


Fig – 5 Rotary spectra of the wind stress ([a]), Codar currents ([b]), and ADCP currents ADCP at subsurface and bottom ([c])

Subsurface currents are on average to the right of surface currents, as predicted by Ekman theory; the veering angle obtained using the complex correlation coefficient well agree with the average value of the angles between surface and subsurface current vectors. Differences are mainly associated with wind forcing on a diurnal time scale (diurnal sea-breeze). An amplitude reduction with depth involves the diurnal band in the rotary spectrum, which is not present in the semidiurnal band. Wind forcing seems to be limited to the upper layer of the water column, where a 50% reduction of K1 tidal ellipse major axis amplitude in the first 5 meters is observed

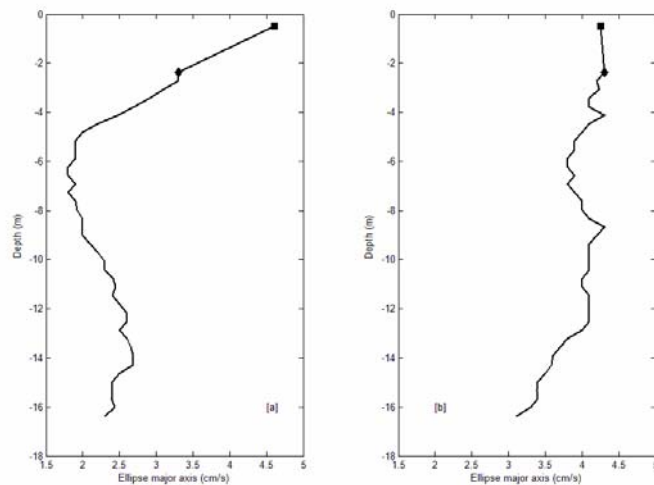


Fig – 6: Vertical distribution of the major ellipse axis for the K1 (left panel; [a]) and M2 (right panel, [b]) tidal constituents. The black squares near the surface refer to the major axis magnitude obtained from Codar, while the black diamonds refer to the major axis magnitude derived from the ADCP current time series.

References

Chapman R.D., Shay L.K., Graber H.C., Edson J.B., Karachintsev A., Trump C.L., Ross D.B., 1997. On the accuracy of HF radar surface current measurements: intercomparison with ship-based sensors. *Journal of Geophysical Research*, 102, C8, 18.737-18.748, 1997.

Graber H.C., Haus B.K., 1997. HF radar comparisons with moored estimates of current speed and direction: expected differences and implications. *Journal of Geophysical Research*, 102, C8, 18.749-18.766, 1997.

Gonella J., 1972. A rotary-component method for analysing meteorological and oceanographic vector time series. *Deep Sea Research*, Vol.19, pp.833-846, 1972.

Kovačević V., Gačić M., Mancero Mosquera I., Mazzoldi A., Marinetti. S., 2004. HF radar observations in the northern Adriatic: surface current field in front of

the Venetian Lagoon. *Journal of Marine Systems*, 51, 1-4, 95-122.

Kundu P. K., 1976. Ekman Veering Observed near the Ocean Bottom. *Journal of Physical Oceanography*, Vol.6, pp.238 – 242, 1976.

Large W.G., Pond S., 1980. Open Ocean Momentum Flux Measurements in Moderate to Strong Winds. *Journal of Physical Oceanography*, vol. 11, pp. 324-336.

Paduan J.D., Rosenfeld L.K., 1996. Remotely sensed surface currents in Monterey Bay from shore-based HF Radar (Coastal Ocean Dynamics Application Radar). *Journal of Geophysical Research*, 101, C9, 20.669-20.686, 1996.

Paduan, J.D., Gačić, M., Kovačević, V., Mancero Mosquera, I., Mazzoldi, A., 2003. Vorticity Patterns Offshore of the Venetian Lagoon from HF Radar Observations. *Linea 3.5 Quantità e Qualità degli Scambi tra Laguna e mare, WBS1 Misure dei Parametri Fisici, WBS1.2. Misure di Corrente con Radar HF, Quinto Rapporto di Ricerca, OGS, Relazione RELI-34/2003 OGA-24.*

Pawlowicz R., Beardsley B., Lentz S., 2002. Classical harmonic analysis including error estimates in MATLAB using T_TIDE. *Computer and Geosciences*, Vol.28, pp. 929 – 937, 2002.

Roberts J., Roberts T.D., 1978. Use of the Butterworth low-pass filter for oceanographic data. *Journal of Geophysical Research*, 83, 5510-5514, 1978.

ESTIMATE OF THE SUSPENDED SOLID MATTER CONCENTRATION FROM THE BACKSCATTER INTENSITY MEASURED BY ADCP

Franco Arena¹, Vedrana Kovačević¹ Andrea Mazzoldi²

¹*Istituto Nazionale di Oceanografia e di Geofisica Sperimentale - OGS, Sgonico (Trieste), Italy,* ²*NR – Istituto di scienze marine (ISMAR), Sezione di Venezia, Italy*

Riassunto.

I correntometri ADCP (Acoustic Doppler Current Profiler) fissi, installati nelle bocche di porto della laguna di Venezia, forniscono il segnale di backscatter, ottenuto dalla onda acustica riflessa dai sedimenti in sospensione. Tramite opportuni algoritmi, questo segnale viene messo in relazione con la concentrazione dei solidi sospesi, mentre le caratteristiche dello strumento e quelle del sedimento nel sito di misura rendono necessario calibrare i dati di backscatter mediante campionamento in situ. La calibrazione del segnale di backscatter è stata effettuata per l'ADCP situato a Lido, allo scopo di ottenere le stime della concentrazione, lungo la colonna d'acqua, in modo continuo per la durata delle misure.

Per tale motivo sono stati utilizzati i dati della concentrazione dei solidi sospesi forniti dal CNR – ISMAR, Sezione di Venezia, impiegando il pacchetto software Sediview. Il lavoro è stato svolto in due fasi. Nella prima fase, la calibrazione del segnale dall'ADCP è stata effettuata utilizzando i dati di concentrazione, ricavati dal CNR-ISMAR di Venezia, mediante analisi gravimetrica dei campioni d'acqua, prelevati alla bocca di porto, in corrispondenza dell'ADCP fisso. Nella seconda fase per la calibrazione si sono utilizzati i dati di concentrazione, ottenuti dai transetti calibrati con Sediview, dal CNR-ISMAR di Venezia. I transetti, ottenuti con un altro ADCP, montato su un'imbarcazione in movimento, che si sposta da una sponda all'altra del canale, rappresentano l'intensità di backscatter sull'intera sezione della bocca, che comprende anche la postazione in cui è ancorato l'ADCP fisso. Il transetto viene calibrato utilizzando sempre gli stessi dati dei campioni d'acqua prelevati in situ.

La calibrazione del segnale di backscatter viene presentata per due distinti periodi di misura, scelti tra le varie campagne effettuate tra luglio 2004 e marzo 2005. In particolare sono state confrontate le concentrazioni nelle varie fasi della corrente mareale. Si ipotizza che alcune discordanze tra le concentrazioni ottenute dall'ADCP fisso e quelle derivanti dai campioni d'acqua e dall'ADCP montato sull'imbarcazione, siano dovute alla non perfetta sincronizzazione spaziale e temporale tra i diversi sistemi di misura. In particolare la disomogeneità spaziale del fenomeno del trasporto solido, sia verticale lungo la colonna che orizzontale lungo la sezione, può spiegare tali differenze.

Abstract

The intensity of the backscatter measured by the bottom-mounted ADCP (Acoustic Doppler Current Profiler) in the Lido inlet is related to the concentration of the particulate suspended solids, determined from the in situ samples taken in two occasions, in July and October 2004 in the vicinity of the deployment site. Moreover, during the sampling intervals, vessel-mounted ADCP was recording a backscatter signal across the inlet passing over the bottom-mounted one. The Sediview [DRL-Sediview, 2003] programme has been used to calibrate the ADCP backscatter, using the same in situ samples. Calibration for the two different periods (July 2004 and October 2004) has been performed and concentrations in the various tidal phases were estimated. The difference between the concentrations from the two methodologies is possibly due to the imperfect synchronism in time and space. The spatially uneven transport of a solid matter, both in vertical and horizontal direction may also be the cause for such differences.

1 Introduction

The long-term current measurements using bottom mounted ADCPs in the inlets of the Venetian Lagoon have been going on since 2001 (Fig. 1). The monitoring will continue for another couple of years, including investigation of the sediment transport in and out of the lagoon.

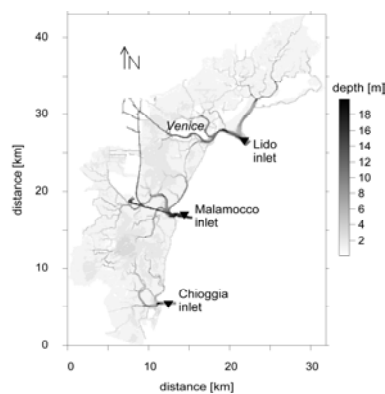


Fig. 1 – Bathymetric chart of the Venetian Lagoon and its inlets. ADCPs are denoted by triangles.

The backscatter signal recorded by the ADCP provides a measure of the suspended sediments in the water column if calibrated carefully [DRL-Sediview, 2003]. Qualitative and possibly quantitative suspended matter concentrations thus could be monitored on the continuous basis during the ADCPs' deployment. Such a methodology could give an insight on the sediment transport variability and provide eventual estimates of the total transport of sediments in and out of the lagoon. A calibration exercise has been performed for the Lido inlet in order to assess the application feasibility for such a methodology in the inlets, and to give the directions on the future design of experimental survey, which would be periodically conducted during the monitoring programme.

2 Data and methods

The bottom-mounted ADCP (for simplicity denoted as ADCP-b) is a Workhorse 600 KHz unit (s/n 1989) deployed in the Lido inlet. The marine currents and the backscatter signal are recorded every 10 minutes at 1 m vertical resolution (for configuration details see Arena and Arcari [2001]). The CTD survey, water samples collection and treatment, and profiling by the vessel-mounted ADCP (ADCP-v) was periodically performed by the ISMAR-CNR Sezione di Venezia (ISMAR-VE) research group in the framework of the projects “Studio del trasporto alle bocche di porto della laguna di Venezia” and “La misura del trasporto solido laguna-mare”. A gravimetric method was applied in order to determine the total suspended matter concentration from the water samples at three depths, near bottom, intermediate, and subsurface levels, in an approx. 12 m of the water column. Details about the methodology are described in [Costa et al., 2005a].

The backscatter signal of the ADCP-b is calibrated in two ways. The first type of calibration uses sediment concentration data determined from the water samples taken at three levels of the water column in the vicinity of the ADCP-b location. The second type is based on calibrated transects across the inlet obtained from the ISMAR-VE [Costa et al., 2005a]. The transects are performed using the ADCP-v with a vertical spatial resolution of 0.5 m. Hence, one or two, sometimes even three cells from the ADCP-v fall in the range of the ADCP-b. In order to avoid repetition, the choice of binding together the closest cells from the two systems has been chosen. Even then there is uncertainty in the height determination in both of them (the instantaneous surface sea level is varying). Finally, concentration values averaged over 30 pings (about 30 seconds, depending on the actual ship speed) at eight levels of the ADCP-v were selected in correspondence to the eight cells of the ADCP-b. These were used as “transect samples”, representing the instantaneous sediment concentration vertically distributed in the water column. The closest ensembles in time from the ADCP-b were then associated with the “transect samples” from the ADCP-v, and the calibration exercise was performed using a Sediview as in the previous case. The time matching can have a range of the order of the sampling interval for the ADCP-b, i.e., 10 minutes.

Both types of calibrations were applied for each of the two surveys described here, using a Sediview software [DRL-Sediview, 2003; Arena, 2004].

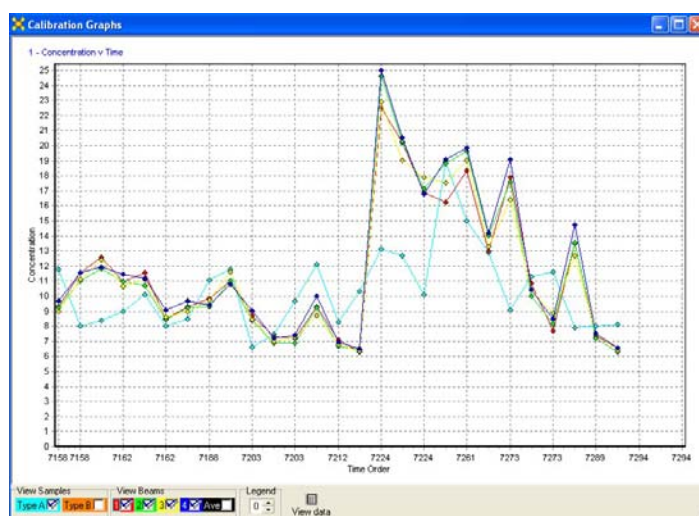
The first survey was conducted on 27-28 July 2004. Nine water samplings were performed during 22 hours of the campaign. In total 27 samples were collected. In addition, twenty subsets of ADCP-v transects were extracted in the time range of about 23 hours.

The second survey was executed on 28 October 2004. Six samplings were performed in the range of about 11 hours (for a detail of the survey see Costa et al. [2005b], and 15 samples were collected for calibrating the ADCP-b. Following the same choosing criteria as in July, nineteen subsets from the calibrated transects were selected as “transect samples”.

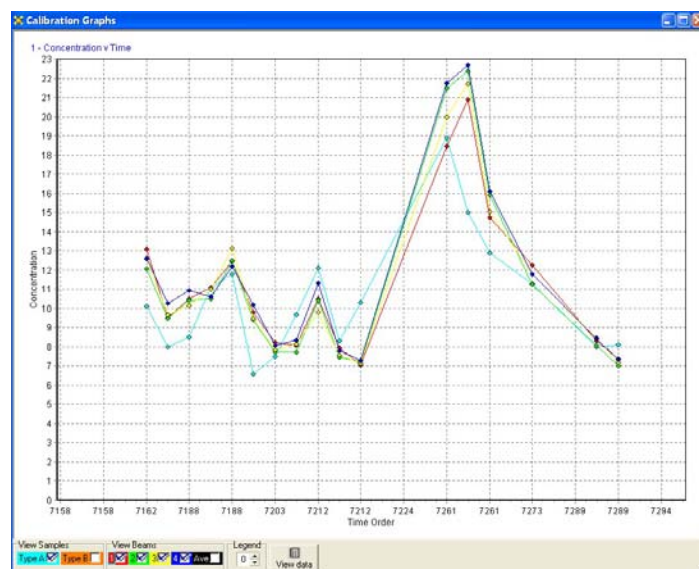
3 July 2004 survey

3.1 ADCP-b backscatter calibration with water samples

It turned out that ten samples were not matching well the ADCP-b values (Fig. 2a). This is possibly due to the imperfect time and space coupling. Therefore they were discarded from the calibration procedure. The degree of matching between each of the four ADCP-b beams and the 17 remaining values from the water samples is indicated in Fig. 2b. Subsequently the ADCP-b derived concentrations were averaged over the four beams.



(a)



(b)

Fig 2 – Initial (a) and final (b) calibration for the July campaign using water samples. Turquoise colour refers to the water samples, and other colours to the four ADCP-b beams. X axis refers to the time order in terms of the ADCP-b ensemble numbers, y axis reports solid concentrations in mg/L.

Dispersion diagram in Fig. 3 shows the agreement between concentrations derived from the ADCP-b and water samples.

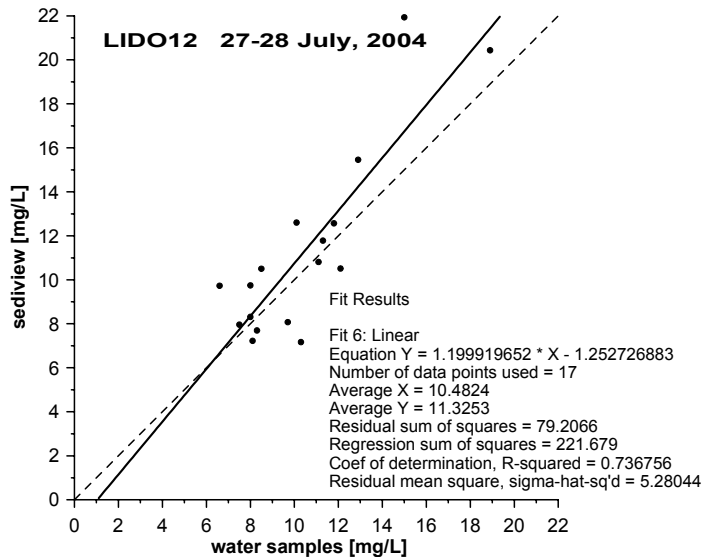


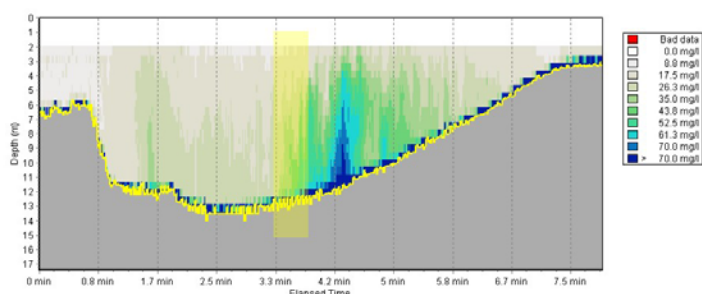
Fig 3 - Dispersion diagram of the concentrations obtained by calibrating the ADCP-b backscatter with the water samples. Values on the sediview axis correspond to the average of the four beams. The bold line represents a linear fit from the data, and a dashed line is a theoretical curve $y=x$.

3.2 ADCP-b backscatter calibration using the ADCP-v

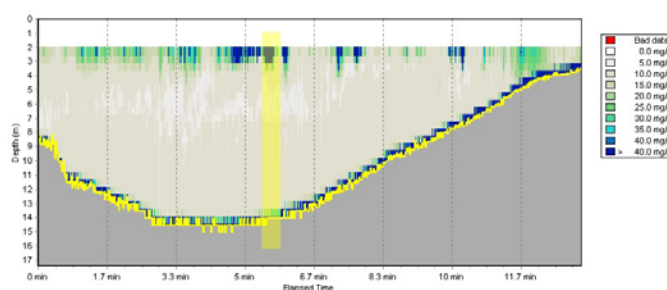
In Fig. 4 the vertical distribution of the sediment concentration during some of the ADCP-v surveys across the inlet is shown along with the subset used as an input transect sample for calibrating the ADCP-b. In particular, the distribution can be spatially uneven over the section (Fig. 4a). The good time and space matching, therefore, is essential for the ADCP-b coupling either with sub-section from the vessel-mounted one, or with the water samples. Moreover, Fig. 4b shows the misleading effect of higher concentration values near the surface caused probably by the air bubbles, formed due either to the waves, or ship wakes, as in Fig. 4c.

A detail of the calibration from the Sediview is presented in Fig. 5a. Unusually high ADCP-v concentration values are achieved in the correspondence of the ADCP-b ensembles 7175, 7176 and 7200 (30-60 mg/L). Some of these are near surface ones (ens. numbers 7175 and 7176), which are supposed to be contaminated by a wave-induced pitch and roll of the research vessel conducting the measurements (Fig. 4b). Such ship movements create air bubbles which affect the backscatter signal and provoke anomalously high concentrations. The ADCP-b is not affected by such a disturbance. High near surface values in correspondence to the ensemble 7200 result from the air-bubbles generated by wakes of other vessels, such as in Fig. 4c. High values

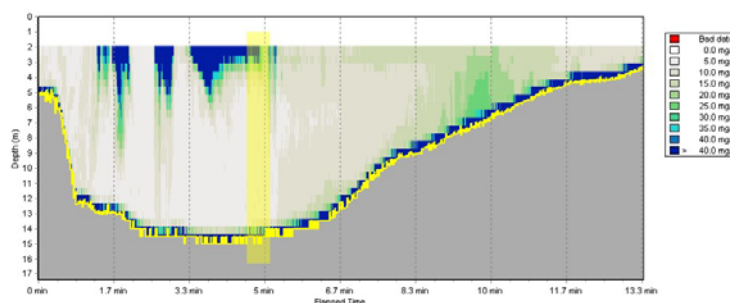
corresponding to the ensemble 7259 are near bed concentrations, detected probably in the vicinity of the high sediment pattern near the ADCP-b location (Fig. 4a).



(a)



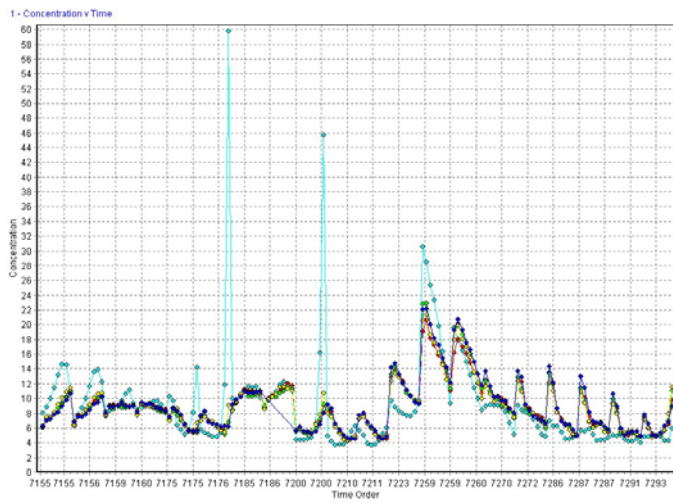
(b)



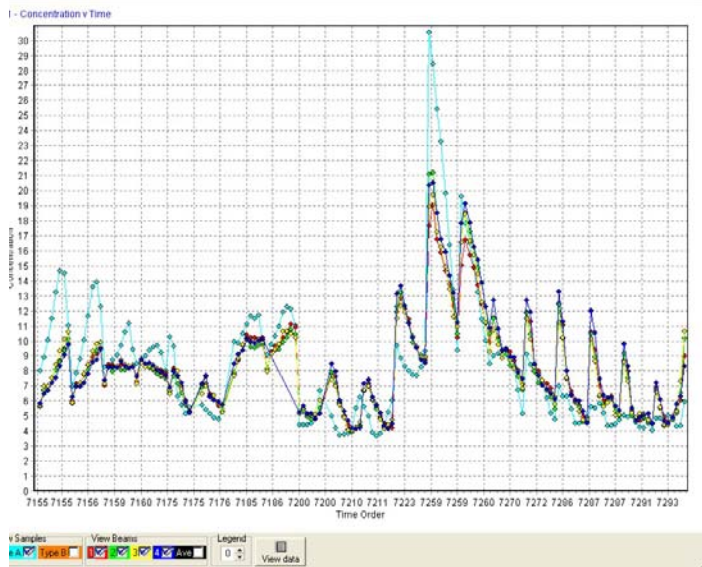
(c)

Fig. 4 – Sediment concentration transects, obtained from the calibrated ADCP-v in the Lido inlet by CNR-ISMAR, Venice, with evident disturbances of different origin: spatially uneven concentration (a), pitch and roll of the vessel (b), ship wake (c). The yellow stripe denotes the 30-ping subset used as a ‘transect sample’ Northern jetty is to the right, southern jetty to the left.

Discarding only those suspicious values for which the cause is readily detected, the final calibration is given in Fig. 5b. But, there again some remaining values are not well coupled with the ADCP-b data. This might be due to the uneven solid matter distribution across the inlet. We have decided to keep them like that.



(a)



(b)

Fig. 5 – Initial (a) and final (b) calibration for the July campaign using subsets of the ADCP-v transects (turquoise colour). The other colours refer to the four ADCP-b beams. X axis refers to the time order in terms of the ADCP-b ensemble numbers, y axis reports solid concentrations in mg/L.

The result of the final fit is shown in Fig. 6. Few outliers at the higher end of the transect samples cause the fit be less efficient, even though there are more data than the water samples.

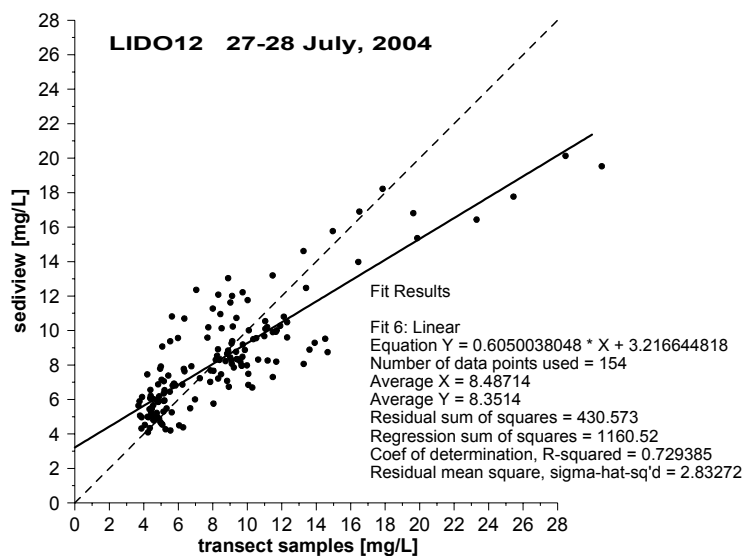


Fig 6 - Same as Fig. 3, except for the concentrations obtained by calibrating the ADCP-b backscatter with the subset of the calibrated ADCP-v transects.

4 October 2004 survey

4.1 ADCP-b backscatter calibration with water samples

The calibration for the October campaign is illustrated in Fig. 7. There are no discarded data.

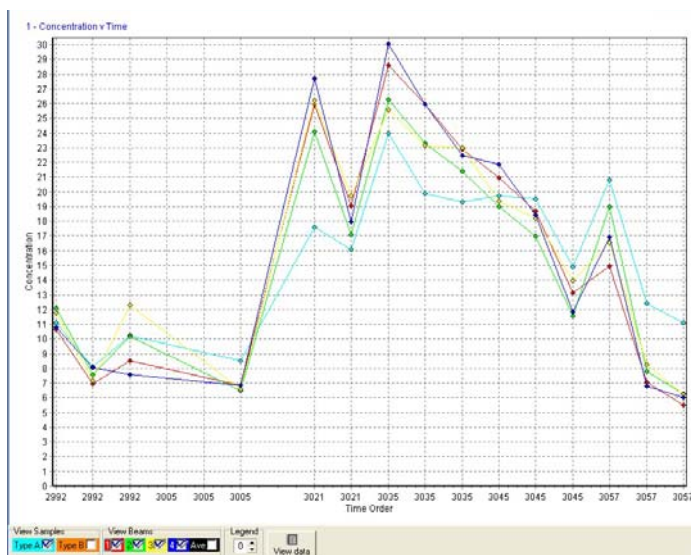


Fig. 7 – Calibration for the October campaign using water samples. Turquoise colour refers to the water samples, and other colours to the four ADCP-b beams. X axis refers to the time order in terms of the ADCP-b ensemble numbers, y axis reports solid concentrations in mg/L.

Matching between the concentrations from the ADCP-b and samples is depicted in Fig. 8.

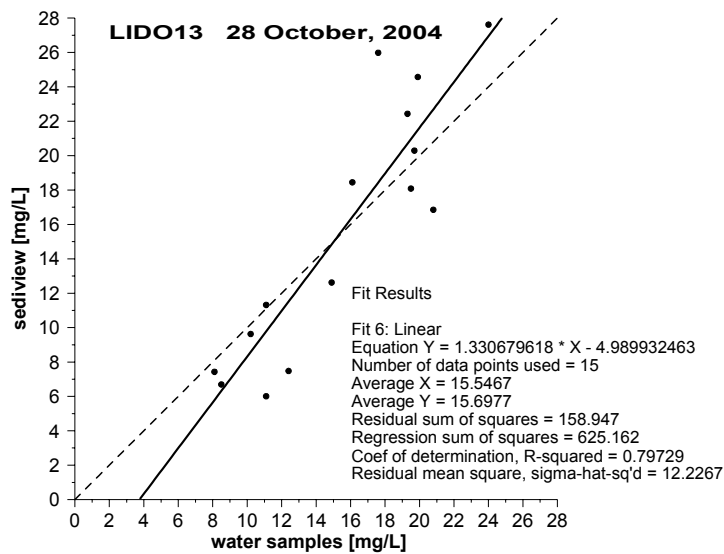
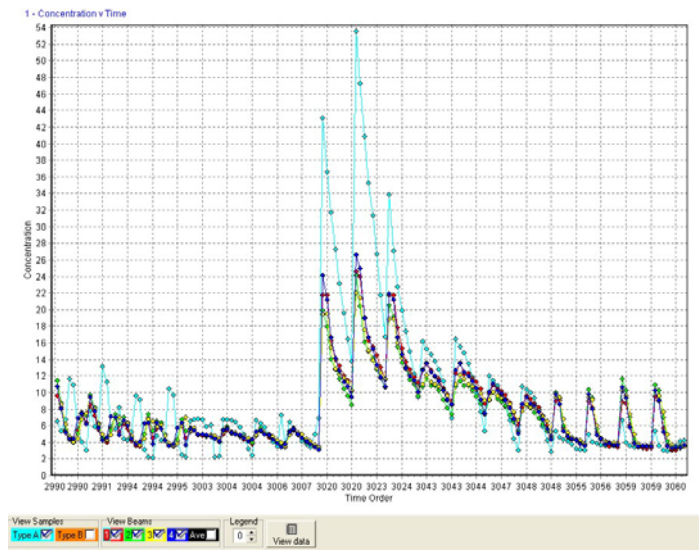


Fig. 8 - Dispersion diagram of the concentrations obtained by calibrating the ADCP-b backscatter with the water samples. Values on the sediview axis correspond to the average of the four beams. The bold line represents a linear fit from the data, and a dashed line is a theoretical curve $y=x$.

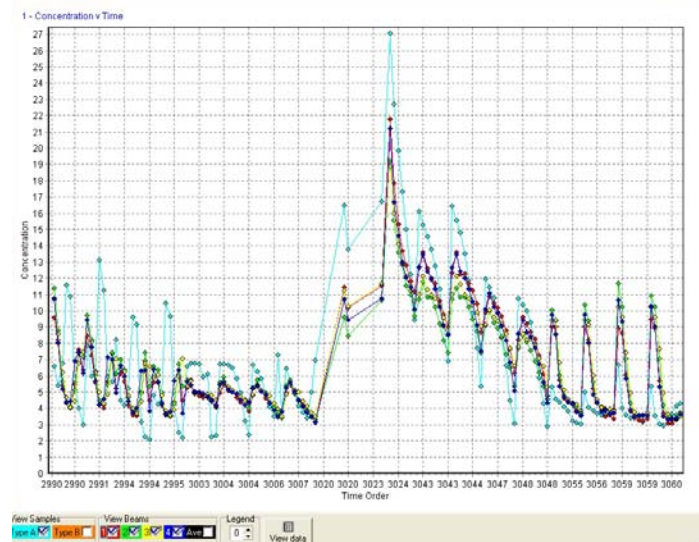
4.2 ADCP-b backscatter calibration using the ADCP-v

Initial calibration curve is reported in Fig. 9a. Unusually high ADCP-v values in the middle of the plot are located in most of the water column (transect not shown), due probably to the resuspension of the bottom sediments during the strong outflow (see Fig. 12, between 12 and 13 o'clock), and only the near surface values match relatively well. Probable space (vertical) and time mismatching of the two systems, ADCP-v and ADCP-b, result in such differences. The final adjustment (after removing some superficial values) through the Sediview procedure is depicted in Fig. 9b.

The result of the final fit is shown in Fig. 10. Like in the July case (Fig. 6), due to few outliers at the higher end of the transect samples, the fit is less efficient than with the water samples.



(a)



(b)

Fig. 9 - Initial (a) and final (b) calibration for the October campaign using calibrated transects (turquoise colour). The other colours refer to the four ADCP-b beams. X axis refers to the time order in terms of the ADCP-b ensemble numbers, y axis reports solid concentrations in mg/L.

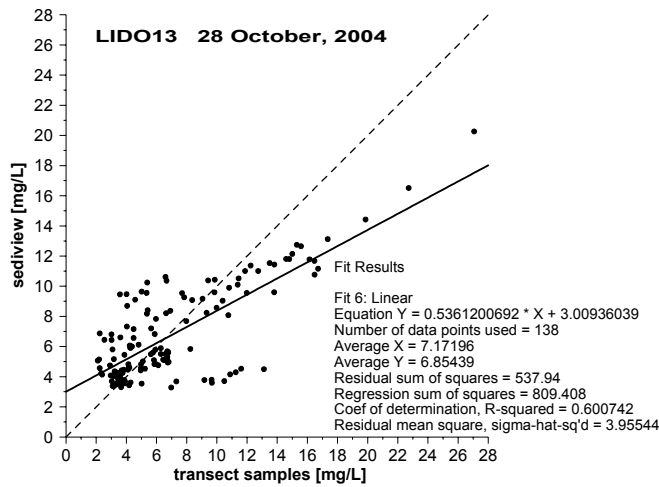


Fig. 10 - Same as Fig. 8, except for the concentrations obtained by calibrating the ADCP-b backscatter with the subset of the calibrated ADCP-v transects.

5 Conclusions

In Table 1 we report the coefficients that determine the conversion of the backscatter (decibel) into suspended solid sediments' concentration (mg/L). They were obtained from the Sediview calibrating procedure of the ADCP-b in two different time periods. The meaning of the K_S and S is reported in DRL-Sediview [2003] and Arena [2004].

Period	Water samples		Calibrated transects	
	K_S	S	K_S	S
July 27-28, 2004	48	28.5	53	29
October 28, 2004	50.6	31.5	58	31

Table 1 – Coefficients K_S and S for conversion of the ADCP-b backscatter signal into concentration using water samples and calibrated transects, for the two campaigns.

The results of the sediment concentration estimates from the ADCP-b in the Lido inlet are summarized in Figs.11 and 12 for July and October surveys, respectively, including the time evolution of the current flow in the inlet during sampling campaigns. The vertical distribution of these two properties is limited to the three levels at different distances above the sea bed, where the water sampling has been performed. These are 2.6 m, 6.6 m and 9.6 m above the sea bed, referring to the near bottom, intermediate, and near surface layers. The flow regime is depicted by the axial current component, aligned with the longitudinal inlet axis, and positive when out-flowing from the lagoon. The flow is almost entirely tidally driven with prevalent semi-diurnal pattern [Gačić et al., 2004].

The time diagram in Fig. 11a represents the flow conditions during the survey in July 2004, between the neap and spring tides (between the first lunar quarter and the full moon). The flow at three levels is quite similar, and the velocity oscillates between -1 m/s and 1 m/s. The suspended sediment concentrations obtained from the water samples are marked by a diamond symbol and coupled with the corresponding sediment concentration time series estimated from a calibrated backscatter signal of the ADCP-b (Fig. 11b).

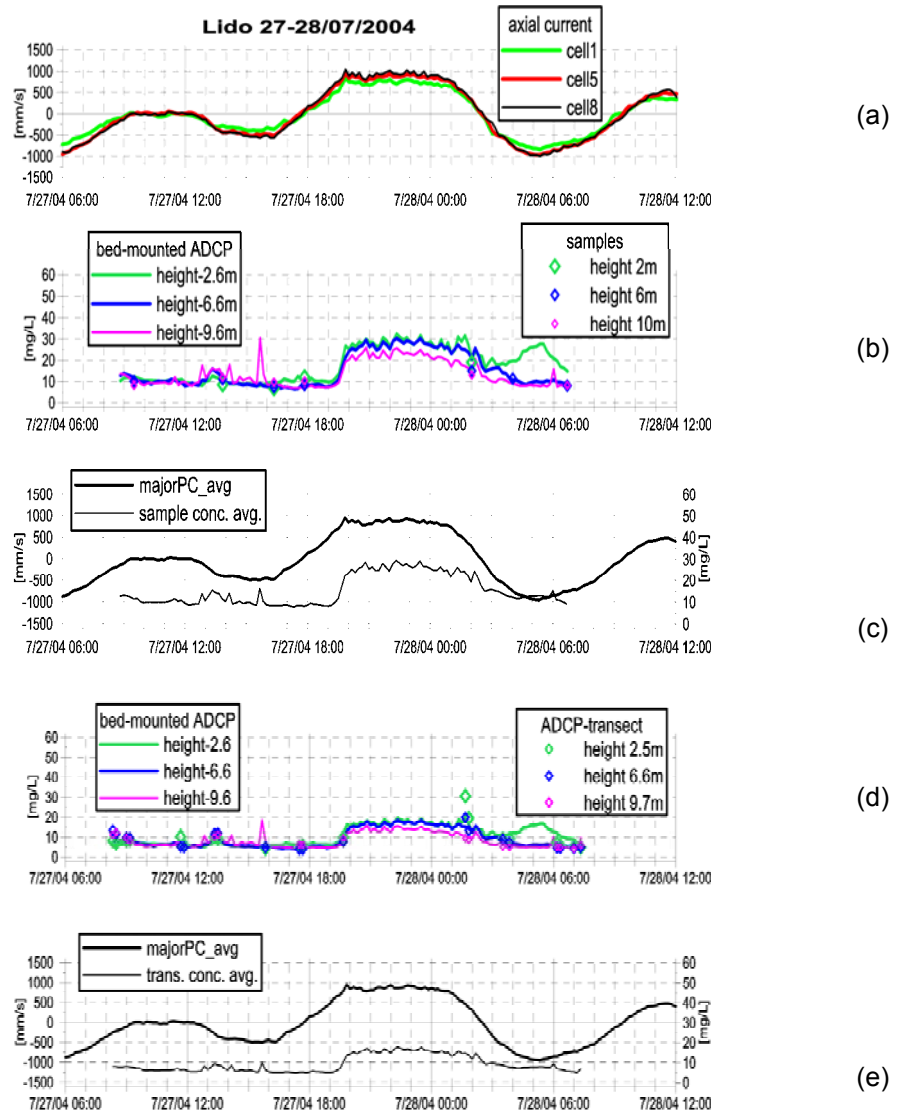


Fig 11 - Time diagram on the 27-28 July: axial current component at three levels, near bed, intermediate and near surface with cell numbers 1, 5 and 8 respectively (a); sediment concentration at three levels corresponding to the cell depths in a, open diamonds - water samples, solid line - ADCP-b values (b); vertically averaged data, axial current is a solid black line and sediment concentration from ADCP-b is a solid grey line (c); same as b but for the samples from calibrated transects of the ADCP-v (d); same as c, but for vertically averaged major concentrations from the calibrated transects (e)

The same colour of the solid line and the symbol denotes the same layer of the water column. It is evident that the sampling data taken into consideration are collected during a moderate current regime (max 50 cm/s). Concentrations are lower during the inflow into the lagoon or during slack waters, while during the outflow from the lagoon the concentration values are higher.

During the inflow, near bottom concentration values increase slightly in correspondence to the maximum current speed, as a probable consequence of the re-suspension. The values from the highest cell located near surface are occasionally disturbed by peaks of high concentrations evident especially during the inflow. Vertically averaged concentrations (Fig. 11c) reflect the pattern seen at three levels, that is the water column is more rich with sediments during the outflow from the lagoon (up to 30 mg/L). The concentration values obtained using the ADCP-v transects are shown in Fig. 11d, for the same three levels, even though the vertical resolution of the transect samples allows comparison at 1 m resolution. In general, the way the sediment concentration varies with time is similar to that obtained from the water samples (Fig. 11b), but the maximum values here do not reach 20 mg/L, while with water samples, the maximum is about 30 mg/L. Accordingly, the vertically averaged concentrations after calibrating the ADCP-b by the ADCP-v (Fig. 11e) are lower than in the case of water samples.

The October survey, coinciding with the spring tide (the full moon), is presented in Fig. 12. The semi-diurnal flow (Fig. 12a) was stronger than in July, and water speed reaches 1.4 m/s. The water samples have been collected at a lower current regime during the first half of the campaign, and near the maximum outflow and inflow during the second half of the survey. Conclusions similar to those observed in July can be drawn, that is, the concentrations of the total suspended matter are higher during the outflow from the lagoon (ebb tide) than during the flood tide. The concentration pattern does not have a distinguished semi-diurnal character, as do the currents. The estimates using the water samples are higher than those using calibrated ADCP-v transects. This results from the fact that coefficient K_S in general is higher when using transect, decreasing consequently the estimated ADCP-b value [DRL-Sediview, 2003; Arena, 2004].

In order to establish the suitable calibration procedure for the ADCP-b, more survey campaigns are going to be analysed, so the number of data will increase and make the estimate statistically more reliable, giving the possibility to evaluate the estimate error as well. The goal is to calibrate the whole time series available from the ADCP-b in Lido, with the best possible pair of coefficient K_S , and S , and establish whether the constant or time dependent values are representing better the sediment variability in the inlet.

In addition, more comparisons will enable treating with a special attention possible difficulties encountered when the ADCP-v concentrations are higher than expected due to the contamination of the backscatter signal by air-bubbles, which are provoked by a ship wake or waves, or when the coupling in time and

space between the ADCP-b and the sampling data (no matter whether they originate from the water sampling or calibrated transects) is not perfect.

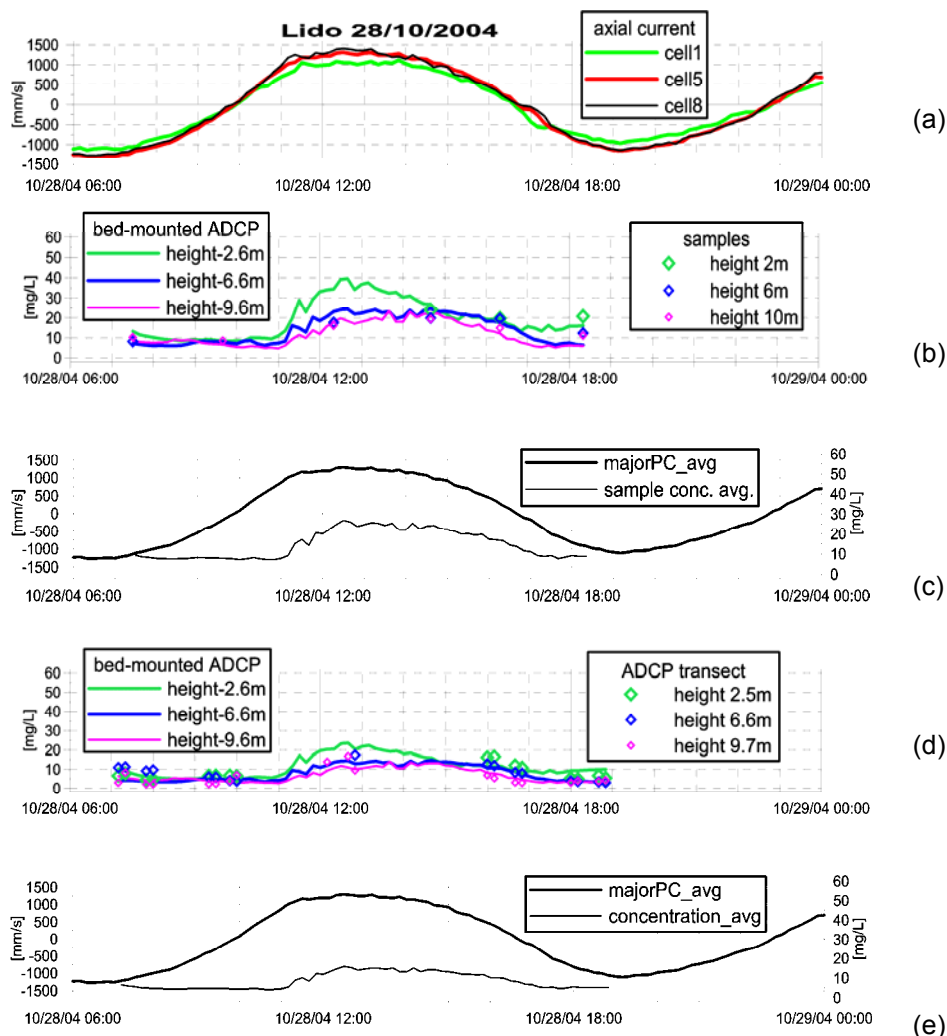


Fig 12 – Same as Fig. 11, except for the 28 October campaign.

References

Arena F. and G. Arcari, 2001. Rapporto tecnico sulle misure correntometriche alle Bocche di Porto di Venezia. Technical Note N. 191, CNR-ISMAR, Sezione di Venezia, Dicembre 2001.

Arena F., 2004. Correntometri acustici autoregistranti – prime calibrazioni dei dati di Backscatter alle Bocche di Porto di Venezia. RELI-47/2004-OGA-18, 48 pp.

Costa F., Defendi V., Zaggia L., 2005a. Campagne di misura per il monitoraggio della produzione di materiale sospeso generato dalle attività di scavo alla Bocca di Porto di Chioggia. Primo Rapporto 15 gennaio 2005, CNR-ISMAR, Venezia.

Costa F., Defendi V., Zaggia L., 2005b. Campagne di misura per stima del trasporto solido alla Bocca di Porto di Lido. Primo Rapporto maggio 2005, CNR-ISMAR, Venezia.

DRL-Sediview, 2003. Acoustic Doppler Current Profiler data processing and analysis. Sediview Procedure Manual. DRL-Software Ltd., July 2003.

Gačić M., Mancero Mosquera I., Kovačević V., Mazzoldi A., Cardin V., Arena F., and Gelsi G., 2004. Temporal Variations of Water Flow Between the Venetian Lagoon and the Open Sea. *J. Mar. Sys.*, 51, 33-47.

MORPHOLOGICAL EVOLUTION AND SAND PATHWAYS IN NORTHERN VENICE LAGOON, ITALY

R. Helsby¹, C. L. Amos¹, G. Umgiesser²

¹ Centre for Coastal Processes, Engineering and Management, University of Southampton, National Oceanography Centre, Southampton, UK, ² ISMAR-CNR S.Polo 1364, Venezia, Italy

Abstract

This paper outlines the morphological changes that have occurred in the approaches to Lido, Lido Inlet, Treporti Canal and Burano Canal between 1930 and 2004. These changes are used to evaluate the sediment transport pathways and net volumes of material in transport. The bathymetric changes have been evaluated on data sets collected in 1930, 1970, 1990, 2000 and 2004. Seabed reflectivity derived from sidescan sonograms and analyses of sand content in samples of bottom sediment show patterns of erosion and deposition as well as sand transport pathways within major morphological features recognised in the study region. This work was undertaken as part of activities defined within Programma di Ricerca 2003-2006 (Allegato A, linea 3.15); that is, to determine non-cohesive sediment exchange between Venice Lagoon and the northern Adriatic.

A link is proposed between the sediment movement in Treporti Canal and the main morphological features of Lido Inlet. The features are: (1) a flood-tidal delta; (2) an ebb-tidal spit; and (3) an ebb-tidal delta. The sand transport pathways indicate that the ebb-tidal features are produced by the net transport of fine sand out of the lagoon and onto the shoreface of the northern Adriatic. The flood-tidal delta, by contrast, appears to be fed by a newly formed sand transport pathway in the flood dominant northern part of Lido Inlet. A south-westerly longshore sand transport on the beaches of Cavallino has formed a beach to the that has prograded seaward to the tip of the eastern jetty. Sand appears to be now passing around the jetty and into Venice Lagoon, where it appears to be contributing to the accumulation of the flood tidal delta

1 Introduction

Venice Lagoon is a restricted, shallow, coastal embayment (Kjerfve, 1994) consisting of a series of canals and mudflats, which are connected to the Adriatic Sea by three inlets. A semi-diurnal micro-tidal circulation from the northern Adriatic flushes the lagoon in 24 hours (CNV, 1996) and results in strong tidal flows in the canals and inlets. The inlets are therefore important sites in controlling the sediment transport and consequent mass balance of the lagoon, despite being confined by long jetties on both sides.

Comparisons between bathymetry collected in 1930, 1970, 1990 and 2000 show that, until 1990, the tidal flats of northern Venice lagoon had accumulated

material at a mean rate of 2 cm/year (Fig. 1A). Since 1990, the region has become deeper at a rate of 5 cm/year (see Fig. 1B).

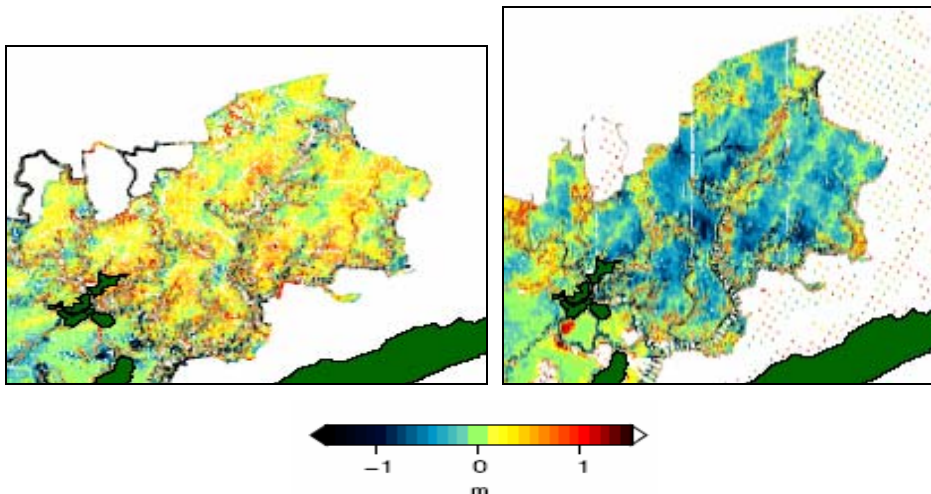


Fig.. 1-Bathymetric comparison of the northern lagoon between 1970 to 1990 (A) and 1990 to 2000 (B).

This study will examine whether this change in trend has been seen within the canals and in the tidal inlet of Lido, which being 900 m wide (Gačić, 2004), is the main conduit to the Adriatic Sea; and if evident, what are the causes of these changes. Umgiesser *et al.* (2005) have predicted that there is a loss of fine sand from the Treporti region to the Adriatic Sea. By contrast, Albani & Serandrei Barbero (2001) have concluded that there is '*no significant mass transport from the lagoon to the gulf*' and cite the apparent lack of ebb-tidal deltas as evidence to this effect. A recent survey off Lido Inlet (Amos *et al.*, 2005) has shown that there is a massive ebb tidal delta off Lido that appears to be classical in form. This delta also appears to be growing. It has been calculated that the mass export of fine grained sediment is $1 \times 10^6 \text{ m}^3/\text{yr}$ (Carbognin & Cecconi, 1997). This (fine) sediment loss is unlikely to be contributing to the evolution of the delta which is composed of sand. There are large areas of sand in the northern lagoon: most of the Lido Inlet, southern Treporti Canal, the margins of Burano Canal and S. Felice Canal (Albani & Serandrei Barbero, 2001). Thus there is a source of sandy material as well as an effective mechanism of transport (Umgiesser *et al.*, 2005). This paper will present the first part of a step-wise analysis of sand transport. That is, the interpretation of morphological changes and the distribution and type of bottom sediments in the regions of morphological change. This will provide the foundation for quantitative analyses of sand transport as defined in Amos *et al.*, (2004).

2 Data collection and analysis

Bathymetric soundings with sidescan sonar were collected in Lido Inlet, Treporti Canal and Burano Canal during February 2003, February 2004 and May 2004.

230 sediment samples were also collected in February 2004 in the Lido Inlet area and Venice Lagoon's beaches and major rivers (see Amos et al., 2005 for details). A further 23 sediment samples collected in Treporti and Burano canals (described in Umgiesser et al., 2005) were included in the analyses.

A single channel echo-sounder (Fishfinder) coupled to a Garmin GPS were used to map bathymetry. NMEA 0182 data strings were logged at 1Hz in ASCII format. A single beam digital sidescan (700 kHz) recorded seabed reflectivity and general morphology online. The bathymetric data were processed to extract: time (GMT); coordinates (latitude and longitude); water depth (m) and water temperature. Tidal corrections were made to reduce soundings to local low water using the tidal predictor of Umgiesser. Seabed reflectivity were determined from sidescan images and assigned mean values that ranged from 1 (lowest) to 30 (highest). Reflectivity is a measure of seabed micro-roughness, grain size and composition. It is largely used to define regions of sand cover as well as to discriminate regions of fine sand (largely derived from the Lagoon) and coarser, micaceous sand (largely derived from the beaches of Cavallino, Gazzi et al., 1973).

Bathymetric data for the entire lagoon were provided by CNR for the periods 1930, 1970, 1990, and 2000. However the approaches to Lido Inlet were surveyed only during 1990 and 2004. Maps were produced of the sidescan and bathymetric data using UNIX programs, primarily GMT (Generic Mapping Tools). Regular grid files of each survey were created and "cleaned" from which surface trends were created illustrating morphology. Surfaces between various years were then subtracted in order to evaluate bed level changes. These changes are presented in a series of colour maps for the entire lagoon, and subsequently in detail for Lido Inlet, and Treporti and Burano canals. Cross sections and associated cross section areas (A) of the canals were also derived for purposes of examining the stability in terms of the standard relationship: $A = xP^n$, where P is the tidal prism at the position of the sections (determined from the model SHYFED).

Subaqueous sediment samples were collected in a 500m spaced grid using a small Van Veen grab. Further samples were collected by hand at 1 km intervals along the barrier beaches of Cavallino, Pellestrina, and Chioggia, and on the tidal flats of Sant'Erasmus. The granulometry was determined by wet sieving to separate the silt, sand, and gravel class sizes. The sand and gravel populations were dried and weighed, and the results subtracted from the initial weight in order to determine fines content.

3 Results

All bathymetry maps show a 15 metre deep channel running along the western edge of the Lido Inlet (a first order channel) and a shallower, 6 metre channel that leads north-easterly towards the second-order Treporti Canal. Field observations substantiated by the model SHYFED show that the deeper navigation channel is ebb dominant and the eastern channel, flood dominant. Associated with these tidal channels are three dominant morphological

structures:

- a shallow flood-tidal delta, joined to the island of Sant'Erasmus, which separates the two flood tidal channels;
- a sub-aqueous ebb-tidal spit (visible only from 1970) off Punta Sabbioni and extending seawards along the eastern edge of Lido Inlet; and
- an asymmetrical ebb tidal delta situated around the Lido Inlet mouth and extending several km seawards.

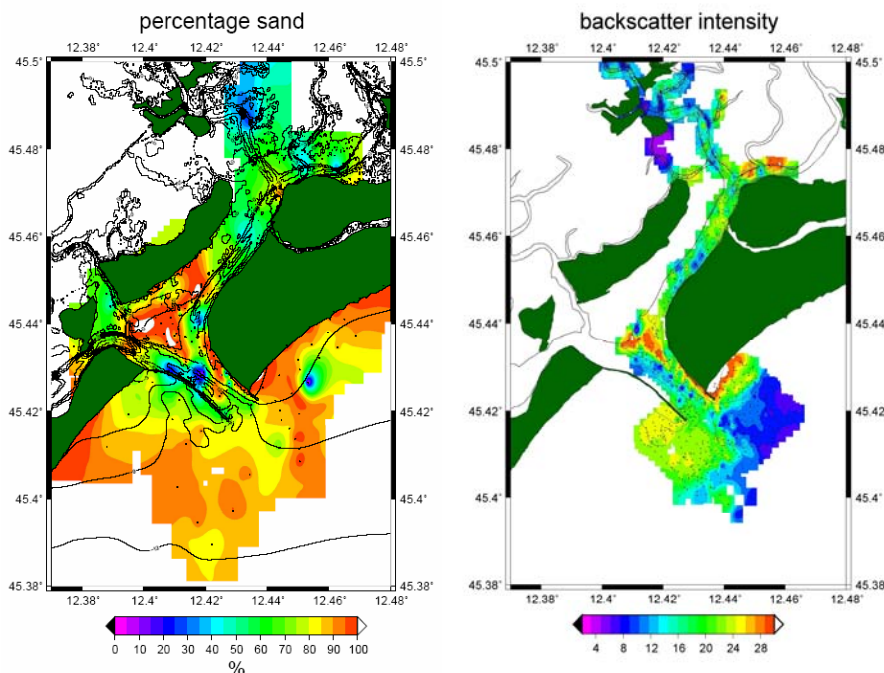


Fig. 2. Percentage sand and backscatter intensity (dimensionless) of Lido Inlet, Treporti Canal and Burano Canal.

The ebb-tidal delta is skewed to the southwest in the direction of long-shore sand transport (Gazzi et al., 1973). Fig. 2 shows that it is composed largely of fine sand (medium reflectivity). The flood-tidal delta and the ebb-tidal spit are also predominantly sandy. Some of this sand appears to be spilling into the main flood-tidal channel. Sand deposition has also taken place in Lido Inlet adjacent to the eastern jetty. The bed of the main channel is 60% sand, which reduces to 30% south of the flood-tidal delta. The percentage of sand southwest of Lido Inlet increases from 75% to 95%; it is this belt of sand that surrounds the Lido Inlet entrance to form the ebb tidal delta, and which is connected to the sand belt of Cavallino Beach. However, about 1 km off Cavallino beach is an area 10% sand, although the extent of this area is unclear from this survey as it is at the edge of the sampling range. The backscatter map shows a large region of low reflectivity, which extends (see Fig.2). Low reflectivity also occurs in the main channel near to the flood-tidal delta and in Burano Canal. High reflectivity occurs in the flood-tidal delta, Cavallino Beach, adjacent to the eastern jetty and

part of San Felice Canal. The remainder of the area is medium high reflectivity.

4 Discussion

4.1 Outer Lido

The outer Lido is dominated by an ebb dominant channel that extends 1.5 km beyond Lido Inlet and by the ebb tidal delta. Scouring up to 4 m deep is prevalent off the jetties and over the extensive ebb tidal ramp. Beyond this ramp deposition is dominant to at least 3 km from the end of the inlet. The ebb tidal delta is thicker and wider towards the south-west and narrow to the north-east due to longshore transport to the southwest. Bathymetric data are currently being collected to determine its extent of the delta. The eastern edge of the delta is bisected by the main navigation channel leading into Lido Inlet, and which appears to have caused some erosion of the ebb-tidal delta.

Erosion of up to 4 m has occurred at the ends of the jetties. Scour off the western jetty is greater than off the eastern one because of the stronger ebb currents in this region. Fig. 3 shows that the erosion extends to the south of the inlet and northeast from the navigation channel. Erosion ends abruptly at a distance between 1 and 2 km from the inlet mouth: within a distance of 500 m, the trend changes from one of net erosion of 1 m to net deposition of 1 m. The region of deposition extends south and west past the limits of the dataset. Thus, at present we cannot estimate at present the volumes of sediment that have been incorporated into the ebb tidal delta. The intermediate seabed backscatter is diagnostic of fine sand similar to that evident in Treporti Canal.

A lateral bar flanks the navigation channel to the north. It is about 1 m high and is linked to the prograding shoreface updrift of the eastern breakwater. It is of high reflectivity and thus coincident with the backscatter off Cavallino. It appears that a portion of the sand moving southwest through longshore transport is being moved seawards to form this feature. The bar has formed subsequent to infill of a large region that had been excavated as part of the jetty extension. This large region shows evidence of progradation of more than 50 m since 1990.

4.2 Lido Inlet

A relatively deep ebb-tidal channel (with an average depth of 12 m) is located along the western edge of Lido Inlet. This channel is flanked by a flood tidal delta, which is attached to and modified by the island of Sant' Erasmo. Also present is a subaqueous ebb tidal spit that extends from Punta Sabbioni and sits between the ebb and flood dominated parts of the inlet (Fig. 4). The water is no deeper than 4 m along its northern flank forming a well defined shelf that continues to the end of the jetty. This shelf is thought to be a sand transport pathway into the lagoon. In general, a comparison between bathymetric surveys show an accumulation of sediment on the south-western flank of the flood tidal delta and over the subaqueous ebb spit. In 1930 (the first dataset), the ebb-tidal spit did not exist.

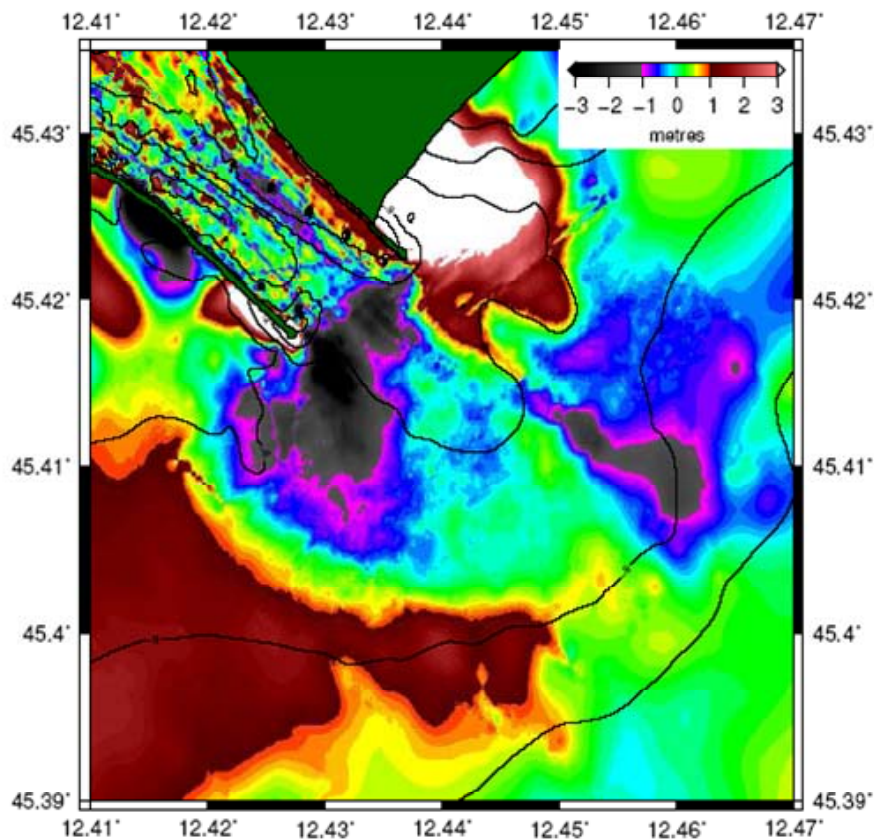
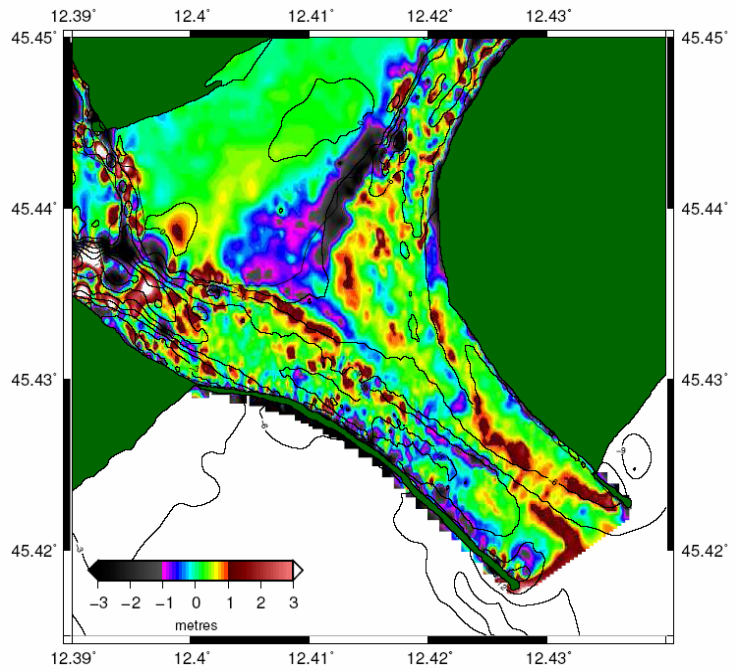
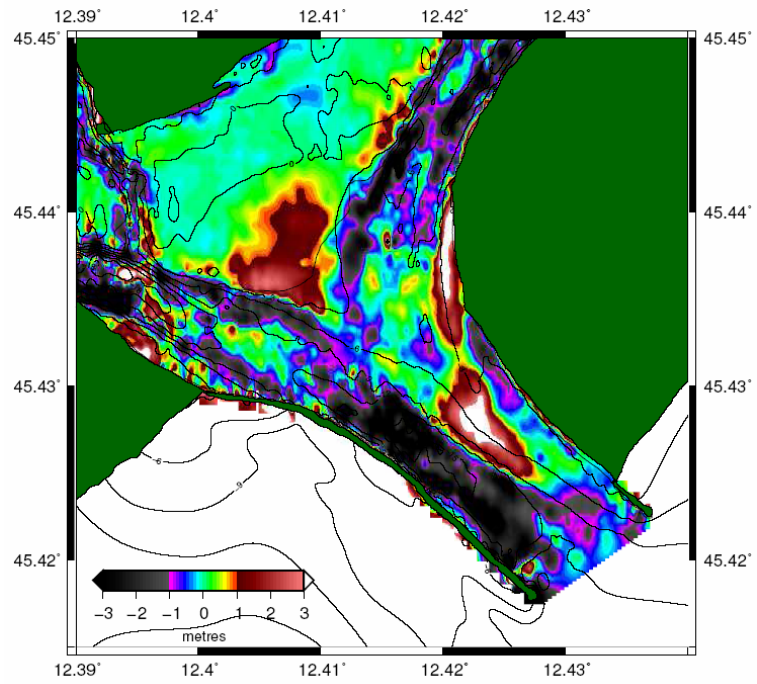


Fig. 3 Comparison of bathymetry between 1990 and 2004 showing part of the ebb-tidal delta. Contours are from the 2004 dataset.

However, it has prograded into Lido Inlet a distance of about 500 m since 1930 and has a present height of almost 3 m. Fig. 2 shows that sand extends into the ebb-tidal channel from the end of the subaqueous spit. The shape of the spit suggests that the sand is derived from Treporti Canal. The flood-tidal delta has grown at a similar rate to the spit since 1930. The delta has prograded south to form a promontory between the two main tidal channels: S. Nicolo and Treporti. Between 1970 and 1990 however, the delta suffered an erosion of between 0.2 and 1 m. Since 1990, the delta has been prograding once again. An average of 3 m of sediment was deposited as an ebb-tidal spit, which extended 1.5 km from Punta Sabbioni into the Lido Inlet (see Fig. 4). Despite beginning as a streamlined feature, the ebb spit widened to about 300 m on reaching the centre of Lido Inlet where up to 5 m of sediment was deposited. The spit is at its narrowest where the two tidal channels converge. Adjacent to the spit in the western channel, an average of 3 m of sediment was removed. This may be a natural response to the formation of the ebb tidal spit. The flood tidal delta, separating the two tidal channels, has remained relatively stable during this period, although up to 3 m of deposition has occurred on the southern flank. Lido Inlet experienced slightly deposition (2cm/yr) in the period 1970 to 1990. The ebb tidal spit had a maximum deposition rate of 5cm/yr.



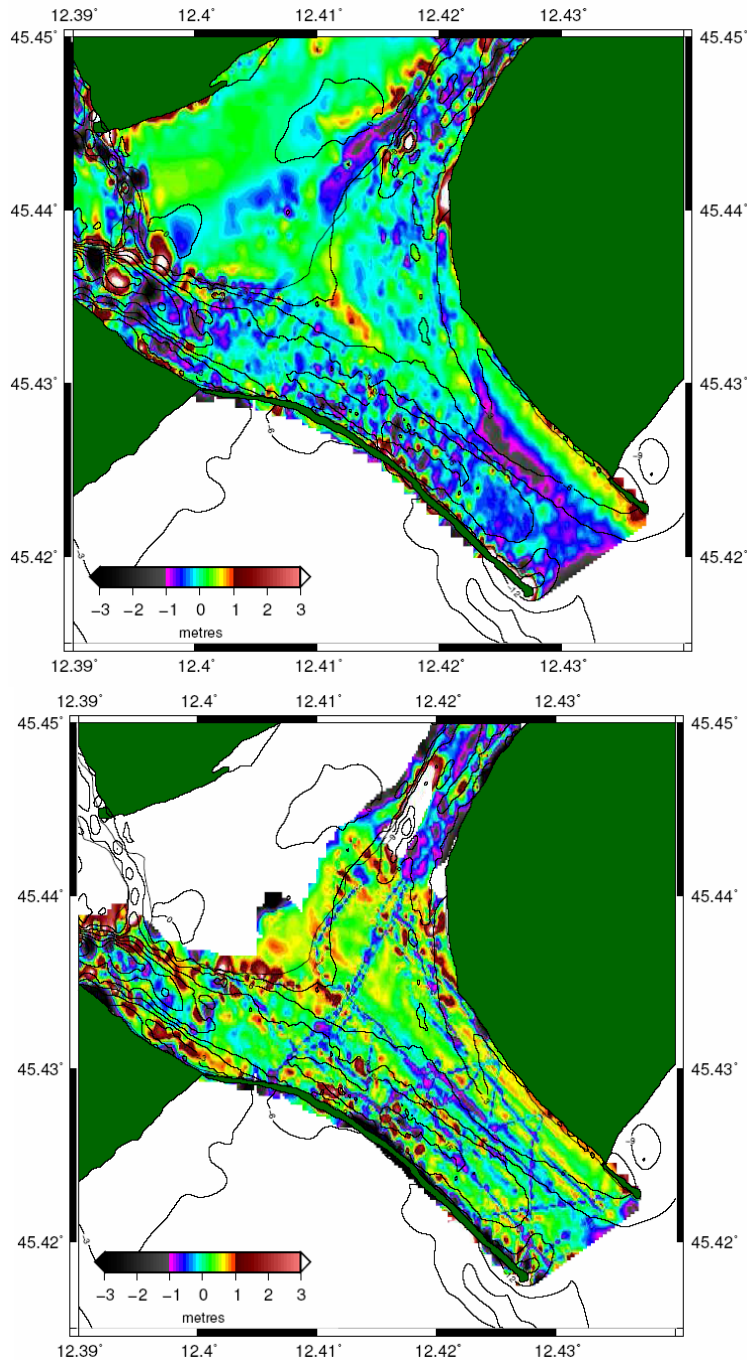


Fig. 4. Bathymetric comparisons from top : 1930-1970; 1970-1990; 1990-2000; 2000-2004.

A zone of accumulation extending from the end of the eastern jetty to the ebb tidal spit could be diagnostic of sand moving into the lagoon. The most obvious change in this time period was the removal of sediment from the flood tidal delta; an average of 0.7 – 1 m was removed over the intervening 20 years. Major engineering works to protect the island of Sant' Erasmo from flooding occurred in the late 1980's. The role of this on sediment accumulation on the flood tidal delta is unclear.

The flood tidal delta became depositional again during the period 1990 - 2004; a maximum of 50 cm accumulated in this time. It appears that the delta was slowly prograding to the southeast into Lido Inlet, as 70-100 cm of sediment was deposited between the two major tidal channels. The most prominent region of deposition was adjacent to the eastern jetty; a deposit of 2 m formed that extended 100 m to the west from the head of the jetty. This may be sediment coming into the lagoon, as other parts of the lagoon have been dredged (clearly seen by the removal of 2 m of sediment from the end of the ebb-tidal spit).

Three cross-sectional profiles (west to east) across Lido Inlet show and compares the bathymetry for all the datasets. It is clear that the inlet is relatively stable; from 1970 to 2004 the greatest change was less than 1.8 m. The exception to this is evident in the middle Lido profile (Fig. 5), where the ebb-tidal spit is prograding. 387 m² of sediment (in the area indicated in Fig. 5) has been deposited over the spit between 1930 and 1970. Conversely, about the same amount of sediment was removed during the same time period from the main channel.

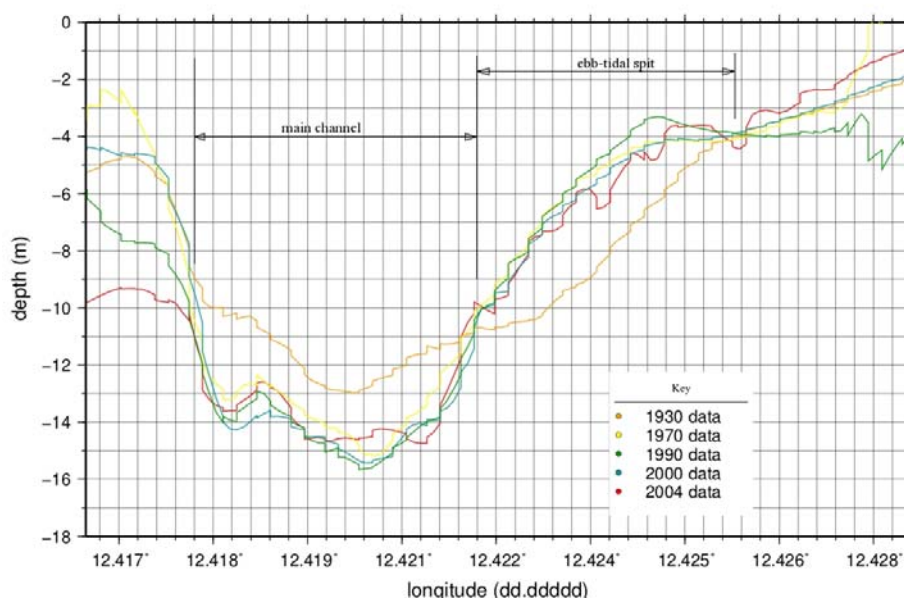


Fig. 5 Cross-sectional profile of midway up the Lido Inlet, showing the depth in 1930, 1970, 1990, 2000 and 2004.

4.3 Treporti Canal

The average depth in Treporti Canal is 7 m, although this increases to around 10 m adjacent to Punta Sabbioni. The predominant feature in this area is a 20 m deep scour hole at the triple junction of Treporti, Burano and San Felice canals. The lee of this scour hole stretches back along Treporti Canal suggesting that scouring occurs mainly during the ebb tidal phase when the waters of Burano and San Felice canals converge. Treporti Canal exhibits net erosion between 1930 and 2004, especially at the edges of the channel where

up to 4 m have been removed. The centre of the canal has also lost an average of 3 m of sediment, which may be due to dredging as this channel is flanked by depositional bars. These bars have accumulated about 1 m since 1930, but are, nevertheless, the most prominent depositional feature in Treporti Canal. This trend incorporates a period of relative stability wherein depth remained within +/- 1 m between 1970 and 2000.

The Treporti scour hole has not extended further up the San Felice Canal but has instead become streamlined. This can be seen in Fig. 6 which shows erosion of over 5 m at the northern tip and at the eastern edge, and deposition of an equal scale on the western edge .

Except for two depositional bars either side of the central channel, Treporti Canal suffered net erosion between 1930 and 1970, losing sediment at an average rate of 3.5 cm/yr. The sides of the canal are highly eroded (over 4 m in places). Treporti Canal was stable during the period 1970 to 1990; no distinct regions of erosion or deposition were detected, although it can be seen that the centre of the channel was still eroding. Between 1990 and 2000 Treporti Canal appears to have ceased depositing sediment in bars flanking the central channel and became entirely erosional. The canal deepened an average of 1 m near Treporti, and a slightly greater amount near Lido Inlet.

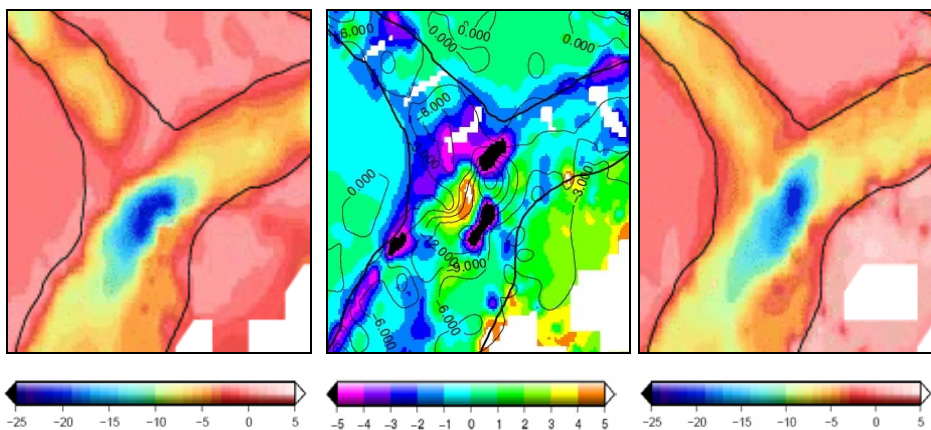


Fig. 6 From left to right; bathymetry 1930, comparison between 1930 & 2000, bathymetry 2000. Warm colours denote areas of deposition, cool colours denote areas of erosion. Scales all in metres.

The net erosion throughout Treporti Canal is clear from the cross-sectional profiles from all datasets. In the first profile, situated just past the influence of the flood tidal delta of Lido, the morphology of the channel changes from a single 'u' shaped channel in 1930 to a 'w' shaped channel in 1970. The depth of the channel increased significantly (2-3 m) from 1930 to 1970, suggesting dredging. From 1970, depth continued to increase in the main channel, causing the form to become increasingly 'v' shaped. The second cross-sectional profile (upstream of the first) also shows a change in morphology from 1930 to 1970 and a stable 3 cm removal of sediment in the main channel from 1970 to 2004.

The morphology here is not 'v' shaped as the previous profile. This can also be seen with the profile running across from Treporti, which, although still slightly erosional, has been stable since 1990. Here, an average erosion of 1 m has taken place since 1970. Interestingly, in this profile, the original 1930 morphology was a 'w' shape, which has become increasingly 'u' shaped, in opposition to the other profiles.

4.4 Burano Canal

Burano Canal is about 4 m deep on average, but has 5 main scour holes that currently reach a maximum depth of 17 m. Most of these scour holes occur at the confluences of minor canals such as Crevan Canal. However, the largest one occurs at the edge of a 90° corner in Burano Canal. These scour holes all lee towards Treporti Canal, suggesting that there are greater turbulent eddies formed during the ebb tide than the flood.

In Fig 7 it can be seen that in the 40 years from 1930, Burano Canal was a region of net deposition, accumulating an average of 2 m. This led to the infilling of scour holes at triple junctions. Only near the confluence of Treporti Canal is there any significant erosion. In the 30 years following 1970, the trend was of net erosion and the canal deepened an average of 1 m. During this period, the scour holes began to expand once again and erosion of up to 3 m occurred within them. This eroded sediment, if carried downstream, may have contributed to the infilling of the northern lobe of Crevan-Burano scour hole, which shallowed in excess of 5 m in this time.

Between 1930 and 1970, Burano Canal exhibited 2 m of accumulation. In the same time period, scour holes present at triple junctions appeared to be moving in the flood tide direction, scouring the sediment at a rate of between 12 cm/yr to 25 cm/yr (at Crevan-Burano junction), whilst infilling the lee of the hole at a similar rate. This suggests a flood dominance of the region. Net infilling of scour holes occurred at the bend of Burano Canal and at the Mazzorbo-Burano Triple Junction, with 7 metres of sediment being deposited at the latter, enough to reduce its size by a third in 40 years. Only the scour hole at Crevan-Burano eroded significantly during this time, expanding in all directions (although predominantly in the flood-tide direction) by removing 2 - 10 m of sediment. A reversal of trend, saw Burano Canal become net erosional, losing an average of 1 m in 30 years. However, in the same period the scour holes became depositional in areas where they had been erosional between 1930 and 1970, reducing in size by half. Only the Crevan-Burano scour hole continued to erode at a rate of 10 cm/yr and doubled its size by extending in both directions along Burano Canal.

Although still net erosional between 1990 and 2004, Burano Canal seems to have stabilized to a degree, with some areas experiencing up to 1 m of erosion, and others, deposition to the same amount. The scour holes at the triple junctions have become erosional, removing up to 7 m of sediment in the ebb-

tidal direction along Burano Canal. This amount of sediment being transported down Burano Canal has overwhelmed the scour hole at Crevan-Burano, as the north-westerly lobe has been almost completely filled in, representing about 10 m reduced depth.

4.5 Sand occurrence and reflectivity

Two major areas of sand occur on the flood tidal delta, and on the ebb tidal spit. In both cases, sand appears to have spilt over into the main navigational channel. As previously discussed, the ebb tidal spit has been extending into the Lido Inlet since at least 1970. Therefore, it is reasonable to assume that this is still an active process. The morphology of the spit suggests that the sand is being exported from the lagoon from Treporti Canal. It may be no coincidence that from 1970, when Treporti Canal became net erosional, the spit began to be a significant feature in Lido Inlet. This feature is not represented strongly in the backscatter map.

The flood tidal delta is, however, clearly represented in both the sand percentage map and the reflectivity map. In both maps it is possible to see sand that appears, by virtue of its decreased width, to be entering the inlet from Cavallino Beach to the north. This may be a source of the sand which is being deposited in the flood tidal delta and indeed both features appear to share the only occurrence of high backscatter in the reflectivity map. The fact that the ebb tidal spit is not visible in the reflectivity map, unlike the other major deposits of sand, may signify two separate sand types and therefore indicate different provenance and transport pathways. Immediately southwest of the western jetty is a large area of relatively low percentage sand (70-85%), which is echoed in the reflectivity map. From field observations it is known that this area is very shelly.

5 Conclusions

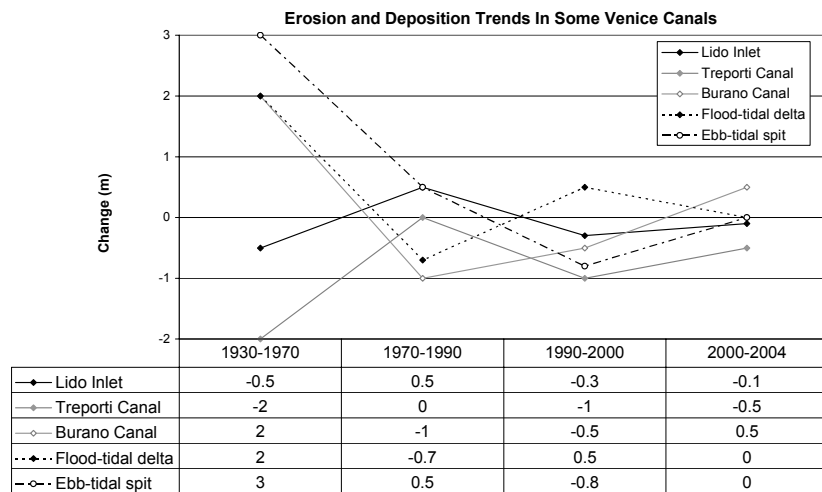
Using these various methods of analysis, it is possible to see that, between 1930 and 1970, Burano Canal was depositing around 2 m of sediment. This sediment is likely to have come from erosional regions of the surrounding salt marshes (although they were mainly stable or depositing). This sediment appears to have been deposited as an ebb tidal spit at the end of Treporti Canal, although does not seem to have been deposited in Treporti Canal, as this channel was net erosional. Lido Inlet was only slightly erosional on average, although the level of sand deposition of the ebb tidal spit was matched by the level of erosion in the adjacent tidal channel.

Between 1970 and 1990, the salt marshes of northern Venice Lagoon were highly depositional resulting in Burano Canal becoming erosional due to a reduction in sediment import. This eroded sediment from Burano Canal appears to have stabilised the erosion in Treporti Canal, before it was transported and deposited in Lido Inlet.

In the decade between 1990 and 2000, the salt marshes underwent a high level

of erosion; Burano Canal was still slightly erosional, although it appears it was in transition to becoming net depositional (as can be seen in the comparison between 2000 and 2004). Treporti Canal had once more become erosional (at a rate of about 0.1 m/yr) as less material was available from the erosion of Burano Canal to continue to stabilize it. Although slightly erosional, Lido Inlet has remained relatively stable from 1990 to present day (2004), with the ebb tidal spit being controlled anthropogenically.

Our results clearly disagree with the conclusions of Albani et al., (1998; 2001) and Rickwood et al., (1992), who stated that there was no discernable ebb tidal delta off Lido. It is clear from the data collected in 2004 that there is a distinct deposition of sand with a clear ebb channel, terminal lobe and channel margin linear bars, surrounding the exit of Lido Inlet (terminology from Mitello & Hughes, 2000).



Tab 1. Table and graph of estimated sediment erosion and deposition by change of depth in metres.

Comparing this data with data collected 14 years previously, it is also apparent that the delta is growing, with the appearance of swash bars. Also apparent however, is the appearance of a sand transport pathway into Venice Lagoon from the longshore transport from the northeast off Cavallino. It is possible that this sand is entering with the flood tide and being deposited on the flood tidal delta, as is shown on the reflectivity map (Fig. 2); Alabani & Serandrei Barbero (2001) have also stated this possibility.

Further grain trend analysis and mineralogical analysis will be undertaken on the sediment samples collected for this linea, therefore, it is hoped that assumptions taken on sand pathways in this paper will be proven one way or another.

References

- Albani A.D., Favero V.M. and Serandrei Barbero R., 1998, Distribution of sediment and benthic foraminifera in the Gulf of Venice, Italy. *Estuarine, Coastal and Shelf Science* 46, 251-265.
- Albani A.D. and Serandrei Barbero R., 2001,. the Distribution of Surface Sediments in the Lagoon of Venice (Italy) in the 1980s. Extract from "Atti Dell'Istituto Veneto di Scienze, Lettere ed Arti" Tomo CLIX (2000-2001) – Classe di scienze fisiche, matematiche e naturali.
- Amos C.L., Helsby R. and Friend P.L., 2004., Final report – CORILA 3.2 – Idrodinamica e morfologia della laguna di Venezia (VELMA). Final Report to CORILA, Venice: , 23p.
- Amos C.L., Umgiesser G., Reed P., Munford G. and Lea J., 2004., The residual tidal circulation and organics in northern Venice Lagoon, Italy. In "Scientific Research and Safeguarding of Venice. Research programme 2001-2003, Volume II", 189-202.
- Amos C.L., Helsby R, Umgiesser, G., Mazzoldi, A. and Tosi, L. 2005, Sand transport in northern Venice Lagoon. In "Scientific Research and Safeguarding of Venice. Research programme 2001-2003, Volume III, 369-384.
- Bonardi M., Tosi L. and Rizzetto F., 2002., Mineralogical Characterization of the Venice Lagoon top sediments. In "Scientific Research and Safeguarding of Venice. Research programme 2001-2003, Volume II", 145-155.
- Bondesan A. and Meneghel M., 2004., Geomorphologia della Provincia di Venezia, Publ. Estrada, Padova: 516p.
- Bondesan, A. et al., 2004., The Geomorphological Map of the Province of Venice. La Cartografia, Publ. Provincia di Venezia.
- Bruun P., 1978., Stability of Tidal Inlets, Theory and Engineering. Elsevier Scientific Publishing Company, Amsterdam,. 506pp.
- Coracci E., Umgiesser G., Scalvo M. and Amos C.L., 2004, Modeling sand transport in the Venice Lagoon inlets. In "Scientific Research and Safeguarding of Venice. Research programme 2001-2003, Volume II", 157-173.
- Carbognin L. and Cecconi G., 1997., The Lagoon of Venice – environmental problems, remedial measures. Meeting of Environmental Sedimentology, IAS, 71p.
- Coastal Engineering Manual. 1998., Engineering Design. COASTAL GEOLOGY. Publ. Dept. of the Army, Washington, Manual No. 1110-2-1810 .
- Consorzio Venezia Nuova., 1996., Measures for the Protection of Venice and it's Lagoon.
- Fitzgerald D.M., 1988. Shoreline erosional-depositional processes associated with tidal inlets. In "Hydrodynamics and Sediment Dynamics of Tidal Inlets". Publ. Springer-Verlag, 189-225.

Gačić M. and Solidoro C., 2004., Lagoon of Venice. Circulation, Water Exchange and Ecosystem Functioning. *Journal of Marine Systems Special Issue 51*, 359p.

Gazzi P., Zuffa G.G., Gandolf G. and Paganelli L., 1973., Provenienza e dispersione litoranea delle sabbie delle spiagge adriatiche fra le foci dell'Isonzo e del Foglia: inquadramento regionale. *Memorie della Società Geologica Italiana 12*, : 1-37.

Kjerfve B, and Magill K.E., 1989., Geographic and hydrodynamic characteristics of shallow coastal lagoons. *Mar Geol 88*, :187-199.

Kjerfve B., 1994., Coastal lagoon processes. Elsevier Scientific Publishing Company. Amsterdam,. 577 pp

Mitello A. and Hughes S.A., 2000., Circulation Patterns at Tidal Inlets with Jetties. ERDC/CHL CETN-IV-29, U.S Army Engineer Research and Development Center, Vicksburg, MS

Oertel G.F., 1982., Inlets, marine-lagoonal and marine fluvial. In "The Encyclopedia of Beaches and Coastal Environments". M.L. Schwartz (ed) Publ. Hutchinson, Ross, : 489p.

Rickwood P.C., Albani A.D., Favero V.M. Serandrei Barbero R., 2002., The geochemistry of unconsolidated sediments from the Gulf of Venice, Italy Technical Contribution Series. 3. Centre for Marine Science, University N.S.W., Sydney.

Umgiesser G., Sclavo M., Carniel S. and Bergamasco A., 2004., Exploring the bottom stress variability in the Venice Lagoon. *Journal of Marine Systems 51*, : 161-178.

Umgiesser G., Ferrarin C., De Pascalis F. and Amos C.L., 2005., Modeling sand transport in a canal system, northern Venice Lagoon. In "Scientific Research and Safeguarding of Venice. Research programme 2001-2003, Volume II", 177-192.

Weltje G.J., 1995., Unravelling mixed provenance of coastal sands: The Po Delta and adjacent beaches of the Northern Adriatic Sea as a test case. In "Geology of Deltas" Oti M.A. and Postma G. (eds), Balkema, Rotterdam,. 181-202.

ASSESSING LONG-TERM CHANGES IN THE KINEMATICS OF INLETS OF THE VENETIAN LAGOON

Mancero Mosquera¹, M. Gačić¹ and A. Mazzoldi²

¹*Istituto Nazionale di Oceanografia e di Geofisica Sperimentale – OGS, Trieste,* ²*Istituto di Scienze Marine – Consiglio Nazionale delle Ricerche (ISMAR-CNR), Venice*

Riassunto

Sono state analizzate le variazioni, su lungo tempo, dei flussi d'acqua attraverso le tre bocche di porto di Venezia, cercando di evidenziare l'eventuale influenza delle dighe foranee costruite di fronte alle bocche di Malamocco e Chioggia negli ultimi due anni. I flussi medi mensili e le deviazioni standard mostrano variazioni sul lungo termine, mediamente su scala stagionale. Statisticamente, cambiamenti nell'orientazione degli assi principali non coincide con la costruzione delle dighe foranee. Inoltre, non sono state individuate importanti variazioni nell'ampiezza delle oscillazioni mareali associabili alle stesse dighe.

Abstract

Long-term variations of the water flow through three Venice lagoon inlets have been analysed seeking possible influence of external barrier that were erected during the measurement period in front of the two inlets (Malamocco and Chioggia). Monthly mean flows and its standard deviation show long term variations, mainly on the seasonal time-scale. Statistically significant changes in the orientation of the polarization axes do not coincide with the barrier erections. Important changes in the amplitude of tidal oscillations possibly associated to barriers have not been documented either.

1 Introduction

Since February 2001 bottom-mounted ADCP measurements have been carried out continuously in the three inlets of the Lagoon of Venice. The long-term records have revealed spatial and temporal characteristics of the flow field and of the water exchange between the lagoon and the open sea that are presented in a series of papers published recently (Gačić et al., 2002; Gačić et al., 2004; Gačić et al., 2005). One of the prominent features of the inlet flow was a very high contribution of tidal currents to the total flow variance that in average reaches even more than 95%. Another important property of the water flow is a strong polarization approximately along the geometrical axis of inlets due to the channel walls constraint. Cross-inlet current components are negligible. Thus, all the data analyses have been performed on the inflowing currents defined as components projected on inlet axis that are responsible for about 99% of the total flow variance. The long-term current records that started in 2001 give also

the possibility to evidence possible low-frequency, seasonal or even year-to-year variations of the inlets' flow properties (Gačić et al., 2005). In 2003, barriers have been constructed in front of Malamocco (March, 2003) and Chioggia (November, 2003) inlets within the framework of the MOSE project for the Venice lagoon defence against the "acqua alta" events. They may change characteristics of the flow in inlets. The aim of this paper is to investigate long-term changes in the current flow characteristics in the inlets in general or as a possible consequence of the barrier constructions.

2 Results and discussion

2.1 Analysis of the major variance axis variations

As shown before, current variability in the inlets is highly polarized along axis of the major current variance. Maximum variance axes are obtained via Principal Component Analysis - PCA (Preisendorfer, 1988). They do not necessarily coincide with the physical (geometric) axis of the inlets due to variability introduced by the bottom topography in inlets. Vertically averaged currents in the inlets are then presented in a new coordinate system, one along the axis of maximum variance of the data, while the second one aligned with the minimum variance direction. The new coordinate system satisfies the second-order statistical independence for which the current components are linearly independent. The percentage of the variance explained along the first principal axis (maximum variance axis) is higher than 99% in each inlet. As an example, inclination angles for September 2003 are shown in the following table, in degrees with respect to the East, defined positive counter-clockwise.

	Geometric	Navigable	1st PC
Lido	-13	-30	-44
Malamocco	-19	-19	-17.51
Chioggia	-5	-5	-9.54

Navigable axis is the one parallel to the navigation channel within the inlet that is not necessarily parallel to the geometric inlet axis as it is the case with Lido. One can see that the polarization axis orientation is rather close to either a geometric or navigable axis except for Lido, the largest inlet that is also characterized by a rather complicated geometry and bathymetry. For Lido the currents polarization angle seems to be closer to the navigable channel orientation than to the geometric axis.

In order to assess if the polarization angles of the currents in the inlets vary with time and whether some changes were induced by the barriers, PCA is applied on a monthly data subsets. Subsequently the temporal evolution of the orientation angle of the major variance axis was presented (Fig. 1). If the barriers did not influence the polarization angles, PCA results would show that

the orientation of the major variance axis does not depart, statistically speaking, from the mean values or that significant changes did not occur simultaneously with the barrier erection. Presented figures illustrate temporal variations of angle of the principal axes for currents in Lido, Malamocco and Chioggia inlets.

Circles indicate points of changes in the angle estimated from statistical tests based on the normalized cumulative sums, under the null hypothesis H_0 :

$$H_0 : \mu_1 = \mu_2 = \dots = \mu_n$$

Statistically significant changes do not coincide with the barrier constructions and thus presumably they do not influence the polarization angle.

In order to quantify the differences in angle before and after the point of the statistically significant change we show the values of the mean angle in degrees calculated for the entire period before and after the estimated point of change (Tab. 1). Mathematical convention is used, i.e. positive counter-clockwise, zero eastward. Important differences before and after the statistically significant angle variations are noted only in Lido and Malamocco, however this change, as mentioned before, does not seem to be associated with the barrier construction.

Angles	point of change	before	after
Lido	March/2003	-47.6	-49.7
Malamocco	January/2003	-19.1	-17.4
Chioggia	May/2003	-10.9	-10.2

Tab. 1

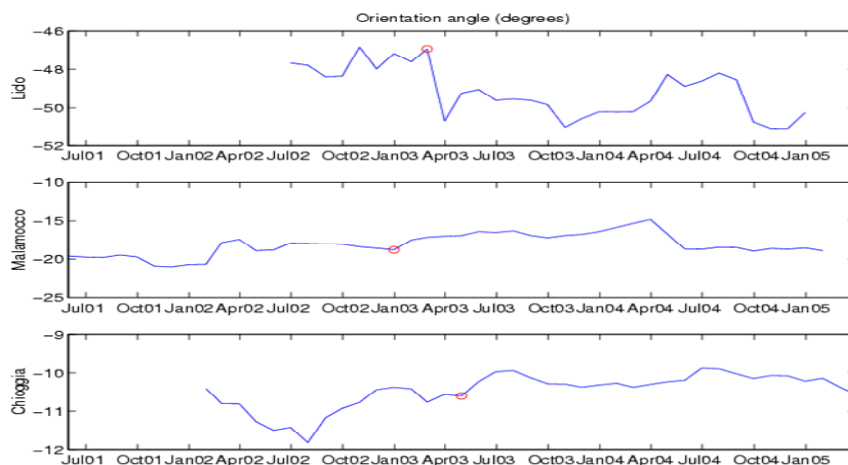


Fig. 1: Monthly mean orientation angle of the maximum variance axis for the three inlets. The angle is defined with the geographical East, negative values means clockwise sense from the east.

In order to seek possible long-term changes in the mean flow and its standard deviations monthly values were calculated for each inlet. Time-series of monthly values of either mean flow or standard deviation (Fig. 2 and 3) show that no prominent long-term change occurs that could possibly be attributed to barrier construction. As one can see, there is a good agreement with previous studies which indicated a prevalent inflow in Lido and an outflow in Chioggia (Gacic et al., 2005). On the other hand, rather prominent seasonal variability in the water exchange is evident in Lido and Chioggia with a maximum inflow and outflow, respectively, in late autumn/early winter. Conversely, monthly mean water flow in the inlet of Malamocco does not show any significant seasonal signal. Time-series of the flow standard deviations show different behavior in Malamocco where the most prominent seasonal signal occurs. Lido shows slightly weaker seasonal signal in the standard deviations, while in Chioggia the seasonal signal can hardly be distinguished from the background noise.

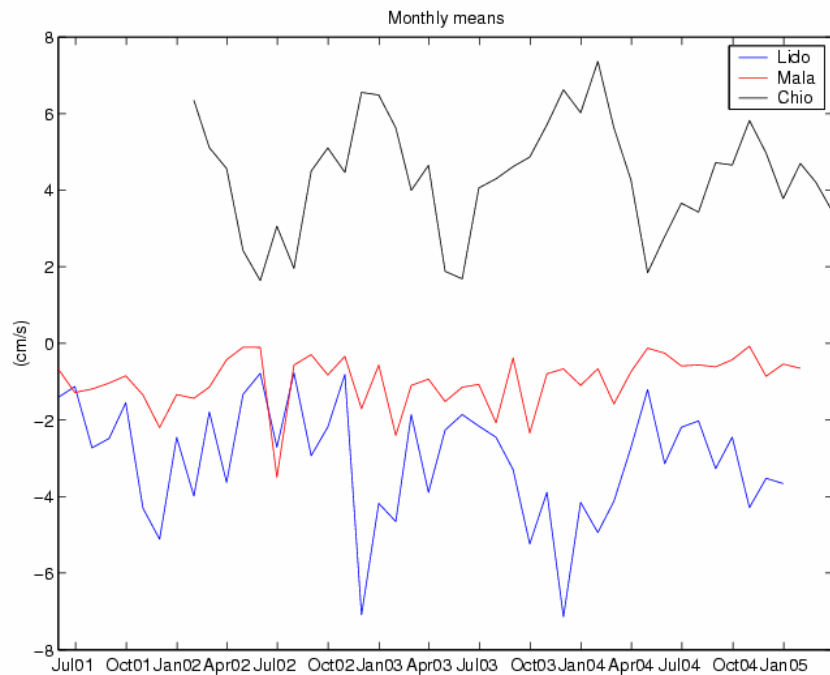


Fig. 2: Monthly mean current component along the maximum variance axis of the three inlets. Negative values stay for the inflow.

2.2 Long-term variations of tidal parameters

Harmonic analysis was applied in order to determine whether any variability in tidal parameters occurred as a consequence of a barrier construction. This technique allows to separate variability due to astronomical forcing by fitting a sum of well known constituents to currents time-series via least-square method. Explained variance due to astronomical forcing in the Venice lagoon inlets reaches about 95% of total variability as already reported in previous papers (see e.g. Gacic et al., 2001). The most important group of constituents is the semidiurnal one with M2 as the most energetic constituent. For current vector

time-series from harmonic analysis, the following estimates of ellipse parameters can be obtained: major-axis amplitude, minor-axis amplitude, phase, orientation angle, and errors of each one.

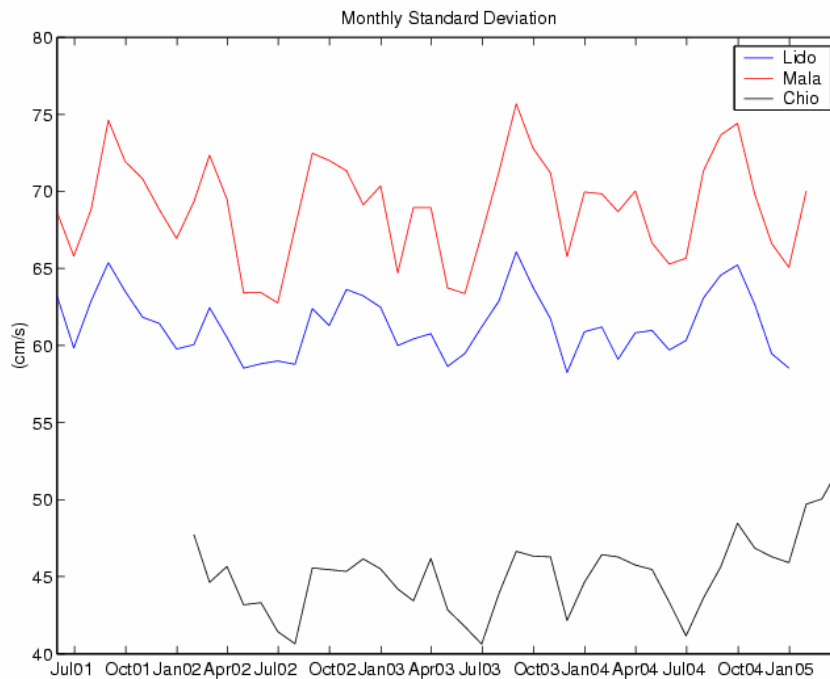


Fig. 3: Monthly standard deviations of the current component along the maximum variance axis of the three inlets.

As expected, tidal variability is also polarized along channel axes anyway, hence estimates of major-axis amplitudes were considered only. The three strongest reported constituents, namely M2, S2 and K1, have been analyzed, and they account for about 87% of total currents variability.

The following table shows results for Lido, Malamocco and Chioggia inlets for two distinct year-long periods that started on 17th June 2001 for the first two. Recording in the Chioggia inlet initiated later so one-year long periods started at 12th February, 2002. So it was possible to compare amplitudes of semi-major axes of these constituents at the beginning and at the end of the available records. Error of amplitudes are also shown in order to see if changes are significant or not.

Since harmonic analysis was applied to PC-decomposed time series, the inclination angle is not absolute but relative to the Principal Axes obtained from PCA. So we present the departures of the orientation angle from the Principal Axis orientation and, in order to estimate if changes are significant, we provided also the errors.

Lido			
		2001-2002	2004-2005
Amplitudes	M2	662.7	660.4
(mm/s)	S2	387.8	382.0
	K1	270.5	273.5
Amplitude	M2	12.2	9.6
errors	S2	10.2	11.8
(mm/s)	K1	16.8	16.2
Inclination	M2	0.02	0.02
(degrees)	S2	0.02	-0.03
	K1	0.18	0.05
Inclination	M2	0.3	0.3
error	S2	0.6	0.4
(degrees)	K1	0.4	0.3
Malamocco			
		2001-2002	2004-2005
Amplitudes	M2	749.251	748.011
(mm/s)	S2	448.302	449.178
	K1	279.661	282.411
Amplitude	M2	12.902	12.105
errors	S2	15.216	11.364
(mm/s)	K1	20.342	15.485

Inclination	M2	-0.01	0.02
(degrees)	S2	0.07	-0.03
	K1	-0.07	0.04
Inclination	M2	0.08	0.09
error	S2	0.13	0.13
(degrees)	K1	0.14	0.18
Chioggia			
		2002-2003	2004-2005
Amplitudes	M2	481.369	495.822
(mm/s)	S2	284.122	296.15
	K1	178.535	190.674
Amplitude	M2	9.784	9.478
errors	S2	10.034	10.667
(mm/s)	K1	10.369	14.344
Inclination	M2	0.01	-0.03
(degrees)	S2	-0.03	0.02
	K1	-0.01	0.09
Inclination	M2	0.1	0.06
error	S2	0.16	0.1
(degrees)	K1	0.18	0.12

Finally, also percentages of explained variance of the three constituents are presented for Lido, Malamocco and Chioggia in the following table.

Lido		2001-2002	2004-2005
%	M2	58.0816	57.9601
Explained	S2	19.8904	19.3931
Variance	K1	9.6726	9.9372
Malamocco		2001-2002	2004-2005
%	M2	59.0571	58.6716
Explained	S2	21.1425	21.1567
Variance	K1	8.2278	8.3632
Chioggia		2002-2003	2004-2005
%	M2	58.7286	56.8725
Explained	S2	20.4599	20.29
Variance	K1	8.0787	8.4107

As evident from the presented data, possible changes in the amplitude are statistically significant for all three constituents only in the inlet of Chioggia where the amplitude increased for about 1 cm/sec from the 2002-2003 to 2003-2004. On the other hand, it is interesting to evidence a significant reduction of the contribution of the M2 constituent in the Chioggia inlet to the total flow variance suggesting an increase of the non-tidal flow variability.

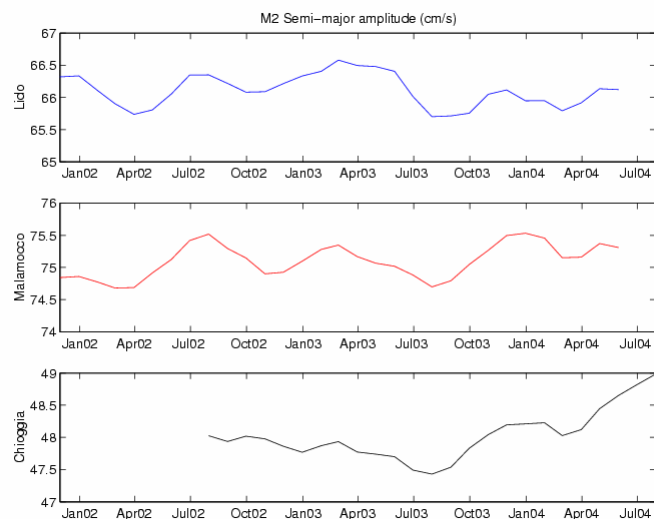


Fig. 4: Amplitude of the M2 tidal constituent as a function of time calculated via harmonic analysis applied on the 13-month moving interval.

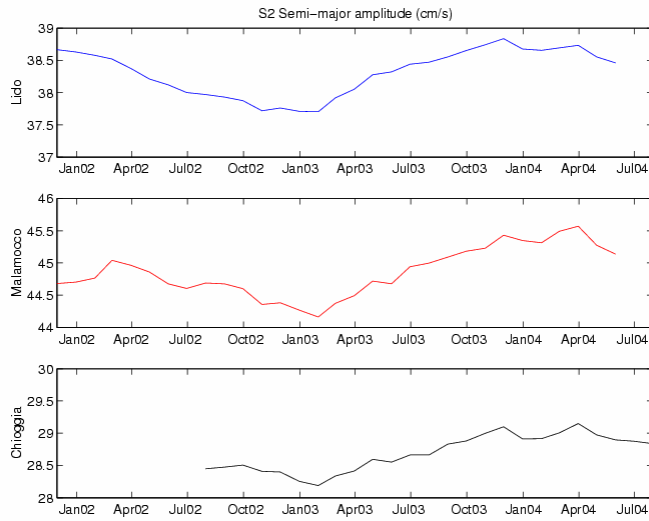


Fig. 5: Amplitude of the S2 tidal constituent as a function of time calculated via harmonic analysis applied on the 13-month moving interval.

The major ellipse orientation for all constituents does not show any important changes.

In order to analyze continuous temporal variations in amplitudes of the three most important tidal constituents (M2, S2 and K1), harmonic analysis was applied to a 13-month moving period for the entire time-series and major ellipse axis are presented in Fig. 4, 5 and 6 as a function of time.

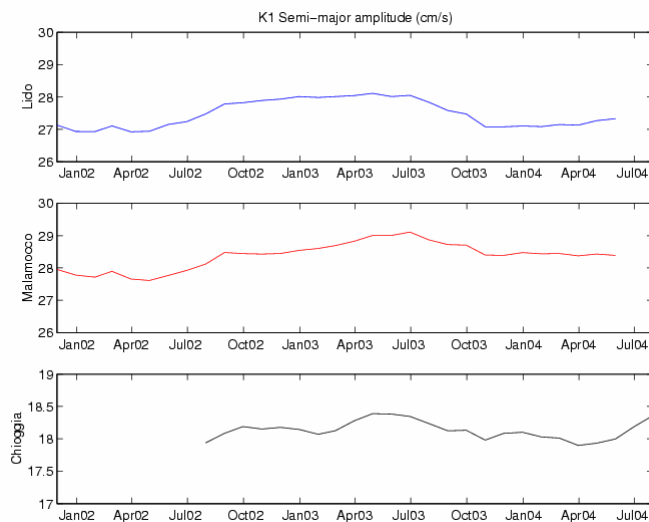


Fig. 6: Amplitude of the K1 tidal constituent as a function of time calculated via harmonic analysis applied on the 13-month moving interval.

Low-frequency variability is the most prominent in the M2 constituent and occurs on the six-month time-scale. S2 shows the most important variability on

the annual time-scale, while the K1 changes very weakly in time. Also, temporal variations of major ellipse axis values for all three inlets result rather highly correlated. From the time-series it can also be seen that no abrupt changes in the tidal constituent amplitude occurred that may possibly be related to barrier constructions. Time-series of the amplitude of the three constituents for the inlet of Chioggia show that differences between the initial and final year-long period that was evidenced earlier is simply due to long-term variations in tidal amplitudes.

3 Conclusions

Long-term variability of the water flow characteristics in the three inlets of the lagoon of Venice was analyzed. A possible changes in flow characteristics could also come from the construction of barriers in front of the inlets of Malamocco and Chioggia. First, long-term variations of the orientation of the major variance axis were considered. Points of the statistically significant changes in orientation were evidenced, but they did not coincide with the barrier erections. Time-series of the monthly mean flow and its standard deviation shows prominent seasonal signal as well as the flow compensation between Lido and Chioggia. Variations in amplitudes of the three most important tidal constituents (M2, S2 and K1) were also analyzed by reconstructing their time-series applying harmonic analysis to a 13-month moving period. Semi-diurnal M2 constituent shows important six-month temporal variations, while the S2 is mainly varying on the yearly time-scale. K1 shows very weak temporal low-frequency variability. Tidal amplitude variations on these long time-scales appear strongly correlated between different inlets, feature that excludes possible influences of the barrier construction on the tidal flow in inlets.

References

- Foreman M. G. G.; 1978: Manual for tidal currents analysis and prediction. Pacific Marine Science Report 78-6, Institute of Ocean Sciences, Patricia Bay, Sidney, British Columbia, Revised edition 1996.
- Gačić M., Kovačević V., Mazzoldi A., Paduan J., Arena F., Mancero Mosquera I., Gelsi G., Arcari G., 2002: Measuring water exchange between the Venetian Lagoon and the open sea. EOS, Transactions, American Geophysical Union, 83, 20, 217-222.
- Gačić M., Kovačević V., Mancero Mosquera I., Mazzoldi A., Cosoli S., 2005: Water fluxes between the Venice Lagoon and the Adriatic Sea. Flooding and Environmental Problems of Venice and Venice Lagoon: State of Knowledge, Cambridge University Press, London, in press.
- Gačić M., Mancero Mosquera I., Kovačević V., Mazzoldi A., Cardin V., Arena F., Gelsi G., 2004. Temporal variations of water flow between the Venetian Lagoon and the open sea. Journal of Marine Systems, 51, 33-47.
- Preisendorfer, R. W., 1988. Principal component analysis in meteorology and

oceanography. Editor: Mobley, C. D. Elsevier Science Publisher, Amsterdam, Oxford, New York, Tokyo.

RESEARCH LINE 3.16

**Characteristics of the lagoon underground
layer**

NEW VERY HIGH RESOLUTION SEISMIC SURVEYS IN SHALLOW WATER TO STUDY THE SUBSURFACE IN THE VENICE LAGOON.

Giuliano Brancolini¹, Luigi Tosi², Federica Rizzetto², Federica Donda¹, Luca Baradello¹, Daniel Nieto¹, Francesco Fanzutti¹, Nigel Wardell¹, Pietro Teatini³, Carl Amos⁴, Maurizio Bonardi².

¹ Dept. Geophysics of the Lithosphere - Istituto Nazionale di Oceanografia e Geofisica Sperimentale, Borgo Grotta Gigante 42/C, 34010, Sgonico, Trieste, Italy, ² Istituto di Scienze Marine - Consiglio Nazionale delle Ricerche, San Polo 1364, 30125, Venice, Italy, ³ Dept. Mathematical Methods and Models for Scientific Applications, University of Padova, Via Belzoni 7, 35131 Padova, Italy, ⁴ Southampton Oceanography Centre, Empress Dock, Southampton, Hampshire, SO14 3ZH, UK

Introduction

After the Last Glacial Maximum the eustatic sea level rise caused the progressive submersion of the Adriatic paleo-plain. The sea reached the southern Gulf of Venice about 11,000 yr B.P. with the maximum ingression about 6,000 yr B.P. A long period of depositional starving (ranging from 6,000 to 10,000 yr) characterized the unconformity at the top of the Pleistocene Low System Tract (LST). This unconformity represents the boundary between the LST and the Holocene Transgressive System Tract (TST) or, mainly in the inner part of the lagoon, the High System Tract (HST), depending on the hiatus.

The upper layer of the LST is often characterized by the occurrence of a clay rich deposit, historically called “caranto” by the Venetians, that shows pedogenesis evidence due to its subaerial exposure.

Since its formation, the morphology of the Venice Lagoon underwent a rapid evolution, that became much more intensive in the last centuries, due to the impact of human activities, e.g. defences for the islands, digging of the channel, dumping of the sediments etc. (Albani et al., 1984, Albani et al., 1995).

The knowledge of the sediment dynamics, with the identification of erosional areas, the sedimentation rate and the flux of sediments, is a fundamental issue for the knowledge of the lagoon evolution and the impact assessment for engineering works. (Umgiesser et al., 2005; Amos et al., 2005).

Our knowledge of the geological settings of the upper Pleistocene and Holocene deposits of the Venice area mainly results from analyses based on cores that, even if collected in a large number, give only local information (Tosi, 1994a; Tosi 1994b). On the other hand, seismic surveys, which can offer the possibility to correlate layers between cores, were rarely carried out in the past because of poor results due to the extreme environment of the lagoon, i.e. very shallow water (McClennen et al., 1997).

In recent years, within the CARG Project, the very high-resolution (VHR) seismic technique has been updated and seismic surveys have been performed

in the lagoon channels, and offshore, to a minimum water depth of 5 m. (Baradello et al., 2002; Tosi et al., 2005a and 2005b).

In order to provide new geological knowledge on the Venetian architecture subsoil, within the Co.Ri.La. Project, a VHR seismic system has been adapted for very shallow water, i.e. 1-2 m depth, and is currently under installation on a dedicated boat. Preliminary surveys have been carried out with this new technique in the lagoon, sea and Sile River. This paper reports and discusses these results and focuses on the characterization of the three main seismic units detected, which relate to the upper Pleistocene Low System Tract (LST), the Holocene Transgressive System Tract (TST) and the Holocene High System Tract (HST). In particular, the target of the investigation was the recognition within these units of features, such as filled paleo-river beds and lagoon channels, ancient littoral ridges and beach rock formations.

1 The single channel acquisition system

The quality of the high resolution seismic surveys in shallow water (less than 3 m) largely depends on the instrument specifications, the survey parameters and the boat characteristics. A seismic source should generate high frequencies, wide band and high repeatability pulses. In the frame of the CARG project in the Venice Lagoon, different sources have been tested (AAVV 2004). The best compromise between high resolution and penetration was reached by a boomer. The system was formed by an electromagnetic transducer UWAK 05 (Figure 1) and a power unit PULSAR 2002. The output power can vary between 150 and 450 Joule/shot and the frequency range is between 300 and 9000 Hz (Figure 2). The transducer is mounted on a sledge with two floats and it is maintained at a constant depth of about 50 cm.



Fig.1: The seismic transducer UWAK05 (left) and the floating sledge with the transducer (right).

The expected resolution for the UWAK05 is about 10 cm. Previous surveys in the Venice area demonstrated that penetration, in good weather conditions, may reach 40 m below sea floor.

Seismic surveys are normally carried out by using a hydrophone streamer for detecting the reflected energy. Depending on the target of the survey, streamer length may vary between few meters, for single channel acquisition, to more

than a thousand meters for multichannel acquisition.

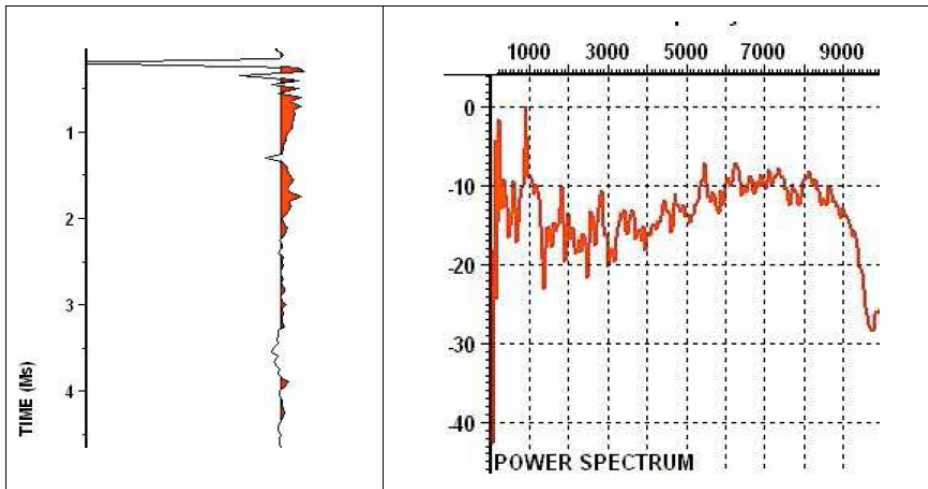
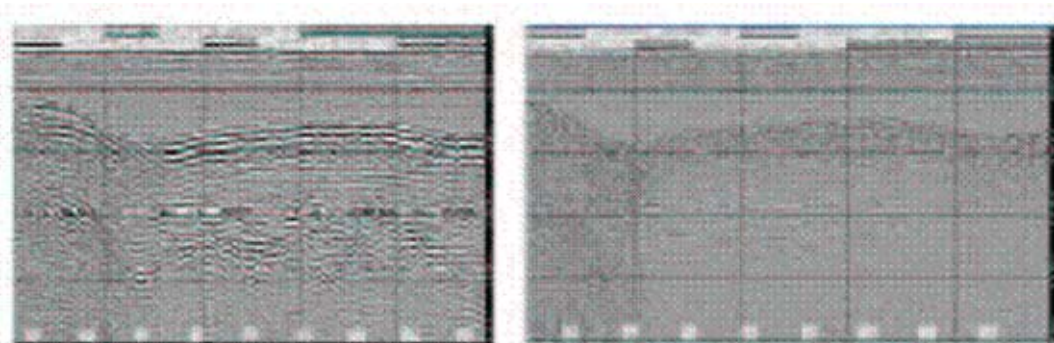


Fig. 2: Signature (left) and amplitude spectrum (right) of the seismic source UWAK05.

In previous surveys in the Venice Lagoon we operated with an EG&G (mod. 265) 320 cm streamer with 8 pre-amplified hydrophones. Multi-hydrophone streamers are useful to improve the level of the recorded energy but, for shallow water and shallow reflector arrivals, these streamers may produce a delay in the arrival time of the order of the dominant wavelet period and therefore may cause a negative interference inside the hydrophone array.



a: streamer B (60 cm length)

b: streamer D (single hydrophone)

Fig. 3: Comparison between a 60 cm streamer (a) and a single hydrophone (b) for sea floor deeper than 5 m

For these reasons, the following different configurations of short to single hydrophone arrays have been tested using the CNR research boat LITUS:

Streamer A: EG&G with 8 hydrophones, active section of 270 cm, pre-amplified

Streamer B: MAE with 3 hydrophones, active section 60 cm

Streamer C: OGS with 3 hydrophones, active section 60 cm

Streamer D: MAE, single hydrophone

Streamer E: OGS, single hydrophone

According to the expectations, the response of the relatively long streamer (B) is much better than single hydrophone (streamer D) in water deeper than 5m (Figure 3). It has not been possible to test the system in very shallow water (less than 3 m), but similar results should be expected. Further test will be carried as soon as the new boat for shallow surveys will be available.

2 The multichannel acquisition system

Single channel systems are very efficient to get data for the shallowest sedimentary section. For targets deeper than the sea floor multiple it is necessary to utilize multichannel seismic systems. The main advantages are; i) to get a drastic attenuation of the multiple reflections, ii) to improve the signal to noise ratio, and iii) to obtain information on the seismic wave velocities.

To improve our capability to obtain high resolution images of the subsurface in the lagoon area, we tested a multichannel technique. Multichannel tests were carried both in the lagoon and in the open sea area close to Chioggia. The energy source was the same Boomer that has been used for the single channel surveys. The acquisition was carried by utilising 6 channel, 2 m group interval streamers, on loan from IFREMER.

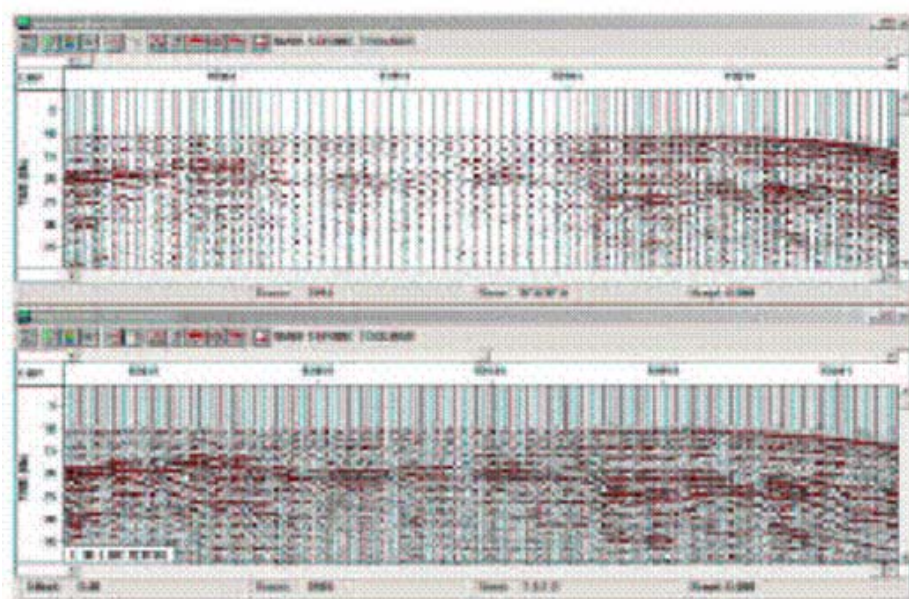


Fig. 4: Example of multichannel seismic section in the Venice Lagoon (below) and the corresponding single channel section from the same line (above). Note that the trace interval in the single channel is not constant due to variations in the boat speed.

Offshore Chioggia, a single cable was used to record a line from the coast out to the beach rocks. This line is shown in Figure 12.

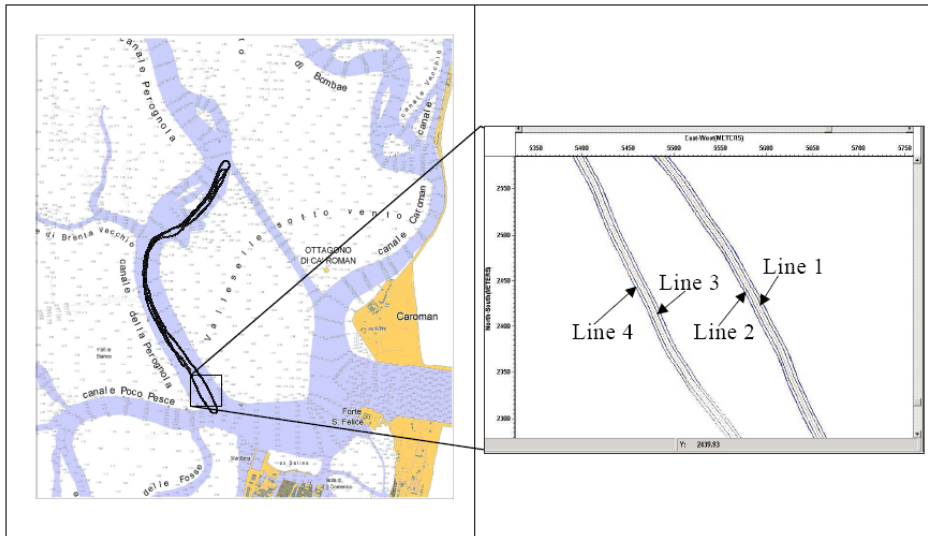


Fig. 5: The position of the 3D multi-channel seismic survey and an enlargement showing the lines displayed in Figure 6.

A comparison between multichannel and single channel data for the lagoon area is shown in Figure 4. Multichannel data produce a notable improvement in the seismic response from the deepest portion of the sedimentary section, but it is still poor in resolution for the shallowest layers. Further tests on the acquisition instruments and processing parameters will be needed to better focus the multichannel methods to the objective of the project.

Within the lagoon, the feasibility of a 3D-acquisition technique was tested. Normally, these tests would be conducted using four streamers, however, due to the limitations of the CNR boat LITUS and the narrowness of the channels, it was only possible to tow two streamers with safety. The streamers were towed parallel at 6m distance from each other, and with an offset of 10 m from the energy source. The distribution of the lines is shown in Figure 5 with an enlargement of part of the survey with two pairs of parallel lines. These four lines are shown, from north-east to south-west, in Figure 6 and demonstrate the lateral variability that can be seen within a cross-line distance of 100 metres. Normally, a denser grid of lines would be acquired using this configuration with similar recording intervals both in an in-line and cross-line direction that would allow a 3D reconstruction of the subsurface to be obtained.

3 Preliminary results of the seismic surveys

Following the results of the tests on the seismic instruments, three field cruises have been carried in the lagoon and open sea area by the ISMAR-CNR boat **LITUS**.

Two single channel seismic profiles have also been recorded along the Brenta and Sile rivers. Processing of the data has not been completed, nevertheless, some preliminary results can be presented and discussed.

Figure 7 illustrates a cross-section of the Venice Lagoon: three depositional

sequences can be identified: the low stand tracts (LST) of the last glacial maximum, the transgressive system tracts (TST) of eustatic sea level rise following the glacial maximum, and the high stand tracts (HST) of the recent sea level still stand.

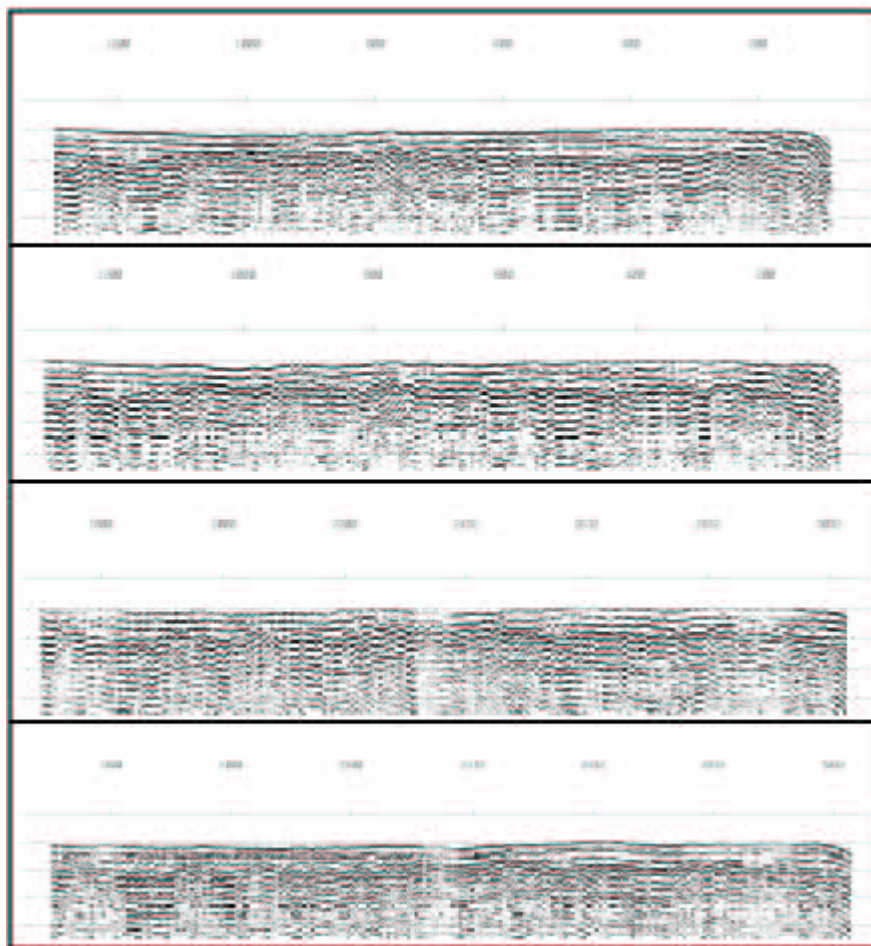


Fig. 6: Multichannel stack sections of the four parallel lines from the enlargement in Figure 5 showing the differences in the cross-line direction.

The LST belongs to the late Pleistocene, and is formed by alluvial plane deposits (generally silt, clay and sand). Locally lacustrine sediments are also present. The top of the TST, is often marked by a overconsolidated paleosoil, named "Caranto". The sequence boundary between the LST (Pleistocene) and the TST (Holocene) is a prominent unconformity, well represented in seismic sections. The Holocene sediments are composed of clay and sand, rich in organic matter, typical of the lagoon environment. The sand content increases toward the sea.

It is not always possible to detect, from seismic data, the maximum flooding surface (mfs) that separate the TST and the HST. Both sequences belong to the Holocene and, unlike the Pleistocene- Holocene transition, the mfs does not show a strong variation in acoustic properties. One of the criteria to recognize the mfs is the presence of an angular unconformity, more common in the outer

portion of the lagoon.

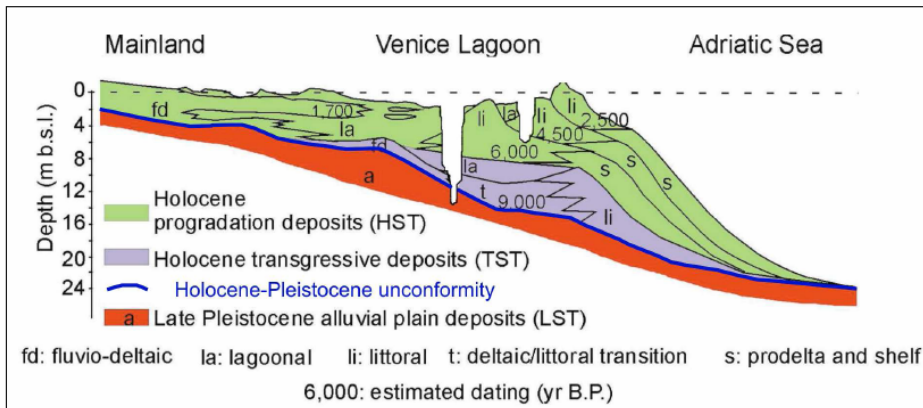


Fig. 7: Depositional sequences in the Venice Lagoon.

The seismic surveys have been carried out in the three most important environments that characterise the Venice area (Figure 8): the rivers, the lagoon and the open sea. Examples from each of them are presented and discussed.

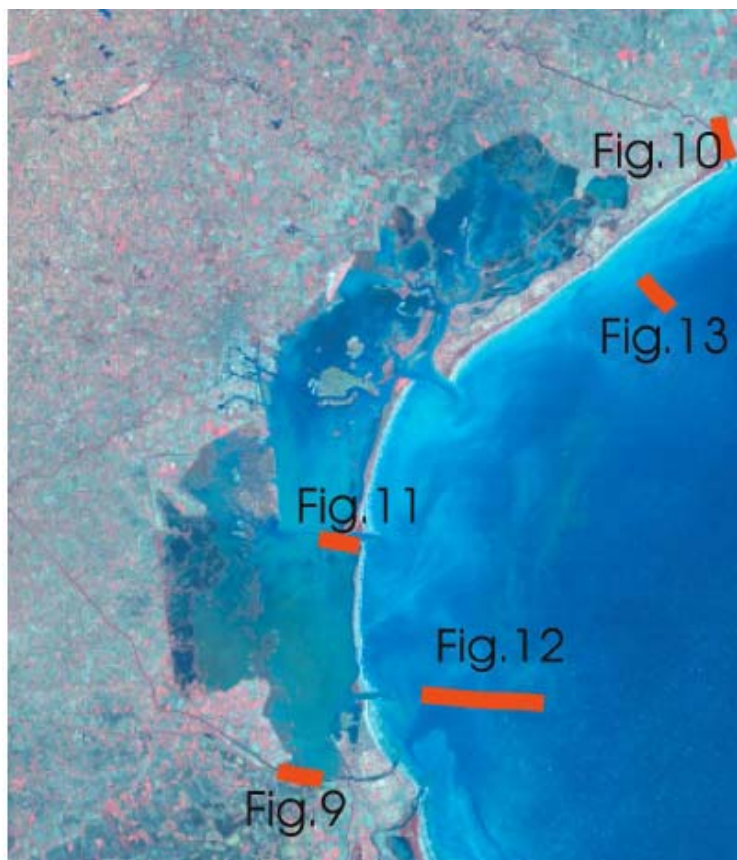


Fig. 8: Map with the trace of the sections presented in this paper

In figures 9 and 10 we present two examples from the Brenta and Sile River. In these sections the setting of the Holocene sequence is controlled by the

interplay between fluvial transport and tidal effects that produced a high variability in the distribution of the sediments. Holocene thickness in fact may vary between 5 and 10 m in a very short distance. The sea floor discordance from the Holocene deposits testifies to the intense anthropogenic excavation that these sectors of the watercourse underwent in recent years.

The irregular and rough morphology of the top of the Pleistocene supports the presence of erosion surfaces belonging to a palaeo-channel channel system.

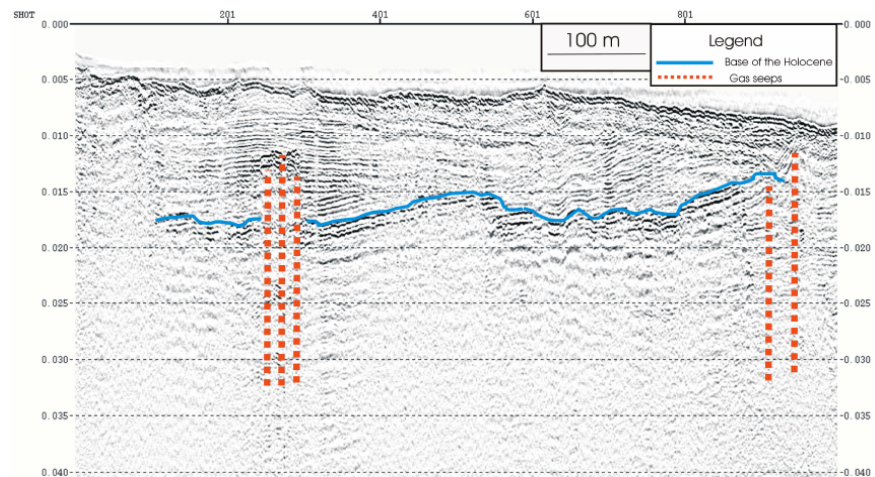


Fig. 9: Example of a single channel seismic section along the Brenta River.

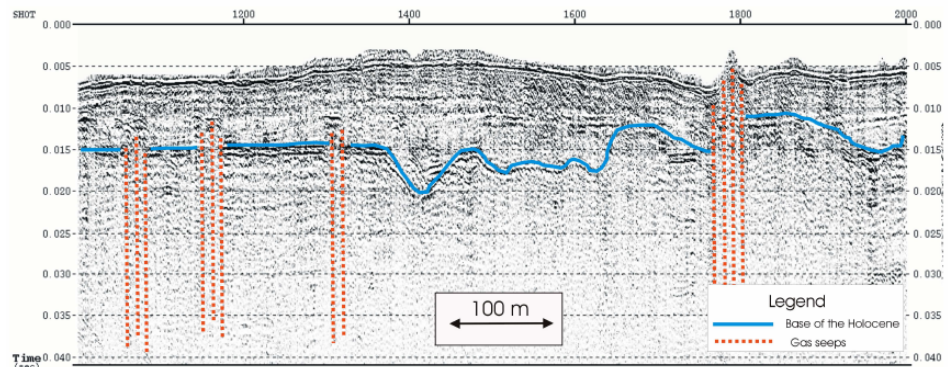


Fig. 10: Example of a single channel seismic section along the Sile River.

Two sequences have been identified inside the Holocene section in the lagoon area. The two sequences are separated by an evident unconformity (Holocene unconformity in Figure 11) and show some peculiar characteristics: the lower sequence is mostly sub-horizontal, with high continuity and low amplitude reflections, while the upper one is formed by continuous high amplitude divergent clinoforms, onlapping on the Holocene unconformity. The upper sequence is often cut by a channel levee system. Considering these characteristics, we attribute the lower sequence to the transgressive system tracts, the upper sequence to the high stand system tracts and the Holocene unconformity to the maximum flooding surface. Also, in these cases, the sea floor is highly discordant compared to the underlying sediments, and proves the

channel excavation of the channel due to human intervention.

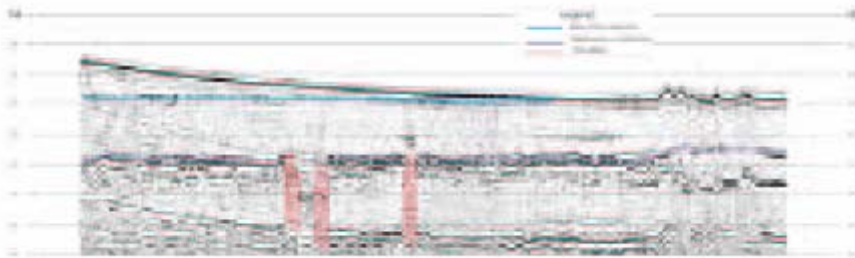


Fig. 11: Example of a single channel seismic section in the lagoon (Malamocco) area.

The Holocene in the open sea area, in front of the Venice Lagoon, is characterized by sedimentary fans downlapping on the Pleistocene sequence boundary (Figure 12). The thickness of the marine sediments rapidly decreases and a few kilometres offshore, the Holocene is very thin (less than 15 cm) or even absent. In front of the fan, the outcrop of the Pleistocene at the sea floor often coincides with a cemented formation, named “beach rocks” or “Tegnue”. The pull-up in the Pleistocene unconformity underlying the beach rocks in Figure 12 testifies to the presence of a positive velocity anomaly, which could be a consequence of the high cementation degree of the formation.

The Pleistocene unconformities in Figures 12 and 13 belong to the continental sequence and are widespread in the entire marine area. There are no evident stratigraphic attributes for these unconformities. As a working hypothesis we consider them as the product of important interstadial climatic changes during the Pleistocene.

In Figure 13, the Holocene has been subdivided into two sequences. The seismic facies constituting both the sequences are not so well defined as in the section in Figure 11, nevertheless we interpret the lower unit as the Transgressive System Tracts and the upper as the High Stand System Tracts.

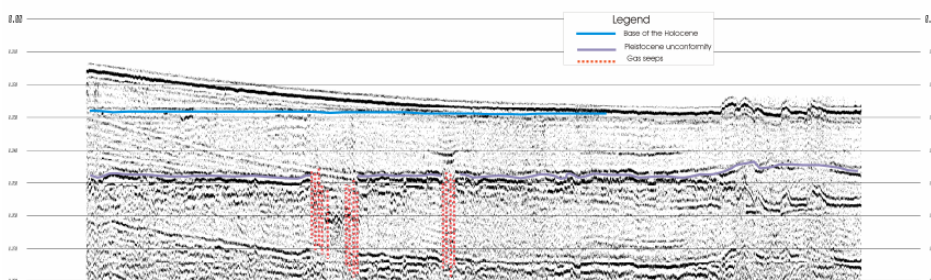


Fig. 12: Example of a multichannel seismic section in the marine area off Chioggia.

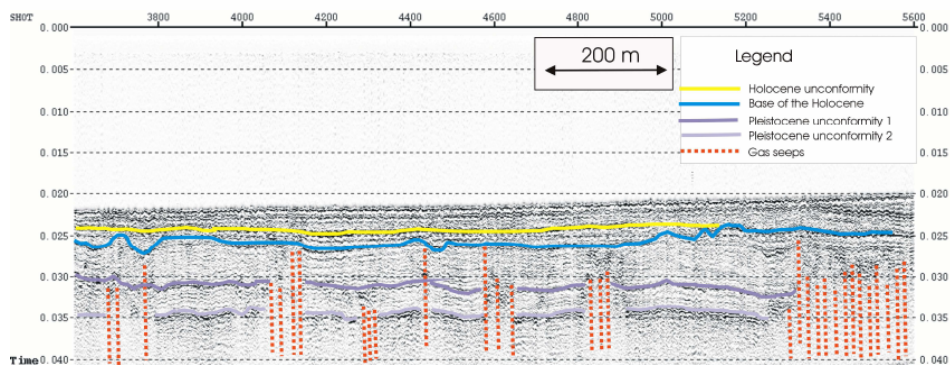


Fig.13: Example of a single channel seismic section in the marine area off Jesolo.

Acknowledgements

This work was carried out with the financial supports of the CO.RI.LA. Subproject 3.16 “New very high resolution seismic methods in shallows to study the Venice lagoon subsoil”. We wish to thank Ing. Pierpaolo Capostrini (Director of Co.Ri.La.) for his continued support in this work.

References

- AA VV. 2004: Rilievo Sismico nella Laguna Veneta, Convenzione 11294, Progetto CARG, Rapporto Finale. Istituto Nazionale di Oceanografia e di Geofisica Sperimentale, Dipartimento di Geofisica della Litosfera 4/2004 OGS,
- ALBANI A., FAVERO V. & SERANDREI BARBERO R. (1984) - Apparatı intertidali ai margini di canali lagunari. Studio morfologico, micropaleontologico e sedimentologico. Ist. Ven. SS. LL. AA., Rapporti e Studi, 9, 137 - 162.
- ALBANI A., FAVERO V. & SERANDREI BARBERO R. (1995) - Condizioni paleoambientali nel sottosuolo di Venezia: la chiesa di S. Lorenzo. Ist. Ven. SS. LL. AA., Rapporti e Studi, 12, 155 - 182.
- AMOS C. L., HELSBY R., UMGIESSER G., MAZZOLDI A., TOSI L. (2005) - Sand transport in northern Venice Lagoon. In: Scientific Research and Safeguarding of Venice. Co.Ri.La. Research Program 2001-2003. Ed. P. Campostrini, Vol. III, 369-383.
- BARADELLO L., FANZUTTI F., RIZZETTO F., TOSI L., (2002) - Rilievo sismico ad altissima risoluzione nel settore meridionale della Laguna di Venezia. Proceedings of the 21th Convegno Nazionale del Gruppo Nazionale di Geofisica della Terra Solida (Rome, Italy), 293-294.
- MC CLENNEN C., AMMERMAN A. & SCHOCK S. (1997) - Framework stratigraphy for the Lagoon of Venice, Italy: revealed new seismic-reflection profiles and cores. Journal of Coastal Research, 13 (3), 745-759.

TOSI L. (1994a) - L'evoluzione paleoambientale tardo-quadernaria del litorale veneziano nelle attuali conoscenze. *Il Quadernario*, 7(2): 589-596.

TOSI L. (1994b) - I sedimenti tardo-quadernari dell'area litorale veneziana: analisi delle caratteristiche fisico-meccaniche. *Geologia Tecnica ed Ambientale*, 2, 47-60.

TOSI L., RIZZETTO F., BONARDI M., DONNICI S., SERANDREI BARBERO R. & TOFFOLETTO F. (2005a) - Note illustrative della Carta Geologica d'Italia alla scala 1:50.000. Foglio 128 – Venezia (in press).

TOSI L., RIZZETTO F., BONARDI M., DONNICI S., SERANDREI BARBERO R. & TOFFOLETTO F. (2005b) - Note illustrative della Carta Geologica d'Italia alla scala 1:50.000. Foglio 148-149 – Chioggia-Malamocco (in press).

UMGIESSER G., AMOS C., BERGAMASCO A., BONARDI M., BRED A., BONSEMBIANTE N., CARNIEL S., CORACI E., CUCCO A., DE PASCALIS F., DONNICI S., FERRARIN C., FRIEND P. L., HELSBY R., RIZZETTO F., SCLAVO M., SERANDREI BARBERO R., STROZZI T., TEATINI P., TOSI L., WEGMÜLLER U., (2005) - Hydrodynamics and Morphology CORILA 3.2. In: *Scientific Research and Safeguarding of Venice. Co.Ri.La. Research Program 2001-2003*. Ed. P. Campostrini, Vol. III, 111-130.

THE ORIGIN OF SAND IN VENICE LAGOON the next step

C.L. Amos¹, R. Helsby¹, C.E.L. Thompson¹, M. Villatoro¹, V. Venturini¹, E. Manca¹, A. Mazzoldi², G. Umgiesser² And L. Tosi²

¹. *Centre for Coastal Processes, Engineering and Management, National Oceanography Centre, Southampton, Hampshire, UK, SO14 3ZH*, ². *Istituto di Scienze Marine, CNR, S. Polo 1364, 30125 Venezia, Italy*

Abstract

This paper outlines progress made within the CORILA programmes 3.15 and 3.16 regarding the origins and transport pathways of sand within the inlets of Venice lagoon. The approach taken is multi-faceted and involves long-term direct measurements within the inlets, inferences based on morphological changes of the bed, direct measurements of sand transport, and geophysical monitoring of key features. Results to date show a clear import of sand into Venice lagoon along the northern margin of Lido inlet. The sand is fine/very fine and is derived from by-passing of the northern breakwater. The sand becomes incorporated within the tidal inlet system of Lido whereupon it contributes to the accumulation of the flood and ebb tidal deltas. We note that there is also a strong import of plant matter subsequent to high river discharge events. This (freshwater) plant material moves close to the bed and is most abundant during flooding tides. The bathymetric and geophysical surveys of the ebb tidal delta of Lido has been completed and show clear progradational foresets diagnostic of rapid accumulation. The ebb delta is a new phenomenon of the shoreface (about 70 years old) and is the product of construction of the jetties. It appears to contain a complete and undisturbed record of sand discharge from Venice lagoon. As such, it should be the site of detailed geophysical and sampling in order to understand the evolution and sand budget of the system as a whole. Accumulation of the ebb tidal delta is largely of fine sand: we speculate that this fine sand is incorporated within the ebb-dominant southern part of Lido inlet and hence reflects the flow patterns of the ebb tidal jet. Thus the innermost part of Lido inlet is a region where two transport pathways intersect: the flood-dominant transport pathway along the northern inlet, and the ebb-dominant transport pathway of Treporti canal and the southern Lido inlet. This region is thus key to understanding the behaviour of sand in northern Venice lagoon. This work should be coupled to a detailed geophysical and stratigraphic evaluation of the ebb tidal delta off Lido. The amount of sand delivered to Lido inlet appears controlled by processing taking place on the shoreface of Cavallino. Yet, we have little in the way of data on sand transport within this region. A final recommendation is for an integrated study of shoreface dynamics off Cavallino.

1 Introduction

The work undertaken in this paper is an extension to activities reported in Amos et al. (2004a) and Amos et al (2004b): that is work originally carried out under

CORILA Linea 3.20. It presently forms part of work activities undertaken in CORILA linee 3.15 (Trasporto solido e circolazione superficiale alle bocche di porto e nella zona costiera) and 3.16 (Caratteristiche del sottosuolo lagunare). As well, this work is strongly linked to Linea 3.14 (Processi di erosione e sedimentazione nella laguna di Venezia). The overarching theme of the work is to determine and characterize the mechanisms of sediment transport in Venice lagoon for purposes of calibration and development of numerical models of sedimentation, and for purposes of establishing a robust sediment budget for the lagoon. Secondary objectives relate to scientific questions regarding the application of general theories of sediment transport to Venice lagoon. Of these, the sedimentation parameters governing cohesive sediment behaviour have been defined. However, the behaviour of fine sand in suspension is yet to be examined. Specifically, the objectives of our work are:

- to validate the ADCP and other acoustical measures of sediment transport in Lido inlet through direct measures of sand transport (Gacic et al., 2004);
- to calibrate/validate the upgraded hydrodynamic/sediment dynamic model of Venice lagoon for purposes of prediction of the residual flux of sand across the main tidal inlets (Umgiesser et al., 2004);
- to evaluate and define the morphology and associated morphodynamics in the vicinity of the inlets to Venice Lagoon subject to active sand transport (Umgiesser et al., 2004);
- to examine the residual fluxes (asymmetries) of sand transport in Lido tidal inlet and which factors control the asymmetry of sand transport (Coraci et al., 2004).

Some important scientific questions remain also to be addressed within the course of this study. These questions are:

- what is the source of sand in the submerged beaches which border Palude della Centrega in Burano and S. Felice canals (Amos et al., 2002) ?;
- to what extent do the submerged beaches (and indeed the entire bed of Venice lagoon) enhance roughness and bed shear stress and hence dissipate tidal and wave energy (Amos et al., 2002) ?;
- insofar as much of the sand in Venice lagoon is relict (Bondesan and Menghel, 2003), what are the sources and sinks of sand in motion and what controls the residual fluxes of sand across the three inlets ?;
- can we define an accurate Rouse parameter to simulate the sand suspension profile in the Lido inlet for purposes of providing accurate concentration profiles within the lower 1 m of water column at the sites of the long-term ADCP measurements ?;
- what are the major morphological features evident as a result of

sand transport and how dynamic are these features in the present day ?

These questions are in the process of being addressed by a series of linked field programmes reported to date in Amos et al. (2004a), and the latest of which is reported herein.

2 Background information

The exchanges of sand across the three inlets of Venice lagoon are fundamental to the evaluation of a complete and accurate estimate of the sediment budget. Coraci et al. (2004), using SHYFEM+SEDTRANS96, has shown that the three tidal inlets behave quite differently showing varying degrees of susceptibility to storm wind effects: sand can be either imported or exported depending on the wind type (Bora or Scirocco) and magnitude: It appears that when Lido imports sand Chioggia exports it; and vice-versa. Umgiesser et al. (2004) has refined this model to incorporate the response of fine sand under waves and tidal currents, showing a strong export of fine sand through Lido inlet under almost all conditions of flow. This result at first light appears counter-intuitive given that most microtidal inlets at their early stages of evolution are flood dominant (van de Kreeke, 1988). Furthermore, the bed of Venice lagoon has a higher sand content than would normally be expected of coastal lagoons (Isla, 1995). So the questions remain: what is the source of the sand, and why is Venice lagoon sandy ? If it is modern, then the source must be inwards through the tidal inlets; if relict, then the source is through in situ reworking and removal of fines. Whilst the removal of fines has been well documented (Carbognin and Cecconi, 1997), the remobilization of sand has not. This because the underlying mechanisms of transport and reworking of fine sand are poorly understood. SEDTRANS96 (linked to SHYFEM and SWAN) was used in the simulations in order to begin studying these mechanisms in the transport of fine sand (Umgiesser et al., 2004). These results show that there is no clear link between the grain diameter of sand within the lagoon, and the magnitude of the bed shear stresses (as one might expect if the sands were in equilibrium within modern day processes). The lagoon is deepening and thus appears to be in transition with the selective removal of fines (Carbognin and Cecconi, 1997) and the coarsening of bottom sediments. Unfortunately, SEDTRANS96 has not been calibrated for fine sand. This is problematic because Bagnold (1966) has shown that there is a transition in sand behaviour around $d_{50} = 125$ microns. Below this median diameter, sand moves entirely in saltation/suspension over a bottom characterized as sheet flow; above this diameter sand moves initially as bedload with the attendant suite of bedforms before entering into suspension. Thus small errors of prediction may result in massive divergences in transport. The experiences gained in CORILA programmes to date have thus been incorporated into an updated version of SEDTRANS which specifically predicts the transport of fine sand. A paper describing this new version (Sedtrans06) is in preparation (Neumeier et al., in prep). The upgrade of the sediment transport model was

undertaken in conjunction with CNR-ISMAR. The updated version also incorporates a new sub-routine for the prediction of the fate of cohesive sediments based on experiences gained during the last round of CORILA funding (Linea 3.20).

A PhD student (Rachel Helsby, funded by CORILA) is mid-way through her studies on the sand transport in the northern lagoon with emphasis on the calibration of the SHYFEM+SWAN+Sedtrans06 model. The calibration of the numerical model will be verified against direct measurements of sand transport in Lido inlet (described in this paper), grain trends as defined by the model of Gao and Collins (1994), and trends in the mineralogical assemblages (after Gazzi et al., 1973). A second PhD student (Monique Villatoro, funded by the Mexican Government) has recently begun a study of sand dynamics in Chioggia inlet. It appears that the two inlets differ in that Lido is influenced by longshore sand transport from the north (the Piave and Sile rivers); Chioggia appears influenced by longshore sand transport from the south (the Brenta river). The two studies will provide a valuable comparison of the inlets.

A third PhD student (Alice Lefebvre, funded by Southampton University) has initiated a study of sand transport in Malamocco inlet. This inlet differs from the two others in that it is strongly controlled by human intervention through maintenance dredging to a depth of 17 m below mean sea level (Cecconi, Pers. Comm., 2005). Bathymetric changes within the central lagoon show that this region is by far the most dynamic having suffered considerable erosion of the bed in the last 10-20 years. The purpose of the study of Lefebvre is to examine the trends in evolution of Malamocco inlet and link them to active processes in the central lagoon. All three PhD studies will examine the nature and development of the ebb tidal deltas that sit off the mouths of the three inlets. The volumes of these deltas, according to Van Rijn (1998), should be a power function of the tidal prism. Reconnaissance surveys undertaken in conjunction with Linea 3.16 show that these morphological features are dynamic, subject to rapid growth, and are recent phenomena. Sampling described in Amos et al. (2004a) show the delta to be largely composed of fine sand. Charts of Venice lagoon (Baso et al., 2003; Bondesan and Menghel, 2004) show that these ebb tidal deltas did not exist at the time of the construction of the breakwaters (starting in 1874) and which now constrain the inlets. In fact, the inlets prior to entrainment were wide and shallow and were "secondary" in form (Galvin, 1971). Such early inlets were classically flood dominant (thus importing sand) and were strongly wave influenced. Entrainment had the effect of transforming the inlets into "primary" types which, as they mature, switch from flood to ebb dominance. Thus, we speculate, the mechanism for the formation of the ebb deltas was created by human intervention in the C19th. However, it is probable that even in 1930 the ebb tidal deltas did not exist. The sand in motion by longshore transport in the exposed surf zones of the barrier islands, which furnishes ebb tidal deltas, was largely trapped behind the breakwaters and was manifested by a rapid seaward progradation of the barrier islands (Cavallino for example). Since 1930, sand has been able to pass around the seaward ends of

the breakwaters and thus become incorporated within the complex transport system of the inlets: manifested by the development of flood and ebb tidal deltas (Smith, 1984). Thus we hypothesise that the ebb tidal deltas off Lido and Chioggia began to evolve around 1930 and so their entire history is to be found in events occurring during the last 70 years or so. If this is true, then we are presented with a unique opportunity. In the first place, we may expect a complete record of sediment transport events of the last 70 years to be preserved within the prograding delta front. Secondly, the volumetric changes of the deltas (flood and ebb) will provide estimates of the sand in transport within the tidal inlets that can be used to supplement measurements of fluxes being undertaken by Gacic, Mazzoldi et al (2004), and budgetary estimates made on bathymetric changes within the lagoon. Thus we may be in a position to define what fraction of the total losses of sediment from the lagoon is sand and what fraction is fines (less than 63 microns in diameter).

3 Field campaign of September, 2005

This field campaign was undertaken in three phases: Phase 1 was the completion of the bathymetric surveying off Lido to encapsulate the entire ebb tidal delta and to survey key regions of the inlet omitted from previous surveys. As well, bottom samples were collected to complete the sampling programme. This was carried out aboard the vessel Corila in collaboration with Tosi et al. (Linea 3.16); Phase 2 was the monitoring of sand transport in Lido inlet undertaken in collaboration with Mazzoldi et al. (Linea 3.15); and Phase 3 was the initiation of surveying and sampling in the Chioggia inlet.

3.1 Phase 1

A total of 144 line km of single beam echo sounding (Fishfinder®) and digital sidescan was carried out in completion of this phase of the programme. These lines supplemented survey lines carried out by Tosi (Pers. Comm., 2005) earlier in the year and provided a complete coverage of the ebb tidal delta (which extends about 4 km seawards of the inlet. The seaward extent of the survey was defined by the closure of progradational foresets seen in high-resolution seismics undertaken by Tosi and which demonstrate clear evidence of seaward growth of the delta front. The formulation of the mass balance of sand in the Lido inlet system is defined in Figure 1. This balance may be subdivided into a series of sub-cells which operate within the coastal sediment transport cell in which the inlet is found. These sub-cells may be defined as: the Cavallino shoreface (Q_{lc}); the ebb tidal delta (Q_{ed}); the flood dominant part of the tidal inlet (Q_f); the flood tidal delta (Q_{fd}); the ebb-dominant portion of the tidal inlet (Q_e); down-drift of the inlet throat (Q_{ls}); and the Lido shoreface (Q_{ll}). The data set now in hand will be used to define the volumetric growth (Q_{ed} and Q_{fd}) of the two deltas between 1990 and the present. By-passing of the inlet will be evaluated by volumetric changes off Lido beach (Q_{ls}). Thus:

$$Q_{tot} = Q_{lc} + (Q_e - Q_f); Q_e > Q_f$$

$$Q_{tot} = Q_{lc}; Q_e < Q_f$$

$$Q_{lc} = (Q_e - Q_f) + Q_{ed} + Q_{fd} + Q_{ls} + Q_{ll}$$

where Q_{tot} is the total quantity of sand within the shoreface transport cell derived from the lagoon and from longshore transport. This will yield a mean annual volume of sand incorporated within the Lido inlet system ($Q_e - Q_f$). The region down-drift of Lido inlet (off Lido beach) was surveyed in order to define the region of accumulation (Q_{ls}) which was seen in part in earlier surveys. The purpose of this is to determine ultimately the degree of inlet by-passing of sand

$$\frac{Q_{ll}}{(Q_{lc})}$$

which is the only natural source of sand to the beaches of Lido. We hope to evaluate Q_{ed} , Q_{ls} , Q_{fd} and Q_f within the course of this study. Q_{lc} will be determined from changes in shoreline position at the downdrift end of Cavallino evident in charts from the C19th. The assumption is made that this rate has not changes over the last 100 years or so. This should be verified by independent measurements of the littoral sand transport rates (Q_{lc} and Q_{ll}).

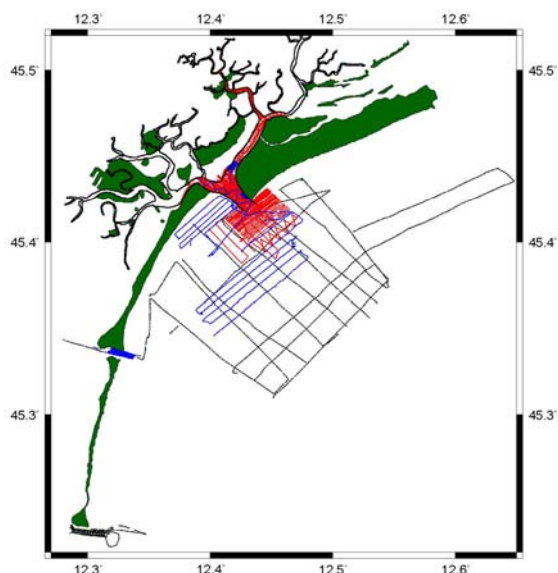


Figure 1. Survey lines undertaken within this programme; red lines are those collected in 2003 and 2004, blue lines are those collected in 2005, and black lines are geophysical lines collected by Tosi (2005).

Such measurements are strongly recommended in the next phase of research. Due to inclement weather and sea state off Lido, survey lines were also carried out off Treporti (in the region of the MOSE construction) and within the inlet of Malamocco (Figure 1).

Bottom samples were collected within the vicinity of Lido inlet for purposes of completing the thesis work of Helsby (R samples) and in support of phase 2 (V samples). The location of these samples are shown in Figure 2A. The samples were in all cases sand and demonstrated that the composition of the ebb tidal delta is also sand. Bottom samples collected within Lido inlet are shown in detail in Figure 2B. These samples will be used for grain trend analysis (Gao and Collins, 1994) in order to compare against other methods of sand transport measurement such as: sand trapping, mineralogical provenance (Gazzi et al., 1973), modeling (Coraci et al., 2004) and long-term monitoring of backscatter (Gacic et al., 2004).

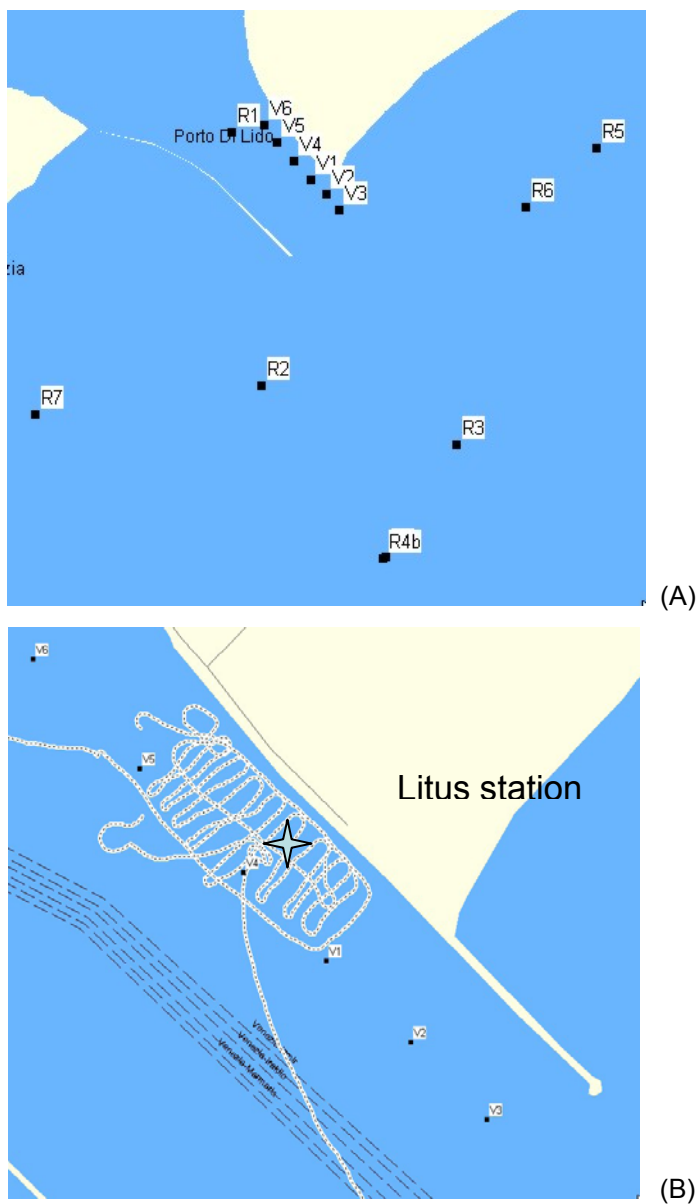


Figure 2. (A) Seabed grab samples collected within Phase 1, (B) Station location within Lido inlet (Lat: 45.46251oN, Lon: 12.42831oW) showing the seabed grab samples collected and the survey lines undertaken.

Latitude (m)	Longitude (m)	Sample
5033906.58	2318118.27	R1
5031260.58	2318335.7	R2
5030588.75	2320397.37	R3
5029438.35	2319608.64	R4
5029429.4	2319575.44	R4b
5033627.07	2321976.08	R5
5033035.37	2321203.3	R6
5031034.5	2315931.18	R7
5033387.57	2318940.32	V1
5033231.35	2319095.87	V2
5033071.35	2319230.94	V3
5033591.15	2318764.37	V4
5033784.72	2318588.9	V5
5033977.84	2318461.97	V6

Table 1. The positions (in Gauss-Boaga coordinates) of bottom grab samples collected in the vicinity of Lido inlet during Phase 1 of this study.

3.2 Phase 2

his phase of the campaign was in support of the long-term monitoring of flows in Lido inlet from the fixed ADCP (Linea 3.15) of Mazzoldi et al. This work was undertaken in conjunction with ADCP transects undertaken hourly by Costa et al. aboard *Henetus* on 20th and 21st September, 2005. Work was undertaken aboard 2 vessels: *Litus* was used for the station monitoring of sand transport; *Corila* was used for seabed sampling and for a detailed site survey of the station (see Figure 2B). The northern site only was occupied: surface tidal currents in excess of 2 m/s prevented any deployments within the vicinity of the ADCP though attempts were made. The station was occupied during 20th -23rd September in water depths between 3.5 and 4.2 m. The survey periods are shown in Figure 3A in cross-hatching. In general, we sampled from mid-flood through high water to mid-ebb. In this fashion, we monitored periods of the

strongest flows. These periods also corresponded to the period of maximum spring tidal range (1.2 m; see Figure 3B). A Bora event took place on 18th September which was accompanied by heavy rain. This was evident as high discharge from the Piave and Sile rivers which (as will be shown) had a strong impact on water column turbidity in the Lido inlet.

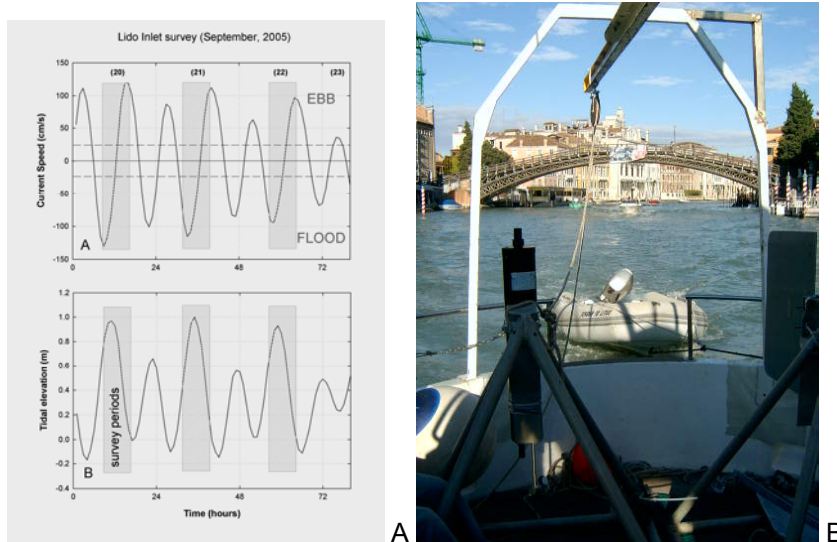


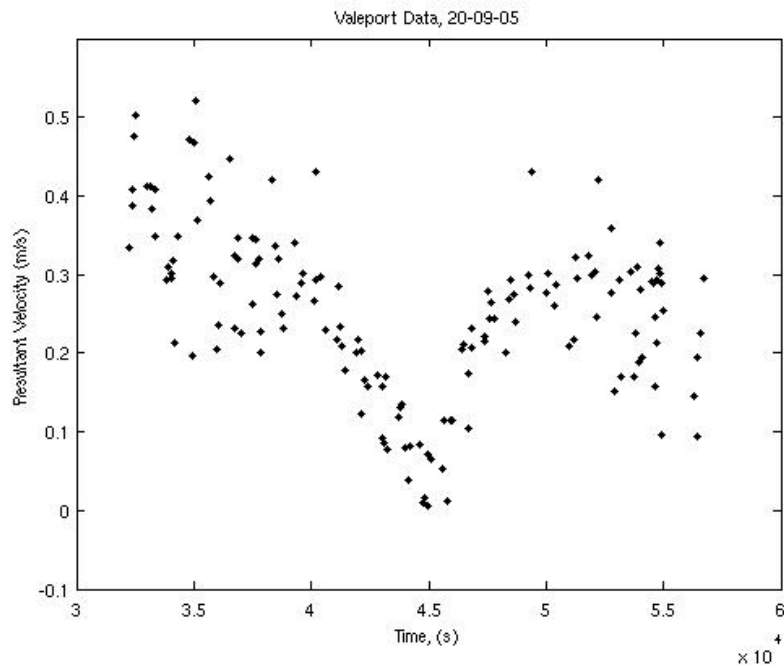
Figure 3. Tidal conditions (predicted current speed (A) and tide height (B) during the anchor station occupied in Lido inlet during 20th -23rd September. Cross-hatching shows the periods at anchor station.. The dashed lines in (A) show the thresholds for fine sand transport; above the threshold sand suspension is predicted to occur. (C) The Valeport® 802 current meter mounted on the deployment frame used in the Lido inlet survey.

The itinerary of events for each day is shown in Table 2. Generally, activities each day followed a common practice. A Valeport® 802 sensor was deployed adjacent to the anchor site.

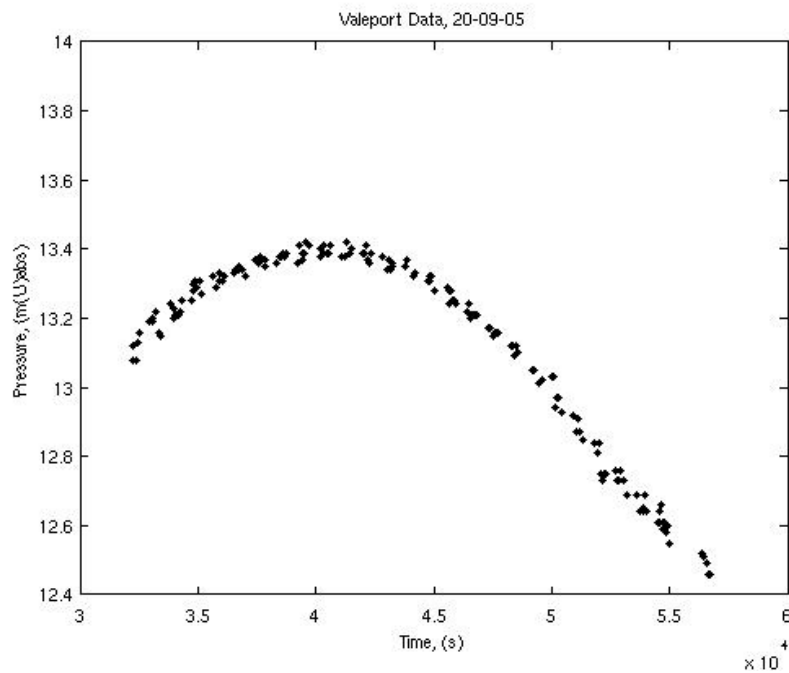
The instrument logged horizontal tidal flows and turbidity at a height of 0.27 m for 20 seconds each 15 minutes at a sample rate of 4 Hz. Water depth was logged in the same protocol from a pressure transducer situated 0.50 m above the bed. Wave climate was evaluated from 2048 measures of water depth and the spectral data so derived were stored by the sensor. All data were logged in BST (Z+1); time was checked against the GPS clock and was within 30 seconds. The instrument logged continuously throughout each of the three days of station monitoring.

The time-series shown in Figure 4 is from the 20th September, 2005. The data are of good quality and the instrument logged continuously without fault. Figure 4A shows the normalized current speed that peaked at about 0.4 m/s on the flood tide and around 0.2 m/s during mid-ebb. The turbidity shown in Figure 4B shows a peak in suspended solids during the mid flood and a steady decrease towards a high tide minimum. The turbidity increases towards mid tide, but is much lower than on the previous flood; a trend also evident in the sand trap

samples. Figure 4C shows the water depth for the deployment period: i.e. late stages of the flood tide, high water and the ebb tide. Notice that slack water and minimum turbidity lags behind high water by about 30 minutes. The velocity data will be compared against predictions for the region; likewise for the water depth time-series; turbidity data will be correlated with the backscatter data and with the sediment trap data described below.



A



B

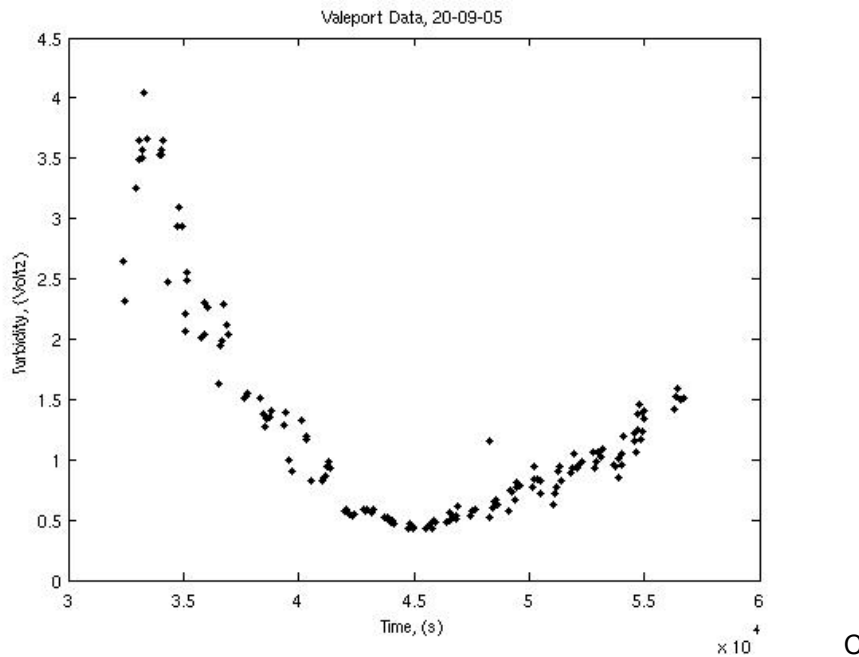


Figure 4 The time-series of data from the Valeport 802 recorded in Lido inlet on 20th September, 2005. (A) resultant velocity (m/s); (B) turbidity (mV); and (C) hydrostatic pressure (mbars).

A frame similar to that of the Valeport® was used to mount the Sediment Imaging Sonar (SIS) which was also deployed adjacent to the Litus. The SIS is a pencil beam acoustic altimeter that emits a sound wave at a frequency of 1.1 MHz. The system measures and records backscatter of the acoustical signal in the time domain. The backscattered signal is mapped in space assuming a sound velocity in seawater of 1400 m/s. The beam width (internal solid angle) is 1.8 degrees, yielding a footprint of approximately 2 cm at a distance of 1 m from the transducer head. The SIS was programmed and controlled from a surface PC connected via a RS-232 cable. Throughout this study, it was programmed to sample at a frequency of 10 microseconds to yield an effective along-beam resolution of 0.7 cm. The instrument was equipped with a rotating head which was used to sweep the region of interest over 360 degrees of arc. The maximum resolution of the sweep angle (0.9 degrees) was used. The signal intensity, pulse length, and gain were also controlled from the PC; these were adjusted according to local conditions. Nadir (zero angle) was set vertically downwards, and the sweep arc was set to a constant 360 degrees. The instrument was mounted on a rigid frame at 0.81 m above the bed. The range was set to a constant of 2 m yielding a total data set of 1.5 Mbytes/sweep of data formatted into: beam angle from nadir (degrees), distance from transducer (m), and intensity of return beam (dB). Each sweep took a constant 53 seconds to complete. The system was set to Auto mode: sweeps were thus repetitive and data storage/file naming was automatic.

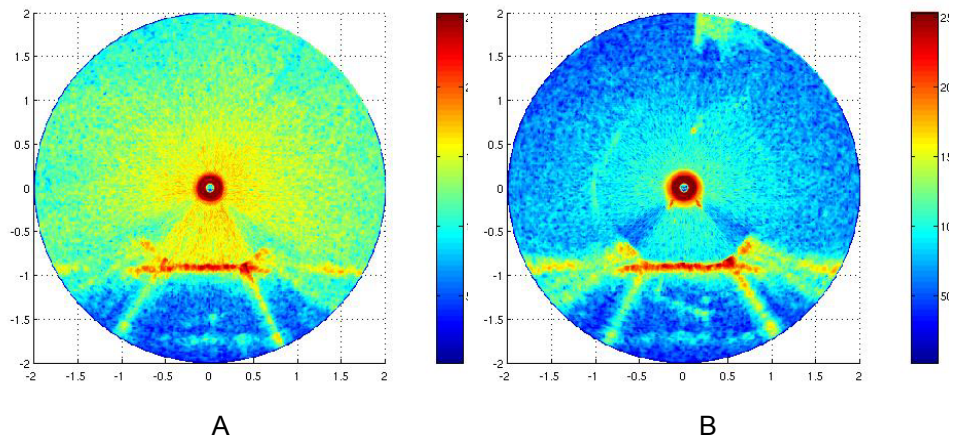


Figure 5. Examples of backscatter images recorded by the SIS. (A) 0832, 20th September, mid flood tidal flow. High turbidity is evident as high backscatter throughout the water column; and (B) 1145, 21st September, early ebb tide, the low backscatter in the water column.

Two examples of the output from the SIS are shown in Figure 5. In general, similar images were generated about once a minute for the period of the anchor stations. Figure 5A shows high turbidity during the flood tide; Figure 5B shows low turbidity during the ebb tide. This pattern persisted throughout the survey showing the strong import of material in the water column along the north side of the inlet. Images show: (1) the source of the beam at the centre and saturation within the near-field region; (2) a strong horizontal reflector 0.8 m below the source which is the seabed; (3) higher backscatter near the bed and lower backscatter towards the surface; (4) two shadowed regions emanating downwards at 45o from nadir caused by the structure of the frame; and (5) two regions of high backscatter below the instruments caused by echoes off the weighted feet of the frame. An Acoustic Doppler Velocimeter (ADV) was attached to the SIS frame for the first day. The sensor head was situated 0.39 m above the bed and monitored flow at 25 Hz for 5 minutes each 15 minutes at a height of 0.30 m above the bed. These time-series will be used to examine the turbulence structure of the flow and to determine the bed shear stresses (τ_o) through the Turbulent Kinetic Energy method (TKE):

$$E = \frac{1}{2} \rho (\overline{u_t^2} + \overline{v_t^2} + \overline{w_t^2})$$

$$\tau_o = 0.19E$$

where u_t , v_t and w_t are the fluctuating components of the mean flow in the two horizontal and vertical directions, and 0.19 is an empirical coefficient defined by Soulsby (1983). Work by Thompson and Amos (2004) has shown that this method is the best predictor of bed shear stress under unidirectional flow provided the measurements are within the turbulent sublayer of the benthic boundary layer. Turbulence was verified through a Reynolds number (Re)

calculation:

$$Re = \frac{\rho U d}{\mu}$$

where $\frac{\mu}{\rho}$ is the kinematic viscosity of the flow, evaluated at $10^{-6} \text{ m}^2/\text{s}$ at 25°C ,

and d is the water depth ($\approx 4 \text{ m}$). Predicted flows varied in magnitude up to 1.5 m/s . At peak flows $Re \approx 6 \times 10^5$ and the mean current speed (U) at which flows became transitional was $U > 0.025 \text{ m/s}$.

Flows may be considered as fully turbulent as the flow Reynolds numbers were in excess of 10^5 , and speeds usually in excess of 0.025 m/s (Komar, 1976). The boundary layer thickness under these conditions (δ) may be expected to vary according to:

$$\delta = 0.38d \left(\frac{\mu}{\rho U d} \right)^{0.2}$$

The logarithmic boundary layer scales to the total water depth, assigning a length scale $d = 500 \text{ m}$ (the distance from the entrance to the anchor station) and $U = 0.5 \text{ m/s}$. We would thus expect fine sand to be suspended to the surface at speeds in excess of this value. The Shield's parameter (θ) for fine sand ($d_{50} \approx 125 \text{ microns}$) is approximately 8×10^{-2} ; according to Bagnold (1966) sand goes immediately into suspension without a phase of bedload transport if θ exceeds the critical value; that is, no ripples are to be expected. The equivalent current speed for the onset of suspension can be determined from the Shield's parameter:

$$\theta = \frac{\tau_{crit}}{(\rho_s - \rho) g d_{50}} > 0.4 \frac{w_s^2}{g d_{50}}$$

$$U_{crit} = \sqrt{\frac{\tau_{crit}}{C_d \rho}}$$

Setting $C_d = 3 \times 10^{-3}$ (Sternberg, 1972), we arrive at $\tau_{crit} = 0.16 \text{ Pa}$, and $U_{crit} = 0.23 \text{ m/s}$. The concentration gradient of suspended sand in theory should follow an exponential decrease with height above the bed within the benthic boundary layer. This decay is governed by the Rouse exponent

$$\frac{w_s}{(\kappa U_*)}$$

where w_s is the sand still water settling rate, κ is von Karman's constant (assumed to be 0.4), and U_* is the friction velocity:

$$U_* = \sqrt{\frac{\tau_o}{\rho}}$$

where τ_0 is the bed shear stress. The concentration (C) at height Z may be determined once C_a , the concentration at a reference height (a), has been measured. Thus:

$$C_z = C_a \left[\frac{\delta - Z}{Z} \frac{a}{\delta - a} \right]^{\frac{w_s}{\kappa U_*}}$$

Helley-Smith sediment traps were used to measure C_a at a reference height $0 < a < 0.15$ m. (assuming a log relationship of C with Z, then mean concentration is a reference height $a = 0.05$ m). The traps were deployed to the seabed on a continuous basis to monitor sand transport. The traps are made of aluminium and are designed to align with the flow (through large tail flights) in order that the sampling mouth is oriented into the flow (Emmett, 1980; Figure 6A). The traps have been used in US rivers for some time and have been extensively calibrated in flume studies (Emmett, 1980). We chose to use the traps with plankton nets of 125 and 250 micron mesh sizes. The larger mesh was used during the first two days and the finer mesh on the last day. The area of the sampling mouth is 0.15×0.15 m. The mouth can be adjusted to be either at the bed or up to 0.4 m above the bed. Initially, the traps were deployed for 20 minutes with the base of the sampling mouth at a height of 0.15 m above the bed. The mouth was lowered to bed level on subsequent days.

The mass transport rate (M) of material per unit width is determined from:

$$M = \frac{V_s}{0.15t}$$

where V_s is total dry mass of material collected, t is the time interval of collection and the constant 0.15 m is the width of the sample region. The volume of water sampled (V_w) is derived from: $V_w = 0.0025U_{0.05}t$ where $U_{0.05}$ is the current speed 5 cm above the bed during sampling ($a = 0.05$ m), and 0.0025 m^2 is the area of the sample mouth.



A

B

Figure 6. (A) The Helley-Smith sand trap ready for deployment aboard Litus; (B) the sand sample from the trap net being removed after a deployment.

The dry sediment mass (m_s) will be determined from a rapid technique where the mass (m_{tot}) and volume (V_{tot}) of the total sample is measured and the dry sediment volume (V_s) estimated (Amos and Sutherland, 1994):

$$m_s = V_s \rho_s = 1.631(m_{tot} - \rho V_{tot})$$

$$V_s = \frac{(m_{tot} - \rho V_{tot})}{1624}$$

$$C_a = 100 \frac{V_s}{V_w} \%$$

where $\rho_s = 2650 \text{ kg/m}^3$ and $\rho = 1026 \text{ kg/m}^3$

The activities undertaken with the Helley-Smith sand traps are presented in Table 2. Eight (8) bottom trap samples were collected on 20th September. In all cases of the flooding tide, the trap returned full. The trapped material was largely composed of plant and leafy organic matter. In general, the traps contained less material on the ebb tide. On 21st September, seven (7) bottom trap samples were collected together with three (3) surface water samples. Surface samples were composed of fine sand in suspension whereas the bottom samples were dominated by organic matter. All samples showed higher masses in suspension on the flood tide than on the ebb tide, as on the previous day. Nine (9) bottom trap samples and three samples from the water column were collected on 22nd September. The samples were low in organic matter and dominated by fine sand. The fine sand mass appeared to co-vary with the magnitude of the tidal flow, and was greater on the flood tide than on the ebb tide. There appeared to be more sand in transport nearer the bed than at the surface and hence a gradient in concentration of sand in the water column was present. This gradient was evident in the backscatter from the SIS which was also highest nearer the bed and lowest towards the surface. We expect to define the concentration gradient through a calibration of backscatter to samples collected in this programme.

Date (dd/mm/yy)	Start Time (UT)	End Time (UT)	Data Collected	Notes
20/09/05	08:17	08:34	sand trap (N1)	mostly organic matter (plant and root)
20/09/05	08:42	09:02	sand trap (N2)	mostly organic matter (plant and root)
20/09/05	09:11	09:41	sand trap (N3)	mostly organic matter (plant and root)
20/09/05	09:49	10:19	sand trap (N4)	mostly organic matter (plant and root)
20/09/05	11:43	12:23	sand trap (N5)	mostly organic matter (plant and root)

20/09/05	12:28	13:08	sand trap (N6)	mostly organic matter (plant and root)
20/09/05	13:16	13:56	sand trap (N7)	mostly organic matter (plant and root)
20/09/05	14:02	14:32	sand trap (N8)	mostly organic matter (plant and root)
21/09/05	08:18	08:58	sand trap (N9)	50:50 organic:inorganic; higher concs close to bed
21/09/05	08:30		surface sample (S1)	50:50 organic:inorganic; higher concs close to bed
21/09/05	09:04	09:44	sand trap (N10)	50:50 organic:inorganic; higher concs close to bed
21/09/05	09:20		surface sample (S2)	50:50 organic:inorganic; higher concs close to bed
21/09/05	09:50	10:30	sand trap (N11)	50:50 organic:inorganic; higher concs close to bed
21/09/05	10:10	10:50	sand trap (N12)	50:50 organic:inorganic; higher concs close to bed
21/09/05	10:10		surface sample (S3)	50:50 organic:inorganic; higher concs close to bed
21/09/05	10:40	11:30	sand trap (N12)	50:50 organic:inorganic; higher concs close to bed
21/09/05			sand trap (N13)	50:50 organic:inorganic; higher concs close to bed
21/09/05	12:05	12:45	sand trap (N14)	50:50 organic:inorganic; higher concs close to bed
22/09/05	12:55	13:35	sand trap (N15)	clean fine sand; little organic matter
22/09/05	08:00	08:30	sand trap (N16)	clean fine sand; little organic matter
22/09/05	08:05		surface sample (S4)	clean fine sand; little organic matter
22/09/05	08:16		bottom sample (B1)	clean fine sand; little organic matter
22/09/05	08:42	09:02	sand trap (N17)	clean fine sand; little organic matter
22/09/05	09:06	09:36	sand trap (N18)	clean fine sand; little organic matter
22/09/05	09:42	10:12	sand trap (N19)	clean fine sand; little organic matter
22/09/05	10:17	10:32	sand trap (N20)	clean fine sand; little organic matter
22/09/05	10:37	11:07	sand trap (N21)	clean fine sand; little organic matter
22/09/05	12:10	12:40	sand trap (N22)	clean fine sand; little organic matter
22/09/05	12:44	13:14	sand trap (N23)	clean fine sand; little organic matter
22/09/05	13:19	13:49	sand trap (N24)	clean fine sand; little organic matter
22/09/05	13:54	14:24	sand trap (N25)	clean fine sand; little organic matter

Table 2. Sand trap deployments in Lido inlet (northern station)

3.3 Phase 3

This phase of the programme was undertaken in the Chioggia inlet in order to provide a data base for a comparison with Lido inlet. A total of 267 line km of bathymetry and sidescan were collected off the mouth of the Chioggia inlet from the prodelta of the Brenta river to the ebb tidal delta off Chioggia. These lines are shown in Figure 7A. The proximal part only of the delta has been surveyed as geophysical evidence provided by Tosi suggests that the ebb tidal delta extends about 4 km offshore. A total of 37 bottom grab samples were collected from the survey region (Table 4). The material collected was largely sandy in composition on the proximal part of the delta, but was muddy for the outermost samples. One sample was collected in the Brenta river about 2 km upstream to provide mineralogical control for provenance studies. We hypothesise that the majority of the sand comprising the Brenta prodelta and the ebb tidal delta is derived from the Brenta river.

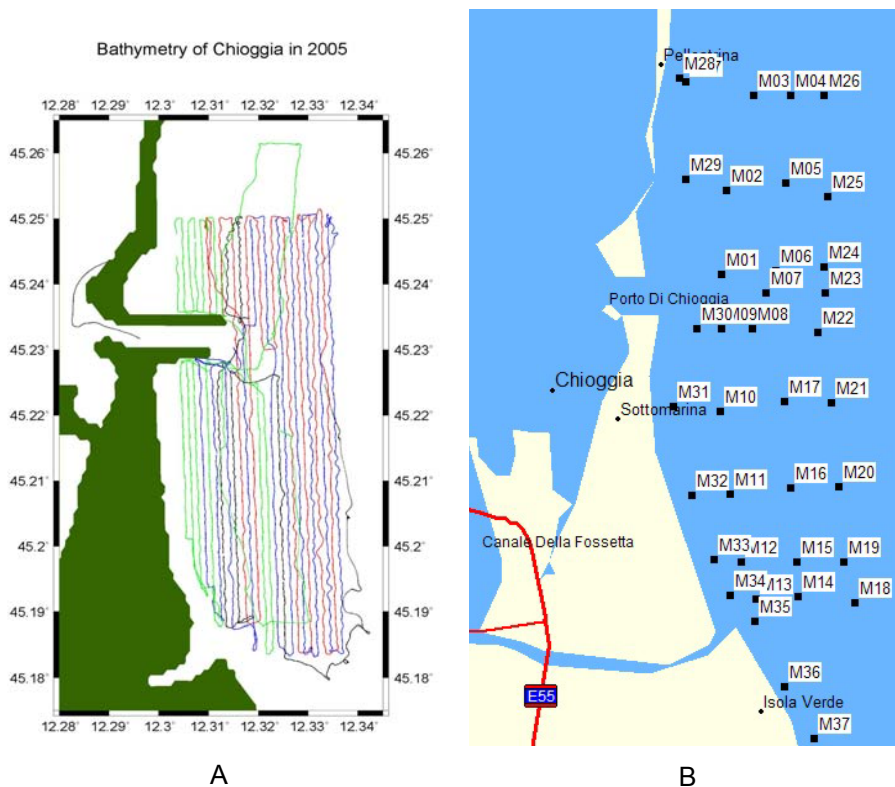


Figure 7 (A) The survey lines undertaken off the Chioggia inlet (red lines – 26 Sept., blue lines – 27 Sept., green lines – 28 Sept., and black lines – 29 Sept.; (B) bottom grab samples collected for grain trend analyses of sand transport.

Unfortunately an attempt to undertake a trial survey of the sidescan sonar on *Bassi fondi* within Venice Lagoon in conjunction with Tosi *et al.* was not possible due to a combination of bad weather, poor visibility, and neap tides (shallow water). It is hoped to undertake work the proposed work in this region during the next field campaign.

Date	Start Time (GMT)	End Time (GMT)	Data Collected
20/09/05	07:56:30	15:00:00	Valeport
20/09/05	08:11:04	08:22:10	SIS
20/09/05	08:25:45	08:30:30	SIS
20/09/05	08:32:00	09:35:00	SIS
20/09/05	09:37:00	09:39:00	SIS
20/09/05	09:46:50	10:15:00	SIS
20/09/05	10:16:40	10:38:28	SIS
20/09/05	11:45:20	11:59:00	SIS
20/09/05	12:13:00	13:00:00	SIS
20/09/05	13:02:30	13:22:00	SIS
20/09/05	13:24:43	13:41:00	SIS
20/09/05	13:42:15	13:50:21	SIS
20/09/05	13:51:35	13:59:00	SIS
20/09/05	14:00:02	14:28:50	SIS
20/09/05	14:29:54	14:30:00	SIS
20/09/05	08:16:08	08:21:00	ADV
20/09/05	08:26:16	08:31:22	ADV
20/09/05	08:36:00	08:41:00	ADV
20/09/05	08:46:00	08:52:35	ADV
20/09/05	08:56:00	09:01:00	ADV
20/09/05	09:06:00	09:11:00	ADV
20/09/05	09:16:00	09:21:16	ADV
20/09/05	09:26:00	09:31:11	ADV
20/09/05	09:38:00	09:39:00	ADV
20/09/05	09:48:00	09:53:46	ADV
20/09/05	09:58:00	10:03:00	ADV
20/09/05	10:08:00	10:13:00	ADV
20/09/05	10:18:00	10:23:00	ADV
20/09/05	10:29:00	10:34:00	ADV
20/09/05	11:46:05	11:51:00	ADV
20/09/05	11:53:30	11:58:30	ADV
21/09/05	08:00:00	13:59:00	Valeport
21/09/05	08:22:16	08:27:35	SIS
21/09/05	08:28:32	09:42:00	SIS
21/09/05	09:43:20	10:17:30	SIS
21/09/05	10:18:30	10:43:00	SIS
21/09/05	10:44:15	11:15:00	SIS

21/09/05	11:16:00	11:40:00	SIS
21/09/05	13:01:45	13:41:00	SIS
22/09/05	07:55:00	14:32:00	Valeport
22/09/05	08:04:40	14:24:25	SIS

Table 3. Activities carried out aboard Litus during Phase 2 operations in Lido inlet.

Latitude ($^{\circ}$)	Longitude ($^{\circ}$)	Sample name
5012585	289134	M01
5013954	289265	M02
5015461	289754	M03
5015443	290349	M04
5014044	290222	M05
5012628	290029	M06
5012268	289854	M07
5011700	289604	M08
5011709	289113	M09
5010382	289045	M10
5009030	289165	M11
5007940	289301	M12
5007330	289522	M13
5007338	290209	M14
5007909	290205	M15
5009110	290156	M16
5010504	290103	M17
5007212	291124	M18
5007883	290975	M19
5009099	290928	M20
5010462	290856	M21
5011611	290679	M22
5012236	290808	M23
5012652	290804	M24
5013802	290912	M25
5015441	290902	M26
5015736	288669	M27
5015799	288576	M28
5014155	288607	M29
5011734	288721	M30

5010488	288298	M31
5009036	288551	M32
5007983	288876	M33
5007395	289112	M34
5006964	289491	M35
5005900	289940	M36
5005038	290402	M37

Table 4. Sites of samples collected off Chioggia inlet in phase 3.

4 Discussion of the results

The results to date from the morphological analysis of Lido inlet shows there is active and ongoing sand transport within the inlet. The source of the sand appears to be largely through the longshore transport of material during storms on the Cavallino shoreface. This sand is then incorporated within the tidal inlet system through by-passing around the northern jetty. The sand appears to diverge once in the inlet: one part appears to move into Lido inlet along the northern margin; the second part appears to become incorporated into the ebb tidal delta whereupon it by-passes the inlet mouth. The import of sand has been verified in phase 2. There is a considerable asymmetry of transport; strongly flood dominant in the northern part of the inlet. The sand moves in suspension. Of particular interest is the prevalence of freshwater organic matter incorporated into this flood load which was present several days after strong rainfall over the Veneto region. We propose that discharges from the Piave and Sile are trapped in the nearshore region and are advected towards Lido inlet whereup they either enter the lagoon or are incorporated within the ebb tidal delta system.

The volume of the ebb tidal delta (V_{eb}) has been shown by Van Rijn (1998) to be related to the tidal prism (P). Results from 44 inlets in the USA yielded the formula: $V_{eb} = aP^{1.23}$ where the coefficient a varies between 0.0055 and 0.0085 (SI units). Results from a further 18 inlets in Florida yielded: $V_{eb} = 0.00055P^{1.4}$. It remains to be seen where the deltas of Venice fall. According to Isla (1995), ebb tidal deltas will accrete material until wave swash impedes the ebb and enhances a flood transport of sediment. At this time, the sand comprising the delta will provide a source to the barrier islands down-drift of the inlet. In the case of Lido inlet, the beaches of Lido island can be expected to benefit from this in the future. It is unclear at the moment how long in the future this process will begin.

The tidal inlet morphology is also worthy of study in relation to the net transport of sand. Hubbard et al. (1979) found that tide-controlled inlets tend to be ebb dominant and wave-controlled inlets tend to be flood dominant. McBride (1987) used the ratio of the tidal prism (P) to longshore transport volume (Q_{lc}) as an index of inlet type. He proposed that where this ratio is less than 50 the inlet is wave controlled, and where it is greater than 150 the inlet is tide controlled; between these values the inlet is intermediate in type showing both flood and

ebb transport patterns and resulting morphological features.

We noted that the magnitude of sand transport into the lagoon appeared to be strongly related to the magnitude of the tidal flow (as expected). The exact relationship will be defined and used as calibration to SHYFEM+Sedtrans06.

5 Future work

There are a number of outstanding issues to be resolved in this study. The first issue is to undertake a second field campaign during September, 2006. The purpose of this will be: (1) to complete the sampling and surveying of Chioggia and Malamocco inlets (in support of two new PhD studies); (2) to complete the bedload sampling within Lido inlet with particular reference to the ebb dominant (southerly) part of the inlet. By working on neap tides, we hope to avoid the difficulties resulting from very strong flows presented during September 05; (3) to undertake measurements of seabed roughness, habitat type and bathymetry at selected sites within the *Bassi Fondi* of central Venice lagoon. The data collected in phase 1 will be used to complete the bathymetric evaluation of the Lido ebb tidal delta. The total accretional volume between 1990 and 2005 will be determined. This will provide valuable data on the net flux of (sandy) material moving within the inlet system. As well, the regions of accretion and erosion will be mapped; this will provide calibration data to the sediment transport predictions of SHYFEM+Sedtrans06. The fine sand entering Lido on the flood tide is probably caught within the subsequent ebb tide and ultimately finds its way to the ebb tidal delta front. We do not know at this stage the mass balance of material within each of the transport sub-cells illustrated in Figure 1. This will be undertaken over the forthcoming winter with a view to the following activities:

(1) define the mass (m_s), concentration (C_a), grain size spectra and still water settling rate (w_s) of sand collected in the sand traps; (2) correlate m_s with mean current speed (U), and friction velocity (U_*); (3) compute the Rousian concentration profiles throughout the water column; (4) correlate m_s with SIS backscatter and map C_a from the SIS profiles at 1-minute intervals; (5) correlate $C_{0.5}$ with Valeport® turbidity and define a high-frequency time-series of sand in suspension at $Z = 0.5$ m; and (6) integrate C with respect to Z to compute the mass flux for the total water depth over the sampled interval.

6 Conclusions

This paper reports on activities undertaken during the field campaign of September, 2005 in support of Linee 3.14, 3.15 and 3.16. That is, the analysis of sand dynamics within the inlets of Lido and Chioggia, and the evaluation of seabed morphodynamics within the inlet system of Lido. Considerable progress has been made in achieving the goals and objectives of the project. Major advances include:

- the mapping of bathymetry and backscatter of the Lido ebb tidal delta. This has been completed. The ebb tidal delta has now been encapsulated and the volumetric estimates of the delta accretion

rate and total delta volume are now underway;

- detection and sampling of sand transport within the flood dominant northern part of Lido inlet have been completed. A Helley-Smith sand trap was used in conjunction with optical and acoustical devices to derive time-series of sand distribution and fluxes throughout the water column. The results show a flood dominance to sand transport. The fluxes are also modulated by tidal current speed and peak during mid tides when fine sand is distributed throughout the water column;
- a new PhD project has begun to evaluate Chioggia inlet sand transport and controlling dynamics with emphasis on the origin and evolution of the ebb tidal delta. A preliminary survey of the inlet has been completed together with a seabed sampling programme; and
- a new PhD project has begun to evaluate Malamocco inlet sand transport and controlling dynamics. The emphasis on this study will be the role of anthropogenic activities on the mass balance of sand in the inlet and on the formation and evolution of the ebb tidal delta.

Acknowledgements

We wish to acknowledge the kindness and support of CNR-IBM for provision of the Foresteria during our stay in Venice. Thanks go also to Matteo Morgantini, Emiglio Valenzasca and Stefania de Zorzi who provided logistical help on behalf of CORILA. Thanks go to P. Capostrini (Direttore, CORILA) for kindly providing boat facilities for the surveying of Lido and Chioggia inlets. Thanks also go to Andrea Cucco for helping with demobilization of this survey, and to the crew of Litus for their friendship, sustenance, and constant support during our field campaign. I also acknowledge Dafydd Lloyd-Jones who helped me with the mobilization of the survey. This is a CCPEM (Centre for Coastal Processes, Engineering and Management) contribution.

References

- Amos, C.L. and Sutherland, T.F. 1994. A rapid technique for the determination of dry sediment mass from saturated marine sands. *Journal of Sedimentary Research* A64(3): 668-670.
- Amos, C.L. Umgiesser, G., Reed, P., Munford, G. and Lea, J. 2002. The residual tidal circulation and organics in northern Venice Lagoon, Italy. *In* Scientific Research and Safeguarding of Venice. Research Programme 2001-2003. Volume III. (P. Capostrini, ed) Publ. CORILA, Venice: 189-202.
- Amos, C.L. Umgiesser, G., Helsby, R. and Friend, P.L. 2004a. The origin of sand in the Venice Lagoon. *In* Scientific Research and Safeguarding of Venice. Research Programme 2001-2003. Volume III. (P. Capostrini, ed) Publ. CORILA, Venice: 161-176.

- Amos, C.L. Helsby, R., Umgiesser, G., Mazzoldi, A. and Tosi, L. 2004b. Sand transport in northern Venice Lagoon. *In* Scientific Research and Safeguarding of Venice. Research Programme 2001-2003. Volume II. (P. Capostrini, ed) Publ. CORILA, Venice: 369-383.
- Bagnold, R.A. 1966. An approach to the sediment transport problem from general physics. US Geological Survey Professional Paper 422: 37p.
- Baso, G., Scarso, M. and Tonini, C. 2003. La Laguna di Venezia nella cartografia storica a stampa del Museo Correr. Publ. Musei Civici Veneziani: 137p.
- Bonardi, M. Breda, A., Bonsembiante, N. Tosi, L. and Rizzetto, F. 2004. Spatial variations of the surficial sediment characteristics of the lagoon of Venice, Italy. *In* Scientific Research and Safeguarding of Venice. Research Programme 2001-2003. Volume III. (P. Capostrini, ed) Publ. CORILA, Venice: 131-144.
- Bondesan, A. and Menghel, M. 2004. Geomorfologia della Provincia di Venezia. Publ. ESEDRA editrice, Padova: 514p.
- Coraci, E., Umgiesser, G., Sclavo, M., and Amos, C.L. . 2004. Modeling sand transport in the Venice lagoon inlets. In: Scientific Research and Safeguarding of Venice. Research Programme 2001-2003. Volume III (P. Capostrini, ed), Publ. CORILA, Venice: 157-173.
- Carbognin, L. and Cecconi, G. 1997. The lagoon of Venice, environment, problems, and remedial measures. Field Guide of IAS Environmental Sedimentology Conference, Venice. Publ. Consiglio Nazionale della Ricerca, Venice: 71p.
- Emmett, W.W. 1980. A field calibration of the sediment-trapping characteristics of the Helley-Smith bedload sampler. US Geological Survey Professional Paper 1139: 28p.
- Gacic, M., Mazzoldi, A., Kovacevic, V., Cosoli, S., Mosquera, I.M., Arena, F. and Cardin, V. 2004. Water fluxes in Venice Lagoon inlets and coastal circulation. *In* Scientific Research and Safeguarding of Venice. Research Programme 2001-2003. Volume III. (P. Capostrini, ed) Publ. CORILA, Venice: 311-321.
- Galvin, C.J. 1971 Wave climate and coastal processes. *In* Water Environments and Human Needs. A.T. Ippen (ed). Publ. MIT, Cambridge.
- Gao, S. and Collins, M.B. 1994 Analysis of grain trends, for defining sediment transport pathways in marine environments. *Journal of Coastal Research* 10(1): 70-78.
- Gazzi, P., Zuffa, G.G., Gandolf, G. and Paganelli, L. 1973. Provenienza e dispersione litoranea delle sabbie delle spiagge adriatiche fra le foci dell' Isonzo e del Foglia: inquadramento regionale. *Memorie della Societa Geologica Italiana* 12: 1-37.

Hubbard, D.K., Oertel, G. and Nummedal, D. 1979. The role of waves and tidal currents in the development of tidal-inlet sedimentary structures and sand body geometry: examples from North Carolina, South Carolina and Georgia. *Journal of Sedimentary Petrology* 49: 1073-1092.

Isla, F. 1995. Coastal Lagoons. *In* *Geomorphology and Sedimentology of Estuaries* G.M.E. Perillo (ed) Publ. Elsevier Science: 241-272.

Komar, P.D., 1976. Boundary layer flow under steady unidirectional currents. *In* *Marine Sediment Transport and Environmental Management*. Stanley, J.D. and Swift, D.J.P. (eds). Publ. John Wiley & Sons, New York: 91-125.

McBride, R.A. 1987. Tidal inlet history, morphology and stability, eastern coast of Florida, USA. *Coastal Sediments '87*. ASCE, New Orleans: 1592-1607.

Neumeier, U., Ferrarin, C., Amos, C.L. Umgiesser, G. and Li, M.Z. in prep. *Sedtrans06: an improved sediment-transport model for continental shelf and coastal waters*. *Computers & Geoscience*.

Smith, D. 1984. The hydrology and geomorphology of tidal basins. *In* *the Closure of Tidal Basins* Publ. Delft University Press, the Netherlands.

Soulsby, R.L. 1983. The bottom boundary layer of shelf seas. *In* *Physical Oceanography of Coastal and Shelf Seas*. B. Johns (ed). Publ. Elsevier, Amsterdam: 189-266.

Sternberg, R.W. 1972. Predicting initial motion and bedload transport of sediment particles in the shallow marine environment. *In* *Shelf Sediment Transport: Process and Pattern*. D.J.P. Swift, D.B. Duane, and O.H. Pilkey (eds). Publ. Dowden, Hutchinson & Ross, Inc, Pennsylvania: 61-97.

Thompson, C.E.L. and Amos, C.L. 2004. Flow deceleration as a method of determining drag coefficient over roughened flat beds. *Journal of Geophysical Research* 109: C03001: 12p.

Umgiesser, G., Albani, A., and others. 2004. Hydrodynamics and morphodynamics. CORILA 3.2. *In* *Scientific Research and Safeguarding of Venice. Research Programme 2001-2003. Volume III*. (P. Capostrini, ed) Publ. CORILA, Venice: 111-130.

Van de Kreeke, J. 1988. Hydrodynamics of tidal inlets. *In* *Hydrodynamics and Sediment Dynamics of tidal inlets*. D.G. Aubrey and L. Weishar (eds). Publ. Springer-Verlag, New York.

Van Rijn, L.C. 1993. *Principles of Sediment Transport in Rivers, Estuaries and Coastal Seas*. Publ. Aqua Publications, the Netherlands.

Van Rijn, L.C. 1998. *Principles of Coastal Morphology*. Publ. Aqua Publications, the Netherlands.

RESEARCH LINE 3.17

Transport phenomena in the hydrological cycle: model of substances release in lagoon

EXPERIMENTAL RESEARCHES ON THE HYDRAULIC BEHAVIOUR OF THE CA' DI MEZZO IN CODEVIGO WETLAND

Vincenzo Bixio¹, Anna Chiara Bixio², Martino Cerni², Andrea Marion¹, Mattia Zaramella²

¹ *Dipartimento di Ingegneria Idraulica Marittima Ambientale e Geotecnica, Università degli Studi di Padova,* ² *Collaboratore del Programma di Ricerca CORILA 2004-2007 presso il Dipartimento di Ingegneria Idraulica Marittima Ambientale e Geotecnica, Università degli Studi di Padova*

Riassunto.

Nella memoria sono riportati i risultati ottenuti nelle ricerche sperimentali eseguite principalmente nel corso dell'anno 2004 presso l'area umida di Ca' di Mezzo di Codevigo, in Provincia di Padova, allo scopo di valutare l'effetto di ambienti di tale tipo sul rilascio di nutrienti, ed in particolare di azoto e fosforo, nel Bacino scolante nella laguna di Venezia.

Abstract.

This paper reports the results of some experimental researches performed, mainly during 2004, in the Ca' di Mezzo in Codevigo Wetland, located in the district of Padova, with the aim of assessing the effects of surface flow wetlands on the release of nutrients (nitrogen and phosphorus) in the catchment basin of the Venetian Lagoon.

1 Introduction

The hydraulic drainage works in the Venetian Lagoon catchment basin have been sensibly developed during the last years, in order to contribute to water depollution by increasing channels storage and constructing wetlands [Bixio, 2000]. In this context, the Ca' di Mezzo Wetland was built in the southern part of the basin, in Codevigo. This is the largest wetland ever constructed in Europe until now, and represents a unique site for experimental researches which aim to assess the effects of humid environments on nutrients release.

2 The Ca' di Mezzo in Codevigo Wetland

The phytodepuration area reconstructed in Ca' di Mezzo – located in the municipality of Codevigo, district of Padova, at the borders with the municipality of Chioggia – was created a few years ago in order to reduce nutrients concentration driven into the Venetian Lagoon by the Altipiano Channel. This channel is named Morto Channel in its final reach before flowing into the Lagoon, after passing under the Bacchiglione and Brenta rivers through the Trezze siphon.

The Ca' di Mezzo Wetland was designed to collect the minimum stream flow

drained from a 8700 hectares catchment area that belongs to the Land Reclamation Consortium Adige Bacchiglione district and is mainly destined to agricultural use (Fig. 1).

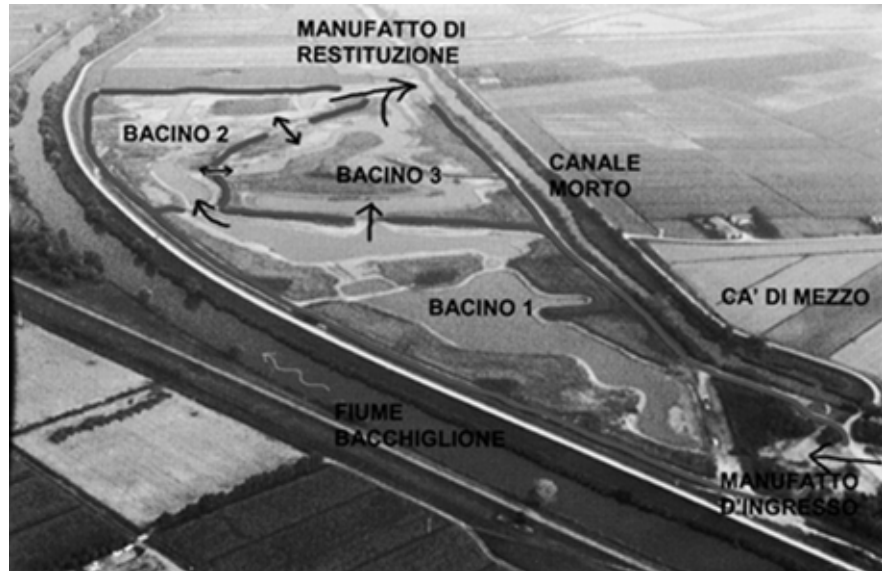


Fig. 1 – Ca' di Mezzo Wetland layout.

The water flows from the Altipiano Channel into the wetland through an inlet structure equipped with check gates and with a second flow stage level control system placed on a downstream bridge. The water is then released into the Altipiano Channel through an outlet structure.

The wetland was designed to treat a few hundreds litres per second discharge, with a mean water stage that varies from 0.20 to 0.30 m a.m.s.l.. The average water depth is about 1 m.



Figs. 2 and 3 – Examples of channel network and flood plain covered by Phragmites in the Ca' di Mezzo Wetland.

The wetland is formed by three independent basins, connected by culverts equipped with control structures.

Areas that are mainly involved in depuration processes are represented by the channel network and the wide flood plains zones (Fig. 2) covered by Phragmites (Fig. 3).

At the inlet and outlet of the wetland there are two couples of sonic level meters

located upstream and downstream the check gates. Check gates are controlled by a level measuring sensor, that allows to determine stored volumes and inlet/outlet discharges. Water levels are available for remote users thanks to the Land Reclamation Consortium Adige Bacchiglione automatic network (Fig. 6). An accurate estimation of the flow rates is important not only to determine the hydraulic behaviour and the hydraulic residence time, but also to assess the removed load of pollutants. The geometry of the wetland has been derived by a 3800 points topographic survey, allowing the description of the phytodepuration areas, constituted by the channels networks and the flood plains (Fig. 4).

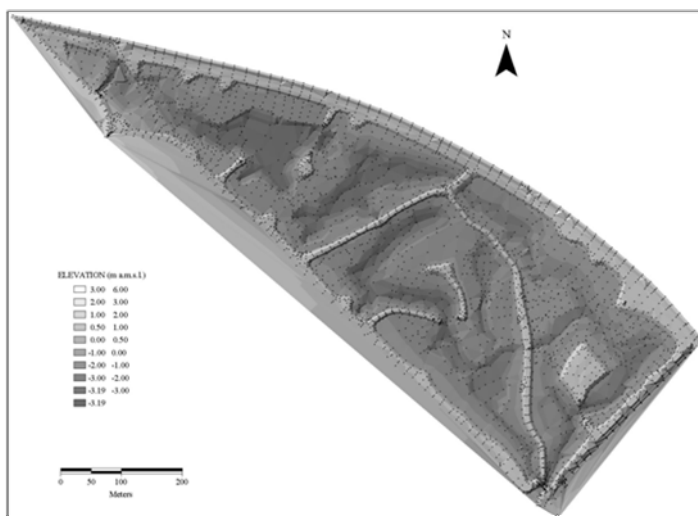


Fig. 4 – Topography of the Ca' di Mezzo Wetland derived through TIN by the surveyed points.

Storage and surface area of the wetland as functions of water elevation are reported in Fig. 5: we can observe that at the medium elevation of 0.20 m a.m.s.l. corresponds a storage volume of about 200'000 m³ and a surface area of 20 hectares .

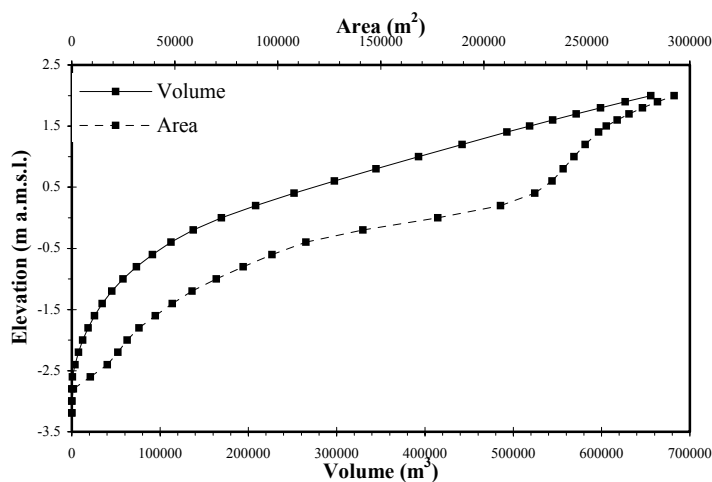
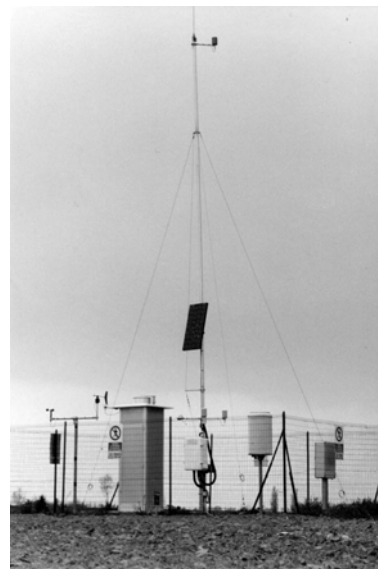


Fig. 5 – Storage volume and water surface area in the Ca' di Mezzo Wetland as functions of water elevation.

3 Meteorological and water quality monitoring of the Altipiano Channel flowing into the Ca' di Mezzo Wetland.

The main climate data (precipitation, air temperature, humidity, solar radiation) are recorded by the ARPAV (Regional Agency for Environmental Protection of the Veneto Region) meteorological station located on the right bank of the Altipiano Channel, just near the wetland (Fig. 7).



Figs. 6 and 7 – Automatic remote control station and ARPAV meteorological station in Ca' di Mezzo.

Water quality monitoring of the Altipiano Channel was carried out starting from 1995, even before the wetland was created. Monitoring allowed to obtain an exhaustive historical frame of local water conditions, and can be useful to evaluate benefits deriving from the wetland construction. The monitoring was performed by the Laboratory for Environmental Systems Analysis (L.A.S.A.) of the University of Padova, Department of Chemical Processes of Engineering. Data concerning both the inlet and the outlet of the wetland have been collected every fortnight starting from 2002, after the phytodepuration basin was completed. Monitored parameters are summarized in Tab. 1.

4 Experimental researches.

During the period running from May to the end of June 2004, many experimental measurements have been carried out inside the wetland, in order to collect useful information about the hydraulic behaviour of the wetland. The experimental works consisted in water velocity sampling within the wetland and in measuring dispersion and hydraulic residence time distribution inside basin 1 (Figs. 1 and 8), using tracers.

4.1 Velocity measurements.

Water velocity measurements have been collected near the inlet structure, the

bridge-footpaths and the culverts connecting the basins as well as in other positions inside the wetland using a small boat. The velocity measurement positions are shown in Fig. 8.

Monitored parameters		
Water temperature	Ammonia nitrogen	Total dissolved inorganic nitrogen
Electrical conductivity	Total dissolved nitrogen	Total nitrogen
Dissolved oxygen	Orthophosphate phosphorus	Non-reactive soluble phosphorus
Dissolved oxygen (saturation %)	Total suspended solids	Total phosphorus
Salinity	Particulate nitrogen	COD and BOD5
Nitric oxide	Particulate phosphorus	Escherichia Coli
Nitrous oxide	Dissolved organic nitrogen	Fecal coliforms

Tab. 1 – Monitored parameters in the Ca' di Mezzo Wetland.

Velocity was measured with an Acoustic Doppler Velocimeter (Fig. 9). The ADV provides the three spatial components of the velocity. It is particularly indicated for measurements inside wetlands because it can record low velocity values up to 1 mm/s. The instrument requires a rigid and stable support and the elimination of all the possible vibrations that may influence and alter the measurements. Particular care must then be given to the wind action that may affect the stability of the instrument both on water surface and along the whole water depth.

The measurements in the culverts were necessary to assess the partition of discharge among basin 2 and basin 3. It was found that about 53% of the total discharge flows into basin 2 while the remaining 47% flows into basin 3.

In spite of a certain variability mainly due to wind action, measurement results show that velocity values inside the wetland can vary from some millimetres per second to some centimetres per second. In the narrowest cross sections, where stream is more concentrated, velocity increases up to 4 cm/s (for instance at the wetland inlet and in point V12, Fig. 8).

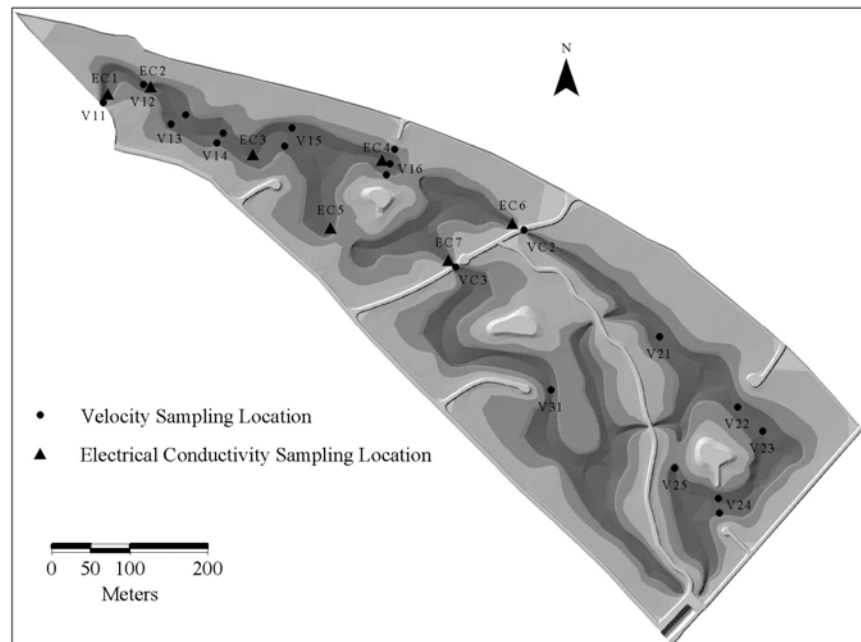


Fig. 8 –Electrical conductivity and flow velocity sampling sites in the Ca' di Mezzo Wetland.



Fig. 9 - Velocity measurements inside the wetland with the ADV probe.

4.2 Tracer tests

Tracer tests have been performed using sodium chloride which is not harmful for the ecosystem. During the first test 300 kg of sodium chloride were opportunely mixed with fresh water and injected at the inlet of the first basin: the breakthrough cloud was monitored with electrical conductivity probes (Fig. 8), in order to determine solute dispersion mechanisms. The test was useful to reach a first understanding of the order of magnitude of the involved parameters.

A second test was then performed injecting at the inlet a constant sodium chloride concentration of about 0.5 g/l for 5 hours. The movement of the plume was then observed with higher precision, but results were satisfactory only at the first measurement positions, up to EC3 (Figs. 14 and 15).

Conductivity and temperature data allowed to obtain some interesting information about the hydraulic behaviour of the wetland and the related dispersion processes. Namely it was possible to measure the travel time of the

tracer near the four measuring placings inside basin 1 (EC2, EC3, EC4, EC5) and the peak time of concentration in the culverts connecting basins 2 and 3 (measuring points EC6 and EC7).



Figs. 10 and 11 – Automatic samplers located in the Ca' di Mezzo Wetland.



Figs. 12 and 13 – Laboratory analysis of the collected water samples.

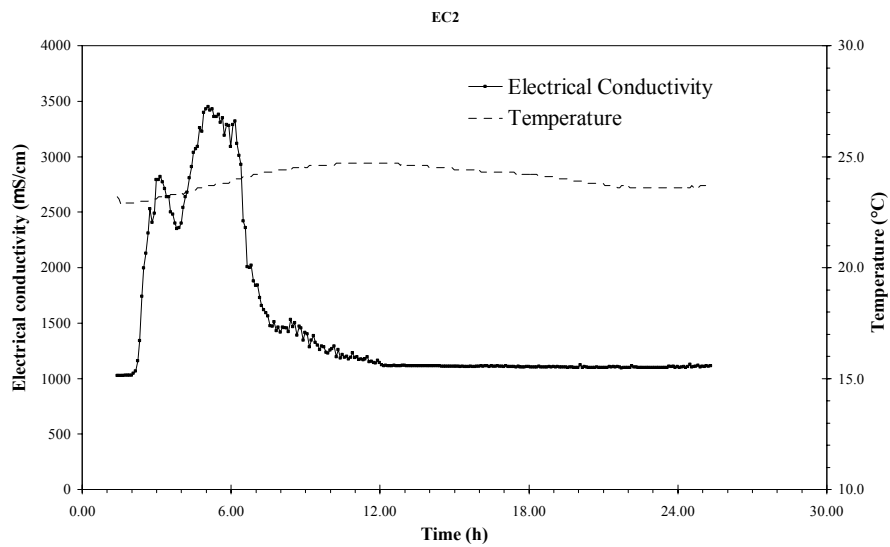


Fig. 14 – Electrical conductivity in measuring placing EC2.

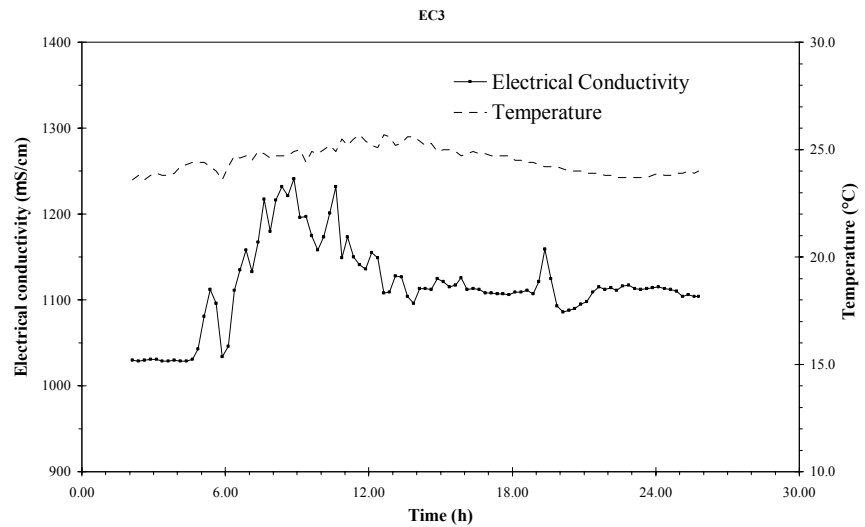


Fig. 15 – Electrical conductivity in measuring placing EC3.

5 Conclusions.

The experimental measurements performed within the Ca' di Mezzo Wetland in Codevigo provided useful information both on the flow field deriving from incoming discharges and on related dispersion processes. Collected data can be particularly useful for the implementation and calibration of hydrodynamic and transport models.

References.

Bixio V., 2000. Water quality improvements in the drainage networks flowing in the Venetian Lagoon . *International workshop on development and management of flood plans and wetlands*. IWF 2000, Beijing, 107-116.

RESEARCH LINE 3.18

**Residence times and hydrodynamical
dispersion in the Venice lagoon**

TIDAL SIMULATION IN VENICE LAGOON

Maria Morandi Cecchi¹, Manolo Venturin¹

¹ Dipartimento di Matematica Pura ed Applicata, Università degli Studi di Padova

Riassunto

Con questo articolo si vuole studiare i principali fenomeni idrodinamici legati alle equazioni delle acque basse nella Laguna di Venezia. Allo scopo, viene utilizzato il modello "dell'onda lunga" per descrivere la fisica che governa questi fenomeni. Sotto questa ipotesi, la lunghezza d'onda risulta molto maggiore della profondità, e quindi il flusso può essere considerato praticamente orizzontale. La risoluzione numerica avviene mediante uso di una procedura di "operator-splitting" basata su elementi finiti.

Abstract

The aim of this paper is to investigate shallow water hydrodynamic phenomena in the Venice Lagoon using the long wave physical model. In such model, the wave length is greater than the depth, so the vertical velocity and accelerations can be neglected, and the flow becomes almost horizontal. The numerical method used is a finite element approach based on a operator-splitting technique.

1 Introduction

The Venice Lagoon is a large natural basin characterized by a complex geometry and bathymetry, see Fig. 1. Several islands and deep canals crossing wide shallow water areas are presents in the lagoon.

The hydrodynamic processes, tidal currents, tidal elevations and secondary circulation between the different parts of the lagoon, are well described by two-dimensional models based on the shallow water equations.

The solution of these equations is of considerable importance for a variety of problems appearing in coastal and environmental engineering. Numerous computer codes using both finite difference [Casulli et al., 1992] and finite element [Morandi Cecchi et al., 1993; D'Alpaos et al., 1993; Umgiesser et al., 1993] approaches have been introduced to investigated shallow water phenomena in Venice Lagoon. The interest in this area is largely motivated by environmental considerations, such as tidal currents, tidal elevations and pollutant dispersion, and the need for prediction of human intervention, such as harbours, barrages, etc.

In this paper we shall present a numerical model for the simulation of tidal elevation and current propagation in the Venice Lagoon. This algorithm is based on an operator split procedure with a finite element space discretization. The calculation step can be carried out either in semi-implicit of fully implicit form.



Fig. 1 – The Venice Lagoon system.

2 Governing Equations

In this section we give a short description of the shallow water equations and their numerical approximation used in the simulations of the tidal motion in the Venice lagoon system. A more detailed discussion can be found in [Morandi Cecchi et al., 1998].

The shallow water equations here presented are based on the commonly used assumptions:

- well mixed hydrodynamics flow;
- the water elevation with respect to the free surface at rest is at any time much smaller than the depth;
- vertical effects (acceleration and diffusion) are negligible;
- horizontal velocities do not vary with the depth.

The equations in conservative form with respect to the Cartesian system of spatial coordinates x_1 and x_2 become in compact form [Peraire et al., 1986; Zienkiewicz et al., 1993]:

$$\frac{\partial U}{\partial t} + \frac{\partial F_1}{\partial x_1} + \frac{\partial F_2}{\partial x_2} = R_s \quad (1)$$

where $U = [h, hu_1, hu_2]^T$,

$$F_1 = \left[hu_1, hu_1^2 + \frac{1}{2}g(h^2 - H^2), hu_1u_2 \right]^T,$$

$$F_2 = \left[hu_2, hu_1u_2, hu_2^2 + \frac{1}{2}g(h^2 - H^2) \right]^T$$

$$R = R_s + \frac{\partial R_{d1}}{\partial x_1} + \frac{\partial R_{d2}}{\partial x_2}$$

with

$$R_s = \left[0, fhu_2 + g(h - H)\frac{\partial H}{\partial x_1} - \frac{g|u|u_1}{C^2H}, -fhu_1 + g(h - H)\frac{\partial H}{\partial x_2} - \frac{g|u|u_2}{C^2H} \right]^T$$

$$, R_{d1} = \left[0, \frac{2\mu_H h}{\rho} \frac{\partial u_1}{\partial x_1}, \frac{\mu_H h}{\rho} \left(\frac{\partial u_2}{\partial x_1} + \frac{\partial u_1}{\partial x_2} \right) \right]^T,$$

$$R_{d2} = \left[0, \frac{\mu_H h}{\rho} \left(\frac{\partial u_2}{\partial x_1} + \frac{\partial u_1}{\partial x_2} \right), \frac{2\mu_H h}{\rho} \frac{\partial u_2}{\partial x_2} \right]^T.$$

Where $H(x_1, x_2)$ is the water depth in the stationary condition over the mean sea level, $\eta(x_1, x_2, t)$ is the height of the free surface, $h(x_1, x_2, t) = H(x_1, x_2) + \eta(x_1, x_2, t)$ is the total height of the fluid, $u_1(x_1, x_2, t)$ and $u_2(x_1, x_2, t)$ are the components of the fluid velocity with respect to the coordinate axes averaged over the depth, g is the acceleration gravity, $C(x_1, x_2)$ and f are the Chèzy and Coriolis coefficients respectively and μ_H and ρ are the viscosity coefficient of turbulence and the density respectively, having omitted the atmospheric pressure.

Under the long-wave hypothesis, omitting advection and viscous terms, and including the forces due to a wind blowing at a speed on the water free surface, one obtains the shallow water system [Morandi Cecchi et al., 1993, Morandi Cecchi et al., 1998]:

$$\frac{\partial U}{\partial t} + \frac{\partial F_1}{\partial x_1} + \frac{\partial F_2}{\partial x_2} = R_s \quad (2)$$

where

$$U = [\eta, u_1, u_2]^T, F_1 = [Hu_1, g\eta, 0]^T, F_2 = [Hu_2, 0, g\eta]^T$$

$$R_s = \left[0, \quad fhu_2 - \frac{g|u|u_1}{C^2H} + \frac{\xi|v|v_1}{H}, \quad -fhu_1 - \frac{g|u|u_2}{C^2H} + \frac{\xi|v|v_2}{H} \right]^T$$

where ξ is a dimensionless constant determined experimentally that models wind-water interaction and v_1 and v_2 are the components of v along the two coordinate axes.

This semi-linear system is to be solved in the two-dimensional domain Ω for η , u_1 and u_2 with the following boundary conditions:

- normal velocities along the boundary Γ ;
- prescribed water elevation and direction of flow at the in/outlets.

In order to solve Equation (2) for the Venice Lagoon, a projection method has been adopted. By taking

$$F_i = F_i^* + F_i^{**}, \quad i = 1, 2$$

and

$$U^{(n+1)} = U^{(n)} + \Delta U^* + \Delta U^{**}$$

with $F_i^* = 0$, $F_i = F_i^{**}$, ΔU^* and ΔU^{**} the corresponding increments in the solution vector from time step n to step $n + 1$ can be split into

$$\frac{\partial \Delta U^*}{\partial t} = R_s \tag{3}$$

$$\frac{\partial \Delta U^{**}}{\partial t} + \frac{\partial F_1^{**}}{\partial x_1} + \frac{\partial F_2^{**}}{\partial x_2} = 0 \tag{4}$$

Next, a semi-implicit scheme is used which consists of solving Equation (3) by an explicit time integration procedure and Equation (4) by an implicit method.

The discretization in time of Equation (3) is obtained by a second-order Taylor expansion which gives for a time step Δt :

$$(\Delta U^*)^{(n+1)} = \Delta t R_s^{(n)} + \frac{\Delta t^2}{2} G R_s^{(n)} \tag{5}$$

where

$$G = \frac{\partial R_s}{\partial \Delta U^*}.$$

For the discretization in space, the point collocation method based on the mesh node is used, and this reduces to a set of uncoupled equations which can be

easily solved by a simple evaluation of the right-hand side at the nodes of the mesh.

The system Equation (4) is integrated in time according to the θ -method. The discretization in space is performed by using linear triangular elements which gives

$$\left[\frac{1}{g} M + \Delta t^2 \theta_1 \theta_2 S \right] (\Delta p^{**})^{(n+1)} = -\Delta t \left(\sum_{i=1}^2 Q_i \left(H \left[u_i^n + \theta_1 (\Delta u_i^*)^{(n+1)} \right] \right) + \Delta t \theta_1 S p^{(n)} \right) \quad (6)$$

$$M (\Delta u_i^{**})^{(n+1)} = -\Delta t Q_i \left[p^{(n)} + \theta_2 (\Delta p^{**})^{(n+1)} \right], \quad i = 1, 2 \quad (7)$$

with $p = g\eta$ and

$$M = \int_{\Omega} [\phi]^T [\phi] d\Omega, \quad S = \sum_{i=1}^2 \left(\int_{\Omega} \frac{\partial [\phi]}{\partial x_i} H \frac{\partial [\phi]^T}{\partial x_i} d\Omega \right), \quad Q_i = \int_{\Omega} [\phi] \frac{\partial [\phi]^T}{\partial x_i} d\Omega.$$

Here, $[\phi]$ is the vector of shape functions at all grid points.

From a computational point of view the solution of system Equation (6) has been obtained using the conjugate gradient method in order to contain the storage requirements, since it allows all quantities needed during an iteration to be evaluated at the element level and then assembled in vector form. For such system, some modules of the Nonsymmetric Preconditioned Conjugate gradient (NSPCG) library have been considered.

The solution of the pair of system in Equation (7) the following iterative method has been adopted

$$\left[(\Delta u_i^{**})^{(n+1)} \right]^{r+1} = M_L \left(f_i^{(n)} - (M - M_L) \left[(\Delta u_i^{**})^{(n+1)} \right]^r \right), \quad r = 0, 1, 2, \dots, \\ i = 1, 2$$

where M_L is the mass lumped *i.e.* the diagonal matrix obtained from M by row summation, $f_i^{(n)}$ is the right-hand side of the i -th system and suffixes r and $r + 1$ stand for two subsequent iterations of then solution process.

To summarize the solution process involves for every single time increment the following steps.

- Evaluate $(\Delta u_i^*)^{(n+1)}$ from Equation (5).
- Solve the system, Equation (6) for $(\Delta \eta_i^*)^{(n+1)}$
- Solve the pair of uncoupled system Equation (7) for $(\Delta u_i^{**})^{(n+1)}$
- Evaluate the new solution vector as $U^{(n+1)} = U^{(n)} + \Delta U^* + \Delta U^{**}$.

3 A Domain Decomposition Approach to Shallow Water for the Venice Lagoon

A domain decomposition and parallel approaches are very useful for shallow water coastal and estuarine circulation problems. With such a type of model good solutions may be given to the problems of preparing a method for the use of parallel computers.

In the domain decomposition idea due to Schwarz the domain Ω is split into sub-domains, a problem is solved in each sub-domain in parallel and then the partial solutions are joined together to get the global solution. This technique can be employed for the solution of problems defined on irregular domain, using the same equations to be solved overall. The parallel code differs from the original serial code only in that it contains communication calls, modified loop limits and also some logical statement to ensure that each processor updates only its sub-region. In other words during the communication phase, each processor computes on its own portion of the data; during the communication phase, the processors exchange data using a message passing library.

In the finite element approach simulations with parallel computer, the fundamental goal is to partition the computation into an appropriate number of communicating processes to be executed concurrently in a way that will keep overhead requirement low. This implies that the meshed computational domain has to be decomposed into sub-domains so that each processor has to do about the same amount of work, and so that the communication time is as small as possible. Clearly, when the region of interest has a simple shape, there may be a natural choice of mesh whose structure is very regular. In the problem at hand, an unstructured mesh has been considered since it can represent the complex geometry of the Venice lagoon more adequately and readily. It can be noted that formally the partitioning unstructured mesh problem is a very hard optimization problem, so called NP-complete [Morandi Cecchi et al., 2002].

The problem to be solved is equivalent to find a partition which evenly balances the load in each sub-domain while minimizing the communication cost. Let $G = G(V, E)$ be an indirect graph of V vertices with E edges which represent the data dependencies in the mesh. When we consider only two processors, it is required to find a partition $V = V_1 \cup V_2$ such that $V_1 \cap V_2 = \emptyset$, $|V_1| = |V_2|$ and the number of cut edges $|C_E|$ defined by

$$|C_E| = | \{ 1 : 1 \text{ in } E; \quad 1 = (v_1, v_2); \quad v_1 \text{ in } V_1, \quad v_2 \text{ in } V_2 \} |$$

is minimized. Here, for a set S , $|S|$ denotes the number of elements in the set.

To partition a graph into more than two sub-graph, cuts are made recursively in order to obtain $2, 4, \dots, 2^s = p$ sub-domains of approximately equal size.

An approach based on Enhanced Sub-domain Generation Method (ESGM) using linear separator [Morandi Cecchi et al., 2002] is used to solve the previous problem. The optimal location of the separator is determined by a Genetic Algorithm (GA) module. This GA is regulated by a fitness function,

which has a maximum value when the numbers of generated elements are equal in both of the sub-domains and the number of interfacing edges (between the sub-domains) is a minimum in the final mesh.

Linear separator	Number of processor				
	2	3	4	5	6
Vertical	33	82	131	162	239
Horizontal	32	64	84	145	155

Tab. 2 –The total number of cut edges.

The results have shown that:

- the elements are (almost) equally distributed at each sub-region.
- it would be better to use horizontal separator due to the geometry of the mesh.

4 Numerical Results

The model is obtained considering different depths of the lagoon and in particular a finer discretization is considered where the wave runs with greater speed, namely along the largest canals.

The geometry, see Fig. 2, and the bathymetry, see Fig. 3 is related to December 2003; the computational mesh is composed by 2173 nodes and 3745 triangles as reported in Fig. 2.

The wind data are given in three station (Chioggia south dam, Malamocco south dam and Grassabò) and their extension to overall domain is necessary to obtain a realistic wind effects. This process consists in an interpolation/extrapolation routine based on inverse proportional distance weight mean and the effect is coupled to then hydrodynamic model via a water-wind coefficient of interaction, ξ , experimentally estimated.

The program has been run for long periods of simulation; many months of simulations have been run successfully with no loss of fluid and perfect behaviour. To validate the program, field data are used taken from the data of the Magistrato alle Acque of Venice. The data have been introduced at the three inlets of the lagoon as boundary conditions on the open boundary.

A comparison has been made between the simulation results and the real data from the internal measurement stations of the lagoon. The comparison is referred to the period 27 November 2003 to 24 December 2003, using a time step, Δt , of 5 sec. The results are reported in Figs. 4, and 5 which shows the good agreement of the model.

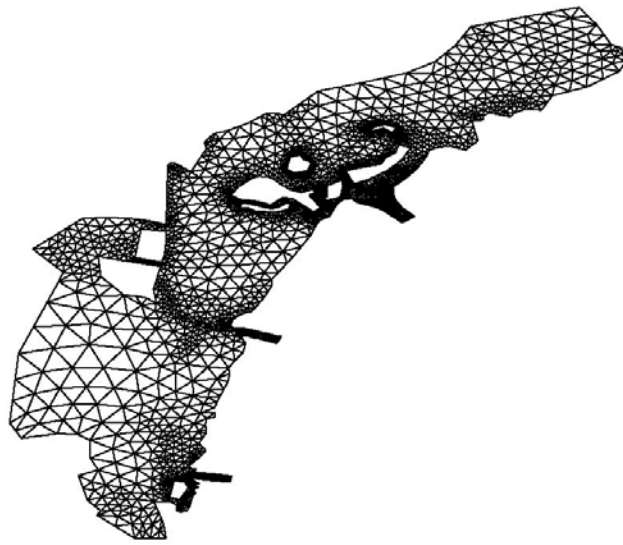


Fig. 2 – The mesh of the Venice Lagoon. 2173 nodes and 3745 elements.

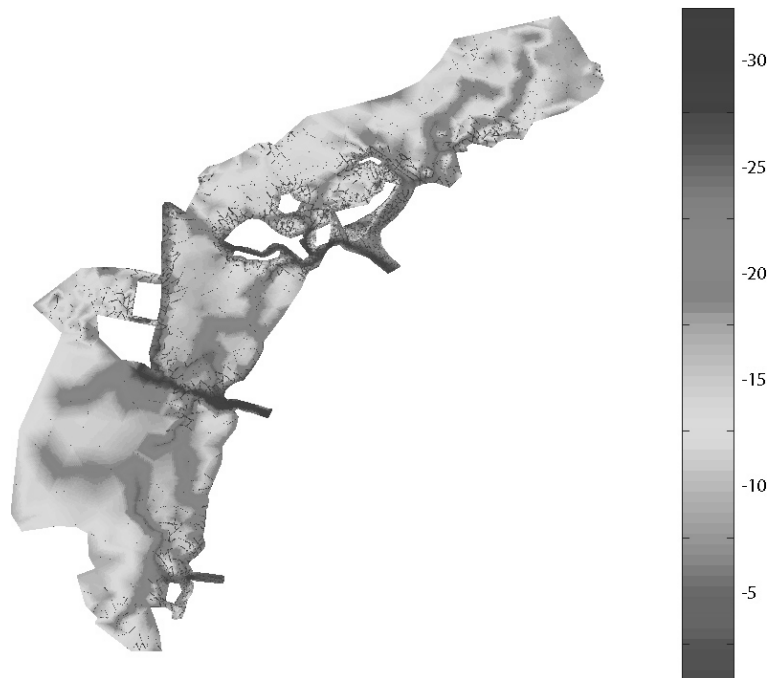


Fig. 3 – The bathymetry of the Venice Lagoon. Depth in meters.

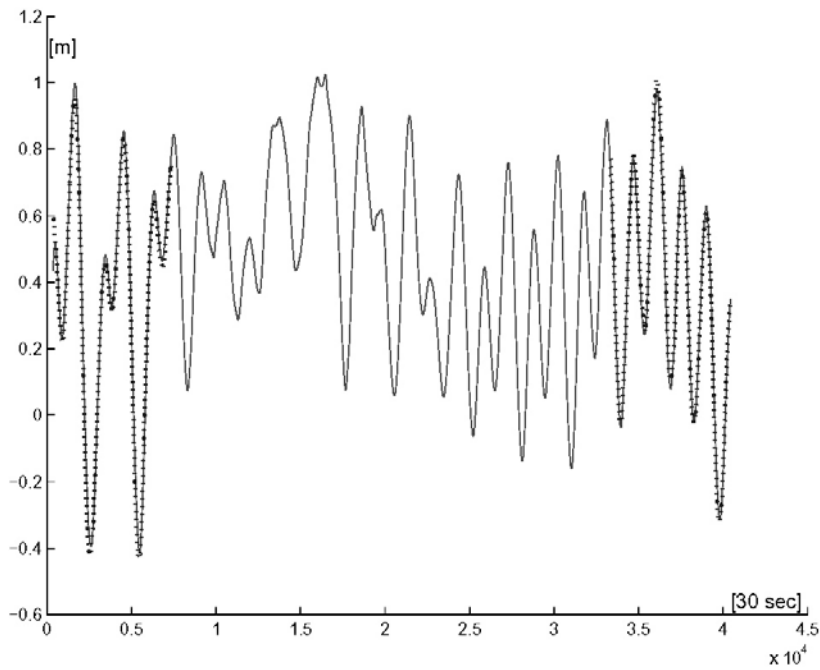


Fig. 4 – 1st and 2nd week of Vigo Chioggia: Simulated computation (continuous line) and experimental data (dotted line).

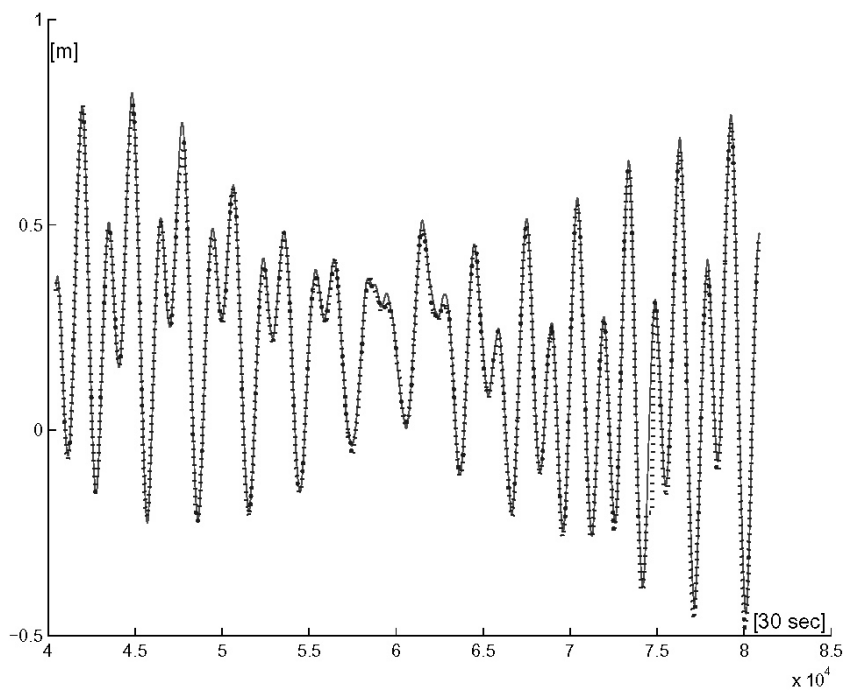


Fig. 5 – 3rd and 4th week of Vigo Chioggia: Simulated computation (continuous line) and experimental data (dotted line).

5 Conclusions

The presented model is shown to be a flexible and efficient tool in order to investigate the shallow water phenomena that occur in a shallow water

modeling. In fact, it permits to treat with complex geometry, with different physical parameters, and several boundary conditions

The numerical model here presented seems to be an useful tool in order to investigate lagoon phenomena and it can be seen as a starting point for future study, such as lagoon pollution, when this model is coupled with advection-diffusion equations.

References

Casulli V., and Cheng R. T., 1992. Semi-implicit finite difference methods for three-dimensional shallow water flow. *International Journal of Numerical Methods in Fluids*, 15, 629-648.

D'Alpaos L. and Defina A., 1993. Venice lagoon hydrodynamic simulations by coupling 2D and 1D finite element models. In Morgan K., Morandi Cecchi M., and Zienkiewicz O. C. (eds), *Finite Elements in Fluids*, Pineridge, Swansea, 917-926.

Morandi Cecchi M., 1988. Domain decomposition method for shallow water flow problems. In Niki N. and Kawahara M. (eds), *Computational Methods in Flow Analysis*, 2, Okayama University of Science, 1322-1329.

Morandi Cecchi M., 1989. Study of the behaviour of oscillatory waves in a lagoon. *International Journal for Numerical Methods in Engineering*, 27, 103-112.

Morandi Cecchi M., Secco E. and Pica A., 1993. Domain decomposition of finite element model of a lagoon. In Morgan K., Morandi Cecchi M., and Zienkiewicz O. C. (eds), *Finite Elements in Fluids*, Pineridge, Swansea, 990-998.

Morandi Cecchi M., Secco E. and Pica A., 1993. Tidal flow analysis with core minimization. In Morgan K., Morandi Cecchi M., and Zienkiewicz O. C. (eds), *Finite Elements in Fluids*, Pineridge, Swansea, 1026-1036.

Morandi Cecchi M., Pica A. and Secco E., 1998. A projection method for shallow water equations. *International Journal for Numerical Methods in Fluids*, 27, 81-95.

Morandi Cecchi M. and Salasnich L., 1998. Shallow water theory and its application to the Venice lagoon. *Computer Methods for Applied Mechanics Engineering*, 151, 63-74.

Morandi Cecchi M. and Marcuzzi F., 1999. Adaptivity in space and time for shallow water equations. *International Journal of Numerical Method in Fluids*, 31, 285-297.

Morandi Cecchi M. and Pirozzi M. A., 2002. A parallel shallow water finite element solver for the Venice lagoon. *International Journal of Computational Fluid Dynamics*, 16(2), 93-99.

Peraire J., Zienkiewicz O. C. and Morgan K., 1986. Shallow water problems: A general explicit formulation. *International Journal for Numerical Methods in Engineering*, 22, 547-574.

Umgiesser G. and Bergamasco A., 1993. A staggered grid finite element model of the Venice lagoon. In Morgan K., Morandi Cecchi M., and Zienkiewicz O. C. (eds), *Finite Elements in Fluids*, Pineridge, Swansea, 659-668.

Zienkiewicz O. C., Wu J. and Peraire J., 1993. A new semi-implicit or explicit algorithm for shallow water equations. *Math. Model. Sci. Comput.*, 1, 31-49.

A FORMULATION OF CONVECTION PROBLEMS FOR SHALLOW WATERS IN VENICE LAGOON

Maria Morandi Cecchi¹, Manolo Venturin¹

¹ *Dipartimento di Matematica Pura ed Applicata, Università degli Studi di Padova*

Riassunto

In questo articolo si vuole presentare il metodo “Characteristic Based Split” particolareggiato alle equazioni delle Acque Basse. Viene fornita una versione a due passi basata su una tecnica di “mass lumping” al fine di stabilizzare le equazioni di convezione diffusione presenti.

Viene inoltre fornita la tecnica di adattività di mesh utilizzata per la gestione della batimetria della laguna.

Abstract

In this paper, we review the “Characteristic Based Split” scheme applied to the shallow water equations. We give a two step version based on a “mass lumping” technique in order to stabilize the convection terms that appears.

We also give a description of the adaptivity technique used to manage the lagoon bathymetry.

1 Introduction

Many Computational Fluid–Dynamics (CFD) problems require a great computational effort to approximate correctly the solution, near strong discontinuities or shocks. Usually, such discontinuities are localized in specific parts of the domain, and may evolve during the computations in time.

The main difficulty is due to the presence of convection operators in the formulation of flow problems based on kinematic description other than Lagrangian. In fact, these operators are non–symmetric and thus the best approximation property in the energy norm of the Galerkin method is lost when convection dominates the transport processes. This property is the basis of success in symmetric cases of the Galerkin method.

In practical cases, solutions to advection–dominated transport problems by the Galerkin method are often corrupted by spurious node to node oscillations that can be severe mesh (and time step) refinement which clearly destroy the practical utility of the method. This has motivated the development of the standard Galerkin formulation which precludes oscillations without requiring mesh refined or time step refinement. Such alternatives are called stabilization techniques and have provided a major feature in finite element modeling of problems in fluid–dynamics.

In truly transient situations, another important issue is to ensure the proper

coupling between spatial and temporal discretizations. In fact, a stable and accurate spatial representation will be quickly spoiled if the algorithm used for transporting the solution in time is not of comparable accuracy. Space–time coupling is indeed particularly crucial when convection dominates the transport process, due to the directional character of propagation of information in hyperbolic problems. Significant progress has also been achieved in recent years in the development of algorithms for accurately solve the transient solutions of highly convective transport problems.

A number of important phenomena encountered in coastal and environmental engineering, are described by the nonlinear shallow water equations. Their interests is largely motivated by environmental considerations, such as the study of tidal currents and water elevations for flood control, and the need for prediction of man–made alterations to the environment by the construction of harbours, barrages, etc.

In the above applications, it is increasingly important to be able to deal with complex geometries with several physical parameters and different boundary conditions. It is also desired to preserve accuracy of solutions in the computational steps and to save simulation time. Hence, the development of sound and flexible numerical tools are important in the investigations of such phenomena in order to have a “true” and “close” description of the reality.

Moreover, transport models, governed by advection–diffusion equations, can also be coupled to the shallow water hydrodynamic model making it possible to study pollutant dispersion or temperature distribution.

In some previous papers [Morandi Cecchi et al., 1998, Morandi Cecchi et al., 2004] only “shallow water diffusive problems” have been considered, using the long–wave hypothesis and omitting advection–viscous terms. Here, a new numerical method based on the Characteristic Based Split method (CBS) is presented for a “advection–diffusion shallow water model” based on primitive variable formulations (retaining velocity and pressure or water elevation as unknowns). The algorithm can treat transient problems, as well as steady state flows both in subcritical or supercritical regime, including “jump” or shock patterns. Moreover, the extension of the algorithm to deal with advection–diffusion equations is straightforward.

During the last years, considerable effort has been focused towards the development of two–dimensional models for the numerical approximation of the shallow water equations both in conservative and non–conservative forms, and many numerical schemes are now available for that purpose. In the past, the most popular methods used for this discretization are based on finite differences and finite volume methods [LeVeque, 2002; Tan, 1992]. Recently, alternative approaches such as spectral element methods [Ma, 1993], and finite element schemes have been proposed [Carey, 1995; Tan, 1992; Zienkiewicz et al. 2000].

2 Governing equations

The shallow water equations can be written as

Continuity equation

$$\frac{\partial h}{\partial t} = \frac{1}{c^2} \frac{\partial p}{\partial t} = - \frac{\partial U_i}{\partial x_i} \quad (1)$$

Momentum equations

$$\frac{\partial U_i}{\partial x_i} = - \frac{\partial}{\partial x_j} (U_i u_j) - \frac{\partial p}{\partial x_i} - Q_i \quad (2)$$

where h or p and u_i are the unknowns. In the expressions, g is the gravity acceleration, ρ is the density of the water, δ_{ij} is the Kronecker delta, τ_{ij} are the viscous stress components given by

$$\tau_{ij} = \mu_H \left(\frac{\partial u_i}{\partial x_j} + \frac{\partial u_j}{\partial x_i} - \frac{2}{3} \delta_{ij} \frac{\partial u_k}{\partial x_k} \right) \quad (3)$$

where μ_H is the eddy viscosity coefficient. The Q_i term contains the source terms, which can be specified as

$$Q_i = f_i - g(h - H) \frac{\partial H}{\partial x_i} + \frac{h}{\rho} \frac{\partial p_a}{\partial x_i} - \frac{1}{\rho} (\tau_i^w - \tau_i^b) \quad (4)$$

where f_i is the i -th component of the Coriolis force $F = [-fhu_2 \quad fhu_1]^T$ with f the Coriolis coefficient, p_a is the atmospheric pressure distribution, τ_i^w is the wind stress traction on the surface and τ_i^b is the bottom friction stress.

The surface wind stress term τ_i^w represents the drag force produced by wind over the water surface and can be expressed as

$$\tau_i^w = \gamma |v| \quad (5)$$

where γ is an experimental constant that models wind–water interactions,

$$v = (v_1 \quad v_2)$$

is the wind velocity field and

$$v = \sqrt{v_1^2 + v_2^2}$$

The bottom friction stress τ_i^b can be modelled by the Chèzy formula

$$\tau_i^b = \frac{\rho g u_i |u|}{C^2 h} \quad (6)$$

where $C(x_1, x_2)$ is the Chèzy coefficient, $u = (u_1, u_2)$ is the flow velocity field and

$$u = \sqrt{u_1^2 + u_2^2}$$

In the case of pollutant dispersion of a passive tracer (scalar variable) T ("passive" meaning the distribution of the tracer does not affect the fluid flow), the following advection–diffusion equations should be solve

Transport equation

$$\frac{\partial(hT)}{\partial t} + \frac{\partial}{\partial x_i}(hu_i T) - \frac{\partial}{\partial x_i} \left(hk \frac{\partial T}{\partial x_i} \right) + R = 0 \quad (7)$$

in which T is the depth–averaged pollutant dispersion, k is the depth–averaged diffusion coefficient, h and u_i are the depth and fluid velocity previously computed, and R is a depth–averaged source ($R > 0$) or sink ($R < 0$) term.

The numerical difficulties, encountered in this problem, in the use of the standard Galerkin finite element method are mainly of three different kinds: the mixed type of the equations, which is due to the coupling of the momentum equation with the incompressibility condition, and subsequently, the treatment of the pressure or water elevation term; the advective–diffusive character of the equations, which have a viscous and a convective term; and finally, the nonlinearity of the problem. In the case of "shallow water diffusive problems" an efficient algorithm may be found in [Morandi Cecchi et al., 1998; Zienkiewicz et al., 1990]. The first is related to the incompressibility of the fluid and exhibits itself when an incorrect combination of element interpolation functions for the velocity and pressure or water elevation is employed. It consists of a constraint on the velocity field which must be divergence free. Then, the pressure has to be considered as a variable not related to any constitutive equation. Its presence in the momentum equation has the purpose of introducing an additional degree of freedom needed to satisfy the incompressibility constraint. The role of the pressure variable is thus to adjust itself instantaneously in order to satisfy the condition of divergence–free velocity. That is, the pressure is acting as a Lagrangian multiplier of the incompressibility constraint and thus there is a coupling between the velocity and the pressure unknowns [Donea et al., 2003; Morandi Cecchi et al., 1998].

Another source of numerical difficulty is due to the presence of nonlinear and non–symmetric convective terms in the momentum equations. As it is well known, the standard Galerkin formulation typically lacks stability when convective effects dominate and alternative spatial discretization procedure

must be used to restore stability without compromising the accuracy.

3 Numerical approximation

As a starting point for the development of the finite element models for the shallow water equations, we consider the CBS algorithm proposed by Zienkiewicz and co-workers [Zienkiewicz et al., 1993; Zienkiewicz et al., 1995; Zienkiewicz et al., 1998] (a detailed description is available in [Zienkiewicz et al., 2000]). Its basis is the fractional step procedure introduced by Chorin [Chorin, 1968; Chorin, 1969] and Temam [Temam, 1969] for incompressible Navier–Stokes equations in the finite difference context.

The main idea of the Chorin–Temam method consists in the decomposition of the time advancement into a sequence of two or more steps that split the numerical treatment of the equation operators into relatively easier subproblems. The principle of the projection method is to compute the velocity and pressure fields separately through the computation of an intermediate velocity, which is then projected onto the subspace of solenoidal vector functions. Basic to the derivation of projection methods is a theorem of orthogonal decomposition due to Ladyzhenskaya, which is based on the Helmholtz decomposition principle [Quartapelle, 1993].

Several implementations have been proposed to perform such splitting and therefore a variety of fractional–step methods exists: fractional steps or splitting methods for evolution equations [Yanenko, 1971], methods based on a projection onto a subspace of the solenoidal vector functions [Temam, 1984]; algebraic splitting methods [Perot, 1993; Quarteroni, 2000] and methods based on pressure or velocity correction [Kovacs et al., 1991; Zienkiewicz et al., 2000]. A detailed exposition of fractional–step methods can be found in [Doneat et al., 2003; Gresho et al., 2000; Quartapelle, 1993; Quarteroni, 1994] and references therein.

The CBS scheme combines the characteristic–Galerkin [Zienkiewicz et al. 2000] method to deal with convection dominated flows with a splitting technique based on velocity correction. The velocity field is computed into two stages with the characteristic–Galerkin method. In the first step, the pressure term (or elevations of the free surface) is retained from the momentum equations and an intermediate velocity field is estimated. Then, the continuity equation is solved using the intermediate vector field value and the pressure is carried out, by means of a Laplacian–type equation, whose self–adjoint form makes the Galerkin space discretization optimal. Finally, the velocity field is corrected using the new computed pressure term.

This leads to the following time–discretization formulae:

Intermediate momentum

$$\Delta U_i^* = \Delta t \left[\frac{\partial}{\partial x_j} (U_i u_j)^n - Q_i^n \right] + \frac{\Delta t^2}{2} u_k^n \frac{\partial}{\partial x_k} \left[\frac{\partial}{\partial x_j} (U_i u_j)^n + Q_i^n \right] \quad (8)$$

Pressure equation

$$\left(\frac{1}{c^2}\right)^n \Delta p - \Delta t^2 \theta_1 \theta_2 \frac{\partial}{\partial x_i} \left(\frac{\partial(\Delta p)}{\partial x_i} \right) = -\Delta t \frac{\partial}{\partial x_i} (U_i^n + \theta_1 \Delta U_i^*) + \Delta t^2 \theta_1 \frac{\partial}{\partial x_i} \left(\frac{\partial p^n}{\partial x_i} \right) \quad (9)$$

Momentum correction

$$\Delta U_i = \Delta U_i^* - \Delta t \frac{\partial p^{n+\theta_2}}{\partial x_i} + \frac{\Delta t^2}{2} u_k^n \frac{\partial}{\partial x_k} \left(\frac{\partial p^n}{\partial x_i} \right) \quad (10)$$

where higher order terms have been neglected.

The approximation of the scalar transport, Eqn. 7, that can be added to the hydrodynamic model, is straightforward, and it requires only the application of the characteristic–Galerkin method. Hence, the characteristic time discretization gives

Transport equation

$$\Delta T = \Delta t \left[-\frac{\partial}{\partial x_j} (u_j T)^n + \frac{\partial}{\partial x_j} \left(k \frac{\partial T}{\partial x_j} \right)^{n+\theta_3} - R^n \right] + \frac{\Delta t^2}{2} u_k^n \frac{\partial}{\partial x_k} \left[\frac{\partial}{\partial x_j} (u_j T)^n + R^n \right] \quad (11)$$

where T is multiplied by h , $\Delta T = T^{n+1} - T^n$.

The procedure has some interesting and useful advantages. The first is that dropping the pressure term, each momentum equation is similar to an advection–diffusion equation and so the characteristic–Galerkin procedure can be applied. The idea of the characteristic–Galerkin scheme is to stabilize advection–diffusion equations using a finite difference discretization of the total derivative along the characteristic. Then, if the discretization of the space is done, a consistent artificial diffusion, which stabilized convective terms, appears. The splitting operation, being self–adjoint, can then be solved optimally using the Galerkin procedure. The second advantage is that removing the pressure from the momentum equations enhances the pressure stability and permits to avoid any restrictions on the nature of the interpolation functions for both velocity and pressure, i.e. the Babuska–Brezzi condition is satisfied. Finally, in the semi–implicit form the algorithm provides a critical time step dependent only on the current velocity instead of the wave celerity [Zienkiewicz et al., 1993; Zienkiewicz et al. 2000].

After Galerkin spatial discretization of the CBS equations, the following algebraic system is obtained:

$$M(U^{n+1} - U^n) = f \quad (12)$$

where M is the mass matrix and f is the right hand side. In order to introduce

an added dissipation and to reduce the second-order scheme to first order near shocks, the consistent mass matrix M is replaced with then diagonal matrix M^L (mass lumping). Furthermore, in order to separate the effect of convective transport from that associated with the added dissipation, it is appropriate to implement the scheme according to the following two-stage procedure [Donea et al., 1988]:

$$\begin{aligned} M(U^* - U^n) &= f \\ M^L(U^{n+1} - U^*) &= d(M - M^L)U^* \end{aligned} \quad (13)$$

where d is the added dissipation parameter. A second order scheme is obtained for $d = 0$ and a first-order method with maximum dissipative effect is obtained when $d = 1$.

4 Mesh generation

The successful implementation of a finite element model for computing shallow-water flow requires the identification and spatial discretization of a surface water region. A broad range of engineering applications use triangulations or meshes as a spatial support in order to solve associated discretization problems. In many of these applications, unstructured triangles are the basic elements to perform the fundamental steps, whose aspect ratios and orientations are chosen to suit the function they interpolate or the Partial Differential Equations (PDEs) whose solution should be approximated. Triangles that are nearly equilateral (isotropic mesh) are excellent for some applications; for others, elements that have a specified direction and elongation may offer better accuracy with fewer elements (anisotropic mesh) [Apel, 1999; George et al., 1998].

For example, in Computational Fluid-Dynamics (CFD) many physical problems are characterized by solutions exhibiting directional features and, in this situation, the effectiveness of the Finite Element Method (FEM) or the Finite Volume Method (FVM) can be improved if the mesh is suitably oriented [Morandi Cecchi et al., 1998; Morandi Cecchi et al., 1999; Morandi Cecchi et al., 2000].

In an iterative mesh generator process, the first step requires — as pre-requisite — an initial adequate meshing of the domain, obtained by Delaunay triangulation [George et al., 1998] or advancing-front methods [Lohner, 1996]. It is important that the initial computational grid has to be “coarse” and “fine” enough to preserve all specific features characterizing the considered problem. The solution obtained is analyzed via a-posteriori error estimators and indicators, which will denote whether or not the process converges. In this case, the role of the error estimate is to localize the part of the domain where is necessary further refinements or un-refinements and new elements size may be determined. Particularly, it is possible to reduce effectively and efficiently the error, refining (or un-refining) the area of the mesh where the error estimate is

higher (or lower) with respect to a certain threshold. Then, a new mesh is produced and the entire process is repeated.

Any adaptive procedure needs a powerful refinement strategy to properly refine the mesh. In the literature, several methods have been developed, in particular it is useful to subdivide them according to:

- *r-refinement*: Using the *r*-method, the connectivity of the mesh remains unchanged, while node relocation is used to move the mesh nodes as desired.
- *p-refinement*: This approach uses the same elements size and increases the order of the interpolation functions.
- *h-refinement*: There are two types of refinement techniques used in the *h*-method and are defined in terms of local or global enrichment. In the local mesh refinement, the subdivision of the elements is obtained without changing their original position. In this process, only the elements where the error, given by the error estimator/indicator, exceeds the prescribed tolerance will be refined. Instead, in the global mesh refinement (re-meshing), a complete discretization is carried out.
- *hp-refinement*: The *hp*-method combines both the *h*-method and the *p*-method.

In the approach here presented, unstructured triangles with local *h*-refinement are used. With these assumptions, the mesh will be refined locally, only when the error exceed the prescribe tolerance. This leads, in general, for a fixed accuracy, to a result very close to the optimal mesh with minimum number of elements. The process is repeated as many times as required.

The basis of adaptivity in FEM/FVM analysis is the computation of a-posteriori error local estimates which are essential for controlling the error within a prescribed tolerance. The error estimators give a (reliable) indication of the global and local error, measured in some norm, and a list of elements which should be refined to efficiently reduce the computational error at the next iteration. In particular, two type of error estimators are considered:

- *Residual based error estimators* [Verfurth, 1996] — Error estimators based on these methods use the residuals of the approximate solution, which fail to satisfy the mathematical model, either in explicit or in implicit form.
- *Recovery based error estimators* or *ZZ-error estimators* [Zienkiewicz et al., 1987; Zienkiewicz et al., 1992] — These types of error estimators are based on the comparison between two different approximations of the solution. The main advantages, over other types of estimators, are the simplicity of their implementation and their cost effectiveness; furthermore, they keep trace of the main error direction element by element.

This information is a key point used in our work, i.e. it is assumed that a-posteriori ZZ-method is implemented, such that, at each iteration, error and error gradient together with its magnitude in some norm are available. This solution will be analyzed by the given a-posteriori error estimator and the result is transformed into criteria directly usable to control the mesh generator process.

The main idea of the algorithm adopted is to introduce an edge almost orthogonal to the error gradient, if possible. This correspond to assume that the solution does not vary across the error gradient i.e., if there are solution discontinuities, these are across and not along the error gradient [Morandi Cecchi et al., 2001, Morandi Cecchi et al., 2004].

The main differences between the anisotropic adaptive algorithm here presented and the existing ones (regular refinement [Bank, 1997] and longest-edge bisection [Rivara, 1984]) are the use of the error and error gradient information computed by an a-posteriori error analysis in the selection of the triangle and edge to be refined instead of pure geometric arguments.

Some results can be found in [Morandi Cecchi et al., 2005].

5 Conclusions

In this paper we have proposed a finite element CBS model based on a two-step version with “mass lumping” technique for the 2D shallow water equations based on triangular elements. The results of our model will be reported in future papers.

We have also presented a scheme for adaptive mesh refinement/un-refinement for unstructured triangular mesh. It allows the use of a standard refinement patterns, and thanks to this approach, its complexity is comparable with respect to “classical scheme”.

References

- Apel T., 1999. *Anisotropic finite elements: local estimates and applications*. Teubner.
- Bank R., 1997. *PLTMG: A software package for solving elliptic partial differential equations. User Guide 8.0*. SIAM.
- Brezzi F., Franca L. P. and Russo A., 1998. Further considerations on residual-free bubbles for advective-diffusive equations. *Comput. Methods Appl. Mech. Engrg.*, 166, 25–33.
- Carey G. F. (editor), 1995. *Finite element modelling of environmental problems: surface and subsurface flow and transport*. John Wiley & Sons.
- Chorin A. J., 1968. Numerical solution of the Navier-Stokes equations. *Math. Comp.*, 22, 745–762.

- Chorin A. J., 1969. On the convergence of discrete approximations to the Navier–Stokes equations. *Math. Comp.*, 23, 341–353.
- Dahmen W., Kurdila A. J. and Oswald P. (editors), 1997. Multiscale wavelet methods for partial differential equations. In *Wavelet Analysis and its Applications*, vol. 6, Academic Press.
- Donea J., 1984. A Taylor–Galerkin method for convective transport problems. *International Journal for Numerical Methods in Engineering*, 20, 101–119.
- Donea J. and Huerta A., 2003. Finite element methods for flow problems. John Wiley & Sons.
- Donea J., Selmin V. and Quartapelle L., 1988. Recent developments of the Taylor–Galerkin method for the numerical solution of hyperbolic problems. In *Numerical methods for fluid dynamics, III*. Oxford Univ. Press, 171–185.
- George P.–L. and Borouchaki H., 1998. *Delaunay triangulation and meshing*. Hermès.
- Gresho P. M. and Sani R. L., 2000. *Incompressible Flow and the Finite Element Method. Vol. 1: Advection Diffusion. Vol. 2: Isothermal Laminar Flow*. John Wiley & Sons.
- Hughes T. J. R. and Brooks A., 1979. A multidimensional upwind scheme with no crosswind diffusion. In *Finite Element Methods for Convection Dominated Flows*, 34, 19–35.
- Hughes T. J. R., Franca L. P., Hulbert G. M., Johan Z. and Sakhil F., 1998. The galerkin least square method for advective diffusion equations. In *Recent Developments in Computational Fluid Mechanics*, Tezduyar T. E. and Hughes T. J. R. , editors.
- Kelley D. W., S. Nakazawa S., Zienkiewicz O. C. and Heinrich J. C., 1980. A note on upwinding and anisotropic balancing dissipation in finite element approximations to convective diffusion problems. *International Journal for Numerical Methods in Engineering*, 15, 1705–1711.
- Kovacs A. and Kawahara M., 1991. A finite element scheme based on the velocity correction method for the solution of a time–dependent incompressible Navier–stokes equations. *International Journal for Numerical Methods in Fluids*, 13, 403–423.
- LeVeque R. J., 2002. *Finite Volume Methods for Hyperbolic Problems*. Cambridge Texts in Applied Mathematics. Cambridge University Press.
- Lohner, R., 1996. Progress in grid generation via the advancing front technique. *Engineering with Computers*, Springer–Verlag, 12, 186–210.
- Ma, H., 1993. A spectral element basin model for the shallow water equations. *Journal of Computational Physics*, 109, 133–149.

- Morandi Cecchi M. and Marcuzzi F., 1999. Adaptivity in space–time finite element approximations. In *Computational Methods in Engineering and Science, Macao*, 1, 327–333.
- Morandi Cecchi M. and Marcuzzi F., 1999. Adaptivity in space and time for shallow water equations. *International Journal for Numerical Methods in Fluids*, 31, 285–297.
- Morandi Cecchi M. and Marcuzzi F., 2000. A directional adaptive scheme for unstructured meshes of space–time finite elements applied to compressible flows. In *Finite Elements in Fluids, Austin, Texas*, 38–39.
- Morandi Cecchi M. and Marcuzzi F., 2001. An algorithm for the anisotropic adaptivity of unstructured triangular meshes. In *2–nd European Conference on Computational Mechanics, Cracow, Poland*, 272–273.
- Morandi Cecchi M., Pica A. and Secco E., 1998. A projection method for shallow water equations. *International Journal for Numerical Methods in Fluids*, 27, 81–95.
- Morandi Cecchi M. and Salasnick L., 1998. The shallow water equations: State of the art and new trends. In Hafez M. and Oshima K., eds., *Computational Fluid Dynamics Review*, 972–993.
- Morandi Cecchi M. and Salasnick L., 1998. Shallow water theory and its application to the Venice lagoon. *Computer Methods for Applied Mechanics Engineering*, 151, 63–74.
- Morandi Cecchi M., M. Venturin, Russo M. R. and Marcuzzi F., 2004. A general framework for error estimation in preserving–shape grid generation in a fluid–dynamic environment and related open problems. In *European Congress on Computational Methods in Applied Sciences and Engineering, ECCOMAS 2004, Finland*, <http://www.mit.jyu.fi/eccomas2004/>.
- Morandi Cecchi M., M. Venturin, 2004. Tidal Simulation in Venice Lagoon. To appear.
- Morandi Cecchi M., M. Venturin, 2005. An algorithm for anisotropic mesh: An application to the Venice lagoon canals. To appear.
- Onate E., 1997. Derivation of stabilized equations for numerical solution of advective–diffusive transport and fluid flow problems. *Comput. Methods Appl. Mech. Engrg.*, 151, 233–265.
- Perot J. B., 1993. An analysis of the fractional step method. *J. Comput. Phys.*, 108, 51–58.
- Quartapelle L., 1993. *Numerical solution of the incompressible Navier–Stokes equations*. Birkhauser–Verlag.
- Quarteroni A., Saleri F. and Veneziani A. Factorization methods for the

numerical approximation of Navier–Stokes equations. *Comput. Methods Appl. Mech. Engrg.*, 188, 505–526.

Quarteroni A. and Valli A., 1994. *Numerical Approximation of Partial Differential Equations*. Springer–Verlag.

Rivara M.–C., 1984. Mesh refinement processes based on the generalized bisection of simplices. *SIAM J. Numer. Anal.*, 21, 604–613.

Temam R., 1969. Sur l'approximation de la solution des équations de Navier–Stokes par la méthode des pas fractionnaires. II. *Arch. Rational Mech. Anal.*, 33, 377–385.

Temam R., 1984. *Navier–Stokes equations*. North–Holland.

Verfurth R., 1996. *A Review of a Posteriori Error Estimation and Adaptive Mesh–Refinement Techniques*. Wiley–Teubner.

Yanenko N. N., 1971. *The Method of Fractional Steps. The Solution of Problems of Mathematical Physics in Several Variables*. Springer–Verlag.

Tan W., 1992. *Shallow Water Hydrodynamics*. Elsevier: Amsterdam, 1992.

Zienkiewicz O. C. and Codina R., 1993. A general algorithm for compressible and incompressible flow. I. The split, characteristic–based scheme. *International Journal for Numerical Methods in Fluids*, 20, 869–885.

Zienkiewicz O. C., Lohner R., Morgan K. and Peraire J., 1986. High speed compressible flow and other advection dominated problems of fluid mechanics. In *Finite Elements in Fluids*, Gallagher et al., editors, 6, 41–88.

Zienkiewicz O. C., Nithiarasu P., Codina R., Vazquez M. and Ortiz P., 1998. The characteristic–based–split procedure: an efficient and accurate algorithm for fluid problems. *International Journal for Numerical Methods in Fluids*, 31, 359–392.

Zienkiewicz O. C. and Ortiz P., 1995. A split–characteristic based finite element model for the shallow water equations. *International Journal for Numerical Methods in Fluids*, 20, 1061–1080.

Zienkiewicz O. C., Szmelter J. and Peraire J., 1990. Compressible and incompressible flow; an algorithm for all seasons. *Comput. Methods Appl. Mech. Eng.*, 78, 105–121.

Zienkiewicz O. C. and Taylor R. L., 2000. *The Finite Element Method. Vol. 3*. Butterworth–Heinemann, Oxford, fifth edition.

Zienkiewicz O. C. and Zhu J. Z., 1987. A simple error estimator and adaptive procedure for practical engineering analysis. *International Journal for Numerical Methods in Engineering*, 24, 337–357.

Zienkiewicz O. C. and Zhu J. Z., 1992. The superconvergent patch recovery and a posteriori error estimates. I. The recovery technique. *International Journal for Numerical Methods in Engineering*, 33, 1331–1364.

Zienkiewicz O. C. and Zhu J. Z., 1992. The superconvergent patch recovery and a posteriori error estimates. II. Error estimates and adaptivity. *International Journal for Numerical Methods in Engineering*, 33, 1365–1382.

Zienkiewicz O. C. and Zhu J. Z., 1992. The superconvergent patch recovery (SPR) and adaptive finite element refinement. *International Journal for Numerical Methods in Engineering*, 101, 207–224.

A 3-D SEDIMENT TRANSPORT MODEL AND BED REWORKING FOR THE VENICE LAGOON

Christian Ferrarin¹, Georg Umgiesser¹, Carl L. Amos²,

¹ ISMAR-CNR, S. Polo 1364, 30125 Venice, Italy, ² Southampton Oceanography Centre, SOC, Empress Dock, Southampton, Hampshire, UK.

1 Introduction

The Venice Lagoon consists of sediments that are mainly cohesive. However, sandy regions can be identified both inside the lagoon and close to the inlets. Venice Lagoon is a tidal-dominated lagoon but with strong wave influences (after Hubbard et al., 1979). It is also classified as restricted (after Kjerfve and Magill, 1989) due to the partial chocking of the lagoon by a well-developed, linked barrier island system made of sand (after Carter et al., 1987). The dominant factor governing the long-term evolution of this coastal lagoonal system is the stability and evolution of this barrier island system which is controlled by the availability and supply of sand.

In order to preserve the delicate lagoon ecosystem a modelling approach that combines hydrodynamics, waves and the sediment dynamics of the Venice Lagoon is highly desirable. This model could be used to estimate the actual loss or gain of sediments from the lagoon to the Adriatic Sea and the importance of the various forcing factors that influence these dynamics.

Coupling SHYFEM finite element hydrodynamic model with an empirical wave model and SEDTRANS05 sediment transport model we obtain a 3-D sediment transport model.

SHYFEM is a three-dimensional hydrodynamic model which uses finite element for horizontal discretization.

Sedtrans05 is a one-dimensional model of sediment transport for sand and mud under either current or combined waves and currents, on the continental shelf and in coastal waters. It applies the combined wave-current bottom boundary theories to derive the near bed velocity profile and bed shear stresses, and then calculates the sediment transport. It uses the sum of grain, bedload and bedform roughness height in the calculation of the total friction factor.

Such a 3-D model resolves the hydrodynamics, computing for every grid point the water level and the barotropic transports and estimating the wave field. The sediment transport module computes the erosion and deposition rates at every element and determines the sediment volume that is injected into the water column for several sediment sizes. After this step the sediments are advected with a transport and diffusion module. For the bedload component a direct advection scheme is used. Multiple grain types are used to track changes in seabed texture, and differential transport of material.

Modifications to bed elevation and to the grain size distribution are updated at

each time step based on the net erosion and deposition. At each location, the bed is modelled as several layers, the uppermost of them represents the surficial active, or mixed, layer. For each size class, the volume of sediment removed from the bed during any time step is limited by the amount available in the active layer. In this way the model takes into account time-dependent and spatial sediment distribution and bed armouring.

The model is freely available on the SHYFEM web page: <https://www.ismar.cnr.it/shyfem>.

2 Hydrodynamic

2.1 Governing equation

The hydrodynamic model used in this work is a three-dimensional finite element model developed at the CNR-ISMAR of Venice and successfully applied to some coastal environments (Umgiesser, 1997; Umgiesser et al., 2003; Ferrarin and Umgiesser, 2005; Scroccaro et al., 2003, 2004).

The model resolves the shallow water equations in their formulations with water levels and transports:

$$\frac{du}{dt} - fv = -\frac{1}{\rho_0} \frac{\partial p}{\partial x} + \frac{1}{\rho_0} \frac{\partial \tau_x}{\partial z} + A_H \left(\frac{\partial^2 u}{\partial x^2} + \frac{\partial^2 u}{\partial y^2} \right) \quad (1)$$

$$\frac{dv}{dt} + fu = -\frac{1}{\rho_0} \frac{\partial p}{\partial y} + \frac{1}{\rho_0} \frac{\partial \tau_y}{\partial z} + A_H \left(\frac{\partial^2 v}{\partial x^2} + \frac{\partial^2 v}{\partial y^2} \right) \quad (2)$$

$$\frac{\partial \zeta}{\partial t} + \frac{\partial H_{L^u}}{\partial x} + \frac{\partial H_{L^v}}{\partial y} = 0 \quad (3)$$

where ζ is the water level, HL the water column depth, f the Coriolis parameter, u and v the velocities in x and y direction, ρ_0 the water density, p the pressure and AH the horizontal eddy viscosity.

Integrating over one level the momentum equations read:

$$\frac{du_i}{dt} - fv_i = -\frac{1}{\rho_0} \frac{\partial p_i}{\partial x} + \frac{1}{\rho_0} \frac{\tau_x^{j-1} - \tau_x^j}{h_i} + A_H \left(\frac{\partial^2 u_i}{\partial x^2} + \frac{\partial^2 u_i}{\partial y^2} \right) \quad (4)$$

$$\frac{dv_i}{dt} + fu_i = -\frac{1}{\rho_0} \frac{\partial p_i}{\partial y} + \frac{1}{\rho_0} \frac{\tau_y^{j-1} - \tau_y^j}{h_i} + A_H \left(\frac{\partial^2 v_i}{\partial x^2} + \frac{\partial^2 v_i}{\partial y^2} \right) \quad (5)$$

with $h_i = H_i - H_{i-1}$ and $H_0 = -\xi$.

The stress terms for each layer could be expressed as:

$$\tau_x^j = -k \left(\frac{\partial u}{\partial z} \right)_i \quad (6)$$

$$\tau_y^i = -k \left(\frac{\partial v}{\partial z} \right)_i \quad (7)$$

with the follow boundary conditions:

$$\tau_x^{\text{sup}} = c_D \rho_a w_x \sqrt{w_x^2 + w_y^2} \quad (8)$$

$$\tau_y^{\text{sup}} = c_D \rho_a w_y \sqrt{w_x^2 + w_y^2} \quad (9)$$

$$\tau_x^{\text{bottom}} = c_B \rho_0 u_L \sqrt{u_L^2 + v_L^2} \quad (10)$$

$$\tau_y^{\text{bottom}} = c_B \rho_0 v_L \sqrt{u_L^2 + v_L^2} \quad (11)$$

with c_B the drag coefficient in the water, c_D the drag coefficient in the air, ρ_a the air density, ρ_0 the water density, (w_x, w_y) the wind velocities and (u_L, v_L) the bottom velocity. The water drag coefficient is computed from the Chezy equation $c_B = g/C^2$ with C the Chezy coefficient which varies with the depth following the relationsheep:

$$C = k_s H_i^{1/6} \quad (12)$$

with k_s the Strickler coefficient.

At the open boundaries the water levels are prescribed in accordance with the Diriclet condition, while at the closed boundaries only the normal velocity is set to zero and the tangential velocity is a free parameter (Umgiesser and Bergamasco, 1995).

The model uses a semi-implicit algorithm for integration in time, which combines the advantages of the explicit and the implicit scheme. The terms treated implicitly are the divergence terms in the continuity equation and the Coriolis term, the pressure gradient and the bottom friction in the momentum equation; all other terms are treated explicitly. It is unconditionally stable for any time step chosen and allows the transport variables to be solved explicitly without solving a linear system. Compared to a fully implicit solution of the shallow water equations the dimensions of the matrix are reduced to one third.

The spatial discretization of the unknowns has been carried out with the finite element method, partially modified from the classic formulation. This approach was necessary to avoid high numerical damping and mass conservation problems, due to the combination of the semi-implicit method with the finite element scheme (Galerkin method). With respect to the original formulation, here the water level and the velocities (transports, and) are described by using form functions of different order, being the standard linear form function for the water level, but stepwise constant form function for the transports. This will result in a grid that resembles more a staggered grid often used in finite difference discretization. A more detailed description of the model equations and of the discretization method is given in Umgiesser et al. (2004).

2.2 Waves

Resuspension of sediments due to wind-generated waves is an important source of sediment to the water column. The wave sub-model utilizes empirical formulations which provide approximate estimates of significant wave height and period. This account refraction, dispersion or wave breaking effect. The formulation of the significant wave height (H_{m0}) and period (T_p) is know empirical prediction equations for shallow water (U.S. Army Experiment Station, 1984):

$$\frac{gH_{m0}}{U_A^2} = 0.283 \tanh \left[0.530 \left(\frac{gh_a}{U_A^2} \right)^{3/4} \right] \tanh \left[\frac{0.00565 \left(\frac{gX}{U_A^2} \right)^{1/2}}{\tanh \left[0.530 \left(\frac{gh_a}{U_A^2} \right)^{3/4} \right]} \right] \quad (13)$$

$$\frac{gT_p}{U_A} = 7.54 \tanh \left[0.833 \left(\frac{gh_a}{U_A^2} \right)^{3/8} \right] \tanh \left[\frac{0.0379 \left(\frac{gX}{U_A^2} \right)^{1/3}}{\tanh \left[0.833 \left(\frac{gh_a}{U_A^2} \right)^{3/8} \right]} \right] \quad (14)$$

where U_A is the wind speed [m/s], g is the gravity [m²/s], h_a is the averaged water depth along the fetch and X is the wind fetch [m]. The wind fetch has been calculated following the wind provenance direction on the finite element hydrodynamic grid, thus considering islands and dry areas. h_a is the weighted average of the element water depth along the fetch using the each element part of the fetch distance as the weights. Using the averaged water depth along the fetch it could appear that the calculated wave height is higher than the real depth. To avoid this overestimation the wave height has been limited to the breaking wave height $H_{br} = 0.55h$ with h the element depth.

This empirical formulation assumes that the wind blows with essentially constant direction (which match the wind direction), over a fetch for sufficient time to achieve steady-state fetch limited values. For shallow water basin, such as the Venice Lagoon, the wave could be considered locally generated by the wind. This assumption is justified, considering that the time required for wave height to decay due to bottom friction is short (minutes) when compared with the wind duration (hours). Further evidence supporting the above hypothesis can be found in Lin et al. (2002), where wind and wave data collected in the Chesapeake Bay show that the mean wave direction closely follows the wind direction. The wind wave module has not been validated, because wave measures in the Venice Lagoon were unavailable.

3 Friction factor and bed shear stress

Sedtrans05 adopts the Grant and Madsen (1986) continental shelf bottom boundary layer theory to predict bed shear stresses and the velocity profile in

the bottom boundary layer. An explicit combined-flow ripple predictor is included in the model to provide time-dependent bed roughness prediction. The model assumes that total bed roughness (z_0) is composed of grain roughness, bedform (ripple) roughness as well as bedload roughness when sediment is in transport. Bed roughness effects on boundary layer parameters are included in the computation of friction factor and bed shear stress (τ_{cs} and τ_{cws}).

For further details, refer to Li et al., 2001 and Neumier et al. (in press).

4 Bedload transport

As bed shear stress increases, sediment particles will first be entrained from their resting position and then start to move along the bed by more or less regular jumps (bedload transport).

Five methods are proposed in SEDTRANS05 to predict the sediment transport for non-cohesive sediments. The bedload methods of Van Rijn (1993) is used here.

4.1 Criteria for initiation of bedload transport

The critical shear stress for initiation of motion reads:

$$\tau_{cr} = \theta_{cr} (\rho_s - \rho) g D \quad (15)$$

with ρ_s the sediment density, ρ the water density, g the acceleration due to gravity, D is the median sieve diameter and θ_{cr} is the dimensionless critical Shields parameter computed according the Yalin's method (Li et al., 2001).

4.2 Bedload transport rate formulation

Van Rijn (Van Rijn, 1993) followed the approach of Bagnold assuming that the motion of the bedload particles is dominated by particle saltations (jumps) under the influence of hydrodynamic fluid forces and gravity. The saltation characteristics have been determined by solving the equations of motions for an individual particle. The bedload transport rate is defined as the product of the particle velocity, the saltation height and the bedload concentration. It is assumed that the instantaneous bedload transport rate is related to the instantaneous shear stress parameter T_m .

For the pure current case the bedload transport rate states:

$$q = \alpha (s - 1)^{0.5} g^{0.5} D^{1.5} D_*^{-0.3} T_m^{2.1} \quad (16)$$

where g is the acceleration due to gravity, D is the median sieve diameter of grains, D_* is the dimensionless grain size, s is the ratio of density of sediment and water, α is a constant equal to 0.053 and T_m is shear stress parameter computed as:

$$T_m = \frac{\tau_{cs} - \tau_{cr}}{\tau_{cr}} \quad (17)$$

with τ_{cs} the instantaneous skin friction current shear stress and τ_{cr} the critical shear stress for initiation of motion.

For combined current and wave case the instantaneous bedload transport rate states:

$$q = 0.25 \alpha D D_*^{-0.3} \left(\frac{\tau_{cws}}{\rho} \right)^{0.5} T_m^{1.5} \quad (18)$$

where ρ is the water density, $a = 1 - (H/h)^{0.5}$ is a calibration factor and T_m now reads:

$$T_m = \frac{\tau_{cws} - \tau_{cr}}{\tau_{cr}} \quad (19)$$

with τ_{cws} the instantaneous skin friction combined shear stress. The time averaged bedload transport rate states is obtained averaging over a wave period.

5 Suspended sediment transport

When the bed shear velocity becomes comparable to that of the particle fall velocity, the particle may go into suspension (suspended transport). Once sediments are in the water column they are transported and diffused by currents and turbulence till the lifting force is greater than gravity force.

Multiple sand grain size classes are considered to behave independently.

5.1 Criteria for initiation of suspended transport

The suspended critical shear stress,

$$\tau_{crs} = \rho (u_{crs}^*)^2$$

is computed following the Van Rijn method (Van Rijn, 1993):

$$\begin{aligned} 1 < D_* \leq 10: & \quad \frac{u_{crs}^*}{w_s} = \frac{4}{D_*} \\ D_* > 10: & \quad \frac{u_{crs}^*}{w_s} = 0.4 \end{aligned} \quad (20)$$

where w_s is the settling velocity based on the formula of Soulsby (1997):

$$w_s = \frac{\nu}{D} \left[\left(10.36^2 + 1.049 D_*^3 \right)^{0.5} - 10.36 \right] \quad (21)$$

where ν the kinematic viscosity. D^* is the dimensionless grain size computed as:

$$D_* = \left[\frac{g(s-1)}{\nu^2} \right]^{1/3} D \quad (22)$$

where s is the ratio of density of sediment and water.

5.2 Advection-diffusion equation

When the bottom shear stress became higher than the suspended critical shear stress sediment particles go in the water column where they are transported by currents.

For each grain size class, transport, settling and diffusion of suspended sediment concentration (SSC) is described by the three-dimensional advection-diffusion sediment equation:

$$\frac{\partial C}{\partial t} + \frac{\partial uC}{\partial x} + \frac{\partial vC}{\partial y} + \frac{\partial wC}{\partial z} - w_s \frac{\partial C}{\partial z} = v_H \left(\frac{\partial^2 C}{\partial x^2} + \frac{\partial^2 C}{\partial y^2} \right) + v_V \frac{\partial^2 C}{\partial z^2} + E \quad (23)$$

where C is the suspended sediment concentration, v_H and v_V are the horizontal and vertical turbulent diffusion coefficients respectively and w_s is the settling velocity. The term E represents external source terms. This equations conserves mass of sediment that is advected with currents, settles due to gravity and diffuse due to turbulence. The model uses finite elements for spatial integration and a semi-implicit algorithm for integration in time.

Vertical boundary condition for the advection-diffusion equation are:

$$\begin{aligned} + v_V \frac{\partial C}{\partial z} + w_s C_{top} &= 0 & z = \text{top of the surface layer} \\ - v_V \frac{\partial C}{\partial z} - w_s C_{bot} &= ED & z = \text{bottom of the surface layer} \end{aligned} \quad (24)$$

where ED is the net sediment water column-bottom flux, corresponding to the difference between resuspension and deposition for each grain class. The term ED is evaluated explicit in case of erosion or implicitly in case of deposition. This approach permits to avoid negative concentration due to deposition higher than the sediment mass present in the water column.

5.3 Sediment exchange with the bed

The net sediment flux between bottom and water column ED is computed as the difference between the equilibrium concentration and the existing concentration in the lower flow level:

$$ED = w_s (\bar{C}_{eq} - C) \quad (25)$$

with w_s the settling velocity,

$$\bar{C}_{eq}$$

the average equilibrium sediment concentration in the lowest layer, calculated from the near-bed equilibrium concentration C_{eq} and assuming a logarithmic velocity and SSC profile (Rouse like profile), and C is the existing suspended sediment concentration in the lowest layer for the considered class.

This equation clearly indicates that when the near bed sediment concentration is less than the equilibrium value a net flux from the bed into the water column occurs ($ED > 0$). Likewise when the concentration exceeds equilibrium, a net flux to the bed occurs ($ED < 0$).

The sediment concentration at the reference height (bed roughness z_0 , see section 2.3.) is calculated using the formula of Smith and McLean (1977) adapted to include the presence of multiple sediment fractions:

$$C_{eq} = \eta_i \gamma_0 C_b \tau_* / (1 + \tau_*) \quad (26)$$

where $C_b = 0.65$ is the volume concentration of bottom sediment, η_i is the relative availability of the sediment fraction i at the bed,

$$\tau_* = (\tau_{cws} + \tau_{cr}) / \tau_{cr}$$

is the normalized excess shear stress, with τ_{cws} being the skin-friction combined shear stress and τ_{cs} the critical shear stress for initiation of motion, and γ_0 is the empirical sediment resuspension coefficient (Li at al., 2001).

6 Morphodynamics

Modifications to the bed elevation are equal to the sum over the sediment fractions of the net change due to suspended and bedload transport.

The net sediment change due to bedload is calculated using the sediment continuity equation, which reads:

$$\frac{\partial h}{\partial t} = \frac{1}{1 + \varepsilon} \left(\frac{\partial q_x^b}{\partial x} + \frac{\partial q_y^b}{\partial y} \right) \quad (27)$$

where h is the change in sediment bed, ε is the sediment porosity and q_x^b and q_y^b are the volumetric bedload transport rate in x and y direction. For the sediment continuity equation for bedload a direct advection scheme is used.

Modifications to the sediment bed caused by resuspension and redistribution of the suspended sediment are calculated as follow:

$$\rho_s (1 - \varepsilon) \frac{\partial h}{\partial t} = -ED \quad (28)$$

with ρ_s is the sediment density and ED is the water column-bottom flux computed as the difference between resuspension and sink (see section 2.5.3.).

7 Bed representation

The sediment bed model uses a three-dimensional grid underneath the hydrodynamic grid. Sediment within each class is exchanged between the bed and the overlying water column through erosion and deposition.

The bed could have spatially different characteristics, such as grainsize composition, sediment density and critical stress for erosion. The authors think

that this is of crucial importance for understanding the dynamics of sediments in lagoons which are by definition considered transition environments. A good representation of the bottom has to be the base for modelling the sediments.

The bed is subdivided in several layers and levels. Each layer is considered homogeneous, well mixed and characterized by its own grainsize distribution (fraction of each class of sediment considered). On the level are defined the dry bulk density ρ_{dry} and the critical stress for erosion τ_{ce} ; it is assumed that these variables vary linearly between two levels (figure 1). These characteristics could vary spatially in the domain.

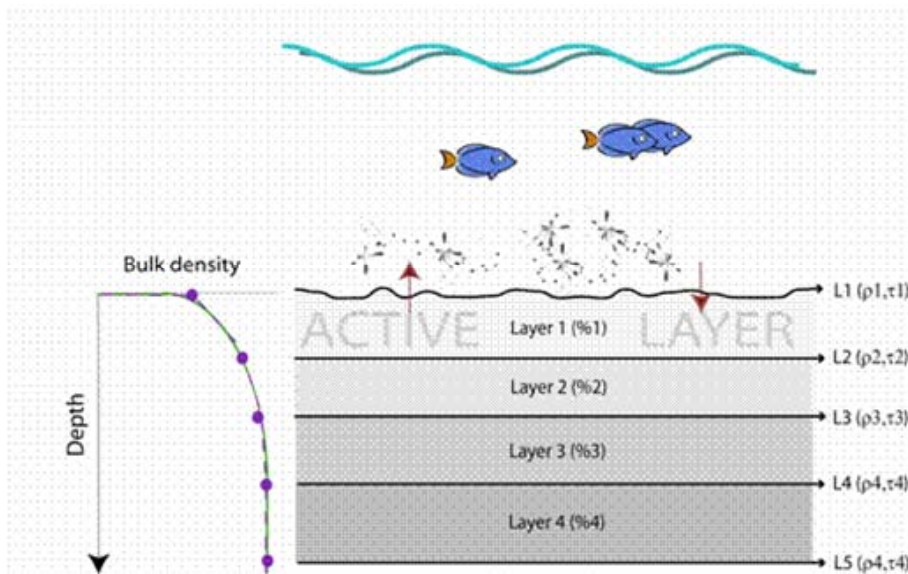


Figure 1: Vertical representation of the bed: the layers are homogeneous for grainsize composition; on the levels are defined the density and the critical stress for erosion which vary linearly between two levels.

At each location the uppermost layer has to be always greater or equal to the surficial active, or mixed, layer that is available for suspension (Courtney and Patricia, 2001). Sediment below the active layer is unavailable for resuspension until the active layer moves downward either because erosion has occurred, or it has thickened due to increase shear stress. As active layer is considered the bottom roughness height considered as the sum of the grain roughness, the bedload roughness and the bedform (ripple) roughness.

If a layer is completely eroded, it is removed and the remaining layers are moved upward. If a layer is only partially eroded, the surface value of ρ_{dry} and τ_{ce} are updated assuming a linear variation in the uppermost layer. When deposition occur a new sediment is added to the top increasing the thickness of the uppermost layer and updating the values of ρ_{dry} and τ_{ce} considering the characteristics of fresh deposited sediments. When the thickness of the uppermost layer exceeds a limit value a new layer is added to the top. Multiple sand grain size classes are considered to behave independently. At each location the average grain size (based on the sediment fractions) is used to compute the bed roughness and critical shear velocities. Modification of the bed

elevation and to the grain size distribution are updated at each time step based on the net erosion and deposition. For each size class, the volume of sediment removed from the bed during any time step is limited by the amount available in the active layer. In this way the model takes into account time-dependent and spatial sediment distribution and bed armouring.

8 Application to the Lido Inlet

The model will be applied to the Lido Inlet to simulate the sand transport between the Adriatic Sea and the Lagoon.

References

- Bagnold, R. A., 1966. An approach to sediment transport problem from general physics. Tech. Rep. 4421, US Geological Survey.
- Carter, R. G., 1988. Coastal Environments. An Introduction to the Physical, ecological and Cultural Systems of Coastlines estuaries and coastal sea. Publ. Academic Press, London, UK.
- Courtney, K. H., Patricia, L. W., 2001. A two-dimensional, time dependent model for suspended sediment transport and bed reworking for continental shelves. *Computer and Geosciences* 27, 675–690.
- Ferrarin, C., Umgiesser, G., in press. Hydrodynamic modeling of a coastal lagoon: the Cabras lagoon in Sardinia, Italy. *Ecological Modelling* .
- Grant, W. D., Madsen, O. S., 1986. The continental shelf bottom boundary layer. *Annual Review of Fluid Mechanics* 18, 265–305.
- Hubbard, D. K., Oertel, G., Nummedal, D., 1979. The role of waves and tidal currents in the development of tidal-inlet sedimentary structures and sand body geometry: examples from North Carolina and Georgia. *Journal of Sedimentary Petrology* 49, 1073–1092.
- Kjerve, B., Magill, K. E., 1989. Geographic and hydrodynamic characteristics of shallow coastal lagoons. *Marine Geology* 88, 187–199.
- Li, M. Z., Amos, C. L., 2001. SEDTRANS96: the upgrade and better calibrated sediment transport model for continental shelves. *Computers & Geosciences* 27, 619–645.
- Lin, W., Sanford, L. P., Suttles, S. E., 2002. Wave measurement and modeling in Chesapeake Bay. *Continental Shelf Research*, 22, 2673–2686.
- Scroccaro, I., Cappelletti, A., Umgiesser, G., 2003. An idealized circulation of the Orbetello lagoon. In: Ozhan, E. (Ed.), *Proceedings of the Sixth International Conference on the Mediterranean Coastal Environment*. Vol. 3. pp. 2087–2098.
- Scroccaro, I., Matarrese, R., Umgiesser, G., 2004. Application of a finite element model to the Taranto Sea. *Chemistry and Ecology* 20, Supplement 1, 205–224.

- Smith, J. D., McLean, S. R., 1977. Spatially averaged flow over a wavy surface. *Journal of Geophysical Research* (82), 1735–1746.
- Soulsby, D., 1997. *Dynamics of marine sands*. ThomasTelford.
- Umgiesser, G., 1997. Modelling the Venice Lagoon. *International Journal of Salt Lake Research* 6, 175–199.
- Umgiesser, G., Bergamasco, A., 1995. Outline of a Primitive Equations Finite Element Model. *Rapporto e Studi, Istituto Veneto of Scienze, Lettere ed Arti XII*, 291–320.
- Umgiesser, G., Melaku Canu, D., Cucco, A., Solidoro, C., 2004. A finite element model for the Venice Lagoon. Development, set up, calibration and validation. *Journal of Marine Systems* (51), 123–145.
- U.S. Army Engineer Waterways Experiment Station, 1984. *Shore Protection Manual*. U.S. Government Printing Office, Washington DC, U.S.
- Van Rijn, L. C., 1993. *Principles of sediment transport in rivers, estuaries and coastal sea*. Aqua Publications, Amsterdam, The Netherlands.

AREA 4

Data management

RESEARCH LINE 4.2

Modeling, analysis and environmental data visualization

ENVIRONMENTAL DATA AND VENICE LAGOON

Renzo Orsini, Francesco Dalla Libera, Stefania De Zorzi, Alessandro Roncato

Dipartimento di Informatica, Università di Venezia

Riassunto

In questo lavoro viene presentato lo stato di avanzamento del progetto "Modellazione, analisi e visualizzazione di dati ambientali", nell'ambito del Secondo Programma di Ricerca del CORILA, programma nato per approfondire le conoscenze sui processi che maggiormente contribuiscono alla contaminazione dell'ambiente lagunare veneziano. Vengono descritte le principali problematiche che si incontrano nella gestione di dati ambientali, e i primi risultati del progetto, volti alla definizione di una base di dati ambientali. Vengono infine presentati gli approcci adottati all'interno di alcune linee di ricerca attualmente in corso di sviluppo e di interesse nell'ambito dell'area delle basi di dati..

Abstract

The current state of the project "Modelling, analysis and visualization of environmental data" is presented, born in the framework of the Second Research Program of CORILA, which is aimed to the increase the knowledge on the pollution processes of the Venice lagoon. In the paper we describe the problems posed by the management of environmental data, as well as the first results of the project for the definition of an environmental database. Moreover we present some of the approaches of the research line currently explored which are of interests in the area of databases.

1 Introduction

The project "Modelling, analysis and visualization of environmental data", jointly developed by people at the Department of Computer Science of the Venice University "Ca' Foscari" and at the National Institute of Applied Sciences (INSA) of Lyon, is driven by a set of different needs:

- allow the systematic collection of data arising from scientific researches in very different areas, like environmental sciences, hydraulics, architecture, social sciences, etc.;
- develop tools and methods to integrate as much as possible such data, also through integration or interchange with other heterogeneous information systems on the Venice lagoon;
- develop tools to allow the use such data both by researchers of the different areas, as well as people responsible of the governance of the territory, in a simple way, through the use of web interfaces, graphical visualization systems or GIS systems;

- develop tools and methods for the analysis of data and the discovery of new knowledge through techniques of data mining, image analysis, spatio-temporal reasoning, complex systems, etc.

The objective of this extended abstract is to give a framework of the project, to present the main results obtained both by this project as well as by previous work devoted to a definition of an environmental database, to discuss some of the research lines currently under development, and to describe a few problems which will be attacked in the rest of the research.

2 The project

A large number of studies currently performed on the Venice lagoon are producing a huge amount of scientific environmental data which are characterized by the complexity, the spread and the heterogeneity. [Smith et al., 1999; Bill et al., 1999a,b; Blair et al., 2002b].

In order to use such amount of information to increase the knowledge on the processes which mainly contribute to the pollution of the environment of the lagoon, so that it would be possible to make careful and useful interventions on the territory, it is essential that: 1) the maximum number of interrelations would be exploited among such heterogeneous data; 2) tools be developed to analyse and extract different types of knowledge, to apply not only to single datasets, but on large set of related data; and 3) tools be made available in order to simplify the access to the interrelated data and to the analysis on them. The project has the objective of producing tools to model, integrate, analyse and access environmental data currently collected by research projects or by external sources, through three workpackages which are devoted to the three aspects cited above.

The first workpackage tackles the problem of modelling the data and integrate them through three different point of view: 1) by defining data structuring mechanisms which can be used to model heterogeneous data in a unified framework; 2) by studying ontologies available in the environmental area, with the production of tools for creating and using them by researchers of the field, and 3) by providing tools for the integration of environmental data available from different data sources and organizations.

In the second workpackage we study different techniques for the analysis of environmental data. A first activity is based on data mining techniques for the extraction of frequent patterns and recurring rules for spatio-temporal referred environmental data and on methods for the reasoning on the extracted knowledge. Another activity concerns the use of techniques for pattern recognition for images, applied to images of buildings, in order to extract significant features and acquire knowledge on their age and state. Another activity concerns the modeling of the lagoon with the use of the theory of Complex Systems, in order to evaluate some of its properties, like efficiency and weak points. The third workpackage is devoted to the development of models and tools for the analysis of continuous data, that is data which model

continuous phenomena and which are derived from continuous fields. Such data are known only on certain points (sampled data). The problem is the building of spatio-temporal interpolations in order to know the phenomenon in each point, and to store not only the sampled points with their coordinates and attributes, but also the spatial and temporal interpolation methods.

3 The database RIVELA

It is well known that the most difficult aspect of structuring an environmental database is the necessity of managing lot of data deriving from completely different areas, like geology, idrology, biology, chemistry, physics, etc. [Michener et al., 2002]. In fact the environment is a really complex system, and each discipline which studies it treat different data with different approaches. The management of the complexity and variety of such data require a database which can accommodate the different research groups and which allows the integration of those data in a single coherent but flexible structure, and, at the same time, which facilitates, through the exploitation of implicit relationships among the data, the discovery and analysis of complex phenomena which span onto different areas.

At the CORILA the relational database RIVELA ("Ricerche su Venezia e la Laguna", Researches on Venice and Lagoon) has been defined and implemented which integrates both biological and chemical-physical data, with the relevant geographical and temporal aspects, as well as any information concerning their acquisition [Campostrini et al., 2001, Campostrini et al., 2002].

The database consists of two main components: a statical one, with auxiliary information, and a dynamic one, concerning field or laboratory data. In Fig. 1 the main sections of the database are shown, and the dynamic component is in the grey area.

The static part maintains the following information:

- Administrative and scientific data concerning the research activities (Research Projects, Workpackages, Activities)
- Geographical location of data (Area, Environmental Units, Locations)
- Information on types of data acquired (Matrices, Sample Types, Parameters)
- Methodologies and Devices of data acquisition

The dynamic part contains four fundamental entities: Measures, Samples, Stations and Sampling Activities. A measure is the value of a parameter which derives from a certain sample, which has exact spatial coordinates (Station) and a temporal location. Samples, on the other hand, are classified according to their type (Sample types), which depend on the environmental matrix.

The database is enriched by a set of web applications which allow the researchers to insert dynamic data, verifying their consistency with the

database, search the data also as datasets through guided queries, or visualize the data with a GIS system.

Finally, note that the current version of RIVELA is more complex than what has been described here, by maintaining semi-structured data, as scientific reports, publications, etc., as well as data collected by researchers of other areas (such as historical, economical or architectural data).

4 The use of Ontologies

In the context previously described, the use of ontologies and thesauri is considered important for the following reasons:

- enhance the sharing of the information among the researchers of different areas (and also in the same area), through normative descriptions of data;
- increase the diffusion of standard ontologies (or metadata) to allow a better classification both of semi-structured data (as technical reports) and of structured data (as the collected datasets) in order to improve the retrieval of the information;
- facilitate the integration of Rivela with other databases through tools and methodologies based on ontologies;
- build a solid information infrastructure for the development of tools of data analysis, model building, etc.;
- experiment tools for the cooperative building of ontologies.

A first analysis of the state of the art has been described in [Casagrande et al., 2005], which has found a few scientific ontologies which could be adopted in the project.

Another of the objectives of the project is the development of a web application to allow to the researchers to cooperate to the building and use of a specific ontology.

5 Database integration

In the project a number of integration aspects must be addressed, and several research problems are tackled. In particular:

- the building of tools to access in a uniform and transparent way both Rivela and other databases internal and external to CORILA;
- the development of methods and tools to integrate into the data model of Rivela data currently maintained in external data sources;
- the building of tools which allows the development of scientific analysis software parametric with respect to the data source, and capable of operating both on databases with different structure that on an integrated view of heterogeneous databases.

An approach currently under development which looks promising is based on the concept of "database interface" [Orsini et al., 2005]. This approach is based on a declarative language which allows the definition of an interface between a database and one or more "external" applications which are not defined on its schema. The interface is used to specify the "minimal" requirements by the applications in order to work correctly with a database. Such requirements are described using the SQLI language, which is used both to give a partial specification of database tables and columns (data structure constraints), and partial specifications of table instances (value constraints).

An important objective of this approach is the possibility of porting an application over a database on which a very restricted set of operations is allowed, typically only a limited access, without the possibility, for instance, of defining user views to adapt the database to the application. The main objective is the isolation of the application from the database, by modifying appropriately the interface when one of the two elements changes.

6 Conclusions.

The project "Modelling, analysis and visualization of environmental data" has been presented, its first results are been described and several promising approaches are discussed. Other activities of the project are in their first stage and for this reason are not yet ready for public discussion.

One important objective of this project is to stimulate the increase of the research on environmental data, both in the area of data modelling and management, as well as in the area of data analysis and visualization. On these arguments a workshop is planned in the next months.

References.

Michener W.K., Brun J.W., 2002. *Ecological Data (Design, Management and Processing)*. Balckwell Science Ltd..

Campostrini P., Dabalà C., De Zorzi S., Orsini R., 2001, *Rivela*, (Database for Research on Venice and the Lagoon): An instrument for Environmental Research, in "Scientific Research and Saveguarding of Venice: CORILA Research Program, 2001 Results", Venezia.

Campostrini, P., Dabalà, C., De Zorzi S., Orsini R., 2002, *Rivela: Database for the research on Venice and the Lagoon*. In "The colour of Ocean Data. International Symposium on Oceanographic Data and Information Management". Brussels, Belgium.

Casagrande A., Orsini R., Dalla Libera F., 2005, *Stato dell'arte su formati, linguaggi e modelli per la definizione e lo scambio dei dati delle Scienze della Terra*. Rapporto Tecnico Dipartimento di Informatica, Università Di Venezia.

Orsini R., Roncato A., 2005, *Interfaces for Databases: Motivations, Definitions and Tools*, Rapporto Tecnico Dipartimento di Informatica, Università di Venezia,

Finito di stampare aprile 2006
Presso Multigraf Industria Grafica Editrice
Spinea - Venezia